Ultraviolet Light Induced Reactions in Polymers

Santokh S. Labana, EDITOR

Ford Motor Co.

An international

symposium sponsored by

the Division of Organic

Coatings and Plastics

Chemistry at the 169th

Meeting of the American

Chemical Society,

Philadelphia, Penn.,

April 8–11, 1975

ACS Symposium Series

Robert F. Gould, *Editor*

Advisory Board

FOREWORD

The ACS SYMPOSIUM SERIES was founded in 1974 to provide a medium for publishing symposia quickly in book form. The format of the SERIES parallels that of the continuing ADVANCES IN CHEMISTRY SERIES except that in order to save time the papers are not typeset but are reproduced as they are submitted by the authors in camera-ready form. As a further means of saving time, the papers are not edited or reviewed except by the symposium chairman, who becomes editor of the book. Papers published in the ACS SYMPOSIUM SERIES are original contributions not published elsewhere in whole or major part and include reports of research as well as reviews since symposia may embrace both types of presentation.

PREFACE

S tudy of the effects of ultraviolet light on polymers has attracted considerable interest for a long time. Some of the early research was directed towards understanding the photodegradation processes in polymers, especially for polymers used in paints and in articles exposed to sunlight. In general this research aimed to make polymers more durable to light. A number of very effective photostabilizers were developed as a result. More recently, because of ecological concerns, notable efforts are being made to develop polymers with controlled rate of photodegradation or to develop polymers which are stable when kept away from sunlight but which degrade rapidly outdoors. Significant progress has been made in this direction in recent years.

Ultraviolet light can be used to induce reactions for making new polymers, modification of existing polymers, crosslinking of polymers, and degradation of polymers. This book deals with the recent developments on both the mechanisms of these reactions and discusses their use. All of these have provided bases for a number of important industrial materials and processes. Various papers describe the use of ultraviolet light for curing of paints, printing inks, microelectronics, photostabilization, photodegradation, and theoretical treatment of the excited species in the photochemical reactions.

The need to reduce solvent emissions and to conserve energy in coatings and printing inks has stimulated investigations of the applications of photopolymerization reactions. The ultraviolet light curable coatings and printing inks generally produce much less organic emissions and cure with less energy consumption as compared with thermally cured compositions. The growth of uv-curable coatings so far has been limited by lack of rapid photopolymerization in highly pigmented or thick (over 25 μ) coatings.

Approximately half of the papers in the book deal with photopolymerization reactions including the role of photoinitiators and photosensitizers. The other half of the papers deal with photodegradation reactions including the use of photostabilizers and photodegradable polymers.

I take pleasure in acknowledging Ford Motor Co. and S. Gratch for their interest in, and support of, this project. I also wish to express my

appreciation to Carol Gestwicki, Joan Gorski, and Anne Oslanci for their secretarial assistance. Finally, I thank the Division of Organic Coatings and Plastics Chemistry, American Chemical Society for sponsoring the Symposium.

Ford Motor Co.   SANTOKH S. LABANA
Dearborn, Mich.
December 16, 1975

Participation of Excited Species in Propagation Step in Photopolymerization
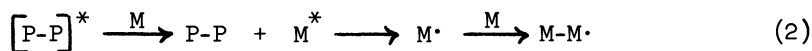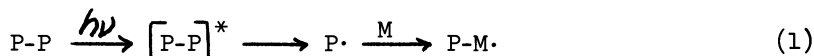
NORMAN G. GAYLORD

Gaylord Research Institute, Inc., New Providence, N.J. 07974

The use of ultraviolet light in polymerization processes takes advantage of the fact that exposure of organic molecules to irradiation results in the generation of reactive species, e.g. excited species, at ambient or lower temperatures. The role of UV light has generally been considered to be restricted to the initiation of polymerization. However, propagation may also involve, or even be limited to, species generated by photo-excitation.

UV Light in Polymerization Initiation

When a polymerizable monomer is exposed to UV light in the presence of a photosensitizer, polymerization may be initiated by radicals generated by dissociation of the excited sensitizer, e.g. benzoin methyl ether. Alternatively, the excited photosen-sitizer may transfer its excitation energy to the monomer which, in turn, undergoes excitation and radical initiated polymeriza-tion.

$$P\text{-}P \xrightarrow{h\nu} [P\text{-}P]^* \longrightarrow P\cdot \xrightarrow{M} P\text{-}M\cdot \qquad (1)$$

$$[P\text{-}P]^* \xrightarrow{M} P\text{-}P + M^* \longrightarrow M\cdot \xrightarrow{M} M\text{-}M\cdot \qquad (2)$$

The initiation of polymerization in the presence of benzo-phenone requires the presence of a hydrogen donor such as a sol-vent or polymer. The excited sensitizer abstracts a hydrogen from the donor resulting in the formation of a radical which initiates monomer polymerization.

$$P \xrightarrow{h\nu} P^* \xrightarrow{SH} PH + S\cdot \xrightarrow{M} S\text{-}M\cdot \qquad (3)$$
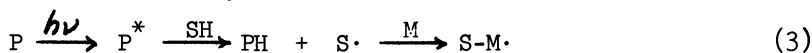
Polymerization of monomers occurs in the absence of a photosensitizer when the functional groups in the monomer undergo
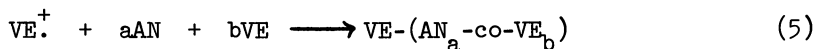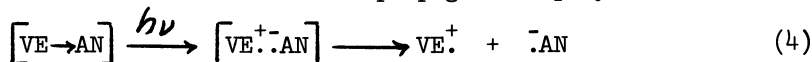
excitation upon exposure to light of the appropriate wavelength,
i.e. energy level.

Although the result of photoactivation of a monomer is gen-
erally the generation of a radical species, ionic polymerization
has been reported where a cationically polymerizable monomer,
i.e. isobutylene, underwent photoionization in the vapor state
and the ionized fragments were separated from their electrons by
an electric field (1).

Irradiation of a donor monomer-electron acceptor charge
transfer complex, e.g. N-vinylcarbazole-sodium chloroaurate (2),
-nitrobenzene (2) or -p-chloroanil (3) and β-propiolactone-uranyl
nitrate (4), results in the initiation of cationic polymerization.

Irradiation of an acceptor monomer-electron donor charge
transfer complex initiates anionic polymerization in the case of
nitroethylene-tetrahydrofuran (5) and radical polymerization in
the case of methyl methacrylate-triphenylphosphine (6).

Free radical copolymerization is initiated upon UV irradia-
tion of mixtures of isobutyl vinyl ether and acrylonitrile (7),
presumably as a result of photoexcitation of the comonomer charge
transfer complexes. The excited complexes dissociate into ion-
radicals which initiate radical propagated copolymerization.

$$[VE \rightarrow AN] \xrightarrow{h\nu} [VE^{+} \cdot^{-} AN] \longrightarrow VE^{+} \cdot \ + \ ^{-} \cdot AN \qquad (4)$$

$$VE^{+} \cdot \ + \ aAN \ + \ bVE \longrightarrow VE\text{-}(AN_a\text{-}co\text{-}VE_b) \qquad (5)$$

Mixtures of styrene and acrylonitrile also yield free radi-
cal copolymers under UV irradiation (Table I) (8).

Table I. Photoinitiated Copolymerization of Styrene and
Acrylonitrile[a]

Light	Time, hr.	Conversion,%	S/AN mole ratio Found	Theory
Dark	24.0	0.0		
2537 A.	0.5	0.5		
3500 A.	0.5	0.9		
	6.0	12.2	58/42	59/41
	18.0	31.6		
3500 A.	1.0	1.8		
Dark	24.0	2.3		

[a] S/AN mole ratio = 1; 30°C

Although initiation by monomer ion-radicals may also be operative
in this case, alternatively, homopolymerization of excited comon-
omer complexes may occur to a limited extent, due to the low con-
centration of such complexes, followed by ion pair coupling or
dissociation to initiate radical copolymerization.

$$[S \rightarrow AN] \xrightarrow{h\nu} [S\overset{+}{\cdot}\overset{-}{\cdot}AN] \longrightarrow (S-AN)_x S\overset{+}{\cdot}\overset{-}{\cdot}AN \tag{6}$$

$$(S-AN)_x S\overset{+}{\cdot}\overset{-}{\cdot}AN \begin{cases} \longrightarrow (S-AN)_x S-AN\cdot & (7) \\ \longrightarrow (S-AN)_x S\cdot + AN & (8) \end{cases}$$

$$(S-AN)_x S-AN\cdot + aS + bAN \longrightarrow (S-AN)_x S-AN-(S_a-co-AN_b) \tag{9}$$

$$(S-AN)_x S\cdot + aS + bAN \longrightarrow (S-AN)_x S-(S_a-co-AN_b) \tag{10}$$
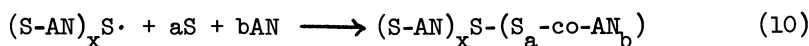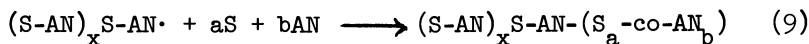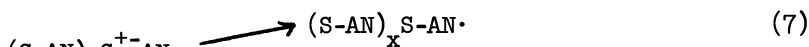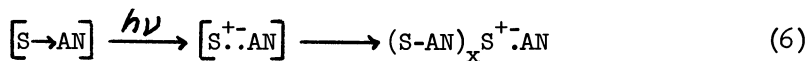
Thus, in these cases, UV radiation provides a method for the initiation of radical or ionic polymerization. After the initiation st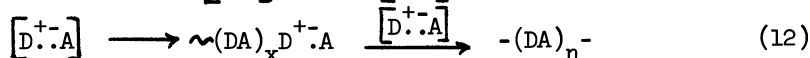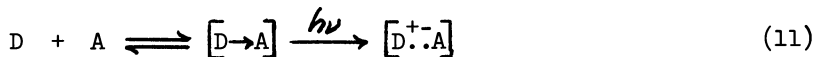ep, chain propagation proceeds as though initiation resulted from the use of conventional catalysts for radical and ionic polymerization.
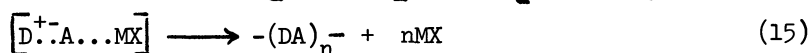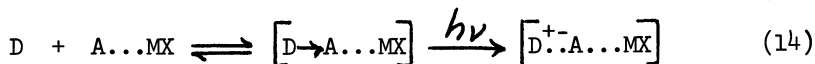
UV Light in Polymerization Propagation

Photoactivated Copolymerization. Although polymerization and copolymerization generally involve the addition of a monomer to a reactive chain end, the ground state charge transfer complex generated by the interaction of an electron donor monomer and a strong electron acceptor monomer, acts as a single unit and, upon excitation of the complex, both monomers enter the chain.

$$D + A \rightleftharpoons [D \rightarrow A] \xrightarrow{h\nu} [D\overset{+}{\cdot}\overset{-}{\cdot}A] \tag{11}$$

$$[D\overset{+}{\cdot}\overset{-}{\cdot}A] \longrightarrow \sim(DA)_x D\overset{+}{\cdot}\overset{-}{\cdot}A \xrightarrow{[D\overset{+}{\cdot}\overset{-}{\cdot}A]} -(DA)_n- \tag{12}$$

The N-vinylpyrrolidone-maleic anhydride charge transfer complex undergoes homopolymerization upon photoexcitation in air to yield the alternating copolymer (9).

Complexation of a relatively poor electron accepting monomer with a Lewis acid or organoaluminum compound converts the acceptor monomer to a stronger electron acceptor, thus promoting the formation of ground state comonomer complexes. The latter undergo photoexcitation and homopolymerization.

$$A + MX \longrightarrow A...MX \tag{13}$$

$$D + A...MX \rightleftharpoons [D \rightarrow A...MX] \xrightarrow{h\nu} [D\overset{+}{\cdot}\overset{-}{\cdot}A...MX] \tag{14}$$

$$[D\overset{+}{\cdot}\overset{-}{\cdot}A...MX] \longrightarrow -(DA)_n^- + nMX \tag{15}$$

Complexation of methyl methacrylate and acrylonitrile with triethylaluminum converts these poor electron accepting monomers into stronger electron acceptors. Ground state charge transfer complexes are generated when styrene is added to these monomers in the presence of triethylaluminum. Photoexcitation of the

complexes under UV irradiation results in the formation of ex-
ciplexes which homopolymerize to yield equimolar copolymers over
a wide range of comonomer ratios (10). Thus, UV light controls
the propagation step by promoting the formation of polymerizable
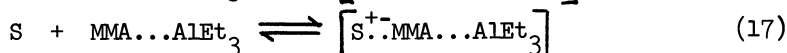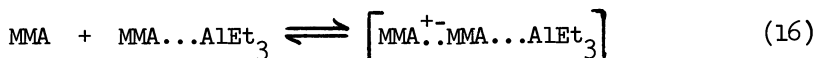species, i.e. comonomer exciplexes.

As shown in Table II, the photoactivated copolymerization of
styrene and methyl methacrylate in the presence of $AlEt_3$ yields
equimolar, alternating copolymers when the initial monomer charge
contains excess styrene. However, when the comonomers are pre-
sent in equimolar ratio, the copolymer is rich in methyl meth-
acrylate.

Table II. Photoactivated Polymerization of S-MMA...$AlEt_3$[a]

Charge S/MMA/Al mole ratio	Conversion, %[b]	Copolymer S/MMA mole ratio	
		Found	Theory
50/50/10	1.74	37/63	50/50
70/30/5	2.79	51/49	60/40
80/20/4	2.83	51/49	70/30
85/15/3	2.95	51/49	75/25
90/10/2	3.19	50/50	84/16

[a] 500W tungsten lamp; 5°C; $\left[AlEt_3\right]$ = 10 mmoles; 2 hr
[b] Based on 1/1 S/MMA

Since MMA...$AlEt_3$ is a stronger electron acceptor than un-
complexed MMA, it forms charge transfer complexes with the latter
as well as with styrene.

$$MMA + MMA...AlEt_3 \rightleftharpoons \left[MMA\overset{+-}{..}MMA...AlEt_3\right] \qquad (16)$$

$$S + MMA...AlEt_3 \rightleftharpoons \left[S\overset{+-}{..}MMA...AlEt_3\right] \qquad (17)$$

The copolymerization of the two complexes yields an MMA-rich co-
polymer. However, when the initial monomer charge contains ex-
cess styrene, there is little or none of the complex from Eq.
(16) and the equimolar copolymer results from the homopolymeriza-
tion of the comonomer complex in Eq. (17).

The copolymerization of styrene and acrylonitrile in the
presence of $AlEt_3$ under UV irradiation yields equimolar, alter-
nating copolymers when the initial comonomer charge is equimolar
or contains excess acrylonitrile and products with compositions
intermediate between that of the equimolar copolymer and that of
the radical copolymer when the initial charge is rich in styrene
(Table III) (10). The intermediate compositions may represent
mixtures of equimolar and radical copolymers, block copolymers
generated as shown in Eq. (6)-(10) or random copolymers resulting
from copolymerization of complexes and monomers.

Table III. Photoactivated Polymerization of S-AN...AlEt$_3$[a]

Charge S/AN/Al mole ratio	Conversion, %[b]	Copolymer S/AN mole ratio	
		Found	Theory
30/70/6	8.81	51/49	54/46
50/50/6	5.67	51/49	59/41
70/30/6	7.12	64/36	67/33
80/20/6	14.33	63/37	74/26
90/10/6	27.10	72/28	84/16

[a] 3500 A. Hg lamp; 30°C; $\left[\text{AlEt}_3\right]$ = 12 mmoles; 2 hr
[b] Based on 1/1 S/AN

Ethylaluminum sesquichloride (EASC) and dichloride are even more effective than AlEt$_3$ in promoting the formation of styrene-methyl methacrylate and styrene-acrylonitrile charge transfer complexes. The concentration of ground state complexes is sufficiently high so that autoexcitation occurs, possibly through collision, and polymerization proceeds even in the dark. However, upon exposure to UV light, the concentration of exciplexes and the rate of homopolymerization are greatly increased to yield alternating copolymers over a wide range of comonomer compositions (Table IV) (10).

Table IV. Photoactivated Polymerization of S-AN...EASC[a]

Charge S/AN/Al mole ratio	Conversion, %[b]	Copolymer S/AN mole ratio	
		Found	Theory
12.5/87.5/5	10.7	48/52	45/55
25/75/5	15.4	50/50[c]	50/50
37.5/62.5/5	16.5	52/48	54/46
50/50/5	21.5	52/48	59/41
62.5/37.5/5	17.1	51/49	62/38
75/25/5	12.3	55/45[c]	69/31

[a] Ambient light; 30°C; $\left[\text{EASC}\right]$ = 10 mmoles; 1 hr
[b] Based on 1/1 S/AN
[c] Alternating structure confirmed by NMR

The influence of UV light on the course of copolymerization, i.e. on copolymer composition, is dramatically shown in the terpolymerization of butadiene, methyl methacrylate and acrylonitrile in the presence of ethylaluminum dichloride. The reaction actually involves the copolymerization of two complexes, i.e. BD-MMA...EtAlCl$_2$ and BD-AN...EtAlCl$_2$. When the reaction is conducted in the dark with an initial BD/MMA/AN = 60/20/20 molar

charge, the terpolymer composition varies with temperature, rang-
ing from a BD/MMA/AN composition of 50/41/9 at 0°C to a 47/17/36
composition at 50°C. In contrast, when the reaction is conducted
under UV light, the composition is essentially independent of
temperature and remains at about 50/33/17 over the 0-50°C range
(Table V) (11). Apparently thermal activation yields differing
relative amounts of the copolymerizable excited complexes as the
temperature is varied while UV light excites all of the ground
state complexes whose relative concentrations are independent of
temperature. The yield of terpolymer is at a maximum between 330
and 350 mμ, consistent with the UV spectra which indicate the
formation of a charge transfer complex with absorption in this
region (12).

Table V. Terpolymerization of BD-MMA-AN in Presence of EtAlCl$_2$
                BD/MMA/AN/Al = 60/20/20/2 mole ratio

Dark					UV Light				
Temp., °C	BD	MMA	AN	MMA/AN	Temp., °C	BD	MMA	AN	MMA/AN
0	50	41	9	4.55	2	50	34	16	2.12
19	52	26	23	1.13	21.5	50	33	17	1.94
30	56	20	24	0.83	30	49	33	18	1.83
40	47	18	35	0.51	40	50	33	17	1.94
50	47	17	36	0.47	50	52	32	16	2.02

        In the terpolymerization of styrene, methyl methacrylate and
acrylonitrile (S/MMA/AN = 50/25/25 mole ratio) in the presence of
EASC, the terpolymer composition is approximately 50/36/14, in-
dependent of the temperature within the range of 10-90°C, whether
the reaction is conducted in the dark or under UV radiation (10).
However, the terpolymerization rate is increased 2-5 times under
UV light.
        The reaction of a conjugated diene such as butadiene or iso-
prene and an electron acceptor monomer such as maleic anhydride
proceeds through a ground state complex which undergoes cycliza-
tion to yield the Diels-Alder adduct. However, under UV light,
in air or in the presence of sensitizers, the adduct is accompa-
nied by the equimolar, alternating copolymer which results from
excitation of the ground state complex, followed by homopolymer-
ization of the excited complex (13), as shown in Eq. (18).
        When the electron acceptor monomer is a relatively weak
acceptor, e.g. acrylonitrile, the reaction with a conjugated
diene such as butadiene, to yield the Diels-Alder adduct, pro-
ceeds slowly. However, in the presence of aluminum chloride, the
acrylonitrile is converted to a stronger electron acceptor and the
formation of the ground state complex and the adduct therefrom
proceeds more rapidly. When the reaction is carried out under UV
irradiation, the yield of adduct is greatly reduced and the equi-

$$(18)$$
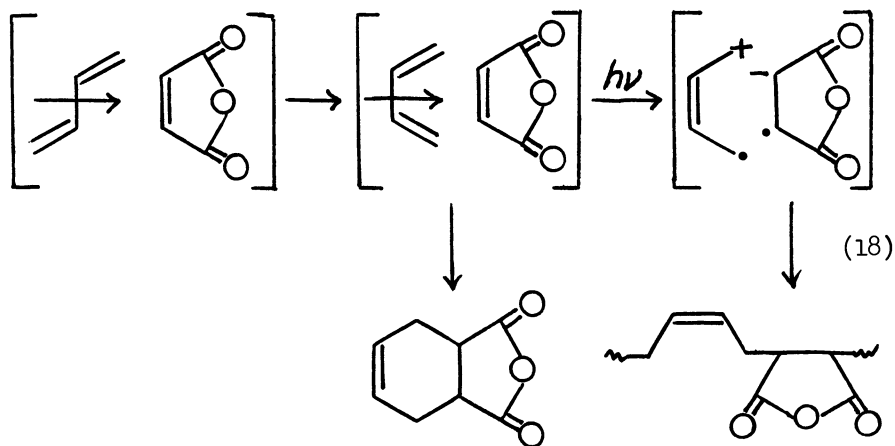
molar, alternating copolymer becomes the predominant product (14) (Table VI), in accordance with the reaction sequence shown in Eq. (19).

Table VI. Photoactivated Copolymerization of Butadiene and Acrylonitrile in Presence of $AlCl_3$ and $EtAlCl_2$[a]

	$AlCl_3$		$EtAlCl_2$	
	Dark	UV	Dark	UV
Adduct BD AN	23.5	12.8	20.0	18.3
Copolymer (BD-AN)$_n$	0	147.3	15.8	126.8

[a] BD/AN/Al = 266/266/2.66 mmoles; $20^{\circ}C$; 40 min
Yield in 10^{-3} mmoles/min

$$(19)$$
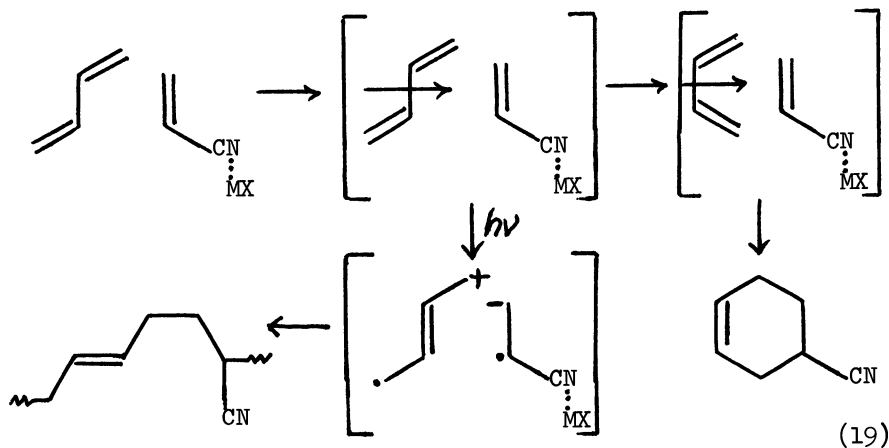
    As shown in Table VI, when the reaction between butadiene
and acrylonitrile is carried out in the presence of EtAlCl$_2$,
autoexcitation occurs even in the dark to yield both adduct and
equimolar, alternating copolymer. Nevertheless, UV light pro-
motes the formation of the copolymer. Thus, in these reactions
excitation under UV light results in a change in the course of
the reaction from adduct formation to copolymerization.

    Photoactivated Homopolymerization. The participation of
excited monomer has been proposed in the polymerization of ethyl-
ene under UV (15,16) as well as gamma irradiation (17) in the
presence of trace amounts of oxygen. It has been suggested that
under irradiation, ethylene undergoes excitation per se or as a
result of the perturbing effect of oxygen, to generate triplet
excited ethylene. The latter reacts with ground state ethylene
to generate a diradical dimer (16) or an excited dimer (17).
Propagation involves addition of the dimer to the growing chain
end which is presumed to be a radical. In one proposal (17),
addition of the excited dimer results in the incorporation of one
ethylene unit into the chain and the regeneration of excited
ethylene monomer.

$$CH_2{=}CH_2 \;\rightleftharpoons\; \left[CH_2{=}CH_2\right]^* \qquad\qquad (20)$$

$$\left[CH_2{=}CH_2\right]^* \;+\; CH_2{=}CH_2 \;\rightleftharpoons\; \left[(CH_2{=}CH_2)_2\right]^* \quad (21)$$

$$\sim\!CH_2\cdot \;+\; \left[(CH_2{=}CH_2)_2\right]^* \;\longrightarrow\; \sim\!CH_2CH_2CH_2\cdot \;+\; \left[CH_2{=}CH_2\right]^* (22)$$
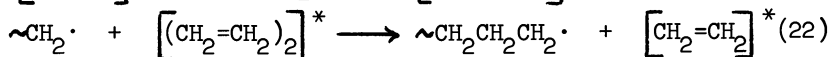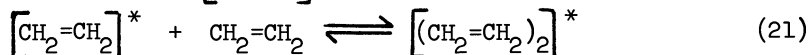
    If the excited ethylene dimer exists as an ion radical pair,
propagation may incorporate both monomeric units of the dimer,
analogous to the behavior of comonomer charge transfer complexes
such as butadiene-maleic anhydride, or only one unit, as noted in
the homopolymerization of N-vinylcarbazole in the presence of
electron accepting monomers such as acrylonitrile and maleic
anhydride.
    Although long considered incapable of homopolymerization,
maleic anhydride is readily polymerized under UV irradiation in
the presence of a photosensitizer (18,19). The polymerization
presumably involves propagation of excited maleic anhydride (20).
It is noteworthy that the structure of poly(maleic anhydride)
contains fused cyclopentanone and succinic anhydride units,
derived from two interacting maleic anhydride units. This sug-
gests that propagation involves excited dimer rather than monomer.

X = H or COOH   (23)
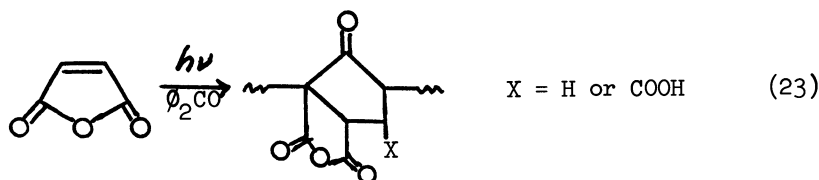
Chemically Induced Photopolymerization in the Absence of Light

The interaction of UV light with organic molecules is not the only method of generating electronically excited species. The same excited species that are formed under irradiation are produced by certain chemical reactions in the absence of light. Such chemically generated excited species undergo the same chemical reactions as the excited species formed by the absorption of light, including the transfer of excitation energy (21).

The altered NMR spectra characteristic of chemically induced dynamic polarization (CIDNP) (22) are observed during the photolytic decomposition of various peroxides in the presence of photosensitizers at ambient temperatures, as well as the thermal decomposition of these peroxides in the absence of light at temperatures where they have a short half-life. The reactions which are responsible for CIDNP are apparently similar in both cases. The precursors of such reactions are photolytically and chemically generated species, respectively, capable of transferring energy to suitable acceptors.

The excitation of comonomer donor-acceptor complexes occurs in the presence of peroxides, under conditions where the latter are undergoing rapid decomposition. The peroxide-induced excited complexes then undergo homopolymerization to equimolar, alternating copolymers. Thus, styrene-methyl methacrylate, styrene-acrylonitrile, α-olefin-acrylonitrile and butadiene-acrylonitrile yield equimolar copolymers in the presence of $AlCl_3$ and/or organoaluminum halides under these conditions. Excited complexes are also the polymerizable species in the peroxide-induced copolymerization of conjugated dienes and maleic anhydride as well as in the formation of copolymers during the retrograde rearrangement of cyclopentadiene-maleic anhydride Diels-Alder adducts.

Ethylene and maleic anhydride undergo peroxide-induced homopolymerization under similar conditions, i.e. in the presence of peroxides undergoing rapid decomposition, presumably through the propagation of excited monomers or dimers.

Summary

Irradiation of a suitable monomer under UV light in the presence of a photosensitizer or complexing agent results in the initiation of conventional radical or ionic polymerization, wherein the monomer adds to the propagating chain end. Irradiation of ground state comonomer charge transfer complexes results in excitation followed by homopolymerization, wherein the comonomer exciplex adds to the propagating chain end to yield equimolar, alternating copolymers, e.g. S-MMA and S-AN in the presence of R_2Al or RAlX. The terpolymerization of BD-MMA-AN in the presence of $RAlCl_2$ yields terpolymers whose composition varies with temperature in the dark and is independent of temperature under UV light. The ground state comonomer complexes from BD-maleic

anhydride and BD-AN-AlCl$_3$ and -EtAlCl$_2$ undergo cyclization to
yield adducts in the dark and excitation followed by homopolymer-
ization under UV light. Excited ethylene monomer or dimer par-
ticipates in the propagation step in the polymerization of ethyl-
ene under UV light in the presence of oxygen. Homopolymerization
of maleic anhydride under UV light in the presence of a photosen-
sitizer proceeds through propagation of the excited monomer or
dimer.

Literature Cited

1. Sparapany, J. J., J. Amer. Chem. Soc. (1966) 88, 1357.
2. Tazuke, S., Asai, M., Ikeda, S., Okamura, S., J. Polym. Sci.,
      Part B (1967) 5, 453.
3. Natsuume, T., Akana, Y., Tanabe, K., Fujimatsu, M., Shimizu,
      M., Shirota, Y., Hirata, H., Kusabayashi, S., Mikawa, H.,
      Chem. Commun. (1969) 189.
4. Sakamoto, M., Hayashi, K., Okamura, S., J. Polym. Sci., Part
      B (1965) 3, 205.
5. Irie, M., Tomimoto, S., Hayashi, K., J. Polym. Sci., Part B
      (1972) 10, 699.
6. Mao, T. J., Eldred, R. J., J. Polym. Sci., Part A-1 (1967) 5,
      1741.
7. Tazuke, S., Okamura, S., J. Polym. Sci., Part A-1 (1969) 7,
      715.
8. Gaylord, N. G., Dixit, S. S., J. Polym. Sci., Part B (1971)
      9, 823.
9. Tamura, H., Tanaka, M., Murata, N., Bull. Chem. Soc. Japan
      (1969) 42, 3042.
10. Gaylord, N. G., Dixit, S. S., Maiti, S., Patnaik, B. K., J.
      Macromol. Sci. (Chem.) (1972) A6, 1495.
11. Furukawa, J., Kobayashi, E., Iseda, Y., Arai, Y., J. Polym.
      Sci., Part B (1971) 9, 179.
12. Furukawa, J., Kobayashi, E., Arai, Y., J. Polym. Sci., Part
      B (1971) 9, 805.
13. Gaylord, N. G., Maiti, S., Dixit, S. S., J. Macromol. Sci.
      (Chem.) (1972) A6, 1521.
14. Furukawa, J., Kobayashi, E., Haga, K., Iseda, Y., Polym. J.
      (1971) 2, 475.
15. Machi, S., Hagiwara, M., Kagiya, T., J. Polym. Sci., Part B
      (1966) 4, 1019.
16. Hagiwara, M., Okamoto, H., Kagiya, T., Kagiya, T., J. Polym.
      Sci., Part A-1 (1970) 8, 3295.
17. Hagiwara, M., Okamoto, H., Kagiya, T., J. Polym. Sci., Part
      A-1 (1970) 8, 3303.
18. Bryce-Smith, D., Gilbert, A., Vickery, B., Chem. Ind. (Lon-
      don) (1962) 2060.
19. Lang, J. L., Pavelich, W. A., Clarey, H. D., J. Polym. Sci.,
      Part A (1963) 1, 1123.

20. Gaylord, N. G., Maiti, S., J. Polym. Sci., Polym. Lett. Ed. (1973) <u>11</u>, 253.
21. White, E. H., Miano, J. D., Watkins, C. J., Breaux, E. J., Angew. Chem. Internat. Ed. (1974) <u>13</u>, 229.
22. Lepley, A. R., Closs, G. L., eds., "Chemically Induced Magnetic Polarization", Wiley, New York, 1973.
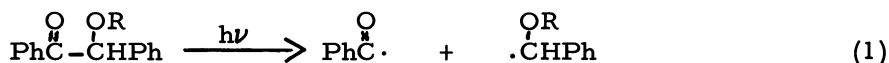
2

Benzoin Ether Photoinitiated Polymerization of Acrylates (1)

S. PETER PAPPAS, ASHOK K. CHATTOPADHYAY (2), and
LELAND H. CARLBLOM

Department of Polymers and Coatings, North Dakota State University,
Fargo, N. D. 58102

Our interest in the photochemistry of benzoin ethers was prompted by two major reasons: (1) a discrepancy existed between recent mechanistic studies on the photochemistry of benzoin ethers and earlier reports on the benzoin ether photo-initiated polymerization of reactive monomers, and (2) the extensive, commercial utilization of benzoin ethers as photo-initiators in uv curable coatings and printing inks warranted further investigation of this discrepancy.

The photochemistry of benzoin ethers (α-alkoxy-α-phenyl-acetophenones) has been examined in considerable detail, recently, by quenching (3, 4), sensitization (4), CIDNP (5), and radical scavenging (6) studies. These investigations indicate that benzoin ethers undergo a facile, photocleavage (Norrish type I) to yield benzoyl and benzyl ether radicals, as shown in eqn 1. This α-scission is not retarded by conventional triplet

$$\underset{PhC-CHPh}{\overset{O\quad OR}{\underset{}{}}} \xrightarrow{\ h\nu\ } \underset{PhC\cdot}{\overset{O}{\underset{}{}}} \ + \ \underset{\cdot CHPh}{\overset{OR}{\underset{}{}}} \tag{1}$$

quenchers which led to the suggestion (3) that reaction occurs via the excited singlet state. However, the sensitization (4) studies are best interpreted in terms of triplet reactivity. The facility of α-cleavage ($k \gtrsim 10^{-10}$ sec^{-1}) (3,4) constitutes an important reason for the effectiveness of benzoin ethers as photoinitiators for uv curing in air (7) since scission is not quenched by oxygen or reactive monomers, such as styrene (8). Unfortunately, the facility of cleavage does not prevent air-inhibition of uv curing by reaction of the initiator or growing polymers radicals with oxygen (7).

Based on the photochemistry of eqn 1, one would reasonably predict that, in the presence of reactive monomer, a conven-

tional radical chain polymerization would occur, initiated by the benzoyl and benzyl ether radicals, as recently proposed (9). One would further predict that a maximum of two initiator fragments would be incorporated per polymer molecule depending upon the relative extent of termination by disproportionation and coupling. However, these predictions are not in accord with earlier studies. Utilizing ^{14}C-labelled benzoin methyl ether as photoinitiator in the polymerization of methyl methacrylate (MMA), Mochel and coworkers reported that 12-14 radioactive fragments or molecules of initiator were incorporated per polymer (10). No radioactivity was incorporated when the polymerization was initiated thermally with α,α'-azobisisobutyronitrile (AIBN) in the presence of radiolabelled benzoin methyl ether (BE_1). Furthermore, based on quantum yield data for benzoin, it was estimated that less than 2 quanta are utilized/polymer molecule formed. Subsequently, these results together with unpublished data were cited as evidence for copolymerization of photoexcited benzoin ethers and benzoin with reactive monomers, such as MMA and styrene (11). This proposal is consistent with the finding that no radioactivity was incorporated when the polymerization was initiated thermally with AIBN in the presence of BE_1 (10). However, the incorporation of 12-14 photoexcited benzoin ether molecules by the absorption of less than 2 quanta requires that about 7 excited molecules be produced/quantum absorbed. This would constitute a chain process for light absorption for which we are unaware of any precedent. We felt that the uniqueness of these results warranted a reinvestigation.

The ^{14}C-labelled benzoin methyl ether (BE_1), utilized by Mochel's group (10), was prepared by methylating benzoin with ^{14}C-methyl iodide. In order to obtain additional information, we also prepared doubly and triply labelled analogs, BE_2 and BE_3, as outlined on Scheme 1.

Irradiations were conducted at 366 nm (Corning 7-83 filter combination) in a merry-go-round apparatus in which the samples rotated about a stationary 450-Watt Hanovia medium pressure lamp for constant light exposure. The samples consisted of degassed 5 ml solutions of the photoinitiators in neat MMA contained in Pyrex tubes. Two initiator concentrations were utilized: 1.05×10^{-3} and 4.11×10^{-2} $\underline{M}$, which corresponded to 16 and > 99% light absorption, respectively. Samples were irradiated to about 7% monomer conversions which required 15 min for the optically dense solutions and 30 min for the tubes with low initiator concentration. The resulting poly-

SCHEME 1

$$PhC\overset{O}{\underset{}{\parallel}}-\overset{OH}{\underset{}{\mid}}CHPh \quad + \quad {}^{14}CH_3I \quad \xrightarrow{Ag_2O} \quad PhC\overset{O}{\underset{}{\parallel}}-\overset{O-{}^{14}CH_3}{\underset{}{\mid}}CHPh$$

BE$_1$

$$Ph{}^{14}CHO \quad \xrightarrow{NaCN} \quad Ph{}^{14}\overset{O}{\underset{}{\parallel}}C-{}^{14}\overset{OH}{\underset{}{\mid}}CHPh$$

$$CH_3I \quad \diagdown \quad {}^{14}CH_3I$$

$$Ph{}^{14}\overset{O}{\underset{}{\parallel}}C-{}^{14}\overset{OCH_3}{\underset{}{\mid}}CPh \qquad\qquad Ph{}^{14}\overset{O}{\underset{}{\parallel}}C-{}^{14}\overset{O-{}^{14}CH_3}{\underset{}{\mid}}CPh$$

BE$_2$ BE$_3$

mers were precipitated in methanol, and the number of mono-
mers reacted/quantum absorbed ($\emptyset_m$) was determined by
simultaneous irradiation of a benzophenone/benzhydrol actino-
meter for which $\emptyset$ was taken as 0.85 (12). The intensity of
light absorbed was approximately 4×10^{17} quanta/min at high
initiator concentration.

After determination of monomer conversions, the polymers
were dissolved in benzene and reprecipitated two additional
times prior to determination of intrinsic viscosities ([η]) and
specific activities. Intrinsic viscosities were obtained in ben-
zene at 30°C with a no. 1 Ubbelohde viscometer (solvent flow
times were 69.1 $\pm$ 0.1 sec). Number average molecular
weights ($\overline{M}_n$) were calculated from the expression: [η] = 8.69
$\times 10^{-5} \overline{M}_n^{0.76}$ (13). Specific activities were determined by
liquid scintillation counting. Polymer activities (A), $\emptyset_m$ and $\overline{M}_n$
values are presented in Table I.

Initiator activities (a) together with average values for
polymer activities (A) are presented in Table II. In marked
contrast to the earlier reports (10, 11), it is seen that polymer
activities are less than that of the corresponding initiator in
each case. Unfortunately, we can offer no rationale for this
discrepancy. However, the present data are readily inter-
preted in terms of benzoin ether photocleavage into benzoyl and
benzyl ether radicals (eqn 1), which initiate MMA polymeri-
zation. The incorporation data may be analyzed by eqns 2-4,
wherein a_1, a_2 and a_3 refer to the specific activities of initiators
BE$_1$, BE$_2$ and BE$_3$, respectively, A$_1$, A$_2$ and A$_3$ represent the
corresponding polymer activities, while B and E are the number

TABLE I.   Photoinitiated Polymerization of MMA

BE ($M \times 10^3$)	$\emptyset_m$	$\overline{M}_n$ $\times 10^{-4}$	A dpm/mol $\times 10^{-4}$
BE_1 (1.05)	1020	8.20	1.73
''	1100	7.86	1.71
''	a	8.54	1.63
BE_2 (1.05)	953	7.97	3.10
''	1030	7.86	3.18
''	1000	8.54	3.39
BE_3 (1.05)	1000	8.08	4.82
''	1070	8.31	4.86
''	1070	8.96	5.00
BE_1 (41.1)	248	6.32	2.59
''	307	4.97	2.46
''	310	5.17	2.52
''	258	5.89	2.87
''	271	5.07	2.53
''	280	5.07	2.47
''	341	6.21	2.94
BE_2 (41.1)	240	5.62	4.62
''	235	5.48	4.17
''	338	5.69	3.58
BE_3 (41.1)	258	5.69	6.78
''	272	5.60	6.49
''	262	5.17	6.30
''	332	4.97	7.00
''	318	5.17	7.15

[a]The weight of the precipitated polymer was inadvertently not recorded in this experiment.

TABLE II. Specific Activities

BE (M x 10³)	a	A
	dpm/mol x 10⁻⁹	
BE₁	3.13	
(1.05)		1.69
(41.1)		2.62
BE₂	6.24	
(1.05)		3.22
(41.1)		4.12
BE₃	9.31	
(1.05)		4.89
(41.1)		6.74

of benzoyl and benzyl ether radicals, respectively, incorporated/polymer. In this context, $\underline{E}$ may be derived independently

$$A_1 = a_1 \underline{E} \tag{2}$$

$$A_2 = \frac{1}{2} a_2 (\underline{E} + \underline{B}) \tag{3}$$

$$A_3 = \frac{1}{2} a_2 (\underline{E} + \underline{B}) + (a_3 - a_2) \underline{E} \tag{4}$$

from eqn 2 and simultaneous solution of eqns 3 and 4. The resulting $\underline{E}$ and $\underline{B}$ values at each initiator concentration are provided in Table III. Average values for $\emptyset_m$, $\overline{M}_n$ and $\emptyset_p$, the corresponding number of polymer molecules produced/quantum absorbed, are also presented in Table III. These values were found to be independent of radiolabel within experimental error, estimated as $\pm$ 10%. However, as shown, they are highly dependent on initiator concentration.

TABLE III. Summary of Data for MMA

[BE] M x 10³	$\emptyset_m$	$\overline{M}_n$ x 10⁻⁴	$\emptyset_p$	$\underline{E}$	$\underline{B}$
1.05	1030	8.25	1.26	0.54	0.49
41.1	280	5.49	0.52	0.85	0.48

The total incorporation at low initiator concentration of approximately one initiator fragment/polymer is in reasonable agreement with values obtained on the polymerization of MMA

utilizing ^{14}C-labeled AIBN (14). The data are indicative of a conventional polymerization, initiated equally effectively by benzoyl and benzyl ether radicals, and terminated predominately by disproportionation of the growing polymer ends. Since the maximum number of polymers/quantum absorbed is 2 for termination by disproportionation, the value of 1.26 for ϕ_p at low initiator concentration corresponds to a minimum quantum efficiency of 63%. This signifies that at least 63% of the absorbed light results in polymer formation.

At the high initiator concentration, initial conversion of monomer to polymer increased by a factor of 1.6 and $\overline{M}_n$ decreased, as expected. However, as shown in Table III, these changes were accompanied by a drop in quantum efficiency to 25% (ϕ_p = 0.52), together with an increase in incorporation of radioactivity (1.33 as compared to 1.03 initiator fragments/polymer). The reduced quantum efficiency may be attributed to self-reactions of the initiator radicals, as well as to chain termination by initiator radicals, i.e., primary radical termination. The increase in incorporation of radioactivity constitutes additional support for primary radical termination. The discrepancy in the incorporation of benzoyl (B) and benzyl ether radicals (E) at high initiator concentration appears to be significant. Further studies on this interesting finding are in progress.

Similar studies are also being carried out with methyl acrylate (MA). In this case, the samples, which were irradiated in triplicate, consisted of degassed 8 ml solutions of the photoinitiators and MA (25% by volume) in benzene. Intrinsic viscosities were obtained in benzene at 35°C with a Cannon-Ubbelohde size 50 viscometer, and number average molecular weights were calculated from the expression: $[\eta] = 1.28 \times 10^{-4} \, \overline{M}_n^{0.714}$ (15). The pertinent results are summarized in Table IV.

As shown in Table IV, the total incorporation values are greater than 2 at both initiator concentrations. Since MA terminates predominately by combination (16), the presence of more than 2 initiator fragments/polymer is suggestive of an additional mode of incorporation. A possible mechanism is H-abstraction from polymer by initiator radicals which provides radical sites for chain branching. However, further discussion of these findings must await confirmation of the molecular weight data by more direct means.

TABLE IV. Summary of Data for MA[a]

[BE] (M x 10^3)	$\emptyset_m$	$\bar{M}_n$ x 10^{-5}	$\emptyset_p$	E	B
1.04	2560[b]	4.48	0.51	1.4	1.3
41.0	1040[c]	2.60	0.35	1.8	1.9

[a]Estimated error ±10%.

[b]15% monomer conversions.

[c]10% monomer conversions.

Literature Cited

1. Taken, in part, from the Ph.D. Thesis of A.K.C., North Dakota State University, 1974.
2. Present address: DeSoto, Inc., 1700 So. Mt. Prospect Road, Des Plaines, Illinois 60018.
3. Heine, H.-G., Tetrahedron Lett. (1972) 4755.
4. Pappas, S. P. and Chattopadhyay, A. K., J. Amer. Chem. Soc. (1973) 95, 6484.
5. Dominh, T., Ind. Chim. Belge. (1971) 36, 1080; Chem. Abstr. (1972) 76, 126080p.
6. Ledwith, A., Russell, P. J. and Sutcliffe, L. H., J. Chem. Soc., Perkin Trans. 2 (1972) 1925.
7. Pappas, S. P., Progr. Org. Coatings (1974) 2 (4), 333.
8. Heine, H.-G., Rosenkranz, H.-J., and Rudolph, H., Angew. Chem., Int. Ed. Engl. (1972) 11, 974.
9. Hutchison, J. and Ledwith, A., Polymer (1973) 14, 405.
10. Mochel, W. E., Crandall, J. L. and Peterson, J. H., J. Amer. Chem. Soc. (1955) 77, 494.
11. Bevington, J. C., "Radical Polymerization," Academic Press, New York, 1961, p. 77.
12. Pappas, S. P., Alexander, J. E. and Zehr, R. D., Jr., J. Amer. Chem. Soc. (1970) 92, 6927.
13. Fox, T. G., Kissinger, J. B., Mason, H. E. and Shuele, E. M., Polymer (1962) 3, 71.
14. Bevington, J. C., Melville, H. W., and Taylor, R. P., J. Polym. Sci. (1954) 14, 463.
15. Sen, J. N., Chatterjee, R. and Palit, S. R., J. Sci. Ind. Research (India) (1952) 11b, 90; Chem. Abstr. (1952) 46, 7847a.
16. Bamford, C. H., Dyson, R. W. and Eastmond, G. C., Polymer (1969) 10, 885.

Photocrosslinkable Polymers

GEORGE B. BUTLER and WILLIAM I. FERREE, JR.

Center for Macromolecular Science and Department of Chemistry,
University of Florida, Gainesville, Fla. 32611

Summary

    This paper describes some polymeric systems which have
recently been shown to undergo photocrosslinking. Photocrosslink-
ing of poly-(m-vinyloxyethoxy)-styrene can be carried out with
several different acceptors, although several others are ineffec-
tive for reasons unknown. The reaction is not quenched apprecia-
bly by H_2O, oxygen, or γ-collidine, but is quenched by triethyl-
amine, and cannot be initiated by azoisobutyronitrile, thus sup-
porting the supposition that the mechanism is cationic but not
protonic. Quenching by hydroquinone may also be consistent with
this conclusion. The reaction is favored by low temperature and
by tetrabutylammonium perchlorate, also supporting a cationic
mechanism.
    Small concentrations of H_2O, added before and after irradia-
tion, induce a postcrosslinking process that proceeds to comple-
tion within a short time and appears to be proton-initiated.
The photocrosslinking is completely quenched by 0.005 M thio-
cyanate ion, and subsequent addition of 0.5 M H_2O causes the
formation of postcrosslinked polymer containing an unexplained IR
absorption band in the carbonyl region.
    Effects of varying light intensity, wavelength, acceptor
concentration, and of rotating the sample tube suggest that the
tetrachlorophthalic anhydride-catalyzed reaction is biphotonic.
The chloranil-catalyzed reaction shows no intensity dependence
but unexplainably will not proceed with 334 nm light, whereas
366 nm light causes very rapid reaction.

Introduction

    The increasing utility of photocrosslinkable polymers in
microelectronics, printing, and UV-curable lacquers and inks is
providing an incentive for development of new varieties of photo-
polymers. After a brief overview of some of the commonly used
materials, some of the interesting recent developments in this

19

field will be discussed. Some recent experimental results obtained in our laboratory on photoionic crosslinking of certain polymers will also be presented.

Photopolymers in Common Use. Increasing industrial use is being made of UV-curable unsaturated polyester formulations. The polyester component is typically prepared from maleic anhydride, an aromatic anhydride, and a diol. This is combined with styrene, a sensitizer, and miscellaneous additives. The unsaturated sites associated with the maleate ester linkages in the polyester chain undergo a radical copolymerization with styrene to effect cross-linking. The sensitizer serves both to absorb light and to generate radicals. Parafin, fatty esters, or similar agents are often included to reduce oxygen inhibition and thus improve surface hardening. The principle use for these formulations is as UV-curable lacquers in the furniture industry. In a typical composition, an unsaturated polyester is prepared from a 1:2:3 mixture of phthallic anhydride, maleic anhydride, and 1,2-propanediol, and a 66% mixture of the polyester in styrene containing 0.1% paraffin, 1% $[(CH_3)_2COCS_2]_2$, and 0.5% sensitizer constitutes the UV-curable polyester. Typical sensitizers are benzoin methyl ether, benzil, xanthone, and acetonaphthone (1). A similar mixture has been used to impregnate fiberglass fabric for UV-hardened orthopedic casts (2).

The efficient light-initiated decomposition of azides has been the basis for commercially important photoresist formulations for the semiconductor industry. A common approach is to mix a diazide, such as diazadibenzylidenecyclohexanone (I), with an unsaturated hydrocarbon polymer. Excitation of the difunctional sensitizer produces highly reactive nitrenes which crosslink the polymer by a variety of paths including insertion into both carbon-carbon double bonds and carbon-hydrogen bonds, and by generation of radicals. The polymer component in the most widely used resists is polyisoprene which has been partially cyclized by reaction with p-toluenesulfonic acid (3). Other polymers used include polycyclopentadiene and the copolymer of cyclopentadiene and α-methylstyrene (4).

A simple, photosensitive polymer that has found wide use as a photoresist and in printing plates is poly(vinyl alcohol) (II) (5). Because radical polymerization of the monomer prefers the cyclopolymerization path, II is prepared by reacting poly(vinyl alcohol) with cinnamoyl chloride. The mechanism of photocross-linking of II has been a matter of controversey, whether proceeding by a radical process, by photodimerization of cinnamate groups to cyclobutanes, or both in competition (6). The initiating species is definitely the triplet, consequently the cross-linking efficiency and absorption bandwidth are greatly increased in the presence of triplet sensitizers (6).

Developments Employing Potentially Photodimerizable Groups.

Most research into new photopolymers has developed along the lines of attaching reactive groups to a polymer backbone. Several polymers containing pendant cinnamate groups are found to improve on the photosensitivity of II. Reaction of poly(β-hydroxyethyl acrylate) with cinnamoyl chloride yields a polymer (III) that when sensitized by 5-nitroacenaphthene is more than twice as reactive as II (7). Poly(glycidyl cinnamate) (IV), prepared by reacting poly(epichlorohydrin) with potassium cinnamate, is a liquid at room temperature and photocrosslinks with an efficiency eight times that of II (8).

A series of similar polymers (V) has been prepared directly from monomers by cationic polymerization of the vinyl ether group of the monomer, the cinnamoyl group being unreactive under these conditions (9).

Poly(vinyl chalcone) (VI) resenbles II in structure, and the mechanism of its crosslinking has similarly been argued in favor of radical or dimerization pathways (10, 11).

One of the more interesting and successful of recent photopolymers is poly(vinyl 2-furylacrylate) (VIII). Its photosensitivity is reported to be more than an order of magnitude greater than that of II, whether sensitized or unsensitized samples are compared. The mechanism of crosslinking is proposed to involve photodimerization of pendant groups to cyclobutanes (12).

Recently, results of incorporating in polymers efficiently photodimerizable groups familiar to modern photochemists have been reported. Reaction of poly(vinyl alcohol) with 1,2-diphenyl-cycloprolenoyl chloride yields a very photosensitive polymer (VIII) that crosslinks by a mixture of cyclobutane ring formation and single bond formation between two diphenylcyclopropene groups after hydrogen-atom transfer (13), mechanisms well characterized in the photochemistry of these moieties (14). Hyde, Kricka, and Ledwith report that N-acryloyldibenz(b,f)azepine (IX) can be copolymerized with styrene, methyl methacrylate, N-vinylcarbazole, or maleic anhydride under radical conditions to provide polymers that photocrosslink by cyclobutane ring formation (15). Two more polymers designed to crosslink by the photodimerization mechanism are X and XI (16). The methoxy substituents are responsible for the efficiency of crosslinking, presumably, in part, by increasing the lifetime of the reactive singlet excited state.

Recent Azido Photopolymers. A class of useful photopolymers that crosslinks by non-dimerizable groups is that containing azido groups. Poly(vinyl-p-azidobenzoate) (XII), prepared from poly(vinyl alcohol), is one example (17). Since no unsaturation is present, crosslinking efficiency depends on the photo-generated nitrene's reactivity toward insertion into carbon-hydrogen bonds and generation of radicals. Various triplet sensitizers increase the efficiency by one to two orders of magnitude.

Reaction of poly(vinylchloride) with sodium azide in dimethyl-formamide incorporates azide groups to yield a photocrosslinkable

polymer (18).

Photocrosslinking of poly(vinyl-p-azidocinnamate) (XIII) is
reported to involve competitive photodimerization of cinnamoyl
groups to cyclobutenes along with the dominant nitrene reactions
of insertion and radical abstraction. The reaction can be
triplet-sensitized (19).

Recent Photopolymers Crosslinked by Radical Processes.
Polymers (XIV) containing the photoreactive acryloyl and methacry-
oyl groups have been prepared by a cationic synthesis similar to
that mentioned earlier (20). Photodimerization is not expected
to play a role in crosslinking in these cases.

A polymer containing pendant benzophenone groups (XV) is
found to photocrosslink. The mechanism is intermolecular coupling
of radicals formed via photoreduction in the triplet state. In
solution, crosslinking is concentration dependent as intramolecu-
lar cyclization competes (21).

Diallylphthalate, which has been converted under radical
conditions to a low polymer, photocrosslinks in the presence of
N-phenylmaleimide and Michler's ketone sensitizer (22). Possibly
the crosslinking involves copolymerization of unreacted allyl
groups with the maleimide.

A large number of examples of polymers containing tertiary
amines are reported to photocrosslink in the presence of alkyl
halides. One combination would be poly(p-dimethylaminostyrene)
and ethyl iodide (23). The mechanism is not reported, but may
involve charge-transfer excitation to form radicals.

The oxidative coupling of monomers such as the dipropargyl
ether of bis-phenol A (XVI) results in photocrosslinkable materi-
al (24). The mechanism is unknown, but the rate is greatest in
examples in which carbonyl groups are attached to the aromatic
rings. A recent study (25) reported on the rates of photocross-
linking and the photosensitivities of poly(vinyl α-cyanocinnamate)
and poly(vinyl α-cyanocinnamoxyacetate). The authors concluded
that photocrosslinking of these polymers proceeded mainly through
radical addition, and that these polymers showed higher photo-
sensitivities than poly(vinyl cinnamate) and poly(vinyl cinnamoxy-
acetate) in spite of the lower rates of photocrosslinking of the
α-cyano-substituted polymers. The photosensitivities and the
rates of photocrosslinking of these α-cyano-substituted polymers
were also compared with that of poly(vinyl β-styrylacryloxy-
acetate).

A recent review (26) covered four-center type photopolymeri-
zation in the crystalline state. Although these photoinitiated
polymerizations by the four-center mechanism may not be considered
to involve a photocrosslinkable step, the extensive discussion of
mechanism by these authors may be of value to those interested in
photocrosslinking as there are some marked similarities between
these two concepts.

Photoionic Crosslinking of Certain Polymers. Certain mono-
mers are readily prepared having two polymerizable functional
groups which propagate exclusively by different mechanism, select-
ing among radical, anionic, and cationic propagation. These
monomers may be polymerized through one functional group and
crosslinked in a separate step by a different class of initiator.
The fact that photoexcitation of charge-transfer complexes can
initiate ionic polymerizations of certain monomers suggested the
feasibility of using photo-generated ions rather than photo-
generated radicals.

The two possibilities available for this purpose are the
photocationic crosslinking of a polymer containing donor olefinic
groups in the presence of an acceptor compound, and the photo-
anionic crosslinking of a polymer containing acceptor olefinic
groups in the presence of a donor compound. The polymer contain-
ing donor olefinic groups, poly-(m-vinyloxy ethoxy) styrene
(XVIII) was prepared in our laboratories by Mr. Shaw Chu (27),
and has a molecular weight of 110,000. The polymer containing
acceptor olefinic groups, poly-[vinyl(2-nitrostyryloxyethyl)
ether], (XIX) was synthesized according to the procedure of
J.W. Schwietert (30) and has a low molecular weight (probably
5000 or less).

Results and Discussion

Initial experiments involved the irradiation of XVIII in the
presence of chloranil in methylene chloride and the irradiation
of XIX in the presence of N,N-dimethylaniline in methylene
chloride. Samples were prepared on the vacuum line with pure dry
materials and with careful removal and exclusion of moisture and
oxygen. However, no trace of photocrosslinking was observable
in either system.

In accordance with the expectation that initiation by a
charge-transfer excited state must be preceded by separation of
the radical cation- radical anion pair by solvent, in order to
compete with reconversion to the ground state within the solvent
cage, more polar solvents were employed to facilitate this step.

$$D + A \rightleftharpoons (D,A) \underset{\Delta}{\overset{h\nu}{\underset{\longleftarrow}{\longrightarrow}}} (D^{+\cdot}, A^{-\cdot}) \rightleftharpoons D^{+\cdot} + A^{-\cdot}$$
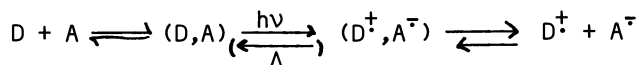
Thus, irradiation of XVIII in the presence of chloranil or tetra-
chlorophthallic anhydride (TCPA) in acetonitrile under dry,
oxygen-free conditions yielded rapid precipitation of crosslinked
polymer. The irradiation of XIX in the presence of N,N-dimethyl-
aniline in dimethylformamide under exclusion of air and moisture
produced a very slight indication of crosslinking occurring.

Until the present time, the fact that the photo-cationic
crosslinking of XVIII is successful while the photo-anionic cross-
linking of XIX is much less so has prompted much further work on

the first and none on the second. Other reasons also exist for the lack of further work on XIX. The photo-anionic crosslinking of XIX is probably quenched by traces of water, and it may be extremely difficult to prepare solutions of the polymer in an absolutely dry state. Also, the polymer partially crosslinks spontaneously by air oxidation during storage, is prepared in low yield, has a low molecular weight, and is very difficult to dissolve, making it less desirable for the purpose intended. Nevertheless, further attempts to crosslink XIX by means of other donors, such as anthracene, would be of interest.

The process apparently being observed in the photo-cationic crosslinking of XVIII is depicted below, where $ROCH=CH_2$ represents XVIII:

$$ROCH=CH_2 + A \xrightarrow[CH_3CN]{h\nu} \overset{+}{R}OCH\text{-}\overset{\cdot}{C}H_2 + A^{\overline{\cdot}}$$

$$\xrightarrow{ROCH=CH_2} \underset{ROCH\text{-}CH_2\text{-}\overset{+}{C}HOR}{\overset{\overset{\cdot}{C}H_2}{|}}$$

$$\underset{ROCH\text{+}CH_2\text{-}CH\text{+}_n X}{\overset{\overset{\cdot}{C}H_2}{|}} \quad \underset{OR}{|}$$

The termination step of a propagating chain could involve proton transfer to monomer, combination with the acceptor radical anion, or electron transfer from the acceptor radical anion to the carbonium ion to yield a terminal radical, as below.

$$\overset{\overset{\cdot}{C}H_2}{|}\ ROCH\text{+}CH_2\text{-}CH\text{+}_n CH_2\text{-}\overset{+}{C}H \xrightarrow{ROCH=CH_2} \overset{\overset{\cdot}{C}H_2}{|}\ ROCH\text{+}CH_2\text{-}CH\text{+}_n CH=CH + ROCHCH_3$$

$$\downarrow A^{\overline{\cdot}} \quad \searrow A^{\overline{\cdot}} \quad \overset{\overset{\cdot}{C}H_2}{|}\ ROCH\text{+}CH_2\text{-}CH\text{+}_n CH_2\text{-}\overset{\cdot}{C}H\text{-}A$$

$$\overset{\overset{\cdot}{C}H_2}{|}\ ROCH\text{+}CH_2\text{-}CH\text{+}_n CH_2\text{-}\overset{\cdot}{C}H + A$$

Presumably the radical sites generated do not propagate but are destroyed in some chain-transfer reaction or radical-radical combination. The charge-transfer complex has not been included in the initiation mechanism for reasons to be discussed.

The effects of different acceptors, oxygen, water, quenchers,

radical initiators, and other additives, temperature, geometry of irradiation vessel, acceptor concentration light intensity, wavelength of light, and spontaneous crosslinking will be discussed.

Effect of Different Acceptors. Although both of the earliest acceptors tested worked, most of the others later examined did not effect photocrosslinking for unknown reasons. Table I lists the acceptors tested, along with two measures of acceptor strength and approximate efficiencies of precipitation of crosslinked polymer. The crosslinked polymer formed with chloranil is predominantly suspended in the liquid while that formed on the tube wall where the light beam impinges. The product of crosslinking XVIII using chloranil or TCPA contains no detectable IR bands due to the acceptors. The IR spectrum of XVIII crosslinked by irradiation in the presence of TCPA is identical to that of XVIII crosslinked by BF_3 by Shaw Chu.

Spontaneous Crosslinking. In the absence of TCPA, evaporated solutions of XVIII can be completely redissolved in fresh solvent in a few minutes. And solutions of 0.05 M XVIII containing 0.007 M TCPA in acetonitrile are stable indefinitely (at least three weeks) at room temperature. However, on evaporation of the solvent under vacuum, the mixture forms a very tough film that is insoluble in acetonitrile or hot DMF, does not melt up to 300°, and is resistant to attack by chromic acid. The IR spectrum is identical to that of XVIII crosslinked BF_3 or by irradiation in the presence of TCPA. Apparently as the solution becomes highly concentrated, crosslinking occurs by thermal excitation of charge-transfer complexes of TCPA and XVIII. The IR evidence and the insolubility behavior appear to discount an alternative possibility of simple association of polymer chains facilitated by the presence of the acceptor compound. The spontaneous crosslinking is also observed with the acceptors chloranil and 1,3,5-trinitro-benzene, and presumably would occur with others.

While the spontaneous crosslinking is interesting and certainly worthy of further investigation, it places limitations on the methods of sample preparation for the photocrosslinking when dry conditions are required. That is, one cannot dry the acceptor and XVIII in the same step by evaporation of a stock solution containing the two to dryness on the vacuum line. The method that was used to avoid the spontaneous crosslinking was to prepare a stock solution of XVIII in dry acetonitrile, evaporate the solvent on the vacuum line, heat the polymer film to 80° briefly, and then allow it to dry under vacuum for one hour, the tube removed from the line and acceptor weighed in, then dry polymer and acceptor dried under vacuum for one hour. Excess dry acetonitrile was condensed into the liquid-nitrogen-cooled tube directly from P_2O_5, melted the excess evaporated by high vacuum, and the tube sealed with a flame. If the drying under vacuum of the combined dry mixture of XVIII and TCPA is carried out for a long period of time, partial spontaneous crosslinking is observed

Table I

Tests of Various Acceptors in the Photo-cationic Crosslinking of XVIII.[a]

Acceptor	Acceptor Strength		$\lambda(+6.4)$, nm	Efficiency[c]
	$E_{1/2}^{red\cdot}/V$	E.A., eV		
Chloranil	+0.01	1.37	334	2.3
Benzoquinone	-0.51	0.77	334 (334, 313, 366)[b]	0.0
1,3,5-Trinitrobenzene	-0.60	0.70	334 (334, 313, 366)[b]	0.0
1,3,5-Tricyanobenzene	(est. -0.8)	(est. 0.4)	300, 275 254, 236	0.0[d]
TCPA	-0.86	0.56	334	0.75
TCPA	-0.86	0.56	275, 236	0.0[e,d]
Phthalic Anhydride	-1.31	----	300	0.75

[a] Concn. XVIII was 0.050 M (in monomer units of M.W. 190) in acetonitrile, concn. acceptor was 0.007 M. Acceptor strength data from book by Forster.
[b] Samples containing 0.50 M H_2O; all others prepared under rigorously dry conditions. All samples sealed under vacuum greater than 10-4 torr.
[c] Expressed in terms of moles of monomer units of polymer precipitated per einstein of protons absorbed.
[d] Irradiated in quartz tubes at room temp. of 25°; all others were Pyrex tubes irradiated while immersed in an ice bath at 3±1°.
[e] A fine precipitate formed that quickly redissolved.

by insolubility in fresh solvent, particularly where the TCPA particles directly contacted the polymer, but there also appears to be some crosslinking caused by TCPA vapor. This process has also been observed with chloranil, which is more volatile than TCPA.

Effect of Oxygen. Although a cationic propagation is generally not affected by oxygen, the excited state giving rise to the photo-cationic crosslinking might be expected to be susceptible to oxygen quenching, particularly if the triplet excited state is involved. To test this, dry reaction samples were prepared on the vacuum line as above, then air admitted through a drying tube and the sample tubes sealed off and irradiated. With TCPA as the acceptor, the photocrosslinking occurred with comparable efficiency to that of tubes kept sealed under vacuum (Table II). Thus both a triplet excited state initiator and a radical propagation mechanism are disfavored by this evidence when TCPA is used. However, with chloranil as the acceptor, photocrosslinking is completely quenched by air. Since several reasons to be discussed below disfavor a radical propagation mechanism for the photocrosslinking, it is believed that the oxygen quenching behavior indicates that the crosslinking is initiated by triplet excited chloranil. Quenching of a singlet excited initiator would have been only partial. It would be of interest to test the hypothesis of triplet initiator by examining the effect of small concentrations (0.02 M) of cyclooctatetraene, a quencher of low triplet energy (39 Kcal.), in the case of chloranil.

Effect of Water. A sample was prepared as described above except that the solvent condensed into the tube containing dry XVIII and TCPA was a measured aliquot of a solution of 0.010 M H_2O in dry acetonitrile. Irradiation produced photocrosslinking in apparently comparable amounts to that for a dry sample. However, after opening the tube and stoppering, then allowing to stand overnight at room temperature, additional crosslinking occurred, as a precipitate that settled to the bottom of the tube, in addition to the patches adhering to the areas where the light beam had impinged. The total conversion isolated was 93% of the 18.1 mg XVIII started with. On repeating the experiment with 0.50 M H_2O, the photocrosslinking occurred with typical efficiency, but after irradiation, as the tube was being allowed to warm to room temperature, the crosslinking resumed spontaneously to fill the solution with heavy precipitate within a few minutes. Total conversion was 95% to the 18.1 mg XVIII started with. The sealed sample had previous to irradiation stood at room temperature overnight with no change. The indication of two separate processes, a photocrosslinking and a water-induced postcrosslinking, hereafter shortened to postlinking, was verified dramatically by the following experiment. A completely dry sample was prepared and irradiated, then the tube opened and enough H_2O (180 mg/2.0 ml aceto-

Table II

Effects of Varying Conditions and of Additives on the
Photocrosslinking of XVIII in the Presence of TCPA or Chloranil.[a]

Acceptor	Additive or Variation	λ[b]	Time Irrad.	mg pcpt.	Effi- ciency[c]
TCPA	-----	334	60 min.	7.3	0.82
TCPA	-----	334	60	6.0	0.68
TCPA	Air	334	60	8.5	0.96
TCPA	0.0010 M TCPA	334	30	0.0	0.00
TCPA	Narrow Slits	334	120	1.3	0.073
TCPA	n-Bu$_4$NClO$_4$ 0.10 M	334	20	4.1	1.4
TCPA	0.0050 M HQ	334	20	0.0	0.00
TCPA	0.010 M Et$_3$N	334	20	0.0	0.00
TCPA	Air, H$_2$O 0.0005 M Et$_3$N	334	10	0.0	0.00
TCPA	0.010 M γ-Collidine	334	10	>0.0	----
TCPA	0.50 M γ-Collidine	334	10	0.0	0.00
TCPA	0.005 M KSCN	334	10	0.0	0.00
TCPA	0.10 M AIBN	366	10	0.0	0.00
Chloranil	-----	366	4	8.3	2.6
Chloranil	Narrow slits	366	12	6.2	2.0
Chloranil	25°	366	8	5.0	0.80
Chloranil	Air	366	8	0.0	0.00
Chloranil	-----	334	10	0.0	0.00

[a]Conc. XVIII was 0.050 M in Acetonitrile; conc. acceptor was
0.0070 M except in the exception noted; irradiations performed on
tubes immersed in an ice bath except where noted.
[b]Dispersion of monochromator was 6.4 nm, except where narrow
slits were employed, reducing dispersion to 3.2 nm. Intensities
for the two slit conditions were, for 334, 4.7 and 1.64 $\times$ 10^{17}
photons/min., and for 366 nm, 2.5 and 0.83 $\times$ 10^{18} photons/min.
[c]Expressed in terms of moles of monomer units of polymer
precipitated per einstein of photons absorbed.

nitrile) to make the solution 0.5 M in H_2O was added and the solu-
tion shaken gently to mix. No change occurred immediately, but on
reexamination after one hour in the dark the whole sample had
crosslinked. Filtration provided 99% conversion.

Dry samples that are irradiated and kept sealed have never
been observed to postlink even after periods of a few days. Addi-
tion of 0.5 M H_2O to an unirradiated sample caused no precipita-
tion for several days in the dark. After six days a milky cast
appeared, and formation of a thin precipitate appeared to have
reached completion in about eleven days.

Effect of Quenchers. The photocrosslinking of XVIII in the
presence of 0.007 M TCPA is quenched completely by 0.010 M tri-
ethylamine or even by 0.005 M triethylamine (air and adventitious
H_2O were present in the latter run). This is believed to be good
evidence that the propagating species is cationic rather than
radical. These samples also do not postlink when 0.5 M H_2O is
added.

The hindered amine γ-collidine (2,4,6-trimethylpyridine) was
then examined as a quencher since it would selectively bond to
protons but not to larger cations. It was observed the 0.010 M
γ-collidine does not quench the photocrosslinking in the presence
of TCPA completely, but postlinking after addition of 0.5 M H_2O
was completely inhibited until two weeks later. This experiment
should be repeated on a larger scale to obtain quantitative
measurements of the inhibition. The experiment appears to prove
that the photocrosslinking is cationic but the initiating species
are not protons, while the postlinking is initiated by protons.
At a concentration of γ-collidine of 0.50 M the photocrosslinking
is completely inhibited, which could be due to competitive charge-
transfer complexation of ground state of excited state TCPA rather
than interfering with cationic propagation. (Forster's book on
charge-transfer complexes shows that γ-collidine can form
complexes.)

Hydroquinone at a concentration of 0.0050 M quenches photo-
crosslinking in the presence of TCPA completely. Possibly the
basicity of hydroquinone is responsible for the inhibition, since
the radical mechanism is disfavored compared to the cationic
mechanism by several other pieces of evidence. The ideal quencher
which was on order, is diphenylpicrylhydrazyl, which affects radi-
cal but not cationic processes.

Effect of Azoisobutyronitrile (AIBN). Although XVIII is
formed from the monomer under radical conditions without radical
propagation occurring along the vinyl ether groups, the possibil-
ity that in the presence of an acceptor such as TCPA or chloranil
the complexed vinyl ether groups would be susceptible to radical
propagation seemed plausible enough to test this possibility.
Thus a sample of 0.050 M XVIII and 0.007 M TCPA containing 0.10 M
AIBN in dry acetonitrile was irradiated at 366 ± 6.4 nm, where

AIBN absorbs and decomposes to radicals with a quantum yield of 0.43 (0.86 radicals per proton) (28). No photocrosslinking occurred. This seemed to show that the crosslinking in this system is not radical-initiated. (It might be mentioned that the only possibility left open by this experiment for a radical process is that direct photo-initiation produces a radical of much greater reactivity than $(CH_3)_2C-CN$ which is able to initiate crosslinking in the presence of the acceptor.)

Effect of Miscellaneous Additives. The source of the protons responsible for postlinking is not yet clear. The results obtained require that irradiation produces either in the crosslinked polymer or the solution an acidic species that does not continue to propagate cationic crosslinking when irradiation is stopped, but which can react with H_2O to release protons. One possibility that has been under consideration is that during photocrosslinking some of the propagating cationic centers become trapped in crosslinked polymer, such that molecules of H_2O could diffuse in and bond to the carbonium ion and then release a proton. Thus H_2O would act as a chain transfer agent. If this theory is correct, other small molecules could similarly intercept the trapped carbonium ions. One approach that was to be attempted is to add via sealed ampoule techniques β-chloroethyl vinyl ether to an irradiated mixture of XVIII and acceptor in acetonitrile and analyze for incorporation of chlorine in the crosslinked polymer, assuming the β-chloroethyl vinyl ether is able to diffuse to the carbonium centers and form grafted chains by cationic propagation. This experiment is preferably to be carried out with an acceptor that absorbs above the Pyrex cutoff of 310 nm and does not contain chlorine. The recently received pyromellitic dianhydride was to be investigated for this purpose.

Another agent investigated as an interceptor of the trapped carbonium ions is potassium thiocyanate, KSCN. This is the only common salt tested that is significantly soluble in acetonitrile. The thiocyanate anion has a molecular size comparable to that of H_2O and its incorporation into the polymer should be easily detected by the strong, sharp infrared absorption near 2100 cm^{-1}. Accordingly, a sample of XVIII and TCPA in dry acetonitrile was irradiated for 20 min. to produce crosslinking, then the tube opened and an equal volume of 0.10 M KSCN in dry acetonitrile added. After standing in ice-water for 2 hours (it was assumed that combination of thiocyanate and carbonium centers would be rapid), the solution was made 0.5 M in H_2O to observe whether the postlinking would occur. After 3 hours at room temperature, no postlinking had occurred, whereas postlinking was complete in an identical irradiated sample not treated with thiocyanate ion. But after three days nearly complete postlinking (93%) had occurred. The infrared spectrum of the filtered polymer showed no detectable band in the 2100 cm^{-1} region nor any other difference from similar samples not treated with thiocyanate ion. However, during the

same set of runs a sample of XVIII and TCPA in dry acetonitrile
containing 0.005 M KSCN was prepared and irradiated, but no photo-
crosslinking occurred. (Although TCPA and KSCN form a yellow
charge-transfer complex in acetonitrile, absorption of the complex
is insignificant at the concentrations used here. It might also
be noted that the stronger acceptor chloranil forms a red complex
with KSCN that spontaneously reacts to form a brown precipitate
that probably results from displacement of chlorines from the 2
and 5 positions by thiocyanate ion.) Addition of an 0.5 M concen-
tration of H_2O produced no postlinking in three hours but complete
precipitation (measured 107% based on starting polymer alone) in
three days. Here we seem to have an example of a more rapid post-
linking in an irradiated sample than in an unirradiated sample
even though no visible precipitation due to photocrosslinking
occurred. Further, although the product does not contain a band
near 2100 cm^{-1}, there is a moderately strong and slightly broad
band at 1737 cm^{-1}, with no other observable difference in the
spectrum from that typical of crosslinked XVIII. Evidently the
species producing the 1737 cm^{-1} band must have incorporated in
the polymer during the irradiation period, otherwise it would also
be present in the product of the experiment described just pre-
viously. One possibility is that the thiocyanate ion quenched
photocrosslinking by combination with the initiating radical
cation or the propagating cation and then was hydrolyzed to a
thiolcarbamate on addition of H_2O. However, the band maximum
does not agree with those reported for N-phenyl- and N-propyl-
thiolcarbamates (29), $R-S(CO)NH_2$, which give sharp doublets in
the 1600-1650 cm^{-1} region and another band near 1300 cm^{-1}. The
position of the band is more typical of an ester or ketone, but
its exact origin is as yet unknown.

The effect of tetrabutylammonium perchlorate was examined,
since it could increase the efficiency of the reaction in two
ways. The perchlorate ion would compete effectively with the
radical anion of TCPA as a counterion to the initiating radical
cation and to the propagating cation, thus possibly decreasing
both radical anion-radical cation recombination and whatever
termination steps the radical anion of TCPA is involved in. It
was found that a sample containing 0.10 M tetrabutylammonium
perchlorate increased the photocrosslinking yield to about double
that observed in the absence of the electrolyte (Table II). The
appearance of the product was also better in that it was whiter
and more coagulated. A possible experiment of interest would be
to irradiate a similar sample in the solvent methylene chloride,
where the presence of the electrolyte might allow the photocross-
linking to proceed and take advantage of the improved propagation
of the cationic process in methylene chloride than in aceto-
nitrile.

Effect of Temperature. In the presence of chloranil, the
efficiency of photocrosslinking at room temperature is decreased

to about one-third of that at an ice-bath temperature (Table II).
This indication of a negative temperature coefficient is strong
evidence that a cationic mechanism is involved in the propagation
of the crosslinking. The effect of temperatures as low as -40°C
would be of interest. In the presence of TCPA, the efficiency of
photocrosslinking also appeared to be reduced at room temperature
but because of filtration difficulties a reliable quantitative
measurement was not obtained in the experiment run.

Effect of Rotating Sample Tube During Irradiation. All of
the early experiments were performed on 2.0 ml samples containing
0.05 M XVIII (19 mg) and usually 0.007 M acceptor. The samples
were irradiated while stationary, usually in an ice bath, and the
tube was turned to a fresh surface at constant frequent intervals.
In the first attempt at obtaining quantitative quantum yield
measurements, a series of 10 ml samples containing 0.05 M XVIII
(95 mg each) and TCPA concentrations of 0.001, 0.003, and 0.007 M
were prepared. These tubes were irradiated while turned by an
electric motor at about 1 r.p.s. and while immersed in an ice
bath, intending to form a uniform coating of crosslinked polymer
on the tube wall rather than the series of patches obtained in the
previous runs. However, under these conditions no significant
solid formed on the tube walls but instead only slightly milky
solutions were produced, decreasing in cloudiness with decreasing
TCPA concentration. Even the precipitate formed in the 0.007 M
TCPA sample was not filterable. However, these irradiated sam-
ples, after unsealing, stoppering, and being left standing for a
week, formed gels occupying the whole liquid volume of the sample.
The gels were no more opaque than the respective original solu-
tions after irradiation, the 0.001 M sample having little opacity.
Apparently adventitious H_2O caused a slow proton-initiated cross-
linking.

Effect of Acceptor Concentration. With the failure of the
rotating-sample-tube experiments, all the quantum efficiency
measurements were performed with 10 ml samples in stationary tubes
turned at constant, frequent intervals to a fresh surface. The
concentration of TCPA used in most of the runs was 0.007 M, which
is near the solubility limit in acetonitrile or methylene
chloride. The absorbance at 334 nm at this concentration for the
0.9 cm pathlength of the tubes is 20, about ten times that neces-
sary to absorb all the light. When a sample containing only
0.0008 M TCPA (absorbance 2.3 for the 0.9 cm pathlength, thus
still absorbing over 99% of the light) was prepared and irradi-
ated, no photocrosslinking was observable within 10 min. A second
sample containing 0.0010 M TCPA produced no photocrosslinking
after 30 min. of irradiation (Table II). This observation
correlates with the qualitative observations in the rotating-tube
run. The observation of a concentration dependence of crosslink-
ing efficiency is very surprising, and a further study of

concentration effects would be of interest.

Effect of Light Intensity. As noted, the failure of the rotated TCPA samples to resemble the behavior of stationary samples during irradiation is very unexpected. However, the decrease of crosslinking efficiency when either the sample tube is rotated or the TCPA concentration is reduced potentially has a common explanation, which is that the reaction efficiency depends strongly on the concentration of excited species. In a stationary tube containing 0.007 M TCPA, there is a high concentration of light-excited species just inside the tube wall where the light beam impinges. Rotating the tube or decreasing the concentration of TCPA decreases local concentrations of excited states without changing their total concentration. (Whether rotation of the tube could significantly affect local concentrations of excited states is by no means certain but is a possibility.) These considerations made a test of the effect of changing light intensity on the reaction imperative, even though photoreactions which are more efficient at higher light intensities (biphotonic reactions) are generally very rare, and the assumed mechanism does not require a biphotonic excitation scheme.

Thus a sample containing 0.0070 M TCPA acceptor was irradiated with narrower slits in the monochromator to reduce light intensity by about two-thirds, and the irradiation time increased proportionately. The observed quantum yield of photocrosslinking was in fact reduced by a factor of ten (Table II), supporting the supposition that a biphotonic process is involved in the reaction catalyzed by TCPA.

On the other hand, a similar experiment with chloranil as the acceptor failed to show a significant effect of decreasing light intensity (Table II). Thus a biphotonic mechanism does not appear to be involved in the chloranil system.

As a side comment, it had been observed in the photopolymerization of fumaronitrile and divinyl ether in methanol that the reaction would not proceed as usual when the sealed sample was magnetically stirred. This may be similar in cause to the effect of rotating the tube above, that is that this reaction also depends on the local concentration of excited states.

Effect of Wavelength. In early test experiments with 0.007 M TCPA acceptor, it was observed that at 366 nm, where absorbance of the solution is less than 0.10, but in which any charge-transfer absorption superimposed on the tail of the acceptor absorption band would be at the optimum percentage of the light absorbed by the solution, no photocrosslinking was observed. Also, in quartz tubes at 275 nm and 236 nm (ice-bath cooling could not be used in these cases since a suitable quartz vessel was not on hand), no photocrosslinking was observed. In the light of subsequent findings that the reaction efficiency decreases markedly with decreased light intensity, these results are adequately

accounted for, since the 275 nm and 236 nm intensities are much
weaker than the 334 nm line, while the 366 nm line is only about
5 to 6 times as intense as the 334 nm line and only a small frac-
tion is absorbed. However, some unexplained wavelength effects
are described below.

When the measurement of quantum yields in the chloranil sys-
tem was to be begun, it was decided to use the 334 nm line rather
than 366 nm since with the high efficiency observed in the test
run with chloranil at 366 nm, it appeared desirable to use a less
intense excitation band in order to have more controllable reac-
tion times, as well as to use the same wavelength used in the TCPA
system for convenience and direct comparison. Surprisingly, no
photocrosslinking watsoever could be initiated at 334 nm in three
different chloranil samples prepared. However, when the excita-
tion wavelength was changed to 366 nm, the same samples produced
photocrosslinking very rapidly. This observation is very puzzling
and deserves further investigation.

Experimental

Acceptor compounds (TCPA, chloranil, 1,3,5-trinitrobenzene,
benzoquinone, phthallic anhydride, and 1,3,5-tricyanobenzene) were
recrystallized and sublimed. Acetonitrile (Mallinckrodt reagent)
was distilled from P_2O_5 and redistilled, retaining middle cuts.
Dichloromethane (Mallinckrodt reagent) was dried over calcium
hydride. XVIII was prepared by Shaw Chu (27) and has a molecular
weight of 110,000 by membrane osmometry. XIX was prepared accord-
ing to the procedure of J.W. Schwietert (30).

The irradiation source is a 2500 Watt Mercury-Xenon lamp
(Hanovia type 929B-9U) contained in the Schoeffel LH 152N/2 Lamp
Housing (supplied with 2¼" diameter variable focus double quartz
condensor, parabolic reflector, cooling fan, and finned heat sinks
for the arc lamp). The output beam is deflected through a
Schoeffel LHA 165/2 Stray Light Reducing & Illumination Predisper-
sion Prism Assembly into a Schoeffel GM 250 High Intensity Mono-
chromator (focal length 0.25 M., linear dispersion 3.2 nm/mm.,
grating blazed at 300 nm with 1180 grooves/mm., aperture ratio
f/3.9). The power supply for the lamp is a Schoeffel LPS 400
equipped with the Schoeffel LPS 400S starter, which operate the
lamp at 50 V and 50 A. A lens supplied by Schoeffel focuses the
exit beam of the monochromator into a vertical narrow line such
that only the center portion of a sample tube is irradiated.

Sample vessels were either Pyrex tubes of 11MM. o.d. (9mm.
i.d.) or 199 mm. o.d. (16 mm. i.d.) or quartz tubes of 12 mm. o.d.
(10 mm. i.d.) sealed to graded seals. The preparation of samples
was as follows. An aliquot of a solution of the polymer in dry
acetonitrile was evaporated to a film in the sample tube on a
vacuum line, heated to about 80° briefly, and dried for one hour.
The tube was removed from the vacuum line, weighed acceptor (and
any nonvolatile additive) were added, the tube reevacuated for one

hour, and excess dry acetonitrile transferred from P_2O_5 by cooling the tube in liquid nitrogen on the vacuum line at 10^{-4} torr or less. The frozen solid is melted and excess solvent evaporated at 25° until the marked volume level is reached, and the tube sealed off with a flame. For experiments in which volatile additives such as triethylamine were used, a measured aliquot of the additive in dry acetonitrile was dried over calcium hydride, degassed by freeze-thaw cycles, and transferred into the sample tube on the vacuum line. Similarly, for testing the effect of H_2O, measured aliquots of mixtures of H_2O in dry acetonitrile were degassed and condensed into the sample tubes on the vacuum line. For testing the effect of air, the sample was prepared as above, air admitted through a drying tube ($CaSO_4$) and the sample sealed off.

The sample tubes were usually irradiated while immersed in an ice bath. The light beam forms an image 24 mm. by 4 mm. on the center of the sample solution. For experiments in which polymer formed on the irradiated wall, the sample tube was turned to a fresh surface at constant, frequent intervals, usually 2.0 min., while use of intervals of twice this long were found to yield nearly equal crosslinking efficiencies. Precipitate was measured by weight after filtration, washing with a large quantity of acetone, and drying two hours under vacuum at 55°.

Light intensities were measured by potassium ferrioxalate actinometry ([31]).

(Note on future experimental: Filtration may be difficult, but is best performed with course sintered glass funnels, which should be cleaned by drawing solvent backwards through them, not using acid. Sample tubes were fused together before final cleaning, soaked overnight with dichromate cleaning solution, washed with water, let stand several hours containing dilute (1–2%) KOH solution, rinsed with distilled H_2O, and dried in an oven.)

Literature Cited

1. Hartmann, H.; Krauch, C.H.; and Marx, M.; Ger. Offen. (Jul.9, 1970), 1,813,011. Chem. Abst. 74, 78650 (1970).
2. Beightol, L.E.; Brit. 1,245,937, Sep. 15, 1971. Chem. Abst. 76, 26114 (1972).
3. Agnihotri, R.K.; Falcon, D.L.; Hood, F.P.; Lesoine, L.G.; Needham, C.D.; and Offenbach, J.A.; Tech. Pap., Reg. Tech. Conf., Soc. Plast. Eng., Mid-Hudson Sect. (1970, Oct. 15–16), 33
4. Kolbe, G.; Schmidt, A.; Schmitz-Josten, R; and Wolff, E.; Ger. Offen. 2,019,598, Nov. 11, 1971. Chem. Abst. 76, 73294 (1972).
5. Minsk, L.M.; Van Deusen, W.P.; and Robertson, E.M.; U.S. Pat. 2,610,120 (1952).
6. Delzenne, G.A.; J. Mac. Sci., Rev. Polym. Technol. (1971), 185.

7. Nishikubo, T.; Watauchi, T.; Maki, K.; and Takaoka, T.;
    Nippon Kagaku Kaishi; (1972); 9, 1626.
8. Taditomi, N.; Ichijyo, T.; and Takaoka, T.; Nippon Kagaku
    Kaishi; (1973), 10, 35.
9. Kato, M.; Ichijo, T.; Ishii, K.; and Hasegawa, M.; J. Polym.
    Sci.(1971); 9; (A-1); 2109.
10. Lyalikov, K.S.; Gaeva, G.L.; and Evlasheva, N.A.; Tr.
    Leningrad Inst. Kinoinzh. (1970). No. 16, 42.
11. Oster, G.; Encyclopedia of Polymer Sci. & Tech.; (1969); 10;
    145.
12. Tsuda, M.; J. Polym. Sci.; (1969); 7; 259.
13. Deboer, C.D.; J. Polym. Sci. (1973); 11; (B); 25.
14. Deboer, C.D.; Wadsworth, D.H.; and Perkins, W.C.; J. Amer.
    Chem. Soc.; (1973); 95, 861.
15. Hyde, P.; Kricka, L.J.; and Ledwith, A.; J. Polym. Sci.;
    (1973); 11 (B); 415.
16. Stuber, F.A.; Ulrich, H.; Rao, D.V.; and Sayigh, A.A.R; J.
    Appl. Polym. Sci. (1969(; 13; 2247.
17. Tsunoda, T.; Yameoka, T.; Nagamatsu, G.; and Hirohashi, M.;
    Tech. Pap., Reg. Tech. Conf., Soc. Plast. Eng., Mid-Hudson
    Sect.; (1970); 25.
18. Takeishi, M. and Okawara, M., J. Polym. Sci., (1969), 7,
    (b), 201.
19. Yabe, A.; Tsuda, M.; Honda, K.; Tanaka, H.; J. Polym. Sci.;
    (1972); 10; (A-1); 2379.
20. Ichijo, T.; Nishikubo, T.; and Maki, K.; Japan Kokai;
    (Oct. 7, 1972); 72; 22,490. Chem. Abst. 78, 30778 (1973).
21. David, C.; Demarteau, W.; and Geuskins, G.; Polymer (1969);
    10; 21.
22. Kleeburg, W.; Rubner, R.; and Kuehn, E.; Ger. Offen. 130,904;
    Dec. 28, 1972. Chem. Abst. 78, 91045 (1973).
23. Hrabak, F.; Bezdek, M.; Hynkova, V.; and Bouchal, K.; Ger.
    Offen. 2,150,076; Apr. 13, 1972. Chem. Abst. 77, 49485
    (1972).
24. Hay, A.S.; Bolon, D.A.; Leimer, K.R.; and Clark, R.F.; J.
    Polym. Sci.; (1970); 8; (B); 97.
25. Nishikubo, T.; Ichiiyo, T.; and Takaoka, T.; J. Applied
    Polymer Sci.; (1974); 18; 2009.
26. Hasegawa, M.; Susuki, Y.; Nakanishi, H.; and Nakanishi, F.;
    "Progress in Polymer Science, Kodansha-Tokyo", Vol. 5;
    pp. 143-210; John Wiley & Sons; New York; 1973.
27. Chu, Shaw, Ph.D. Dissertation, University of Florida, 1974.
28. "Photochemistry,: Calvert & Pitts.
29. Sadtler Standard Infrared Spectra No. 4291.
30. Schwietert, J.W.; Ph.D. Dissertation; University of Florida;
    1971.
31. Hatchard, Parker, Proc. Roy. Soc. (London) A235, 518 (1956).

Synthesis of New Photocrosslinkable Polymers Derived from Cinnamic Acid

C. P. PINAZZI and A. FERNANDEZ

Laboratoire de Chimie et Physico-Chimie Organique et Macromoléculaire,
Equipe de Recherche Associée au CNRS N° 311, Route de Laval—Le Mans, France

Dimerization of trans-cinnamic acid under ultraviolet radiations is a well known phenomenon since it has been studied a long time ago by Bertram and Kürsten (1). Presence of cinnamic structures in macromolecules leads, after irradiation, to crosslinking polymers which have found applications in modern lithographic techniques and electronic microminiaturization (1).

Photodimerization of cinnamic acid only occurs in the solid state and irradiation of its melt or solutions does not give dimer. One control factor in such reaction is the geometry of the crystal structure of the species (2). Photocrosslinking of polymers carrying cinnamic structures cannot be explained by the only cyclobutanic structures formations. Nakamura and Kikuchi have proposed according to EPR data the intervention of two different kinds of radical intermediates, one of them being produced by hydrogen abstraction from the main chain of the polymer (1).

The photocrosslinking of cinnamic polymers is accelerated by introduction of organic compounds. The absence of fluorescence of these sensitizers and their high intersystem crossing efficiencies $(S_1* \longrightarrow T_1*)$ show that triplet state is the precursor of the reaction.

Introduction of these photocrosslinkable structures in macromolecular chains can be performed by esterification of hydroxylated polymers with cinnamoyl chloride. Cellulose (3), condensation products (4,5) and mainly poly(vinyl alcohol) have been treated(6) by this method. Other chemical modifications have been studied as ester interchange of poly(vinyl acetate) (7) and Knoevenagel reaction on polyesters (8). Very few results on the synthesis of such photocrosslinkable polymers by polymerization have been reported. Therefore free radical polymerization of cinnamic acid vinyl derivatives did not lead to the expected polymers, but to insolubilization reactions. Howewer cationic procedure can be a good way in some cases since Kato et al. could polymerize by this way with high yields p-vinyl phenylcinnamate (9) and β-vinyloxyethyl cinnamate (10).

In this paper, synthesis of new photosensitive polymers

derivated from cinnamic acid are described and their insolubili-
zation properties pointed out. In connection with this work pro-
tective abilities of new polymeric absorbers derived from 2-hy-
droxy benzophenone and phenylbenzoate are examined.

Synthesis And Polymerization Of Photosensitive Polymers

Monomers have been prepared in benzene solvent by Knoevanagel
reaction between 4-vinyl benzaldehyde and malonic derivatives at
room temperature, by use of two catalysts chosen according to the
nature of compounds (Table I). For carboxylic acids as malonic or
cyanacetic acids piperidine can be used ; for esters as ethylmalo-
nate or ethyl cyanacetate piperidinium benzoate is prefered.
Monomers 1,2 and 4 have been purified by recristallization.
Compound 3, an oil, is heated at 100°C under reduced pressure to
drive off the aldehyde and used without further purification.No
decarboxylation of the carboxylic acid derivatives has been obser-
ved in this step.
Polymerizations have been carried out under nitrogen in THF
or benzene with azobisisobutyronitrile (3% weight) as initiator
(Table II). The results are different according to the nature of
the cinnamic double bond substituents. Monomers 1 and 2 and cor-
responding polymers can indeed lose one acid function during poly-
merizations carried out at reflux temperature. This decarboxyla-
tion is in relation with the yield of gel product and molecular
weight. Therefore monomers 3 and 4 for which no decarboxylation
could occur, have been polymerized without gel formation with
high yields. Likewise decarboxylation reaction seems to induce
transfert reaction.

Irradiation Of The Photosensitive Polymers

Different methods have been used to follow crosslinking reac-
tions. When polymers were irradiated by U .V. light in dilute THF
solution above 200 nm (Method A) or 300 nm (Method B), the inso-
lubilization reaction was followed by measuring the solution ultra
violet absorbance versus time. Likewise the course of disappea-
rance of cinnamic structure was measured on polymers films placed
on quartz at 9cm of the lamp and irradiated above 200 nm (Me-
thod C). Lamp used for methods A and C was a PCQ 9 G-1 which emits
in the U.V. region at 253.7 (2.5 W), 312.5, 365 nm , the other
rays being in visible. A Pyrex filter was placed beetween 450 W
Hanovia lamp and solution when only higher wave lenghts were
expected. Lamps powers were controled before and after irradia-
tion with a Black-Ray Ultra-Violet Intensity Meter.
Nitro-2 fluorene (E_T=59 kcal/mole) and Michler's ketone
(E_T=61 kcal/mole) are efficient sensitizers for poly(vinylcin-
namate) and poly (vinylfurylacrylate) (11). For this reason, we
have tested their efficiency in the case of synthesized polymers.
Ravve et al. found that xanthene-9 one (E_t=74 kcal/mole) increa-

$$Ph - CHO \longrightarrow Ph - CH = C\binom{R}{R'}$$

$$CH_2\binom{R}{R'}$$

	R	R'	Yield %	Mp°c	ν_{vinyl} cm^{-1}	ν_{CO} cm^{-1}	ν_{CN} cm^{-1}
1	CO$_2$H	CO$_2$H	75	210	925	1680-1710	-
2	CO$_2$H	CN	75	138	910	1680	2230
3	CO$_2$Et	CO$_2$Et	-	-	915	1725	-
4	CO$_2$Et	CN	70	76.5	915	1720	220

TABLE I . Synthesis and caracteristics of 4-vinyl cinnamic derivatives.

	Soluble Polymer %	Gel%	Solvent	Decarboxylation % on polymer	$\overline{Mn}$	λ max (nm)	ε max
Poly-1	40	20	(THF)	70	900	290	-
Poly-2	40	10	(THF)	<8	2,000	312	18,400 (b)
Poly-3	60	0	(C$_6$H$_6$)	-	2,500	288.5	21,400
Poly-4	70	0	(THF)(a)	-	24,300	311	18,500

TABLE II . Caracteristics of polymersobtained from monomers 1,2,3,4.

Yields were calculated from initial monomer quantity. Polymerization conditions : 100g/l with 3% weight AIBN at solvent reflux during 5 hours, except (a) : 12 hours. Number average molecular weightswere obtained from GPC in THF with polystyrene references. λ max was found on a DK2A Beckmann Spectrophotometer in THF. For ε max, concentrations were taken in unit-mole/l (unit/l). (b) : ε max was calculated from pure diacid polymer concentration.

sed the rate of disappearence of the carbon-carbon double bound
of a similar polymer.It is why we have carried out a study with
this compound. The results are collected in Tables III, IV and V.
The polymer issued from monomer 4 showing the poorest efficiency
towards photocrosslinking has not been more studied.

The increasing order of photocrosslinking efficienties of
polymers is nearly the same for each type of irradiation. Poly 2
is the most sensitive polymer with a low presure lamp since in
THF solution, 92% of polymer is precipitated in one minute. To
obtain the same result with Poly 1, it is necessary to wait for
five times more, while this result is not reached after 7 minu-
tes with Poly 3 solution. These results are in agreement with the
substitution degrees of the cinnamic double bond on one hand and
with absorption characteristics of Poly-2 (λ max = 312 nm) ,
Poly-1 (290 nm) and Poly-3 (288,5 nm) on the other hand.

The same classification is found in presence of photosensi-
tizers. Poly-1   insolubilization above 290 nm is accelerated
by nitro-2 fluorene, Michler's ketone and especially by xanthone.
On the other hand when irradiation is carried out on films with
additional 253.7 nm ray, nitrofluorene only gave an effect. The
results obtained with the same sensitizers were similar in the
case of Poly-3. The observations are quite different with Poly-2,
the photochemical reaction of which is very sligthly improved by
the presence of xanthone and greatly reduced by the two other com-
pounds perhaps because of quenching effect.

Synthesized polymers showed excellent ability towards photo-
crosslinking and it could be thought that they can be used to
check the protective ability against U.V. light of new polymers.

Testing Of New Polymeric Photoprotector

The protective ability of orthohydroxylated benzophenones is
well known. They can act as U.V.absorbers, i.d optical screeners
or as quenchers with some polymers such as polystyrene (12). We
have synthesized a polymer containing such structures : the poly
(4-vinyl 2'-hydroxy 4'-methoxy benzophenone) (Poly-5) (13,14). In

Poly-5   Poly-6   Poly-7
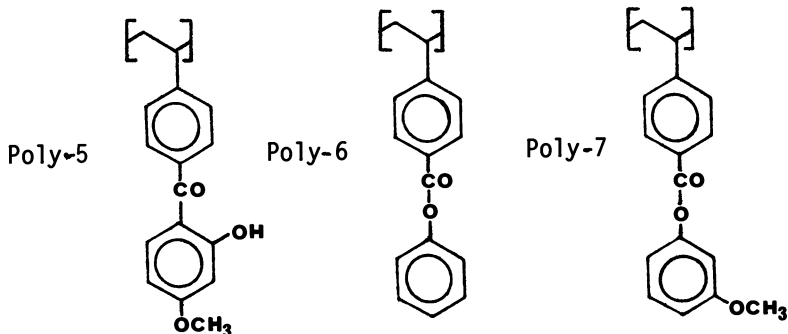
TIME , s	10	30	60	90	180	300	420
Poly-1	9.5	32.5	51	69	79.5	89	94
Poly-2	9.5	44	92	97	98	-	-
Poly-3	3.5	16	35.5	42	73	83	91

TABLE III : Decrease of the concentration of 5.10^{-5} unit/l solution % (Method A)

TIME , mn		5	10	20	30	60	90	120	180
Poly-1	Control	16	24	36	46	65	73.5	78.5	84
	2% nitro-fluorene	22	30.5	37	47.5	67	76	81	87
	2% Xan-thone	9	16	28	39	54.5	62	69	78.5
Poly-2	Control	17	30	42	53	72	78.5	82	85
	2% nitro-fluorene	14	21	33	42	59	69	74	80
	2% Xan-thone	17	32	47	64	77	80	82	84
Poly-3	Control	5	10	16	23	40	52	63	72
	2% nitro-fluorene	7	13	19	26	45	58	66	75
	2% Xan-thone	5	11	16	24	42	53	58	66
Poly-4		3	8	14	20	32	40	50	57

TABLE IV : Loss of C=C % (Method C)

TIME , mn		3	10	20	45
Poly-1	control	5	37	71	
	2% nitro-fluorene	4.5	41	75	
	2% MK	10	43	76	
	2% Xanthone	17	54.5	78.5	
Poly-2	control	12	68	97	
	2% nitro-fluorene	9	41	87	
	2% MK	13.5	58	97	
	2% Xanthone	22	51.5	83	
Poly-3	Control	1	12.5	32.5	41
	4% nitro-fluorene	2	25.5	40	55
	4% MK	16	31	41	55
	4% Xanthone	1	14	40	55

TABLE V . Decrease of the concentration of 5.10^{-5} unit/l
solution % (Method B)

MK : Micher's ketone

a similar purpose, derivatives of phenyl benzoate have been sug-
gested (15,16). They undergo photoFries reactions which can give
hydroxybenzophenones, when they are submited to U.V. light :
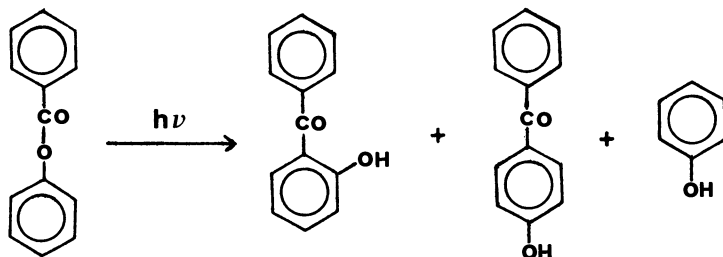
Agreement is not entirely done on the multiplicity of the
precursor excited state. Howewer, it is generally agreed that
triplet quenchers have no effect on the rearrangement (18). Two
mechanisms have been suggested which call into play either a con-
certed process or cage recombination (19), although, recent works
show intervention of free radicals during the reaction (19,20,21).
At last, if phenol has always been found in variable quantities,
products derived from the corresponding acyl part could not al-
ways be defined.

In a study on chemical Fries reaction, polymers of 4-vinyl
phenyl benzoate (6) and 4-vinyl 3'-methoxyphenylbenzoate (7) have
been prepared (17). The inconvenience of the use of such compounds
for protection is the formation, beside the orthohydroxybenzophe-
none, of the pararearrangement product which can act as a photo-
sensitizer and not as an U.V.protector. In order to check the
respective proportions of ortho and para rearrangement we have
studied the irradiation of poly-6 and Poly-7 solutions. Beside
the hydroxylated benzophenones formation, other products can occur
in side reaction : phenols, poly(4-vinylbenzaldehyde) and poly
(4-vinyl diphenyl ether) units by example. Crosslinking reactions
have been pointed out for long irradiations of esters solutions
in THF (48 hours for Poly-6 and 64 hours for Poly-7). These reac-
tions are of very poor importance when irradiation time does not
go beyond 12 hours at the end of which the greatest quantity of
recovered polymer is soluble. Phenols have never been isolated
after polymer precipitation. On the other hand a small insoluble
part has always been found, the structure of which could not be
determined. Thus after 6 hours of Poly 6 irradiation in THF, the
isolated product represents 94% of the original polymer weight.
The remaining 6% appears as white needles insoluble in usual or-
ganic solvents as in acid or basic solutions. The absorption of
the different side products of the reactions and of the esters
are negligible between 360 and 300 nm. So, with a slight error, it

has been possible to estimate on the U.V. spectra of irradiated
solutions the rates of ortho and para rearrangement from the
extinction coefficients of the hydroxylated poly (4-vinyl benzo-
phenones).

PhotoFries Rearrangement Of Poly (4-vinyl phenyl benzoate).
Ultraviolet irradiation of this polymer allows to obtain in the
chain, poly (4-vinyl 2'-hydroxybenzophenone) (Poly-8) and poly
(4-vinyl 4'-hydroxybenzophenone) (Poly-9) units as described in
Figure 1. Poly-8 and Poly-9 synthesis have already been described
(13,14,17). The ultraviolet caracteristics between 300 and 360 nm
of Poly-6, Poly-8, Poly-9 and poly (4-vinyl benzaldehyde), which
is a possible side product, are given in Table VI. The results
obtained from the U.V. spectra of irradiated solutions of Poly-6
are given in Table VII. The first possible observation is the
speed of the reaction which is finished after 5 minutes time.
Longer irradiation changes no more polymer composition. Ortho/para
ratio which is important at the beginning shows tendancy to
decrease versus time till a limit after 5 minutes reaction. The
same study carried out in the case of a longer irradiation of
a more concentrated THF solution gives a similar ratio value.

PhotoFries Rearrangement Of Poly (4-vinyl 3'-methoxy phenyl
benzoate). Unit structures obtained in this reaction are those of
the poly (4-vinyl 2'-hydroxy 4'-methoxy benzophenone) (Poly-5)
and poly (4-vinyl 4'-hydroxy 2'-methoxy benzophenone) described
in Figure II. For spectroscopic caracteristics we have compared
the para-hydroxy derivative to poly (4-vinyl 2',4'-dimethoxy ben-
zophenone)(Poly-10) which is an intermediary in the synthesis of
Poly-5 (13). Here too, absorption of the reaction products in the
range of 300-360 nm were sufficient to estimate the ortho/para
rearrangements ratio. The ultraviolet caracteristics of Poly-7,
Poly-5, Poly-10 and results of irradiations of Poly-7 are listed
in Tables VIII and IX. In the same conditions of irradiations,
ortho/para ratio and yields are smaller than the values obtained
in the case of Poly-6. But, as in the previous case, benzophenones
are obtained very rapidly and the ortho product formation is
greater than the para one. It is thus possible to consider poly
(4-vinyl phenyl benzoates) as U.V. protectors.

Checking Of The Polymeric U.V. Protector. 2-Hydroxy 4-metho-
xy benzophenone (11) has been included in this study to compare
the protections brought by a small organic molecule and that
brought by a polymer. This comparison is not entirely exact since
polymer advantage must reside in the permanence of effect in a
long time and that irradiations have never exceeded 3 hours. It can
give yet an idea of the respective protective abilities. The same
experimental conditions as previously described have been used on
solutions (Methods A and B) and films (Method C) of the photosen-
sitive polymers containing the additives in the weight proportion
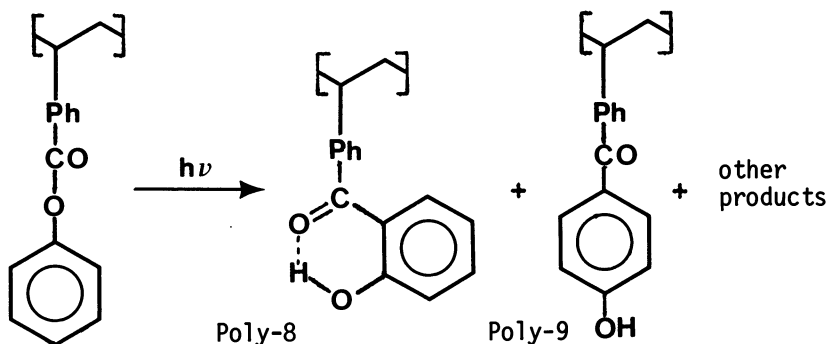
Figure 1.   PhotoFries rearrangement of poly(4-vinyl phenyl benzoate)

	360 nm	325 nm	300 nm
Poly-6	0	80	240
Poly-8	3,060	5,150	2,680
Poly-9	0	630	12,300
Poly VB	50	100	200

TABLE VI . Extinction coefficient of some products of the photo
            Fries reaction of poly (4-vinyl phenyl benzoate).
            Poly VB : Poly (4-vinyl benzaldehyde) obtained by
            treating the copolymer with its dimethyl acetal by
            acidic solution.

	Irradiation time,mn	Poly-8/Poly-9	(Poly-8 + Poly-9)%
A	1	2,4	45
	2	1,9	70
	5,15,30,60	1,7	74
B	360	1,6	62

TABLE VII. Ortho and para rearrangement of Poly-6 versus time.
            A. $8.93 \cdot 10^{-5}$ unit/l solution in 1,2-dichloroethane (DCE)
            B. $2.2 \cdot 10^{-2}$ unit/l solution in THF
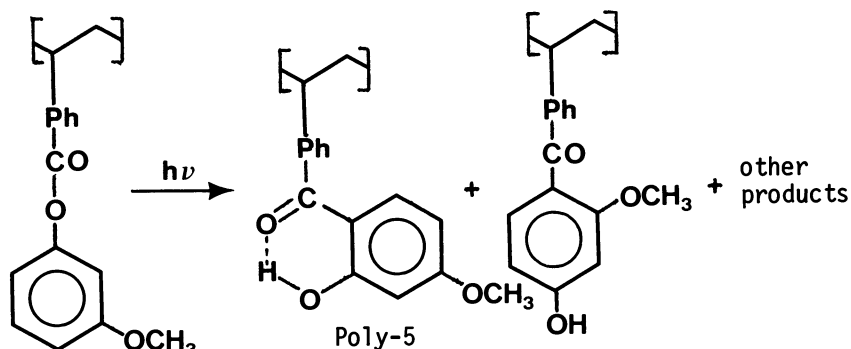
Figure 2. PhotoFries rearrangement of poly(4-vinyl 3'-methoxy phenyl benzoate)

	360	325	300
Poly-7	0	0	1500
Poly-5	3,480	10,000	11,100
Poly-10	440	2,270	5,950

TABLE VIII . Extinction coefficients of some products of the
             photoFries reaction of poly(4-vinyl 3'-methoxy
             phenyl benzoate).

	Irradiation,mn,	Poly 5·/ Poly-10	(Poly-5+Poly-10)%
A	2	1.1	46
	5,10,20	1.1	48,5
B	420	1.7	40

TABLE IX. Ortho and para rearrangement of poly(4-vinyl 3'methoxy
          phenyl benzoate) versus time.

          A. $5.55.10^{-5}$ unit/l solution in DCE
          B. $3.24.10^{-2}$ unit/l solution in THF

Additive \ Time,s		10	30	60	90	180	300	420
Poly-1 (a)	none	9.5	32.5	51	69	79.5	89	94
	11	1	10.5	29	45.5	77	91	94
	Poly-5	3	13	26	39	71	90	91.5
	Poly-6	5	16.5	35	72	85	94	96
	Poly-7	1	4	29	35	75	91.5	92.5
Poly-2 (a)	none	9.5	44	92	97	98	-	-
	11	2.5	24	54	73	86	98	-
	Poly-5	4	16	52	74	87	98	-
	Poly-6	6	38	84	96	98	-	-
	Poly-7	6.5	39	85	96	97	-	-
Poly-3 (b)	none	3.5	16	35.5	42	73	83	91
	11	3.5	15	34	41	79	92	93
	Poly-5	4.5	16	29	38	74	89.5	94
	Poly-6	1	15	30	33.5	78.5	90.5	96
	Poly-7	0	5	30	40	73	93	95

TABLE X . Effects of additives on the photocrosslinking yield
of photosensitive polymers versus time (Method A).

Concentration : 5.10^{-5} unit/l

Additive concentrations : a = 2% in weight
                          b = 4% in weight

Additive	Time, mn	3	10	20	45
Poly-1 (a)	none	5	37	71	
	11	4	39	70	
	Poly-5	5	39	66.5	
	Poly-6	6	38	72	
	Poly-7	3	32	64	
Poly-2 (a)	none	12	68	97	
	11	2	56	97	
	Poly-5	6	54	97	
	Poly-6	8	55	98	
	Poly-7	9.5	51	96.5	
Poly-3 (b)	none	1	12.5	32.5	41
	11	2.5	12	29.5	42
	Poly-5	3.5	15	30	40
	Poly-6	3	11	30	39
	Poly-7	3.5	14	33	42

TABLE XI . Effects of additives on photocrosslinking yield
of photosensitive polymers versus time (Method B)
Concentration : 5.10^{-5} unit/l

Additive concentrations : a = 2% in weight
b = 4% in weight

	Time ,mn Additive	5	10	20	30	60	90	120	180
Poly-1	none	16	24	36	46	65	73.5	78.5	84
	11	20	31	49.5	62	78.5	84.5	85.5	86.5
	Poly-5	12.5	28	41	46	59	64	68.5	69.5
	Poly-6	17	30	44.5	55.5	71.5	79	83	85.5
	Poly-7	2.5	4.5	8.5	12.5	28	42	48	55.5
Poly-2	none	17	30	42	53	72	78.5	82	85
	11	8	12.5	20.5	26.5	38	47	51.5	60
	Poly-5	11.5	20	36	48	69	76.5	81	86
	Poly-6	19	28.5	43	53.5	71.5	79.5	83	86
	Poly-7	13.5	22	39.5	52	71.5	79.5	83	86
Poly-3	none	5	10	16	23	40	52	63	72
	11	6.5	12	21	30.5	57.5	72	77.5	84
	Poly-5	5	6	9	14	37	60	71	77.5
	Poly-6	3	6	10	17	30.5	41	48.5	58
	Poly-7	8	15	25	35	59	68.5	75	79.5

TABLE XII . Effects of additives on C=C loss yield
of photosensitive polymers (Method C).

Additive concentration : 2% in weight

of 2 or 4%. The results of irradiations are listed in Table X, XI
and XII. The most interesting observation concerns the use of poly
(4-vinyl phenyl benzoates). The high rate of photoFries reaction
is again pointed out since protection proceeding with this reac-
tion does not generally exceed 1 minute (cf. Table X). Likewise
the polymer giving the best rearrangement yield, i.e Poly-6, shows
the poorest protective effect, except in one case (Poly-3 irradia-
ted in film). On the other hand, similarities between Poly-7 and
Poly-5 show that, in the cases of aromatic esters, only the pro-
ducts issued from photoFries reaction have realy some importance.
The best example of protection is pointed out during the irradia-
tion of Poly-1 containing the poly (4-vinyl 3'-methoxy phenyl ben-
zoate). Poly-5 is more active than molecule 11 which does not decrease
the photocrosslinking yields excepted in the case of Poly-2.
      As a conclusion, if it is possible to foresee if a compound
can be a protective agent, only experimentation allows to know
what polymers it can protect. Furthermore a compound can have op-
posite effects on two polymers, even if they have similar absorb-
tion properties. Protection of polymers is the result of several
factors, at least in the case of orthohydroxylated benzophenones :
the screening effect is less important than compatibility and
quenching effect.

LITERATURE CITED

1. In G.A.Delzenne,Eur.Polym.J. (1969), Supplement, 55-91
2. M.D.Cohen and G.M.J.Schmidt, J.Chem.Soc.(1964), 1996-2000
3. L.M.Minsk, J.G.Smith, W.P.Van Deusen and J.F.Wright (1959)
    J.Appl.Polym.Sci., 2, 302
4. Algraphy Ltd.Br.Pat.Spec. 921530, cf reference 1
5. J.S.Shim and S.Kikuchi, Kogyo Kagaku Zasshi (1965), 68, 387,
    cf reference 1
6. M.Tsuda, Makromolek.Chem. (1964), 72, 183, cf reference 1
7. M.Tsuda and Y. Minoshima, Kogyo Kagaku Zasshi (1964), 67, 472
    cf reference 1
8. A.Ravve, G.Pasternack, H.K.Brown and S.B.Radlove, J.Polymer
    Sci.Chemistry, (1973), 11, 1733-52
9. M.Kato, Polym.Lett. (1969), 7, 605-8
10. M.Kato, M.Hasegawa and T.I.Chijo, Polym.Lett. (1970),8,263-5
11. F.S.Prout, A.A.Abdel Latif and M.R.Kamal, J.Chem.Eng.Data
    (1963), 8, 597, cf reference 8
12. G.A.George, J.Appl.Polym.Sci. (1974), 18, 117-24
13. C.P.Pinazzi and A.Fernandez, Makromol.Chem. (1973), 167, 147
14. C.P.Pinazzi and A. Fernandez, Makromol.Chem. (1973), 168, 19
15. L.W.A.Meyer and M.H.Broyles.U.S. 2,811,460 (1957) in CA 52
    2451g
16. G.C.Newland and G.R.Lappin, US 3,519,599 (1970) in C.A. 73
    56812
17. C.P.Pinazzi and A.Fernandez I.U.P.A.C. International Symposium
    on Macromolecules (1974), Madrid

18. D.Bellŭs, Advan.Photochem. (1971), 8 , 109
19. All references in J.W.Meyer and G.S.Hammond, J.Amer.Chem. Soc. (1972), 94, 2219
20. W.Adam, J.A. de Sanabia, M.Fischer,J.Org.Chem.(1973),38,2571
21. C.E.Kalmus and D.M.Hercules, J.Amer.Chem.Soc.(1974), 96, 449

5

Photosensitized Crosslinking of Polymers

ZDZISŁAW HIPPE

I. Łukasiewicz Technical University, 39-959 Rzeszów, Poland

    Synopsis.Some results of broad research project
on the photosensitized crosslinking of poly(vinyl buty-
ral) and unsaturated polyester resin, are presented.
Various aspects of data obtained are briefly discussed.

    Introduction. It is the purpose of this article[*]
to report the present status of a research program
which has as its goal photoinduced crosslinking of va-
rious industrial polymers. The results received for
poly(vinyl butyral) and for unsaturated polyester resin
in mentioned project, are dealt with.
    Photosensitized crosslinking of polymers has been
the subject of numerous publications [1 - 30] , concer-
ned mainly with poly(ethylene), poly(vinyl alcohol),
various vinyl copolymers, copolymers of maleic anhy-
dride and/or phtalic anhydride with styrene and some
polymers derivated from cinnamic acid. The following
compounds were used as sensitizers: benzophenone, 4-
chloro- and 4,4-dimethylbenzophenone [1, 3-6, 8, 9] ,
α -and β -derivatives of anthraquinone [3, 23] aceto-
phenone, hydroquinone, triphenylmethane and pyridine
[4] , chlorobenzene and no less than trichlorinated n-
paraffins [6] , a complex of zink chloride with o-dia-
nizidine [11], potassium bichromate [12] , anthracene
[13, 14] 2,5-methoxy-4-amino-trans-stilbene [15], ben-
zylideneacetophenone [16-18],ω -thiophenylacetophenone,
ω -thiophenyl-ω -phenylacetophenone, thiophenyl carbo-
nate and p,p-disubstituted dibenzoyldisulphide [19],

---

[*] Note. Some parts of presented investigations were
    carried out at the Paint Research Institute, 44-100
    Gliwice, Poland.

benzilmonoacetal [21, 22], hydantoine[24], rhodamine
[25], triphenylphosphine [26], triethylaluminium [27],
ferrocene + carbon tetrachloride 28 , titanocene di-
chloride [29] and some donor-acceptor complexes [30];
of these substances, benzophenone, antraquinone and
their derivatives have attracted most attention.

Poly(Vinyl Butyral)

Experimental. Thin films of investigated polymers,
contained about 125 x 10^{-3} mole of sensitizer per 100g
of pure polymer, were spread out on glass substrate.
For crosslinking, light was used with the radiation
below 315m eliminated by glass filter. The source was
120W high-pressure Q-400 mercury lamp with total effi-
ciency of 30 lumens/W. The spectrum of incident beam
contained 254 (2.09), 302 (1.74) and 313mμ (3.48W) lines.
The incident light intensity measured by means of
Hatchard and Parker technique [31] was 18 x 10^{15} qu-
anta.cm.$^{-2}$sec.$^{-1}$; the doses applied differed according
to aim of the test performed. In constant temperature
crosslinking experiments, the temperatures of the speci-
mens during exposure did not exceed 23°C $\pm$ 2°C. The
sensitizer efficiency was followed by estimation of
sol-gel relation (extraction with ethyl alcohol for
1 hour in a Soxhlett apparatus). IR - spectra of the
crosslinked polymer (not cited here) were run on UR-10
(C. Zeiss, Jena) double-beam spectrometer; thermal pro-
perties of the polymer were estimated with the use
Hitachi-Perkin-Elmer calorimeter model DSC-1B; elastic
modulus determination was done on ultrasonic elasto-
meter the type 501, (Unipan, Poland); studies of sur-
face topography were performed on electron microscope
type UM-100A (U.S.S.R.) using samples prepared by means
of a two-stage replica system [poly vinyl alcohol -
chromium preshadowed carbon replica] . All computations
were done on the ODRA-1013 electronic digital computer
Elwro, Poland and, in some cases, on Hewlett-Packard
model 9100A desk-top electronic calculator.

Results and discussion. In the course of our stu-
dies on light induced crosslinking of poly(vinyl buty-
ral) , new class of effective photosensitizers, namely
organic sulphoxides, was discovered. [41] It should be
noted, that four years after our invention, the use
diphenyl sulphoxide simultaneously with o-ethylbenzo-
ine and H$_2$O$_2$ as effective sensitizer for crosslinking
of polymers, was reported [23].
In the aliphatic series of saturated, symmetrical

and unsymmetrical sulphoxides, the sensitizing action
rised linearly with the SO mole fraction in the sensi-
tizer molecule. This finding may be understood if we
consider the S→O bond character. Examination of the
molar refraction or of the parachor leads to the con-
clusion that in the aliphatic sulphoxides the S O
bond is predominantly a single coordinate covalent bond
 32, 33 . Saturated aliphatic sulphoxides display -
notwithstanding the chain length - a chromophoric ab-
sorption near 210mμ , which indicates that the S→O
bond is rather unchangeable in character. Therefore, a
definite and constant influence of the sulphur-oxygen
bond on the sensitizer efficiency may be expected. This
influence diminished as the SO mole fraction in the
sulphoxide molecule is decreased. As regard the aroma-
tic sulphoxides, even though the sulphoxides are not
planar (and $\pi - \pi$ conjugation actually does not exist),
possibly the p-d orbital interactions may be involved
[34], which resulted in a more rigid S-O bond. This
phenomenon may also be explained on the basis of the
inductive effect of the electron - withdrawing aromatic
ring which reduces the contribution of the resonance
form >S=O ←→>S-O and increases the force constant of
the bond. This was revealed by the spectral shift of
the SO band in the infrared, in accordance with the
electron - attracting ability of the S-attached substi-
tuents (in transition from n-alkyl-SO-n-alkyl to Ph-SO-
Ph the spectral shift of the band $1008.0 cm^{-1}$ up to
$1042.0 cm^{-1}$, was discovered). It seems that in the case
of aromatic or mixed sulphoxides, the S-O bond charac-
ter will be the most important factor determining the
sensitizer effectiveness; the mole fraction of the SO
grouping is here of secondary importance.
        Among the investigated compounds, diphenyl sulpho-
xide, the structural analogue of classical sensitizer
- benzophenone - was found to be the most effective.
        According to several authors [1] , effective sen-
sitizers seem to be substances that decompose photoche-
mically to free radicals. It has already been found [8]
that, during the photolysis of benzophenone, the radi-
cals $\overset{\cdot}{C}_6H_5$ and $C_6H_5\overset{\cdot}{C}O$ are produced, the latter decom-
posing partly to $\overset{\cdot}{C}_6H_5$ and CO. This finding means in
fact that in the irradiated system, the concentration
of the sensitizer decreases owing to its gradual decom-
position. Speaking of benzophenone [9, 35] the triplet
state formation is postulated in which the hydrogen
atom is abstracted from the polymer molecule giving a
macroradical [36], whereas benzophenone itself gives

benzopinacol [37, 38] or benzohydrol [1] . In contrast,
other workers e.g. Schenck [39] expected that the
sensitizing agent would transfer the absorbed energy on
the polymer molecules initiating the reaction of cross-
linking, without entering into the reaction itself, i.
e. its molecules would be regenerated after termination
of the kinetic chain. The investigations performed pro-
ved, that in conditions used, the sulphoxides act as
thrue sensitizers for crosslinking: the excitation
energy was transferred to polymer molecules but the
sensitizers did not change photochemically themselves,
i.e. they regenerate their initial molecules when the
kinetic chain was completed. The above postulated view
may be well assumed in the case of sensitation of solid
state reactions since the possibility of recombination
of the radicals formed of a sensitizer molecule has
been advanced to account for the cage-effect of Franck
- Rabinovitsch [40] .

The properties of tridimensional network formed in
the poly(vinyl butyral) on irradiation were estimated
by means of ultrasonic and thermal methods. It was
found, for instance, that the elastic modulus changed
over from 3.33×10^{10} dynes cm.$^{-2}$ to 4.03×10^{10} dynes
cm^{-2} for gel content increase from 0.082 up to 0.923.
Simultaneously, the thermal stability of the crosslin-
ked polymer rised from 167°C up to 417°C. [42]

In completion of above mentioned studies, the
dependence between incident light intensity, I_a, and
the crosslinking yield, was estimated. It has been
found, that the dependence explored may be represented
by the equation:

(1)   gel content (% by wt.) $= (1.5I_a + 45.1) + I_a^{1/2}$

Assuming that the yield for gel fraction is pro-
portional to the rate of crosslinking, it seemed that
the observation on possibility of resolving the experi-
mental results into terms proportional to I_a and
$I_a^{1/2}$, points out the dual mechanism of photoinduced
crosslinking of poly(vinyl butyral). The over all cha-
racter of the equation (1) suggests that the main role
in the discussed reaction plays the relation: gel con-
tent $\propto I_a$, connected possibly with direct coupling of
two adjacent polymeric radicals. On the other hand,
negligible meaning has the relation: gel content
$\propto I_a^{1/2}$, which seems to be associated with the diffu-
sion of radicals and transport of active centers along
the polymeric chain. More detailed treatment of derived
relation is difficult as the reaction occurs in solid

state and besides in thin film. In that case the
diffusion of radical scavengers eg. atmospheric oxygen
should be taken into consideration.
     The relation of gel content to film thickness for
a fixed radiation dose , obeyed, as was anticipated,
the general equation:

$$(2) \qquad\qquad g = a\,e^{-bL}$$

where g is the quantity of gel in the polymeric film
($\%$ by weight), e - base of logarithms, L - film thic-
kness [cm.], a,b - empirical coefficients. Under the
conditions applied, the coefficient a [$\%$] (its numerical
value equals 95$\%$) characterizes the limiting value for
the gel content in the polymeric film, as its thickness
approaches zero. It might be supposed that for high
doses of radiation applied, the weight-fraction gel
formed throughout the film, approaches the cross-lin-
king yield at the incident surface. However, since de-
gradiation processes take place during exposure, it is
practically impossible to obtain a totally cross-linked
polymer.
     The numerical value of coefficient b (32cm^{-1}) is
in satisfactory agreement with the value of the so
called integral absorption coefficient, as was estima-
ted in independent experiment. An examination of the
influence of the initial molecular weight on gel frac-
tion yield showed the reciprocal relation between these
two parameters.
     Also, the influence of the temperature of exposure
(for a fixed radiation dose) on gel fraction yield, was
tested. The relation studied is described by the equa-
tion:

$$(3) \quad \text{gel content } (\% \text{ by wt.}) = -134.13+9.48t-0.13t^{2}+$$

$$+0.006t^{3}$$

where t is temperature, [$^{\circ}$C]. It should be stressed
that the equation (3) is refined for the dark crosslin-
king. [42] The inspection of the above mentioned equa-
tion points out that the photoinduced crosslinking of
poly(vinyl butyral) proceeds to a slight extent as
endothermic process.
     It seemed interesting to follow the formal kine-
tics of the reaction. It has already been reported [42]
that within the entire range of radiation doses used,
the reaction is reversible, i.e. the polymer underwent

simultaneous cross-linking and degradation, but the
final effect in macro-scale depends on the ratio of the
rates of both reactions. In the initial phase the rate
of cross-linking exceeds that for scission, and for
higher doses both reactions take place at similar ra-
tes, so that overall yield for the process approaches
asymptotically a fixed value. Theoretically, in this
phase of the reaction the number of cross-links per ti-
me unit equals the number of scissions. It was found,
that the discussed reactions might be interpreted in
terms of reversible first order reaction [42]. The
solution of equations given in [43] for reversible
first-order reactions yielded $k_1^{40^o}= 146.8 \times 10^{-4}$,
$k_2^{40^o}= 41.9 \times 10^{-4}$, $k_1^{50^o}= 332.8 \times 10^{-4}$ and $k_2^{50^o}= 78.1 \times$
$\times 10^{-4}$ [hr^{-1}]. Using Arrhenius equation for reversible
systems, the thermal activation energies (16 kcal/mole
and for reverse reaction 12.51 kcal/mole), and change
of enthalpy over the range 40° - 50°C, was calculated
(ΔH = 3.94 kcal/mole).

The effectiveness of diphenyl sulphoxide as sensi-
tizer of poly(vinyl butyral) exceeds over twenty times
that of the benzophenone [42] . More-over the use of
the compound shifted the spectral region of usefull ra-
diation towards longer wavelengths. This enabled to
acquire interesting results with crosslinking of the
polymer by solar radiation. It may be stated that the
process of the tridimensional network formation sets in
at early phase of the exposure, for instance after the
lapse of 6 days the amount of insoluble fraction was
found to be roughly 50 - 60% by weight. Afterwards, the
yield of crosslinking rose gradually and after one
month approached the limiting value 75% by wt. The ac-
tion of solar radiation on the polymer brings about -
as in the case of steady illumination under laboratory
conditions - crosslinking and degradation, but the
final effect on macro-scale depends on the ratio of the
rates of both reactions. It is an interesting contribu-
tion that the effect of solar radiation dose on the
crosslinking of the polymer may be satisfactorily in-
terpreted with the use of Charlesby's treatment, ori-
ginally developed for describing of the molecular chan-
ges produced in linear polymers by ionizing radiation.

One of the most interesting problems was evalua-
tion of quantum yield for light induced crosslinking of
poly(vinyl butyral) in the presence of diphenyl sulpho-
xide. Mathematical treatment of the molecular changes
produced in polymers by light is based on that by ioni-
zing radiation. In our case, as the changes above the
gel point were examined, the only suitable approach

seemed to be that of Shultz [44] . However, using spe-
cially designed computer programs [45, 46] , it was
found that three distinct solutions of Shultz's equa-
tions:

I $R^* > R_0$

$$(4) \qquad g = 0$$

II $R_0 \geqslant R^* \geqslant R_L$

$$(5) \quad g = (0.5 - X)(kL)^{-1} \ln\left(\frac{R_0}{R^*}\right) + C(kL)^{-1}\left(\frac{R^*}{R_0} - 1\right) +$$
$$+ 2(kL)^{-1}\left[(B+C)^{0.5} - \left(B + C\frac{R^*}{R_0}\right)^{0.5}\right] +$$
$$+ 2B^{0.5}(kL)^{-1}\left[\text{ctnh}^{-1}\left(1 + \frac{CR^*}{BR_0}\right)^{0.5} - \text{ctnh}^{-1}\left(1 + \frac{C}{B}\right)^{0.5}\right],$$

III $R_L \geqslant R^*$

$$(6) \quad g = (0.5 - X) + C(kL)^{-1}\left(\frac{R^*}{R_0} - \frac{R^*}{R_L}\right) + 2(kL)^{-1}\left[\left(B + C\frac{R^*}{R_L}\right)^{0.5} - \right.$$
$$\left. - \left(B + C\frac{R^*}{R_0}\right)^{0.5}\right] + 2B^{0.5}(kL)^{-1}\left[\text{ctnh}^{-1}\left(1 + \frac{CR^*}{BR_0}\right)^{0.5} - \text{ctnh}^{-1}\left(1 + \frac{CR^*}{BR_L}\right)^{0.5}\right].$$

have no general character and may be put in use with
caution. [in equations (4), (5) and (6), X is ratio of
quantum yield for degradation, to quantum yield for
crosslinking; $B = 0.25 + X$, $C = 2 - X$, R_0 is the
energy absorption at the incident surface (photons g^{-1}),
R_L - the energy absorption in lamina L centimeters
below the incident surface, whereas R - is the gela-
tion energy . Thus, the specified intervals of gel
content were estimated, for which the X has had nega-
tive, physically unreal values. The results of computa-
tions (bisection with convergence acceleration of ite-
rational process by δ^2 Aitken method) for the case of
$R_0 \geqslant R \geqslant R_L$ are summarized in the Table I.

TABLE I. The $R_o \gg R^* \gg R_L$ case.

Energy absorption at the incident surf. $\dfrac{quanta}{g} \times 10^{20}$	Gel content interval	$X = \Psi_d / \Psi_c$
280.80	$0.00032 < g < 0.00979$	$-0.0700 > X > -0.2400$
561.60	$0.05714 < g < 0.13631$	$0 > X > -0.2400$
842.40	$0.11840 < g < 0.24709$	$0 > X > -0.2400$
1123.2	$0.16582 < g < 0.33311$	$0 > X > -0.2400$
2246.4	$0.28309 < g < 0.54938$	$0 > X > -0.2400$
4492.8	$0.39895 < g < 0.76403$	$0 > X > -0.2400$

Gelation energy: 226.1×10^{20} quanta/g, film thickness 0.08 cm.

and for the case $R_L \gg R^*$ - in the Table II.

TABLE II. The $R_L \gg R^*$ case.

Energy absorption at the incident surface, R_o $\dfrac{quanta}{g} \times 10^{20}$	Gel content interval	$X = \Psi_d / \Psi_c$
280.8	$0.00120 < g < 0.17924$	$-0.0300 > X > -0.2400$
561.6	$0.40437 < g < 0.74589$	$0 > X > -0.2400$
842.4	$0.49277 < g < 0.88924$	$0 > X > -0.2400$
1123.2	$0.51884 < g < 0.94312$	$0 > X > -0.2400$
2246.4	$0.52778 < g < 0.97993$	$0 > X > -0.2400$
4492.8	$0.51728 < g < 0.95284$	$0 > X > -0.2400$

Gelation energy: $R^* = 226.1 \times 10^{20}$ quanta/g, film thickness $L \sim 0.00408$ cm.

The results presented proved our assumption that the use of Shultz's equations, should be in some circumstances dissuaded. Even Shultz himself suggested in [47] that in some circumstances (as in the crosslinking of methyl methacrylate - ethylene dimethacrylate system) negative, physically unreal X values were obtained. In this case, a special factor (e.g. - 1) has to be used

for making a change of the sign. The origin of the fac-
tor is not quite clear.
    Equations (4), (5) and (6) were derived under the
assumption that the absorption coefficient k remains
constant during the exposure. It may thus be supposed
that the derivation of relation between X and gel frac-
tion content of the polymer, with the assumption that
the absorption coefficient changes during irradiation
may yield useful results. If the light absorption by
polymer film is properly measured, the following formu-
la may be derived:

$$(7) \qquad g_{R_i} = \frac{R_i - R_i^*}{R_i + 2R_i^*}$$

where g_R is gel fraction content of the polymer after
energy R_i has been absorbed; R_i - integral energy
absorption by the film, and R_i - integral energy absor-
ption at gelation point. Relation (7) was tested for
poly$($vinyl butyral$)$, and recently, for other polymers.

Polyester   of Maleic/Phtalic Anhydrides   and Ethylene Glycol in   Styrene [a]

    Experimental. The general conditions of experime-
nts, and methods of investigations were similar to
those described previously.However, extremely precise
and reproducible results of crosslinking were achieved
owing originally developed device for exposure $($Fig 1$)$
in which the specimens may be rotated with chosen rate.
Additionally, the selection of UV-sensitizers was ex-
tented, and besides diphenyl sulphoxide, also dinaphtyl
sulphoxide, methyl - benzyl sulphoxide, bis- p-chloro-
phenyl sulphoxide, bis- 2,4-dichlorophenyl sulpho-
xide, were used. Also, some other compounds were exa-
mined, namely: diphenyl sulphide and its p-nitro-p-
amino- as well o,o-dicarboxy-derivatives, methiomethy-
lene-diethyl phosphate and uranyl acetate.

---

[a] This part of work was done with collaboration of
    Mrs. B. Guzowska   and Mr. J. Lipiński
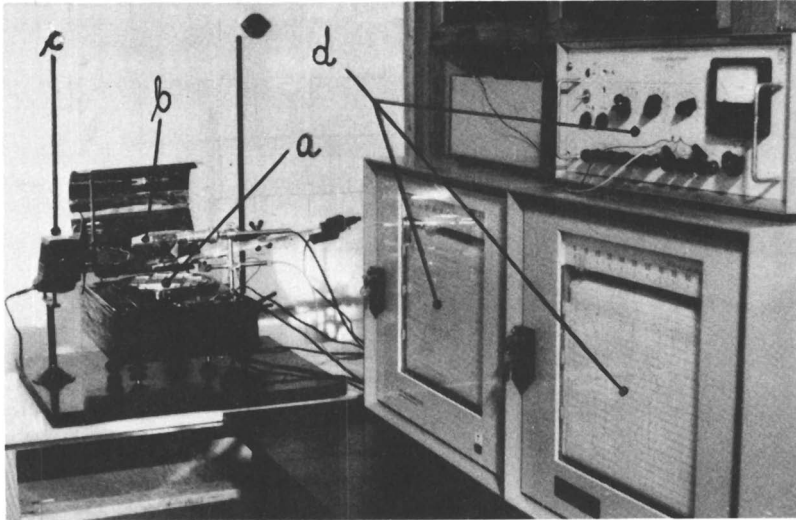
Figure 1. Device for controlled irradiation of polymer films—rotating plate with specimens (a), source (b), ventilator (c), and electronics for controlling of light intensity, specimens temperature, and rate of rotations, (d)

Results and discussion. The most effective substance was found to be (among the S-compounds) diphenyl sulphide. On the other side, p-nitro-p-amino-diphenyl sulphide showed nearly complete lack of activity. In the group of substituted sulphoxides and sulphides, may be noticed the dependence of sensitizing efficiency on the electromeric effects in the molecule. At present status of the work it is imposible to predict whether this result has as its own basis an I - or M - effect. However, decrease of sensitizing ability of discussed compounds may also be connected with disturbance of coplanarity of photosensitizers structures.

High activity of uranyl acetate as crosslinking sensitizer should be noted. Possibly, this may be explained from different points of view: uranyl acetate belongs to the compounds that yield easily to photocemical excitation, and also uranyl acetate as radioactive compound may produce itself free radicals in neighboring polyester molecules.

The detailed investigations along these lines are now in the course.

Literature Cited

1. Oster, G., Oster, G.K., Moroson, H., J.Polym.Sci.,
   (1959), 34, 671
2. Oster, G.K., Oster, G., Int.Symposium on Macromolec.
   Chemistry, Moscow, 1960, section 3, 289-292
3. Oster, G., Polymer Letters, (1964), 2, 1181
4. Luck, W., Hrubesch, A., Suter, H., German Pat.
   1,046,883 (1958)
5. Wilski, H., Angew.Chem., (1959), 71, 612
6. Wilski, H., German Pat. 1,062,007 (1959)
7. Soumelis, K., Wilski, H., Kunststoffe,(1961), 52,471
8. Pao-Kung Chien, Ping-Cheng Chiang, En-Chien Hou, K o
   Hsueh T ung Pao 1958 , 663 (Chem.Abstr.(1959), 53,
   120151)
9. Pao-Kung Chien, Ping-Cheng Chiang, Yu-Chen Liao,
   Ying-Chin Liang, Hsia-Yu Wang, Chni-Chang Fang, Sci.
   Sinica,(1962), 11, 903 (Chem.Abstr. (1965), 61,10539e)
10.- ibid.,(1962), 11, 1513 (Chem.Abstr. (1963), 58,
   10320e)
11.Tsunoda, Yamaoka, J.Appl.Polymer Sci., (1964) , 9,1763
12.Ducalf, B., Dunn, A.S., ibid.,(1964), 8, 1763
13.French Pat. 1,091,323 (1955)
14.French Pat. 1,229,883 (1960)
15.Stuber, F.A., Ulrich, H., Rao, D.V., Sayigh, A.A.R.,
   J.Appl.Polym.Sci., (1969), 13, 2247
16.US Pat. 2,816,091 (1957)
17.UK Pat. 820,173 (1959)
18.UK Pat. 825,948 (1959)
19.Hutchison, J., Redwith, A., Advances in Polymer Sci.
   Vol. 14, p.
20.German Pat. 2,102,366 (1971)
21.German Pat. 2,232,365 (1971)
22.German Pat. 2,337,813 (1971)
23.Andruntchenkho, A.A., Bogdan, L.S., Khatchan, A.A.,
   Shrubovitsch, W.A., Vysokho Molekh.Soiedin.(1972),
   14, 594
24.US Pat. 2,719, 141 (1954)
25.Marimoto, K., Hayashi, I., Inami, A., Bull.Chem.Soc.
   Japan (1963), 36, 1651
26.Tsubahiyama, K., Fujisaki, S., J.Polym.Sci., (1972),
   B, 10, 341
27.Gaylord, N.G., Dixit, S.S., Patnaik, B.K., ibid.,
   (1971), B 9, 927
28.Ogawa, T., Taninaka, T., ibid.,(1972) , A-1, 10, 2056
29.Kaeriyoma, K., Shimura, Y., ibid.,(1972), A-1, 10,
   2833
30.Dack, M.R., J.Chem.Educ., (1973), 50, 109

31. Hatchard, C.G., Parker, C.A., Proc.Roy.Soc. (1956),
    A235, 518
32. Strecker, W., Spitaler, R., Chem.Rev. (1926),59, 754
33. Vogel, A.J., J.Chem.Soc.(London), (1948), 1820, 1833
34. Gillis et all, R.S., J.Am.Chem.Soc. (1958), 80, 2999
35. Charlesby, A., Grace, C.S., Pilkington, F.B., Proc.
    Roy.Soc., (1962), A268, 205
36. Yang-Hsu Liang, Hsia-Yu Wang, Chni-Chang Fang, Ping-
    Cheng Hsiang, Pao-Kung Chien, Sci.Sinica (1962), 11
    903 (Chem.Abstr. (1965) , 62, 10589a)
37. Trudelle, I., Neel, I., Compt.Rend.Hebd.Seances
    Acad.Sci. (1965), 260, 1950
38. Charlesby, A., Rad.Chemistry Proc.Tihany Symp.,
    Tihany, 1962
39. Schenck, G.O., Ind.Eng.Chem. (1963) , 55, 40
40. Franck, I., Rabinovitsch, E., Trans.Faraday Soc.,
    (1934), 30, 120
41. Hippe, Z., Bull.Acad.Polon.Sci.,Ser.Sci.Chim.,(1967)
    15, 261
42. Hippe, Z., The P.R.I.Research Project No
43. Stevens, B., Chemical Kinetics, Chapman and Hall,
    London, 1961, p. 78
44. Shultz, A.R., J.Chem.Phys., (1958), 29, 200
45. Hippe, Z., Dębska, B., Bull.Acad.Polon.Sci.,Ser.Sci.
    Chim., (1972), 20, 1001
46. Hippe, Z., Dębska, B., ibid., (1972), 20, 1075
47. Shultz, A.R., J.Am.Chem.Soc. (1958), 80, 1834

6

Polymerization and Crosslinking by the Benzene–Bismaleimide Photoaddition Reaction

MALCOLM P. STEVENS

Chemistry Department, University of Hartford, West Hartford, Conn. 06117

Maleimide and N-substituted maleimides undergo photoaddition to benzene and alkylbenzenes to form 2:1 adducts (1).[1-3] Intermediate in the reaction is homoannular diene (formed by initial 2 + 2 cycloaddition) which subsequently undergoes 2 + 4 (Diels-Alder) cycloaddition to give diimide (Reaction 1). Maleic anhydride reacts similarly[4,5] to give a dianhydride (2) having the analogous pentacyclic structure; however, it has

Reaction 1

(R=H, alkyl)   (R'=H, alkyl, aryl)
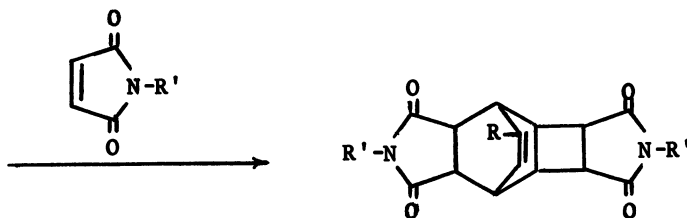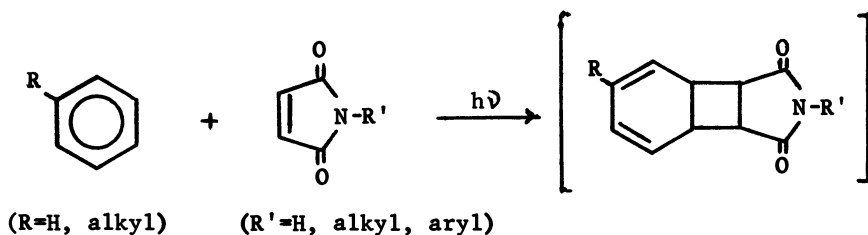
1

been shown[6,7] quite conclusively that the mechanism in this case involves an excited charge-transfer intermediate rather than homoannular diene.

2 (R=H, alkyl)
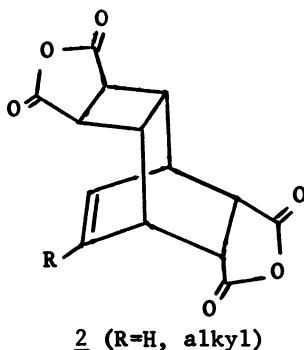
In the case of photoaddition to alkylbenzenes, the substituent R group has been shown, on the basis of ultraviolet[8] and NMR[9] spectroscopy, to be located principally on the double bond of the adduct (as shown), but the actual direction of cycloaddition has also been shown to vary with temperature.[10] Thus it is quite probable that isomer mixtures result in the photopolymerization reactions described below. It has also been reported that N-phenylmaleimide and meta- and para-substituted N-phenylmaleimides give very poor yields of photoadduct.[6] This has been attributed to the existence of low-lying, excited states that quench the photoexcited maleimide when the benzene and maleimide rings are coplanar. With N-alkylmaleimides and N-phenylmaleimides having ortho substituents (which prevent coplanarity), photoaddition proceeds readily.[1] More recent work[11] has shown that N-phenylmaleimides substituted in the para position with strongly electron-attracting groups (NO_2, CO_2CH_3, $SO_2C_6H_5$) also form photoadducts with benzene in good yield.

A logical extension of maleimide photoaddition is the light-catalyzed cyclopolymerization reaction of bismaleimides with benzene or alkylbenzenes to form polyimides. This reaction, and the application of bismaleimide photoaddition to polystyrene crosslinking, are discussed in the following sections.

Polyimide Formation

Under the influence of light, benzene and alkylbenzenes copolymerize with bismaleimides by successive 2 + 2 and 2 + 4 cycloaddition reactions[12-14] (Reaction 2). Although only the head-to-tail repeating unit is shown in Reaction 2, it should be recognized that head-to-head and tail-to-tail units can

also form depending upon the sequence of cycloaddition reactions during propagation. Following is a review of polyimide syntheses performed in our laboratories.[12,13] Similar results have been reported by Zhubanov and Akkulova.[14]

<div align="center">Reaction 2</div>

(R=H, alkyl)   (R'=alkyl,aryl)

3

+ head-to-head
and tail-to-tail
structures
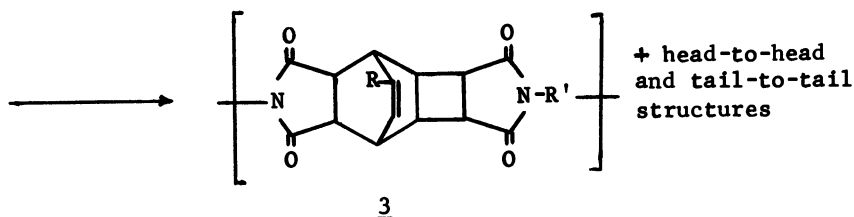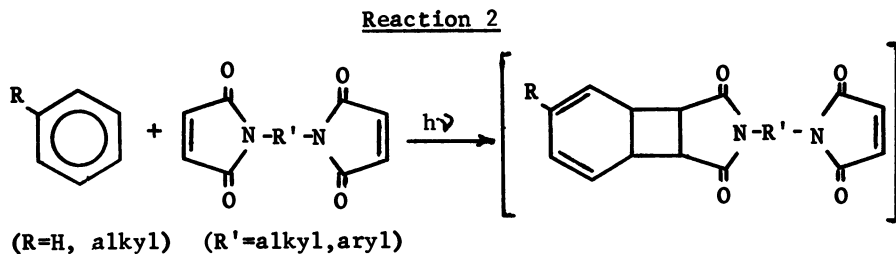
    The photopolymerization reactions may be carried out in ordinary borosilicate glassware, using acetone to effect solubility of the bismaleimides and acetophenone as photo-sensitizer. A water-cooled Hanovia 450-W ultraviolet lamp was used in this work, although ordinary sunlight is also effective. Polymers precipitated as pale yellow or white powders or were deposited as brittle films on the walls of the irradiation tubes. They were insoluble in the usual solvents, including N,N-di-methylformamide, N,N-dimethylacetamide, trifluoroacetic acid, and hexamethylphosphoramide, probably because of crosslinking during polymerization. This could occur via copolymerization of maleimide groups with the double bond arising from cyclo-addition.
    Polymer structure was established from the following observations:
    1. Infrared spectra closely resembled those of the corre-sponding polyimides prepared from dianhydride, 2, and the corre-sponding diamines, although absorptions arising from unreacted amine and anhydride were present in the latter. (A comparison is shown in Figure 1, along with the spectrum of a model compound.)
    2. Elemental analyses of representative polymers were con-sistent with structure.
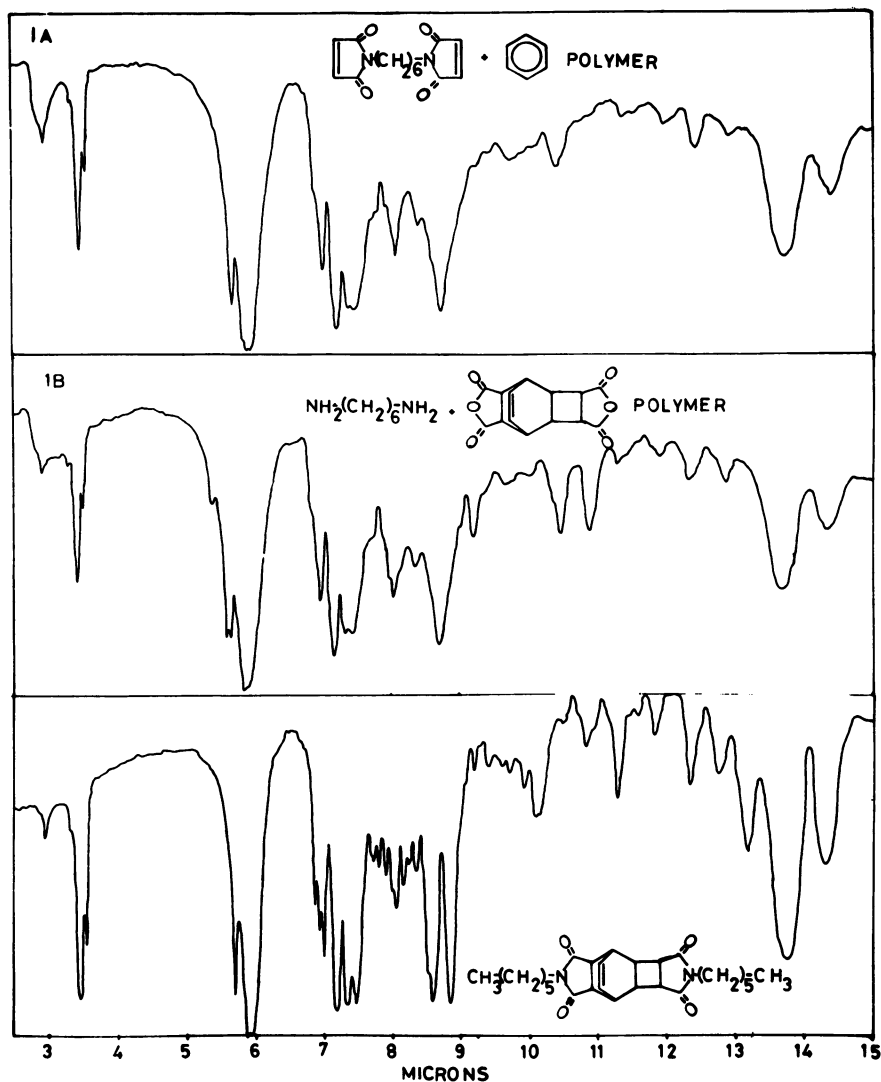
Figure 1. Infrared spectra (KBr) of (A) polyimide prepared by photolysis of benzene solutions of N,N'-hexamethylenebismaleimide; (B) polyimide prepared from benzene-maleic anhydride photoadduct (2) and 1,6-hexanediamine; and (C) the N,N'-bis(n-hexyl) derivative of diimide 1
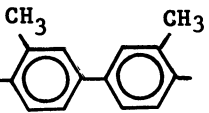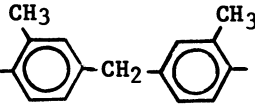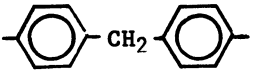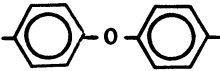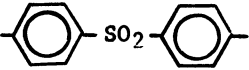
    3. Ultraviolet spectra of acetonitrile extracts of polymers
exhibited maxima consistent with both maleimide and homoannular
diene end groups.
    4. The NMR spectrum of dilute trifluoroacetic acid extracts
of one polymer was consistent with structure. (Solubility was
too low for the others.)
    5. Polymers underwent thermal decyclization at 420 to 485°C
regardless of bismaleimide structure; and DTA thermograms of
polyimides prepared photochemically closely resembled those
of the model polyimides.

TABLE 1

Polyimides Prepared with Bismaleimides and Benzene[12]

R' of Bismaleimide	Approx. Yield, %[a]	Initial dec. Temp.°C[b]
$-(CH_2)_2-$	95	420
$-(CH_2)_3-$	80	420
$-(CH_2)_6-$	70	410
dimethyl-substituted biphenyl (CH_3 groups on two phenyl rings)	65	485
two tolyl rings (CH_3) joined by CH_2	80	440
two phenyl rings joined by CH_2	15	420
two phenyl rings joined by O	30	420
two phenyl rings joined by SO_2	85	450

[a]After irradiation for 18 hr.

[b]Approximate temperature observed in melting point capillaries.

   Table 1 shows approximate yields and initial decomposition
temperatures of polyimides prepared from a variety of aliphatic
and aromatic bismaleimides. DTA thermograms, which confirmed
the initial decomposition temperatures, also exhibited strong
endothermic transitions in the range 480-510°C corresponding
to more extensive decomposition. Polymer yields from aliphatic
bismaleimides decreased with chain length, possibly because of
competing intramolecular cyclization.[15] Aromatic bismaleimides
having <u>ortho</u> methyl groups gave higher yields than the
unsubstituted ones with the exception of 4,4'-bismaleimido-
diphenylsulfone which contains a strongly electron-attracting
group.[11]

   Percentage yields and decomposition temperatures for a
series of polyimides prepared from three bismaleimides and
four alkylbenzenes are given in Table 2, together with the same
data for the corresponding polyimides prepared from benzene.
Best yields from alkylbenzenes were obtained from toluene
and t-butylbenzene with all three bismaleimides. This probably
reflects a balance between inductive effects, which would favor
both 2 + 2 and 2 + 4 cycloadditions in the order <u>t</u>-butyl >
i-propyl > ethyl > methyl, and steric effects which would hinder
the reaction in the same order. Additional steric effects a-
rising from the <u>ortho</u> methyl groups of N,N'-4,4'-(3,3'-
dimethylbiphenyl)bismaleimide are evident since no polymer
was formed from this monomer with ethylbenzene or i-propylbenzene
(Zhubanov and Akkulova reported[14] their best yields were obtained
with 1,10-decamethylenebismaleimide and i-propylbenzene.)

   Other workers[16] have reported the homopolymerization of
certain substituted bismaleimides in solution by successive
2 + 2 cycloaddition reactions, and they have appropriately de-
fined this type of process as a true photopolymerization; i.e.
a polymerization in which every chain-propagating step involves
a photochemical reaction. Another such example is the solid-
phase 2 + 2 cyclopolymerization of divinyl monomers.[17] By
contrast, the polymers described above result from a combina-
tion of photocycloadditions and Diels-Alder cycloadditions.
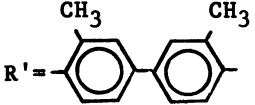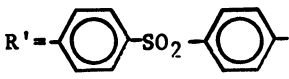
Polystyrene Crosslinking

   The extension of bismaleimide photoaddition to polystyrene
crosslinking represents a practical application of photopoly-
merization with potential in the area of light curable coatings.
Initial crosslinking experiments have been concerned with the
effect of both aliphatic and aromatic bismaleimides on gelation
times of polystyrene solutions. A commercial atactic poly-
styrene with number average molecular weight of 270,000 was used
for this work.

   Both dimethylene- and hexamethylenebismaleimide were
found effective in gelling methylene chloride solutions of
polystyrene in sunlight at bismaleimide concentrations as low as

TABLE 2

Polyimides Prepared with Bismaleimides and Alkylbenzenes[13]
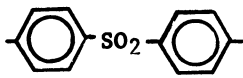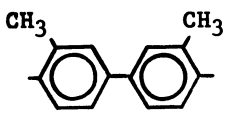
	Benzene	Toluene	Ethyl-benzene	i-Propyl-benzene	t-Butyl-benzene

$R' = -(CH_2)_6 -$

	Benzene	Toluene	Ethyl-benzene	i-Propyl-benzene	t-Butyl-benzene
Irradiation time, hr.	18	24	24	24	24
Approx. yield, %	70	40	23	28	34
Dec. temp. °C[a]	410	380	390	390	425

$R' =$ (4,4'-biphenyl with two CH_3 substituents)

	Benzene	Toluene	Ethyl-benzene	i-Propyl-benzene	t-Butyl-benzene
Irradiation time, hr.	18	40	40	40	40
Approx. yield, %	65	45	0	0	44
Dec. temp. °C[a]	485	390	-	-	370

$R' =$ (diphenyl-SO_2-)

	Benzene	Toluene	Ethyl-benzene	i-Propyl-benzene	t-Butyl-benzene
Irradiation time, hr.	18	5	5	5	5
Approx. yield, %	85	89	50	60	85
Dec. temp. °C[a]	450	400	360	420	400

[a]Approximate temperature observed in melting point capillaries.

1 mole percent based on phenyl equivalents in the polymer. Results are shown in Table 3. Surprisingly, gelation time did not decrease with increasing bismaleimide concentration. In the case of hexamethylenebismaleimide, several test runs confirmed the shortest gelation time for the unsensitized solution containing 1.0 mole percent bismaleimide. Somewhat different results were obtained using an artificial ultraviolet source (G.E. 375 watt sunlamp), as shown in Table 4. The data in this table are for a distance of 60 cm between lamp and sample. Much faster gelation times were observed at shorter distances (2 hr. for 5% bismaleimide at 15 cm.).

Aromatic bismaleimides were much less effective (Table 3), partly because of low solubility in the polystyrene solutions and partly because the rates of photoaddition were much lower than those of the aliphatic bismaleimides. Not unexpectedly (in view of the results shown in Table 2), the bismaleimide prepared from o,o'-dimethylbenzidine (o-tolidine) was least effective. Only in the case of 4,4'-bismaleimidodiphenylsulfone did photosensitizer (benzophenone) noticeably shorten gelation

TABLE 3

Polystyrene Crosslinking[a]

R' of Bismaleimide	Bismaleimide Conc. Mole %[b]	Sensitizer Wt. %[c]	Gelation	Time Hr.
$-(CH_2)_6-$	20	0	Yes	16
	10	0	Yes	$9\frac{1}{2}$
	5.0	0	Yes	$6\frac{1}{2}$
	5.0	0.5	Yes	$6\frac{1}{2}$
	2.5	0	Yes	$4\frac{1}{2}$
	1.0	0	Yes	3
	1.0	0.5	No	40
	0.5	0	No	40
	0.1	0	No	40
$-(CH_2)_2-$	10	0	Yes	7
	5.0	0	Yes	7
	2.5	0	Yes	5
	2.5	0.5	Yes	$5\frac{1}{2}$
	1.0	0	Yes	$5\frac{1}{2}$
	1.0	0.5	Yes	11
	0.5	0	Yes	$16\frac{1}{2}$
	0.1	0	No	40
phenyl–SO_2–phenyl	1.0	0	No	40
	1.0	0.5	Yes	30
	1.0	1.0	Yes	27
CH_3-substituted biphenyl	1.0	0	No	40
	1.0	0.5	No	40
	1.0	1.0	No	40
	0.5	0	No	40
	0.1	0	No	40

[a] Methylene chloride solutions of polystyrene ($\overline{M}_n \approx 270,000$), 10% w/v, irradiated in Gardner viscosity tubes in sunlight.

[b] Based on phenyl equivalents.

[c] Benzophenone, based on polystyrene.

TABLE 4

Polystyrene Crosslinking with Hexamethylenebismaleimide Using a UV Lamp[a]

Bismaleimide Conc.[b]	Gelation	CH_2Cl_2 soln. Time, hr.	$ClCH_2CH_2Cl$ soln. Time, hr.
0	No	40	40
0.5	No	40	40
1.0	No	40	40
2.0	Yes	11	16
3.0	Yes	11½	12
4.0	Yes	12	12
5.0	Yes	13½	13½

[a]G.E. 375 watt sunlamp, 60 cm from samples. Sample temp. 28°C. No photosensitizer added. Polystyrene conc. 10% w/v in CH_2Cl_2 or $ClCH_2CH_2Cl$.

[b]Mole percent based on phenyl equivalents.

time. Change in viscosity of the solutions (as measured in Gardner tubes by comparison with standards) was relatively insignificant until close to the gelation point.

Polystyrene alone or with photosensitizer was unaffected under photolysis conditions, apart from some yellowing, and polystyrene-bismaleimide solutions appear to be stable indefinitely in the dark. Bismaleimides have been used previously in peroxide-induced crosslinking of polymers;[18] however, polystyrene was reported to be unreactive under these conditions. Thus, the crosslinking reactions described here are not free radical in nature and are best formulated according to Reaction 3. Bismaleimides have also been reported to accelerate the radiolysis-induced crosslinking of elastomers.[19]

Clear polystyrene films containing up to 2 mole percent hexamethylenebismaleimide (based on phenyl equivalents) were cast from 1,2-dichloroethane. Higher concentrations gave cloudy films. Irradiation of the films with the G.E. 375 watt sunlamp resulted in rapid changes in the carbonyl absorption, as shown in Figure 2. The major peak at 1710 cm^{-1} broadens and a new absorption at 1770 cm^{-1} characteristic of maleimide photoadducts[11] appears. Other significant changes include the disappearance of bismaleimide peaks at 1405 and 830 cm^{-1} (the former is probably the cis olefinic C-H in-plane bending of the maleimide group) and the appearance of a new peak at 1390 cm^{-1}. Irradiated films do not redissolve in solvent. Spectra of polystyrene films containing no bismaleimide are not significantly affected by irradiation, and the films retain their solubility.

Reaction 3
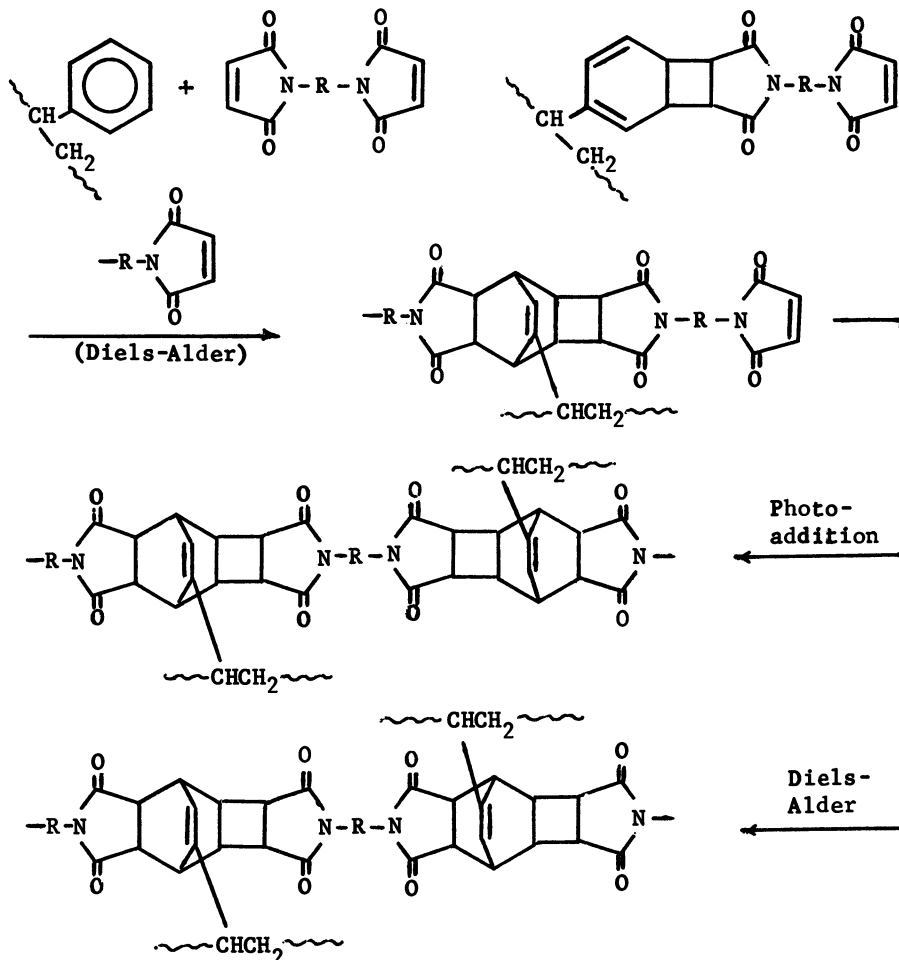
Studies in this area are now being directed toward synthesis of polystyrene containing pendant maleimide groups. Other workers have reported the photochemical modification of polystyrene with maleic anhydride[20-22] and maleimide.[22]

Acknowledgment
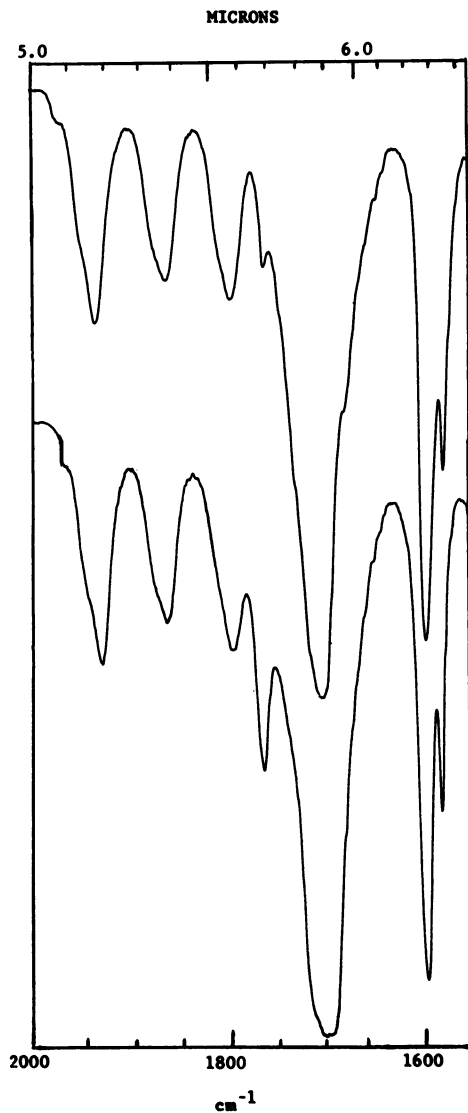
Figure 2. Infrared spectra of polystyrene film containing 2% hexamethylenebismaleimide. Upper curve, preirradiated; lower curve, after irradiation for 5 hr with a G.E. 375W sunlamp.

Literature Cited

1.   Bryce-Smith, D., Hems, M. A., Tetrahedron Lett. (1966) 1895.
2.   Bradshaw, J. S., ibid. (1966) 2039.
3.   Bradshaw, J. S., (to Chevron Research Co.), U. S. Pat. 3,366,642 (1968); Chem. Abstr. (1968) 69, 26863 h.

4. Angus, H. J. F., Bryce-Smith, D., Proc. Chem. Soc. (1959) 326; J. Chem. Soc. (1960) 4791.
5. Grovenstein, E., Jr., Rao, D. V., Taylor, J. W., J. Amer. Chem. Soc. (1961) 83, 1705.
6. Bryce-Smith, D., Pure Appl. Chem. (1968) 16, 47.
7. Bryce-Smith, D., Deshpande, R., Gilbert, A., Grzenka, J., Chem. Commun. (1970) 561.
8. Bryce-Smith, D., Gilbert, A., J. Chem. Soc. (1965) 918.
9. Bradshaw, J. S., J. Org. Chem. (1966) 31, 3974.
10. Bryce-Smith, D., Gilbert, A., Chem. Commun. (1968) 19.
11. Kardush, N., Stevens, M. P., J. Chem. Eng. Data. (1973) 18, 440.
12. Musa, Y., Stevens, M. P., J. Polym. Sci. A-1, (1972) 10, 319.
13. Kardush, N., Stevens, M. P., ibid. (1972) 10, 1093.
14. Zhubanov, B. A., Akkulova, Z. G., Vysokomol. Soedin. Ser. B. (1973) 15, 473; Chem. Abstr. (1973) 79, 105611j.
15. DeSchryver, F. C., Bhardwaj, I., Put, J., Angew. Chem. Int. Ed. (1969) 8, 213
16. DeSchryver, F. C., Boens, N., Smets, G., J. Polym. Sci. A-1 (1972) 10, 1687.
17. Wegner, G., in "Polymerization Reactions and New Polymers," (Platzer, N. J., ed.), American Chemical Society, Advances in Chemistry Series No. 129, Washington, D. C., 1973.
18. Kovacic, P., Hein, R. W., J. Amer. Chem. Soc., (1959) 81, 1187, 1190.
19. Miller, S. M., Roberts,R.,Vale, R. L., J. Polym. Sci. (1962) 58, 737.
20. Waack, R., (to Dow Chemical Co.), U. S. Pat. 3,214,416 (1965); Chem. Abstr., (1965) 63, 18291g.
21. Hrdlovič, P., Lukač, I., J. Polym. Sci., Symposium No. 47, (1974) 319.
22. Schulz, R. C., Pure Appl. Chem., (1973) 34, 305.

7

Photocrosslinking of Polyethylene Using Polyethylene–acryloxybenzophenone—A Physical Study

R. M. IKEDA, F. F. ROGERS, S. TOCKER, and B. R. GELIN

E. I. du Pont de Nemours & Co., Inc., Experimental Station, Wilmington, Del. 19898

Abstract

The photocrosslinking of polyethylene//poly
(ethylene/acryloxybenzophenone) blends was investi-
gated. Rather modest (50% - 70%) maximum gel frac-
tions and crosslink densities were found and a two-
phase model proposed to account for these observa-
tions and the "low" phenone UV extinction coefficients
measured in the blends. The particle size of the dis-
persed crosslinking phase should have a significant
bearing on the degree of crosslinking and blend param-
eters related to the dispersion were found to corre-
late with the maximum gel fractions. The two-phase
model was also extended to relate the observed UV
phenone extinction coefficient to the polymer/polymer
dispersion, and agreement was found.

Introduction

The use of monomeric benzophenones as photoactive
crosslinking agents in polyethylenes has been known
for some time (1). To minimize exudation in blends,
a polymeric form of these sensitizers was prepared by
the copolymerization of ethylene with minor amounts of
acrylic esters containing benzophenone (2). Subse-
quent evaluation of these polymeric photosensitizers
in crosslinking polyethylene blends showed their gross
behavior to follow the monomeric experience. Light
absorbed by the phenone led to the expected cross-
linking and, if one accounted for the non-migrating

character of the reactants and products, the kinetics
of the photolysis reaction were predictable. Evalua-
tion also uncovered two seemingly unrelated anomalies.
First, the benzophenone UV extinction coefficients
determined from the samples were much lower and more
variable than expected from monomeric model compounds.
Second, gels produced from the photolyzed blends were
fragile, the maximum gel fractions were low and "ex-
cessive" scatter was found in the correlation of the
maximum gel fraction with the sensitizer concentra-
tion. A two-phase model of the blends is proposed to
account for these observations.

Experimental

    Sensitizer Preparation. Detailed recipes for the
preparation of the 4-acryloxybenzophenone (ABP) and
poly(ethylene/acryloxybenzophenone) (E/ABP) have been
reported (2). Specific E/ABP polymers used in this
study are listed in Table I showing their range of
melt indices and ABP concentrations.

TABLE I
COPOLYMER SENSITIZERS

No.	WT % (ACRYLOXYBENZOPHENONE)	MELT INDEX
1	7.0	7.2
2	7.1	22
4	5.4	38
5	2.4	906
6	6.1	51
7	3.1	845
8	10.9	14.4
9	4.5	8
10	1.2	-*

* VISCOSITY AVG MOLECULAR WEIGHT = 70,000

    Blend Preparations. Blends were made from the
E/ABP sensitizers and several polyethylenes (E). We
used a branched polyethylene, Alathon® 15 polyethylene
resin, a medium density polyethylene designated Super
C, and two high-density polyethylenes, Alathon® 7030
and 7040. The E to E/ABP volume ratios ranged from
4/1 to 22/1 and the overall ABP concentrations from

0.1 to 1.2 weight per cent.

To prepare the E//E/ABP blends (the double slash indicates a physical blend), polyethylene pellets were mixed with dry ice and powdered in a Wylie mill. After drying, the powder was mixed with the E/ABP fluff and the mixture extruded into film (1-5 mils thick) using a 3/4" Killion extruder at 200° to 225°C.

<u>Sensitizer Concentrations</u>. The ABP concentrations were measured using the infrared 1670 cm^{-1} band (benzophenone carbonyl). Both a Beckman Infracord and a Beckman IR12 were employed. The extinction coefficient (base 10) was determined from model compound mixture studies and found to be 0.0341 (mil-wt % ABP)$^{-1}$. Film thicknesses were adjusted to obtain absorbances in the 0.3 to 0.7 range for measurement precision.

<u>UV Measurements</u>. For the UV extinction coefficient measurements, absorption spectra were made with a Bausch and Lomb 505 or a Cary Model 14 spectrophotometer.

<u>UV Exposures</u>. The film samples were crosslinked by exposure to a GE UA-3 medium pressure mercury vapor lamp. Forced draft cooling maintained a constant lamp temperature and the samples were kept at 25°C by a water-cooled backing plate. Light-to-sample geometry was kept constant.

<u>Gel Fractions</u>. Weighed samples were placed in 300 mesh stainless steel baskets and extracted 16 hours in a vapor-jacketed Soxhlet extractor with p-xylene. The insoluble fraction was dried in a vacuum oven with a nitrogen bleed at 80°C overnight and the gel content determined from the initial and final weights.

For gel swelling, the gels were removed from the Soxhlet extractors and placed in p-xylene at the desired temperature (in most cases refluxing p-xylene). After reaching equilibrium, they were blotted, weighed, dried as described above, and reweighed. The swelling ratios were calculated from the weights and the material densities.

Results

Absorption Characteristics of the Blends. The UV spectrum of an E//E/ABP film shows three absorptions between 200 and 500 nm - Figure 1 - a weak peak in the 330 - 350 nm region, a strong absorption maximum near 255 nm and a very strong absorption at or below 210 nm.
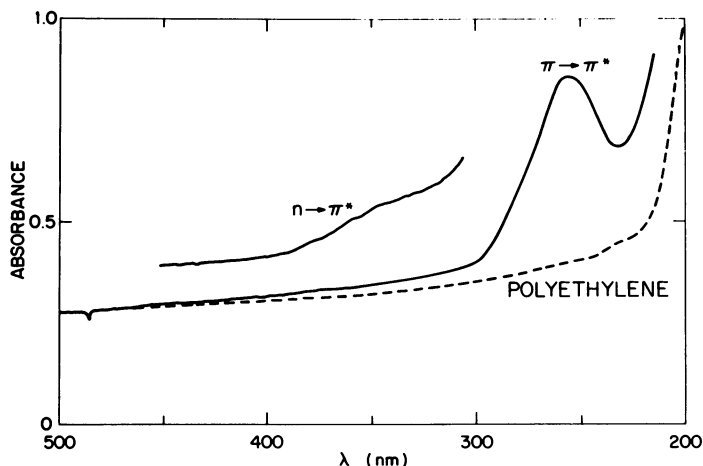
Figure 1. Typical uv spectrum of E//E/ABP system

From comparisons with model compound spectra, we attribute the 330-350 nm absorption to the n→π* transition of the benzophenone moiety and the 255 nm absorption to the π→π* transition of the same group. The absorption below 210 nm is attributed to the sensitizer aromatic absorption and/or the absorption by additives and structural imperfections present in the host polymer.

For our studies, the π→π 255 nm absorption is of primary importance. The extinction coefficient of the n→π band is too small to be very active and the strong absorption below 210 nm does not overlap a significant portion of our lamp's emission.

Baseline Determinations and Relative Extinction Coefficients. For the 255 nm absorption baseline determination, we define polyethylene as transparent

at 450 nm and subtract the absorption at that wave-
length from all other values. Next, we obtained a
measure of the surface and/or interior scattering of
the films and possible base polymer absorption. The
spectra of several Alathon® 15 polyethylene films of
different thicknesses were measured and, for wave-
lengths greater than 220 nm, the $A(\lambda)-A(450$ nm) values
were identical for all samples. This indicated that
the polyethylene "absorption spectrum" was primarily
due to surface scattering and could be used as the
baseline for the 255 nm absorption maximum.

We examined the spectra of 5 blend samples to
investigate the possibility of peak overlap effects.
After subtracting baselines, the π→π* absorptions
ranged from 0.3 to 1.0; and in each case, the ab-
sorptions were determined at a series of wavelengths
between 220 and 380 nm. Relative extinction coeffi-
cients were obtained for each sample at the various
wavelengths by dividing the individual absorptions by
the maximum absorption (257.5 nm). These values were
then averaged and plotted versus the reciprocal wave-
length. The resulting symmetrical peak is shown in
Figure 2.
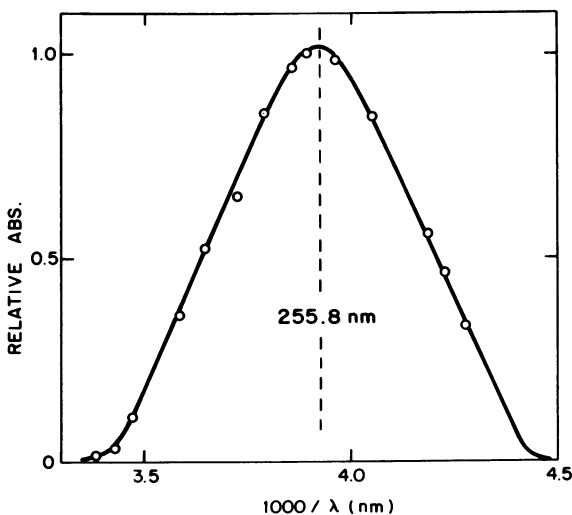
Figure 2.   Sensitizer π → π* absorption

We conclude that our baseline determination permits a reasonable determination of the sensitizer π→π absorption characteristics.

With linear polyethylenes, the scattering correction was thickness dependent. While extensive computations were not carried out with these samples, the thickness-adjusted scattering corrections appeared to be as satisfactory in the baseline determination as was found for Alathon® 15.

Extinction Coefficients.

$\underline{255 \text{ nm absorption}}$. Table II summarizes our measurements of the apparent extinction coefficient for this band. There is considerable scatter in the data but error analysis of the individual experiments showed that most of the variations could not be attributed to random measurement errors. The extinction coefficient (base e) for the model compound, p-benzoyl phenyl isobutyrate was measured as 5.47×10^4 1-mole^{-1}-cm^{-1} - a significantly greater value than most of the numbers in Table II.

TABLE II
255 nm EXTINCTION COEFFICIENTS

	BASE	Co(Wt %) (IR)	(255 nm) A_corr	t(mils)	$\frac{<A_{corr}>}{t}$	ε(e)(1/mole-cm)×10⁻⁴
371-31-1A	A15	0.493	1.220	1.55		4.06
371-31-2A	A15	0.493	1.143	1.84		3.20
371-31-5A	A15	0.336	0.700	1.33		3.96
-5B	A15	0.336	1.745	3.20		4.11
371-31-6A	A15	0.420	0.734	1.12		3.96
371-31-8A	A7040	0.343	0.439	0.92		3.53
-8B	A7040	0.343	1.97	3.55		4.11
371-31-9A	SUPER C	0.269	0.417	1.23		3.20
-9B	SUPER C	0.269	1.143	3.03		3.48
371-31-10A	A15	0.495	0.900	1.37		3.35
371-31-11A	A15	0.214	0.516	1.55		3.96
371-31-12A	A15	0.502	1.549	1.75		4.47
371-148-2A	A15	0.102	<0.172>	<0.98>		4.36
-2B	A15	0.106	<0.539>	<2.88>		4.47
371-148-3A	A15	0.119	-	-	0.269	5.74
-3B	A15	0.142	-	-	0.268	4.77
371-148-4A	A15	0.172	-	-	0.372	5.47
-4B	A15	0.176	-	-	0.315	4.54
371-148-5A	A15	0.188	-	-	0.304	4.11
-5B	A15	0.220	-	-	0.403	4.64
297-21-A	A15	0.56				2.89
373-105-5	A15					2.89
367-69	A7030	0.5				2.79

$\underline{340 \text{ nm absorption}}$. The data available for this absorption are summarized in Table III. The corrected absorptions are small and the variations of the computed extinction coefficients in Table III can be attributed to random errors.

TABLE III
340 nm EXTINCTION COEFFICIENTS

SAMPLE	$\epsilon(e)(1/mole-cm) \times 10^{-2}$
371-31-1A	7.7
-2A-1	5.1
-2A-2	4.8
-2B	5.8
-2C	5.6
AVG	(5.8 ± 1.3)

Gel Measurements. An example of the gel
fraction data is given in Figure 3 with gel fraction,
G, plotted against the fraction of sensitizer reacted,
x. The solid line is given by:

$$G = \frac{(x - x_c)}{\frac{(1 - G_{max})}{G_{max}}(1 - x_c) + (x - x_c)}$$

The terms are defined in the figure. We can only
specify Xc in the 0.1 to 0.2 wt % ABP range. G_{max}
is modest (50% - 70% range) with the blends and
there is a definite correlation with the total ABP
concentration although the scatter in the correlation
is excessive relative to the experimental precision,
Figure 4.
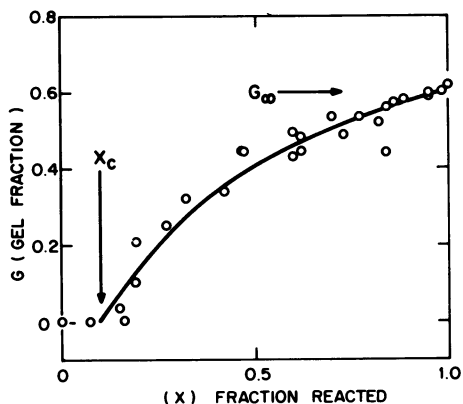
Figure 3. Gel fraction and the fraction reacted
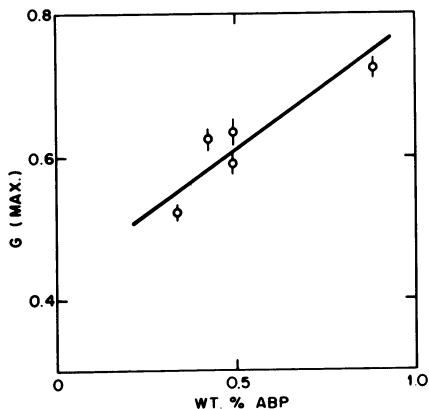
Figure 4. Maximum gel fraction and the init. sensitizer concentration

Using well-known relationships for swollen gels (3), we computed "apparent crosslink densities" from the gel swell ratios and the solvent-polymer interaction parameter determined from the temperature dependence of those ratios (4). With lower ABP concentrations, the gels produced from the blends were fragile, leading to appreciable experimental uncertainties. With the higher ABP concentrations, more meaningful information was obtained.

In comparison experiments, we used two samples, each with 1.2 wt % ABP - one an E/ABP copolymer and the other an E//E/ABP blend. Due to the sample thickness (2 mils) and the high ABP concentration, nearly 100% of the incident radiation was absorbed by the samples in the initial part of the reaction. The samples were irradiated for various periods and the gel fractions and crosslink densities determined. These data are tabulated in Table IV and plotted in Figure 5.

TABLE IV
COPOLYMERS & BLENDS
GEL FRACTIONS & CROSSLINK DENSITIES

EXPOSURE (MIN)	COPOLYMER		BLEND	
	G^1	Q^2	G^1	Q^2
1	40	1.62	21	0.70
2	49	3.58	31	1.13
5	60	9.26	35	1.61
0	85	21	65	6

^{1}WT. %
^{2}CROSSLINKS/5000 C-ATOMS
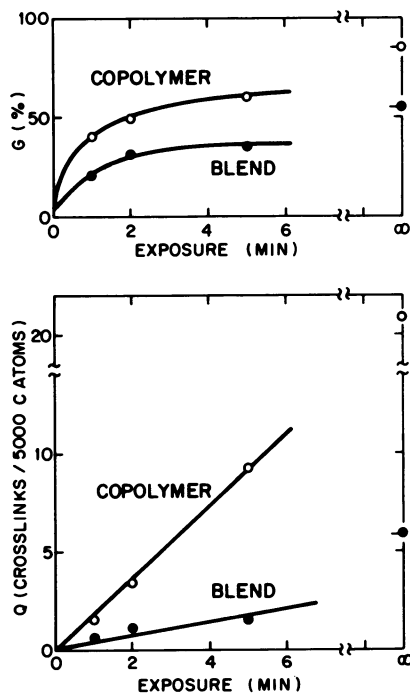
Figure 5. *Gel fractions and crosslink densities for copolymers and blends*

Two factors were worthy of note. First, as we expected from the total absorption of the incident radiation, initially there is a linear increase in the "apparent crosslink density" with time. Secondly, the "apparent crosslink density" efficiency of the sensitizer moiety is greater with the copolymer sample and much more of the total polymer (i.e., 90%) can be involved in the crosslinked portion.

Discussion

The gel swelling results can be explained by assuming that the E//E/ABP blends are two-phase materials with domains of E/ABP dispersed in a polyethylene matrix. In this picture, a significant fraction of the matrix would have no contact with the crosslinking copolymer and would remain soluble after photolysis, leading to low maximum gel fractions. The gel from such blends should have a "tight" core (10% - 20% of the gel) surrounded by a more open

structure which would have few crosslinks. The over-
all appearance would be that of a fragile, lightly
crosslinked gel.

The G_{max} correlation can be sharpened by the two-
phase argument. With the crosslinking agents con-
fined to their own phase, the quantity of gel should
be determined by the total surface area of that phase
and, hence, the dispersion of the E/ABP in the poly-
ethylene matrix. If we assume that better blending is
achieved by matching the component melt viscosities,
then G_{max} should be dependent on the sensitizer melt
index (MI), the relative volumes of the components -
blend ratio, BR - and the total sensitizer concentra-
tion (Co). From least squares analyses of our re-
sults, we find:

$$G_{max} = 0.174 + 0.0296 \log MI + 0.475 \, Co + 0.0149 \, BR$$

The fit of this expression to the experimental data is
excellent as indicated by the last two columns in
Table V and underscores the usefulness of the two-
phase proposal.

<div align="center">

TABLE V

MAXIMUM GEL FRACTION CORRELATIONS

</div>

No.	log MI	Co (WT %)	BLEND RATIO	GEL (MAX) EXP	GEL (MAX) CALC
371-31-1	0.857	0.493	13	0.638	0.628
-31-2	-0.143	0.493	13	0.593	0.598
-31-3	2.060	0.883	4.63	0.724	0.724
-31-5	2.958	0.336	6	0.512	0.511
-31-6	1.710	0.420	13.65	0.626	0.628

The two-phase model can also explain the low
values of our measured 255 nm extinction coefficients
and their variability. Consider a clear polyethylene
matrix with strongly absorbing dispersed domains of
E/ABP. If the dispersion is gross (i.e., large
particles), then some photons will pass through the
film and see no ABP. Other photons will pass through
one domain and be mostly absorbed while still others
will pass through more than one domain. For the
latter, passage through the second, or third, domain

will remove very little of the incident radiation
since most of the beam was absorbed passing through
the first domain. Because of this strong absorption
by the domains, when the total absorption is averaged
over the entire film surface, the effect will be a
low apparent absorption.

This notion can be quantified in a model. Assume
that the E/ABP phases are cubes with sides, d/Z.
Here, d is the film thickness and Z is some large
integer. Divide the film volume into a matrix of
such cubes and randomly disperse the sensitizer in
this matrix. The light transmitted by such a sample
is:

$$I = \sum_{n=0}^{Z} P(n)\, I(n)$$

where P(n) is the probability of finding a column of
Z cubes containing n E/ABP cubes and I(n) is the
light transmitted by such a column and is given by
the expression:

$$I(n) = I_0(\exp)\left(\frac{-A_t n}{Z}\right)$$

Here I_0 is the incident radiation and A_t is the true
absorbance (base e) for a molecularly dispersed system.
The probability, P(n) is the same as that for flipping
a coin Z times and coming up with n heads. Thus:

$$P(n) = \frac{Z!}{n!(Z-n)!}\, V^n (1-V)^{Z-n}$$

where V is the volume fraction of E/ABP. Sub-
stituting and rearranging the terms, we obtain:

$$e^{-A_a} = (1-V)^Z + \sum_{n=1}^{Z} \left\{ (1-V)^{Z-n} \prod_{i=1}^{n}\left[\frac{(Z+1-i)}{i} V\right] \right\} e^{\frac{-A_t n}{Z}}$$

This expression is useful since it contains measurable true and apparent absorbances (A_t and A_a); measurable volume fractions, V; and only one unknown, the size parameter, Z. Some typical computational results are shown in Figure 6 where A_a/A_t values are plotted versus the size parameter, Z. Note that A_a approaches A_t for very large Z's, i.e., molecular dispersion.
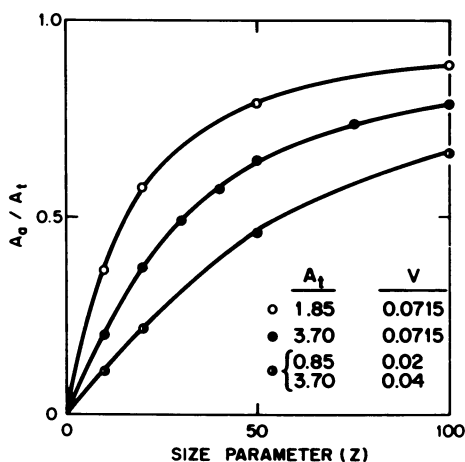
Figure 6. Apparent absorption and the size parameter

For A_t, we can use the extinction coefficient measured for the model compound, p-benzoyl phenyl isobutyrate (5.47×10^4 l-mole^{-1}-cm^{-1}) and then use the experimental A_a's to compute the E/ABP phase sizes, (d/Z). These are shown in Table VI.

TABLE VI

COMPUTED PARTICLE SIZES

SAMPLE	ϵ (1/mole-cm) × 10⁻⁴	BLEND RATIO	PHASE SIZE (μm)	$\left\lvert \log \dfrac{MI^*}{4} \right\rvert$
371-31-1A	4.06	13	0.49	0.255
-2A	3.20	13	0.91	0.745
-4A	3.70	10.7	0.80	0.976
-5A(B)	4.04	6	1.40	2.355
-6A	3.96	13.65	0.58	1.109
-8A(B)	3.53	9	1.26	2.325
-9A(B)	3.32	9	2.19	2.325
-10A	3.35	22	0.40	0.559
-11A	3.96	22	0.60	0.301
-12A	4.47	8.58	0.43	0.301

*MELT INDEX OF THE POLYETHYLENE = 4

The calculated phase sizes have reasonable dimensions. As a check on the calculations, we again assume that the blending will be better (i.e., particles smaller) if the polyethylene and the E/ABP have the same viscosity. We have chosen to use the melt index (MI) function:

$$\left\lvert \log \frac{MI_{E/ABP}}{MI_E} \right\rvert$$

as a measure of the similarity, or dissimilarity of the viscosities and have plotted this parameter versus the computed-phase sizes in Figure 7. There is a positive correlation which supports this hypothesis.
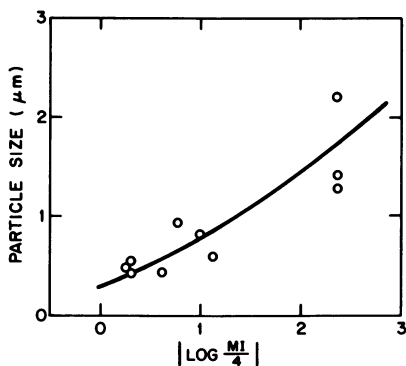
Figure 7.   Particle size and the melt index mismatch

Summary

The crosslinking behavior of blends of polyethylene and E/ABP photosensitizers can be explained on the basis of a two-phase mixture. The particle size of the disperse phase (E/ABP) has a significant bearing on the degree of crosslinking, approaching theoretical as particle size decreases. Improved dispersion can be attained by matching the melt viscosities of the components. The behavior of such similar materials underscores the difficulty in getting molecular compatibility with polymers.

Literature Cited

1. M. J. Roedel, U.S. Patent 2,484,529, 10/11/49

2. S. Tocker, U.S. Patents, 3,214,492 (1965), 3,265,772 (1966), and 3,315,013 (1967)

3. R. F. Boyer, J. Chem. Phys., 13 363 (1945)

4. M. L. Huggins, Annals, N.Y. Acad. Sci., 44 431 (1943)

8

Calorimetric Analysis of Photopolymerizations

J. E. MOORE, S. H. SCHROETER, A. R. SHULTZ, and L. D. STANG

General Electric Corporate Research and Development, Schenectady, N. Y. 12345

The present high level of industrial activity in the field of light initiated polymerizations has stimulated research in basic polymerization phenomena including polymerization kinetics.([1-4]) Unfortunately, previously used methods of determining monomer conversion such as dilatometry or measurements of unreacted monomers are not easily adapted to thin coating films. In addition, the presence of multifunctional monomers yielding networks at low conversion in photopolymerizable formulations also complicates analyses.

Differential scanning calorimetry (DSC) has been used to investigate addition and condensation polymerizations in bulk, solution, and emulsion systems.([4-8]) Both isothermal and temperature scanning modes have been employed. In the present preliminary work we demonstrate the utility of DSC in studying the kinetics of light initiated free radical polymerizations. Differential calorimetry was chosen because it was anticipated that direct, continuous monitoring of the reaction exotherm would give the most information on rapid acrylate polymerizations. Lauryl acrylate provided a monomer of low volatility upon which recent conventional kinetic studies ([9,10]) existed. 1,6-Hexanediol diacrylate, neopentyl glycol diacrylate and trimethylol propane triacrylate were chosen to determine the capability of the differential calorimetric approach as applied to network-forming photopolymerizations.

Experimental

Materials. Lauryl acrylate was freed of inhibitor by three separatory funnel extractions with 5% sodium carbonate solution, three deionized water washings, followed by three crystallizations from methanol. Residual methanol and water were removed by 24 hour sparging with nitrogen at room temperature. Both original (inhibited) and purified lauryl acrylate (LA) were polymerized. 1,6-Hexanediol diacrylate (HDDA), neopentyl glycol diacrylate

90

(NPGDA), trimethylol propane triacrylate (TMPTA), Trigonal 14 (Noury Chem. Corp.; mixture of benzoin butyl ethers), benzoyl peroxide, and t-butyl perbenzoate were used as obtained from commercial suppliers without further purification.

Apparatus. A Perkin-Elmer DSC-1B differential scanning calorimeter was modified by replacing the glass windows of the sample holder cover with quartz windows. Figure 1 displays schematically the modified DSC-1B sample holder (A), reference holder (B), sample holder cover (C), a readily moved super structure containing neutral density filters (D), shutter (E), circulating water heat filter (F), and a General Electric H3T7 medium pressure mercury lamp (G) mounted in a reflector enclosure. This apparatus was employed in the initial screening studies. The major portion of the data reported here were obtained with a modified Perkin-Elmer DSC-2 instrument. This is well-represented by Figure 1 except that the irradiation superstructure was mounted in a pressed-wood composition board platform containing a rectangular quartz window. The bottom of this platform rested on a rubber O-ring gasket seated directly on the surface of the refrigerated block (turret removed) containing the sample holders. A two pen, strip chart recorder (Hitachi model 56) was connected to the DSC-2.

Procedure. Solutions were prepared by weighing. All concentrations of initiators are stated as weight initiator per total weight of mixture. Since the solutions were prepared in air, all solutions should be assumed essentially equilibrated with air.

The DSC instruments were calibrated by the heat of fusion of indium (6.80 cal gm-1). Total incident light intensity (UV + visible) was determined in the DSC-2 apparatus by painting the sample holder with a thin layer of carbon (Aquadag), adding 10 mg of Uvinul N-539 to cover the carbon with a liquid layer, and illuminating the sample holder (rest of sample holder cavity shielded) with the reference holder and cavity shielded from the light. The differential heating rate was 3.52 mcal sec-1 over a 0.503 cm^2 area or 6.99 mcal cm^{-2} sec-1 for the H3T7 lamp on a type LD-S ballast at 400W. An empty aluminum cup with crimped-on lid was used as a secondary, working standard for subsequent intensity measurements. The total sample holder cavity was illuminated. A factor of 2.28 was required to convert observed mcal sec-1 to intensity in mcal cm^{-2} sec-1 using this secondary standard. Long pass filters show 71% of the light energy lies below 470 nm wavelength and 58% of the light energy lies below 380 nm wavelength. The principal UV light energy output of the H3T7 lies in the three regions around 254 nm, 313 nm, and 365 nm.

Thermally-activated peroxide initiated polymerizations were performed in the normal scanning temperature mode (+20° min-1, 40 mm min-1 chart speed) with the unmodified DSC-2 apparatus. The scan baseline was obtained by a second scan of the reacted material. Temperature range 30°-250°C. The curve area integrations

were achieved by Xeroxing the curves, cutting, and weighing.

A typical light-initiated polymerization involved weighing 7-9 mg of acrylate with initiator into the standard DSC aluminum cup. The cup was placed in the DSC sample holder and an empty aluminum cup was placed in the reference holder. The usual nitrogen flow within the cell enclosure was established with the UV lamp, filter, and shutter assembly positioned over the holders. The guillotine shutter was operated manually. A holder temperature of 52°C was used with the DSC-IB while isothermal temperatures from 0° to 80° were employed with the DSC-2. A recording chart speed of 4 cm min⁻¹ was used with the DSC-2 with most runs observed for 15 minutes. The two pens were set at different sensitivities so that one trace would remain on scale throughout the exotherm while the second trace amplified the later, low rate curve section. Curve area integrations and digital rate data were obtained by tracing the curves on a CALMA digitizer, storing the digital coordinate data on magnetic tape, and processing the data files on a GE 600 series digital computer.

Results and Discussion

The results of peroxide initiated and Trigonal 14 photoinitiated polymerizations of lauryl acrylate (LA), 1,6-hexanediol diacrylate (HDDA), neopentyl glycol diacrylate (NPGDA), and trimethylol propane triacrylate (TMPTA) will first be presented. These experiments were designed to observe total heats of polymerization under prescribed conditions. The results of more extensive rate studies on Trigonal 14 photoinitiated LA polymerizations will then follow.

Mono-, Di-, and Tri-Acrylate Polymerizations: Peroxide Initiation. Table I presents the observed heats of polymerization of LA, HDDA, NPGDA, and TMPTA containing 1% benzoyl peroxide +1% t-butyl perbenzoate upon +20°/min thermal scanning from 30° to 250°C. The combined peroxide initiator system assured a high probability of reaction of nearly all "accessible" double bonds in the network-forming monomers. The -19.2 kcal mol⁻¹ (-80.0 cal gm⁻¹) total heat of polymerization found for LA is close to the -18.8, -18.6, and -18.6 kcal mol⁻¹ reported for methyl, ethyl, and n-butyl acrylates,(11,12) respectively. The -17.6, -16.7, and -15.4 kcal per mole of C=C observed for HDDA, NPGDA, and TMPTA, respectively, are believed to show the progressively decreasing heats of polymerization due to unreacted carbon-carbon double bonds on the polymer networks.

Mono-, Di, and TriAcrylate Polymerizations: Trigonal 14 Photoinitiation. The heats of polymerization of the monomers achieved by photoinitiation (light intensity approximately 5.2 mcal cm⁻² sec⁻¹) using Trigonal 14 at approximately 1% concentration (Table I) were obtained from rate vs. time DSC-2 traces similar to the one shown in Figure 2 (cf. seq.). Due to the rapid
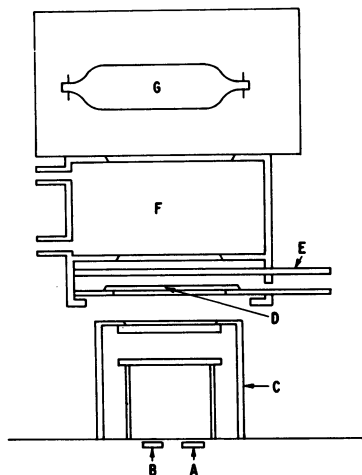
Figure 1. Schematic of modified DSC–IB apparatus: (A) sample holder, (B) reference holder, (C) sample holder cover with quartz windows, readily moved superstructure with (D) neutral density filters, (E) guillotine shutter, (F) circulating water heat filter, and (G) G. E. H3T7 medium pressure mercury lamp in a reflector enclosure

TABLE I

Heats of Polymerization of Acrylic Monomers

Thermally-activated Peroxide Initiation. Scan 30°–250°C.
Photo-activated Trigonal 14 Initiation.** 40° and 60°C.

Monomer	Initator	Initiator Conc. $10^2C(gm\ gm^{-1})$	Temp. °C	$-\Delta H_p$ cal gm^{-1}	kcal mol^{-1}C=C
LA	peroxides	1 + 1	scan	80.0	19.2
(C-13)	TR-14	0.989	30	73.	17.5
(C-5)	TR-14	1.01	40	71.	17.0
(C-19)	TR-14	1.13	40	74.	17.8
HDDA	peroxides	1 + 1	scan	155.4	17.6
	TR-14	1.312	40	99.	11.2
	TR-14	1.000	40	106.	12.0
	TR-14	1.312	40	106.	12.0
	TR-14	1.000	60	147.	16.6
NPGDA	peroxides	1 + 1	scan	157.5	16.7
	TR-14	1.236	40	76.	8.1
	TR-14	1.236	40	78.	8.3
	TR-14	1.236	60	91.	9.7
TMPTA	peroxides	1 + 1	scan	156.1	15.4
	TR-14	1.045	40	94.	9.3
	TR-14	1.045	40	94.	9.3
	TR-14	1.045	40	88.	8.7
	TR-14	1.045	60	103.5	10.2

**400W H3T7 lamp; no filter, approximately 5.2 mcal cm^{-2} sec^{-1}

initial polymerization rates of the multifunctional monomers, sample weight had to be restricted to 2-3 mg. The 40° photoactivated, Trigonal 14 initiated runs yielded polymerization heats of -17.4, -11.7, -8.2, and -9.1 kcal per mole of C=C for LA, HDDA, NPGDA, and TMPTA, respectively. Assuming $\Delta H_p = -19.2$ kcal per mole of C=C for complete conversion, the LA, HDDA, NPGDA, and TMPTA photopolymerization conversions at 40° were 91%, 61%, 43%, and 47%. Based on their particular polymerization heats in the thermal scans, the LA, HDDA, NPGDA, and TMPTA photopolymerizations at 40° were 91%, 66%, 49%, and 59%, respectively, of their "ultimate" possible conversions. The multifunctional acrylates exhibit increased conversion during photopolymerization at 60°. Based on -19.2 kcal per mole of C=C for complete conversion, the 60° photopolymerization conversions of HDDA, NPGDA, and TMPTA are 86%, 51%, and 53%, respectively. Again, based on their particular polymerization heats in the thermal scans, the HDDA, NPGDA, and TMPTA photopolymerizations at 60° were 94%, 58, and 66%, respectively, of their "ultimate" conversions. The increased mobility of the networks brought about by raising the temperature probably accounts for the increased conversion of C=C bonds in going from 40° to 60°. Two further conclusions may be drawn. First, the greater flexibility and resultant configuration possibilities of HDDA network units relative to NPGDA network units permit for the former slightly higher C=C bond conversions in the thermal scans and markedly higher conversions at 40° and 60° in the photopolymerizations. Secondly, the photopolymerization of TMPTA at 40° and 60° is slightly more efficient than that of NPGDA in spite of a lower "ultimate" conversion of TMPTA suggested by the thermal scan. It is interesting to speculate on the possibility that the polymer network produced by the TMPTA polymerization provides greater accessibility for reaction of the pendant double bonds at 40° and 60° than that which exists in the NPGDA network.

Lauryl Acrylate Polymerization by Photo-activated Trigonal 14 Initiation. A more extensive preliminary study of the capability of calorimetry to follow rapid photopolymerization reactions was made of the kinetics of LA polymerization initiated by photo-activated TR-14.

    Figure 2 is a tracing of an isothermal exotherm curve of LA containing TR-14 during continuous irradiation by a 400W H3T7 medium pressure mercury lamp. At high light intensities and high TR-14 concentrations no induction period is seen. Differential heating is noted at about 2 sec after shutter opening; t=0 is taken at this point. The differential heating peak (exotherm peak) is seen to occur at about t=7 sec with subsequent decline as monomer (and initiator) concentration diminishes. The upper curve is the base line obtained by repeating the irradiation cycle after 15 min irradiation. The "rate at peak" is used in the following data presentation as a convenient comparator of rates. The subsequent computer treatment of the data reveals for this run that

10% of the total polymerization heat (69.4 cal gm^{-1} for this sample) is observed prior to the peak. It is possible to extrapolate the rate vs. conversion curve to zero conversion (cf. section Monomer Concentration Effect), but for the present this is not done. The reader's attention is directed to the fact that these are very rapid polymerizations being described here. 50% of the total heat appears by t=25 sec in the run represented by Figure 2.

Data obtained from curves such as the one shown in Figure 2 are presented in Tables II through V.

The dependence of LA polymerization rate on temperature, initiator concentration, light intensity, and monomer concentration (conversion) is discussed in the following sections.

Temperature Effect. Table II lists data on LA polymerization rate at the exotherm peak in the temperature region 0°–80°C at two light intensities. A 1% TR-14 concentration was used. The data are presented graphically in Figure 3. For the high light intensity series a low apparent activation energy of 0.63 kcal mol^{-1} is observed from the temperature dependence of the rate at exotherm peak. (This activation energy is calculated from the cal gm^{-1} sec^{-1} rates rather than from mol l^{-1} sec^{-1} rates. Use of the latter would decrease the calculated activation energy since about one-third of the rate increase would be diminished by the specific volume increase in the 50° temperature interval. Of course, the initiator concentration on a mol l^{-1} basis would also decrease about 5%.)

The log (rate at peak) vs. l/T data (Series II) at low light intensity appear complex (Figure 3). No attempt will be made at this time to explain the observed negative apparent activation energy for the reaction in the 0°–30° temperature range.

Initiator Concentration Effect. Table III presents data for five series of photopolymerizations of LA using various concentrations of TR-14. The series differ from one another in incident light intensity and/or temperature. Also, Series III was performed with LA monomer still containing free-radical inhibitor. Figure 4 represents the data of Series IV, V, and VI run in the modified DSC-2 apparatus plus a non-tabulated series on inhibited monomer in the DSC-1B apparatus. Series III data (not plotted) would lie slightly below and parallel to the Series V data. One notes that the data (C=.001 to .01) at high intensity illumination may be approximated by straight line relations in Figure 4. The slope of these lines yields (rate at peak) $\propto C^{0.35}$. The (rate at peak) $\propto C^{0.35}$ represents the data for Series III and V (400W lamp operation) less well and over a more limited concentration range. The same power relation appears to approximate the low intensity data (Series VI; 400W lamp operation with neutral density filter) only in the region near C = .01.

The complexity of the initiator mix, film thickness variation, and oxygen presence in these photopolymerizations does not
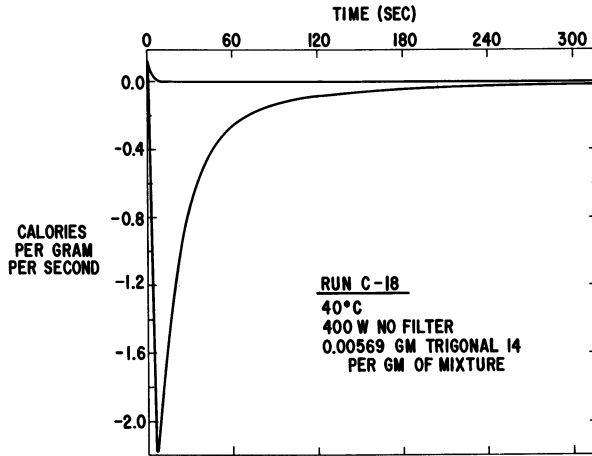
Figure 2. Photopolymerization exotherm trace. Rate of sample heat change vs. time at 40°C. Photoactivated Trigonal 14 initiation of lauryl acrylate polymerization.

TABLE II

Temperature Effect
Lauryl Acrylate Photopolymerization

Series*	Run	T(°C)	Rate at Peak $-dH/dt$ (cal gm^{-1} sec^{-1})
I	T-1	10	2.29
	T-2	30	2.47
	T-3	40	2.50
	T-4	50	2.69
	T-5	60	2.68
II	T-6	0	0.615
	T-7	10	0.601
	T-8	20	0.586
	T-9	30	0.563
	T-10	40	0.573
	T-11	60	0.601
	T-12	80	0.729

*Series I   800^{+} watts; intensity 16.7 mcal cm^{-2} sec^{-1};
T-14 10^2C = 0.989 gm gm^{-1}

Series II   400 watts, 0.1 neutral density filter;
intensity 0.88 mcal cm^{-2} sec^{-1};
T-14 10^2C = 0.989 gm gm^{-1}

TABLE III

Initiator Concentration Effect
Lauryl Acrylate Photopolymerization

Series*	Run	Trigonal 14 10^2C (gm gm^{-1})	Rate at Peak $-dH/dt$ (cal gm^{-1} sec^{-1})	Total Heat $-\Delta H_p$ (cal gm^{-1})	Half Reaction Time, $t_{0.5}$ (sec)
III	C-1	0.101	0.80	34.	30
	C-2	0.205	1.19	47.	28
	C-3	0.405	1.68	57.	25
	C-4	0.604	1.88	71.	29
	C-5	1.01	2.05	71.	25
	C-6	2.01	2.11	74.	26
	C-7	4.03	2.42	79.	26
IV	C-8	0.0101	0.023	--	--
	C-9	0.0375	0.59	17.	25
	C-10	0.159	1.74	48.	21
	C-11	0.352	2.33	59.	18
	C-12	0.634	2.79	68.	17
	C-13	0.989	3.34	73.	17
V	C-14	0.107	1.01	39.	28
	C-15	0.140	0.92	39.	32
	C-16	0.257	1.56	60.	29
	C-17	0.257	1.59	54.	24
	C-18	0.569	2.18	69.	25
	C-19	1.13	2.55	74.	22
	C-20	2.06	2.65	77.	21
	C-21	4.59	2.55	(83.)	25
VI	C-22	0.107	0.057	5.5	64
	C-23	0.140	0.046	4.6	68
	C-24	0.159	0.132	14.6	82
	C-25	0.257	0.262	30.	90
	C-26	0.352	0.313	35.	91
	C-27	0.569	0.515	54.	101
	C-28	0.634	0.451	42.	79
	C-29	0.989	0.546	52.	86
	C-30	1.13	0.570	52.	85
	C-31	1.13	0.637	57.	85
	C-32	2.06	0.693	65.	95
	C-33	4.59	0.588	68.	122
	C-34	4.59	0.612	70.	116
VII	C-35	0.0375	(0)	(0)	--
	C-36	0.159	0.182	23.	116
	C-37	0.352	0.352	41.	120
	C-38	0.634	0.432	47.	122

*Series III 400 watts; intensity 6.6 mcal cm^{-2} sec^{-1}; T=40°C;
inhibited monomer
Series IV 800$^+$ watts; intensity 16.7 mcal cm^{-2} sec^{-1}; T=30°C
Series V 400 watts; intensity 6.3 mcal cm^{-2} sec^{-1}; T=40°C
Series VI 400 watts; 0.1 neutral density filter; intensity
0.89 mcal cm^{-2} sec^{-1}; T=40°C
Series VII 400 watts; 0.1 neutral density filter; intensity
0.89 mcal cm^{-2} sec^{-1}; 60°C.
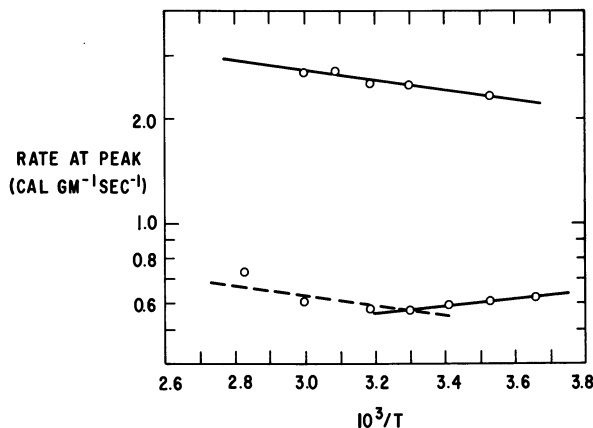
Figure 3. Temperature dependence of $-dH/dt$ exotherm rate at peak for lauryl acrylate containing 0.989 gm gm^{-1} of Trigonal 14 (cf. Table II). Upper points at 16.7 mcal cm^{-2} sec^{-1} total light intensity; lower points at 0.88 mcal cm^{-2} sec^{-1} total light intensity.
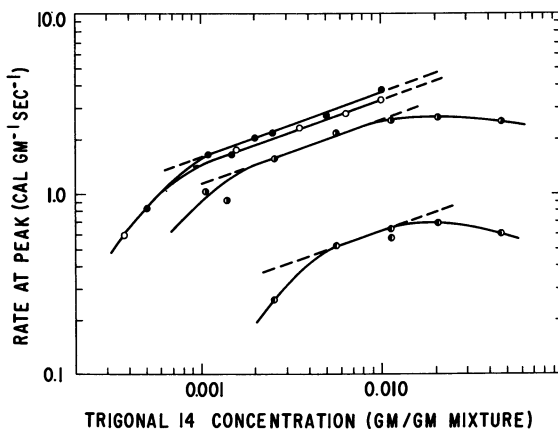
Figure 4. Dependence of $-dH/dt$ exotherm rate at peak on initial Trigonal 14 concentration in photopolymerizations of lauryl acrylate. ●, 800 + W, inhibited monomer, $T = 52°C$, DSC-1B; ○, 800 + W, $T = 30°$ (Series IV); ◐, 400W, $T = 40°C$ (Series V); ◖, 400W, 0.1 neutral density filter, $T = 40°C$ (Series VI).

encourage detailed analysis of the initiator concentration effect. However, the rapid decrease in the peak rate with lowering of C below 0.001 appears associated with initiator loss to side reactions, most likely to depletion due to oxygen presence. At very low C an extended inhibition period is noted in the isothermal DSC photopolymerizations leading in extreme instances, e.g., run C-35, to no observed polymerization. The accentuated drop-off at low light intensity (Series VI) in the peak rate with initiator concentration decrease is not readily explicable. We presently ascribe the decrease in the rate at peak at high TR-14 concentrations to optical thickness effects. This aspect requires study with better film thickness geometry, single initiator species, and limited wavelength ranges.

Figure 5 displays the variation of total heat of reaction with initial initiator concentration for Series IV, V, VI, and VII. This effect is most assuredly associated with initiator depletion throughout the continuous irradiation. Some enhancement of total conversion at given initiator concentration is noted in raising the polymerization temperature from 40° (Series VI) to 60° (Series VII). A large decrease in total heat of reaction is noted in going from the 16.6 mcal cm^{-2} sec^{-1} and 10 mcal cm^{-2} sec^{-1} illuminations to the 0.89 mcal cm^{-2} sec^{-1} illuminations.

Light Intensity Effect. The effect of light intensity upon the polymerization rate at peak is displayed by three series of runs (cf. Table IV). The series differ slightly in initial TR-14 concentration and temperature. Figure 4 presents these data as log (rate at peak) vs. log (intensity). The rates plotted have been converted to rates at C = 0.0100 and T=313°K (40°C) by using $R^0_{313}{}^{100} = R^C_T \times (C/.01)^{0.35} \times e^{+316(T^{-1}-313^{-1})}$. Considering the 30-fold intensity range 0.48 mcal cm^{-2} sec^{-1} to 14.3 mcal cm^{-2} sec^{-1} (Figure 6) and first averaging the rate at peak values at given intensities, we find that the least-squares straight line through the resulting ten data points yields a slope corresponding to (rate at peak) ∝ (intensity)$^{0.53}$. This is near the expected dependence of polymerization rate upon the square root of the light intensity for simple initiator photolysis and radical + radical termination of kinetic chains in solution.

Monomer Concentration Effect. In bulk polymerizations such as those conducted in the present study, the dependence of polymerization rate on monomer concentration can be determined only on the basis of the dependence of rate on the extent of reaction. Reduction of the rate vs. time DSC traces to digital data files permits computer calculation of reaction rate as a function of monomer conversion. A computer program which yields print-out of the rate and time at given fractions of the total heat release allows computation of the order of reaction with respect to carbon-carbon double bond concentration. Assuming -80.0 cal gm^{-1} represents the
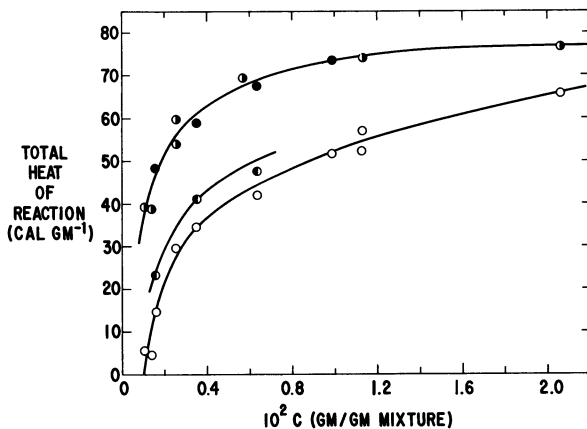
Figure 5. Total heat of reaction, $-\Delta H_p$, plotted against initial Trigonal 14 concentration, C, for lauryl acrylate polymerizations (cf. Table III). ●, Series IV; ◑, Series V; ○, Series VI; ◐, Series VII.

TABLE IV

Light Intensity Effect
Lauryl Acrylate Photopolymerization

Series*	Run	Light Intensity (mcal cm^{-2} sec^{-1})	Rate at Peak $-dH/dt$ (cal gm^{-1} sec^{-1})
VIII	I-I	0.69	0.70
	I-2	1.42	1.00
	I-3	3.52	1.91
	I-4	9.0	2.26
	I-5	14.3	3.32
IX	I-6	0.34	0.074
	I-7	0.34	0.059
	I-8	1.53	0.727
	I-9	1.53	0.763
	I-10	14.3	2.74
	I-11	14.3	3.02
X	I-12	0.107	0.007
	I-13	0.214	0.187
	I-14	0.48	0.197
	I-15	0.48	0.504
	I-16	0.84	0.80
	I-17	2.80	1.59
	I-18	4.34	1.96
	I-19	4.34	1.93

*Series VIII   800$^+$ watts; TR-14 10^2C = 1.00; 52°C;
              inhibited monomer; DSC-1B
 Series   IX   800$^+$ watts; TR-14 10^2C = 0.989; 30°C
 Series   X   400 watts; TR-14 10^2C = 1.13; 40°C

total ΔH_p of LA, the residual heat of polymerization at time t_x, $H_R(t_x) = 80.0 - \int^{t_x} (dH/dt) \cdot dt$, is proportional to the unreacted monomer concentration in the system at that time. Figures 7 and 8 are plots of the exotherm rates, $-(dH/dt)_{t_x}$ vs. $H_R(t_x)$ on log-log coordinates for the Series IV and Series V data. t_x at which the points are shown are $t_{0.2}$, $t_{0.3}$, $t_{0.4}$, etc., in which 0.2, 0.3, 0.4, etc., are the fractions of total heat for each run. Thus, the upper four points on the top curve of Figure 7 represent for run C-13 the rates of reaction at 0.2 x 73 = 14.6, 0.3 x 73= 21.9, 0.4 x 73 = 29.2, and 0.5 x 73 = 36.5 cal gm^{-1} for -H cumulative = $-\int^{t_x}_0 (dH/dt)dt$, x = .2, .3, .4, .5. If there were little initiator depletion and other factors remained constant, one would expect the curves in Figures 7 and 8 to be parallel straight lines whose slopes would be the order of reaction with respect to monomer concentration. Obviously, curvature exists in the plots and the curve slopes in the early stages of conversion appear to increase as the initial initiator concentration is lowered. Despite these deviations we may expect the slopes of the curves in Figures 7 and 8 at low conversion and high initial initiator concentrations to represent nearly the order of reaction with respect to monomer concentration.

Table V presents the results of least-squares fitting of straight lines to the 0.2, 0.3, 0.4, and 0.5 fractional heat points of the log-log plots (of Figures 7 and 8) of polymerization rates $(-dH/dt)_{t_x}$ and residual heats of reaction for Series III, IV, and V data. The slopes, B, progressively increase as initial initiator concentrations decrease. However, restricting our consideration to the ten runs in which $-\Delta H_p > 68$ cal gm^{-1} the average B is 1.65. For the six runs (Series IV and Series V) for which $-\Delta H_p \geq 68$ cal gm^{-1} and no free radical inhibitor was initially present the average B is 1.57. We therefore conclude, with considerable reservation, that $-dH/dt \propto [M]^{1.6}$ for LA where [M] is the monomer concentration.

Summary. The foregoing sections lead to the conclusion that for the photo-activated Trigonal 14 polymerization of lauryl acrylate, the rate of polymerization may be approximately expressed as

$$-d[M]/dt = K_1 \times (-dH/dt)$$
$$= K_2 \, C^{0.35} \, I^{0.53} [M]^{1.6} e^{-316/T} \tag{1}$$

where C is the Trigonal 14 concentration, I is the incident light intensity, [M] is the lauryl acrylate monomer concentration, and T is the absolute temperature. This expression holds best for the higher light intensities, $0.001 \leq C \leq 0.010$ range, and $[M]/[M]_0 \geq 0.5$ region.

Although the foregoing information was obtained on lauryl acrylate initially equilibrated with air and initiated by a complex commercial photo-initiator, it is still profitable to compare
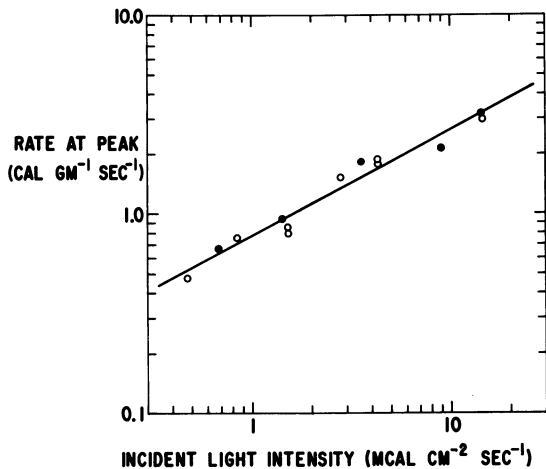
Figure 6.   Exotherm rate at peak, −dH/dt (peak), vs. incident light intensity for photoactivated Trigonal 14 initiated lauryl acrylate polymerizations (cf. Table IV). ●, Series VIII; ○, Series IX and Series X.
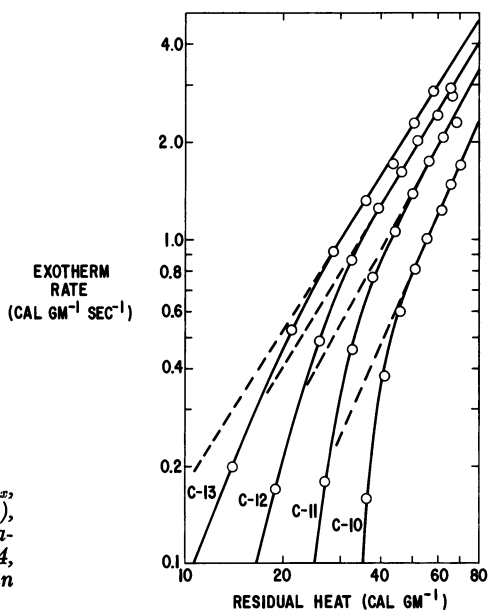
Figure 7.   Exotherm rates, (−dH/dt)$_{tx}$, vs. residual polymerization heats, $H_R(t_x)$, for Series IV lauryl acrylate polymerizations. Points correspond to 0.2, 0.3, 0.4, etc., fractional conversions for each run based on its total −ΔH$_p$.
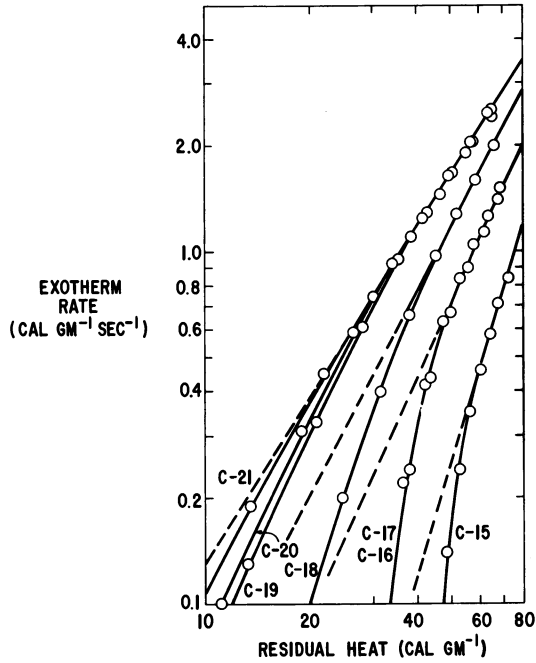
Figure 8. Exotherm rates, $(-dH/dt)_{tx}$, vs. residual polymerization heats, $H_R(t_x)$, for Series V lauryl acrylate polymerizations. Points correspond to 0.2, 0.3, 0.4, etc., fractional conversions for each run based on its total $-\Delta H_p$.

TABLE V

Polymerization Rate Dependence on Residual Polymerization Heat
Lauryl Acrylate Photopolymerization

Run	TR-14 10^2C (gm gm^{-1})	$-\Delta H_p$ (cal gm^{-1})	A	B
C-13	0.989	73	-4.476	1.34
C-12	0.634	68	-5.156	1.47
C-11	0.352	59	-6.182	1.67
C-10	0.159	48	-8.835	2.20
C-21	4.59	83	-5.618	1.56
C-20	2.06	77	-5.756	1.60
C-19	1.13	74	-5.463	1.52
C-18	0.569	69	-7.278	1.90
C-17,16	0.257	57	-9.631	2.37
C-15	0.140	39	-14.12	3.29
C-7	4.03	79	-5.789	1.59
C-6	2.01	74	-6.824	1.81
C-5	1.01	71	-7.019	1.83
C-4	0.604	71	-7.146	1.84
C-3	0.405	57	-9.318	2.31
C-2	0.205	47	-10.817	2.57
C-1	0.101	34	-16.729	3.83

ln R_p = A + B lnΔH (residual)

$-R_p$ = rate (cal gm^{-1} sec^{-1})

ΔH(residual) = 80.0 - (-ΔH cumulative [cal gm^{-1}])

ΔH cumulative = integrated heat to chosen fraction of total
heat

    A and B obtained from least-squares line according to above
equation using 0.2, 0.3, 0.4, and 0.5 fractional heat data points.

    B = 1.65 average for the ten runs having $-\Delta H_p \geq 68$ cal gm^{-1}.

the calorimetric study of polymerization rate with more conven-
tional dilatometric studies. (9,10) Our present data are in
agreement with the observation of no Trommsdorf effect in LA bulk
polymerization. (9) Our determination of approximate monomer or-
der 1.6 for the very rapid photopolymerizations is higher than the
1.4 order found previously for bulk polymerization and near the
1.6 order found for solution polymerization. (9) It should be
recognized that the rates of polymerization in the present work
are as much as 300 times the rates in the dilatometric study. The
effect of initiator depletion on the computed monomer order in the
present treatment is to increase the apparent order. The 0.35 or-
der in Trigonal 14 concentration corresponds qualitatively with
the 0.45 order in initiator concentration found in the dilato-
metric work. It is interesting that although the Trigonal 14 or-
der is approximately 0.35, the order in light intensity is near
0.5.

  The present preliminary study of rapid photopolymerization
reactions by differential calorimetry shows this method to have
great potential utility. Future studies involving simpler reaction
systems and better controlled reaction conditions will display the
power and sophistication of the differential calorimetric tech-
nique in photochemical research.

Abstract

  Differential calorimetry has been applied to the study of
rapid photopolymerizations. This new technique holds great promise
for basic and applied research on photopolymerization and other
photochemical reactions. The method requires only a few milligrams
of sample, can be used on network-forming systems, and can approx-
imate actual conditions of thin film and coating technologies.

  Lauryl acrylate polymerizations initiated by a photo-acti-
vated mixture of benzoin butyl ethers (Trigonal 14) were performed
in Perkin-Elmer model DSC-1B and DSC-2 apparata modified by attach-
ment of a heat-filtered medium pressure mercury lamp. Within spec-
ified variable limits, the rate of polymerization may be approxi-
mated by the relation $R_p = const. \; I^{0.53} C^{0.35} [M]^{1.6} e^{-316/T}$. I is
light intensity; C is initiator concentration; [M] is monomer con-
centration; T is absolute temperature.

  Peroxide initiated polymerizations (scan 30°-250°C) of lauryl
acrylate (LA), 1,6-hexanediol diacrylate (HDDA), neopentyl glycol
diacrylate (NPGDA), and trimethylol propane triacrylate (TMPTA)
revealed total polymerization heats per mole of C=C of 19.2, 17.6,
16.7, and 15.4 kcal, respectively. Photoactivated Trigonal 14 in-
itiated polymerizations at 40° yielded total polymerization heats
per mole of C=C of 17.4, 11.7, 8.2, and 9.1 kcal for LA, HDDA,
NPGDA, and TMPTA, respectively. At 60°C the photopolymerization
heats for the latter three monomers increased to 16.6, 9.7, and
10.2 kcal per mole of C=C, respectively.

Literature Cited

 1. McGinnis, V.D., Holsworth, R.M. and Dusek, D.M., A.C.S. Coat-
    ings and Plastics Preprints, (1974), Vol. 34, (No. 1), p. 669
 2. Osborn, C.L. and Sander, M.R., ibid., p. 660.
 3. Schroeter, S.H., Moore, J.E. and Orkin, O.V., ibid., p. 751.
 4. McGinnis, V.D. and Dusek, D.M., J. Paint Tech., (1974), 46,
    23.
 5. Faru, R.A., Polymer, (1968) 9, 137.
 6. Horie, K., Mita, I. and Kambe, H., J. Poly. Sci., (1968), Vol.
    6, (A-1), 2663.
 7. Burrett, K.E.J. and Thomas, H.R., Brit. Polymer J., (1970),
    Vol. 2, p. 45.
 8. Willard, P.E., Polym. Eng. and Sci., (1972), Vol. 12, (No. 2),
    120.
 9. Scott, G.E. and Senogles, E, J. Macromol. Sci.,-Chem., (1970),
    A4, 1105.
10. Scott, G.E. and Senogles, E., ibid., (1974), A8, 753.
11. Joshi, R.M., Makromol. Chem., (1963), 66, 114.
12. Joshi, R.M., J. Polymer Sci., (1962), 56, 313.

Applications of Radiation Sensitive Polymer Systems

W. MOREAU and N. VISWANATHAN

IBM Corp., Systems Products Division, E. Fishkill, N.Y. 12533

Over the last five years, significant advances have
been made in the radiation processing of commercial
products. The products range in size from cured films
on automobiles to picosecond microelectronic devices
500A° in three dimensional size. Four major techno-
logical areas encompass the scope of the applied tech-
nologies, (cf., Table I). These include; (1) the
radiation curing or alteration of coatings and fibers,
(2) the photoproduction of lithographic printing plates,
(3) the processing of fabricating electronic devices
with resists, and (4) the commercial development of
photodegradable plastics. The treatment of photocon-
ductive polymers for xerography will not be reviewed
but is treated in several reviews (see bibliography).
In this report we will survey the catagories of applica-
tion by examining the chemical classes of polymeric
systems, the processing sequences, and the efficiency
of the various systems.

The exposure of polymeric systems has involved the
full electromagnetic spectrum (Table II). The irradia-
tion wavelength is usually in excess of the bond energy
of the carbon bonds or in excess of the activation
energy of chemical reaction. High energy x-rays,
gamma, ion, electron, ultraviolet and infrared beams
have been used to degrade, polymerize, or crosslink
polymeric films. The most widely used wavelengths are
the 3000-5000A° region of mercury lamps for the expo-
sure of polymer films. The thicknesses of exposed
films range from Angstroms to thousands of microns
(cf., Table III).

TABLE I

Radiation Processing of polymers

Polymerization	Grafting	Cross-linking	Degradation
Polymer Synthesis	Fiber treatment	Negative resists	Positive resists
Ink Curing	Membrane	Ink curing	Photo-degrading plastics
Coating curing	"Casing"	Coating curing Dental coatings Heat shrinks	Plastic weathering Paint weathering Polymer analysis

TABLE II

Exposure Sources of Polymer Systems

Radiation Source	Approximate Wavelength A°	Energy Kcal	Application
X-Rays	1-10	290 x10^3	Resist exposure
Gamma(1MEV)	0.01	28 x10^6	Polymer synthesis
E-Beam(100KV)	0.008	35 x10^5	Resist exposure
E-beam(10eV)	1200	250	Plasma processing
UV	1000-3000	190	UV curing
UV	3000-4000	100	Ink Curing Lithography
UV	4000-5000	60	Photoresists Graphic Arts
Laser	3000-6000	70	Holography Resist exposure
Laser	10.6 μ	3	Plastic Evaporation
ION(100KV)	0.13	2 x10^6	Resist Etching
ION (10ev)	1000	300	Plasma Chem. treatment of films, fibers, membranes.

The polymeric systems are usually composed of a polymer which imparts the majority of physical properties and actinic additives. In simple systems such as curing films or electron beam resists, the polymer is also the radiation sensitive species. In most cases, the formulations behave similarily in their response to high energy irradiation. Practically any polymer can be made radiation sensitive by direct exposure to ionizing energies or by formulation with additives such as free radical precursors. Thermally sensitive polymers are also likely to undergo a similar reaction when exposed.

The processing of polymer films involves wet and dry techniques. Some systems are solventless laminates such as dry resists. In most cases one-dimensional films require only coating and exposure. For multidimensional images, solvents are used to form images by dissolution of unwanted areas. A general trend for economic and ecological purposes will involve solventless coatings and dry processing.

The increased interest in energy sensitive polymers probably evolves from the shortcomings of the conventional image recording media-silver halide emulsion. It is both difficult and expensive to apply emulsion films as protective layers or use as printing plates or etch resists. Synthetic polymers are one to two orders of magnitude less radiation sensitive than halide emulsion, but their unique properties of chemical and physical resistance easily overcome this disadvantage, (cf., Table IV).

Radiation sensitive films are available from a wide source of cheap synthetic monomers or polymers. The resolution of polymeric films greatly exceeds that of silver emulsion. Images as microscopic as 50A° lines and spaces (200,000 lines/mm.) have been recorded in resist films by exposure in a scanning electron microscope. Molecular additives such as diazonium salts or organic halides can be added to produce colored images of high opacity. Polymeric systems can be envisioned as meeting a majority of technological needs for information recording and in the fabrication of miniature electronic or mechanical components.

In the applied technologies, the curing of paints or inks by electron beam or ultraviolet light has

TABLE III

Exposure Penetration in Processing Polymers

Exposing Radiation	Depth of Penetration	Polymer Thickness
Plasma (UV Emission)	1–10 μ	Surface Treatment
Plasma (1–10eV)	0.005–0.05 μ	Surface Treatment
Ion (60KV)	2 μ	0.1 – 1 μ
E–Beam (20KV)	8 μ	0.1 – 2 μ
E–Beam (1MEV)	150 μ	25 – 200 μ
X–Rays (60KV)	10 μ	0.5 – 2.0 μ
UV (3650A°)	1–125 μ	0.1 – 10 μ

Table IV

Comparison of Conventional Silver Emulsion
and Unconventional Polymer Image Recording

Silver Emulsion Film	Polymeric Films
Higher cost	Low cost
Higher proprietary formulations	Wide patent base
Precoated films	Easily applied
Thickness restriction	Molecular films
Resolution to 1μ	Resolution to .001μ
Wet Chemical Process	Dry and Wet Processing
High speed (10^{-3}cm^2/erg)	Slow speed (10^{-6}cm^2/erg
Poor chemical resistance	Excellent resistance
Poor physical resistance	Excellent resistance
One or two dimensional images	Multi-dimensional images
Quantum amplification	Low quantum amplification
200–1000 nm sensitivity	200–500 nm sensitivity

finally been accomplished on an industrial scale.
The electron beam curing of coatings has for some time
attracted a great deal of attention since it is claimed
that coatings can be fully cured in a fraction of a [1]
second. The coatings are primarily based on the cross-
linking of acrylic or epoxy resins in a polyurethane
or polyester base (i.e., modified paints).

Electron beam curing has reached fully commercial
stages in the USA and Europe.[2] Protective coatings
have been electrocured on automotive finishes, wood
products, plastic products, and structural metals.
The products usually have to be flat for the most
efficient processing. The high sensitivity of sol-
ventless coatings coupled with more efficient sources
has enabled process speeds to attain 50-100 feet per
minute.[3]

Since the electron beam (150 KV) penetrates and
cures films up to 50 mils in thicknesses, the films
can be highly pigmented (preferably with high atomic
number additives to enhance electron absorption).

The ultraviolet curing of inks and coatings has
also received new attention. The renewed interest in
curing inks has been influenced by ecological and eco-
nomic considerations.[4] The inks can be formulated as
solvent free systems which are sensitized to mercury
3650A° irradiation. The curing energy is only a frac-
tion of that needed with heat curable systems.

The ink formulations usually contain an unsatu-
rated monomer or prepolymer, a radical precursor and/
or an actinic sensitizer, a polymer vehicle base, and
pigmentation. Recent formulations include polyunsatu-
rated polyenes, and polyacrylates with thiol or ben-
zoin radical sources.[5] The acid or hydroxyl content
of the resin base is usually varied to adjust the
water or oleophillic wetting action of the composition.

Although the penetration range of ultraviolet
light is only about 25 microns (1-2 mils), the curing
time is in the second range and throughputs approach
the speeds of electron beam cured films. The electron
and ultraviolet curing of radiation can be compared as
follows. Electron curing has a wider range of appli-
cation and is suitable for thicker, pigmented systems.
Electron beam sources are more expensive to operate and
not readily adapted to a small industrial scale or for

small parts.   Both techniques overcome the solvent
pollution of heat curable coatings but are still re-
stricted to mainly flat surfaces.

In the printing industry one of the applications
of photopolymerization is in the area of generating
lithographic printing plates.   As is commonly known in
all lithographic systems, the printing plates could be
generated by positively or negatively acting resist
systems.   The printing plates can be broadly classified
as Surface plates or Deep etch plates.

In the former class, the photopolymerised coating
is a hard residue on the developed plate; and the
polymerised material is usually oleophillic and hydro-
phobic.   The background (usually a metal substrate) in
contrast is usually hydrophillic and oleophobic.   In
actual practice, the background metal lands are peri-
odically desensitized with a suspension of colloidal
particles in an acidic medium.

The Deep etch plates, on the other hand, are
usually etched metal plates using a negatively working
photoresist and an etching lacquer.   In the industry
the Deep etch plates have found wider usage in view of
their mechanical stability towards printing more
copies.

From the materials point of view, the printing
industry has used all possible compositions of photo-
polymerizable prepolymers.   Commonly used systems are
materials with unsaturated moieties as esters, ketones,
ethers, and modifications of these.   Of these classes,
broadest patent coverage seems to center around acrylic
esters and derivatives of acrylate systems, especially
in the areas of surface printing plates.   The major
emphasis in this type of lithographic plates seems to
be on the mechanical stability of the polymerized
image to sustain repeated impacts without serious loss
of resolution and deformation of the images.   From
this point of view, increased mechanical strength ob-
tained by extraneous crosslinging agents have found
the widest applicability to obtain rigid structures.
On the other hand, in the areas of Deep etch plates,
the emphasis seems to be on the stability and etch
resistance of the images (to withstand chemical agents)
necessitate the use of chemically stable compositions
(such as cyclized isoprene, epoxidised esters).   Ad-
ditional factors such as adhesion of the photoresist

to the metal plate affect the quality of the final
image.

   The sensitizers and initiators used in the prin-
ting plate industries are basically well known sensi-
tizers in the photochemical field. Most of these have
strong absorption in the near UV-visible sources, Hg
lamps occupying the major role in present-day techno-
logy. Table V is a comprehensive summary of some im-
portant sensitizers and prepolymers used in the photo-
lithographic field.

   From processing point of view, emphasis has been
placed heavily on substituting hard plastics in the
place of metals used in the past, with the major ad-
vantage of reduced costs involved in fabrication. Al-
most every possible physical and chemical property
has been experimented with to obtain the necessary
contrast between the exposed and unexposed areas of
the lithographic plates. Physical property distinc-
tions based on adhesion, thermal properties (melting
point, for example) have paved the way for the long
sought after dry processing techniques. The trend
seems to be in the direction of departing from wet
chemical processing (such as solubility methods)
techniques. It should also be noted that emphasis
seems to be in the direction of avoiding processing
steps under darkroom conditions. Several commercial
compositions are obtainable in the laminate form,
usually with an inert oxygen insensitive top film to
avoid quenching effects caused by oxygen during expo-
sures.

   To improve the mechanical strength and hardness
call for the use of curing agents (usually activated
by a bake step after development) in the photopoly-
merizing composition. Typical curing agents mentioned
have been alkyl hydroperoxides, bifunctional amines,
acids, etc. The last class of compounnds have been
the most popular additives to the epoxy based polymer
compositions. Additionally, the use of inert fillers
 is also known.

   A recent example of newer classes of compounds
in photosensitive printing plate industry is the use
of sulfenyl carboxylates and aryl sulfonyl diazo-
methane derivitives.[6] In the same report, examples of
negative working diazoindole based polymers are shown.

The concepts of positive or negative systems are by no means a strict classification since modifications of the original pre-polymer with additives, with suitable changes in the development processes can be utilized to obtain positive resists whilst the unmodified material is a negative resist. For example, tetrachloro diazo cyclopentadienes in general are polymerisable by UV light to obtain negative resist systems. By using these materials with novolak type (phenol-formaldehyde for example) resins, and using aqueous developers, one can obtain a preferential solubility of the exposed areas, a positive working system. In this context it should be mentioned that most of the newer materials suffer from the disadvantage of having absorption peaks around 3000A°, a region restricted for use only with quartz optics and dearth of high intensity light sources.

The photo- and electron (ion and x-ray) beam resists are divided into two classes (cf., Fig. 1) of solubilization in developing an image. A positive resist is more soluble in the developer in regions irradiated while a negative resist is insolubilzed in the exposed regions. The solubility differences between the exposed and unexposed regions are used to form three dimensional images which protect desired materials during the etching of the substrate. The photoresists are exposed through a mask by contact or projection printing with the 3650, 4050, and 4350A° mercury lines. Electron beams 5-30KV and x-rays 2-10A° have also been employed. The positive resist reproduces the mask or image in a direct positive replication while a negative resist reproduces an image reversal of the opaque portions of the mask.

The resist are about one to two microns thick for silicon semiconductor fabrication of two to ten micron devices and about three to twenty-five micron thick for printed circuit board packaging. The resists are mainly used in subtractive masking for etching by chemicals or, most recently, by plasmas of fluoride ions. Since positive resists are soluble in organic solvents, they are exclusively used in an additive cycle to define metal lands in a lift-off scheme. Most of the resists are in the liquid form, but recently solventless dry film resist for thick film applications have been introduced.[7] Dry films protect plating holes in circuit boards.

TABLE V

List of commonly used prepolymers in photolithography

Acrylates   Acrylonitriles   Allyl Esters
Cellulose esters   Epoxies Ethylenic (unsaturated)
hydrocarbons   Poly-hydroxy esters(eg: Pentaerythritol
tetramethacrylate,Ethylene Glycol diacrylate)
Polyolefins   Vinyl compounds(esters,acids)
Vinylidene compounds.

Common Sensitizers

Class	Typical Examples
Carbonyl compounds	Benzoin,Quinones,Benzophenone
Azo compounds	Diazonium compounds,
Organic Sulfur Cpds.	Mercaptans , Disulfides
Redox systems	Per acids , Fe^{2+} - Fe^{3+}
Halogen compounds	Silver Halides, CBr_4,$HgBr_2$
Dyes	Eosin/Amine,Cyanine dyes
	Methylene blue
Organometallics	Metal alkyls
Metal Carbonyls	$M(CO)_x$
Photoconductors	ZnO
Triplet	Benzophenone,Benzothiazoles
	Nitroaromatics
Singlet	Eosin dyes.

RESIST PROCESSES

POSITIVE   NEGATIVE

ETCH

LIFT-OFF
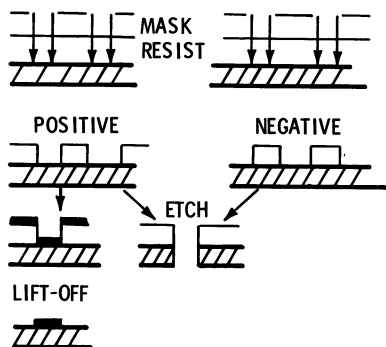
Figure 1.   Resist processes

The commercial positive photoresists are based on the photoinduced Wolf rearrangement of a diazoquinone to a indene carboxylic acid[8]
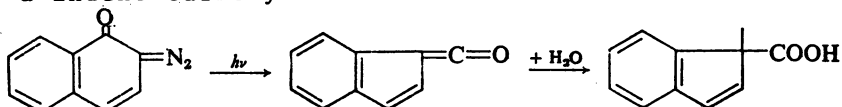
The ketene intermediate reacts with water present in the phenolic polymer base or in subsequent alkaline developer to form a soluble indene carboxylic acid.

Recent work by Russian Workers has revealed a more reasonable explanation of the photoinsolubilization of a phenolic resin by the decomposed diazoquinone. The ketene intermediate was found to be grafted onto the phenolic resin through the formation of a carboxylic acid ester[9]
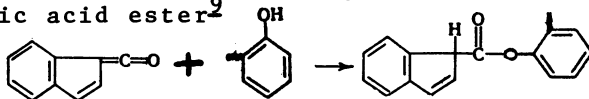
The grafted polymer is soluble in the alkaline ph.-12 developer. The unexposed phenolic resin protected by the insoluble napthoquinone diazide is unaffected by the developer. Since the polymers are photosensitive to 5500A°, they could eventually be useful spinoffs as photodegradable polymers soluble in alkaline soils.

In contrast to dry film plating or etching negative resists such as Dupont's Riston[10] no dry film positive resists have been marketed. The positive resists offer versatile processing alternatives. In Figure 1, the additive lift-off or subtractive etch process is outlined. Since the positive resists are soluble in organic solvents, metal films can be patterned and "lifted off" in undesired regions. Negative resists are not soluble in organic solvents. Harsh strippers such as alkali or strong acids are used. These agents would attack metals such as copper or aluminum deposited over negative resists.

Negative resists have been exclusively used in lithographic plate production. They have been adopted to electronic manufacture of printed circuit boards and microscopic semi-conductor devices. Micro-electronic grade negative resists free of particles or metal ions have been exclusively marketed. Negative resists have been formulated on all aspects of photo-polymerization, crosslinking, and insolublizing reactions of unsaturated monomers or polymers. Since high molecular weight polymers or crosslinked insoluble polymers are desired to produce a "negative" (image area exposed is insoluble in developer), various

sensitizers and vinyl or allyl based polymers have
been used. Three successful resists exemplify basic
paths to obtain an insoluble high polymer. These are
based on triplet $\underline{11}$ sensitized crosslinking of poly-
vinylcinnamate. Over 300 patents have been disclosed
on this reaction.

$$
\begin{array}{cccc}
C_6H_5 & C_6H_5 & C_6H_5 & C_6H_5 \\
| & | & | & | \\
HC & CH & HC\text{————}CH \\
\| \;+\; \| & \longrightarrow & | & | \\
HC & CH & HC\text{————}CH \\
| & | & | & | \\
COOH & COOH & COOH & COOH
\end{array}
$$
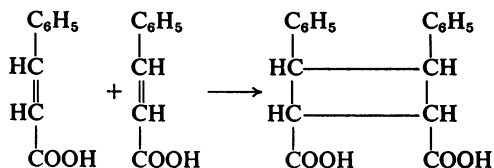
The second example of a basic reaction is the bisazide
    bisnitrene crosslinking of cyclized polyisoprene
(P)

$$
N_3RN_3 \xrightarrow{\;h\nu\;} :NRN: \xrightarrow{\;\sim\!\!P\!\!\sim\!\!P\!\!-\!\!} \sim\!\!P\text{——}P\!\!\sim
$$
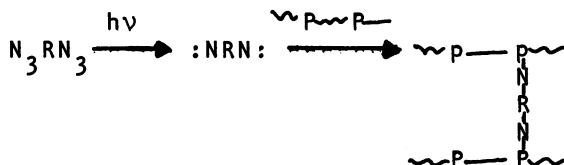
In thin films $\langle 2\mu$, the system is limited to 3650A° ex-
posure and is not suitable for projection printing.
Recently, the spectral sensitivity of the conjugation
associated with azide chromophore has been extended
to 4350A° for projection exposure. $\underline{12}$ In very thin
layers   5000A°, the presence of oxygen will quench the
nitrene crosslinking by conversion into a nitroso
derivative. $\underline{12}$
    Prepolymers especially di, tri, and tetrafunc-
tional acrylates or diallylpthalates sensitized by
triplet or radical photosensitizers form the third
class of negative resists.   These resists are also
useful as examples of radiation curable coatings,
paints, or inks.
    The benzoin-sensitized insolubilization of dia-
llypthalate prepolymers and the t-butyl anthraquione
sensitized gelation of pentaerythritol acrylates are
examples of thick film wet and dry negative resists. $\underline{10}$
        The systems are oxygen sensitive.   Rapid

insolubilization is achieved through spatial poly-
merization in all dimensions.

It is expected that thermoset epoxy prepolymers
will be eventually used as high speed negative resists
once the shelf life can be extended. Heat sensitive
polymers could be activated by adding the photo-
sensitizer immediately before exposure. Highly
sensitive negative resists are more difficult to pro-
cess since insoluble residues arising from "dark"
polymerization cannot be tolerated in the developed
(unexposed) regions. Solventless compositions will
eventually be required for high speed negative
resists. Ideally, thermally stable (up to 300°C) but
radiation sensitive polymers are needed in the field
of three dimensional image recording.

In comparison of positive and negative resists,
the nature of the substrate and etching conditions
eventually dictate the choice of resists. In Table VI
is a comparison of a commercial positive diazoquione
resist with a commercial negative resist. The
positive resists have higher resolution but slower
speed and less etch resistance. Since glass and metal
films with a multitude of etchants or processes are
used, both resists are widely used in semiconductor
manufacture. Hydrophillic and hydrophobic surfaces
are encountered. A universal resist with adhesion
and high etch resistance but soluble in organic
solvents can be envisioned as the next generation
material.

In the semiconductor technology, a major effort to
produce microcomputer circuits with enormous memories
has been undertaken in the last decade. This has
increased the demand for the development of circuits
with dimensions near the wavelength of light 0.5μ.
Higher resolution exposure using X-rays, ion beams
and electron beams have been investigated. Since the
electron beam can be accurately moved by deflection
in equipment such as in a scanning electron micro-
scope, various resists based on degrading or cross-
linking polymers have been investigated.

The negative electron beam resists as shown in
Table VII are based on vinyl polymers [13]

$$\text{\raisebox{0pt}{$\sim\!\!\sim\!\!\sim$}}\!-\!\!\left[\!-CH_2-\underset{R}{\overset{H}{C}}\!-\!\right]\!-$$
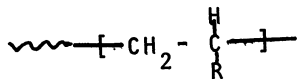
with eliminating or decomposing side chains such as

$$-Cl \ , \ -Si(CH_3)_3 \ , \ -\underset{O}{\overset{\|}{C}}-OCH_3 \ , \ -O\underset{O}{\overset{\|}{C}}OCH_3$$
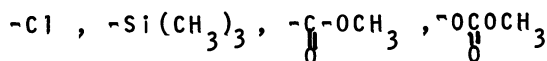
TABLE VI

Comparison of Positive and Negative Resists

	Positive Diazoquinone	Negative Bis-Azide
Spectral Sens.	3650-5000A°	3650A°
Oxygen Sens.	no	yes
Exposure ergs/cm^2	2×10^6	4×10^5
Resolution/mm	800 lines	300 lines
Etch Resistance	acid but not alkali.	acids& alkalis
Strip	organic solvents	acids
Lift-Off	Yes	No

TABLE VII

Electron Beam Polymers

POSITIVE - DEGRADING TYPE

	Min. Dose Coul/cm^2
POLYMETHYL METHACRYLATE	10^{-5}
POLY T-BUTYL METHACRYLATE	10^{-6}
POLYMETHYL ISOPROPENYL KETONE	10^{-5}
CROSSLINKED POLYMETHYL METHACRYLATE	10^{-5}
POLY OLEFIN SULFONES	10^{-6}
POLY HEXYL ISOCYANATE	10^{-5}
DIAZOQUINONE PHOTORESIST	10^{-5}

NEGATIVE - INSOLUBILIZING TYPE

AZIDE PHOTORESIST	10^{-6}
POLY DIALLYL ORTHO PHTHALATE	10^{-6}
POLYSILOXANES	10^{-6}
EPOXIDIZED RUBBERS	10^{-7}
POLYGLYCIDYL METHACRYLATE	10^{-7}

Crosslinking side chains of R such as epoxy, olefin, or conjugated ketones have also been investigated. Traditionally all coatings cured by heat, MEV electrons, gamma rays, or UV light may find useful applications as high speed (thin film (0.1-1.0μ)) electron beam resists. The resolution of the negative electron beam resists at 1-2μ range is not as good as the equivalent positive electron beam resists. Since no photosensitizers are needed, it can be expected that thousands of vinyl polymers could be formulated into negative resists.

Since polymers with tetrasubsituted centers are difficult to synthesize, two main types of positive resists have been disclosed. Polymethylmethacrylate[14]or polymethyl isopropenyl ketone[15]which undergo side chain elimination and subsequent main chain fracture have been used as positive electron beam resists (cf. Table VII).

The incorporation of a weak link in the main chain of a olefin sulfone copolymer such as poly - 1 - butene sulfone is a recent example of polymers with high G value[10]and high sensitivity 10^{-7}coul/sq. cm. needed to read and write patterns in minute throughput times.[16] The low ceiling temperature ($\sim25°C$) of some highly radiation sensitive sulfones severely limits the practical processing of resists. Polymer films which are deposited as cold films at low temperature by gas phase reactions including radiation processing such as plasma or UV, can be envisioned as the next generation of solventless resists of high sensitivity.

The equipment for processing polymers performs three major steps: coat-dry, expose, and develop-readout. Coating films greater than a micron is accomplished by paint techniques such as roll, dip, spray, or laminate. Thin coatings such as in microelectronics are applied by spinning the object and applying the resist solution. Ultrathin films are applied by polymerization of activated monomers onto the substrate. Solvent coatings can be dried by conduction, connection or other forms of energy such as infrared, microwave, or induction heating. After drying the films can be flood exposed by mercury vapor lamps or sprayed with KV electrons. Thin resist films are contacted printed with light or digitally patterned with submicron electron beams. The images are usually developed by organic or alkaline solvents by static or spray processing.

The efficiency of the exposure source is a critical cost and thruput factor. Ultraviolet sources output up to 10% of the input energy while 150 KV electron cure sources can be 70% efficient. To record high

resolution images, point sources are used but at a
sacrifice of low output intensity and efficiency.
Electron beams are the most accurately controlled than
deflected light, ion, or x-rays.

The processing equipment in resist technology has
advanced from the traditional batch tanks for develop-
ing, etching, and stripping to fully automated coating,
baking, exposing developing, etching, and stripping
systems. The automation of thick resist for printed
circuits was achieved in the late sixties and the
automation of thin films resist for semiconductor pro-
cessing has been made commercially available.[17] The
exposure of resists has switched from contact to
proximity to projection printing in a effort to extend
mask life. More durable masks of chrome or iron oxide
on glass have overcome the limited life of silver
emulsion masks. In the future electron beams are
envisioned to replace masked exposure.

Besides using the resists to etch copper boards,
metal parts, or silicon surfaces, new applications
have been disclosed. Spatial images have been holo-
graphically recorded in resists.[18] The resist systems
of siloxanes can be converted after imaging by oxida-
tion into passivated glass for direct formation of
insulated circuits.[19] The resist can be filled with
glass[20] or metals[21] and fired to form circuits
directly. In one application, the resists are filled
with electroless plating sensitizer for deposition of
metal films.[22] The resists can be used in the litho-
graphic sense as relief printing plates.[23] The
chemical milling of small machine parts is a economical
means of mass production. The general improvements in
various properties such as chemical and thermal
stability are desirable for extensive future appli-
cations. The commercial suppliers of resist have
established engineering labs to experience the customer
applications on multifarious insulator or conductive
substrates and to improve by experience the performance
of resist formulations.

In the last category of radiation sensitive
polymers, the development of ecologically sound photo-
degradable polymers has been a noteworthy application.

Polymers have been traditionally formulated with
ultraviolet absorbers or anti-oxidants to prevent
oxidative, photochemical, thermal, or biodegradation
during processing or in consumer products. Consumer
packaging products have been sensitized to photo-
degrade by the incorporation of ketone groups to absorb
3000A° sunlight exposure.[24] The Norrish elimination
of the adjacent alkane groups in ethylene carbon mon-
oxide copolymers with chain scission is proposed as a

likely degradation mechanism. In a realistic sense,
very little 2537 A° radiation is available from the
polluted atomsphere for photodecomposition. The poly-
meric additives in commercial plastics have to be
eliminated if reasonable degradation is to occur. The
biodegradable systems are more effective than photo-
degradation since uniform exposure is difficult to
achieve for waste materials. Perhaps, a combination
of bio-, photo-, or heat degradable plastics will be
produced for food products. Up to this point we have
surveyed the various applications of radiation
sensitive polymers, the compositions and chemical
parameters and briefly examined the processing
sequences.

Finally, the comparison of the efficiency of
various radiation sources is of imminent interest.
Each application requires a particular combination of
the material absorption and the radiation source. In
order to assess the efficiency of each of the systems,
several factors have to be taken into consideration.
Notable among these are the thickness of the film,
the absorption cross section, and the subsequent
chemical reactions in the exposed phase. As noted
before in Table II, the spectrum of energies used
range from high energy (MeV) electrons to lower
energy (KeV) electrons and x-rays to the lowest energy
(eV) ultraviolet rays. In some cases the absorption
cross sections are depth dependent functions as
typified by electron penetration into polymers (cf.,
figure 2). Hence the choice of electron beam energies
is strictly a matter of the penetration range desired
in the exposed medium. For thin resist films $(1-4\mu)$,
5-30kV electron beams are used in semiconductor
fabrication. The curing of thicker films $(10-1000\mu)$
requires a higher energy (0.05-2MeV) electron beam.

The image readout efficiency (a simple contrast
function for lithographic resist) can be related to
the ratio of the chemical or physical properties of
the exposed to unexposed molecular weights. A
relative comparison is given in Table VIII of various
exposable compositions.

The greatest change or contrast in material
properties occurs between a monomer (M) and a
polymer. (Pz) The

$$nM \longrightarrow Pn \rightleftharpoons Pz \longrightarrow P_{\infty}$$

radiation intiated polymerization has the highest
efficiency since amplification (up to 10^4) occurs
after initiation by conventional polymerization at
low (~5kcal.) activation energies. As the reaction
proceeds to high conversion, the propagating inter-
mediates are deactivated by the viscous media.

Secondly, low viscosity monomers cannot form films use-
ful in coating or ink curing and as resists.   Thus,
the amplification and contrast gain is lost by using
prepolymers Pn to obtain film forming properties.   From
a photochemical viewpoint, a polymerizable composition
would have a high speed but for practical imaging
contrast, the crosslinking reaction is the second best.

Although crosslinking (Pz⟶P∞) or scissioning
(P∞⟶Pz) have about the same G values (0.1-10) and
activation energies, (10-40 kcal/mole), a greater
change in physical properties for equivalent doses
occurs in going from a uncrosslinked to a crosslinked
polymer instead of lowering the molecular weight by
degradation.   Only two crosslinks per chain are needed
to achieve infinite molecular weight.   By the same
reasoning, the selective degradation of crosslinks in
a polymer network would form a high speed "positive"
resist or photodegradable film.

The crosslinking of polymers can be achieved by
three major reactions:(1) polymerization of multi-
functional monomers (e.g., tetraacrylates), (2) self-
crosslinking polymers (e.g., polyvinylcinnamates) and
(3) crosslinking agents (e.g., bisazides).   For the
choice of exposure source and cost, it appears that
high resolution imaging for small exposed areas is
achievable by ultraviolet or low KV electrons for sub-
micron dimensions.   In figure III, the exposure costs
for larger areas are considered to be lower than
thermal curing.

In thin films for microelectronics (1μ) the
exposure systems can be compared in Table IX.   As can
be seen, the typical ultraviolet (3650A°) exposure is
absorbed much more efficiently than electron or x-rays.
However, the higher energy electron beam can be focused
to submicron dimensions while the x-ray   exposure [25]
through a mask has a large depth of focus.

From the materials viewpoint, it is of interest to
examine the thermodynamics of radiolysis of polymers.
Since gamma radiolysis data is readily available,
polymers can be compared as in Table X.   Note that
materials having a large heat of polymerization tend
to crosslink under radiolysis.   The same polymers are
thermally resistant to degradation.   Degrading polymers
have low ceiling temperatures (<150°C) and low heats
of polymerization.

The G values (chemical events/100 ev absorbed) are
also indications of the tendency of a polymer to
degrade or insolubilize under any form of radiation
in excess of bond energies.   In Table XI, a compilation
of the G values is noted along with the expended energy
for each bond broken or formed.   In the case of

PENETRATION OF ELECTRONS
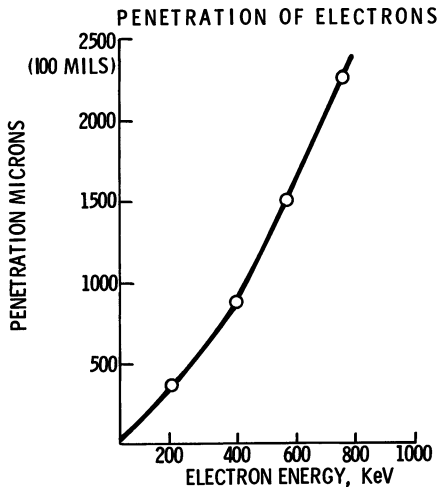
Figure 2. *Penetration of electrons*

TABLE VIII

Image Differentiation

IMAGING PROPERTY	TYPE OF IMAGE	
	Positive	Negative
Solubility Rate	Inc	Dec
Volatilization Rate	Inc	Dec
Tackiness		Dec
Adhesion		Inc
Adsorption	Inc	Dec
Viscosity	Dec	Inc
Solidification	Dec	Inc
Permeability	Inc	Dec
Transmission	Inc	Dec
Refraction	Dec	Inc

COST COMPARISON OF CURING
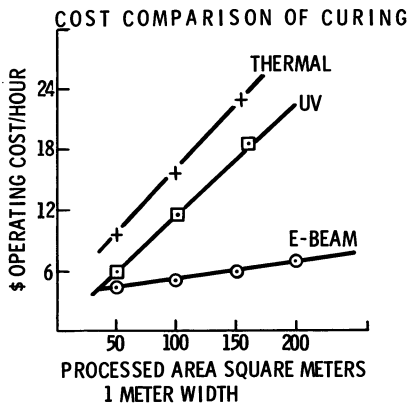
Figure 3. *Cost comparison of curing*

TABLE IX

Efficiency of Radiation Reactions in Films

Energy System	Typical absorption percent	Reaction efficiency percent	Overall efficiency percent
E-Beams,Ion beams(20-50KV)	4 - 1	1	0.01
X-Rays,Gamma (50KV-1MEV)	1 - 0.01	0.5-1	0.0005
UV (typ.3650A°)	50	25	12.5

TABLE X

Comparison of Crosslinking Vs Scission of Polymers

Polymer	Radiation Effect	Heat of Polymn. Kcal/mole	Monomer yield on pyrolysis %
Poly-			
-Ethylene	Crosslink	22	0.025
-Propylene	" "	16.5	2.0
-Methyl acrylate	" "	19	2.0
-Isobutene	Scission	10	20.0
-Methyl methacrylate	" "	13	100.0
-alpha-Methyl styrene	" "	9	100.0

from D.E.Roberts,J.Res.Natl.Bur.Std., **44**,221,(1950)

degrading polymers, the sulfones expend the least energy (12.5ev/bond) which is still in excess of the bond energy (4-5ev). Competing reactions such as emission, charging, and thermal dissipation of the absorbed energies reduce the effectiveness of absorbed ultraviolet electron, x-ray, or ion beams.

From Table XI, it can be seen that polymers have spectrum of doses necessary to obtain maximum readout efficiency. We will examine in the following example the imaging of a positive electron beam resist as a function of dose and molecular weight-solubility changes.

A positive resist system can be of either two types. The classical diazoquinone system represents a photochemical rearrangement reaction which is the basis of commercial photoresists. Scissioning or degradation of a polymer chain by light or electrons is a later example of solubility induced change. We will examine this change in detail.

A positive electron beam resist image is developed by immersion in a solvent which dissolves the exposed region at a rate (Sf)which is faster (approx. 10X) than the unexposed rate (Si . The rate of dissolution of a linear polymer is related to its molecular weight M by the Uberreiter function (26):

$$S = k M^{-\alpha} \qquad [1]$$

where α is the solvent-polymer solubility parameter. In figure 4, the increase in solubility or decrease in viscosity is illustrated for a corresponding decrease in molecular weight.

In a positive resist the image readout efficiency for a particular exposure dose is defined as the ratio of solubility rates:

$$SR = \left[\frac{S_f}{S_i}\right] = \left[\frac{M_i}{M_f}\right]^{-\alpha} \qquad [2]$$

The image readout can be derived and related the exposure dose by the equation(27):

$$SR = (1 + k\phi\varepsilon Q M_o)^{\alpha} \qquad [3]$$

where k is a constant, ϕ is the quantum efficiency or "G" value, Q is the dose, E is the absorption co-efficient of the resist, and Mo is the initial molecular weight. The exposure produces a randon scissioning of the polymer chain which at low dose is more sensitive to high molecular weights. In figure 5, a

TABLE XI

Radiation Efficiency in Polymeric Systems

Class of Polymer	Typical Examples	Efficiency* of Radiation reaction /100 ev	Overall Bond breakage or formation energy- ev
Degrading (mainly side chain)	Poly- -MIPK -TBMA -Isobutene Cellulose	1.4 2.5 2.4 6-10(??)	71 40 42 16-10
Degrading (Main chain scission)	-sulfones -esters	8 1.4	12.5 71
Crosslinking	vinyl compounds	0.3-1.0	300-100
Polymerization (solid phase)	Acrylo- -nitrile Styrene	0.15 0.6	670 170
(liq.phase)	Styrene	0.7	142

*Arbitarily for 100 eV absorbed,typical G values
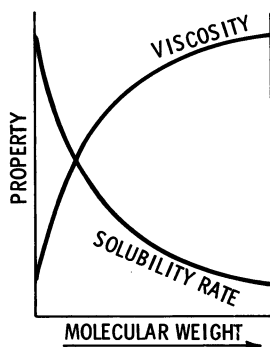
Figure 4. Contrast by molecular weight

typical plot for this relation is shown. For practi-
cal readout, a solubility ratio of 8-10 is used to
diminish the unnecessary loss of unexposed resist in
the development step. In the same figure is noted the
lower doses required to image a negative electron or
photoresist. Negative resists use crosslinking re-
actions which are more efficient than a simple poly-
merization (reverse of scissioning in positive
resists) reaction to form high molecular weights.

     Negative resists in principle should require the
same dose and can be treated by equations 1-3, if
polymerization or scissioning where simple reversible
processes. In practice, however, multifunctional
monomers or crosslinking reactions are used to achieve
more efficient insolubilization of polymer formula-
tions. The theory of crosslinking (28) and multi-
center polymerization with monomers is very complex
and difficult to experimentally corroborate due to
the insolubility of the polymer formed. From a
elementary viewpoint, the crosslinking reaction as
illustrated in Figure 6, is proportional to dose. The
corresponding change in molecular weight or solubility
for a linear polymer (as described by eqn 1.) is very
large and proportional to a large power function of
molecular weight.

     Tetrafunctional monomers or polymers with vinyl
side chains offer the unique possibility of quantum
amplification by spatial polymerization. This re-
action is also shown in Figure 6. Multicentered
polymerization by chain reaction provides high speed
and the mechanical-physical strength of a crosslinked
polymer. However, because of the rapid increase in
viscosity, the amplification may not be as large as
expected.

     In summary, the radiation processing of polymer
films has become a major technological process. One
dimensional films are rapidly processed as eco-
nomically as conventional thermal curing. Image
recording requires coating-drying, exposure, and
developing processing. The thruput decreases and
the cost increases with the miniaticrization of image.
The costs are incurred in the sophistication of
mechanical, electronic, and optical equipment used to
record high density information which will eventually
only be seen in an electron microscope.

     The processed products range from cured laminates
or inks to lithographic plates and copy papers to
memory and logic computer circuits. The curing
systems are a new technology which offers low costs,
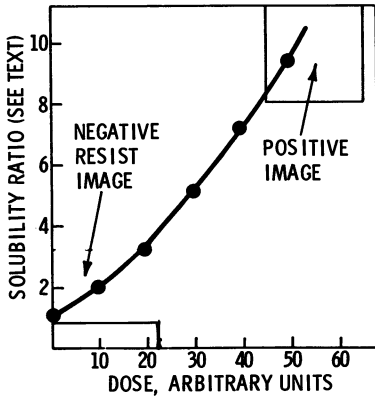
Figure 5.   Solubility ratio for photoresist
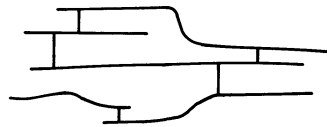
Typical Crosslinking : Each link requires at least one
Radiation Event
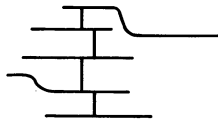
Network Formation   : Requires only one Radiation
By Chainlinking   Event

*Figure 6.   Radiation insolubilization of poly-
mers*

fast cure, and solventless coatings. Resist materials
have improved in material consistency, purity, and in
performance. More efficient energy sources are needed
to conserve electrical energy and to lower the cost of
processing.(cf.Table XII)

     Materials or formulations used in a specific
application should be considered for broader applica-
tions in other areas. Curing laminates or inks may be
useful as lithographic resists or as microelectronic
negative electron beam resists. Positive photoresists
may be applicable as photodegradable plastics. The
basic compositions of sensitive polymers range from
polymerizable monomers to crosslinking or degrading
high polymers. One component systems are mainly found
in systems exposed by electrons or other forms of high
energy radiation. Photoexposure predominates the
radiation processing of polymers but electrons are
finding increased usage in processing coatings or in
fabricating sub-micron electronic circuits. The most
efficient process is the photocrosslinking or photo-
insolubilization of a polymer composition. Images can
be read out or developed by a wide variety of pro-
perties including solubility, adhesion, volatization
and fixing by chemical coupling. The images are
either permanent films able to withstand agents and
repeated mechanical impact as in printing or temporary
etch stencils for electronic circuit fabrication.

     At present, very little amplification of the
quantum of absorbed energy occurs in insolubilizing or
degrading systems. Only polymerization in the bulk
provides a mobile reaction media for amplification of
one intiator fragment into several units of prepoly-
mers. Basic research is needed in amplification by
chemical agents which can diffuse into a polymeric
media and initiate crosslinking or further degradation.
The continued research and development of radiation
sensitive polymers will lead to a broader base of
applications. If the sensitivity could be enhanced to
the speed of the slowest emulsion, each specific
application would be significantly lower in exposure
costs. Future images will range in sophistication
from one-dimensional protective coatings to multi-
dimensional colored holographic images.

TABLE XII

Comparison of Radiation Processing of Polymers

Property	Most Efficient System
Penetration Depth	
microns	Low energy electrons (20KV)
mils	High energy electrons(50 KV to 1 MEV)
Particle energy	Short UV , Electrons
Energy Transfer (Ions,electrons radicals and Charge transfer)	Thermal radical propagation (typical gel-prepolymer system)
Chemical Efficiency	Insolubilizing polymerizations (Ideal if monomer is highly soluble in polymer, but to obtain high contrast polymer should be highly insoluble in monomer,hence contradicting limits)
Equipment	
cost	UV and low KV e-beams for small substrates
availability	UV
throughput	E-Beams(large areas) UV (small areas) small area substrates- UV

References

1.   W. Deninger and M. Patheiger.
     J. Oil. Col. Chem.Assoc. 52, 930-45, 1969.
2.   K. Morganstern, Organic Coating and Plastic
     Chemistry Preprints, American Chem.Society 165th
     Meeting, 1973, pp. 256-265.
3.   H. Diepstraten, Trans. of Inst. of Metal Finishing
     51, 199, 1973.
4.   C. Southwick, Modern Packaging, 64-70, 1972.
5.   S. Schroeter, Organic Coatings and Plastics-Chem-
     istry Preprints, Amer. Chem. Soc. 164th Meeting
     1972, pp. 401-410.
6.   A. Poot, G. Delzenne, R. Pollet and V. Landou,
     J. Photographic Sci., 19, 88 (1971).
7.   J. Celeste and R. Hecart in Soc. of Photog.
     Science and Eng. Proceedings of Applications of
     Photopolymers,1970, pp.42-53.
8.   Ger. patent, 865, 860 (1953), U.S.patent,3,046,120
     (1962).
9.   Chem Abstr., 81 97720 t (1974)
10. U.S. patents 3,462,267; 3,448,089 (1969)
11. W.Moreau, Polymer Preprints, American Chem.Society
     10, 362-367 (1969).
12. N. Clecak, R. Cox, and W. Moreau, Soc. of Plast.
     Eng. Regional Technical Conference on Photopoly-
     mers, 1973, pp. 43-50, U.S. pat. 3,695,886.
13. G. Paal, V. Strahle, and G. Kielhorn, J. Electro-
     chem Soc., 120, 1714 (1973).
14. M. Hatzakis, J. Electrochem. Soc., 116, 1033 (1969)
15. A. Levine, M. Kaplan, and J. Fech, J. Poly. Sci.,
     Part A-1, 11, 311 (1973).
16. L. Thompson and M. Bowden, J. Electrochem. Soc.,
     120, 1722 (1973).
17. Anon, Electronic Pkg. and Production, July 1974,
     Vendor Equipment Guide.
18. R. VanRenesse, Optics and Laser Technology, 24-27
     (1972).
19. E.D.Roberts, Third International Conf., Electron,
     Ion Beam, and Laser Technology, 1968, p.571.
20. U.S.patent, 3, 474, 718 (1969).
21. D. Ulrich-Electronic Pkg.& Production, 14, 226
     (1974).
22. N. Feldstein and T.Lanscek, RCA Rvw 439-442 (1970)
23. T.Protzman, SPE Jrnl, 29, 14 (1973).

24. American Chem Soc.-<u>Polymer Preprints</u>., "Symposium
     on Plastics in Ecology" 13,626-665(1972).U.S.
     patents,3,767,401;3,679,777 (1972) 3,853,814(1974)
25. P.V. Lanzo and E.G. Spencer, Appl. Phys. Letters,
     <u>24</u> 289 (1974)
26. K. Ueberreiter and F. Asmussen
     J. Poly. Sci., <u>57</u> 187 (1962)
27. N. Viswanathan, C. Ting, and M. Hatzakis, Sixth
     International Conference on Electron, Ion, and
     Laser Technology, Electrochemical Society, 1975,
     P532
28. O. Saito, Chapter 11 in <u>Radiation Chemistry of
     Macromolecules</u>, M. Dole, Editor, Academic Press
     1972, Volume I.

Bibliography

A: <u>General Interest</u>
i)   J. Kosar,"Light Sensitive Systems",John Wiley
     (1965)
ii) M.S.Dinaburg,"Photosensitive Diazo Compounds".
     Focal Press, (1965)
iii) SPE Symposia, Photopolymers: Principles, Processes
     Materials, Soc.of Plastic Engineers,Mid-Hudson
     Section,(1967,1970,1973).
iv) M.Dole,"Radiation Chemistry of Macromolecules",
     Academic Press, (1973).
v)   SPSE Symposia-"Unconventional Photographic Systems"
     1964, 1967, 1971

B.   <u>Microelectronics</u>
i)   M. Crooke and S. Wiltstock, Trans. S. African In-
     stitute of Elec. Engineers <u>64</u>, 194 (1973).
ii) K. G. Clark, Microelectronics <u>3</u>, 450 (1971).
iii) L. Maissel and R. Glang "Handbook of Thin Film
     Technology", McGraw-Hill, N.Y., (1970).
iv) Kodak Seminars on Microminiaturization & Photo-
     resists (Professional, Commercial, Industrial
     Marketing Div. Eastman Kodak Co.)1965-1974.
v)   J.B.Lounsbury and D.L.Klein, Electronics Packaging
     <u>14</u>, 60 (1974).
vi) IEEE Symposia on Electron, Ion, Laser Beam Tech-
     nology, San Francisco Press, 12 volumes.
vii) International Conf. on Electron & Ion Beam Tech-
     nology, Electrochemical Society, 6 volumes.

viii)G.Brewer, IEEE Spectrum, Jan. 1971 (29-45).

ix) M.Hatzakis, Kodak Symposium on Microminiaturiza-
     tion, Atlanta, Oct. 1973.

C: Electron & UV Curing
i)   W.H.T.Davison, J.Oil & Color Chem.Assoc.,52,947
      (1969)
ii)   H.M.P.Diespraten, Trans.Inst.Metal Finishing, 51,
      199 (1973).
iii) M.W.Ranney, "Electrodeposition & Radiation Curing
      of Coatings" Noyes Data Corp.,Park Ridge,NJ(1970)
iv)   W.Deninger and R.Pethiger, J.Oil & Color Chem.
      Assoc.,52, 930 (1969).
v)   D.J.Garlick, Modern Packaging, p.64, Dec. 1972.

D: Lithographic Printing Plates
i)   A. Poot, G. Delzenne, R. Pollet, and U.Laridon,
      J.Photographic Sci., 19, 88 (1971).
ii)   P. Walker, V.J.Webers and G.A.Thommes, J.Photo-
      graphic Sci., 18, 150 (1970).
iii) T.F.Protzman, SPE Journal, 29, 14 (1973).
iv)   D. Derenzo, "Polymers in Lithography". Noyes
      Data Corp., Park Ridge, N.J. 1971.

E: Photoconductive Systems
i)   C. Claus in SPSE Symposium on unconventional
      photographic systems, "Electropohtographic Pro-
      cesses and Materials" State of Art, 1971.
ii)   A. Tweet, ibid., "Electrophotography" State of
      Art, 1971.

F: Plasma Treatments
i)   J.R. Hollahan and A.T. Bell, Techniques and
      Applications of Plasma Chemistry, John Wiley,
      1974

Ultraviolet Curing of Pigmented Coatings

VINCENT D. McGINNISS

Glidden-Durkee, Div. of SCM Corp., Strongsville, Ohio 44136

It has now been well established that UV-curing
of coatings can be achieved and there have been many
references in the literature as to the development and
descriptions of these coatings and the UV-curing
art.[1,2] Most of these literature references describe
commercial curing of clear finishes as well as UV-
curable inks.[3-6] This paper explores some of the
parameters associated with non-ink low viscosity pig-
mented UV-curable coatings.

Pigmentation Effects on UV-Curable Coatings. Pig-
ments cannot be thought of as inert additives in the
UV-curing of opaque or colored coatings. The folowing
are some of the considerations on the effects of pig-
ments during the curing process:

(1) Light scattering (internal) or external reflect-
     ance) and penetration of energy.[4]
(2) Refractive index and wavelength of light absorp-
     tion of the pigment.
(3) Free radical catalytic activity and viscosity
     effects.
(4) Particle size and degree of dispersion.
(5) Amount of pigment and film thickness in relation
     to hiding power and effects on cure speed.
(6) Photophysical properties of pigments.[7]

The refractive index of a pigment at each wave-
length is determined by its crystal structure. Titan-
ium dioxide pigments (rutile and anatase) differ from
each other and from other white pigments or crystalline
substances, like silicon dioxide, in the proportion of
radiant energy that is transmitted, absorbed, or re-

flected at each wavelength by a film in which it is
contained. The maximum energy absorption of SiO$_2$ is
about 150 to 200 nm and the maximum for anatase TiO$_2$
is in the near UV region and rutile TiO$_2$ is nearer to
the visual portion of the spectrum (Figures 1 and 2).
Refractive index is highest at a wavelength slightly
longer than the wavelength of maximum absorption and
decreases as the wavelength energy increases (Figure
1).

The optical properties of rutile and anatase TiO$_2$
are different in that anatase is more reflective than
rutile at 380 nm and rutile is very strongly UV-absorb-
ent at 380 nm (Figure 2).[8] The optical properties
of the various pigments strongly effect photosensitizer
absorption and photochemical activity.

   Photosensitizers or Photoinitiators. The primary
component in the UV-curable coating system is the
photosensitizer or photoinitiator (a light sensitive
catalyst that upon absorption of energy results in a
free radical species that can initiate acrylic monomer
polymerization).[9]

The first rule of photochemistry is that in order
for a light sensitive reaction to take place, light
energy, at the appropriate wavelength, must be absorb-
ed by the reacting molecule (photoinitiator).[10] In
opaque or colored coatings there is competition between
pigment and photocatalyst in that the photoinitiator
must

(1)   absorb light energy in the same region of the ab-
      sorption spectrum as the pigment. In this case,
      the molar extinction coefficient (ϵ) of the photo-
      initiator must be large or a large concentration
      of photosensitizer is necessary to effect photo-
      polymerization.
(2)   not absorb light energy, or have a different ab-
      sorption spectrum, in the same region as the pig-
      ment. In this case, the molar extinction coeffi-
      cient of the photoinitiator may be small and
      smaller concentrations of photoinitiators can be
      used.

In each of these cases, the thickness of the coat-
ing film is very important (inks 2 to 10 microns versus
a fluid coating of 0.5 to 2 mils) on the amount of
light energy absorbed by the photoinitiator. The
amount of pigment, dispersion, and reflectance of the
paint film are also important for light absorption by
the photocatalyst.
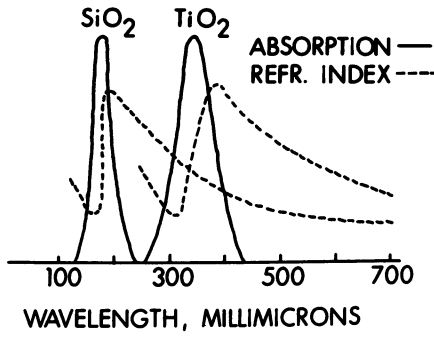
Figure 1.
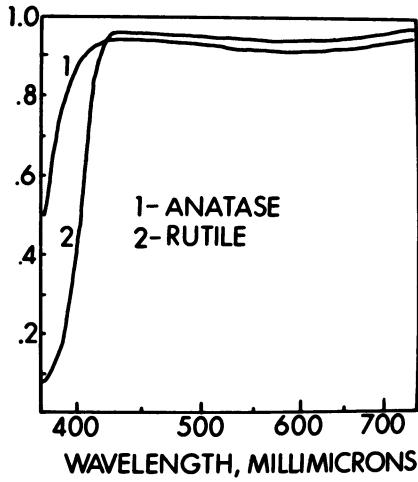
Figure 2.

In Figure 3 are the plots of absorption versus wavelength of four photoinitiators used in the UV-curing of pigmented coatings:
Michler's Ketone derivatives 4,4'-bis(diethylamino) benzophenone (DEABP), λ max 352 nm, ε = 40,700;
Thioxanthone (TX), λ max 366 and 378 nm,
ε = 5,200 and 6,100
2-Chlorothioxanthone (2CTX), λ max 370 and 385 nm,
ε = 4,040 and 4,650
Benzanthrone (BZA), λ max 380 nm, ε = 10,900
       In Figure 4 one can see a comparison of photo-sensitizer absorption λ max superimposed onto the UV-visible absorption-reflectance spectra of rultile ti-tanium dioxide. Michler's Ketone derivatives (DEABP) absorb energy in the same region as the very strong UV-absorption of rutile TiO_2 but these compounds have large extinction coefficients in this region and are acceptable photocatalysts for curing of a pigmented coating. Thioxanthone derivatives (TX and 2CTX) have λ max values near the absorption edge of rutile TiO_2 while benzanthrone (BZA) is outside of this absorption edge and absorb energy in the visible region of the spectrum. All of these photoactive compounds can be used to cure opaque coatings systems.
       Some other factors to consider in the photocuring of coatings are self quenching of photoinitiators at high concentrations and the various effects of light intensity as well as spectral output of the light source. Pigmentation may also quench photosensitive initiation reactions through energy transfer of photo-physical deactivation pathways as well as radical ter-mination reactions.(7)
       After light absorption by the photocatalyst, the next step is photoproduction of free radicals that initiate polymerization of the acrylate unsaturated monomers, oligomers, and polymers contained in the UV-curable coating system.

Mechanisms of Photoinitiation
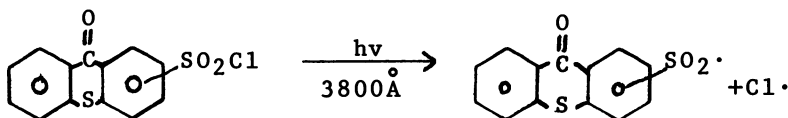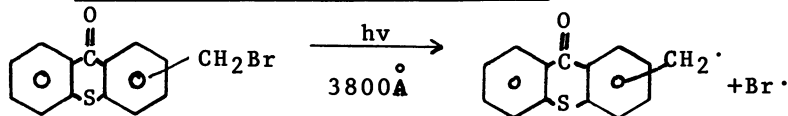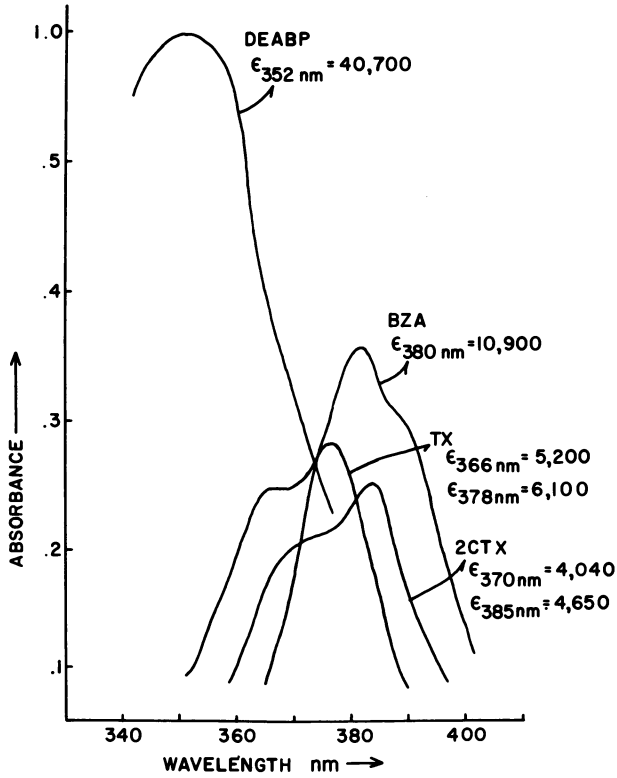
Figure 3.
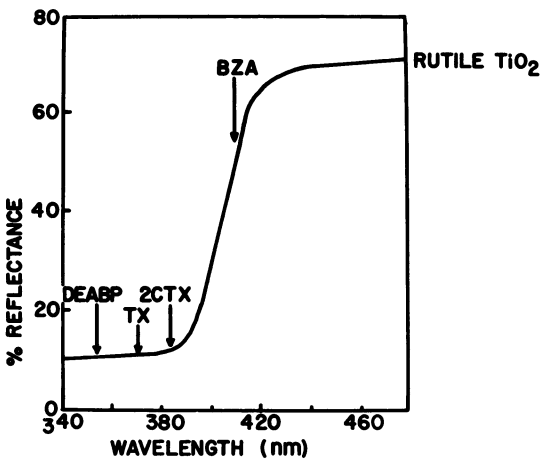
Figure 4.

Direct Photofragmentation
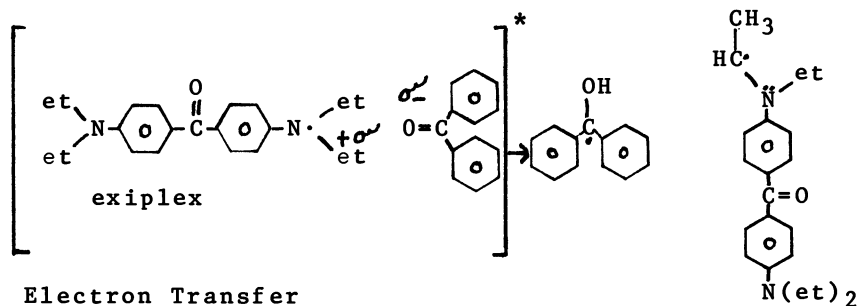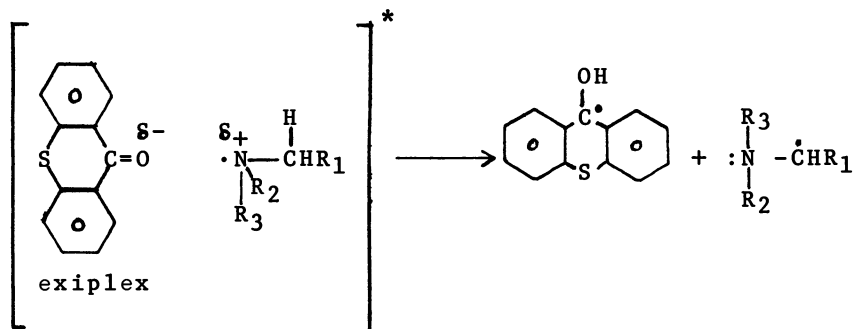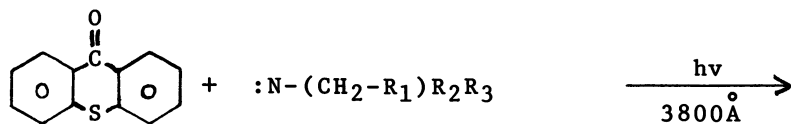
Electron Transfer

Some basic mechanisms of photoinitiation are:

(1)   Direct photofragmentation into free radicals.
(2)   Electron transfer followed by proton transfer and
      formation of free radicals.

In direct photofragmentation, the thioxanthone
derivative absorbs light at about 380 nm which results
in homolytic cleavage of the methylene-halogen or sul-
fonyl-halogen bonds of the parent molecule to produce

free radical species.[11]

In electron transfer reactions, the thioxanthone derivatives absorb light at 380 nm and then forms an exiplex in which an electron is transferred from the nitrogen atom to the excited carbonyl of the thioxanthone. This exiplex then undergoes proton transfer followed by production of initiating free radicals.[12] Michler's ketone derivatives absorb UV-energy at 360 nm and forms an exiplex, through electron transfer of the nitrogen atom, with a ground state benzophenone molecule. This exiplex then decomposes into free radical species via proton transfer and reduction of the benzophenone into a benzpinacol radical.[13,14]

Thioxanthone
(TX)

Quinoline Sulfonyl Chloride
(QSC)

$(TX)_0$ donor $\xrightarrow{hv}$ $(TX)_3$* excited state donor

$(TX)_3$* + [structure SO_2Cl] $(ground state acceptor)\longrightarrow$

$(TX)_0$ + [excited acceptor structure SO_2Cl]* $\longrightarrow$ [free radical products structure $SO_2\cdot$] + $Cl\cdot$
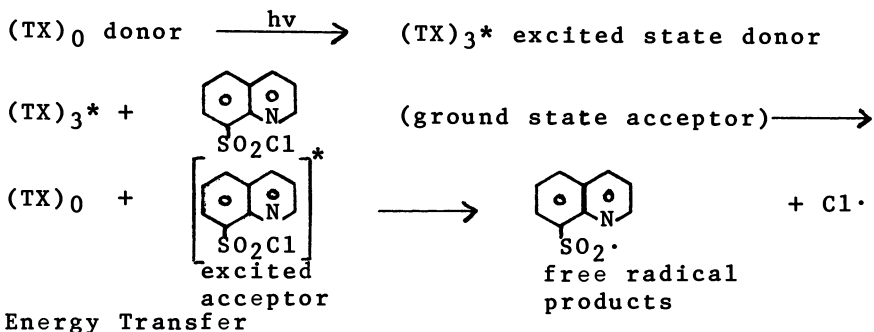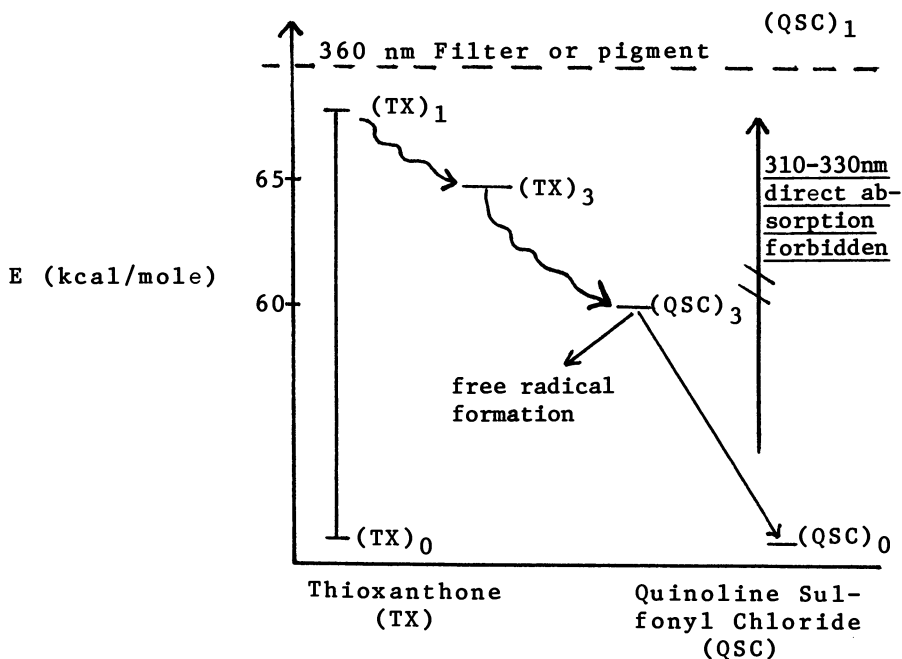
Energy Transfer

In this type of energy transfer reaction, thio-
xanthone (TX) is the only active light absorbing
species (cut off filters or titanium pigments strongly
absorb radiation below 360 nm) contained in the re-
active paint system. Thioxanthone alone does not
photoinitiate polymerization of vinyl unsaturated
monomers. Quinoline sulfonyl chloride (QSC) absorbs
light at approximately 310-330 nm which results in
homolytic cleavage of the sulfonyl-chloride bond to
produce initiating free radical species (clear reactive
systems).
        In filtered or pigmented coating systems all light
transmitted at 310-330 nm is absorbed by the filters
or pigment so direct absorption or excitation by QSC
is not allowed. The only way a photochemical initia-
tion can take place is through the light absorption of
energy (370-380 nm) by TX which can then transfer its
absorbed energy to a ground state QSC molecule and re-
sult in free radical formation (see diagram).[15]
        The triplet energy for TX is 65 kcal/mole and the
triplet energy for QSC is 60 kcal/mole (ΔE = 5 kcal/
mole excess) which meets one of the basic requirements
for efficient energy transfer i.e. E_t donor (TX) > E_t
acceptor (QSC).[10]

Experimental

        The same experimental conditions were used as
previously described in reference 13 for the photo-
polymerization of methyl methacrylate (MMA) with 4,4'-
bis(diethylamino) benzophenone (DEABP) 1×10^{-2}M in com-
bination with 3×10^{-2}M benzophenone. The dilatometric
irradiation equipment is shown in Figure 5. This
apparatus allows the following of rates of photopoly-
merization (R_p) of MMA in the presence of various con-
centrations of pigments and also allows measurement of
changes in light intensity (I_o) as % transmittance (T).
The pigment used in these experiments was untreated
chloride process rutile titanium dioxide (Glidden Pig-
ments Division, Baltimore, Md.). This was obtained as
a water slurry (pH 1-3) and was screened before using.
Ultraviolet spectra of various photosensitizers (in
THF) were taken with a Perkin Elmer 350 spectrophoto-
meter.

Results and Discussion

        One of the unusual features of the UV-curing of
pigmented coatings is that the apparent rate of poly-
merization (R_p) appears to be somewhat faster than the

conventional clear coatings. One example in the lit-
erature is the thermal and photochemical polymeriza-
tions of MMA in the presence of silica gel pigments.
These results show that the addition of colloidal
silica to MMA markedly decreases the time required to
complete the polymerization. These effects could be
caused by the change in viscosity of the dispersion
due to the silica because an increase in viscosity
would be expected to reduce the rate constant (k_t) for
termination and effect the overall rate of polymeriza-
tion (R_p k_t-1/2). The acceleration of the rate of
polymerization or conversion was shown to occur at
concentrations of silica where there was little effect
on viscosity of the dispersion. Another mechanism is
the stabilization of free radicals on the pigment sur-
face which reduces mutual termination reactions of
growing radical chains but the Authors found no evi-
dence of polymer grafting onto the silica surface.
The silica pigment was thought to exert some sort of
catalytic effect on the rate of polymerization.[16]
     In the photopolymerization of MMA in the presence
of rutile TiO_2 it was noticed (Figure 6) that as one
increases pigment concentration there is a correspond-
ing decrease in light transmission (I_o) through the
reaction cell. The R_p for the reaction shows a slight
increase up to a limiting value of pigment concentra-
tion at which point the R_p decreases corresponding to
the decrease in I_o. This relative increase of R_p at
decreasing I_o could be a measure of catalytic activity
or light reflectance and scattering of the pigment.
     Clear or pigmented liquid photocurable coatings
can be applied to a flexible substrate (metal, poly-
ethylene or filter paper) and the relative rate of
cure or network formation as a function of changes in
dynamic mechanical properties versus exposure time can
be determined.
     Figures 7 and 8 contain a diagram and the energy
calculations for a simple flash lamp circuit. This
xenon flash lamp (L_1) was used to cure films on a
torsion pendulum (Figure 9). The theory and manufact-
ure of conventional torsional pendulums have been des-
cribed elsewhere but a simple diagram and basic calcu-
lations for the pendulum are shown in Figures 9 and
10.[17,18]   Both pigmented and clear coatings were
cured by this technique either with flash or steady
state illumination from a 450 watt medium pressure mer-
cury lamp (L_1). Figure 11 shows a sample trace of the
torsional pendulum before and after irradiation. Be-
fore irradiation the coating is a fluid viscous liquid
and exhibits a high degree of damping (peak to peak

Figure 5.

Figure 6.

R_I — LAB RHEOSTAT
T_I — 15 KV, 30MA (neon sign trans.)
D_{1-4}—RCA CR-110, 10 KV
R_2 — 250 K, HIGH VOLTAGE
R_3 — (10) 25K, 10 WATT

V — VOLTMETER
S_{1-3}-HIGH VOLTAGE SWITCHES
S_4—SPARK GAP
C — 20KV 10 μF CAPACITOR
L — XENON FLASH LAMP
       XENON CORP
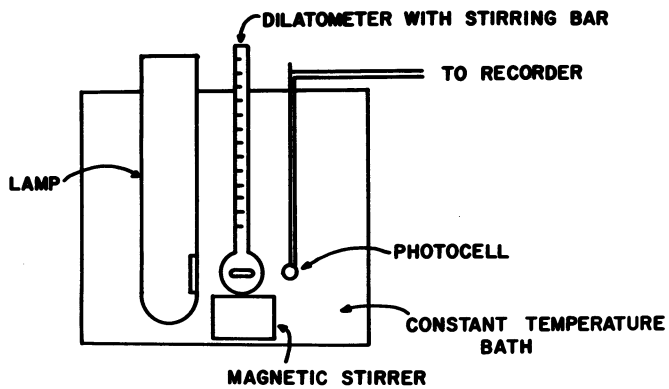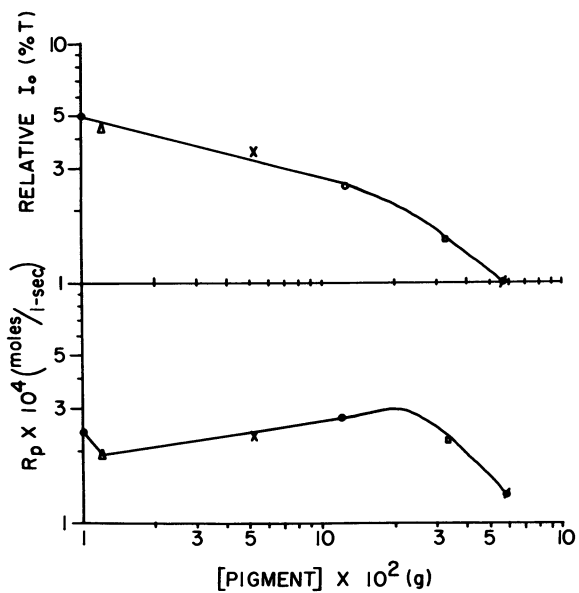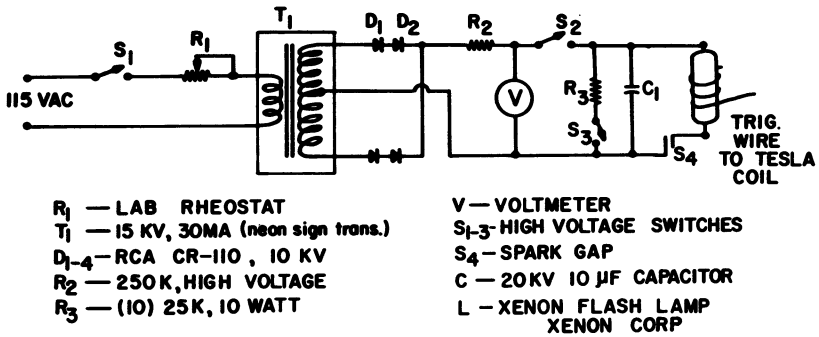
Figure 7.

$$E = \frac{CV^2}{2}$$

C—STORAGE CAPACITY IN FARADS
V—VOLTAGE ON C IN VOLTS

C = 10 μF
V = 5000 VOLTS
E = 125 J

$$P = \frac{CV^2}{2} \times F$$

P—AVERAGE POWER DELIVERED TO
    FLASH TUBE
F—FLASHES PER SECOND
FLASH DURATION TO 50% PEAK $\cong$ 20–
    40 μ SEC.
QUANTA FLASH (200–400 nm) $\cong 10^{20}$ QUANTA

Figure 8.
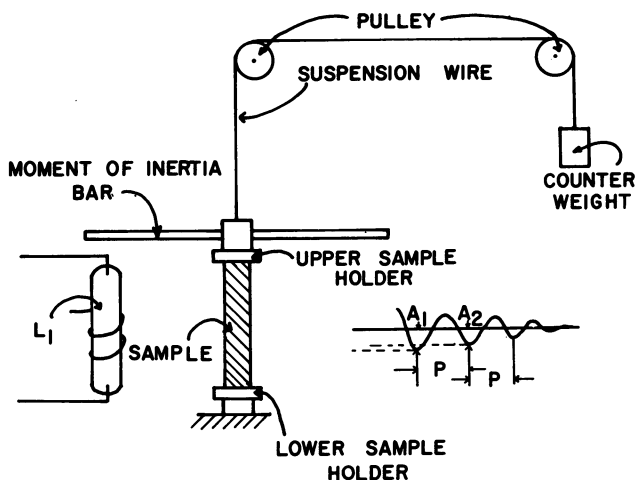
Figure 9.

$$G = K \frac{I}{P^2}$$

$$K = \frac{38.54 \, LI}{CD^3 \mu P^2}$$

G—SHEER MODULUS IN DYNES/CM^2
L—SAMPLE LENGTH IN INCHES
C—SAMPLE WIDTH IN INCHES
D—SAMPLE THICKNESS IN INCHES
I—POLAR MOMENT OF INERTIA BAR
    IN G—CM^2
P—PERIOD OF OSCILLATION IN SEC.
μ—SHAPE FACTOR C/D

$\Delta - \ln\left(\frac{A_1}{A_2}\right) = \ln\left(\frac{A_2}{A_3}\right) = \cdots$

Δ—LOG DECREMENT

Figure 10.
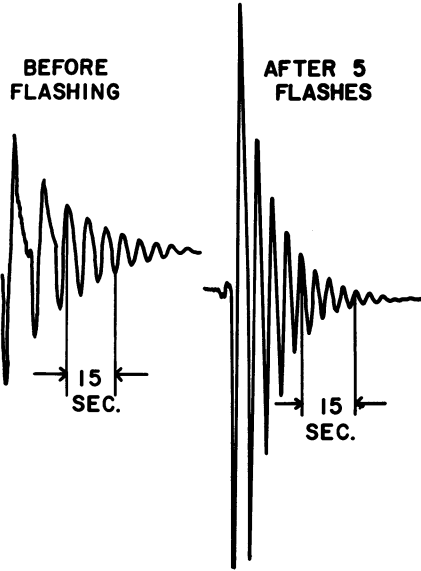
Figure 11.
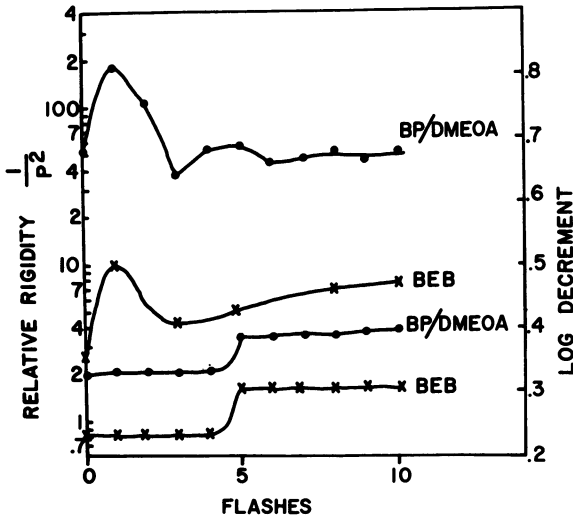
Figure 12.

distances are large and there is a large rapid decrease
in amplitude). After irradiation the coating under-
goes curing which influences the relative rigidity of
the sample and the degree of damping becomes lower
(peak to peak distances are shorter and the relative
change in amplitude of the waveform is smaller or shows
less damping).[19]

In Figure 12 is a typical curing curve for a coat-
ing as a function of relative rigidity (K^1/p^2), log
decrement ($\ln \Sigma\,A^n/Am+1$) and flash irradiation. The
coating (0.1g sample), pentaerythritoltriacrylate
(PETA) sensitized with 2% n-butyl ether of benzoin
(BEB) or 2% benzophenone (BP)/3% methyldiethanolamine
(MDEOA), was cured between thin polyethylene sheets
and as the curing reaction took place, relative rigid-
ity stayed fairly constant until a final breaking point
was reached after 5 irradiation flashes (5,000 volts/
flash). A damping increase occurred after initial
radiation then decreased rapidly at the onset of
further gelation.

In pigmented coatings the relative increase of
change in rigidity or decrease in damping as a function
of exposure time for different pigments at equal PVC
follow the order: SiO_2 > anatase TiO_2 > rutile TiO_2.
The relative changes in rigidity (K^1/p^2) or log de-
crement are a measure of cure for the coating.

The data at this time is only qualitative but
efforts are being made to develop the torsional pen-
dulum-UV-curing techniques and to quantify relation-
ships between relative rigidity, damping, gel-point,
vitrification, and irradiation intensity or exposure
time for clear as well as pigmented photocurable coat-
ings.

Further work is planned to determine the exact
parameters associated with photocuring of pigment coat-
ings and the development of more efficient photoiniti-
ators.

References

1. Kinstle, J., Paint Varnish Prod., 17, June (1973).
2. Special Radiation Cure, Issue Paint Varnish Prod.,
    August (1974).
3. Bassemir, R. W. and Bean, A. J., paper presented
    at 26th Annual Meeting of TAGA, St. Paul, Minn.,
    May 13-15, 1974; to be published in TAGA Pro-
    ceedings.
4. Wicks, Z. W., paper presented at 14th Annual
    Coatings Symposium, North Dakota State University,
    Fargo, North Dakota, June 3-5, (1974).

5.   Vanderhoff, J. W., ibid.
6.   Huemmer, T. F., Journal of Radiation Curing, $\underline{9}$, July (1974).
7.   Allen, N. S., et al, Polymer Letters, $\underline{12}$, 241 (1974).
8.   Patterson, D., "Pigments", Elsevier Publishing Co., New York, (1967).
9.   McGinniss, V. D., and Dusek, D. M., J. Paint Tech., $\underline{46}$, 23 (1974).
10. Turro, N. J., "Molecular Photochemistry", W. A. Benjamin, Inc., New York, (1967).
11. McGinniss, V. D., U. S. Patent 3,827,956; 3,827,957; 3,827,958; 3,827,959; 3,827,960 (1974).
12. Sander, M. R., Osborn, C. L., and Trecker, D. J., J. Polymer Sci., $\underline{10}$, 3173 (1972).
13. McGinniss, V. D., and Dusek, D. M., Am. Chem. Soc. Div. Polymer Chem. Preprints 15, 480 (1974).
14. McGinniss, V. D., Paper presented at 14th Annual Coatings Symposium, North Dakota State University, Fargo, North Dakota, June 3-5, (1974).
15. McGinniss, V. D., U. S. Patent 3,857,769 (1974).
16. Manley, T. R., and Murray, B., European Polymer Journal, $\underline{8}$, 1145 (1972).
17. Pierce, P. E., and Holsworth, R. M., J. Paint Tech., $\underline{38}$, 263 (1966).
18. Nielsen, L. E., "Mechanical Properties of Polymers", Reinhold Publishing Corp., New York, (1962).
19. Gillham, J. K., J. Macromol. Sci. Phys., $\underline{89}$ (2), 209 (1974).

11

Oxygen Insensitive Resins and Coatings for High Energy Curing

D. D. PERRY, W. ROWE, A. CIRIGNANO, and D. S. DAVIS

Polychrome Corp., Clark, N. J. 07066

For the past several years, Polychrome Corporation has had under development a family of energy-curable resins which have been given the trade name of Uvimer^{TM}.* Several of these materials have reached the commercial stage while others are in an advanced state of development. The present paper describes representative members of the Uvimer^{TM} family of resins in terms of their basic physical and chemical properties and how these relate to specific end-uses.

Basic Considerations and Approaches

In approaching the development of an energy-curable resin system, we have attempted to solve a number of problems with which the ultimate user of these types of materials is faced, namely:

1. Oxygen inhibition of cure which exists in
    many energy-curable resins necessitating
    the use of inert blanketing.

2. The desire to minimize the number of han-
    dling and formulating operations.

3. The necessity for good shelf-life, both
    in sensitized and unsensitized formulations.

4. The desire to limit the number of items in
    the product line, while permitting the tailor-
    ing of properties for a variety of end-uses.

5. The need to minimize costs without sacri-
    ficing essential properties.

* Patents Applied For.

150

We will attempt to show in this paper how these goals have been approached.

Much has already been published concerning the composition of energy-curable resin systems for use in coatings and inks, and the basic approach to the development of such vehicles is well known (Refs. 1, 2, 3). A typical formulation contains an oligomer, which may or may not contain reactive functional groups (e.g., double bonds), a cross-linking agent, a reactive diluent (for viscosity control), and a photosensitizer or photoinitiator.

Control over the properties of the cured resin vehicle may be exercized in a number of ways:

1. Via the structure of the oligomer backbone, including such factors as:

   (a) Degree of chain branching
   (b) Types of functional groups
   (c) Number and type of double bonds
   (d) Molecular weight

2. Functionality and level of cross-linking agent.

3. Nature and level of reactive diluent.

4. Sensitizer or photoinitiator.

It was our initial aim to develop a basic oligomer or family of oligomers that, in suitably formulated systems, were relatively unaffected by the usual inhibiting action of molecular oxygen. It was fortunate that in the early stages of the synthetic investigations such materials were obtained. Consequently, these newly synthesized oligomer structures became the basis for the Uvimer[TM] resins. Variants on the basic structures were later developed to obtain specific end-use properties.

Description of Typical Uvimers[TM]

The principal members of the Uvimer[TM] series are uniquely designed unsaturated urethanated oligomers. One method of incorporating unsaturated functionality is by reaction of pendant isocyanate groups with unsaturated compounds containing active hydrogen (See, e.g., Ref. 1).

$$R-NCO + H-R^1-\overset{\overset{\text{11}}{R}}{C}=CHR^{11} \longrightarrow$$

$$R-NHCO-R^1-\overset{\overset{\text{11}}{R}}{C}=CHR^{111} \qquad (1)$$
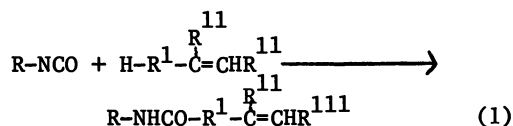
Where R   = Oligomer backbone structure
and R^1 = $-OCH_2CH_2OOC-$, $-OCH-CH_2OOC-$, $-OCH_2$, or
                                    CH_3
           $-NHCH_2-$, for example
      R^{11} = H- or CH_3-
and R^{111} = H- or C_6H_5-

Polyol and isocyanate components may be reacted to afford
isocyanate-terminated oligomers which can then be subjected to
the general reaction illustrated in equation 1 above. Together
with other synthetic modifications, this permits the preparation
of a wide variety of oligomers. One may vary, for example:

(1) The hydroxyl functionality of the polyol.
(2) The molecular weight of the polyol.
(3) The backbone structure of the polyol.
(4) The type of other functional groups present
    in the polyol.
    Similar modifications may be made in the
    structure of the polyisocyanate component.

The oligomers employed in our work are based on commercially
available materials. However, they embody unique synthetic modi-
fications made on the starting materials prior to their being
converted to oligomers.
    In regard to the relative insensitivity of the Uvimer[TM] ma-
terials to oxygen inhibition, the mechanism of this is not fully
understood at present. However, we believe that it relates to a
common structural feature in all of these resins, namely the
occurrence of the ethylenic double bonds in a particular position
relative to the other functional groups in the oligomer.
    Selected reactive diluents are employed to reduce the vis-
cosity of Uvimer[TM] formulations and to impart a greater flexi-
bility to the cured product. The choice of a monomer or reactive
diluent for a Uvimer[TM] is based on a number of factors, including
compatibility with the base resin, odor, volatility, toxicity,
and its effect on specific properties such as adhesion. Changing
the diluent monomer does not drastically alter the basic proper-
ties of the resin so that it is possible to supply a given
Uvimer[TM] with a choice of diluents in order to comply with par-
ticular user requirements.
    The Uvimer[TM] designation thus represents a generic struc-
tural type, while the diluent may be varied for the reasons
explained above. For the purposes of this paper, a Uvimer[TM] may
be shown with a particular reactive diluent or combination of
diluents, although this composition is not currently offered com-
mercially. We consider the Uvimer[TM] type to be independent of
the particular diluent or diluents employed.

We will describe typical members of the Uvimer^{TM} series in terms of their composition and physical properties. Uvimer^{TM} 530, the first member of the series, is a relatively hard, brittle and fast-curing resin which is suitable for use as an ink vehicle and as a coating on rigid substrates. The table below gives basic formulation and cured film properties of this Uvimer^{TM}:

TABLE I – UVIMER^{TM} 530

A. **Composition**

Component	Parts
Urethane Oligomer A	60
PETA	40

B. **Physical Properties**

Viscosity, poises	375–600
Color, Gardner	2–3
Weight/vol., lbs./gal.	9.80 ± 0.05
Non-volatile cure loss	0%
Sward Hardness	>50
Abrasion Resistance*	No visible effect

C. **Cured Film Characteristics**: Hard, glossy, brittle, fast-curing resin; highly chemically resistant.

D. **End-Uses**: Ink vehicles, particle board coatings.

* (ASTM Method D-968-51, Falling Sand Method)

Uvimer^{TM} 530 exhibits outstanding chemical resistance as evidenced by the data presented in Table II.

Uvimer^{TM} 530 and the other members of the Uvimer^{TM} series may be cured with benzoin ether type photoinitiators and with di-ethoxyacetophenone.** Table III presents data on the cure speed of Uvimer^{TM} 530 formulated with butyl benzoin ether. These data were obtained in air without the use of inert blanketing. Films of 3 mil thickness were irradiated on a moving belt using a 5000 watt Addalux uv lamp (Berkey Photo, Inc.) focussed on one linear inch. This is a low pressure lamp incorporated in an experimental unit. Faster cure speeds (up to 200 ft. per minute/lamp) were obtained in later studies with a unit employing two medium pressure, 200 watts/linear inch Hanovia lamps.

** Union Carbide Corporation

TABLE II – CHEMICAL RESISTANCE OF UVIMER[TM] 530

   Test Conditions: 3.5 mil film cured at 0.6 sec. per linear
inch of travel using 5,000 watt Addalux lamp (400 watts/linear
inch) at 3" above work surface. Tests were done under watch glass
where applicable. Substrate was particle board.

Test Liquid	Duration of Test (Hours)	Condition	Remarks
70% Hydrofluoric acid	48	No effect	
70% Hydrofluoric acid	144	Very slight dis-coloration	Film intact
Sulfuric acid (50%)	48	No effect	
Sulfuric acid (98%)	144	Moderate dis-coloration	Film intact
35% Nitric acid	48	No effect	
70% Nitric acid	144	Heavy dis-coloration	Film intact
Glacial acetic acid	144	No effect	
20% Sodium hydroxide	48	No effect	
40% Sodium hydroxide	144	Very slight dis-coloration	Film intact
Ammonium hydroxide, 26° Baumé	144	No effect	
Ferric nitrate (50%) (conc. copper etching solution)	144	No effect	
10% Iodine in Xylene	144	Very slight dis-coloration	Film intact
10% Iodine aqueous solution	48	Slight dis-coloration	Disappears in 2 hrs.
Dimethyl formamide	144	No effect	
Dimethyl sulfoxide	144	No effect	
Phenol (90%)	144	No effect	
1-Methyl-2-pyrrolidone	144	No effect	
Trichlorethylene	144	No effect	
Aromatic solvents	144	No effect	
Aliphatic solvents	144	No effect	
Oxygenated solvents	144	No effect	
Methyl ethyl ketone	1000 rubs	No effect	

TABLE III – CURE SPEED OF UVIMER^{TM} 530

Formulation:

Uvimer^{TM} 530   100 parts
Butyl Benzoin Ether   4 parts

Speed	Effective Exposure Time	Condition of Film*
16 fpm	0.30 secs.	No effect – film intact
36 fpm	0.14 secs.	No effect – film intact
50 fpm	0.10 secs.	Slight dulling – film intact
65 fpm	0.08 secs.	Slight dulling – film intact

* Determined by rubbing 100 times with cloth
  saturated with methyl ethyl ketone.

A pigmented Uvimer^{TM} 530 formulation coated on particle
board was successfully cured in an electron beam accelerator
using one-half the normal nitrogen flow. In the complete absence
of nitrogen blanketing, partial curing was obtained. The formu-
lation used was as follows:

Uvimer^{TM} 530   51.5 parts
2-Ethylhexyl acrylate   5.0 parts
Styrene   5.0 parts
TiO_2 15.4 parts
$CaSO_4$ 23.0 parts
Stabilizer   0.1 parts

Another member of the Uvimer^{TM} series is Uvimer^{TM} 545 whose
properties are summarized in Table IV.
    A third member of this series is Uvimer^{TM} 580 whose proper-
ties are summarized in Table V.
    The above resins gave hard, rigid, highly cross-linked films,
suitable for use on rigid substrates or as ink vehicles. They are
also relatively high in viscosity in the uncured state. We recog-
nized early the need for softer, more flexible film-formers, as
well as for lower viscosity formulations for certain applications.
This was achieved by significant modification of the oligomer
structure. This approach is illustrated by four members of the
Uvimer^{TM} 700**series: 720, 740, 765, 775.
    Uvimer^{TM} 720 (Table VI) is softer and more flexible than 530,
540, and 580 and exhibits improved adhesion to most substrates.

** Patents applied for.

TABLE IV – UVIMER^{TM} 545

A. Composition

Component	Parts
Urethane Oligomer B	40
Reactive Diluent	60

B. Properties

Viscosity, poises	400–600
Color, Gardner	3 max.
Weight/vol., lbs./gal.	10.00 ± .05
Non-volatile cure loss	0% (60 secs.)
Chemical resistance	Same as Uvimer^{TM} 530, but less resistant to strong oxidizing acids.

C. General Characteristics and End-uses: Same as 530; overprint varnish (offset printing).

TABLE V – UVIMER^{TM} 580

A. Composition

Acrylate Oligomer A-1	83.5
Reactive Diluent	16.5

B. Properties

Viscosity, poises	150–300
Color, Gardner	2–3
Weight/vol., lbs./gal.	9.63 ± .05

C. General Characteristics: Fast curing, hard, brittle.

TABLE VI - UVIMER^{TM} 720

A. <u>Composition</u>

Urethane Oligomer C	91
RD-30	9

B. <u>Properties</u>

Viscosity, poises	500-700
Color, Gardner	5 max.
Weight/vol., lbs./gal.	9.10 ± 0.05
Non-volatile cure loss	0% (60 secs.)

C. <u>General Characteristics</u>: Flexible, tough, abrasion resistant, moderately fast cure.

D. <u>End-Uses</u>: Tile coatings, photopolymer liquid plate.

Because of its superior flexibility and adhesion to many substrates, Uvimer^{TM} 720 was considered a prime candidate for a floor tile coating. Table VII presents data on two formulations developed for this application. The primary consideration in this instance was abrasion resistance, with resistance to curl running a close second. Both formulations showed good abrasion resistance, but the formula containing the increased level of diluent was significantly better as shown by comparison of the results with the 1000 gram weight.

Data on Uvimer^{TM} 740 is presented in Table VII, while Uvimers^{TM} 765 and 775 are compared in Table VIII. Uvimer^{TM} 740 is somewhat stiffer and harder than either 765 or 775, primarily due to the difference in the structures of oligomers D and E. It should also be noted that Uvimers^{TM} 765 and 775 have better color and do not exhibit yellowing on aging. Since the latter two resins employ the same basic oligomer, it is evident that on the basis of viscosity reduction 2-ethoxyethyl acrylate is a more effective diluent than the 2-ethylhexyl acrylate/hydroxyethyl acrylate combination. Thus, it is possible in Uvimer^{TM} 775, to employ a lower level of reactive diluent and thereby obtain a harder, stiffer, faster-curing formulation.

The use of Uvimer^{TM} diluent RD-30 in a 740 formulation gives a higher viscosity than 2-ethoxyethyl acrylate. However, the odor level is significantly reduced.

TABLE VII - FLOOR TILE COATINGS BASED ON UVIMER^{TM} 720

Formulation

	A	B
Uvimer^{TM} 720	100	100
Reactive diluent	5	10
DEAP	3	3.3
Accelerator	1	1.1
Leveler	3	3.3
Slip Additive	2	2.2

Properties

Viscosity, poises, Brook-field, RVT, #5/20 rpm/80° F.	200	155
Taber Abrasion*, 500 g.	8	--
Taber Abrasion, 1000 g.	25	16
Curl, 12 hrs./120° F.	None	None

* CS-17 wheel for 1,000 cycles, tested on 2 mil coatings

TABLE VIII - UVIMER^{TM} 740 FORMULATIONS

A. Composition

Urethane Oligomer D	66	65
2-Ethoxyethyl Acrylate	34	--
RD-30	--	35

B. Physical Properties

Viscosity, poises	22-27	100-140
Color, Gardner	4-5	4-5
Weight/vol., lbs./gal.	9.27 ± 0.05	9.47 ± 0.05
Hardness, Shore A	90	--
Hardness, Shore D	45	--

C. General Characteristics: Moderately fast cure, medium soft, flexible.

D. End-Uses: Coatings for flexible substrates; insulating tape.

TABLE IX – COMPARISON OF UVIMERS[TM] 765 AND 775

A. Composition	765	775
Urethane Oligomer E, parts	52	67
2-Ethylhexyl acrylate	34	—
Hydroxyethyl acrylate	14	—
2-Ethoxyethyl acrylate	—	33

B. Properties

	765	775
Viscosity, poises	22–27	18–22
Color, Gardner	1	1
Weight/vol., lbs./gal.	8.65 ± 0.05	9.10 ± 0.05
Hardness, Shore A	68	90
Cure Speed* ft./min./lamp	15	37

* Determined on 3.5–4.0 mil film using two 200
  watts/linear inch Hanovia lamps over moving
  belt 3 inches from work surface. Sensitized
  with 3% by wt. diethoxyacetophenone (DEAP).

C. End-Uses: Flexibilizing additive; strapping tape;
   fabric coatings; and paper coating.

Pressure Sensitive Adhesive

Recently, Dowbenko et al (Ref. 4) of PPG Industries des-
cribed two approaches to the development of energy-curable
pressure sensitive adhesives. One involved the incorporation of
low molecular weight acrylic polymers into hot melt formulations;
the second employed radiation polymerization of monomer-polymer
syrups.

We have taken a somewhat different approach. By employing
mixed molecular weight oligomers, we have been able to develop an
extremely promising uv-curable adhesive system.

Data on the composition and properties of this adhesive are
presented in Tables X and XI. In Table X, two formulations with
different reactive diluents are shown.

In Table XI, data are shown on the properties of the cured
adhesive with and without a plasticizer type additive.

Shelf-life of Uvimer[TM] Resins

The Uvimers[TM] exhibit excellent shelf-life, as demonstrated
by room temperature and 60° C. aging experiments. All of them
are indefinitely stable in air at room temperature, and for three

TABLE X — PRESSURE SENSITIVE ENERGY-CURABLE ADHESIVES

	Uvimer[TM] 1793	Uvimer[TM] 1818
A. Composition		
Oligomer F	90	90
RD-31	10	--
RD-30	--	10
B. Physical Properties		
Viscosity, poises, Brookfield, RVT	1106	520
Viscosity, Gardner-Holdt	Z_9-$\frac{1}{2}$	Z_7
Color	Water White	Water White
Wt./vol., lbs./gal.	8.60 ± .05	8.61 ± .05
Cure Speed, ft./min.	35	35

TABLE XI — PROPERTIES OF ADHESIVES BASED ON UVIMER[TM] 1793

A. Formulation		
Uvimer[TM] 1793	100	100
Sensitizer	3	3
Accelerator	1	1
Plasticizer	35	--
B. Cured Adhesive Properties *		
Shear strength/$\frac{1}{4}$ in.^{2}, min.	$>$120	$>$72
135° hold, sec.	88	60
180° peel strength, oz./in.^{2}	$>$ 30	25-30
Quickstick	Very Good	Very Good
Adhesive Offset	None	None

* 1.5 mil adhesive films cured on paper or Mylar
  backing at 70 ft./min. with two 200-watts/linear
  inch Hanovia mercury vapor lamps.

months or more at 60^U C. In addition, formulations sensitized with 3% DEAP have shown virtually unlimited shelf-life in the dark at room temperature.

Specifically, Uvimer^{TM} 775, sensitized with 3% DEAP, has been aged for 23 days at 60° C. without appreciable change. Upon longer aging (48 days), there was a significant increase in viscosity, but no gelation. Formulations containing RD-30 and RD-31 have stability at least equivalent to those containing other diluents. Both 530 and 545 are stable in sensitized form at 60° C. for 30+ days.

It is, therefore, possible to supply sensitized formulations to the user in order to minimize handling of the materials in their uncured state.

Summary

The Uvimers^{TM} comprise a useful new group of energy-curable resins suitable for a wide variety of applications. Special features which should be of interest to potential users include:

1. The low degree of oxygen inhibition of cure.

2. The wide range of properties available from the members of the series. These can be augmented by additional formulation by the user.

3. Excellent shelf-life.

4. Good stability of sensitized formulations.

Literature Cited

1. Carden, C. H. and O. W. Smith "Coatings and Plastics Preprints", 34 (1), 664-668 (1974).

2. Koch, S. D. and J. M. Price, Ibid, 34 (2), 432-434 (1974).

3. Fussa, A. D. and S. V. Nablo, Ibid, 34 (2), 422-431 (1974).

4. Dowbenko, R; R. M. Christenson; C. C. Anderson; and R. Maska, "Chemtech", 1974 (September) 539-543.

12

Ultraviolet Light Cured Inks—A Review

J. W. VANDERHOFF

National Printing Ink Research Institute, Lehigh University, Bethlehem, Penn. 18015

The printing ink industry with annual sales of about $0.7 billion is a small but vital part of the $37-billion-a-year graphic arts and communications industry (1). This industry is founded upon technical service because the ink formulations are tailored to the specific printing application. It is estimated that one million new ink formulations are produced each year, with another 4-5 million older formulations still available (2).

Printing Processes

This very large number of formulations is necessitated by the several different printing processes and the varying requirements of each printing application. There are three main printing processes:
1. letterpress; 2. lithography; 3. gravure. Figure 1 shows schematic representations of these three processes. In letterpress or relief
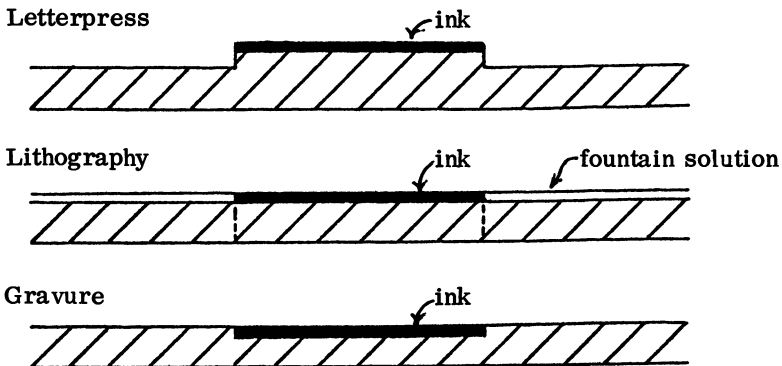
Figure 1. Schematic of printing processes

162

printing, the image area is raised above the plate surface. The ink is applied only to the image area (type-face) and then transferred to the paper substrate in the type-face plane. Flexography is a special type of letterpress printing in which the plate is rubber instead of metal. In lithography or planographic printing, the image is essentially co-planar with the non-image area. The image area is hydrophobic (i. e. , ink-receptive) while the non-image area is hydrophilic (i. e. , not receptive to ink). The hydrophobic ink film is applied to the image area and aqueous fountain solution to the non-image area; the ink film is transferred to the blanket roll and then to the paper substrate. In gravure or intaglio printing, the image area is recessed below the plate surface. Ink is applied to the plate and forced into the image cavities; the remainder is "doctored" off the plate surface. During printing, the paper substrate is forced into the cavities, picking up the ink.

Preparation and Characteristics of Printing Inks

Printing inks consist of a dispersion of a pigment or dye in a fluid vehicle. Most inks also contain a polymeric or resinous component that forms a continuous film upon drying. The pigments may be black (carbon black, furnace black, lampblack), white (opaque or transparent), inorganic colors, or organic colors; dyes may also be used. The vehicles may consist of non-drying oils, drying oils, resin-solvent solutions, resin-oil combinations, or resin-wax combination. In addition to the pigment and vehicle, the ink may also contain driers, waxes, compounds, greases, lubricants, reducing oils, body gums, binding varnishes, antioxidants, antiskinning agents, or surface-active agents.

The mode of drying is as varied: absorption (non-drying oils); oxidation (drying oils); evaporation of solvent (resin-solvent solutions); cold-set (resin-wax combinations); quick-set (resin-oil combinations); heat-set (resin-oil-solvent combinations).

Printing inks are usually prepared by dispersing powdered pigment in a vehicle by mechanical mixing. The powdered pigment consists of agglomerates and aggregates of primary particles, e. g. , some carbon blacks consist of 30-100μ-diameter agglomerates and aggregates of the 0. 02-0. 03 μ-diameter primary particles. The dispersion process usually consists of premixing and mixing steps during which the large pigment agglomerates and aggregates are broken down to a colloidal dispersion of small aggregates and primary particles. A much finer degree of dispersion is required for printing inks than for other types of coatings because the ink films are much thinner (perhaps only 1-2μ thick). Moreover, for all pigments, there is an optimum degree of dispersion (or particle-size distribution) for maximum opacity or color strength (3), and ink makers devote much effort to dispersing pigment agglomerates and aggregates to

this desired size range.

Table I (4) shows that the pigment content and viscosity of printing inks vary widely according to the printing process and application.

Table I

Composition and Viscosity of Printing Inks

Printing Process	% Pigment	Viscosity, poises
lithography	20–80	100–800
letterpress	20–80	10–500
flexography	10–40	1–100
gravure	10–30	0. 5–10
news–ink	8–12	2–10

The paste inks used in letterpress and lithography have relatively high concentrations of pigment, while the low-viscosity liquid inks used in flexography and gravure have much lower concentrations. The differences in the viscosities are due to the different pigment and solvent concentrations.

Figure 2 shows a schematic representation of the ink transfer process.
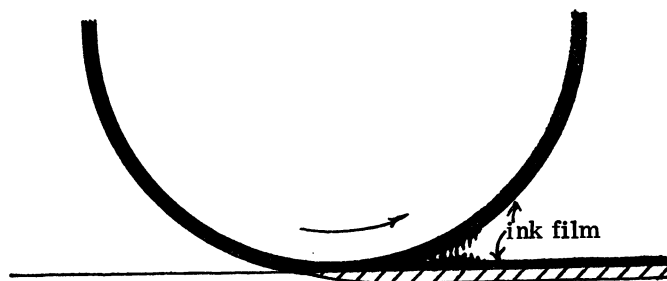
ink film

Figure 2.   Schematic of ink transfer process

The ink transfer rolls apply a uniform film of ink to the printing plate or roll; this ink film is transferred directly to the paper substrate, or first to the printing blanket and then to the paper substrate. During printing, the ink film penetrates into the porous paper substrate, and that part of the ink film remaining between the substrate and the plate splits, leaving part of the film on the substrate and part on the plate. This ink film splitting is described by the Walker-Fetsko equation (5):

$$y = b + f(x - b)$$

where y is the amount of ink transferred per unit area of the print, x the amount of ink originally on the plate, b the amount of ink immobilized by penetration into the substrate, and f the fraction of ink film between the substrate surface and the plate that is transferred to the substrate. For a wide variety of printing processes and conditions, f is about 0.4 for non-absorbent substrates and about 0.2 for absorbent substrates (6).

New Developments in Printing Inks

Stimulus for Development of New Inks. Many inks are formulated with solvents to control the viscosity of the formulation, and during printing these solvents evaporate into the atmosphere. For example, the rapid-drying heat-set inks widely used in webfed printing contain 35-45% of volatile hydrocarbon solvents, which must be removed quickly in the dryer if fast printing speeds are to be maintained. However, recently-enacted or impending legislation by the federal, state, and local governments administered by the Environmental Protection Agency restricts the amount of solvent that can be vented to the atmosphere in all types of coating operations. Moreover, increased concern has been expressed by individuals and unions over the possible toxic effects of prolonged exposure to solvents, and the establishment of the Office of Safety and Health Administration has given the organizational means to monitor and control such exposures. For printers and converters, this means that all but the smallest companies must reduce sharply the amounts of solvent vented to the atmosphere.

There are three possible approaches to elimination of solvent emission: 1. incineration of solvents emitted from solvent-based inks; 2. recovery of solvents emitted from solvent-based inks; 3. use of solventless inks. The choice that a printer or converter must make is influenced by the energy shortage, which makes procurement of additional natural gas or fuel oil difficult, and the raw material shortage, particularly the solvents used in printing inks.

The incineration of solvents is an approach worth considering for

printers and converters who use letterpress or lithographic printing processes. The solvents contained in the heat-set inks can be burned at 1500°C to produce carbon dioxide and water; however, a supply of natural gas or fuel oil is required. Therefore, although this approach is technically and economically feasible, the energy shortage is certain to limit its adoption.

The recovery of solvents is an approach worth considering for printers and converters who use gravure or flexographic printing processes. These inks contain high concentrations of low-boiling solvents, and the usual practice is to dilute them further in the press room. The large volume of solvents emitted makes incineration impractical, but these solvents may be absorbed on activated charcoal, and removed by steam distillation when the charcoal is saturated. The recovered solvents may be re-used or sold; however, it may be impractical to fractionate some recovered solvent blend that boil in the same temperature range, which lessens their value considerably. Therefore, although this approach is also technically and economically feasible, the difficulty in procuring the solvents used for dilution may restrict the continued use of these solvent-based inks and, hence, the adoption of solvent recovery approach.

The use of solventless inks avoids the emission of solvents during drying. The development of such inks has been a major goal of the printing ink industry for the past several years and has resulted in the development of several different types: 1. ultraviolet light–cured inks; 2. electron beam–cured inks; 3. thermally-catalyzed inks; 4. water-based inks; 5. solventless oil-based inks plus overcoat; 6. low-smoke low-odor inks.

Radiation Curing Methods. There are three types of radiation curing systems that are adaptable to the rapid cure of polymer films: 1. micro-wave; 2. electron beam; 3. ultraviolet light. Microwave radiation is most useful for drying aqueous or highly-polar systems, e. g. , water-based gravure or flexographic inks, but not for the non-polar letterpress or lithographic inks. Electron beam radiation because of its high intensity cures both thick and thin films rapidly, and it is readily adaptable to paste and liquid inks; however, its capital cost is high, and it requires safety shielding for the x-rays produced and an inert atmosphere to prevent the formation of ozone. Ultraviolet light radiation is a good compromise in that its capital cost is relatively low and it is easily shielded, yet it gives a reasonably high radiation intensity. At present, this latter system is the most advanced of the various approaches to produce solventless inks.

Ultraviolet Light-Cured Inks. Ultraviolet light-cured inks are a distinct departure from conventional printing inks in that their mechanism of

curing is vinyl addition polymerization. The vehicles consist of mixtures of polyfunctional vinyl monomers and photoinitiators, which upon exposure to ultraviolet light form free radicals that initiate a rapid crosslinking polymerization to form a three-dimensional polymer network.

An important advantage of these ultraviolet light-cured inks is that they give excellent film properties at fast printing speeds and thus have potential for further technical and economic development. Also, the non-volatile vinyl monomers and prepolymers used in their formulation completely eliminate the emission of solvents. Moreover, since the ink film is cured at temperatures only slightly above room temperature, the paper substrate is not degraded, and therefore lower-quality paper may often be used. Anti-offset spray is not needed, and wet-trapping can be eliminated because of the rapid curing; in multi-color printing, the colors may be dried between stations. In addition, the ultraviolet lamps occupy less space than the heat-set ink dryers they replace.

The disadvantages are that the present cost of the ultraviolet lamps is relatively high, and the cost of lamp replacement can be greater than that of oven maintenance. Moreover, oxygen inhibition of the photoinitiated vinyl polymerization must be overcome, and paper printed with these inks cannot be recycled in the processes currently used (8), thus lowering the return on the sale of scrap (9).

Electron Beam-Cured Inks. Electron beam-cured inks are similar in principle to ultraviolet light-cured inks except that no photoinitiator is needed. Vinyl polymerizations may be initiated by any form of ionizing radiation, e.g., neutrons, α-particles, γ-rays, and x-rays, as well as by high-energy electrons (β-rays). The mechanism of initiation is more complex than that of photochemical initiation in that radiation of vinyl monomers gives cations and anions as well as free radicals; however, most radiation-initiated polymerizations are radical-initiated because the cations and anions formed are not stable at the temperature of polymerization and therefore dissociate to form radicals.

Although similar in principle to ultraviolet light-curing, electron beam curing offers higher intensities and, hence, faster rates of curing (at least for thick ink films). However, the impingement of high-energy electrons upon metals gives secondary x-radiation, a more highly penetrating form that requires elaborate shielding for safety. The lower-intensity electron beam generators currently offered (10) may lessen the safety problems somewhat, but probably at the expense of reduced intensity (although this reduced intensity is sufficient to cure ink films). Also, as with the ultraviolet light-cured inks, paper printed with these electron beam-cured inks cannot be recycled in the processes currently used.

Thermally-Catalyzed Inks Thermally-catalyzed inks are stable at room temperature, but crosslink rapidly when heated to dryer tempera-

tures. There are two types: 1. acid-crosslinkable prepolymers; 2. prepolymers that become reactive at dryer temperatures.

The acid-crosslinkable prepolymers are polyester-alkyd, urea-formaldehyde, or melamine-formaldehyde resin adducts combined with a "blocked" acid catalyst that becomes "unblocked" at the dryer temperatures (7, 11, 12), e.g., a melamine-polyester resin adduct with "blocked" p-toluenesulphonic acid catalyst (12). These acid-crosslinkable prepolymers are stable on the press distribution system but are converted to three-dimensional polymer networks by heating to 275–325° F.

The prepolymers that become reactive at dryer temperatures are styrenated-alkyd adducts (11). Inks formulated with these vehicles contain small concentrations of high-boiling solvents, which are not evaporated during drying and presumably remain in the film.

Letterpress and lithographic inks can be formulated from these thermally-catalyzed vehicles. Their main advantage is that they can be cured with the present flame or hot-air dryers, to give carbon dioxide and water plus small amounts of alcohols and formaldehyde. Moreover, the properties of these inks films are very good, particularly their resistance to scuffing, abrasion, or scratching. In addition, they handle well on the press distribtion system or on the printing plate, and their shelf life is adequate (3–6 months).

The main disadvantage is that web temperatures of 275–325° F are required to cure the film. These temperatures affect the paper properties adversely, and therefore higher-quality, more-expensive paper must be used. Even so, blistering or cracking in the folder may be a problem. Moreover, the solvent emission, although reduced significantly, is not eliminated, and, as with the ultraviolet light-cured inks, paper printed with these thermally-catalyzed inks cannot be recycled in the currently used processes (8, 9).

Water-Based Inks. In this context, the term "water-based" means a preponderance of water as the solvent rather than an absence of organic solvents. For example, water-based flexographic inks may contain as much as 20% alcohol. However, since Rule 66 and other governmental regulations allow emission of these quantities of alcohols (at least in certain geographic areas), these inks are a suitable approach to solve the printers' problems.

These water-based inks use water-based polymer vehicles. There are three main types of water-based polymer systems: 1. latexes; 2. water-soluble polymers; 3. water-solubilized polymers. The latexes are colloidal dispersions of submicroscopic polymer spheres; the latex viscosity is dependent primarily upon the interactions between the colloidal particles and is independent of the molecular weight of the

polymer. Thus, the concentration of polymer in a low-viscosity latex may be 50% or more. Aqueous solutions of water-soluble polymers are true solutions, i. e., molecular dispersions of polymer molecules; the viscosity of these solutions is dependent upon both the concentration and molecular weight of the polymer. High-molecular-weight polymers can be used only at the expense of polymer concentration, and vice-versa. The water-solubilized polymers lie between the latexes and polymer solutions; i. e., between the colloidal and molecular sizes. These water-solubilized polymers are often prepared by the neutralization of carboxyl-containing latex particles with base, to give swelling and partial disintegration of the particles.

A review (13) of water-based inks points out that ink vehicles must have "tack" for printability and that high solution viscosities are required to give this tack. The viscosity of most latexes is too low to give this tack, so water-soluble or water-solubilized polymers are usually used. Upon drying, however, these polymers must no longer be soluble in water. Therefore, most water-based ink vehicles are ammonium hydroxide-neutralized alkaline solutions of carboxyl-containing polymers; when the solution is dried, the ammonia evaporates, leaving the polymer in its water-insoluble carboxyl form.

The main advantage of these water-based inks is the elimination of non-exempt solvent emission without resorting to solvent recovery or incineration. In addition, microwave radiation can be used to dry these inks rapidly because of the high dielectric constant of water.

Their main disadvantage is that the heat of vaporization of water is greater than that of the organic solvents usually used, e.g., 1043 BTU/lb as compared with about 180 BTU/lb for toluene, methyl ethyl ketone, and ethyl acetate. Also, the utility of these inks is limited: they cannot be used in letterpress printing because they dry too rapidly on open roller systems, and they cannot be used in web-offset lithography because they are miscible with the aqueous fountain solution. Moreover, the water may swell the paper substrate and give poor register, and paper printed with some water-based inks cannot be recycled in the presently-used processes.

These inks can be used in gravure printing on absorbent substrates, where their slow drying speed, low gloss, and limited adhesive qualities are offset by their non-flammability, easy wash-up, and dilution with water. These inks are also used in flexographic printing on absorbent paper and paperboard substrates; alcohols and glycol ethers are often added to these formulations to improve printability and drying speed.

Solventless Oil-Based Inks Plus Overcoat. The principle of this approach developed some years ago (14) is to protect the wet ink film on a printed surface by applying a thin, transparent, film-forming polymer

solution while the ink is still wet. In present practice, solventless oil-
based inks, which require several hours to dry by oxidation, are over-
coated with a thin, transparent coating that protects the ink film while it
dries (15). These solventless oil-based inks are the same types used
before the development of heat-set and quick-set inks. The polymer
coatings are oxygen-permeable abrasion-resistant alcohol-soluble pro-
pionate resins (16) or water-soluble polymers.

The main advantage of this approach is that solvent emission (except
that from the coating solution) is eliminated. In addition, the printed
films show high gloss and good abrasion resistance. Moreover, paper
printed by this process can be recycled without complication, and both
alcohol-based and water-based coatings are available.

The main disadvantage is the capital cost of the additional coating
operation. Also, the whole sheet must be coated (not a disadvantage in
some applications), and the complete drying of the ink film under the
protective coating requires a long time.

Low-Smoke Low-Odor Inks. Low-smoke low-odor inks are refine-
ments of the solvent-based heat-set inks currently used. These inks
contain lower concentrations of solvents (e.g., 20% instead of 40%), with
a smaller proportion of saturated hydrocarbon solvents and none of the
photochemically-reactive solvents, yet have printing and ink-film pro-
perties typical of heat-set inks. Some of these inks contain exempt
solvents (e.g., low-boiling azeotropic mixtures), some contain high-
boiling co-solvents (e.g., long-chain alcohols), others contain emulsified
water.

The main advantage of these inks is that they can be used in the pres-
ent drying systems without installing new equipment. Moreover, some
can be dried at temperatures as low as 220°F instead of the usual 275° F.
Their main disadvantage is that the solvent emission, although reduced
significantly, is not eliminated. Nevertheless, they can serve as satis-
factory interim replacements for the heat-set inks until the next gener-
ation of solventless inks is fully developed.

Composition of Ultraviolet Light-Cured Inks

The formulations of ultraviolet light-cured inks are proprietary, and
at present, the best source of information as to their composition is the
rapidly-growing patent literature. However, it is risky to infer the
composition of inks used in the field from those described in the patent
literature because only a small proportion of patented compositions ever
become commercial products, and the compositions used in the field may
be the subject of patent applications not yet granted, or may be held as
technical secrets without applying for patents. Nevertheless, the patent

literature is presently the only available source of information on the composition of ultraviolet light-cured inks. The wide variety of compositions described in the patent literature are difficult to classify, but can be divided into five main types:

1. esters of unsaturated acids and polyhydric alcohols combined with a photoinitiator (17-25);
2. acrylate- or methacrylate-ester derivatives of conventional ink vehicles combined with a photoinitiator (26-39);
3. acrylate- or methacrylate-ester derivatives of epoxy resins combined with a photoinitiator (40-43);
4. unsaturated polyester prepolymers combined with a photoinitiator (44-46);
5. conventional ink vehicles (i. e., whose polymerization mechanism is not vinyl polymerization) combined with a photoinitator (47-51).

The first type of composition is exemplified by: 1. A mixture of an acrylic acid ester of a di- or trihydric alcohol (e.g., trimethylolpropane triacrylate) and a p-toluenesulfonamide-formaldehyde resin combined with a halogenated photoinitiator (17); 2. A mixture of an acrylic acid ester of pentaerythritol dipentaerythritol, or polypentaerythritol with an aryl sulfonamide-formaldehyde resin combined with a halogenated photoinitiator (18); 3. An acrylic acid ester of pentaerythritol, dipenta-erythritol, or polypentaerythritol combined with a halogenated photo-initiator (19); 4. An acrylic acid ester of a di-, tri-, or tetrahydric alcohol combined with a halogenated photoinitiator (20); 5. An acrylic, methacrylic, or itaconic acid ester of pentaerythritol combined with a halogenated photoinitiator (21); 6. A mixture of pentaerythritol tetra-methyacrylate and a 70:30 acrylic acid-styrene copolymer esterified with glycidyl methacrylate combined with a mixture of 1,2-benzanthraquinone and benzoin methyl ether photoinitiators (22); 7. A 63:37 β-(vinyloxy) ethyl methacrylate-trimethylolpropane trimethacrylate adduct combined with a 2-ethylanthraquinone photoinitiator (23); 8. A mixture of penta-erythritol tetraacrylate and a 63:37 monobutyl maleate-styrene copolymer combined with a photoinitiator (24); 9. Poly-β-[(2-furyl)acryloyloxy] ethyl methacrylate combined with a 5-nitroacenaphthene photoinitiator (25).

The second type of composition is exemplified by a wide variety of acrylate- or methacrylate-ester derivatives of conventional ink vehicles combined with a photoinitiator: 1. The reaction product of tung oil fatty acids, glycidyl methacrylate, p-benzoquinone, and 2-methyl-imidazole mixed with tung oil and treated with tolylene diisocyanate, combined with benzoin methyl ether (26); 2. Glycerol-linseed oil-isophthalic acid alkyd reacted with isocyanate-containing prepolymer (formed by reaction of tolylene diisocyanate, p-henzoquinone, 2-hydroxypropyl acrylate in ethyl acetate solution) using dibutyltin diacetate catalyst, combined with tung oil, synthetic varnish, and benzoin methyl ether (27); 3. Epoxidized

soybean oil acrylates or their methyl isocyanate or tolylene diisocyanate derivatives, trimethylolpropane-tall oil fatty acid-adipic acid alkyd, and the reaction product of tolylene diisocyanate-2-hydroxyethyl acrylate adduct combined with a photoinitiator having a triplet energy of 42-85 kcal/mole (28,29); 4. Maleic acid-modified tung oil-4,4-isopropyli-denebis (3,5-dichlorophenolpropylene oxide) adduct and trimethylolpro-pane triacrylate-pentaerythritol tetraacrylate-1,4-butanediol diacrylate copolymer combined with Aroclor 5460, hydroquinone, and stannous chloride (30); 5. Co Resyn I unsaturated polyester-2-hydroxyethyl acrylate-neopentyl glycol diacrylate mixture with 2,2-dimethoxy-2-phenylacetophenone (31); 6. Tolylene diisocyanate-2-hydroxyethyl meth-acrylate-α, α-bis(hydroxymethyl)propionic acid adduct combined with benzoin methyl ether (32); 7. Unsaturated polyester-methyl methacrylate-tetrahydrofurfuryl methacrylate-2-ethylhexyl acrylate adduct combined with benzoin methyl ether and zirconium oxide (33); 8. Adduct of tolylene diisocyanate, 2-hydroxyethyl methacrylate, and p-benzoquinone with a 15:15:35 :35 acrylic acid-2-hydroxyethyl methacrylate-ethyl acrylate-methyl methacrylate copolymer combined with benzoin ethyl ether (34); 9. A mixture of nitrocellulose, a hydroxyethyl acrylate-tolylene diiso-cyanate adduct, and a tripolycaprolactone Triol A-tolylene diisocyanate-hydroxyethyl acrylate monoisocyanate adduct in toluene-2-ethoxyethyl acetate-ethyl acetate-butyl acetate solution combined with benzophenone (35); 10. A mixture of a DER 332(bisphenol A diglycidyl ether)-acrylic acid-pelargonic acid adduct, a DER 332-polyethylene glycol diglycidyl ether adduct, pentaerythritol tetraacrylate, and polyethylene glycol diacrylate combined with 1-chloro-2-methylanthraquinone (36); 11. A castor oil fatty acid-trimethylolpropane-triethanolamine-phthalic anhy-dride alkyd-glycidyl methacrylate adduct combined with benzoin methyl ether, cobalt octanoate, and a rare earth octanoate (37).

The third type of composition is exemplified by acrylate- and methacrylate-ester derivatives of epoxy resins combined with a photo-initiator: 1. Epoxy prepolymers (e.g., glycidyl methacrylate-allyl glycidyl ether copolymers or Ciba ECN 1299) combined with a photo-sensitive aryldiazonium compound (e.g., p-nitrobenzenediazonium hexaflourophosphate) (38,39); 2. Epoxy prepolymers (e.g., a diglycidyl ether of disphenol A-(3,4-epoxycyclohexyl)-methyl-3,4-epoxycyclohex-anecarboxylate-alkyl glycidyl ether mixture) combined with a photo-sensitive aryldiazonium compound (e.g., p-chlorobenzenediazonium hexafluorophosphate) and 1-methyl-2-pyrrolidone gelation inhibitor (40); 3. A mixture of GY-280 epoxy resin, ethylene glycol diacrylate, and crotonic acid combined with hydroquinone monomethyl ether and N,N-dimethylaniline (41).

The fourth type of composition is exemplified by unsaturated polyester prepolymers combined with a photoinitiator: 1. A mixture of a tolylene diisocyanate-modified maleic anhydride-phthalic anhydride-propylene

glycol copolymer with styrene combined with a benzoin-propylene oxide
addition product (42); 2. A mixture of maleic acid-phthalic acid-1, 2,-
propanediol copolymer and styrene combined with benzoin ethyl ether,
hydrogen peroxide (color stabilizer), and diphenyl disulfide (hydrogen
peroxide stabilizer) (43); 3. A wood oil-maleate resin adduct diluted
with spindle oil and combined with Fanal Pink B and benzoin ethyl ether
(44); 4. A fumaric acid-propylene glycol-diethylene glycol-trimethylol-
propane-trimethylolpropane diallyl ether copolymer combined with 4-
benzoylbenzal   chloride (45).

The fifth type of composition is exemplified by formulations which are
not usually considered to polymerize by a free radical mechanism:
1. A mixture of acid-hardening resins, physically-drying resins,
solvents boiling at less than 150°, and pigment dyes containing acid-
releasing photoinitiators (e.g., halomethylated benzophenones or
α -(sulfonyloxymethyl)benzoins) (46); 2. Pigmented drying oil mixtures
combined with azides, diazo compounds, naphthoquinone azides, or
diaminodiphenyl ketones (47); 3. Conventional fast-drying ink comprised
of alkyds, polyesters, aluminum compounds, driers, carbon black, and
solvent combined with an 8:1 benzophenone-Michler's ketone mixture (48);
4. Air-drying alkyd resin lacquer without photoinitiator (49); 5. A mix-·
ture of short oil alkyd, butanolic urea, and melamine urea resins com-
bined with 2-chloro-4-tert-butylacetophenone (50); 6. A plasticized
urea-formaldehyde resin in butanol-xylene-dimethylcarbinol solvent
mixture combined with 2, 2-dichloro-4-tert-butylacetophenone (51).

Curing of Ultraviolet Light-Cured Inks

Theoretical Aspects. Ultraviolet light-cured inks are cured by free
radical-initiated vinyl addition polymerization. The photochemical
initiation of vinyl polymerization has been the subject of many investi-
gations dating back more than 30 years, to the first systematic studies
of polymerization kinetics. Photochemical initiation offered a reprodu-
cible source of radicals that is not dependent upon temperature, as is the
thermal decomposition of free radical initiators. However, despite
these early studies of its mechanism and kinetics, only recently has
photochemical initiation become of practical interest, mainly because
of the recent development of ultraviolet lamps suitable for production
curing of printing inks and coatings.

Other authors (52, 53) have described the mechanism and kinetics of
photochemically-initiated polymerization in detail; therefore this subject
will be reviewed only briefly here.

Free radicals can be initiated by ultraviolet irradiation of pure mono-
mer or monomer containing initiators or photosensitizers. For a pure
monomer $\underline{M}$, the reaction can be expressed as:

$$M + h\nu \longrightarrow (M)^* \longrightarrow R\cdot + \cdot R' \tag{2}$$
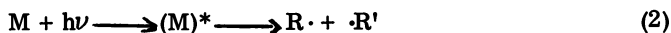
The identity of the activated compound $(M)^*$ has not been well-established, even for such standard monomers as styrene. However, the rate of initiation R_i and the rate of polymerization R_p can be expressed as:

$$R_i = 2\,f\,I_a = 2\Phi\,\epsilon\,I_o\,[M] \tag{3}$$

$$R_p = k_p[M]^{3/2}\{\Phi\epsilon\,I_o/k_t\}^{1/2} \tag{4}$$

where I_a is the intensity of absorbed light (moles light quanta/liter-sec), f the number of pairs of radicals produced per light quantum absorbed, Φ the quantum yield for radical production, I_o the light intensity incident upon the monomer, ϵ the molar absorptivity, k_p the rate constant for propagation, and k_t the rate constant for termination. In this case, the rate of initiation varies directly with incident light intensity and monomer concentration, and the rate of polymerization varies with the 1.5 power of the monomer concentration and the 0.5 power of the incident light intensity.

The light absorption, which varies with the thickness of the reaction vessel, can be approximated using Beer's law:

$$I = I_o\,e^{-\epsilon[M]b} \tag{5}$$

where I is the incident light intensity at distance b in the reaction vessel. In this case, the rates of initiation and polymerization can be expressed as:

$$R_i = 2\Phi\epsilon\,I_o\left\{1 - e^{-\epsilon[M]b}\right\} \tag{6}$$

$$R_p = k_p[M]\left[\Phi I_o\left\{1 - e^{-\epsilon[M]b}\right\}/k_t\right]^{1/2} \tag{7}$$

In this case, the rate of initiation varies directly with incident light intensity, but varies in a complex manner with monomer concentration; the rate of polymerization varies with the 0.5 power of incident light intensity, but also varies in a complex manner with monomer concentration.

The same initiators that undergo thermal decomposition to produce radicals are also subject to photochemical decomposition. Usually, radicals of the same structure are produced. However, a wider range of compounds undergo photochemical decomposition than thermal decomposition, e.g., ketones, benzoin, alkyl halides, and organometallic compounds.

ketones
$$\underset{\substack{|| \\ O}}{R-C-R'} + h\nu \longrightarrow \underset{\substack{|| \\ O}}{R-C\cdot} + \cdot R' \qquad (8)$$

benzoin
$$\underset{\substack{|| \quad | \\ O \ \ OH}}{C_6H_5-C-CH-C_6H_5} + h\nu \longrightarrow \underset{\substack{|| \\ O}}{C_6H_5-C\cdot} + \underset{\substack{| \\ OH}}{\cdot CH-C_6H_5} \qquad (9)$$
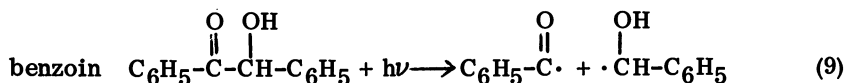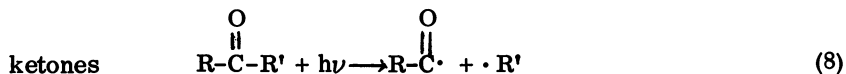
In systems that contain an initiator In, the rates of initiation and polymerization can be expressed as:

$$R_i = 2\Phi\epsilon I_0 [In] \qquad (10)$$

$$R_p = k_p [M] \left\{ \Phi I_0 (1 - e^{-\epsilon[In]b})/k_t \right\}^{1/2} \qquad (11)$$

In this case, the rate of initiation varies directly with the incident light intensity and initiator concentration, and the rate of polymerization varies directly with monomer concentration and the 0.5 power of incident light intensity, but varies in a complex manner with initiator concentration.

A photosensitizer Z is a compound that brings about the reaction of monomers or initiators that do not undergo sufficient excitation at the available frequencies of light. The reactions can be expressed as:

$$Z + h\nu \longrightarrow (Z)^* \qquad (12)$$

$$(Z)^* + C \longrightarrow Z + (C)^* \qquad (13)$$

$$(C)^* \longrightarrow R\cdot + \cdot R' \qquad (14)$$

In this case, the activated compound (C)* cannot be produced by direct irradiation with light of frequency ν. Instead, the activated photosensitizer (Z)* transfers energy to the monomer or initiator C at an appropriate frequency that can be absorbed by C. Typical photosensitizers used in photochemically-initiated polymerizations are benzophenone, fluorescein, and eosin.

Practical Aspects. The foregoing theoretical relationships are difficult to apply to the curing of ultraviolet light-cured printing inks for several reasons. First, the polymerization kinetics of the complex monomers and prepolymers used in the ink formulations have not yet been investigated under conditions that can be correlated with theory (i.e., low concentrations of reactants, constant temperature, simple model formulations). Second, the ultraviolet light-cured inks are polymerized in bulk to high conversion; the polyfunctional nature of the

monomers and prepolymers and the autoacceleration of the polymerization rate almost always observed are difficult to correlate with theory. Third, the ink is applied to the substrate as a thin film, which is almost immediately exposed to a high-intensity ultraviolet light lamp for a very short time and then is moved down the line out of the light path; during this brief exposure, sufficient radicals must be generated to complete the polymerization despite the oxygen inhibition (the conditions are ideal for inhibition by oxygen diffusing from the air into the very thin ink films). Finally, most inks are pigmented, and the dispersed pigment particles absorb part of the ultraviolet light energy and thus mask off part of the film. Nevertheless, the present ultraviolet light-cured inks cure very rapidly upon exposure to ultraviolet light despite the presence of pigment and inhibition by oxygen.

Intensity of Irradiation. The intensity of irradiation varies with position relative to the ultraviolet light lamp (55, 56). The relative intensity of irradiation was determined by scanning along the three coordinate axes $\underline{X}$, $\underline{Y}$, and $\underline{Z}$ shown in Figure 3 (55). For a Hanovia 200 watt/in quartz
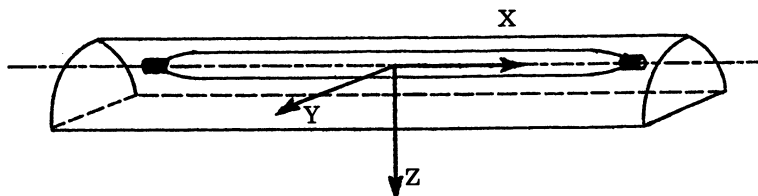
Journal of Paint Technology

Figure 3. Schematic of coordinate system used to determine intensity of ultraviolet light irradiation (55)

lamp with a Hanovia reflector of semi-elliptical cross-section, the relative intensity along the vertical (Z) axis dropped off rapidly with increasing distance to a minimum at about 3 cm, then increased to a maximum at about 8 cm and then dropped off rapidly once more (Figure 4); this curve was interpreted (55) as a composite of the two types of irradiation: 1. direct emission from the lamp; 2. elliptically-reflected from the reflector. Figure 5 shows the variation of relative intensity with distance along the horizontal (Y) axis as a function of the vertical distances (Z)

Figure 4. *Variation of relative intensity of ultraviolet light irradiation with distance along Z axis* (55)

Figure 5. *Variation of relative intensity of ultraviolet light irradiation with distance along Y axis as a function of Z* (55)

corresponding to the arrows in Figure 3 (55). The asymmetric shape of the radiation pattern was attributed to minor misalignment of the lamp relative to the reflector. The areas under these curves were found to be the same, so that a printed substrate moving at a given speed would be exposed to the same overall intensity of irradiation independent of the value of Z. Figure 6 shows that the variation of relative intensity along

Figure 6. *Variation of relative intensity of ultraviolet light irradiation along X axis* (55)

the axis of the lamp (X) was approximately the same independent of the value of X throughout the 25.5-in arc length (55); the slight asymmetry was attributed to misalignment of the lamp relative to the reflector.

These results were confirmed by another study (56) using a Hanovia 200 watt/in quartz lamp with a 100A. $\frac{1}{2}$band centered at 2537A., equipped with a Sun Graphics elliptical reflector. Figure 7 shows that the relative intensity decreased, then increased to a maximum at the focal distance, and then decreased again with vertical distance in a similar manner (compare with Figure 4). Figure 8 shows that the variation of
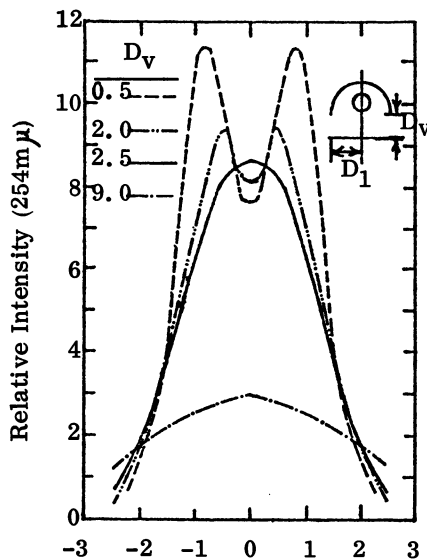
Figure 8.   Variation of relative intensity of ultraviolet light irradiation with distance along Y axis as a function of Z (56)
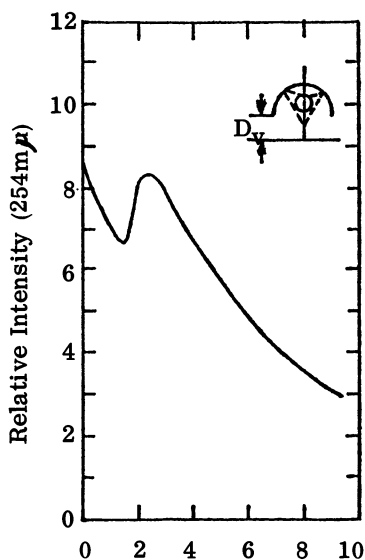
Figure 7.   Variation of relative intensity of ultraviolet light irradiation with distance along Z axis (56)

relative intensity with lateral distance from the centerline was also similar (compare with Figure 5), i. e., two-peaked at distances smaller than the focal distance, single-peaked and high at the focal distance, and single-peaked, low, and broad at distances greater than the focal distance.

Both of these studies (55, 56) emphasize the importance of optimizing the position of the moving web of printed substrate relative to the ultraviolet light lamp.

Experimental Measurement of Rate of Cure.   The rate of cure was measured experimentally in several studies (54-58). Three of these (54, 57, 58) used the dilatometric method to determine the rate of

polymerization, which, although of great value for mechanistic studies and exploratory development of new coating formulations, is not directly applicable to the curing of very thin printed ink films. Only one study, (56) has examined in detail the curing of very thin ink films containing a colorant.

In this work (56), three empirical methods were used to evaluate the rate of cure of a given formulation: 1. the maximum rate of cure (in ft/min/lamp) that gave tack-free (TF) films; 2. the maximum rate of cure that gave thumb-twist-free (TTF) films (rotary twisting motion with downward pressure of 5 kg); 3. the maximum rate of cure that gave scratch-free (SF) films. Ink films of about 3μ thickness were applied to glass slides and cured at various rates. Figure 9 shows the variation of log cure rate in ft/min/lamp with log relative intensity as a function of the colorant used: magenta, yellow, cyan, or black (56). In no case did the rate of cure vary with the 1.0 or 0.5 power of the intensity as predicted by theory, but instead with a higher power according to the colorant: the fastest rates of cure were observed with the magenta and the slowest with the black.

Figure 10 compares the maximum rates of cure (ft/min/lamp) that gave tack-free and thumb-twist-free films for the same four colorants (56)

TAGA Proceedings
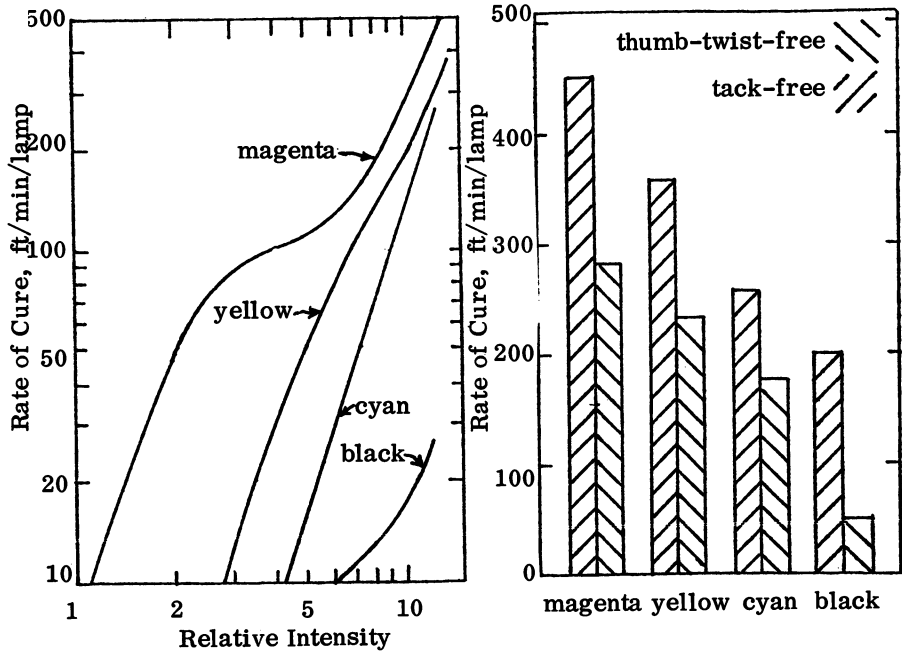
Figure 9. Variation of log rate of cure with log relative intensity of ultraviolet light irradiation (56)

TAGA Proceedings

Figure 10. Maximum rate of cure that gave thumb-twist-free and tack-free films (56)

Again, the magenta gave the fastest rate of cure and the black the slowest. Moreover, the maximum rates of cure for a given colorant were always greater for the tack-free than for the thumb-twist-free test.

These differences in rates of cure observed for the different colorants were attributed to different absorbances of these colorants over the wavelength range 220-350 mμ (56). Figure 11 shows the percent transmission-wavelength curves of 10% suspensions of these colorants in mineral oil.
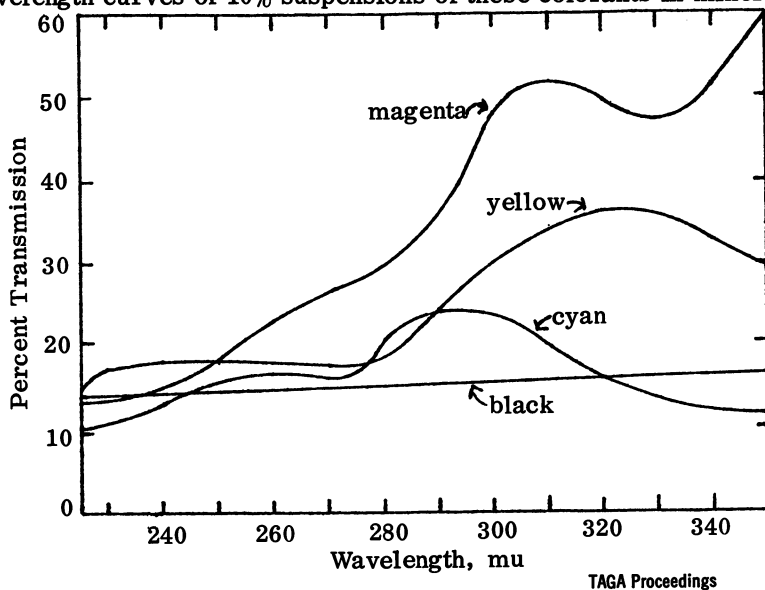
Figure 11. Variation of % transmission with wavelength (56)

Although the percent transmission curves vary with wavelength, that for magenta generally showed the highest percent transmission at a given wavelength, followed by yellow, cyan, and black in that order.

The presence of colorant was also shown to affect the behavior of the photosensitizer (56). Figure 12 compares the curing efficiency of photo-sensitizers A, B, and C with and without 10% black pigment. In both
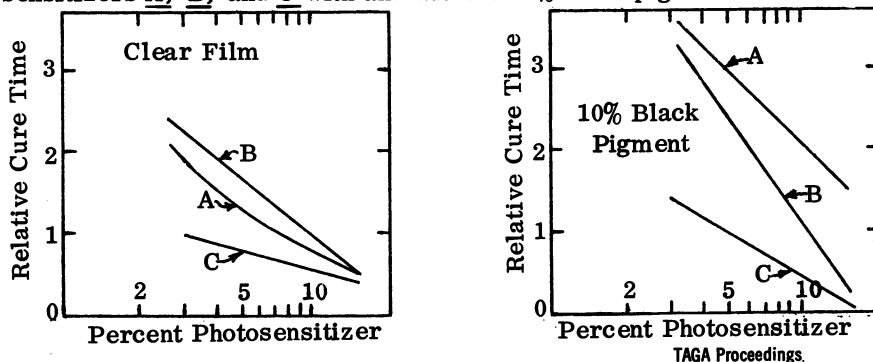
Figure 12. Variation of relative cure time with log photosensitizer (56)

cases, the fastest rates of cure were obtained with photosensitizer C̲ , but the relative efficiencies of photosensitizers A̲ and B̲ were reversed when 10% black pigment was added to the clear film.

As expected, the rate of cure decreased slightly with increasing film thickness (56̲). Figure 13 shows that the decrease of log rate of cure with film thickness was linear and about the same for the four colorants;
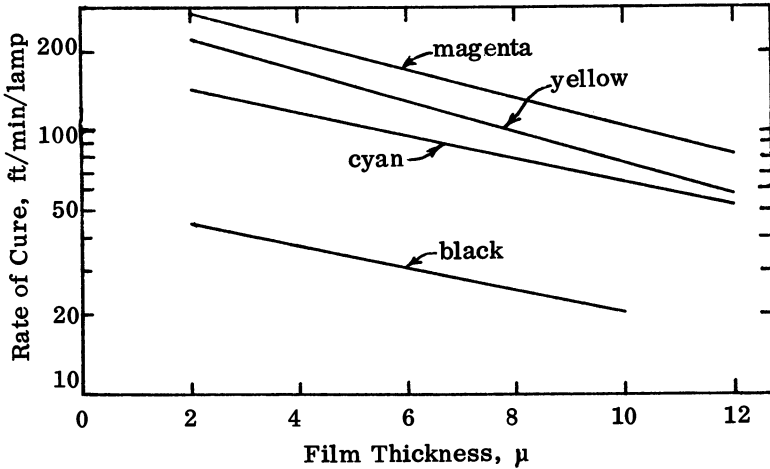
TAGA Proceedings

Figure 13.   Variation of log rate of cure with film thickness (56)

in the film-thickness range of 2-12μ , the rate of cure was approximately halved for each 5μ increase in film thickness.

The effect of wavelength was also studied by substituing a Hanovia "ozone-free" lamp for the standard type (56̲). Figure 14 shows the ratio
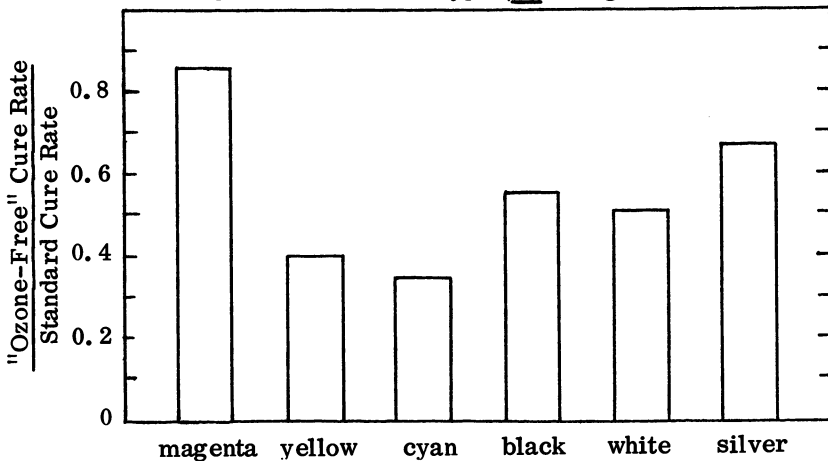
TAGA Proceedings

Figure 14.   Ratio of "ozone-free"/standard cure rate (56)

of cure rates for the "ozone-free" lamp relative to the standard lamp for films containing various colorants. In all cases, the rate of cure was slower for the "ozone-free" lamp, but the decrease was greatest for cyan and yellow and least for magenta. This difference in cure rates was attributed to the different spectral output of these lamps (56). Figure 15 shows that the relative emission-wavelength curves for the

TAGA Proceedings
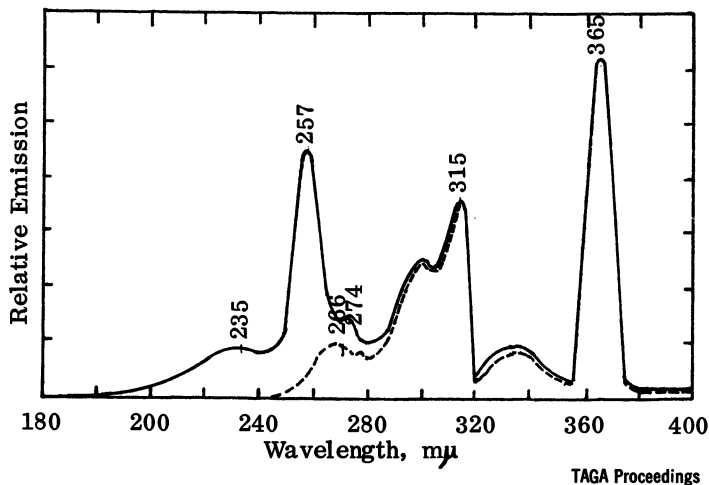
Figure 15. Variation of relative emission with wavelength for Hanovia "ozone-free" and standard lamps (56)

"ozone-free" lamp was lower than that of the standard lamp in the wavelength range 200-280 mμ, particularly near the peak at 257mμ.

The foregoing results illustrate the complexity of these systems and emphasize the importance of studying the ultraviolet light-cured ink system in addition to its individual components.

Cost of Ultraviolet Light-Cured Inks

Inevitably, the cost of ultraviolet light-cured inks is higher than that of the conventional solvent-based inks they are designed to replace. Part of the increased cost is offset by their higher concentrations of vehicle and pigments (volatile solvents are replaced by reactive monomers and prepolymers) so that the potential volume of ink film per lb of ink is greater; however, in practice, only part of this difference is realized as greater mileage.

It is difficult to specify the increased cost of thse ultraviolet light-cured inks with any accuracy. For example, in one case, the cost of the ink was estimated to be 30-50% higher (7), but an estimate made in 1971 cannot be expected to apply today when raw material costs are increased on a monthly or even weekly basis. In another case, the overall cost of

operating a web-offset lithographic press using ultraviolet light-cured inks was estimated to be 88% higher than for the conventional solvent-based heat-set inks plus incineration; however, this cost analysis was also made 2-3 years ago and is probably not applicable today. In any event, although the cost is higher, the rate of increase in cost of the ultraviolet light-cured inks is often less in today's rapidly changing market than the corresponding increase of the conventional solvent-based inks.

Summary

Ultraviolet light-cured inks have been formulated and used successfully in letterpress, lithographic, gravure, and flexographic printing as a substitute for the solvent-based paste and liquid inks currently used. These new ultraviolet light-cured inks offer advantages other than the elimination of solvent emission, notably, a combination of excellent film properties with fast printing speeds. The great interest in their development is shown by the large number of patent citations describing various compositions that can be cured by ultraviolet light. Although the future of these new inks must be determined by commercial trial, it appears that their most promising future is in the paste inks used in letterpress and lithographic printing rather than in the liquid inks used in gravure or flexographic printing.

References

1. 1972 U.S. Census of Manufacturers; cited in American Ink Maker 52(5), 19 (1974).

2. National Association of Printing Ink Manufacturers, 101 Executive Boulevard, Elmsford, New York 10523.

3. P. D. Mitton, "Opacity, Hiding Power, and Tinting Strength," in Printing Ink Handbook Vol. III, T. C. Patton, editor, John Wiley & Sons, New York, 1973, p. 289-339; J. W. Vanderhoff, "Rheology and Dispersion of Printing Inks," ibid., p. 409-416.

4. A. C. Zettlemoyer and R. R. Myers, "The Rheology of Printing Inks," in Rheology Vol. 3, F. R. Eirich, editor, Academic Press, New York, 1960, p. 146.

5. W. C. Walker and J. M. Fetsko, American Ink Maker 33(12), 38 1955.

6. J. M. Fetsko, Tappi 41(2), 49 (1958).

7.   R. W. Bassemir, Preprints, 8th TAPPI Graphic Arts Conference,
     Miami, Fla., Oct. 19-22, 1971, p. 21.

8.   J. W. Vanderhoff, American Ink Maker 51(4), 38 (1973).

9.   J. W. Matheson, "Tech Talk #5," American Paper Institute, 1971.

10. S. V. Nablo, B. S. Quintal, and A. D. Fussa, paper presented at
     the Annual Meeting, Federation of Societies for Paint Technology,
     Chicago, Ill., Nov. 1973.

11. M. H. Bruno, "State of the Art of Printing in the U. S. A.," paper
     presented at the 11th International Conference of IARIGAI, Rochester,
     N. Y., May 12-19, 1971.

12. A. Morano, "Catalytic Thermo-Cured Web Inks," talk presented at
     the New York Printing Ink Production Club meeting, Sept. 20, 1972.

13. H. Dunn, paper presented at the 8th TAPPI Graphic Arts Conference,
     Miami, Fla., Oct. 19-22, 1971; published in Penrose Annual.

14. J. P. Costello (to Fred'k H. Levey Co., Inc.), U. S. 2,696,168,
     Dec. 7, 1954.

15. W. A. Rocap, Jr., Meredith Printing Co., Des Moines, Iowa,
     private communication, October 1972.

16. Eastman Chemical Products Publication X-214, "Alcohol-Soluble
     Propionate (ASP) in Printing Inks," and Customer Service Report
     217-1, "Alcohol-Soluble Propionate in Flexographic and Gravure
     Printing Inks."

17. R. W. Bassemir, R. Dennis, and G. I. Nass (to Sun Chemical Corp.),
     U. S. 3,551,235, Dec. 29, 1970.

18. R. W. Bassemir, D. J. Carlick, and G. E. Sprenger (to Sun
     Chemical Corp.), U. S. 3,551,246, Dec. 29, 1970.

19. G. I. Nass, R. W. Bassemir, and D. J. Carlick (to Sun Chemical
     Corp.), U. S. 3,551,311, Dec. 29, 1970.

20. R. W. Bassemir, R. Dennis, and G. I. Nass (to Sun Chemical Corp.),
     U. S. 3,552,986, Jan. 5, 1971.

21. R. W. Bassemir, D. J. Carlick, and G. I. Nass (to Sun Chemical Corp.), U.S. 3,661,614, May 9, 1972.

22. K. Hosoi, H. Sagami, and I. Imai (to Ashai Chemical Industry Co., Ltd.), Ger. Offen. 2,164,518, July 20, 1972; CA 78, 45224c (1973).

23. T. Ichijo, T. Nishibuko, and K. Maki (to Japan Seal Oil Industry Co., Ltd.), Japan Kokai 72 22,490, Oct. 7, 1972; CA 78, 30778n (1973).

24. R. E. Beaupre, M. N. Gilano, and M. A. Lipson (to Dynachem Corp.), Ger. Offen. 2,205,146, Nov. 23, 1972; CA 78, 59876d (1973).

25. C. Osada, M. Satomura, and H. Ono (to Fuji Photo Film Co., Ltd.), Ger. Offen. 2,222,472, Nov. 23, 1972; CA 78, 45221z (1973).

26. Y. Nemoto, M. Shiraishi, and T. Syuto (to Dainnippon Ink and Chemicals, Inc.), Ger. Offen, 2,157,115, June 22, 1972; CA 77, 90224t (1972).

27. Y. Nemoto and S. Takahashi (to Dainippon Ink and Chemicals, Inc.), Ger. Offen. 2,158,529, June 22, 1972; CA 77, 90225u (1972).

28. J. F. Ackerman, J. Weisfeld, R. G. Savageau, and G. Beerli (to Inmont Corp.), U.S. 3,673,140, June 27, 1972.

29. J. F. Ackerman, G. Beerli, R. G. Savageau, and J. Weisfeld (to Inmont Corp.), U.S. 3,713,864, Jan. 30, 1973.

30. G. Pasternak (to Continental Can Co., Inc.), U.S. 3,712,871, Jan. 23, 1973.

31. M. R. Sandner and C. L. Osborn (to Union Carbide Corp.), Ger. Offen 2,261,383, June 20, 1973; CA 79, 127478y (1973).

32. T. Kakawa and T. Kato (to Kansai Paint Co., Ltd.), Japan Kokai 73 43,729, June 23, 1973; CA 78, 93572g (1973).

33. S. Nakabayashi and I. Sumiyoshi (to Nippon Paint Co., Ltd.), Japan Kokai 73 47,534, July 6, 1973; CA 79, 106212s (1973).

34. H. Morishita (to Kansai Paint Co., Ltd.), Japan Kokai 73 54,135, July 30, 1973; CA 80, 5033z (1974).

35. J. E. Gaske and R. E. Ansel (to De Soto, Inc.), U.S. 3,749,592, July 31, 1973.

36. S. B. Radlove, A. Ravve, and K. H. Brown (to Continental Can Co., Inc.), Ger. Offen 2,317,522, Oct. 31, 1973; CA 80, 84858y (1974).

37. M. Shiraishi, Y. Yanagida, and H. Hisamatsu (to Dainippon Ink and Chemicals, Inc.), Japan Kokai 73 85,628, Nov. 13, 1973; CA 80, 97460n (1974).

38. S. I. Schlesinger (to American Can Co.), Ger. Offen. 2,035,890, Jan. 27, 1972; CA 77, 68565h (1972).

39. S. I. Schlesinger (to American Can Co.), U.S. 3,708,296, Jan. 2, 1973.

40. W. R. Watt (to American Can Co.), U.S. 3,721,617, Mar. 20, 1973.

41. T. Nishibuko, S. Ugai, and T. Ichijo (to Japan Seal Oil Industry Co., Ltd.), Japan Kokai 73 55,280, Aug. 3, 1973; CA 80, 72185p (1974).

42. E. Guertler, R. Kiessig, P. Herte, H. Schuelert, R. Zenker, and P. Noekel, Ger. (East) 81,929, Oct. 5, 1971; CA 78, 59875c (1973).

43. H. Seidl, H. Meyer, and H.-J. Twittenhof (to Peroxid-Chemie G.m.b.H.), Ger. Offen. 2,102,366, Aug. 3, 1973; CA 78, 31569q (1973).

44. A. Bassl, Ger. (East) 91,706, Aug. 5, 1972; CA 78, 59891e (1973).

45. K. Fuhr, H. J. Traencker, H. J. Rosenkrant, H. Rudolph, M. Patheiger, and A. Haus (to Farbenfabriken Bayer A.-G.), Ger. Offen. 2,221,335, Nov. 15, 1973; CA 80, 49390t (1974).

46. H. Rosenkranz, A. Haus, and H. Rudolph (to Farbenfabriken Bayer A.-G.), Ger. Offen. 2,105,179, Aug. 10, 1972; CA 78, 31603p (1973).

47. V. S. Lapatukhin, L. P. Savanov, and V. P. Tikhonov, U.S.S.R. 355,203, Oct. 16, 1972; CA 78, 86137v (1973).

48. R. G. Savageau and P. J. Whyzmuzis (to Inmont Corp.), Ger. Offen. 2,216,154, Oct. 19, 1972; CA 78, 45254n (1973).

49. C. Sander (Robert Hildebrand Maschinenbau G. m. b. H.), Ger. Offen. 2,213,831, Sept. 27, 1973; CA <u>80</u>, 16596m (1974).

50. AKZO N. V., Neth. Appl. 72 05,394, Oct. 23, 1973; CA <u>80</u>, 72142x (1974).

51. R. Havinga and P. D. Swaters (Akzo G. m. b. H.), Ger. Offen. 2,317,846, Oct. 31, 1973; CA <u>80</u>, 49372p (1974).

52. J. J. Bulloff, Polymer Eng. Sci. <u>11</u>(5), 405 (1971).

53. J. Kinstle, Paint Varnish Prod., June 1973, p. 17.

54. V. D. McGinniss and D. M. Dusek, J. Paint Tech. <u>46</u>(589), 23 (1974).

55. H. Rubin, J. Paint Tech. <u>46</u>(588), 74 (1973).

56. R. W. Bassemir and A. J. Bean, paper presented at 26th Annual Meeting of TAGA, St. Paul, Minn., May 13–15, 1974; to be published in TAGA Proceedings.

57. V. D. McGinniss and D. M. Dusek, Am. Chem. Soc. Div. Polymer Chem. Preprints <u>15</u>(1), 480 (1974)

58. V. D. McGinniss, R. M. Holsworth, and D. M. Dusek, Am. Chem. Soc. Div. Org. Coatings Plastics Chem. <u>34</u>(1), 667 (1974).

13

Use of the Interaction of Ultraviolet Light With Chain Molecules to Study the Rate of Conformational Transition

H. MORAWETZ

Polytechnic Institute of New York, Brooklyn, N. Y. 11201

In the study of the solution properties of flexible chain polymers, a great deal of emphasis has been placed on methods by which the mean extension of the chain molecule can be characterized. The mean square radius of gyration of the molecular chain, $<s^2>$, is obtained rigorously from the angular dependence of light scattering intensity ($\underline{1}$) and a less rigorous but experimentally more convenient estimate of this quantity can be derived from the intrinsic viscosity ($\underline{2}$). As is well known, $<s^2>$ may be represented by $<s_0^2>\alpha^2$, where the "unperturbed" mean square radius of gyration $<s_0^2>$ depends on the conformational distribution in the chain backbone determined by short-range interactions, while the "expansion coefficient" α arises from long-range interactions which lead to an excluded volume effect depending on the polymer-solvent interactions and the length of the chain molecules ($\underline{3}$).

Relatively much less is known about the rate at which conformational transitions take place. In comparing such a process in a long chain molecule and in an analogous molecule of low molecular weight, we are faced with a conceptual difficulty: If the conformational transition involves rotation around a single bond in the backbone of the polymer, a long chain would have to swing rapidly through a viscous medium and such a process would lead to a prohibitively large dissipation of energy. It was, therefore, suggested that conformational transitions take place by a coordinated rotation around two bonds, so that only a short section of the chain is involved in a "crankshaft-like motion" ($\underline{4}$)($\underline{5}$). This concept is illustrated in Figure 1. However, the requirement of such a coordinated motion would necessarily lead to a pronounced increase of the free energy of activation and one should, therefore, expect conformational transitions in long chain molecules to be slower than in their low molecular weight analogs. We have looked for such an effect by using an NMR technique for the study of conformational transitions in piperazine polyamides and their low molecular weight analogs, but found that there is no significant difference between the rates of their conformational transitions ($\underline{6}$).

<u>Photochemical and Thermal Isomerization Rates of Polymers
Containing Azobenzene Residues</u>. The NMR technique for studying
rates of conformational transitions suffers from two limitations.
(1) High resolution spectra are obtainable only in systems of low
viscosity and the technique cannot, therefore, be applied to a
study of conformational transitions in concentrated polymer sys-
tems. (2) Analysis of the data leads only to a mean rate cons-
tant and the method is, therefore, not suitable for detecting
differences between the conformational mobility of chemically
similar groups. Both these limitations are eliminated if we
follow by ultraviolet spectroscopy the photochemical or thermal
isomerization of azobenzene residues in the backbone or the side
chains of polymeric molecules. The photochemical trans-cis
isomerization leads to a shift of the absorption peak to shorter
wavelength and the thermal reverse reaction to the more stable
trans form takes place at convenient rates in the neighborhood
of ambient temperatures. A Nylon 66-type polyamide containing a
small number of azodianiline residues

$$-CO(CH_2)_4CONH-\bigcirc-N=N-\bigcirc-NHCO(CH_2)_4CONH(CH_2)_6NH-$$

was prepared and its behavior was compared with that of the
analog

$$C_6H_{11}CONH-\bigcirc-N=N-\bigcirc-NHCO\ C_6H_{11}$$
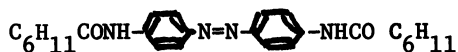
It was found that in 95% formic acid solution the ratio of the
dark reaction, following photoisomerization to the cis form, was
the same, within experimental error, for the polymer and the small
molecules (*7*). Moreover, this equivalence held even for polymer
solutions containing 15 weight % of Nylon 66 and 15 weight % of
its low molecular weight analog, N-propylpropionamide, although
at this concentration the polymer molecules would be heavily
intertwined.

These results seem incompatible with the assumption of a
"crankshaft-like motion". We believe that they can be understood
if we assume that the transition from the cis to the trans form
does not take place in a single step but rather by a large number
of oscillations around the bond angle by which the transition
state is approached. If we then impede these oscillations by
incorporating the azobenzene group into a polymer chain, we reduce
equally the rate at which the transition state is approached and
the rate at which a strained bond relaxes to its initial shape.
The transition state is then still in equilibrium with the ground
state and incorporation of the azobenzene residue into a polymer
chain has no effect on its rate of isomerization.

It may be noted that this argument is similar as in the case
of bimolecular reactions, which have reaction rates independent of
the viscosity of the medium as long as they are characterized by

high activation energies. This is so since a large number of
collisions are required for the reaction and an increasing visco-
sity slows down both the approach of the reagents towards each
other and their diffusion apart.

The behavior of the polyamides described above could not be
studied in bulk because the polymer is crystalline and is not
transparent. However, with a methyl methacrylate copolymer
carrying a small number of azobenzene residues in side chains
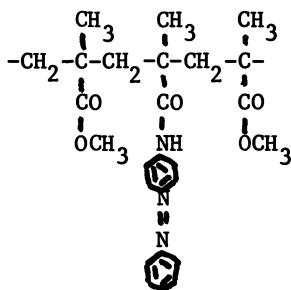
Copolymer ABA-MMA

data could be collected over the entire concentration range, from
dilute solution to the glassy polymer in bulk (8). The results
for the thermal reaction following photoisomerization are shown
in Figure 2. It may be seen that the rate of isomerization is
almost identical for a dilute polymer solution in butyl acetate
and a polymer film plasticized with 30% of dioctyl phthalate.
Even more surprising is the behavior of the unplasticized polymer:
Here the isomerization deviates from first-order kinetics exhibi-
ting an anomalous component faster than in dilute solution! We
believe that this is due to azobenzene residues which are trapped
during the photoisomerization in high energy conformations from
which they may return more easily to the stable trans form. This
concept is supported by the observation that samples irradiated
above the glass transition temperature and cooled under irradia-
tion do not exhibit this anomaly. In any case, the results consti-
tute an interesting chemical demonstration of the micro-hetero-
geneity of the glassy state. Similar results were obtained with
the isomerization of azonaphthalene and 4-ethoxyazobenzene dis-
solved in a glassy polymer (9).

A comparison of the photochemical behavior of azobenzene
residues in the backbone and the side chains of polymers is of
special interest since the short lifetime of the excited state
makes it more difficult for the chain to undergo long-range con-
formational changes favoring the trans-cis isomerization process.
In fact, the photochemical process is much less sensitive to the
rigidity of the system if the azobenzene is attached as a side
chain. Copolymer ABA-MMA exhibited a quantum efficiency only 4-5
times lower in a glassy film then in dilute solution (8). By
contrast, Figure 3 shows the relative quantum efficiencies for the
trans-cis isomerization of a copolyamide of isophthalic acid with
4,4'-diaminodiphenyl sulfone containing a small proportion of
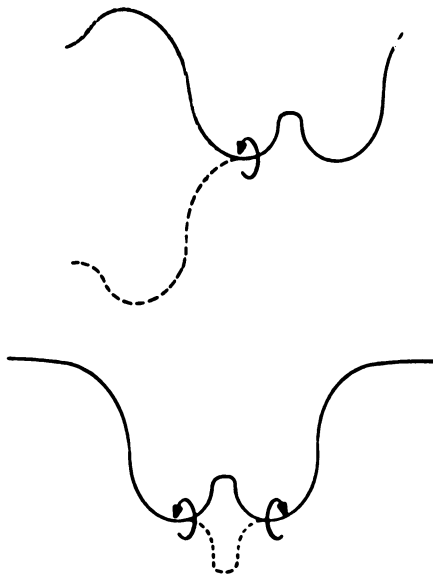
Figure 1.   Schematic of a conformational transition in a polymer chain. Top, rotation around a single bond; bottom, correlated rotations around two bonds in a crankshaft-like motion.
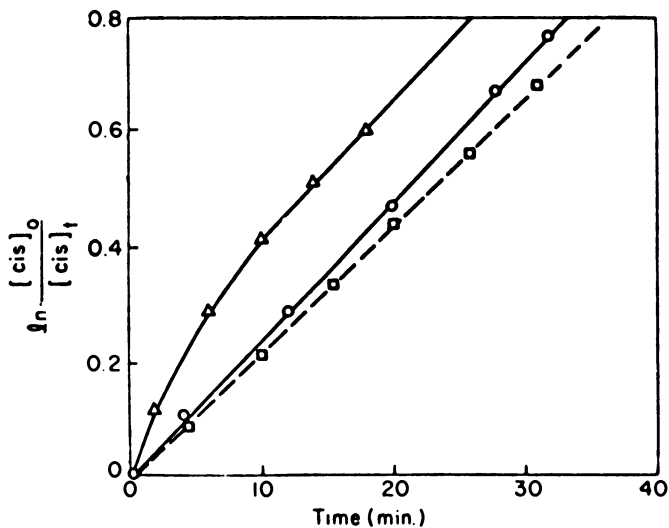
Figure 2.   Medium-dependence of the rate of cis–trans isomerization of copolymer ABA-MMA. ☐, dilute solution in butyl acetate; △, polymer in bulk; ○, polymer plasticized with 30% DOP.
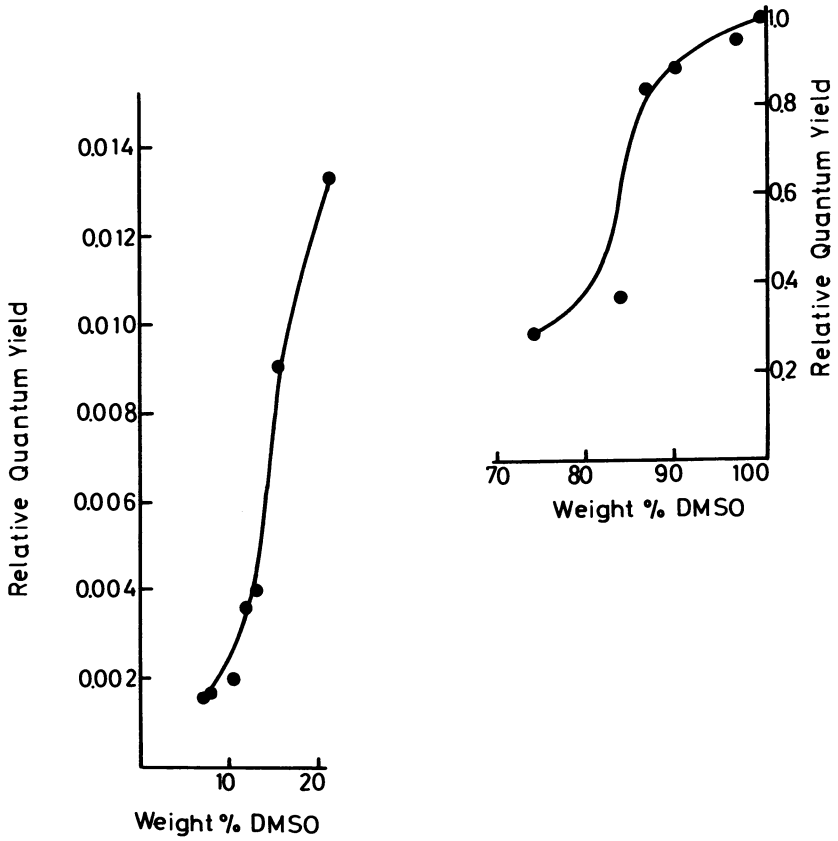
Figure 3. Photoisomerization of isophthalic acid copolyamide with 4,4'-diamino-diphenylsulfone and 4,4'-diaminoazobenzene

4,4'-diaminoazobenzene residues

$$-NH-\underset{}{\bigcirc}-N=N-\underset{}{\bigcirc}-NHCO-\underset{}{\bigcirc}-CONH-\underset{}{\bigcirc}-SO_2-\underset{}{\bigcirc}-NH-$$

as a function of the dilution of the polymer with dimethylsulfo-
xide (10). It may be seen that with the azobenzene residue in the
chain backbone, there is a very sharp drop in the quantum efficie-
ncy of the photoisomerization in solutions containing about 15
weight % of polymer. In glassy films containing small proportions
of DMSO, the quantum efficiency is extremely low. Unfortunately,
we were not able to determine it in the completely unplasticized
polymer, since it is soluble only in non-volatile solvents which
cannot be completely removed.

Intramolecular Excimer Fluorescence Studies in Polymers
Carrying Aromatic Side Chains. Some years ago, it was shown that
certain excited aromatic molecules may form a complex with a simi-
lar molecule in the ground state, which is characterized by a
structureless emission band red-shifted relative to the emission
spectrum of the monomer. The formation of such complexes, called
"excimers", requires the two chromophores to lie almost parallel
to one another at a distance not exceeding about 3.5A$^\circ$ (11). Later,
it was found that intramolecular excimer formation is also possi-
ble. In a series of compounds of the type $C_6H_5(CH_2)_nC_6H_5$, excimer
fluorescence, with a maximum at 340nm, was observed only for n=3 –
all the other compounds had emission spectra similar to toluene,
with a maximum at about 280nm (12). Similar behavior was observed
in polystyrene solutions, where the phenyl groups are also separ-
ated from one another by three carbon atoms (13).

It is obvious, that the conformation of a section of poly-
styrene which is required to make two neighboring phenyl residues
lie parallel to one another (at a distance of about 2.5A$^\circ$) would
be characterized by a prohibitive potential energy and such a
conformation would not be expected to be significant in the
ground state. This conclusion is also supported by the fact that
polystyrene exhibits the normal UV spectrum of alkylbenzene, while
benzene rings constrained to lie parallel to one another at such a
short separation have characteristically distorted absorption
spectra (14). We must, therefore, conclude that excimers are
formed by a conformational transition during the lifetime of the
excited state. This transition is assisted by the large exother-
micity of excimer formation which is characterized by ΔH values of
–5.1 and –3.9 kcal/mole for benzene and toluene, and by –5.8
and –6.9 kcal/mole for naphthalene and the methylnaphthalenes (11).

Recent studies in our laboratory were aimed at defining more
closely the conditions governing intramolecular excimer formation
in dilute polymer solutions (15). An alternating copolymer of
styrene with maleic anhydride or methylmethacrylate showed no
excimer emission, confirming that interactions of other than
neighboring phenyl residues made no significant contribution to

the effect. Poly(α-methylstyrene) had an even larger fraction of its emission in the excimer band than polystyrene; presumably, this polymer is highly strained in all its conformations and the additional energy requirement for the conformation in which neighboring phenyl groups are parallel to each other is smaller than in the less hindered polymer containing no quaternary carbons in the chain backbone. It was, however, quite enexpected that the alternating copolymer of stilbene and maleic anhydride

(-CH-CH-CH-CH-)$_n$
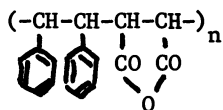
had an excimer emission band, since this had been found absent in both 1,2-diphenylethane and 1,4-diphenylbutane (12). We see here, that the peculiar conformational restrictions of a polymer chain can produce effects which are not easily simulated in low molecular weight analogs.

An interesting problem arises with polyacenaphthylene

(-CH-CH-)$_n$
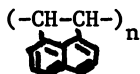
where the rigidity of the chain clearly precludes a face-to-face orientation of two neighboring naphthalene residues. Yet, this polymer does exhibit excimer fluorescence and this has been assumed to arise by interaction of next-to-nearest neighbors (16). We have confirmed this interpretation by showing that the alternating acenaphthylene-maleic anhydride copolymer behaves in a very similar manner as the homopolymer. Table I lists the ratio I_D/I_M of the quantum yields of dimer and monomer fluorescence of alternating acenaphtylene copolymers with maleic anhydride and other comonomers. There is a striking contrast between the copolymers with acrylonitrile or methyl acrylate, where there is very little excimer formation, and copolymers with methacrylonitrile or methyl methacrylate, where excimer emission is much more pronounced than in polyacenaphthylene. It is seen that excimer emission is a sensitive indicator of a change in the conformational distribution of the polymer chain.

Table I. Ratio of Quantum Efficiencies of Excimer and Normal Emission in Acenaphthylene Homopolymer and Equimolar Copolymers

Comonomer	I_D/I_M
None	1.2
Maleic Anhydride	1.2
Methyl Acrylate	0.3
Acrylonitrile	0.3
Methyl Methacrylate	2.2
Methacrylonitrile	3.3

Since a conformational transition during the short lifetime of the excited state is required for excimer formation, excimer fluorescence is potentially a powerful tool for studying conformational changes involving relatively low energy barriers. The feasibility of this approach has recently been demonstrated on 1,3-di(α-naphthyl)propane by following the time-dependence of the excimer fluorescence intensity (17). In ethanol solution at 25°C, a rate constant of $1,2 \times 10^8$ sec^{-1} was measured and this rate constant was found to decrease with an increase in the viscosity of the medium. We have prepared the monomer N,N'-dibenzylacrylamide and copolymerized it with a large excess of methyl methacrylate to study the effect of the rigidity of the medium on excimer formation in a group attached to a polymer chain. As would be expected, excimer fluorescence was observed in dilute solution, but not in the glassy polymer film. However, a trace of dibenzyl ether dissolved in poly(methyl methacrylate) did exhibit some excimer emission. We intend to expand studies of this type of compare the results with experiments on the viscosity dependence of excimer emission requiring conformational transitions in the chain backbone. Data of this kind should clarify the validity of theories dealing with the role of potential energy barriers and the viscosity of the solvent medium in determining rates of conformational transitions (18).

Acknowledgement

Literature Cited

1. Zimm, B.H. J.Chem.Phys. (1948) 16, 1099.
2. Flory, P.J. J.Chem.Phys. (1949) 17, 303.
3. Flory, P.J. "Statistical Mechanics of Chain Molecules", Interscience Publ., New York (1969).
4. Schatzki, T. Polymer Prepr., Am.Chem.Soc., Div.Polym.Chem. (1965) 6, 646.
5. Helfand, E. J.Chem.Phys. (1971) 54, 4651.
6. Miron, Y., McGarvey, B.R., and Morawetz, H. Macromolecules (1969) 2, 154.
7. Tabak, D., and Morawetz, H. Macromolecules (1970) 3, 403.
8. Paik, C.S., and Morawetz, H. Macromolecules (1972) 5, 171.
9. Priest, W.J., and Sifain, M.M. J.Polym.Sci. (1971) A-1, 9, 3161.
10. Chen, D.T., and Morawetz, H.,unpublished results.
11. Birks, J.B. Progr.Reaction Kinetics (1970) 5, 181.
12. Hirayama, F. J.Chem.Phys. (1965) 42, 3163.
13. Vala, Jr., M.T., Haebig, J., and Rice, S.A. J.Chem.Phys. (1965) 43, 886.

14. Cram, D.J., Allinger, V.L., and Steinberg, H. J.Am.Chem.Soc.
     (1954) $\underline{76}$, 6132.
15. Wang, Y.C., and Morawetz, H. Macromol.Chem., $\underline{176}$ (in press).
16. David, C., Lempereur, M., and Geuskens, G. Eur.Polym.J.
     (1972) $\underline{8}$, 417.
17. Avouris, P., Kordas, T., and El-Bayoumi, M.A. Chem.Phys.Lett.
     (1974) $\underline{26}$, 373.
18. Peterlin, A. J.Polymer Sci. (1972) $\underline{B10}$, 101.

Photochemical Reaction of Monosubstituted Amino-azidobenzoic Acid Derivatives in Novolak

TAKAHIRO TSUNODA and TSUGUO YAMAOKA

Faculty of Engineering, Chiba University, Japan

We found that when 4.4'-diazidodiphenylamine in novolak was irradiated by UV light, novolak was insolubilized in alkali aqueous solution and colored in black.[1] But it is impossible to use it as photopolymer for plate-making because 4.4'-diazidodiphenylamine is very dangerous causing explosion during storage.

We investigated the photosensitive azide compounds that was stable and made a deep color image by UV irradiation. We synthesized monosubstitutedamino azidobenzoic acid derivatives which made a deep color image and caused insolubilization of novolak in alkali aqueous solution by UV irradiation. These photosensitive azide compounds including some couplers gave more deep color image by UV irradiation. 2.4-Dichloronaphthol was the most important coupler to photodecomposed monosubstitutedamino-azidobenzoic acids. The photosensitive layer (thickness: about 3.7μ) containing 2-(p-methylphenylamino)-5-azidobenzoic acid, 2.4-dichloronaphthol and novolak had the color density 1.48 by UV irradiation. The polyester film coated with this photocolored polymer was exposed by UV light through a negative film and then

washed out by dilute alkali aqueous solution to re-
move the unexposed area. The produced color image on
polyester film may be used as negative or positive
intermediate film for plate-making instead of silver
salt emulsion film.

Experimental

       1) Synthesis of 2-monosubstitutedamino-azido-
benzoic acid derivatives

  a) 2-Monosubstituted(R)amino-5-nitrobenzoic acid(I)
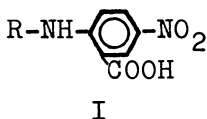
A mixture of 2-chloro-5-nitro-
benzoic acid and amine derivati-
ves in glycerol was stirred with
heat adding potassium carbonate.
After reaction, the solution was
filtered and acidified with hy-

R-NH-⟨O⟩-NO$_2$
      COOH
       I

drochloric acid. The precipitation was the reaction
product. Table 1 shows the reaction condition, pro-
ducts and yield.

  b) 2-Monosubstituted(R)amino-5-aminobenzoic acid
(HCl-salt)(II)
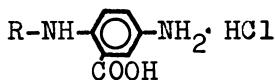
A mixture of I, methanol and
hydrochloric acid was refluxed
with tin powder for 3-5 hours
and then filtered. From the aci-
dified filtrate with hydrochlo-
ric acid, the reduced product,

R-NH-⟨O⟩-NH$_2$·HCl
      COOH

amine derivative was separated as hydrochloric acid
salt. Table 2 shows the reaction condition, products
and yield.

  c) 2-Monosubstituted(R)amino-5-azidobenzoic acid
(III)

  II was diazotized with nitrosyl sulfuric acid or
sodium nitrite in aqueous solution of acetic acid or

hydrochloric acid. After filtration, the diazotized II was azidotized with sodium azide. The precipitation was azide compound III.
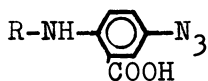
$$R-NH-\bigcirc-N_3$$
$$\text{COOH}$$
III

Table 3 shows the reaction condition, products and yield.

Table 1 / Table 2
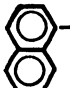
R-	Temp. °C	Reaction hour hrs	Yield %	Melting point °C	Reaction hour hrs	Yield %	Melting point °C
Cl-◯-	140	5	46.1	251-3	3	63.9	232-5
◯-	130	6	94.4	246.5-7.5	4	61.9	216-7
CH₃-◯-	140	5	81.9	146-8	5	97.2	207-8
CH₃O-◯	140	4	80.8	186-7	5	69.8	226-9
◯◯ (naphthyl)	140	5	13.0	258-9	3	45.7	214-5

Table 3

R-	Reaction hour(hrs) Diazo	Reaction hour(hrs) Azido	Yield %	Melting point °C	Compound
Cl-◯-	1	1	74.4	over 250	2-(p-chlorophenyl-amino)-5-azidobenzoic acid III$_a$
◯-	1	1	90.1	253-4	2-phenylamino-5-azidobenzoic acid III$_b$
CH₃-◯-	1	4	46.8	257-9	2-(p-methylphenyl-amino)-5-azidobenzoic acid III$_c$
CH₃O-◯-	1	1	56.5	156 decom.	2-(p-methoxyphenyl-amino)-5-azidobenzoic acid III$_d$

	1	1	51.7	162 decom	2-(α-naphthylamino)-5-azidobenzoic acid III_e

2) Novolak resin

m-Cresol type novolak, Alnovol 429K (Chemische Werke Albert Wiesbaden-Biebricht) was used.

3) Couplers

2.4-Dichloronaphthol(mp.107°C), 4-methoxynaphthol (mp.125°C), 1-phenyl-3-methylpyrazolone(mp.129°C) and 2.5-dichloroacetacetanilide(mp.95°C) were used as coupler to photodecomposed 2-monosubstitutedamino -5-azidobenzoic acids.

4) Measurement of Infrared spectra

Infrared spectra were measured by Hitachi EPI-S2 type spectrophotometer.

5) Measurement of spectral sensitivity

Spectral sensitivities were measured by Narumi RM-35 monochromator equipped with grating and 450W Xenon arc lamp.

6) Measurement of optical density of colored image.

Macbeth densitometer was used for measurement of transmittance density.

7) Exposure equipment

Vacume printer equiped with ten 40W chemical lamps (Dainippon Screen P-113-B) was used. The distance from lamp to negative film was 4.4 cm.

8) Photodecomposition and separation of photodecomposed products

In 500 ml of benzene, 0.5g of azide compound was solved. In a flask equipped with UV light source, the azide in benzene was photodecomposed passing nitrogene gass. The photodecomposed products were separated by column chromatography with developement

solvents of chloroform and acetone.

Result and discussion

Table 4 and 5 show the color and optical density of photodecomposed 2-monosubstitutedamino-5-azidobenzoic acid. The colors in table 4 were produced by UV irradiation to a filter paper absorbed with 30% methanol solution of azide compounds. The colors in table 5 were produced by UV irradiation to a grained aluminum plate or polyester film coated with 10% solution of mixture of novolak and azide compounds (10:3) solved in methylethylketone.

Table 4 The color of photodecomposed azides coated on filter paper without novolak

Table 5 The density of photodecomposed azides coated on polyester film with novolak

Compound	Exposure time (min.)	Color	Exposure time (min.)	Color	Optical density
					coating thickness (micron) after wash out
III$_a$	1 3 5	light G. light G. light G. (G:gray)	-	————	————
III$_b$	1 3 5	light G. black black	2	black	0.30
III$_c$	1 3 5	light G. black black	2	black	0.30
III$_d$	1 3 5	light G. black black	2	green black	0.32
III$_e$	1 3 5	light G. black black	1	black	0.36

The transmittance densities of the colored image
were measured on polyester film after UV irradiation
or after irradiation and washing out in 2% aqueous
solution of sodium phosphate.
  Fig. 1 shows the spectral sensitivities of these
azide compounds. The mechanism of the color reaction
is not clear, but it is assumed that the various rea-
ction products of nitrenes from photodecomposed azi-
de compounds produce the mixed coloring matter.
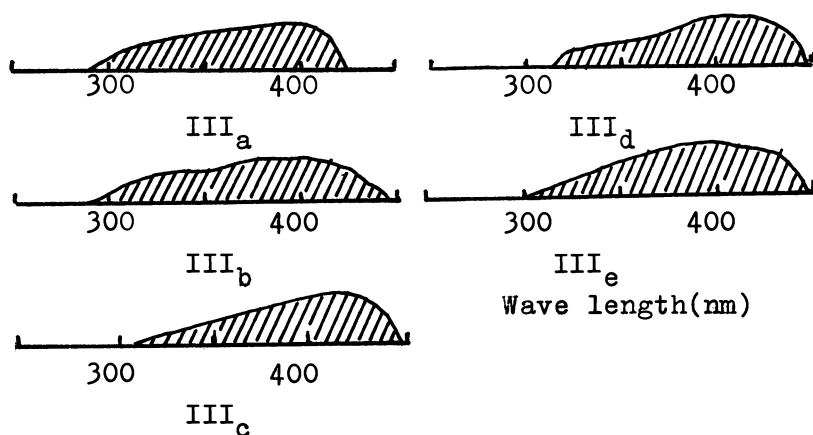
Figure 1. Spectral sensitivities of 2-monosubstituted-amino-5-azidobenzoic acids

  In this photocolor reaction of 2-monosubstituted-
amino-5-azidobenzoic acid, the imino and carboxilic
groups in the molecules are very important. The com-
pounds(IV and V) which hydrogen of these groups are
substituted with alkyl group are very hypsochromic
when they are photodecomposed. The reason why the
photodecomposed IV and V are hypsochromic may be due
to the fact that they can not have inner salt struc-
ture like VI .
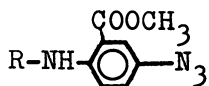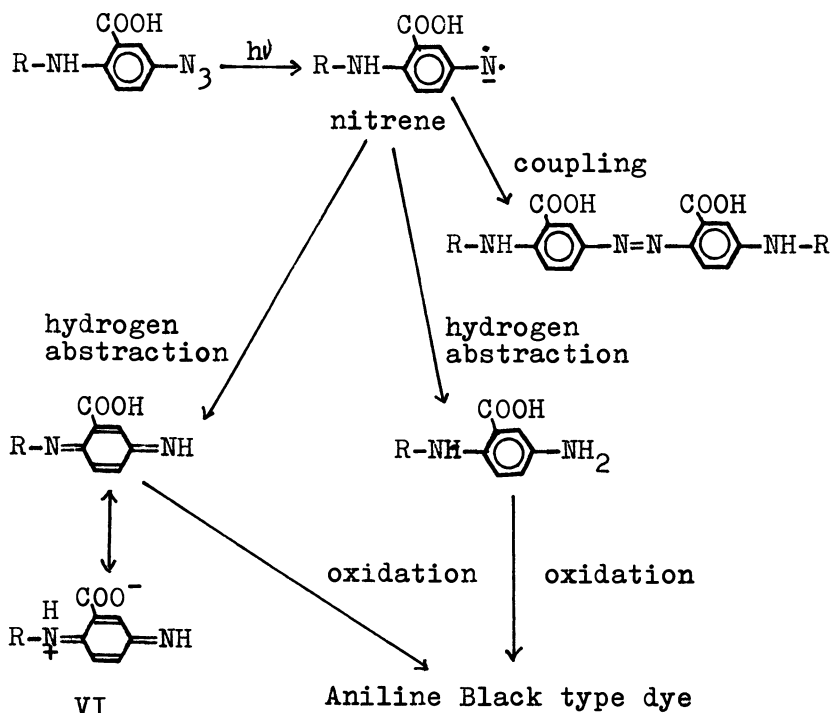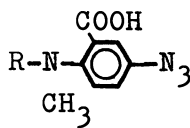
When the mixture of 2-monosubstitutedamino-5-azido-
benzoic acid and novolak was irradiated by UV light,
photocolor and photocure occured at the same time. In
this case, it is considered that quinonimine derivat-
ives are also produced by the photoreaction between
azide compounds and novolak.[2]

quinonimine
compound
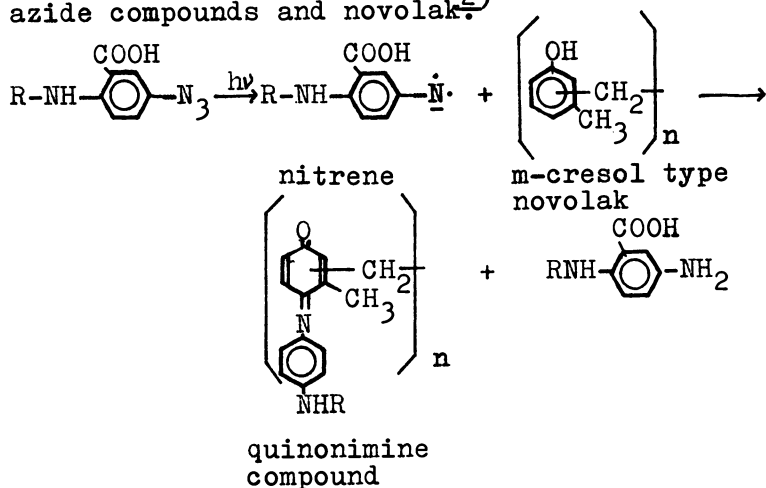
Fig. 2 shows the Infrared spectra of 2-phenylamino-
5-azidobenzoic acid III_b and the photodecomposed pro-
duct in KBr tablet by UV irradiation.
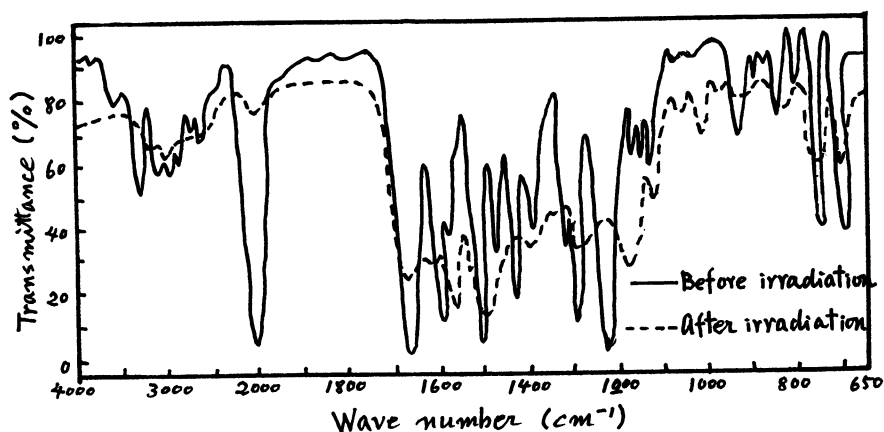
Figure 2. Infrared spectra of 2-phenylamino-5-azidobenzoic acid and the photode-
composed product

2-Phenylamino-5-azidobenzoic acid III$_b$ was photo-
decomposed in benzene without oxygen, and then the
photodecomposed products were separated by column
chromatography. Fig. 3 shows the Infrared spectrum of
the photodecomposed component obtained from the deve-
loped layer of the column.
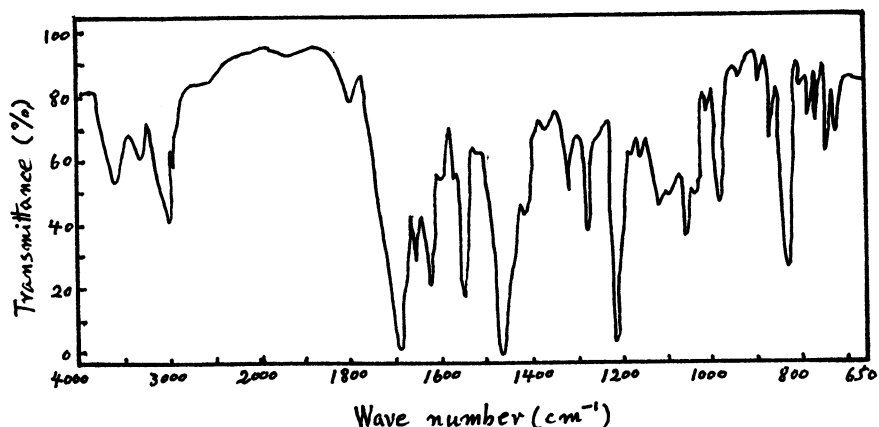
*Figure 3.   Infrared spectrum of the one component from photodecomposed 2-phenyl-
amino-5-azidobenzoic acid*

A mixture of 2-monosubstitutedamino-5-azidobenzoic
acid and coupler gave deep color image by UV irradi-
ation. It seems that the dye produced by coupling
photodecomposed azide with coupler added to the pho-
tocolor of monosubstitutedamino-azidobenzoic acid.
For example, the coupling reaction is as follows[3];
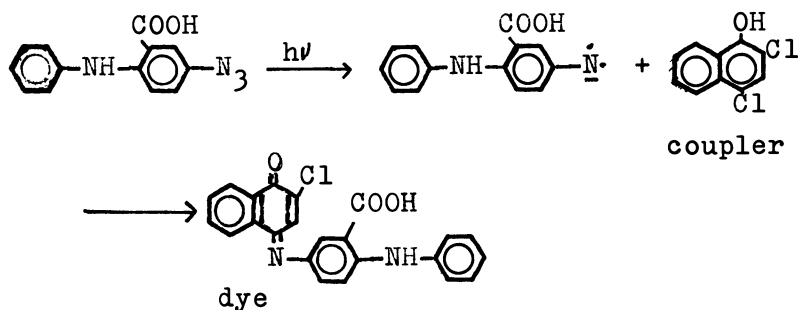
The following example is the coating solution cont-
aining azide compound, novolak and coupler. The ave-
rage thickness of coating layer was 3.7μ. All parts
given are by weight percent.

azide compound	5
novolak(alnovol)	32
coupler	4
methylcellosolve	59

Table 6 shows the transmittance densities of the
color images produced by UV irradiation to the coat-
ing layer of the mixture of azide compound, novolak
and coupler on polyester film, and then by washing
out in 2% aqueous solution of sodium phosphate. The
color image from the mixture of 2-(p-methylphenylam-
ino)-5azidobenzoic acid(III$_c$) and 2.4-dichloronaphth-
ol gave the highest density 1.48 .
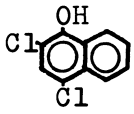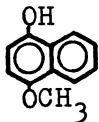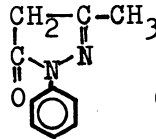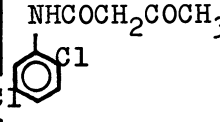
Conclusion

        2-Monosubstitutedamino-5-azidobenzoic acid der-
ivatives are very useful for photocoloring matter.
The density of the photocolor image increases by add-
ing a proper coupler to the azide compound. It is
possible to fix the colored image using the photo-
polymers containing these azide compounds and novo-
lak. In future, it may be possible to use this photo-
color film for plate making instead of silver halide
emulsion film.

Acknowledgment

Table 6

C \ A	E	Cl—C₁₀H₆(OH)Cl Filter R	G	C₁₀H₆(OH)OCH₃ Filter R	G	CH₂-C-CH₃ azolone Filter R	G	NHCOCH₂COCH₃ Cl Filter R	G
IIIb	1	0.42	0.59	0.63	0.88	0.57	0.54		
	2	0.58	0.75	0.63	0.89				
	3	0.58	0.80	0.56	0.81	0.55	0.52		
	4	0.65	0.95	0.63	0.90				
	5	0.62	0.88	0.62	0.86	0.49	0.48		
IIIc	1	0.96	1.19	0.54	0.67	0.38	0.25	0.53	0.38
	2	0.97	1.20	0.57	0.64	0.40	0.29	0.57	0.40
	3	1.00	1.33	0.56	0.69	0.40	0.33	0.67	0.98
	4	1.07	1.48	0.58	0.68	0.41	0.32	0.69	0.47
	5	1.10	1.48	0.57	0.69	0.39	0.34	0.62	0.41
IIId	1	0.79	1.05			0.45	0.42		
	2	0.82	1.12			0.48	0.43		
	3	0.74	1.o5			0.51	0.44		
	4	0.76	1.17			0.58	0.55		
	5	0.84	1.18			0.56	0.52		
IIIe	1	0.61	0.90	0.56	0.66	0.26	0.24		
	2	0.60	0.89	0.51	0.56				
	3	0.62	0.92	0.59	0.69	0.39	0.33		
	4	0.65	0.91	0.58	0.73				
	5	0.60	0.88	0.55	0.67	0.38	0.34		

C:Coupler, A:Azide compound, E:Exposure time(min.)
R:Red filter, G:Green filter

Literature cited

1) T.Tsunoa, T.Yamaoka and Y.Yamaguchi: Japanese Patent pending

2) Takahiro Tsunoda: Technical Papers of Photopolymer Conference (1973) 20

3) J.J.Sagura and J.A.Van Allan (Kodak Co.): U.S. Pat. 3.062.650 (1962)

15

Photodegradation of Polyvinyl chloride

ERYL D. OWEN

Chemistry Department, University College, Cardiff, Wales

1. Introduction

The mechanisms of the thermal and photochemical degradation of poly(vinyl chloride) (PVC) continue to be active areas of research in polymer chemistry mainly because its high chemical resistance, comparatively low cost and wide variety of application make PVC one of the most widely used thermoplastic materials. The wide variety of forms which the material can take includes pastes, lattices, solutions, films, boards and moulded and extruded pieces and depends to a very large extent on the good electrical and mechanical properties of the polymer. In spite of these advantages the even wider application of the material has been restricted by its low thermal and photochemical stability. Thermal instability is a problem since processing of the polymer is carried out at about $200^{\circ}C$ and the photochemical instability places a limit on the extent of the outdoor applications which can be developed.

Both thermal and photochemical processes take the form of a dehydrochlorination reaction which leads to discolouration as well as extensive changes in the internal structure of the polymer which has an unfavourable effect on the desirable electrical and mechanical properties. It has become apparent that considerable similarity exists between the two degradation processes and that it is neither easy nor desirable to make a vigorous distinction between the two. Information gained from experiments on thermal degradation are often directly relevant to the analogous photochemical process.

The reaction involved may be written:-

$$\wedge\wedge CH_2 \cdot CHCl \cdot CH_2 \cdot CHCl \wedge\wedge \xrightarrow{h\nu} \wedge\wedge CH_2 \cdot CHCl \cdot CH=CH \wedge\wedge + HCl$$
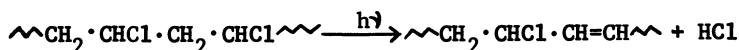
leading eventually to -

$$\wedge\wedge (CH_2 \cdot CHCl)_n \wedge\wedge \xrightarrow{h\nu} \wedge\wedge (CH=CH)_n \wedge\wedge + n \ HCl$$
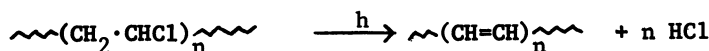
where $n = 5\text{-}10$[1,2]. The absorptions of these extended polyene structures spread into the visible region and makes the

208

material appear coloured. This is by no means the only change
which takes place since even in inert media the increase in
molecular weight inferred from viscosity measurements indicates
that cross linking of the chains occurs with the formation of an
insoluble three dimensional structure. When the reaction is
carried out in oxygen, attack on the original polymer and on the
polyene sequences takes place. The presence of $\rangle C=0,-00H$ and
OH groups can readily be detected in the photo-oxidised polymer
showing that the cross linking is accompanied by chain scission.
     Degradation can be minimised by the incorporation of
various types of stabilisers into the film. These have been
developed in a totally empirical way and their performance is
far from being totally satisfactory. Further improvements in
their performance however requires a more detailed understanding
of the mechanism of the degradation process and the point at
which the stabilisers intercept it. Areas at present under
investigation in this context may be classified as follows
a) the nature of the absorbing species which leads to a
   degradation reaction and hence the nature of the initiating
   step
b) the nature of the propagation step and the involvement of
   O_2,HCl or other components of the system
c) the extent of chain scission and cross linking and the effect
   that these have on the physical and mechanical properties
d) the mechanism by which the stabilisers act and the development
   of more efficient materials
     Because of the transparency of PVC in the visible and near
ultraviolet regions of the spectrum, the accent is on sensitized
processes considered both from the point of view of preventing
degradation (stabilization) and in some applications of
encouraging it (photodegradability).

Initiation and Polymer Structure
     It is now quite clear that the act of absorption which
initiates the degradation process has little to do with the
$\sim\sim(CH_2CHCl)\sim\sim$ repeat unit since absorptions arising as a result
of interaction of radiation with this chromophore will lie in the
far ultraviolet. Rather, structural irregularities which depend
strongly on the method of preparation of the polymer (i.e. bulk,
suspension, emulsion or solution), chromophores such as carbonyl
or hydroperoxy arising as a result of oxidative processes taking
place during the processing or the presence of impurities such as
traces of catalyst, surfactant or metal ions are likely to be the
dominant causes of absorptions which initiate the degradation
process.
a) Structural irregularities. Studies of the thermal stability
of a large number of model compounds including 2,4 dichloro-
pentane and 1,3,5-trichloroheptane show that they decompose at an
appreciable rate only above 200°C in the liquid phase[3,4] and only
above 300°C in the gas phase[5,6,7]. Pyrolysis of these compounds
in the gas phase is a homogeneous first order process with an

activation energy around 210 kJ mole^{-1}. The introduction of
further CH$_2$CHCl groups makes little difference which suggests
that chain length is not an important factor. PVC on the other
hand decomposes at 100°C so clearly structural irregularities
contribute to both thermal and photochemical instability.

The direct photolysis (254 nm) of the various isomeric
dichlorobutanes proceeds with the formation of HCl, 1 and 2
chlorobutanes and various unspecified chlorobutenes[8-10]. The
1,3 isomer is the simplest repeat unit present in PVC while the
2,3 and 1,4 isomers correspond to head to head and tail to tail
structures respectively. In the case of the 1,4 isomer a signi-
ficant amount of 1,4 1,3 isomerisation also occurs. The
mechanism proposed begins with dissociation of the C-Cl bond and
is followed by abstraction of hydrogen from a molecule of DCB by
the chlorine atom with the formation of HCl. The mechanism
proposed is essentially the same as that proposed by Benson and
Willard[11] for the HCl catalysed free radical isomerisation of
n-propyl Cl→isopropyl Cl but in this case nineteen hydrocarbon
products were detected in addition to various organic chlorides.

The alkyl aryl ketone sensitised photolysis (313 nm) of
hexane solutions of t-butyl Cl reported by Harriman[12] also gave
HCl as a major product together with 2-methyl propene. Quantum
yields ranged from 0.19 when benzophenone was the sensitiser to
0.313 for ϕEtC=O and the involvement of the triplet state was
confirmed by the quenching of the reaction by 2,5-dimethyl-hexa-
2,4 diene. Comparison of the range of E$_T$ values (280 – 330 kJ
mole^{-1}) of the sensitisers with the dissociation energy of the
C-Cl bond (327 kJ mole^{-1}) led these authors to suggest that some
charge transfer interaction was involved since there was ample
evidence for such a process occuring between triplet ketone
acceptors and amine[13] or sulphide[14] donors. In contrast,Golub[10]
has concluded that the photolysis of 1,4 DCB sensitised by a
variety of aliphatic ketone sensitisers is a singlet state
reaction. There is ample evidence that this is also the case
when aromatic hydrocarbons act as sensitisers in a variety of
processes. Finally Whittle has shown that hexafluoroacetone is
able to sensitise the elimination of HCl from a variety of alkyl
chlorides. It appears that the triplet or singlet state may be
involved and there is a strong possibility that the actual
elimination process occurs from a vibrationally excited ground
state. Clearly then different groups of workers favour the
singlet, triplet or vibrationally excited ground state as the
precursor for the elimination process.

There is little evidence to clarify the extent to which
catalyst end groups arising from initiation or termination of
the polymer –

i.e. R· + CH$_2$=CHCl $\longrightarrow$ R-CH$_2$-$\overset{\bullet}{\text{C}}$HCl

or $\sim\!\!\sim\!\!\overset{\bullet}{\text{C}}$HCl + R· $\longrightarrow$ $\sim\!\!\sim$CHClR
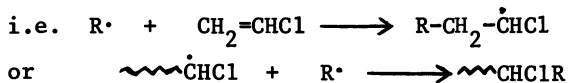
influence the photochemical stability but this will clearly be
determined by the nature of R and its absorption and photo-
chemical characteristics.

Effects of R on the thermal stability are contraversial
since all of the studies carried out so far have been plagued
by the presence of traces of unreacted catalyst present not as
a polymer end group but trapped within the polymer. These
traces of free catalyst are undoubtedly much more effective
than those present as end groups particularly since transfer
reactions mean that only 20-40% of the polymer have R ends.
Similar conclusions can be drawn regarding end group unsaturation
since the nature of the chromophore is such that absorptions
would be in the far ultraviolet unless the unsaturation was an
extended system of conjugation. Thermal stability of these
systems however is much more clearly defined and it may be
concluded that end group unsaturation contributes to the
instability of low molecular weight polymers only, while the
instability of high molecular weight fractions is more strongly
influenced by some other factor, probably the presence of
branch points or internal double bonds.

Many of the attempts which have been made to implicate
particular structural features as a cause of thermal or
photochemical instability have utilised low molecular weight
model compounds and there are several considerations which
severely limit any extrapolations which can be made from such
studies. Firstly although small model compounds undergo
unimolecular homogeneous reactions, the introduction of a
surface component could cause a dramatic reduction in the energy
of activation and so any possible surface effect could be very
important. Secondly many of the studies which have been
carried out in solution are complicated by factors such as
solvent participation or the catalytic effect of HCl. Thirdly,
as well as requiring information on the effect of particular
structural features, the frequency of their occurrence in the
polymer is also essential. Before enough information of this
type is available however much more information on the kinetics
of vinyl chloride polymerisation are required.

b) <u>Chromophores</u>. It is possible to imagine many
chromophores which could arise during processing of the
polymer but the most effective in affecting photostability
are probably $>C = 0$, $-OOH$ and metal ions M^{R+}. Ketones and
hydroperoxides have low intensity absorptions in the
ultraviolet region and there is no reason why these should be
much affected by attachment to a polymer chain. Some comments
have already been made regarding the ketone sensitised photolysis
of model compounds which occurs by transfer of energy from the
ketone to the alkyl chloride. In addition, several other
possible mechanisms of initiation are possible. For example the
ketone may decompose by the Norrish Type I mechanism with the
formation of free radicals thus:-

$$-\overset{|}{\underset{|}{C}}-\overset{O}{\overset{\|}{C}}-\overset{|}{\underset{|}{C}}- \quad \xrightarrow{h\nu} \quad -\overset{|}{\underset{|}{C}}-\overset{O}{\overset{\|}{C}}\cdot + \cdot\overset{|}{\underset{|}{C}}- \quad \longrightarrow \quad -\overset{|}{\underset{|}{C}}\cdot + \overset{O}{\overset{\|}{C}} + \cdot\overset{|}{\underset{|}{C}}-$$
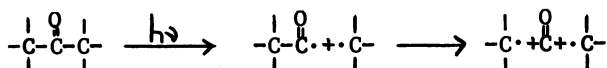
Alternatively the Norrish Type II process may operate since the
possibility of a γ hydrogen being available in the polymer is
high

$$-\overset{O}{\overset{\|}{C}}-\overset{|}{\underset{|}{C}}-\overset{|}{\underset{|}{C}}-\overset{|}{\underset{|}{C}}- \quad \xrightarrow{h\nu} \quad -\overset{OH}{\overset{|}{C}}=\overset{|}{C} + \overset{|}{\underset{|}{C}} = \overset{|}{\underset{|}{C}}$$

$$\overset{O}{\overset{\|}{C}}-\overset{|}{\underset{|}{C}}-$$
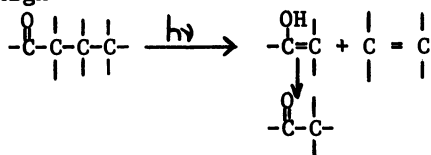
A further and very important possibility is the transfer of
energy from the ketone sensitiser to molecular oxygen forming
one of the two low lying singlet states of oxygen

$$^3\text{ketone} + \ ^3O_2 \ (^3\Sigma^-) \longrightarrow \text{ketone} + \ ^1O_2 \ (^1\Sigma_g^+ \text{ or } ^1\Delta).$$
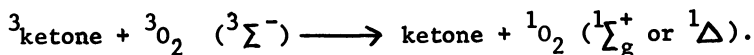
Reactions of singlet oxygen with isolated olefins having allylic
hydrogen atoms are extremely rapid and in this sense isolated
double bonds at any point in the polymer are a source of
photochemical instability

$$-\overset{|}{C}=\overset{|}{C}-\overset{|}{\underset{|}{C}}- + \ ^1O_2 \ (\Delta) \longrightarrow \overset{OOH}{-\overset{|}{\underset{|}{C}}-\overset{|}{C}=\overset{|}{C}}$$
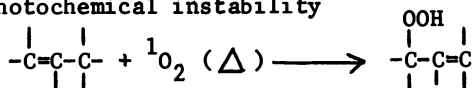
Yet another possible mode of initiation is hydrogen
abstraction thus:-

$$^3\text{ketone} + RH \longrightarrow \text{ketone}\cdot\text{-H} + R\cdot$$

so that at least four well documented mechanisms exist by
which a triplet ketone sensitiser can initiate photodegradation
namely i) decomposition with the formation of free radicals,
ii) energy transfer to the polymer, iii) energy transfer to
molecular oxygen, iv) hydrogen abstraction with consequent
formation of free radicals.

Alkyl hydroperoxides which may also be formed if oxygen
is present during processing have an absorption which extends
to about 320 nm which may lead to the formation of free radicals
thus:-

$$ROOH \xrightarrow{h\nu} RO\cdot + \cdot OH$$
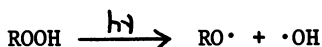
Metal ions act as efficient sensitisers for this process as well
as forming free radicals by the process:-

$$M^{n+}{}_nX^- \xrightarrow{h\nu} M^{(n-1)+}{}_{(n-1)}X^- + X\cdot$$
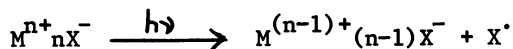
The nature of X^- may effect the position of λ_{max} very
considerably.

c) Impurities. Two main classes of impurities affect the photostability of PVC. The first type, traces of catalyst, have already been discussed in section (a) while the second type, traces of solvent, are important when the polymer is in the form of thin films which have been cast from a solvent. Such traces are extremely difficult to remove completely and are undoubtedly responsible for much of the irreproducibility and disagreement which is apparent in the literature. One of the best solvents for PVC is tetrahydrofuran (THF) but this solvent is particularly difficult to remove. Its removal is very necessary however since it reacts very readily with dissolved oxygen to form a photolabile peroxide whose decomposition products are very effective in initiating the photodegradation reaction.

Mechanism of the Reaction

It is probable that once the initiation has been accomplished, the mechanisms of the thermal and photochemical reactions have much in common. For that reason it is profitable to make some comments about the mechanism of the reaction, most of which result from work on the thermal process. Until about ten years ago most workers in the field believed that a radical mechanism operated. This view depended to a large extent on analogy with the results of the thermal decomposition of other polymers. In 1959 two mechanisms were put forward simultaneously by Winkler [15] and by Stromberg [16] which differed in the details of the initiation process but agreed that propagation occurred by a "Zipper" process which may be written

$$\text{\scriptsize\textasciitilde\textasciitilde\textasciitilde} \ \dot{C}HCHCl \text{\scriptsize\textasciitilde\textasciitilde\textasciitilde} \longrightarrow \text{\scriptsize\textasciitilde\textasciitilde\textasciitilde} CH{=}CH \text{\scriptsize\textasciitilde\textasciitilde\textasciitilde} \ + \ Cl\cdot$$

$$\text{\scriptsize\textasciitilde\textasciitilde\textasciitilde} CH{=}CH \text{\scriptsize\textasciitilde\textasciitilde\textasciitilde} \ +Cl\cdot \longrightarrow \text{\scriptsize\textasciitilde} CH{=}CH\cdot\dot{C}H\cdot CHCl\text{\scriptsize\textasciitilde\textasciitilde} \ +HCl$$
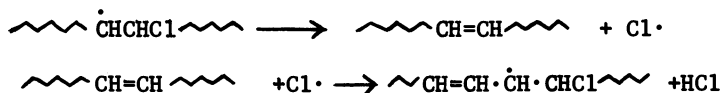
and was supported to some extent [17] by earlier work on the gas phase decomposition of alkyl chlorides. At about the same time it was found that the presence of small quantities of salts like $FeCl_3$ or $ZnCl_2$ had a strong accelerating effect on the rate of the dehydrochlorination reaction [18-21] which led some authors to believe that an ionic mechanism could be operative at least in the absence of oxygen. Support for the idea that at least a partial separation of charge in the transition state was possible began to grow and gained impetus from the following observations:- a) typical radical inhibitors like hydroquinone did not affect the rate of dehydrochlorination in a nitrogen atmosphere, b) chlorine has never been detected as a reaction product, c) the catalytic effect of HCl in the absence of oxygen [21-24] is difficult to explain by means of a radical mechanism but easier to explain in terms of a non-radical process proceeding via a cyclic, six membered transition state, d) the effect of solvent, in particular nitrobenzene, first

mentioned by Goto and Fujii[25] and later confirmed by
Bengough[15,17] as well as the relation between the rate of
dehydrochlorination and the dielectric constant of the solvent[23]
is typical of non-radical processes, e) the low molecular
weight model compounds which undergo thermal decomposition in
the gas phase by a homogeneous, first order, monomolecular
process, probably do so via a polar transition state.

   In spite of the increasing support for an ionic mechanism
and the evidence which has been advanced for the presence of
carbonium ion species in PVC[28,29] there are still many workers
who support a free radical mechanism. The work of Bamford[30]
is typical and involves carrying out the degradation in labelled
$C_6H_5CH_2T$ or $C_6H_5C^{14}H_3$ toluene at 180°C where it is found
that both T and C^{14} are incorporated into the polymer chain.
The evidence for both types of mechanism is so convincing and
the conditions so difficult to standardise that it is tempting
to speculate that both mechanisms may operate given the right
con.itions. Indeed Guyot[31] has suggested that the initial step
has an ionic mechanism and that this might initiate a radical
process which predominates when high concentrations of HCl are
present. Papko and Pudov[32] have gone one step further and
suggested that radical, molecular and ionic mechanisms may make
contributions which depend on the conditions. In particular
they suggest that the presence of HCl may induce an ion-molecule
reaction. It is becoming apparent from results such as these
that the presence of HCl may be very important and its presence
may dictate which mechanism predominates.

Termination and Extent of Dehydrochlorination

Various estimates have been made of the length and distribution
of the polyene sequences which result from the dehydrochlorinat-
ion reaction. Guyot[2] suggested a range of 5-12, Geddes[33]
thought that 13-15 was more typical while Braun[34] believed that
values as high as 25-30 were possible. More recent work[35,36]
favours the shorter range $\leq$ 12 while the more sophisticated
computer based spectrum matching procedure of Daniels and Rees[37]
shows that the range 3-14 applies to the sample degraded under
their carefully defined conditions but that the temperature
and duration of degradation may be critical. The method used
by most workers to analyse the distribution of polymers is
ultraviolet spectroscopy and this is undoubtedly the main
reason for the considerable disparity in the results obtained
by different investigators. Polyene sequences are very reactive
and the spectra may be considerably affected by interaction
with a) the solvent, b) solvent derived peroxides, c) molecular
oxygen, d) HCl, or by undergoing intramolecular or intermolecular
Diels-Alder type reactions.
a) Russian authors[38] have shown that the NMe_2 group of
dimethylformamide causes a bathochromic shift of polyene

absorptions while Daniels and Rees[37] have had to assume shifts in
order to obtain agreement between their experimental and
synthetic spectra.
b) Many workers suspected that the behaviour of PVC films which
had been cast from solution depended on the nature of the
solvent used. Some authors[38] attributed the improved resistance
to discoloration of films prepared from THF to the fact that
oxygen containing impurities in the solvent retarded the
formation of poly enes. In a very careful study however, Daniels[39]
has shown that of the various products of both dark and photo-
chemical reactions of oxygen with tetrahydrofuran only the
α -hydroperoxytetrahydrofuran reacts with the polyene sequences.
This reaction takes the form of an addition to the terminal
double bond of the polyene sequence. Films cast from THF and
containing trace amounts of this solvent will therefore be
subject to variable behaviour unless oxygen is rigorously
removed.
c) As well as reacting with the solvent to form unstable
peroxidic products, molecular oxygen in the gas phase or in
solution may have a very profound effect on the degradation
process. The mechanisms by which it reacts are undoubtedly
very complex and have been summarised in several good reviews
of the photooxidation of polymers[40,41]. Its accelerating
effect on the degradation (measured by HCl evolution) is due
at least in part to the formation of $>$C = 0 and $-$OOH
chromophores which sensitise further decomposition. It also
undergoes a very rapid photochemical reaction with polyene
sequences which make the measurement of the extent of degradation
in the presence of oxygen by spectroscopic measurements in the
visible and ultraviolet regions meaningless.
d) The effect of HCl on the rate and extent of the degradation
reaction has long been a matter of controversy. Technologists
involved with the processing of PVC have long interpreted the
stabilising effect of HCl acceptors as evidence that HCl is a
catalyst for the degradation process. The opposite view held
by Arlman[1] and Druesdow[42] however was widely accepted for many
years. The definate catalytic effect found by Rieche[21] and
Talamini[43] however has been amply confirmed by more recent work[44]
and is now generally accepted. Our own work has shown [49]
conclusively that a rapid photochemical addition of HCl to the
polyene sequences of degraded PVC results in a bleaching
reaction which is the reverse of the photodehydrochlorination.
The reaction, which is wavelength dependent reaches a photo
stationary state in which a new polyene distribution is formed
which depends on the wavelength of the irradiating light and
the concentration of HCl. Results for the photo addition of
HCl to the model compound diphenyloctatetraene (DPOT) indicate
that the reaction is slower in ethanol than in hexane and
therefore do not support an ionic mechanism. The thermal
dehydrochlorination reaction in the liquid phase on the other

hand is undoubtedly accelerated by the presence of free HCl[3,4]
o-nitrophenol[45] or strong electrophiles such as $ZnCl_2$ [46] or
$SnCl_4$ [47] especially in polar solvents while non-polar solvents
inhibit. In these systems, the rate of reaction depends on the
dielectric constant and on the electron accepting power of the
medium, results which lead to the inevitable conclusion that an
ionic mechanism or at least a strongly polarised transition state
is involved. Clearly the role played by HCl is not completely
understood. Its presence may facilitate ionic mechanisms which
may not be significant when its concentration is low. Since its
concentration may vary very considerably from one experimental
arrangement to another the mechanisms involved may vary
accordingly.

e) It is necessary to mention one other factor which effectively
terminates the dehydrochlorination reaction when the PVC is in
the form of thin films. This is the formation of the polyenes
in a thin strongly absorbing surface layer which effectively
protects the bulk of the film from further degradation[48]. When
this layer is separated from the bulk of the film it is found to
be highly insoluble and therefore cross linked to some extent.
Any spectrophotometric analysis of degraded films therefore
should take this fact into account since the polyenes are not
homogeneously distributed throughout the film as is often
assumed. In order to overcome this problem the films described
in our work[49] were cast from solutions using PVC which had been
thermally degraded and were homogeneous so that the surface
layer did not present a problem.

Stabilisation of PVC

At least four types of additives have been used to stabilise
PVC towards photodegradation.

The first type are merely strong ultraviolet absorbers
which function by dissipating as thermal energy light which
would otherwise be absorbed by a sensitiser and initiate
photodegradation. Some of the most effective are of the
hydroxybenzophenone or 2'-hydroxybenzotriazole type which
utilise internal hydrogen bond formation in the dissipative
mechanism.

A second type of stabilisers are quenchers which can
accept the energy of an excited sensitiser molecule and convert
it harmlessly into heat. One molecule which can do this very
effectively is oxygen but the singlet oxygen so formed may be
more damaging than the original sensitiser. For this reason
quenchers should be as non selective as possible ie. they
should quench as large a range of excited states as possible.
One very useful class of molecules in this respect are Ni(II)
chelates which quench both triplet sensitiser and singlet
oxygen. It is interesting though that diamagnetic square
planar complexes are more effective in stabilising polypropylene

than paramagnetic ones. One explanation which has been suggested
is that energy transfers to the higher energy triplet ligand
states of the paramagnetic compares are endothermic while
transfers to the lower energy ligand field states of the
diamagnetic complexes are exothermic though sterically hindered.
Essentially similar results have been obtained for polystyrene[51].
The efficiencies of this type of quenchor are generally higher
than those of the absorber type discussed above but the fact
that they are coloured may be unacceptable.

The third class of stabilisers are included only for the
sake of completeness but the mechanism by which they operate
are probably the best understood. They may be described as
antioxidants and are effective because they intercept the
radical chain carriers or decompose the peroxides or
hydroperoxides which are potential radical initiators.

The fourth class which are peculiar to PVC have one thing
in common namely an ability to react with HCl. They include
such diverse substances as inorganic lead salts, heavy metal
soaps, organo-tin compounds, epoxides and many others. Although
their ability to react with HCl may be a contributory factor
their main function is undoubtedly to react with and deactivate
potential sites of initiation such as branch points or areas
of unsaturation.[52]

References

1. Arlman E.J., J.Polymer.Sci., (1954), 12, 547.
2. Guyot A., Benevise J.P. and Trambouze Y., J.Appl. Pol. Sci., (1962), 6, 103.
3. Suzuki T., and Nakamura M., Japan Plast., (1970), 4,16.
4. Mayer Z., Obereigner B. and Lim D., J.Polym.Sci., (1971), C33, 289.
5. v Erbe F., Grewer T. and Wehage K., Angew.Chem., (1962), 74, 988.
6. Asahina M. and Onozuka M., J.Polym.Sci., (1964), 2, 3505.
7. Chytry V., Obereigner B. and Lim D., Eur.Pol.J.Suppl., (1969), 379.
8. Golub M.A., J.Amer.Chem.Soc., (1969), 91, 4925.
9. Golub M.A., J.Amer.Chem.Soc., (1970), 92, 2615.
10. Golub M.A., J.Phys.Chem., (1971), 75, 1168.
11. Benson H.L., and Willard J.E., J.Amer.Chem.Soc., (1961), 83, 4672, (1966), 88, 5689.
12. Harriman A., and Rockett B.W., J.Chem.Soc., Perkin 2, (1974), 5, 485.
13. Cohen S.G. and Parson G., J.Amer.Chem.Soc., (1970), 92, 7603.
14. Davidson R.S., and Steiner P.R., J.Chen.Soc., (C), (1971), 1682.
15. Winkler D.E., J.Polym.Sci., (1959), 35, 3.
16. Stromberg R., Strauss S. and Achhammer B.G., J.Polym.Sci., (1959), 35, 355.
17. Barton D.H.R., and Howlett K.E., J.Chem.Soc., (1949), 155.
18. Imoto M., Mem.Fac.Eng.Osaka City Univ., (1960), 2, 124.
19. Baum B., SPEJ., (1961), 17 71.
20. Hartmann, A., Kolloid-Z., (1956), 149, 67.
21. Rieche A., Grimm A. and Mucke H., Kunststoffe, (1962), 52, 265.
22. Braun D., and Bender R.F., Eur.Pol.J.Suppl., (1969), 269.
23. Marks G.C., Benton J.L., and Thomas C.M., Soc.Chem.Ind., (London) Monograph, (1967), 26, 204.
24. Geddes W.C., Eur.Pol.J., (1967), 3, 267.
25. Koto K., and Jujii H., Nippon Gomu Kyokaishi, (1959), 32, 90.
26. Bengough W.I., and Sharpe H.M., Makromol.Chem., (1963), 66, 31,45.
27. Bengough W.I., and Varma I.K., Europ.Polym.J., (1966), 2, 49, 61.
28. Scalzo E., Mater.Plast.,(1962), 28, 682.
29. Schlimper R., Plaste Kautschuk, (1966), 13, 196.
30. Bamford C.H., and Fenton D.F., Polymer, (1969), 10, 63.
31. Guyot A., and Bert M., J.Appl.Polym.Sci., (1973), 17, 753.
32. Papko R.A., and Pudov V.S., Vyoskomol.Soedin., (1974), A16, 1409.
33. Geddes W.C., Eur.Polym.J., (1967), 3, 747.
34. Braun D. and Thallmaier M., Makromol.Chem., (1966), 99, 59.
35. Smirnov L.V. and Popov K.R., Vyoskomol.Soedin., (1971), A13, 1204.

36. Minsker K.S., and Krac E.O., Vyoskomol Soedin., (1971), A13, 1205.
37. Daniels V. and Rees N.H., J.Polym.Sci., (1974), 12, 2115.
38. Smirnov L.V. and Popov K.R., Int.Symp.Makromol.Chem., Prepr.(1969), 5, 461.
39. Daniels V. Ph.D. thesis Univ.of Wales, (1974).
40. Cicchetti O., Adv. Polymer Sci., (1970), 7, 70.
41. Karspukhin O.N. and Slobodetskaya E.M., Russ.Chem.Revs., (1973), 42.
42. Druesdow D. and Gibbs C.F., Nat.Bur.Stds Circ., (1953), 525.
43. Talamini G., Cinque G. and Palma G., Mat.Plast., (1964), 30, 317.
44. Corsato-Arnaldi A., Palma G. and Talamini G., Mat.Plast., (1966), 32, 50.
45. Mayer Z. and Obereigner B., Eur.Polym.J., (1973), 9, 435.
46. Kimura G. Yamamoto K. and Sueyoski K., Yuki Gosei Kagaku Kyokaishi, (1965), 23, 136.
47. Leprince P. Rev. Inst. Fr. Petroli Ann Combust. Liquides (1959), 14, 339.
48. Bailey R.J., Ph.D. thesis, Univ.of Wales (1972).
49. Owen E.D. and Williams J.I., J.Polym.Sci., (1974), 12, 1933.
50. Adamczyk A. and Wilkinson F., J.Appl.Polym.Sci., (1974), 18, 1225.
51. Harper D.J. and McKellar J.F., J.Appl.Polym.Sci., (1974), 18, 1233.
52. Anderson D.F. and McKenzie D.A., J.Polym.Sci., A-1, (1970), 8, 2905.

16

Dielectric Studies of the Photochemistry of Polystyrene Films

R. GREENWOOD and N. A. WEIR

Chemistry Department, Lakehead University, Thunder Bay, Ontario, Canada

The photochemistry of polystyrene has been the subject of a considerable amount of research during the past twenty-five years. Two main approaches have been employed: (a) analyses of gaseous products liberated or absorbed during photolyses, and (b) analyses of the polymer residue after the absorption of a given amount of radiation.

Analyses of the photolysis products has been achieved by mass spectrometry[1,2] and by gas chromatography[3], and absorption of O_2 during photo-oxidation has been indicated by differential manometry[4,5]. Structural changes in the polymer residue have been monitored spectroscopically (I.R.[6,7,8], U.V.[3,9,10], N.M.R.[7], e.s.r.[11,12] and fluorescence[13,14]) and by molecular weight determinations[15,16,17]. These studies have shown that the mechanisms of the photolyses reactions are very sensitive to experimental conditions, in particular the wavelength of the radiation and presence of oxygen critically control both primary and secondary photochemical processes. It is possible to distinguish four principle systems: 1) short-wave U.V. (λ=254nm) photolysis under high vacuum conditions, 2) short-wave U.V. photolysis in presence of O_2, 3) long-wave U.V. photolysis (λ>300nm) under high vacuum, and 4) long-wave photolysis in presence of O_2.

Absorption of short-wave radiation by the phenyl chromophores results in the formation of the vibrationally excited singlet state, S_1^*, which undergoes rapid vibrational relaxation to S_1, which rapidly becomes deactivated to form the excimer[18]. The very small excimer-triplet (T_1) splitting facilitates intersystem crossing from the excimer to T_1. Excimer fluorescence is also observed, but no singlet (S_1) fluorescence has been observed for the solid polymer at room temperature[19]. The primary photochemical process involves fission of the tertiary C-H bond[3,12], and this step presumably involves both singlet and triplet states, since each have associated with them degrees of excitation in excess of the C-H bond dissociation energy (estimated to be 80±3 kcal. mole^{-1}), provided that this energy can be concentrated in the C-H bond. The tertiary radicals subsequently interact with

themselves and add to benzene rings to form cross-links[13] and molecular H_2 is formed by combination of H-atoms and by inter- and intra-molecular abstractions of hydrogen from the polymer, the latter process being responsible for the formation of conjugated sequences in the polymer chain[3,13,20,21]. Recent studies of pulsed photolysis of the polymer indicate that main chain C-C bonds are also broken, but the quantum yield is much lower than that for C-H fission[22].

In presence of O_2, the tertiary radicals produce peroxy radicals, which in turn yield the hydroperoxides via inter- and intra-molecular H-atom abstractions[23]. Hydroperoxides may undergo further photolytic decomposition or decompose as a result of energy transfer from the excimer[14], presumably by an exchange interaction, to yield chain-end carbonyl compounds with concomitant chain scission. Acetophenone, which has recently been observed as a reaction product, could conceivably be formed from the carbonyl compound by a Norrish type II reaction.

Polystyrene has no long-wave U.V. ($\lambda > 300$nm) chromophores, and the initial formation of radicals during long-wave irradiation is difficult to reconcile with the structure of the pure polymer. However, it has been shown that long-wave irradiation under vacuum produces small extents of random chain scission[17,24], which has been attributed to the photolysis of O-O bonds which are incorporated into the chains as a result of the free radical copolymerization of small amounts of O_2, and in support of this hypothesis, it has been shown that anionically prepared polymers (which should not contain such impurities) show considerably greater stability when treated under identical conditions[17]. Ketonic impurities, resulting from small extents of purely thermal oxidation of the polymer, have also been invoked[14] as possible chromophores for long-wave U.V., and acetophenone has been identified as such an oxidation product[7].

Initiation of the long-wave photodegradation can be achieved by photolysis of such impurities into radicals which can, by means of H-atom abstraction produce radical centers on the polymer[24]. It would appear that the small radicals produced from, for example, acetophenone would, because of their high mobilities and reactivities, act as efficient initiators. In addition, excited triplet states of such aromatic ketones, which can result from intersystem crossing following absorption of long-wave U.V., are capable of H-atom abstraction from the polymer[14]. In the presence of O_2, the polymer radicals will undergo oxidation, admittedly at a lower rate, to the hydroperoxide in a similar sequence to that outlined above. Hydroperoxide decomposition is qualitatively similar to that outlined above, however, because of the broad absorbance in the long-wave region, direct photolysis is possible[25]. The resulting ketonic products are similarly photolabile. The general kinetic characteristics of the long-wave photo-oxidation are significantly different from those of the 254nm initiated reaction, in that appreciable induction periods are

observed[23], and it would seem that these times are associated with the production of macro-radicals. Also, since the absorption characteristics of the two types of radiation are completely different, the long-wave reaction is likely to be homogeneous throughout the films.

Most of the results obtained by the above techniques inevitably refer to relatively advanced stages of the photo-reactions, as it is often very difficult to detect with any degree of accuracy, the small structural modifications of the polymer which occur in the very early stages of the reaction. Since polystyrene has a very low dielectric loss (typically $\varepsilon''=4.5 \times 10^{-4}$ at 10^5Hz)[26], and since photodegradation introduces polar groups, e.g. C=O groups and polarizable groups (conjugated C=C sequences) into the polymer, it can be predicted that the dielectric characteristics will be significantly modified by the presence of relatively low concentrations of polar impurity. Hence, measurements of changes in dielectric properties as a function of time of degradation appear to offer a sensitive monitor of the incorporation of polar and polarizable groups into the polymer. Dielectric properties depend largely on the surface characteristics (e.g. resistance) of the sample and, where thin films are used, the surface layers constitute a major proportion of the total volume of the sample. Since most of the photo-reaction occurs in the surface layers, dielectric measurements reflect fairly accurately the effects of photolysis. It can also be readily predicted that such modifications of non-polar polymeric insulators and dielectrics will be reflected as less desirable insulating and dielectric properties of these polymers. However, despite the consequences of deteriorating electrical and dielectric properties brought about by the inevitable exposure of these materials to potentially photodegradative environments, few systematic studies have been made.

The effect of γ-radiation in air on the dielectric properties of polyethylene has been studied[27] and it was shown that both the dielectric constant and the dissipation factor increased gradually with increasing radiation dose. The effects of the radiation were frequency dependent and more pronounced changes in both ε' and tan δ were observed in the 10^5-10^6Hz region. Outdoor aging of polyvinyl chloride for a period of six months results in an enhanced dielectric dispersion, and dielectric constant and increased a.c. conductivity at low frequencies (30-50Hz) has been used to determine the kinetics of the HCl elimination reaction[28]. Irradiation of polyvinylidine chloride with 254nm U.V. results in increased conductivity[29], and similar treatment of polyethylene rapidly increases the dielectric constant, and power factor (sinδ)[30]. Photo-oxidation has also been used as a tracer in the assignment of dielectric relaxations. The assignment of the dielectric relaxations. The assignment of the dielectric α-relaxation in polyethylene has been the subject of considerable controversy, and this was resolved by introducing C=O groups, by means of photo-oxidation, into crystalline polyethylene[31,32,33].

Results demonstrated that the α–relaxation is associated with re-orientations occurring in the crystalline region.

The object of the present work was to investigate the kinetics of the various photo–decompositions of polystyrene, in particular the early events in these reactions, using dielectric techniques, and to compare the results with those previously obtained. The results will, in addition, provide information regarding the effects of such photo–degradations on the dielectric properties of the polymer.

Dielectric measurements were made using a Hewlett–Packard Model 4342–A Q–Meter for the high frequency range (22kHz–70MHz) and a 1620–AP General Radio Capacitance Bridge for the lower frequency range (10 Hz–20kHz).

The Q–meter was used in conjunction with a 1620–AP G. R. capacitance measuring assembly mounted on a 4342 mounting jig (Rutherford Research) without with which reproducible results were not obtained. The test cell for the G. R. Bridge was a 3–terminal spring–loaded parallel plate capacitance cell. Good electrical contact was ensured by attaching metal foil to the surfaces using thin grease films. In order to reduce the effect of variable atmospheric humidity, the cells were flushed with dry nitrogen and a dry N_2 atmosphere was maintained in the cells during measurements.

Polystyrene was prepared from carefully purified monomer both thermally without initiator and anionically using an established method[34]. Purification consisted of repeated precipitation of the toluene solutions from pure methyl alcohol. Precipitates were dried at 65°C under high vacuum for at least 100 hours before use. Characteristics of the polymers used are as in Table 1. Dielectric measurements were made in 5 cm circular discs 0.075 mm thick which were made by solvent evaporation from toluene solutions or were moulded from powdered polymer using a press and die. U.V. irradiations were carried out in the presence of oxygen and in vacuum, the discs being mounted in a fused silica vessel. The U.V. sources used were a General Electric High Pressure Hg Lamp fitted with a Pyrex filter for long–wave irradiation and a P.C.Q. low pressure Hg arc (Ultra Violet Products) which emitted predominantly 254nm radiation, the incident flux of which was 7.8×10^{-9} $Ecm^{-2}sec^{-1}$. The total flux of long–wave U.V. i.e. the flux integrated over the wavelength range 300–366nm was $2.4 \times 10^{-8} Ecm^{-2}sec^{-1}$.

When a voltage is applied to an "ideal" dielectric, polarization of the dipoles occurs instantaneously, and there is no lag between the orientation of the molecules and the variation of the electric field. Under these conditions the current has a displacement of $\pi/2$ relative to the e.m.f., and no loss of electrical energy occurs. This is illustrated in (a). For a real dielectric the situation is quite different. Firstly, there is an inertia associated with the orientation polarization of a dipole, and a finite time is required for the dipole to become oriented, and secondly, the dipoles tend to undergo a relaxation to the original

Table 1
Characteristics of Polystyrenes

Polymer	Polymerization Temperature (^{o}C)	$\overline{Mn}x10^{-4}$
Anionic	50	2.1
"	50	4.8
"	50	10.1
"	50	24.2
"	50	58.0
"	50	87.0
"	50	200.0
Radical	60	160.0
"	72	94.2
"	80	51.0
"	90	18.7

random orientations which they would adopt in the absence of the
field. As the frequency of the applied field, E, increases the
polarization, P, lags behind it. The applied field which varies
as $E=E_0 Sin\omega t$, and the polarization takes the form $P=P_0 Sin(\omega t-\delta)$.
Because of the phase lag and the existence of a finite period of
dielectric relaxation, part of the electrical energy is dispersed
as heat. It can be seen from illustration (b) that the current is
no longer out of phase with the e.m.f. by $\pi/2$, but by $(\pi/2-\delta)$
where δ is the phase displacement or loss angle. The loss can be
equated with the product of the e.m.f. and the in-phase component
which the current acquires, i.e. $isin\delta$. Another consequence of
the lag is that the permittivity decreases at higher frequencies
where the loss angle is appreciable. The permittivity may be
represented by the complex function:

$$\varepsilon^* = \varepsilon'-j\varepsilon'' \qquad \ldots\ldots\ldots\ldots\ldots\ldots (1)$$

where ε' is the real permittivity or dielectric constant, and ε''
is the dielectric loss (imaginary component) and $j=(-1)^{\frac{1}{2}}$, is the
algebraic operator. From Figure 1(c) it can be seen that:

$$\tan\delta = \varepsilon''/\varepsilon' \qquad \ldots\ldots\ldots\ldots\ldots\ldots (2)$$

in which $\tan\delta$ is the dissipation factor. The Q values obtained
from the Q-Meter are related to $\tan\delta$ as $Q=(\tan\delta)^{-1}$.
    Removal of the external field results in a reorientation of
dipoles and the polarization decays with time according to the
equation,

$$P_{(t)} = P_0 exp(-t/\tau) \qquad \ldots\ldots\ldots\ldots (3)$$

where P_0 is a constant and τ is the relaxation time for the polar-
ization, i.e. the time required for the polarization to be reduced

to 1/e of its original value.

Since relaxation involves rotational rearrangements, there are energy barriers associated with the process. τ is related to the energy (H) by the equation,

$$\tau = \tau_0 \exp(-H/kT) \quad \ldots\ldots\ldots\ldots (4)$$

where τ_0 is a constant and k is Boltzmann's constant. τ is further related to the frequency at which maximum loss occurs, (f_m), for a given relaxation by the equation,

$$\tau = 1/2\pi f_m \quad \ldots\ldots\ldots\ldots\ldots (5)$$

The frequency dependence of the complex dielectric constant can be expressed by the Debye equation,

$$\varepsilon^* = \varepsilon_\infty' + \frac{\varepsilon_0' - \varepsilon_\infty'}{1 + j\omega\tau} \quad \ldots\ldots\ldots (6)$$

where ε_∞' and ε_0' are the dielectric constants at very high and very low (static) frequencies. It can be shown that ε' and ε'' are related to frequency by combining (1) and (6):

$$\varepsilon' = \varepsilon_\infty' + \frac{\varepsilon_0' - \varepsilon_\infty'}{1 + \omega^2\tau^2} \quad \ldots\ldots\ldots (7)$$

and

$$\varepsilon'' = \frac{\varepsilon_0' - \varepsilon_\infty' \; \omega\tau}{1 + \omega^2\tau^2} \quad \ldots\ldots\ldots\ldots (8)$$

In the present work ε_0' and ε_∞' are not readily determinable, particularly since the chemical nature of the polymer is changing. However, for a given relaxation, if it can be assumed that there is a symmetrical distribution of relaxation times ε_∞' and ε_0' can be related by the Kramers-Kronig equation[35], or by the following alternative expression[36],

$$\Delta\varepsilon' = \varepsilon_0' - \varepsilon_\infty' = 2\Delta H/R\pi \int_0^\infty (\varepsilon'')d(1/T) \quad \ldots (9)$$

where ΔH is the activation energy and R is the gas constant.

$\Delta\varepsilon'$ is a measure of the intensity of the dielectric relaxation spectrum (the relaxation strength) and it is in turn related to the number of relaxing dipoles (N) per unit volume by the equation[37,38],

$$\Delta\varepsilon' = \frac{4\pi N g \mu^2}{3kT} \left(\frac{n^2 + 2}{3}\right)^2 \left(\frac{3\varepsilon_0'}{2\varepsilon_0' + \varepsilon_\infty'}\right) \quad \ldots\ldots\ldots (10)$$

where μ is the dipole moment, n is the refractive index, g is the Kirkwood g factor and k is Boltzmann's constant. The variation of

$\Delta\varepsilon'$ with degradation is a useful measure of the accumulation of polar groups in the polymer. However, there appears to be considerable overlapping of multiple peaks, and in the early stages of the reaction, $\Delta\varepsilon'$, which is determined from areas under curves in the ε'' vs $1/T$ plots is not readily accessible. The relaxation peaks are fairly symmetrical and ε'' values at the frequency of maximum loss have been used as alternative data to follow reactions.

Dielectric constants of the radically and the anionically prepared polymers are comparable over the frequency range investigated (Fig. 2) and the frequency dependence shown is similar to that previously reported[39]. Values of the corresponding dielectric losses are shown in Figs. 3 and 4, and the frequency dependence of each is qualitatively very similar to what has already been demonstrated[36,39]. However, the actual losses, in particular those in the 10^4–10^6Hz region, are numerically lower than those previously determined, and these values may reflect the lower concentrations of polar impurities that are introduced into the chains during the present polymerizations. It is significant that anionic polymers, in which incorporation of polar groups is much less probable than in free radical polymerization, have lower losses over the entire frequency range. Dissipation factors ($\tan\delta$) are frequently used as a measure of dielectric loss, and these data, shown for the anionic polymer (Fig. 3), are qualitatively similar to the ε'' data. However, during degradation ε' values vary in a complex manner, and the use of $\tan\delta$ values to monitor degradation tends to obscure the real effects of degradation on dielectric losses.

Since molecular weight changes are frequently associated with photochemical reactions, the effects of molecular weight or dielectric properties of both types of polymer were investigated in order to avoid possible complications arising from varying molecular weights. The data shown in Figs. 5 and 6 indicate that polymers with low molecular weights (10^4) have relatively higher losses, particularly at low and very high frequencies, and these figures perhaps reflect the relative importance of impurities in the low molecular weight polymers, the effective ratio of polar to non-polar material being higher.

The maxima in the loss curves at around 8×10^5 are not immediately explicable, however, dynamic mechanical loss moduli (E'') show a similar variation with molecular weight[40]. The smaller losses associated with higher molecular weight material ($\overline{Mn}>10^6$) are perhaps a consequence of chain entanglement which increases with increasing molecular weight[41], and which would inhibit to some extent group rotations and other co-operative movements which are prequisites for dielectric dispersion. The following work has been carried out using the polymers ($\overline{Mn}\sim10^5$) which have the lowest losses over a wide frequency range, in order to extend the sensitivity of the technique.

Photo-oxidation of polystyrene (254nm, 400torr oxygen)

IDEAL DIELECTRIC   DIELECTRIC LOSS
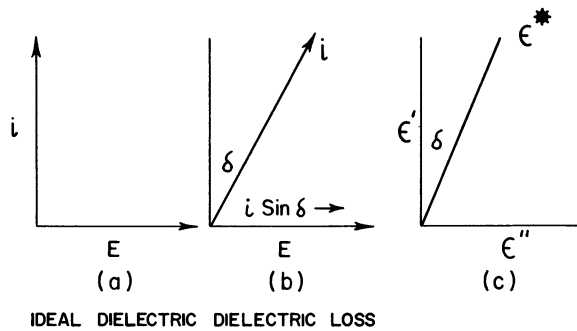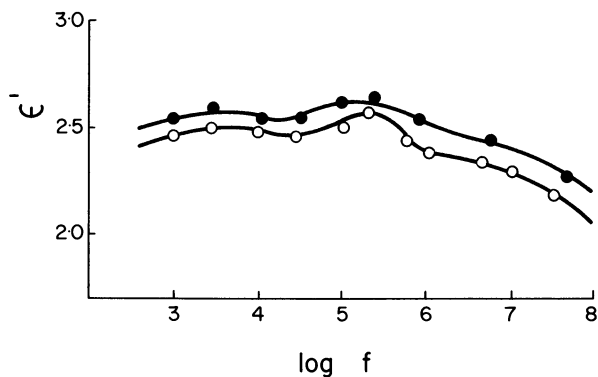
Figure 1.

Figure 2. Dielectric constants (ϵ') as a function of frequency (f). ○, anionic; ●, radical polymers ($\overline{M}n = 10^5$ and 1.87×10^5, respectively).
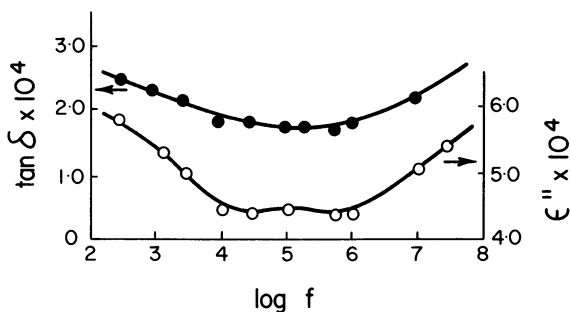
Figure 3. Dielectric loss (ϵ'') and loss tangent (tan δ) as a function of frequency. Anionic polymer ($\overline{M}n = 10^5$).
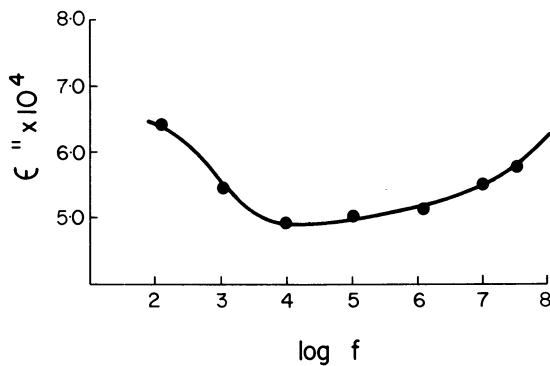
Figure 4. Dielectric loss (ϵ'') as a function of frequency. Radical polymer ($\overline{M}n = 1.87 \times 10^5$).
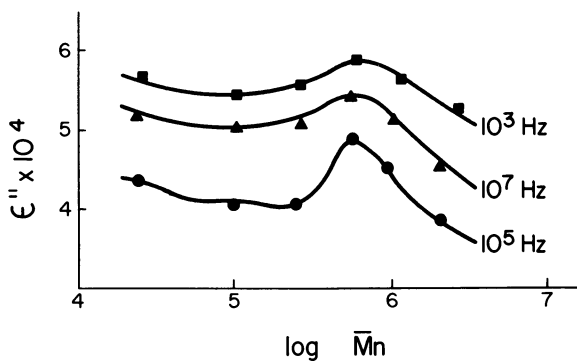
Figure 5. Dielectric loss (ϵ'') as a function of molecular weight ($\overline{M}n$). Anionic polymer.
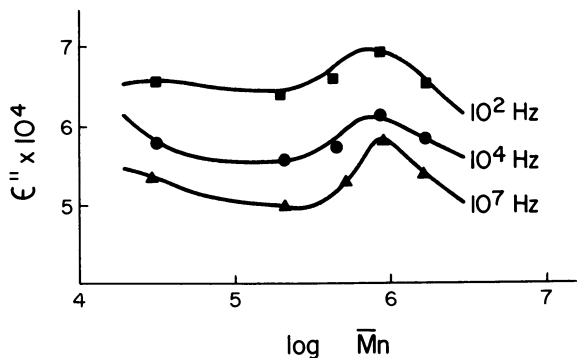
Figure 6. Dielectric loss (ϵ'') as a function of $\overline{M}n$. Radical polymer.

results in increased dielectric constants and losses (Figs. 7 and 8) over the entire frequency range. Three distinct areas of maximum loss appear in the dielectric spectrum with increasing degradation, a low frequency band around 2.5×10^2Hz, another centered on 10^4Hz and a pronounced peak around 2×10^6Hz. Radically prepared polymers show identical behaviour. It is obvious that the general increase in dielectric parameters results from overlapping of multiple relaxations of a range of oxidation products, however, the three areas of more pronounced dispersion were further investigated.

The variation of dielectric constant with increasing extents of degradation is shown in Figure 9 and it can be seen that the actual pattern of increase in ε' is complex and also frequency dependent. The apparent "levelling off" of the ε' at high frequencies could be indicative of some type of inhibition occurring, but it is probably the result of decreasing dielectric constants, the orientation polarization decreasing as the relaxing dipoles interact with the high frequency field. It would therefore appear that interpretation of such data cannot be made unequivocally.

Increases in dielectric losses occurring at the frequency regions of highest loss are shown as a function of degradation time (short-wave U.V. in O_2) in Figure 10, and it can be seen that the losses increase with increasing degradation in a similar fashion in each of the frequency ranges. However departures from the linearity with time of degradation occur at around 180 minutes degradation, and this is probably attributable to the photodecomposition of some of the polar entities which contribute to the dielectric losses, small molecules forming and diffusing out of the films. It is possible also that mobilities of polar groups are restricted somewhat by cross-linking.

The three main dispersion regions are discussed in more detail as follows:

(a) The 2.5×10^2Hz region. It is likely that the lowest frequency loss is associated with D.C. conductivity and possibly also Maxwell-Wagner interfacial polarization. Dielectric losses are due to dielectric relaxation and to a number of other processes related to D.C. conduction by the sample. The total loss ε_T'' can be equated with these component losses as follows[42].

$$\varepsilon_T'' = \varepsilon'' + k\sigma/f \qquad \ldots\ldots\ldots\ldots (11)$$

where σ is the D.C. conductivity and k is a constant. It can be seen that D.C. conductivity will contribute significantly only at low frequencies. Interfacial scattering of radiation also occurs at phase boundaries when particles of one material are suspended in another which has a different dielectric constant (Maxwell-Wagner polarization)[43], and dielectric losses similar to those due to dipolar relaxations are observed, often at low frequencies[44]. Small highly cross-linked matrices formed in the
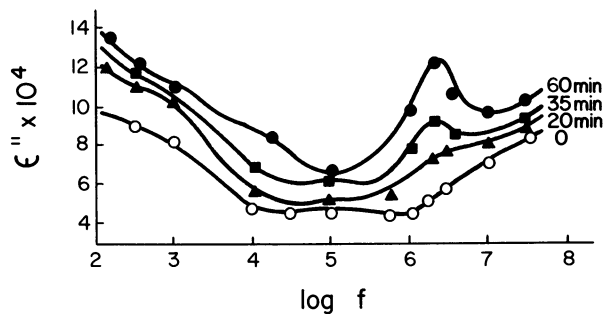
Figure 7.   Changes in dielectric loss as a function of f with irradiation at 254 nm in O_2 (400 torr) ($\overline{M}n = 2.4 \times 10^5$). Anionic polymer.
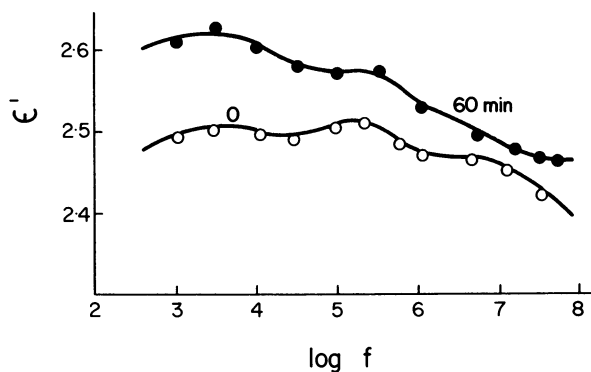
Figure 8.   Changes in ϵ' as a function of f on irradiation (254 nm) in O_2 (400 torr). Anionic polymer $\overline{M}n = 2.4 \times 10^5$. ●, no irradiation; ○, after 60 min.
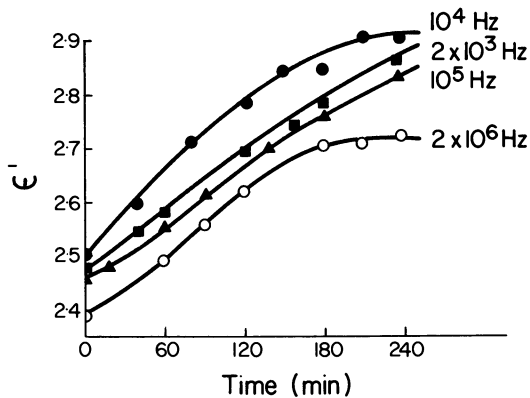
Figure 9.   Increases in ϵ' with time of irradiation (254 nm) in O_2 (400 torr). Anionic polymer ($\overline{Mn} = 2.4 \times 10^5$).
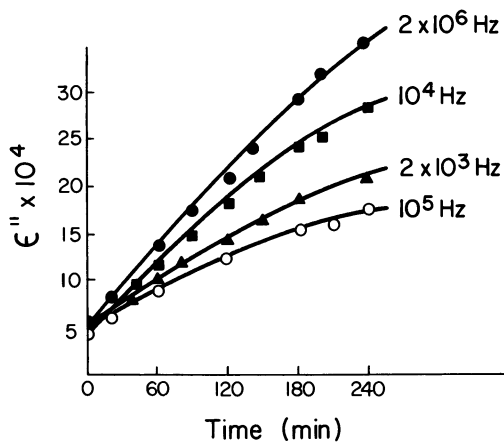
Figure 10.   Dielectric loss as a function of time of irradiation (254 nm) in O_2 (400 torr). Anionic polymer ($\overline{Mn} = 2.4 \times 10^5$).

surface layers in particular could constitute the suspended parti-
cles, which, by extensive modification due to degradation, would
have completely different dielectric properties from those of the
polymer.

The magnitudes of such losses depend critically on the geom-
etry of the particles, and since it was not possible to obtain
such information for the cross-linked polymer, the effect was not
further investigated.

(b) The 10^4Hz region. The low temperature dependence of the
10^4Hz dielectric loss of an oxidized film (254nm in O$_2$) was inves-
tigated and the results are shown in Figure 11. Oxidation results
in the formation of a broad loss peak with a maximum at 232°K,
which overlaps the very small loss peak at around 220°K in the
pure polymer. The latter peak, designated as the γ-relaxation
peak[45], has been ascribed to oscillatory motion of the phenyl
groups around the C-C$_6$H$_5$ bond accompanied by a small amplitude
twist of the main chain of the polymer.

It has been shown[45] that thermal degradation of polysty-
renes containing peroxide linkages leads to a similar enhancement
of the γ-relaxation peak, and this has been attributed to the
presence of small degradation products of these peroxides. That
the large loss peak in Figure 11 is associated with small, vola-
tile polar photo-oxidation products (e.g. ketones) was demonstra-
ted by heating the oxidized sample to 75°C at 10^{-6}torr and deter-
mining the dielectric loss as a function of heating time. It can
be seen (Figure 11) that after 16 hours heating, the loss peak has
largely disappeared and after 30 hours heating, the losses in the
oxidized film are very similar to those in pure sample. It would
appear that the enhancement of the γ-peak is related to the co-
operative motions of the small molecules and the phenyl groups,
orientation of the small occluded molecules being made possible
by phenyl rotations.

(c) The high frequency relaxation at 2×10^6Hz. The loss peak
at 2×10^6Hz was unaffected by heat treatment in vacuum, and it can
be concluded that it is due to the relaxations of dipoles which
are chemically bound to the polymer chain. The temperature varia-
tion of this loss peak is shown in Figure 12 and the activation
energy (E) associated with the relaxation was determined from the
variation in relaxation time (τ) with temperature (T) using the
equation,

$$\tau = \tau_0 \exp(-E/RT) \qquad \ldots\ldots\ldots\ldots (12)$$

where, τ$_0$ is a constant.

A value E = 12.4±1.5kcal mole^{-1} was obtained. Since this
value is comparable with the values of energy barriers to rotation
observed for aromatic ketones (measured in a polystyrene ma-
trix)[46] which also show loss maxima around 5×10^6Hz, it is
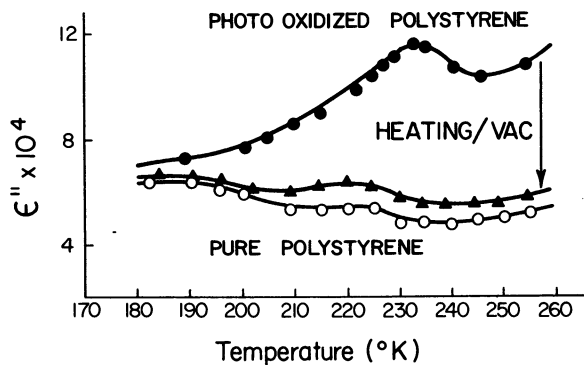
Figure 11. *Dielectric loss of oxidized anionic polystyrene (1.5 hr at 254 nm in 400 torr O_2) at low temperatures (f = 2.4 × 10^4 Hz) $\overline{M}n = 10^5$*
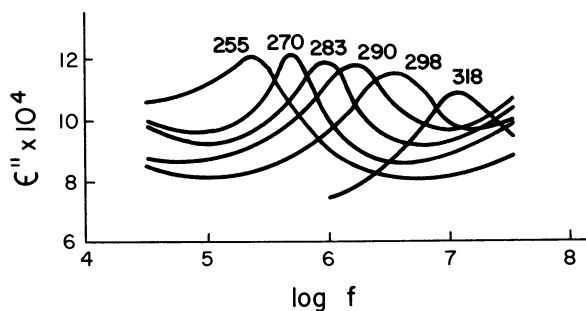
Figure 12. *High frequency relaxation of oxidized anionic polystyrene (1.2 hr at 254 nm in 400 torr O_2). Effect of temperature.*

reasonable to associate the high frequency loss peak with relaxations of ketonic groups in the polymer.

Terminal ketonic groups have been found in oxidized polystyrene[14,16] and the relaxation process could be envisaged as rotation of the C_6H_5-CO group around the 1-2 C-C bond.

$$-\overset{2}{CH_2}-\overset{\overset{\displaystyle O}{\overset{\|}{C}}\overset{1}{}}{\underset{C_6H_5}{|}}$$
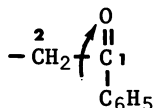
Kinetically both anionically and radically prepared polymers conform to the following relationships, the rate of photo-oxidation being expressed as the rate of increase of the high frequency loss $(d\varepsilon''/dt)$.

$$\text{Rate} = d\varepsilon''/dt = K\phi(I_0)^m(O_2)^n \quad \dots\dots \quad (13)$$

where K is a constant, ϕ is the quantum yield, I_0 is the incident U.V. intensity, and m and n are exponents.

Two limiting cases can be distinguished: (a) at low O_2 pressures, $P_{O_2}<150$torr, n=1 and m=0 and (b) at higher pressures, $P_{O_2}>150$torr, n=1 and m=0. The variation of rate with increasing oxygen pressure is shown in Figure 13.

These results can be rationalized in terms of O_2 solubilities and diffusion coefficients. At low pressures, both of these quantities are small and the oxidation is essentially a diffusion controlled process, and since the radical flux is relatively higher than the local concentration of O_2 within the films, the rate is independent of I.

However, beyond about 150torr, the diffusion coefficient is independent of the O_2 pressure[47], and consequently the rate of oxidation becomes independent of oxygen pressure. Diffusion coefficients are subject to further reductions due to concomitant cross-linking, which is more probable when the O_2 scavenger concentrations are low[48].

The first order dependence on I_0 is explained as follows:

$$\text{Rate of radical formation} = \phi I_0\{1-\exp(-\beta\ell)\}..(14)$$

where ℓ is the thickness of film and β is the effective absorption coefficient.

For the films under study, $\exp(-\beta\ell)<<1$, hence Rate = ϕI_0

Short-wave irradiation of the polymer under high vacuum conditions following rigorous degassing at 10^{-6}torr for 24 hours, gives rise to significant losses in the low frequency region (at 10^2-10^3Hz) only (Figure 14). However, if the degassing procedure is not observed, small, but detectable losses also occur in the 10^6Hz region.

It has been shown that such treatment results in the formation of conjugated sequences in the polymer chains, and it is
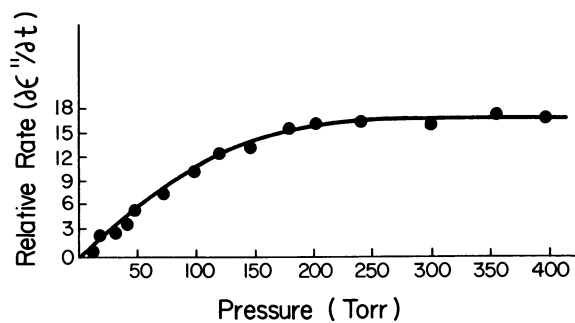
Figure 13. Effect of O_2 pressure on rate of increase of loss at 2.25×10^6 Hz (254 nm, anionic polymer $\overline{Mn} = 2.4 \times 10^5$)
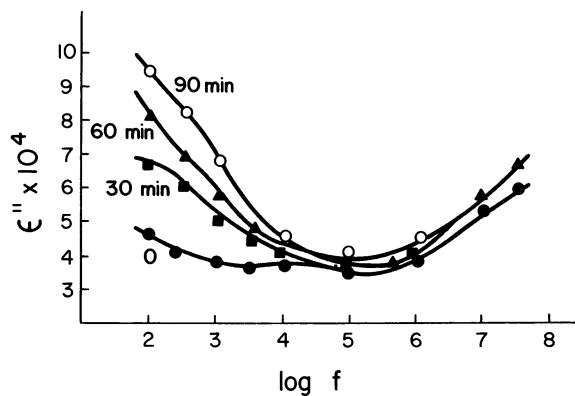
Figure 14. Irradiation (254 nm) of anionic polymer at 10^{-6} torr. Effect of photodegradation on loss.

possible that these have semi-conducting characteristics similar
to these exhibited by polyenes, and the low frequency dispersion
could be related to D.C. conductivity. Under these conditions the
polymer becomes highly cross-linked and there may also be formed
sufficient cross-linked particles containing polyenes to give rise
to some interfacial polarization.

Long-wave ($\lambda > 300$nm) irradiation in O_2 results in much less
rapid increases in dielectric losses, however it would appear from
the ε'' versus log f data (Figure 15) that the products of oxida-
tion are very similar to those formed on short-wave irradiation.
The more rapid oxidation of the radically prepared sample perhaps
reflects its high concentration of photo-labile impurities which
can act as initiation centers[17]. The higher reactivity of the
radically prepared sample is further demonstrated by the shorter
induction period (than that for the anionic polymer) shown in
Figure 16. The general behaviour shown in Figure 16 is qualita-
tively in agreement with the results of Grassie and Weir[23],
however, the induction periods are significantly shorter than
those previously determined. Since it is highly unlikely that the
present polymers contain higher concentrations of photolytic
impurities, the discrepancy is not a function of the polymer, but
is rather more likely to be related to the relative sensitivities
of the dielectric and manometric techniques for determining the
induction periods. The present technique would appear to be a
sensitive monitor of polymer modification.

Kinetically, long-wave oxidation after the induction period,
may be represented by the expression,

$$\text{Rate} = d\varepsilon''/dt = K'\phi'(I_0)^m(O_2)^n \qquad \ldots\ldots\ldots \text{(15)}$$

in which K' is a constant, ϕ' the quantum yield for photolysis
(in the linear region) and m and n are exponents.

(a) at low O_2 pressures, n=1 and m≈1
(b) at higher O_2 pressures (>60torr) n=0, m≈1

It would appear that after the induction period, initiation is
brought about by photolysis of the initially formed oxidation
products, and the O_2 pressure dependence (Figure 17) is attrib-
utable to the very low radical concentrations i.e. only at very
low O_2 pressures is the radical flux higher than the available O_2
concentration. Because of the low reaction rates, intensity expo-
nent data cannot be accurately measured, however, a low chromo-
phore concentration (C), would lead to first order dependence on
I_0, since

$$I_0\{1-\exp-(C\beta'\ell)\} \quad I_0 C\beta'\ell \quad \text{for low extents of absorption.}$$

The relaxation strength ($\varepsilon_0' - \varepsilon_\infty'$) of the dipole which shows
the high frequency absorption is related to the dipole moment, μ,
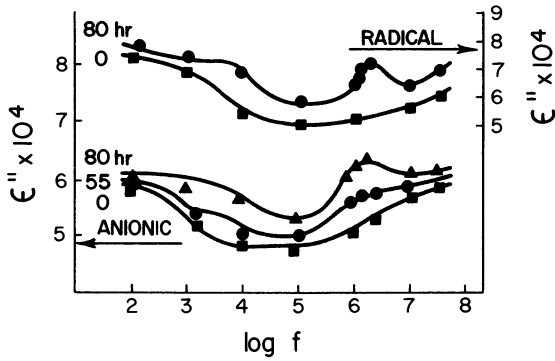
Figure 15. Irradiation of anionic $(\overline{M}n = 2.4 \times 10^5)$ and radical $(\overline{M}n = 10^5)$ polystyrenes at $\lambda \geq 300\,nm$ in O_2 (400 torr). Losses as a function of time degradation.
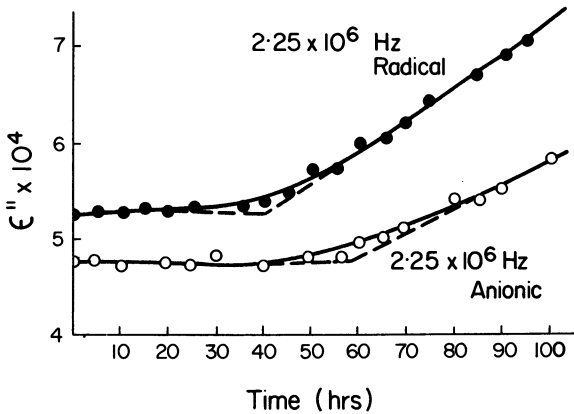
Figure 16. Characteristics of loss increases for anionic $(\overline{M}n = 2.4 \times 10^5)$ and radical $(\overline{M}n = 10^5)$ polystyrenes. Reactions at $\lambda \geq 300\,nm$ in O_2 (400 torr).

and the number of dipoles per unit volume, N, by the following
form of the Onsager equation,

$$\Delta\varepsilon' = \varepsilon'_0 - \varepsilon'_\infty = \frac{\xi N\mu^2}{T}\left(\frac{\varepsilon'_\infty + 2}{3}\right)^2 \left(\frac{3\varepsilon'_0}{2\varepsilon'_0 + \varepsilon'_\infty}\right) \quad ..(16)$$

where ξ is a constant ($\xi=4\pi g/3k$). For polymers used in this
study, $\Delta\varepsilon'/3\varepsilon'_0 \ll 1$ and $3\varepsilon'_0/(2\varepsilon'_0+\varepsilon'_\infty)$ 1 and it can reasonably be
assumed that $g\{(\varepsilon'_\infty+2)/3\}^2$ is a constant for both oxidized and
unoxidized polymer, since the extent of oxidation is small. Thus,
$\Delta\varepsilon'=\zeta N\mu^2/T$, where $\zeta=\xi(\varepsilon'_\infty+2/3)^2$.

$\Delta\varepsilon'$ values can be obtained from the areas of ε'' vs $1/T$
curves. However, all the dipoles in the system can contribute to
some extent to this area because of the limits of the integration
and the precise delineation of the absorption (in terms of the
temperature axis) is difficult. $\Delta\varepsilon'$ as determined is essentially
a sum of contributions from various dipoles, some admittedly very
small, and this can be allowed for as follows. The contribution
from the ith component is $\Delta\varepsilon'_i=\zeta N\mu_i^2 x_i/T_i$ where x_i is the mole
fraction.

The total dielectric relaxation strength as indicated by the
ε'' vs $1/T$ plot is,

$$\Sigma\Delta\varepsilon_i T_i = \zeta\Sigma N x_i \mu_i^2 \qquad \ldots\ldots\ldots\ldots (17)$$

The main contributions are from a carbonyl compound and from poly-
styrene and the above equation can be approximately written as,

$$\Sigma\Delta\varepsilon_i T_i = \zeta N\{x_c\mu_c^2 + (1-x_c)\mu_p^2\} \qquad \ldots.. (18)$$

where x_c and x_p are the mole fractions of carbonyl and styrene
units, respectively. The value of N depends on x_c since the vol-
umes of carbonyl and styrene are not the same. Since x_c is small,

$$N \simeq N_s\{1-(V_c-V_p/V_p)x\}$$

where N_s is the number of styrene units per unit volume and V_c and
V_p are the volumes of the carbonyl and styrene units.

$$\Sigma\Delta\varepsilon_i T_i = \zeta N_s\{1-(V_c-V_p/V_p)x\}\{x_c\mu_c^2+(1-x)\mu_p^2\}$$

Differentiation with respect to x gives

$$\partial(\Sigma\Delta\varepsilon_i T_i)/\partial x = N_s\zeta(\mu_c^2-\mu_p^2)-N_s\zeta\mu_p^2(V_c-V_s/V_s)$$

The second term is small, thus the gradient of the plot of $\Sigma\Delta\varepsilon_i T_i$
vs x is $N_s\zeta(\mu_c^2-\mu_p^2)$ and the intercept is $N_s\zeta\mu_p^2$. The intercept
has previously been evaluated as 22k/erg[45] and using this value
a plot was made (Figure 18) of $\Sigma T_i\Delta\varepsilon_i$ (obtained from the ε'' vs $1/T$
plot) versus the carbonyl concentration x as determined by U.V.
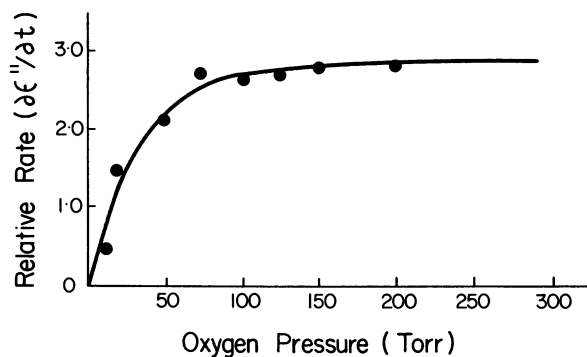
Figure 17.   Effect of O_2 pressure on rate of increase of loss at 2.25×10^6 Hz.   Irradiation at $\lambda \geq 300$ nm in O_2 (400 torr). Anionic polymer $\overline{M}n = 2.4 \times 10^5$.
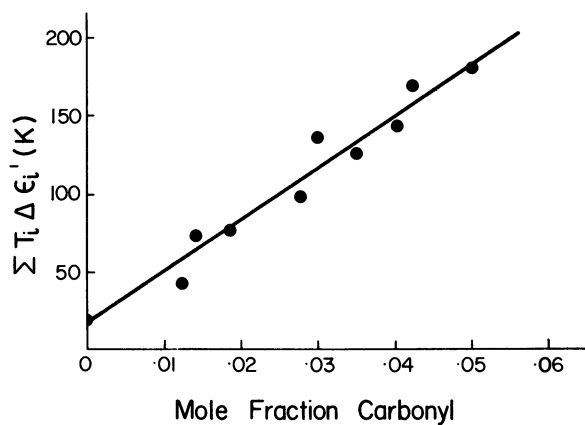
Figure 18.   Relaxation strength for the 2.25×10^6 Hz loss as a function of carbonyl concentration (determined by uv spectrometry.   Photooxidation at 254 nm in O_2 (400 torr). Anionic polymer ($\overline{M}n = 2.4 \times 10^5$).

spectrophotometry.

Although the data are scattered, a least mean squares value of μ_c=1.8±0.2D can be obtained for the dipole moment of the carbonyl oxidation product. This value is in reasonable agreement with the accepted value of 2.3D for the carbonyl group, considering the assumptions that have been made in the above analysis. The agreement could, however, be fortuitous.

Literature Cited

1. Achhammer, B. G., J. Polym. Sci., (1952), 8, 555.
2. Achhammer, B. G. in "Polymer Degradation Mechanisms", Chap.14, N.B.S. Circular, 525, (1953).
3. Grassie, N. and Weir, N. A., J. Appl. Polym. Sci., (1965), 9, 975.
4. Grassie, N. and Weir, N. A., J. Appl. Polym. Sci., (1965), 9, 963.
5. Lawrence, J. B. and Weir, N. A., J. Appl. Polym. Sci., (1974), 18, 1821.
6. Achhammer, B. G., Reiney, M. J., and Reinhart, F. W., J. Res. Nat. Bur. Stand., (1951), 47, 116.
7. Beachell, H. C. and Smiley, L. H., J. Polymer Sci., (1967), A-1, 5, 1635.
8. Zapolskii, O. B., Vysokomolekul. Soedin., (1965), 7, 1635.
9. Selivanov, P. I., Kirillova, E. I., and Maksimov, V. A., Vysokomolekul. Soedin., (1966), 8, 1418.
10. Wall, L. A., Harvey, M. R., and Tryon, M, J. Phys. Chem., (1956), 60, 1306.
11. Selivanov, P. I., Maksimov, V. L., and Kirillova, E. I., Vysokomolekul. Soedin., (1969), A11, 482.
12. Cozzens, R. F., Moniz, W. B., and Fox, R. B., J. Chem. Phys., (1968), 48, 581.
13. Weir, N. A., J. Appl. Polym. Sci., (1973), 17, 401.
14. Geuskens, G., Paper presented at International Symposium, "Degradation and Stabilization of Polymers", Brussels, 1974.
15. Jellinek, H. H. G. and Kragman, J. F. in "Photochemistry of Macromolecules", (Ed. R. F. Reinisch), 91, Rlenum, New York, 1970.
16. Lawrence, J. B. and Weir, N. A., Chem. Comm., (1966), 257.
17. Lawrence, J. B. and Weir, N. A., J. Polym. Sci., (1973), A1 11, 105.
18. Vala, M. T., Haebig, J, and Rice, S. A., J. Chem. Phys., (1965), 43, 886.
19. David, C., Piers, M., and Geuskens, G., Europ. Polym. J., (1973), 9, 533.
20. Weir, N. A., J. Macromol. Sci. Chem., (1972), A6, 125.
21. Grassie, N. and Weir, N. A., J. Appl. Polym. Sci., (1965), 9, 999.
22. Greenwood, R. and Weir, N. A., unpublished data, (1974).

23. Grassie, N. and Weir, N. A., J. Appl. Polym. Sci., (1965), 9, 987.
24. Lawrence, J. B. and Weir, N. A., "Kinetics and Mechanisms of Polyreactions", (1969), 5, Section 11, 323, I.U.P.A.C. Symposium, Budapest, 1969.
25. Calvert, J. G. and Pitts, J. N., "Photochemistry", John Wiley, New York, 1966.
26. Greenwood, R. and Weir, N. A., A.C.S. Preprints, International Symposium on U.V. Light Induced Polymer Reactions, Philadelphia, 1975.
27. Clark, F. M., "Insulating Materials for Design and Engineering Practice", John Wiley, New York, 1963.

28. Hedvig, P., J. Polym. Sci., (1971), C33, 315.
29. Oster, G., Oster, G. K., and Kryszewski, M., J. Polymer Sci., (1962), 57, 937.
30. Myers, C. S., Ind. Eng. Chem., (1952), 44, 1095.
31. Fuijnman, C. A. F., Polymer, (1963), 4, 259.
32. Reddish, W. and Barrie, J. T., I.U.P.A.C. Symposium, Wiesbaden Kurtzmitteilung, (1959), 1A3.
33. Michailov, P., Kabin, S. P., and Krylova, T. A., Sov. Phys. Tech. Phys. (1957), 2, 1899.
34. Altares, T., Wyman, D. P., and Allen, V. R., J. Polym. Sci., (1964), A12, 4533.
35. Böttcher, C. J. F., "Theory of Electric Polarization", Elsevier, Amsterdam, 1952.
36. McCrum, N. G., Read, B. E., and Williams, G., "Anelastic and Dielectric Effects in Polymeric Solids", John Wiley, New York, 1967.
37. Onsager, L., J. Am. Chem. Soc., (1936), 58, 1486.
38. Boyer, R. F. in Encyclopedia of Polymer Science and Technology H. F. Mark, Ed., Vol. 13, 257, John Wiley, New York, 1970.
39. Boundy, R. H. and Boyer, R. F., "Styrene, Its Polymers, Copolymers and Derivatives", Reinhold, New York, 1952.
40. Mathur, M. S. and Weir, N. A., unpublished data, (1974).
41. Bueche, F., "Physical Properties of Polymers", Wiley-Interscience, New York, 1962.
42. Davies, M. M., "Molecular Behaviour", Pergamon, London, 1965.
43. North, A. M. and Block, H., Adv. Mol. Relaxation Processes, (1970), 1, 309.
44. Harrop, P. J., "Dielectrics", Butterworks, London, 1972.
45. Yano, O. and Wada, Y., J. Polym. Sci., (1974), A2, 12, 665.
46. McLellan, K. and Weir, N. A., unpublished data, (1973).
47. Jellinek, H. H. G. and Igaroski, S., J. Phys. Chem., (1970), 74, 1409.
48. Greenwood, R. and Weir, N. A., J. Appl. Polym. Sci., in press, (1975).

17

Weak Links and Energy Sinks in the Photooxidation of Styrene Polymers and Copolymers in Solution

R. B. FOX, T. R. PRICE, and R. F. COZZENS

Naval Research Laboratory, Washington, D. C. 20375

Photodegradation is one of the most common light-induced reactions in polymers. An understanding of the phenomena involved is important in both the stabilization of polymeric materials and in solid waste disposal, where degradation is a desirable reaction. Impurities in a polymer system may control the course of photoreactions by acting as donors or acceptors in energy transfer processes. Chain impurities may play a special role as weak links or energy sinks and thereby control the act of chain scission in photoreactions of polymers. These impurities will be of particular importance wherever energy migration can take place within the system, since they can become the locus of photoreactivity.

Intrachain singlet and triplet energy migration is well known in polyarenes such as polystyrene (PS). It has been shown (1) that sequences of methyl methacrylate (MMA) units in a PS chain inhibit electronic energy migration and that vinyl-naphthalene (VN) units or chain impurities such as those produced by oxidation can act as traps for migrating energy. The very efficient process of excimer formation in PS is an energy-trapping process.

Our interest in polymer photodegradation has led us to an investigation of the competition for migrating energy by chain impurities and "defects" such as excimer-forming sites. To isolate the intrachain phenomena, photooxidation of polymer solutions in dimethoxymethane have been carried out. As an example of a very photostable excimer-forming polymer, PS has been selected. Since poly(methyl methacrylate) (PMMA) is known to be far less stable than PS on a quanta-absorbed basis, MMA units have been incorporated into the chain to act as weak links. For energy sinks, 1-VN and 2-VN units have been made part of the chain.

Experimental

Most of the polymers and copolymers have been described previously (1). The sample designated PS-41 is an anionic polymer prepared in tetrahydrofuran with α-methylstyrene tetramer as the initiator. The method of Bamford and coworkers (2), with the Mn(III) chelate of 1-phenyl-1,3-butanedione as initiator, was used to synthesize PS-B. Most of the chains of PS-B are considered to have $-CH(COCH_3)(COC_6H_5)$ end groups based on the method of synthesis and the spectral properties discussed below. The polymers and copolymers, along with their initial number-average molecular weights, determined by osmometry, are listed in Tables I and II. Dimethoxymethane (DMM), used as the solvent for most of the photooxidations, was purified by distillation from $LiAlH_4$; 1 cm of the neat liquid had no significant absorbance at wavelengths above 250 nm and no difference in absorbance was detected between aerated and degassed solvent. Neither prompt nor delayed emission was observed in aerated DMM under our conditions.

Stirred solutions of each polymer or copolymer at a concentration of 10 mg./ml. were irradiated in air at 25°C in a quartz vessel with the light from a low-pressure mercury lamp at an absorbed intensity of 2.95×10^{14} quanta $ml^{-1}sec.^{-1}$. Polymer films, evaporated from DMM or methylene chloride solutions on quartz cuvettes or plates and vacuum dried, were irradiated in air at about 35°C in a Rayonnet Model RPR-100 Photochemical Reactor containing 12 low-pressure mercury lamps; the incident radiation at the films was 1.3×10^{15} quanta $cm^{-2} sec^{-1}$. Emission spectra were measured with the equipment and techniques described in our earlier reports (1).

Quantum yields for chain scission, ϕ_s^O, were determined from the initial slopes of plots of the number of scissions, s, per average chain against the quanta absorbed by the average chain or from plots of s against the quanta, q, absorbed per g of polymer and calculated from the relation $\phi_s^O = (A/\overline{M}_n^O)$ (s/q). The course of the scission process was followed viscometrically and s was estimated from $([\eta]^O/[\eta])^{1/\alpha}-1$; an approximation of α was taken as 0.65 for all solutions in DMM.

Results and Discussion

The choice of solvent for solution degradations of PS with 254 nm radiation is somewhat limited (3). For the present purpose, DMM was selected because it lacked a strong oxygen charge-transfer absorption band such as that observed in aerated tetrahydrofuran or dioxane. In DMM, ϕ_s^O for PS-7 were similar to those observed in tetrahydrofuran or methylene chloride.

In Figures 1 and 2 are given plots of chain scissions against quanta absorbed per polymer chain for various PS

TABLE I

Quantum Yields for Scission in Styrene Polymers and
Copolymers in DMM

Sample	Initiator	$\overline{M}_n^o \times 10^{-5}$	$\phi_s^o \times 10^4$
PS-41	anionic, α-methyl-styrene tetramer	4.9	16
PS-7	AIBN	3.2	26
PS-7(LiAlH$_4$-treated)	AIBN	2.6	26
PS-1	$(C_6H_5CO)_2O_2$	0.38	49
PS-B	Mn(III) chelate of $C_6H_5COCH_2COCH_3$	6.5	200
P(S-co-MMA)(99:1)[a]	AIBN	0.78	58
P(S-co-MMA)(50:50)	AIBN	1.1	142
P(S-co-MMA)(3:97)	AIBN	9.6	630
P(S-alt-MMA)(52:48)	$(C_2H_5)_{1.5}AlCl_{1.5}$	0.33	630

[a]Mole-percent compositions based on ultraviolet absorption
spectra and absorption coefficients assumed from model
compounds

TABLE II

Quantum Yields for Scission[a] in Vinylnaphthalene-Containing
Polymers and Methylnaphthalene Mixtures in DMM

Sample	Initiator	$\overline{M}_n^o \times 10^{-5}$	$\phi_s^o \times 10^4$
P[(S-<u>co</u>-2VN)-<u>alt</u>-MMA](I) (59:1:40)[b]	$(C_2H_5)_{1.5}AlCl_{1.5}$	14.4	76
P(S-<u>alt</u>-MMA)(52:48) + 2-methylnaphthalene (spectrally matched to I)	$(C_2H_5)_{1.5}AlCl_{1.5}$	0.33	550
P(S-<u>co</u>-2VN)(II)(94:6)	AIBN	0.28	c
PS-7 + 2-methylnaphthal-ene (spectrally matched to II)	AIBN	3.2	26
P(S-<u>co</u>-1VN)(99:1)	AIBN	0.73	d
P(S-<u>co</u>-2VN-<u>co</u>-MMA) (56:2:42)	AIBN	0.85	62
P(S-<u>co</u>-2VN-<u>co</u>-MMA) (90:4:6)	AIBN	1.04	115

[a]Based on quanta absorbed by the S-units only

[b]Mole percent compositions based on ultraviolet absorption
spectra and absorption coefficients assumed from model
compounds

[c]No viscosity change after absorption of 16 quanta/polymer
molecule

[d]No viscosity change after absorption of 34 quanta/polymer
molecule; some crosslinking observed in later stages of
irradiation
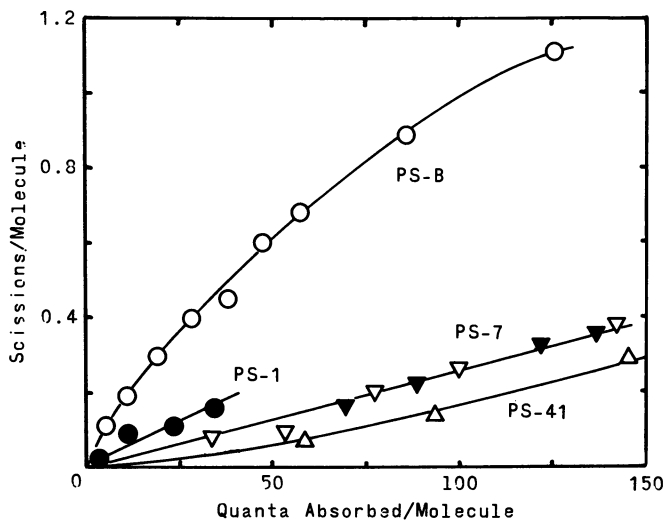
Figure 1.   Chain scission in PS homopolymers in aerated DMM.
▼*, PS-7 after LiAlH₄ treatment.*
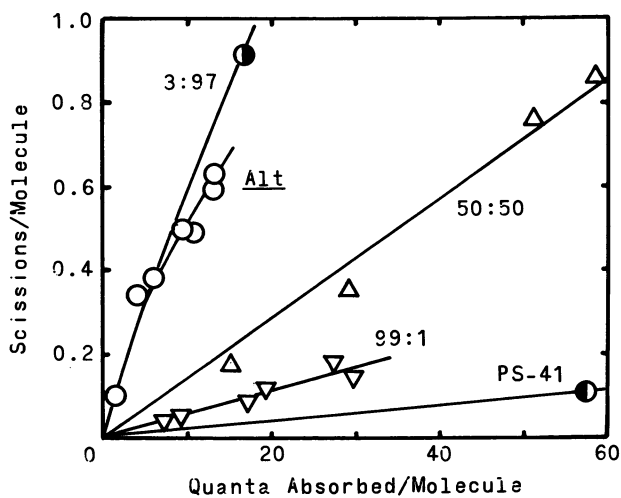
Figure 2.   Chain scission in S-MMA copolymers in aerated
DMM. Plots for 3:97 and PS-41 are derived by extrapolation
from longer exposures.

homopolymers and for S-MMA copolymers. Except for PS-B and the alternating copolymer, these plots are linear within experimental error. If s is plotted against q, a slight upward curvature is noted for PS-41 and PS-7. Intercepts are always at the origin in either type of plot. Therefore, extremely photolabile weak links such as those reported by Lawrence and Weir (4) are not reflected in these data. The data given for PS-7 includes photooxidation of the polymer before and after refluxing for 16 hours in tetrahydrofuran with LiAlH$_4$. This treatment reduced the average chain length by about 25%, clearly indicating a degradation process, yet the photooxidative scission process appeared to be unaffected.

The ϕ_s^O derived from these data are summarized in Table I. With the single exception of PS-B, the PS homopolymers are more photostable than the copolymers. Among the random copolymers, the quantum yield for scission increases as the proportion of S-units decreases. The least stable copolymers are those in which the S-units are separated by one or more MMA-units; excimer fluorescence is not observed in these copolymers (1). As the ratio of excimer fluorescence to fluorescence increases, the quantum yield for scission decreases. Wherever a migrating singlet exciton is trapped at an excimer site, it is less likely to contribute to the scission process.

Poly(methyl methacrylate) is intrinsically a less photostable polymer than PS; its ϕ_s^O is on the order of 0.07 in aerated dioxane or methylene chloride (5). An MMA-unit in a PS chain may thus constitute a weak link in that chain. In P(S-alt-MMA) and in P(S-co-MMA)(3:97), essentially every photon absorbed by the polymer is absorbed by an S-unit situated next to an MMA unit.

At least in regard to excited singlets, the ϕ_s^O in most of these polymers may generally reflect (a) the probability that the photon is absorbed by an S-unit adjacent to a weak link, usually an MMA-unit, and (b) the probability that the absorbed photon will migrate to an excimer site before it reaches a weak link. Superficially, for an individual polymer chain in solution, a competition for the absorbed energy exists between the excimer site, which is an energy sink, and the MMA-unit, which is a weak link.

Clearly, this is a simplistic view, since there is a considerable variation in ϕ_s^O among the PS homopolymers. Yet the excimer fluorescence to fluorescence ratio in DMM solutions is very similar from polymer to polymer. A possible alternative, or additional, route to chain scission may involve intramolecular triplet energy migration and transfer processes. It has been shown (1) that intramolecular triplet migration is facile in both PS and P(S-alt-MMA), but that sequences of two or more MMA-units interrupt the migration process. If an excited triplet trapping site can release its excess energy without bond scission,

the ϕ_S^0 will be lower than if that site is itself a moiety that can undergo scission or it can transfer its energy to a nearby scission-prone weak link.

Ketonic groups are logical triplet traps in styrene polymers, whether they arise from the scission of main chain peroxide linkages (4), pendant peroxide groups (6), or result from impurities incorporated during polymerization or from oxidation reactions themselves. The close similarity between the phosphorescence of acetophenone and polystyrene films photo-oxidized by light of $\lambda > 290$ nm has been noted (6)(7)(8), and it has been suggested that such groups are responsible for scission, either directly or indirectly, in these polymers.

The phosphorescence spectra of dilute solutions of PS in a rigid glass at 77°K consist of a single band at about 400 nm, with τ_p of 2.6, 1.9, and 3.7 sec. for PS-1, PS-7, and PS-41, respectively, which suggests that different concentrations of triplet quenchers are present in the three polymers. On the other hand, the phosphorescence of a dilute solution of PS-B is structured (peaks at 399, 423, and 454 nm) and almost ident-ical to the phosphorescence of 1-phenyl-1,3-butanedione, from which its end groups are derived. The excitation spectrum for the PS-B phosphorescence, however, is the same as the excitation spectra for the phosphorescence of the other PS homopolymers in solution, and this indicates that intramolecular triplet migra-tion and trapping does indeed take place in PS-B. The dione end groups may well be the primary source of the scission process in PS-B in DMM, via abstraction of a hydrogen atom from the solvent and attack by the resulting solvent radical at some point on the original or another polymer chain.

A sample of PS-B photooxidized in DMM, reprecipitated and cast as a film, produced a delayed emission spectrum having a new phosphorescence band, λ_{max} 505 nm, with an excitation maximum in the 380-410 nm region. The emission spectrum is shown in Fig. 3. Similar treatment of P(S-alt-MMA) and PS-41 degraded in DMM showed a corresponding weak phosphorescence at about 507 and 515 nm, respectively, but neither showed an excitation maximum in the 400 nm region. Irradiation of films of each of the polymers and copolymers given in Table I also generated the phosphorescence in the 515 nm region. Concom-itantly, the intensity of the structured short-lived phosphorescence in the 400-450 nm region that is generated in the early stages of film photooxidation of these films is decreased. Examples of these spectra are shown in Fig. 3 for films of PS-41, PS-B, and a poly(methyl methacrylate) film containing 1-phenyl-1,3-butanedione, the model for the end group for PS-B. Neither acetophenone nor benzaldehyde in poly-(methyl methacrylate) films yield similar phosphorescence in the 515 nm region upon irradiation in air. Zapol'skii (9) also observed luminescence at 515 nm in photooxidized PS films and ascribed it to a benzil-like moiety.

As film irradiation is continued and triplet traps undergo
the changes noted, both fluorescence and excimer fluorescence
are increasingly quenched. Thus, the singlet and triplet
processes are interdependent. It is clear that the photooxida-
tion reactions in polystyrene and related polymers are complex
and far from resolved. Nonetheless, it is also clear that
singlet and triplet trapping processes can control access of
migrating absorbed light energy to the weak links that generate
main chain scission in this type of polymer.

Changes in the absorption spectra of PS undergoing photo-
oxidation have been frequently utilized to assess the extent of
degradation. We observed no significant differences between
the infrared spectra of undegraded PS-41 and PS-B and samples
that had been irradiated in DMM, reprecipitated, and cast as
films. These samples of PS-41 and PS-B had been degraded to the
extent of 0.7 and 0.8 scission per average chain, respectively.

It is well known that photooxidation of PS films leads to
the formation of absorption bands in the 280-300 nm region
of the spectrum; these bands may be due to styrene monomer (10).
A broad absorption band centered at about 340 nm is also readily
observed in an irradiated film, and this band has been attributed
to a benzalacetophenone-like moiety (10). Absorption bands at
280 and 310 nm in films of PS irradiated under 600 Torr of
oxygen may be the result of polyene formation (6). We have
observed absorption bands in the same spectral regions in PS
solutions in halogenated solvents irradiated in the absence of
air (5)(11).

At concentrations of 10 mg/ml in DMM, PS solutions
irradiated in air show a general increase in absorbance in the
235-400 nm region of the spectrum; in the absence of air, this
increase occurs very slowly and no band formation was observed.
In solutions irradiated in air, however, specific absorption
bands appear in the spectra. Typical examples are shown in
Fig. 4; these changes in absorbance remain with the polymer
after reprecipitation. The increases in absorbance at 282 nm
are directly proportional to the quanta absorbed per unit weight
of polymer. These bands are formed in DMM solutions of all of
the polymers and copolymers listed in Table I. Plots of the
increase in absorbance at 280 nm against quanta absorbed per
polymer molecule give slopes that might be termed "quantum
yields for band formation," ϕ_{280}. In Fig. 5, ϕ_{280} is shown to
be linearly related to $1/\overline{M}_n^o$ for all of the polymers in Table I
except PS-B and P(S-alt-MMA), suggesting that the absorption
has its origin in only a few sites in each polymer chain; an
end group is a logical possibility.

A second absorption band at 365 nm appeared in irradiated
aerated DMM solutions of all of the materials listed in Table I
except P(S-co-MMA)(3:97) and P(S-alt-MMA); it was absent in an
irradiated solution of toluene in DMM. For PS-41, the 365 nm
band was also observed in irradiated tetrahydrofuran or
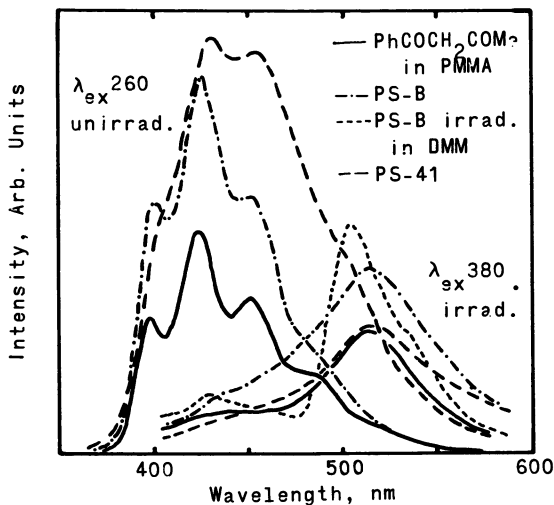
Figure 3. Phosphorescence spectra from films. Intensities are not comparable; the unirradiated films give the same spectra, except for intensity, from λ_{ex} 260 and λ_{ex} 380 nm.
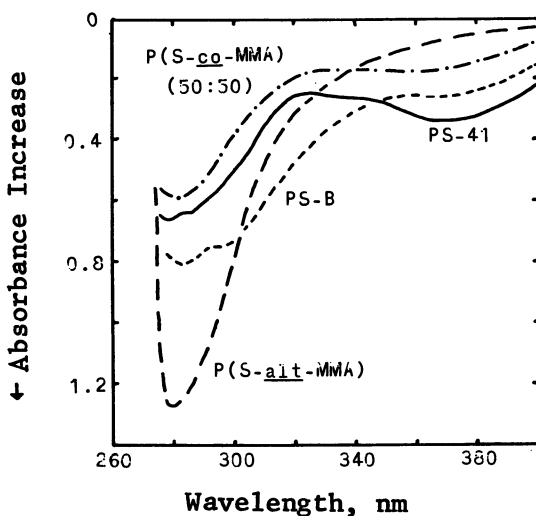
Figure 4. Changes in absorption spectra during irradiation of aerated DMM solutions, 1 cm path, 10 mg/ml., 3×10^{-4} Einstein/g polymer

cyclohexane, but not in methylene chloride solutions. The ϕ_{365} is only approximately related to $1/\overline{M}_n^0$, as indicated in Fig. 5. In the early stages of irradiation, the 365 nm band is generated more slowly than the 280 nm band with the PS samples other than PS-B, but eventually the ratio of the two absorbances becomes constant. This is shown in Fig. 6, which also depicts the behavior of PS-B.

No meaningful relationship could be adduced between any function of ϕ_s^0 and the changes in absorption just described. The 365 nm band also cannot be associated with the 515 nm phosphorescence generated during irradiation, since the latter was observed in P(S-alt-MMA) degraded in DMM. Except to note that the 365 nm band is formed only with those polymers that show excimer fluorescence, identification of the responsible entities must remain speculative.

The energy sinks thus far considered have been excimer sites, photooxidation products, or adventitious impurities. From spectroscopic evidence (1), 1- or 2-vinylnaphthalene (VN) units in PS or P(S-alt-MMA) chains are efficient traps for migrating triplet energy, although the photochemistry of the traps themselves is unknown. The photooxidation of DMM solutions of a number of styrene polymers and copolymers containing VN-units was therefore undertaken. The course of scission process for the alternating copolymer case is shown in Fig. 7. To eliminate filter effects, a spectrally-matched solution of P(S-alt-MMA) and 2-methylnaphthalene is compared to the alternating terpolymer, whose alternating structure is inferred from the method of synthesis and its emission spectra (1). Results with other polymers containing VN-units are summarized in Table II.

It is clear that the introduction of VN-units into a PS or a P(S-alt-MMA) chain acts to stabilize the polymer chains in regard to the scission process in aerated DMM solution. The mechanism by which this occurs is not as clear, except that it is likely to involve intra-chain interactions. From the very nature of the material, the trapping species (the VN-units) are close to the energy donor in the same chain. The probability of dipole-dipole singlet energy transfer is high in the alternating case, since the overlap between the donor fluorescence and VN-unit absorption bands is good. In the PS case, excimer emission does not overlap the VN-unit absorption band, and therefore dipole-dipole interaction is less likely. An intrachain migration and transfer process involving either singlet or triplet excitons may also be invoked to explain these results, particularly if the ϕ_s^0 for the random terpolymers is considered. In these cases, the MMA-units may play the role of both weak link and interruptors of the migration process. If some energy transfer process other than migration is involved, the MMA-units would be expected to have little effect.
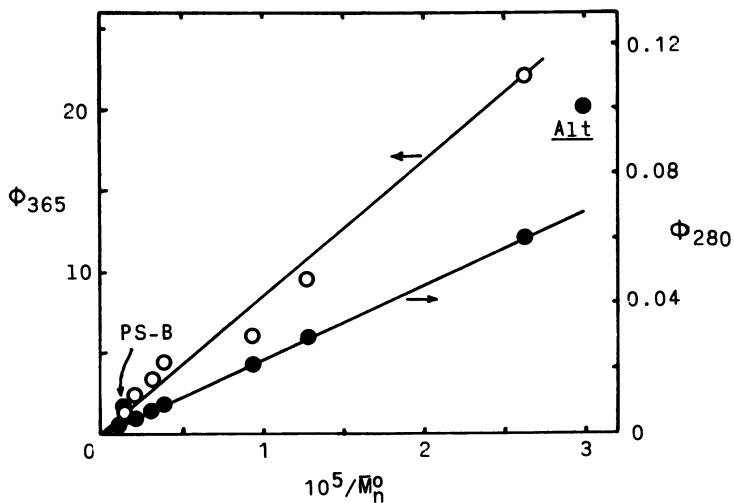
Figure 5. Relationship of absorption spectra changes to polymer chain length
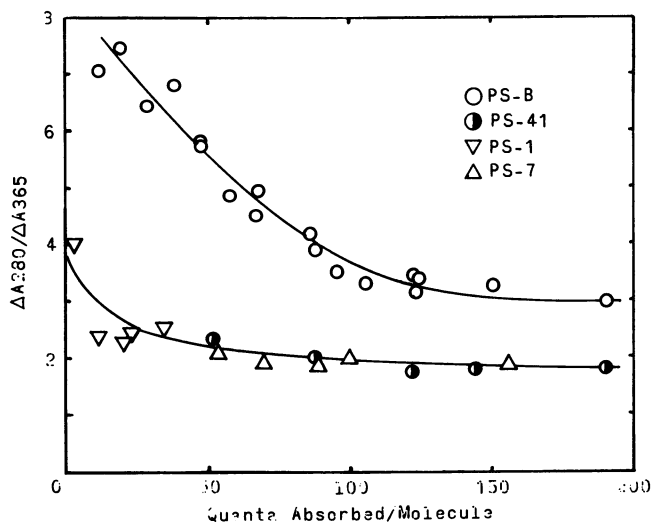
Figure 6. Relative absorption band changes in irradiated PS solutions in DMM
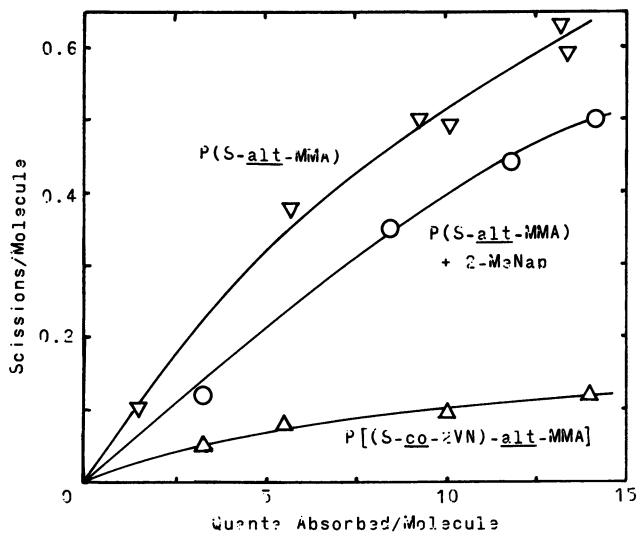
Figure 7. *Effect of energy sinks on chain scission in irradiated alternating copolymer solutions in DMM*

Summary

Photooxidation of styrene-based polymers and copolymers in solution involves a complex group of related and unrelated reactions. In part, the main chain scission process is subject to the competition for migrating absorbed energy by various labile moieties that can be termed weak links and by energy-trapping species that may themselves be weak links or the source of subsequent degradation reactions. The intentional introduction of suitable trapping species can also serve as a means for the reduction of the rate of the scission process.

In this work, we have shown that aromatic diones may be a significant product in the photooxidation of polystyrene and some of its copolymers. As an end group, a dione can be the source of secondary scission processes. Diones and other chain oxidation products appear to function as both energy sinks and weak links. An excimer site in a chain of S-units constitutes a physical energy sink that has a photostabilizing influence With the introduction of MMA-units in the chain, weak links are established, in part through a reduction in the number of excimeric sites. The sequence in which S- and MMA-units appear in the polymer chain is therefore important, as shown by the differences in the behavior of an alternating and a random S-MMA copolymer of similar composition. A decisive influence on the overall photooxidation process in an individual polymer chain may be exercised by introducing other aromatic species into the chain that can act as energy traps without themselves undergoing degradation.

Literature Cited

1. Fox, R. B., Price, T. R., Cozzens, R. F., and Echols, W. H., Macromolecules (1974) 7, 937.
2. Bamford, C. H. and Lind, D. J., Proc. Roy. Soc. (1968) A302, 145.
3. Price, T. R. and Fox, R. B., Polymer Letters (1966) 4, 771.
4. Lawrence, J. B. and Weir, N. A., J. Polymer Sci., Polymer Chem. Ed. (1973) 11, 105.
5. Fox, R. B. and Price, T. R., J. Appl. Polymer Sci. (1967) 11, 2373.
6. Geuskens, G. and David, C., presented at the Intl. Sympos. on the Degradation and Stabilization of Polymers, Brussels, Sept. 1974.
7. Burchill, P. J. and George, G. A., J. Polymer Sci., Polymer Lett. Ed. (1974) 12, 497.
8. George, G. A., J. Appl. Polymer Sci. (1974) 18, 419.
9. Zapol'skii, O. B., Vysokomol. Soedin. (1965) 7, 615.
10. Wall, L. A., Harvey, M. R., and Tryon, M., J. Phys. Chem. (1956) 60, 1306.
11. Price, T. R. and Fox, R. B., Naval Res. Lab. Report 6323, Oct. 1965.

Photosensitized Degradation of Polymers

J. F. RABEK

Department of Polymer Technology, The Royal Institute of Technology,
Technical University, Stockholm, Sweden

Photosensitization of polymers has been found to be important
for a variety of purposes such as 1) Photopolymerization, 2)
Photomodification (photo-grafting), 3) Photodegradation, and 4)
Photostabilization (1). In commercial polymers photodegradation
reactions are usually photosensitized by the presence of alien
groups in the chain or by the presence of trace impurities (2,3).
The first group of impurities is formed during storage and
processing of polymers in the presence of air. Hydroperoxide,
carbonyl and hydroxyl groups, and also unsaturated bonds, belong
to the internal impurities. These groups are mainly formed
during the moulding operations which require heat and pressure
to shape the polymer into the required form. The thermal history
of a polymer has been shown to have a marked effect on its subse-
quent photostability (4-8). Such groups may also be formed on
the polymer surface during the exposure to sunlight.
Second group of impurities consists of traces of compounds
added for the synthesis of the polymers, e.g., catalysts, modi-
fiers, emulsifiers, solvents, etc.
It has been suggested that the nomenclature used for the de-
scription of photosensitized reactions should precisely be applied
(9), namely:
1. "Photoinitiator" is a compound which absorbs light and is
excited by it to a higher energy state having a total energy con-
tent in excess of that required to effect a homolytic scission of
some bonds in polymer molecule to form free radicals, which pro-
mote secondary reactions.
2. "Photosensitizer" is a compound which by absorption of light
is transferred to excited states and then donates the energy to
another compound by inter- or intramolecular energy transfer.
3. "Photosensitized reactions" are strictly speaking such reac-
tions which are activated by photoinitiators or photosensitizers.
In many cases a chemical compound may, in dependence upon the
conditions of a photochemical reaction, behave either as a photo-
initiator or as a photosensitizer.

Free radical reactions

The study of the photochemistry of inorganic and organic compounds gives valuable information on their photolysis during which free radicals are formed (10-12). Extensive studies have especially been made in the field of photo-chemistry of aliphatic ketones, ethers and peroxides (12-14). All these compounds have been found to be good photo-initiators which initiate degradation and crosslinking of polymers. The mechanism of these reactions seems to be simple:

$$RH + h\nu \longrightarrow R\cdot + H\cdot$$
$$RR + h\nu \longrightarrow R\cdot + R\cdot$$
$$PH + R\cdot \longrightarrow P\cdot + RH$$
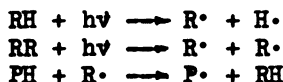
where: RH(RR)-photoinitiator, PH-polymer molecule. Free radicals formed during the photolysis of a compound abstract hydrogen from the polymer backbone or from side groups and form macroradicals. This simple photolysis mechanism is however complicated by:

1. The formation of charge-transfer complexes between initiators and polymer macromolecules. The absorption of charge-transfer complexes is more intense than that of the components and is shifted towards long wavelengths.

2. The formation free radicals in solid state, the diffusion of free radicals into polymer matrix, the kinetics of hydrogen atom abstraction.

3. In the case of photodegradation in solution the cage effect due to solvent molecules which surround the radical pairs formed and enclose them as in a cage (15-16).

4. Reactions of free radicals with oxygen and formation of peroxy radicals.

Photodegradation influenced by the presence of solvents

The finding of a best method for introducing photo-initiators and photosensitizers into polymers is a very important practical problem. Two main methods are in this case applied: a polymer film is cast from a solution with the respective photosensitizer added, or the photosensitizer is pressed into the film at an elevated temperature. In the first method it is sometimes very difficult to remove all traces of solvent, which may influence the photoreactions observed. In the second method conditions of pressing (temperature of 100-200°C and pressure of 100-200 atm) may alter the polymer and compound added.

Many common solvents are usually considered to be inert in photochemical reactions. Only few solvents, such as alcohols and paraffinic hydrocarbons are indeed inert when irradiated in the range of 200-700 nm. Other solvents, such as ketones, aromatic hydrocarbons, tetrahydrofurane, chloroform and carbon tetrachloride are in this range photolyzed (3).

Photo-oxidative reactions may occur in many solvents in the presence of oxygen. Photochemical reactions of several common solvents are presented below:

1. Ketones ($\underline{10,11,13}$)

KETONES

$$RCOR' \xrightarrow{+h\nu} R\overset{\bullet}{C}O + R' \cdot \longrightarrow R \cdot + CO + R' \cdot$$

NORRISH TYPE I

NORRISH TYPE II

2. Benzene ($\underline{17-20}$)

BENZENE

FULVEN

BENZALVEN

OHCICH=CH$_2$CHO
TRANS-TRANS-2,4--HEXADIENE-1,6-DIAL

OHCICH=CH$_5$CHO
2,4,6,8,10-DODECA--PENTAENEDIAL
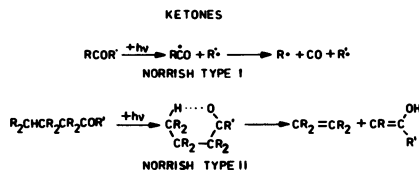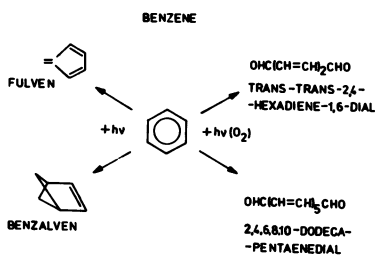
Figure 1. *Formation of the absorption spectra of trans-trans-2,4-hexadiene-1,6-dial and 2,4,6,8,10-dodecapentaenedial during uv irradiation of pure benzene in the presence of air*
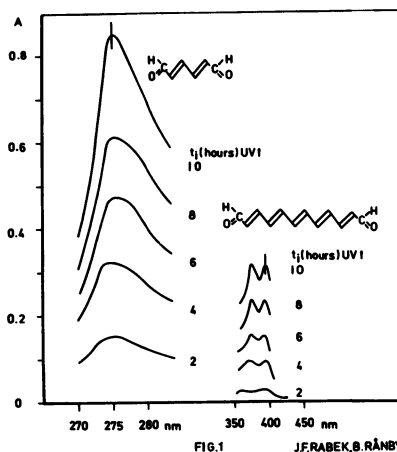
3. Tetrahydrofurane ($\underline{21-24}$)
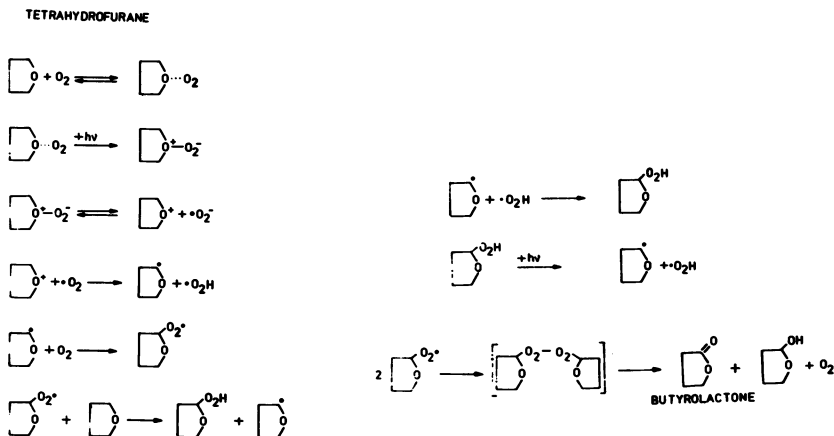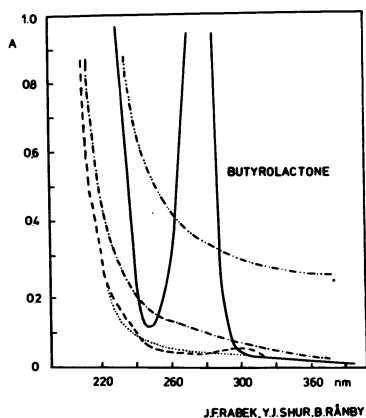
TETRAHYDROFURANE

Figure 2. (left) Formation of the absorption spectra of butyrolactone in PVC film casted from tetrahydrofurane during uv irradiation in the presence of air. (-- and ···) PVC film free from THF, (-·-) and (-··-) after 1 and 5 hr uv irradiation, respectively. (below) Formation of ir-spectra of butyrolactone in PVC film casted from THF during uv irradiation in the presence of air.
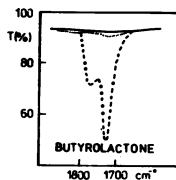
Recently it has been found (25) that tetrahydrofurane (THF) retained by poly(vinyl chloride) (PVC) in amounts of 2 to 6 % may influence the photodegradation of polymers. Free radicals which are formed during the photolysis of THF in PVC matrix are capable of abstracting hydrogen and forming macroradicals. If the effects of solvent traces are ignored a false interpretation of observed phenomena may result.

    4.Carbon tetrachloride (26-29)

CARBON TETRACHLORIDE

$$CCl_4 \xrightarrow{+h\nu} \cdot CCl_3 + \cdot Cl$$
$$CCl_4 \xrightarrow{+h\nu} \cdot CCl_2 \cdot + Cl_2$$
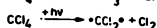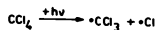
It has been found that the photodegradation of several polymers is strongly influenced by chlorinated solvents,e.g. poly(methyl methacrylate) by 2-chloroethanol (30),methylene chloride (31),chloroform (32,33).

Energy transfer reactions

    The well known process of the transfer of the electronic excitation energy from organic compounds to macromolecules may occur in the liquid or solid state (3,11,34,35). The transfer of energy normally takes place in five steps:
    1.Absorption of a light quantum by a donor molecule followed by the formation of the excited state (Fig.4).
    2.When the excited state of the donor has a higher vibrational energy than the surrounding medium,e.g.solvent, thermal relaxation occurs in a very short time of 10^{-13}-10^{-12}

sec.,and the energy state of the donor drops to lower
vibrational levels until a thermal equilibrium is established.

3.When an acceptor molecule is in the vicinity of an
excited donor the transfer of energy may take place
by one of the following processes: a.Resonance excitation
transfer,b.Exchange energy transfer. The theory of such
energy processes is well developed (34,35).

4.When the excited state of the acceptor after energy
transfer has a higher vibrational energy than the surrounding
molecules the thermal relaxation takes place and the energy
state of the acceptor drops to lower vibrational levels.

5.The excited state of the acceptor macromolecules can be
deactivated by the emission or by other non-radiative
processes.
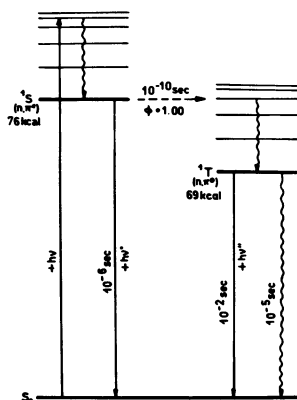
Figure 4. Energy levels and electronic
states for benzophenone in modified
Jablonski diagram
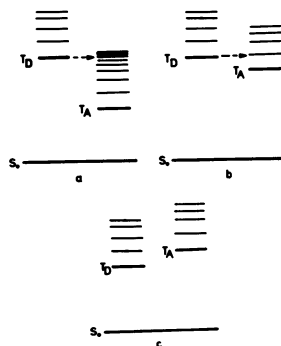
Figure 5. Diagram of energy transfer.
a, high energy transfer efficiency; b, low
energy transfer efficiency; c, no energy
transfer.

In photosensitized degradation of polymers it is most
important to know whether the transferred energy is sufficient
to effect the scission of bonds in acceptor macromolecules.
The main process probably consists of the excitation of
chromophores present in various polymers. This process may be
followed by the formation of free radicals.

Energy transfer reaction have an important role in the
formation of singlet oxygen (2,3,36-40).

Transition metal photosensitizers

The majority of polymers manufactured on an industrial
scale contain a number of various metallic impurities,such as
metal oxides and salts,and also residue of metal organic

catalysts. Some of these impurities are formed during the
manufacture by absorbing products of chemical and atmospheric
corrosion of apparatus used. Other impurities may originate
from packing materials or from processing mechinery,e.g.
rollers,calenders,extruders. Photoactivity of metal oxides
may be attributed to the radical oxygen anions (O_2^-. and O^-.)
(41-43):

$$ZnO + O_2 \xrightarrow{+h\nu} (ZnO)^+ + O_2^-$$
$$O_2^- + H_2O \longrightarrow HO_2\cdot + HO^-$$
$$2 HO_2^- \longrightarrow H_2O_2$$
$$H_2O_2(ZnO) \xrightarrow{+h\nu} 2 HO\cdot$$
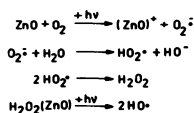
The interaction of O_2^-. with water leads to the formation of
$HO_2\cdot$ radicals.
     The hydroxyl and hydroperoxy radicals may abstract hydrogen
atoms from the macromolecules and thus initiate degradation.
A number of authors reported that TiO_2 (44-49) and ZnO
accelerates the photodegradation rate of nylons,and CuO and
Cu_2O that of natural rubber (50).
     Inorganic salts are well known photoinitiators.The transfer
of electrons from one ion to another or to a solvent molecule
is very important in the majority of inorganic photoreactions:

$$X^n H_2O \xrightarrow{+h\nu} (X^{n+1} H_2O^-)$$
$$(X^{n+1} H_2O^-) + H^+ \longrightarrow X^{n+1} + H_2O + H\cdot$$
$$(X^{n+1} H_2O^-) \longrightarrow X^{n+1} + HO^- + H\cdot$$

$$X^n H_2O \xrightarrow{+h\nu} (X^{n-1} H_2O^+)$$
$$(X^{n-1} H_2O^+) + OH^- \longrightarrow X^{n-1} + H_2O + HO\cdot$$
$$(X^{n-1} H_2O^+) \longrightarrow X^{n-1} + HO\cdot + H^+$$
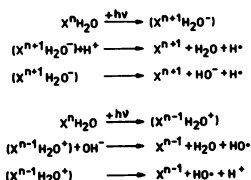
Cations which are photoreduced by the electron transfer
process include:
     $H_g^{2+}(1800Å),Cu^{2+}(2000Å),Pb^{2+}(3085Å),Fe^{3+}(2300Å)$ and Ce^{4+}
     about $(3200Å)$.
Aqueous solution of these cations show a strong absorption.
The absorption spectra of ion pairs of these cations with
various anions are shifted towards the visible region and
the magnitude of that shift is almost directly proportional
to the decrease in electron affinity of the anion (51).

Thus for $Fe^{3+}Cl^-$(λ_{max}=3200Å),$Fe^{3+}Br^-$(λ_{max}=3800Å) and $Fe^{3+}SCN^-$ (λ_{max}=4600Å). It may be concluded that in such ion pairs the anion carriers the electron and the primary act of absorption is for example:

$$Fe^{3+}X^- + h\nu \longrightarrow Fe^{2+}X$$
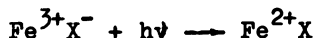
This reaction is followed by various reactions of the inter- mediate compounds including the dissociation of the compound:

$$Fe^{2+}X \longrightarrow Fe^{2+} + X$$
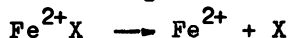
It has been found that $FeCl_3$ accelerated photodegradation of poly(methyl methacrylate)(52-54),poly(vinyl chloride)(55).

Organometallic compounds,e.g.ferrocene,may accelerate the polymer degradation. The photosensitized isomerization and dimerization of conjugated dienes by ferrocene has been investigated in some detail (56-58). Ferrocene is usually believed to be a light-stable compound,but in organic halide solvents it decomposes upon exposure to light; the decomposi- tion results in the formation of free radicals (59,60). The UV spectrum of ferrocene in CCl_4 contains a new strong and broad absorption band in the wavelength region from 300 to 390 nm (60,61). This new band is due to a charge-transfer complex formed between ferrocene and CCl_4 (62,63).The iron atom serves as an electron donor and the chlorine atom as an electron acceptor. Under UV-irradiation the photochemical dissociation of this charge-transfer complex takes place:

FERROCENE   CT-COMPLEX
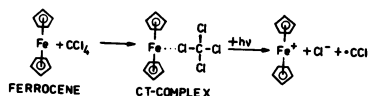
Ferrocene may accelerate the embrittlement of chlorinated polymers (64). This mechanism also involves a charge-transfer complex with a C-Cl bond in PVC and ferrocene. The formation cation,chloride ion and a polymer macroradical are formed:
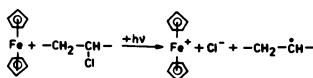
Another organic ferric compound,namely the ferric acetyl acetonate ($Fe^{III}AcAc$) has been found to be an effective initiator for the photodegradation of polyethylene (65) and poly(vinyl chloride)(66). These ferric compounds are easily oxidized and photolyzed.The following mechanism for radical formation in polyethylene sample was proposed (67,68):

$$Fe^{3+}(OCOC_{18}H_{37})_3 \longrightarrow Fe^{2+}(OCOC_{18}H_{37})_2 + C_{18}H_{37}COO\cdot$$

$$C_{18}H_{37}COO\cdot \longrightarrow CO_2 + \cdot C_{18}H_{37}$$

$$\cdot C_{18}H_{37} + -CH_2-CH_2- \longrightarrow C_{18}H_{38} + -CH_2-\overset{\cdot}{C}H-$$
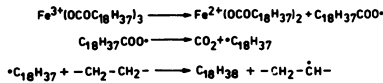
It has recently been found that thermal stabilizers containing a metal, e.g.:
    dibutyltin-S,S'-di(isooctylthioglycolate)(Irgastab 17)
    dibutyltin-di(2-ethylhexylmaleate)(Thermolite 25)
    dibutultin-dilaurate (Stanclere DBTL)
photo-sensitize oxidative degradation of poly(vinyl chloride) (69). The following radicals could be identified by ESR-spectroscopy (Fig.6 and Fig.7):

DIBUTILTIN-S,S-DI(ISOOCTYLTHIOGLYCOLATE)

DIBUTYLTIN-DI(2-ETHYLHEXYLMALEATE)

J.F.RABEK, G.CANBÄCK, B.RÅNBY
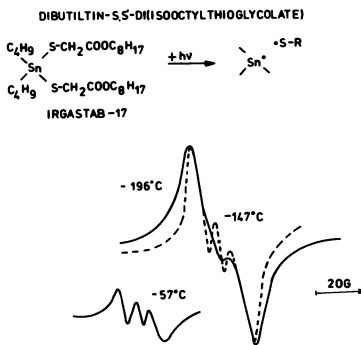
Figure 6. ESR-spectra of Irgastab 17 obtained after 20 min uv irradiation and further warming
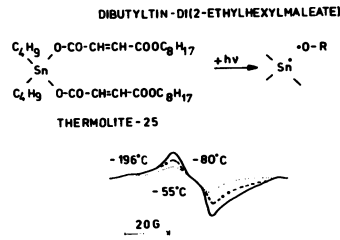
Figure 7. ESR-spectra of Thermolite 25 obtained after 20 min uv irradiation and further warming

On the other hand several transition metal complexes, e.g. dithiocarbamate and 2-hydroxylacetophenone oxime partixipate in the photostabilization of polymers (3,70-76).

Copolymerized sensitizing groups

It is well known that several monomers, such as styrene, α-methylstyrene, isoprene, vinyl acetate (77) have shown formation of charge-transfer complexes in the presence of oxygen. Polystyrene peroxide is formed by photoirradiation of charge-transfer complex in the initial stage of polymerisation and the further photoinduced decomposition of the polystyrene peroxide initiates the polymerisation of styrene. On the other way, the reaction between excited state of styrene and oxygen may induce the formation of an alternating copolymer with peroxide groups -O-O- in backbone.

Among other copolymerized sensitizing groups promoting
the photodegradation of polymers the carbonyl group is most
common. Ethylene-carbon monoxide copolymers for example
contain carbonyl groups built in the main chain (78,79).
Other types,e.g.polyesters and some vinyl copolymers,are
prepared by copolymerization of monomer units containing
carbonyl groups (80-86). On exposure to UV irradiation these
copolymers are photolysed by Norrish type I and Norrish type
II reactions (78,79):

$$
-CH_2-CH_2-C-CH_2-CH_2- + h\nu
\begin{cases}
-CH_2-CH_2-\overset{O}{\overset{\|}{C}}\cdot \ + \ \cdot CH_2-CH_2- \text{ Norrish type I} \\[2ex]
-CH_2-CH_2-\overset{O}{\overset{\|}{C}}-CH_3 \ + \ CH_2\!=\!CH-\text{Norrish type II}
\end{cases}
$$
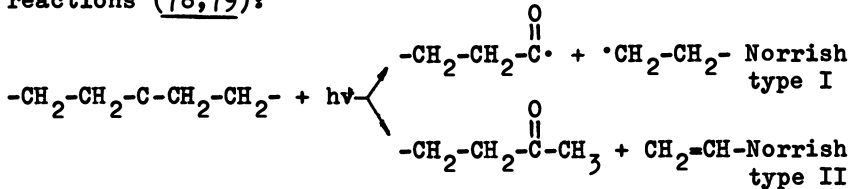
An other important group of polymers with sensitizing
groups consists of polymers with carbonyl group in the side-
chain group,e.g.polyethylene with side-chain keto-ether
groups (87). Photodegradation proceeds through a primary
process with the generation of ketone and keto groups in
chains. A secondary photochemical process sensitized by these
two units leads to oxidative photodegradation.

The intramolecular transfer of excitation energy along a
polymer chain is especially interesting. In the case of
chromophore groups with a long life of their excited states
there always is a possibility of energy transfer between
different parts or segments of the same macromolecule.
Poly(methylvinyl ketone) in which carbonyl groups are also in
side-group photolyse by the Norrish Type II reaction (88,89).
It has been shown,that when the ketone groups are isolated
from each other by copolymerization of methyl vinyl ketone
with methyl acrylate,the photodegradation process increases
(90). This effect can be partially explained by intramolecular
energy transfer.

A new model of representing macromolecules consider
van der Waals inter-and intramolecular interactions. The
latter are responsible for the formation of loops in polymer
main-chain. Energy transfer may occur between adjacent groups
and also between two groups in the vicinity of the loop
interaction points,when the respective distances are less
than 100 Å (3). Polarity and steric factors are very important
in intramolecular energy transfer.

In crystalline regions of a polymer with a high degree of
symmetry the excitation energy is not localized in one point
but it may wander along the chain:

$$-A^x-A-A-A-A-A- \longrightarrow -A-A-A^x-A-A-A-$$

The lifetime of migrating exciton is 10^{-8} sec. During that
time the exciton may "visit" several molecules over a long

distance of 10^2-10^6 Å. Such migrating exciton may be captured
by impurities or traps (e.g.physical defects in the crystal)
and loses its energy which is then transformed into the
vibrational energy of an atom or a molecule. The exciton
energy transfer can occur in many polymers with an adequate
symmetry.

Photosensitized reactions of polymer degradation

The classification of photosensitized reactions according
to the polymer structure seems to be a resonable approach,but
unfortunately the quantitative evidence necesary for such
classification is still inadequate. In practice it is
convenient to group the sensitized reactions according to the
photochemical reactions of the initiators and sensitizers,e.g.

Benzophenone

The triplet state is the photochemically reactive state of
this compound (9-12,91).
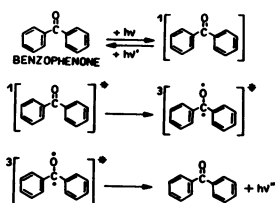
It has been found that only ketones,in which the lowest
triplet state has the n,π^* configuration,are highly active for
the hydrogen abstraction reactions:
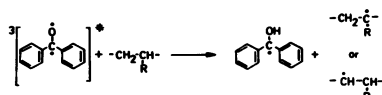
This reaction was reported for the benzophenone photosensiti-
zed degradation of polypropylene (92),polystyrene (93),
poly(vinyl alcohol) (94),polyisoprene (95,96),polyurethane
(97) and polyadenylic acid (98). In solid state benzophenone
also produce an extensive crosslinking of polyethylene
(99-103). It has also been found that benzophenone and its
derivatives caused an initial rapid oxidation,increasing with
ketone concentration (70). Currently the relative importance
of singlet oxygen formation in energy transfer reaction
between excited benzophenone and molecular oxygen is discussed
(92,104):
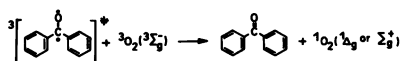
Quinones

On exposure to UV irradiation the reactions of quinones involve their carbonyl groups and the ring double bonds. Quinones arecapable of abstracting hydrogen atoms from various hydrogen donors. The singlet and triplet states of quinones are considered to be the initial reactive intermediate in the reaction:
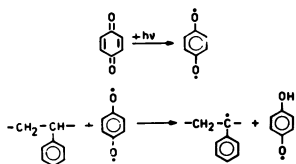
Quinones are effective compounds for the photodegradation of polystyrene (105-107),polyisoprene (108,109),polypropylene (110),polyamides (111),polyurethanes (97) and cellulose (112). During the quinone-sensitized photooxidative degradation of polystyrene film and its solution in benzene,an initial rapid decrease of average molecular weight has been observed by viscosity measurement (Fig.8) and GPC (Fig.9) (107).
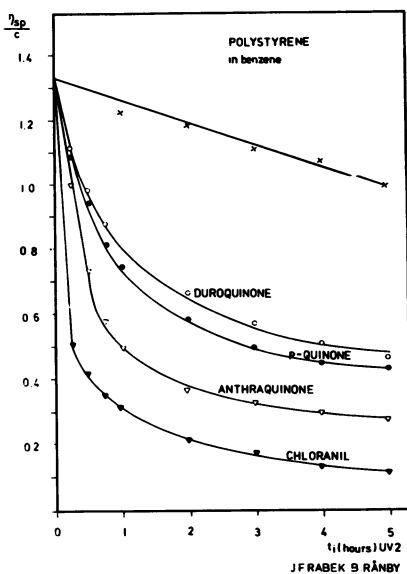
Figure 8.
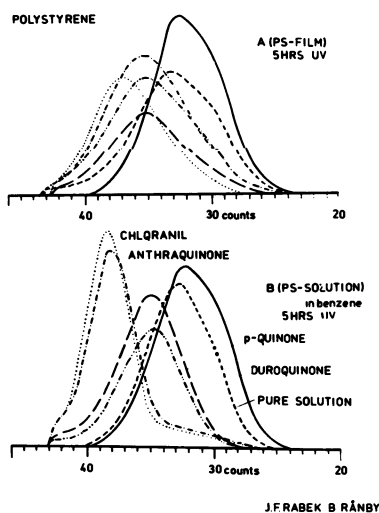
Figure 9.

(Legends on following page)

Figure 8.   (page 262, left) Change of viscosity number in benzene solution during uv irradiation in the presence of air and (●) p-quinone, (○) duroquinone, (▽) anthraqui-none, (▼) chloranil, and (✕) without quinone. Molar ratio of styrene units to quinone = 88:1.

Figure 9.   (page 262, right) Gel permeation chromatograms of (—) undegraded polymer and polystyrene degraded after 5 hr uv irradiation with (– –) p-quinone, (–·· –) duro-quinone, (· · ·) chloranil, (–·–) anthraquinone, and without quinone (– – –). (A), polysty-rene as film; (B), polystyrene in benzene solution. Molar ratio of styrene units to qui-none = 88:1.

The reaction rates are strongly increased by quinone such as p-quinone,duroquinone,anthraquinone,and chloranil.It has been suggested (107) that this photosensitized degradation of polystyrene occurs by a singlet oxygen reaction which might be related to an energy transfer mechanism from excited triplet states of quinone to molecular oxygen.

Peroxides

They are especially important in the process of thermal and photodegradation of polymers. The primary photo-dissociation of alkyl and aryl peroxides takes place in the first absorption region. The weak RO-OR' bond is disrupted:

$$RO-OR' + h\nu \longrightarrow RO\cdot + \cdot OR'$$

Below 220 nm alkyl peroxides dissociate in another way:

$$RO-OR' + h\nu \begin{cases} RO_2\cdot + R'\cdot \\ R\cdot + R'\cdot + O_2 \end{cases}$$
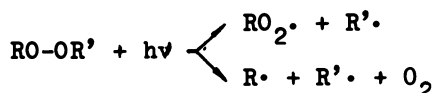
sometimes very important differences of the natures of the radicals produced in thermal and photochemical dissociation are found. It was shown (113) that the peroxide molecules are dissociate by heat to pairs of benzyloxy radicals,some of which may dissociate further to phenyl radicals and carbon dioxide. Photochemical dissociation leads to the direct production of some phenyl radicals (114).

It has been found that the photodegradation of several polymers such as poly(vinyl chloride)(115),polyisoprene (109, 116),bisphenol A polycarbonate (117) is sensitized by peroxides.

Polycyclic aromatic hydrocarbons

They are well known as compounds which are photochemically very reactive. The excited singlet and triplet states are the photochemically reactive states,and they also can participate in energy transfer reactions (2,3,10,11). Some of these compounds such as anthracene,phenanthrene,pyrene added to polyethylene effect the photodegradation of polymer (118,

119). They can sensitize the abstraction of the allylic hydrogen of unsaturated groups in polyethylene. Photoexcited triplet state transfers its excess energy to the unsaturated bond to excite it,and the excited unsaturated groups release their allylic hydrogen atom,producing an allylic radical.

Hexahydropyrene sensitized chain scission of polypropylene and polyisobutylene during light irradiation (120).Polycyclic hydrocarbons have a important role in sensitized photo-oxidation of polyisoprene (122),polystyrene (123), poly(methyl methacrylate) (123-126). It is quite probable that these reactions can also occur with participation of singlet oxygen.

Polymers readily degraded by light

The photosensitizing degradation may considerable contribute to the solution of the plastic-litter problem. In order to improve the standards of our environment the amounts of plastic litter should be reduced and this aim may easily be achived by the use of plastics which would readily degradable by sunlight. This practical problem has been fully reviewed by the following publications (3,127).

Conclusions

It has been demonstrated in this short review that the understanding of the photosensitization mechanism in polymers may be applied for the improvement of their photostability and for the development of polymers with controlled lifetime.

References

1.J.F.Rabek,Photochem.Photobiol.,7,5 (1968).
2.J.F.Rabek,in "Degradation of Polymers",Comprehensive Chemical Kinetics,(ed.C.H.Bamford and C.F.Tipper),Elsevier, Oxford,vol.14,p.265 (1975).
3.B.Rånby and J.F.Rabek,"Photodegradation,Photo-oxidation and Photostabilization of Polymers",Wiley‚London,1975.
4.R.F.Moore,Polymer,4,493 (1963).
5.I.B.Kuznecov and G.O.Tatevosyan,Plast.Massy,9,36 (1964).
6.A.Anton,J.Appl.Polym.Sci.,9,1631 (1965).
7.D.G.M.Wood and T.M.Kollman,Chem.Ind.(London),1972,423.
8.G.V.Hutson and G.Scott,Chem.Ind.(london),1972,725.
9.J.F.Rabek,in Conference on "Photopolymers",SPE Mid-Hudson Section,Ellenville,New York,October 1973,p.27.
10.J.G.Calvert and J.N.Pitts,Jr.,"Photochemistry",Wiley,New York,1966.
11.N.J.Turro,"Molecular Photochemsitry",Benjamin,New York,1966.
12.N.J.Turro,in "Technique of Organic Chemistry" (ed.P.A. Leermakers and A.Weissberger),Wiley-Interscience,New York, 1969,vol.14,p.133.
13.J.N.Pitts Jr.,and J.K.S.Wan,in "Chemistry of Carbonyl Compounds" (ed.S.Patai),Interscience,New York,1966.

14. M.B.Rubin,Fortsch.chem.Forsch.,13,251 (1969).
15. R.M.Noyes,in "Progress in Reaction Kinetics" (ed.G.Porter),
    Pergamon Press,New York,1961,vol.1,p.129.
16. T.Koening and H.Fischer,in "Free Radicals" (ed.J.K.Kochi),
    Wiley-Interscience,New York,1973,vol.1,p.157.
17. H.J.F.Angus,J.McDonald and D.Smyth-Bryce,J.Chem.Soc.,1960,
    2003.
18. H.R.Ward and J.S.Wishnok,J.Am.Chem.Soc.,90,1085 (1968).
19. K.E.Wiltzbach,T.S.Ritscher and L.Kaplan,J.Am.Chem.Soc.,
    89,1031 (1967).
20. K.Wei,J.C.Mani and J.N.Pitts Jr.,J.Am.Chem.Soc.,89,4225
    (1967).
21. B.C.Roquitte,J.Am.Chem.Soc.,91,7664 (1969).
22. V.I.Stenberg,R.D.Olson,C.T.Wang and N.Kulevsky,J.Org.Chem.,
    32,3227 (1967).
23. N.Kulevsky,C.T.Wang and V.I.Stenberg,J.Org.Chem.,34,1345
    (1969).
24. V.I.Stenberg,C.T.Wang and N.Kulevsky,J.Org.Chem.,35,1774
    (1970).
25. J.F.Rabek,Y.J.Shur and B.Rånby,J.Polym Sci (in press).
26. C.S.Marvel,E.J.Prill and D.F.deTar,J.Am.Chem.Soc.,69,52
    (1947).
27. K.Pforde,J.Prakt.Chem.,5,196 (1957).
28. E.P.Abramson,B.M.Buchhold and R.F.Firestone,J.Am.Chem.Soc.,
    84,2285 (1962).
29. M.F.Abd-El-Bary,Dissertation in Leigh Univ.USA,1969.
30. H.H.G.Jellinek and J.C.Wang,Kolloid-z.s.Polym.,202,1 (1965).
31. R.B.Fox and T.R.Price,J.Appl.Polym.Sci.,11,2373 (1967).
32. H.Mönig,Naturwiss.,45,12 (1958).
33. D.Braun and J.Berger,Kolloid-z.z-Polym.,248,871 (1971).
34. M.Burnett and A.M.North,"Transfer and Storage of Energy by
    Molecules",Wiley-Interscience,New York,1969.
35. A.A.Lamola,in "Technique of Organic Chemistry" (ed.P.A.
    Leermakers and A.Weissberger),Wiley-Interscience,New York,
    1969,vol.14,p.17.
36. D.R.Kearns,Chem.Rev.,71,395 (1971).
37. D.R.Kearns and A.U.Khan,Photochem.Photobiol.,10,193 (1969).
38. E.A.Ogryzlo,Photophysiology,5,35 (1970).
39. J.F.Rabek,Wiadom.Chem.,25,293,365,435 (1971).
40. J.F.Rabek and B.Rånby, Polym.Eng.Sci.,15,40 (1975).
41. J.H.Lunsford and J.P.Jayne,J.Chem.Phys.,44,1487 (1966).
42. A.J.Tench and T.Lawson,Chem.Phys.Lett.,7,459 (1970).
43. A.J.Tench and T.Lawson,Chem.Phys.Lett.,8,177 (1971).
44. G.S.Egerton,Nature,204,1153 (1964).
45. G.S.Egerton and K.M.Shah,Text.Res.J.,38,130 (1968).
46. G.H.Kroes,Rec.Trav.Chem.,82,979 (1963).
47. B.Marek and F.Lerch,J.Soc.Dyers Colour.,8,481 (1965).
48. N.D.Shcherba,Z.A.Bazilevich and A.N.Tynnyi,Fiz.Khim.Mekhn.
    Mater.,8,114 (1972).
49. H.A.Taylor,W.C.Tincher and W.F.Hanmer,J.Appl.Polym.Sci.,14

141 (1970).

50. J.C.Ambelang,R.H.Kline,O.M.Lorentz,C.R.Parks,C.Wandelin and J.R.Shelton,Rubber Chem.Technol.,36,1497 (1963).

51. N.Uri,Chem.Rev.,50,375 (1952).

52. Yu.A.Mikheev,G.B.Pariskii,V.F.Shubnyakov and D.Ya.Toptygin, Khim.Vysok.Energii,5,77 (1971).

53. G.B.Pariskii,E.Ya.Davydov,N.I.Zaitseva and D.Ya.Toptygin, Izv.Akad.Nauk SSSR,1972,281.

54. Yu.A.Mikheev,T.S.Popravko,L.L.Yashina and D.Ya.Toptygin, Vysokomol.Soedin.,A15,2470 (1973).

55. V.T.Kagiya,in Conference on "Degradability of Polymers and Plastics",Inst.Electrical Engineers,London,Nov.1973,p.8/1.

56. J.J.Dannenberg and J.H.Richards,J.Am.Chem.Soc.,87,1626 (1965).

57. J.P.Guillroy,C.F.Cook and D.R.Scott,J.Am.Chem.Soc.,89,6776 (1967).

58. R.S.H.Liu and J.Edmani,J.Am.Chem.Soc.,90,213 (1968).

59. A.M.Tarr and D.M.Wiles,Can.J.Chem.,46,2725 (1968).

60. J.C.D.Brand and W.Snedden,Trans.Faraday Soc.,53,894 (1957).

61. L.Kaplan,W.L.Kester and J.Katz,J.Am.Chem.Soc.,74,5531(1952).

62. R.E.Bozak,in "Advances in Photochemistry" (ed.J.N.Pitts Jr. G.S.Hammond and W.A.Noyes),Wiley-Interscience,8,p.227(1971)

63. T.Tsubakiyama and S.Fujisaki,J.Polym.Sci.,B10,341 (1972).

64. A.W.Birley and D.S.Brackman,in Conference on "Degradability of Polymers and Plastics",Inst.Electrical Engineers,London, Nov.1973,p.1/1.

65. G.Scott,in Conference on "Degradability of Polymers and Plastics",Inst.Electrical Engineers,London,November,1973 p.6/1.

66. B.Rånby,J.F.Rabek,Y.J.Shur,Z.Joffe and K.Wikström,in Symposium on "Degradation and Stabilization of Polymers", Bruxelles,1974,p.35.

67. T.Tsuji,Rep.Progr.Polym.Phys.Japan,16,565 (1973).

68. K.Tsuji,J.Polym.Sci.,B11,351 (1973).

69. J.F.Rabek,B.Carnbäck,J.Lucky and B.Rånby (in preparation for publication).

70. M.U.Amin and G.Scott,Europ.Polym.J.,10,1019 (1974).

71. P.J.Briggs and J.F.McKellar,J.Appl.Polym.Sci.,12,1825 (1968).

72. D.J.Harper and J.F.McKellar,Chem.Ind.,1972,848.

73. J.C.W.Chien and W.P.Connor,J.Am.Chem.Soc.,90,1001 (1968).

74. A.Adamczyk and F.Wilkinson,J.Chem.Soc.Faraday,68,2031 (1972).

75. D.C.Mellor,A.B.Moir and G.Scott,Europ.Polym.J.,9,219(1973).

76. J.P.Guillory and R.S.Becker,J.Polym.Sci.,A12,993 (1974).

77. T.Koidara,K.Hayashi and T.Ohnishi,Polym.J.,4,1 (1973).

78. G.H.Hartley and J.E.Guillet,Macromolecules,1,165 (1968).

79. M.Heskins and J.E.Guillet,Macromolecules,1,97 (1968).

80. Y.Amerik and J.E.Guillet,Macromolecules,4,375 (1971).

81. P.I.Plooard and J.E.Guillet,Macromolecules,5,405 (1972).

82. A.C.Somersall and J.E.Guillet,Macromolecules,5,410(1972).
83. M.Kato and Y.Yoneshige,Makromol.Chem.,167,159 (1973).
84. M.Kato,in Conference on "Degradability of Polymers and
    Plastics",Inst.Electrical Engineers,London,Nov.1973,p.5/1.
85. E.Dan,A.C.Somersall and J.E.Guillet,Macromolecules,6,228
    (1973).
86. E.Dan,and J.E.Guillet,Macromolecules,6,230 (1973).
87. E.Cernia,W.Marconi,N.Palladino and P.Bacchin,J.Appl.Polym.
    Sci.,18,2085 (1974).
88. J.E.Guillet and R.G.W.Norrish,Proc.Roy.Soc.,A233,172
    (1955).
89. K.F.Wissbrun,J.Am.Chem.Soc.,81,58 (1959).
90. Y.Amerik and J.E.Guillet,Macromolecules,4,375 (1971).
91. R.S.Cooke and G.S.Hammond,Chem.Soc.Spec.Publ.London,No.24,
    1970.
92. D.J.Harper and J.F.McKellar,J.Appl.Polym.Sci.,17,3503
    (1973).
93. E.D.Owen and R.J.Bailey,J.Polym.Sci.,Al,10,113 (1965).
94. Y.Trudelle and J.Noel,C.R.Acad.Sci.,Ser.C.,260,1950(1965).
95. J.F.Rabek,Chem.Stosow.,11,53 (1967).
96. J.F.Rabek,J.Polym.Sci.,Ser.c,No.16,949 (1967).
97. H.C.Beachell and I.L.Change,J.Polym.Sci.,Al,10,503 (1972).
98. M.Charlier,C.Helene and W.L.Carrier,Photochem.Photobiol.,
    15,527 (1972).
99. A.Charlesby,C.S.Grace and F.B.Pilkington,Proc.Roy.Soc.,
    A268,205 (1962).
100. G.Oster,J.Polym.Sci.,22,185 (1956).
101. G.Oster,G.K.Oster and H.Moroson,J.Polym.Sci.,34,671(1959).
102. Tsao-Gun,Chian-Pin-Chen,Hoy En-Chian,Vysokomol.Soedin.,
    1,635 (1959).
103. H.Wilski,Kolloid-z.z-Polym.,188,4 (1963).
104. A.M.Trozzolo,Adv.Chem.Ser.,No.77,167 (1968).
105. K.Nakamura,T.Yamada and K.Honda,Chem.Lett.(Japan),1973,35.
106. J.F.Rabek and B.Rånby in IUPAC Symposium on "Photochemical
    Processes in Polymer Chemistry",Leuven,June 1972.
107. J.F.Rabek and B.Rånby,J.Polym.Sci.,Al,12,295 (1974).
108. J.F.Rabek,Chem.Stosow.,11,89 (1967).
109. J.F.Rabek in XXIIIrd IUPAC Congress,Boston,USA,1971,
    ed.Butterworths,London,vol.8,p.29.
110. M.Kitano,Japana Pat.71 24,796 (1971).
111. M.V.Locl and F.B.Sugar,Proc.Chem.Soc.,1960,358.
112. C.Kujirai,S.Hashiya,K.Shibuya and K.Nishio,Kobunski
    Kagaku,25,193 (1968).
113. J.C.Bevington,Proc.Roy.Soc.,239,420 (1957).
114. P.K.Sengupta and J.C.Bevington,Polymer,14,527 (1973).
115. W.H.Gibb and J.R.McCallum,J.Polym.Sci.,Symp.,No.40,9
    (1973).
116. J.F.Rabek,Chem.Stosow.,11,183 (1967).
117. G.B.Pariskii,D.Ya.Toptygin,E.Ya.Davydov,O.A.Ledneva,Yu.A.
    Mikheev,and V.M.Karasev,Vysokomol.Soedin.,B14,511 (1972).

118.T.Takeshita,K.Tsuji and T.Seiki,J.Polym.Sci.,Al,<u>10</u>,2315
     (1972).
119.K.Tsuji,T.Seiki and T.Takeshita,J.Polym.Sci.,Al,<u>10</u>,3119
     (1973).
120.L.M.Baider,M.V.Voevodkaya and N.V.Fok,Khim.Vys Energ.,
     <u>5</u>,422 (1971).
121.J.F.Rabek,Scientific Report,Wroclaw Technical University,
     1971.
122.J.F.Rabek,Scientific Report,Uppsala University,1968.
123.H.Mönig and H.Kriegel,Z.Naturfosrch.,<u>15</u>,333 (1960).
124.H.Mönig and H.Kriegel,Proc.Intern.Congr.Photobiol.,
     3rd.Copenhagen,1960,p.618.
125.H.Mönig and H.Kriegel,Biophysik,<u>2</u>,22 (1964).
126.R.B.Fox and T.R.Price,J.Appl.Polym.Sci.,<u>11</u>,2373 (1967).
127.B.Baum and R.D.Deanin,Polym.Plast.Techn.Eng.,<u>2</u>,1 (1973).

19

Photodegradation of Vinyl Chloride–Vinyl Ketone Copolymer

M. HESKINS
EcoPlastics Ltd., 201 Consumers Rd., Willowdale, Ontario, Canada M2J 4G8

W. J. REID,* D. J. PINCHIN,** and J. E. GUILLET
Department of Chemistry, University of Toronto, Toronto, Ontario, Canada M5S 1A1

Recently it has been shown that photodegradable polymers suitable for use in packaging applications can be prepared by copolymerization of ethylene or styrene with vinyl ketone monomers (1). Since PVC is the third important plastic used for packaging, we have investigated the possibility of using the same method to develop photodegradable PVC compositions.

Experimental

Synthesis. The copolymers were prepared by suspension polymerization using a 1 gal stainless steel reactor operating at the autogenous pressure of vinyl chloride at 50° C. The vinyl chloride (Matheson) was purified by passing the gas over KOH pellets. A 9:1 ratio of water to vinyl chloride was used, the suspending agent being methyl cellulose (Methocel 25 cps, Dow Chemical). Percadox 16 (Noury Chemical Corp.) was the catalyst. Because the calculated reactivity ratios indicated that the vinyl ketone would be used up faster than the vinyl chloride, the methyl vinyl ketone was added at frequent intervals throughout the run to maintain an approximately constant feed composition. Yields of 70–85% copolymer were obtained for the copolymers in 5–6 hr. The properties of the resulting copolymers are given in Table I.

Film Preparation. The PVC homopolymer and the copolymers were reprecipitated from THF solution with methanol. Experimental compositions were made up containing 100 parts PVC homopolymer or PVC copolymer, 3 parts Ferro 75-001 (Ba–Cd stabilizer), 1 part Mark C (organic phosphite chelator), and 4 parts Drapex 3.2 (Epoxy plastici-

Present address:
 *Uniroyal Limited, Research Laboratories, Guelph, Ontario, Canada.
**Cavendish Laboratories, Cambridge University, Cambridge, England.

TABLE I. Copolymers of Vinyl Chloride and Methyl Vinyl Ketone

Ketone content mol-%	$[\eta]$ dl/g	M_v	Tensile strength, psi	Elongation at break, %
6	0.72	54,000	4400	130
1.6	0.95	78,000	4900	130
0	0.83	65,000	4900	110

zer). This stabilizer system was found to be more effective for the co-polymers than other systems tried, including the tin salts. The above ingredients were dissolved in THF (15 ml/gm) and subsequently cast onto glass plates. The glass plates rested on mercury in order to en-sure constant film thickness. Films of thickness 0.08, 0.20 and 0.25 mm were prepared in this manner. The presence of Drapex 3.2 im-parts a slight plasticization to the film.

Degradation. The films were weathered either on wooden racks placed on the roof of the Chemistry Department (University of Toronto), facing south at 45°, or in an American Ultraviolet Accelerometer (Model NS-1200). The temperature in the weatherometer was 37° C.

Molecular Weight. The viscosity average molecular weight of the homopolymer and copolymers was determined from single point deter-minations of viscosity of a 0.25% solution in Fisher purified cyclohexane at $30.0 \pm 0.01°$ C. The molecular weight is calculated from the intrinsic viscosity, $[\eta]$, using the relationship (2)

$$[\eta] = 1.63 \times 10^{-4} M_v^{0.77}$$

Results

Preliminary experiments showed that when thermally stabilized thin films (80 μ thickness) of vinyl chloride–methyl vinyl ketone copoly-mers were subject to UV radiation they became brittle without color for-mation. When the ketone concentration in the copolymer was approxi-mately 6 mol-%, the time to brittleness in the Accelerometer was less than 20 hr, whereas 40 to 50 hr were required if the ketone concentra-tion was only 2%. Samples of PVC homopolymer, identically stabilized, were photolyzed along with the copolymers. No color or chemical change was apparent in these samples, even after 100 hr photolysis. Quantitative information was then obtained on the degradation pro-cess by irradiating 0.2 mm thick film samples in the Accelerometer for varying periods of time and subsequently measuring their elongation at

break. The results are shown in Fig. 1, while Fig. 2 shows how the molecular weight varied with photolysis time for both the homopolymer and copolymer. The molecular weight results are plotted in the form of $[(1/M) - (1/M_0)]$ which gives the number of breaks per chain, corrected for differing initial molecular weight. As expected, the molecular weight and percent elongation remaining decreased with time for the copolymer, while little change was noted for the homopolymer.

Outdoor weathering of the various samples confirmed the high susceptibility to UV degradation of the copolymer relative to the homopolymer. The elongation, tensile strength and molecular weight all decreased rapidly outdoors. The results are shown in Figs. 3-5. Figure 3 shows that the copolymer with 6% ketone degrades rapidly for the first three weeks outdoors. The film rapidly turns a brown color thereafter, possibly because the barium soap has been exhausted and the cadmium chloride is catalyzing the formation of color centers. The same discoloration was noticed after 30 hr in the Accelerometer. The homopolymer stabilized in the same way and exposed to the same conditions remains colorless for much longer periods of time. The stabilizers appear to be depleted in the copolymers at a higher rate than in the homopolymer. Moreover, the depletion rate increases with ketone content as the films with approximately 1.5% present were still colorless after six weeks outdoor exposure.

Infrared spectra of the crude copolymer showed a main carbonyl peak at ~1710 cm^{-1} with a small peak at 1770 cm^{-1}. Reprecipitation of the copolymer removed the 1770 cm^{-1} peak completely. Upon irradiation of the purified copolymer, the 1710 cm^{-1} peak immediately began to decrease while the 1770 cm^{-1} peak together with another peak at 1725 cm^{-1}, reappeared. These effects are shown in Fig. 6, which shows the IR spectrum of the irradiated film in the carbonyl region using an unirradiated film as reference. However, when the degraded polymer was reprecipitated at an early stage of photolysis, the 1770 cm^{-1} band again disappeared. Continued photolysis leads to a broadening of the 1770 cm^{-1} peak and the eventual disappearance of the 1710 cm^{-1} peak. The rates of appearance and disappearance of these bands were unaffected by the stabilizer system since a copolymer sample without stabilizer showed similar rates of change.

Discussion

Previous studies by Hartley and Guillet (3) and by Amerik and Guillet (4) have shown that polymers containing ketone groups undergo photolysis by the Norrish type I and type II reactions. The relative proportions of type I and II depend on the polymer concerned and the particular environment of the carbonyl group. These reactions are
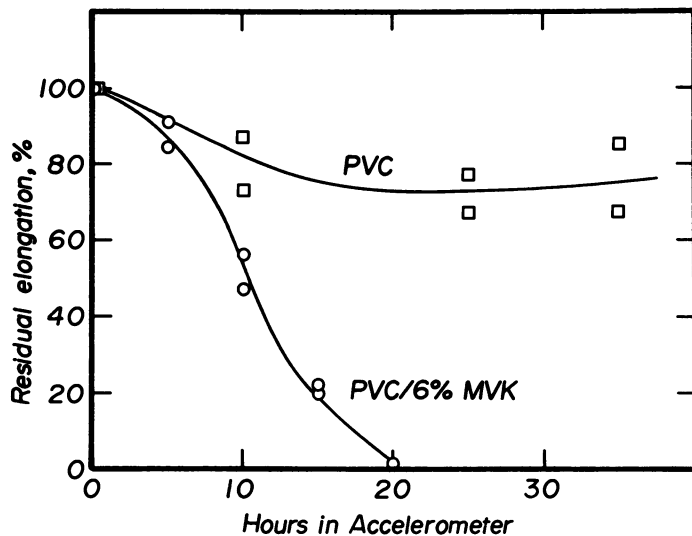
Figure 1.   Percent elongation remaining with irradiation in the accelerometer; film thickness, 0.2 mm
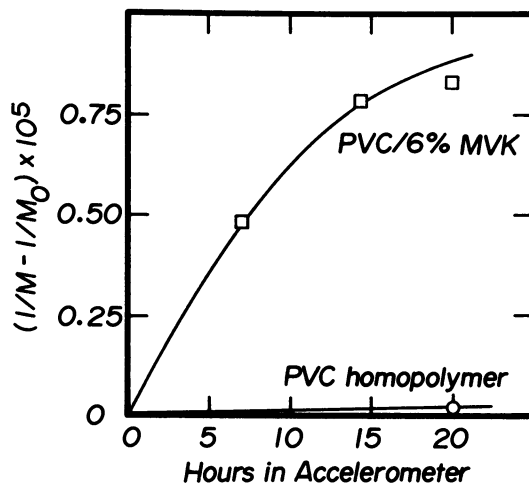
Figure 2.   Normalized chain breaks with irradiation in accelerometer; film thickness, 0.2 mm
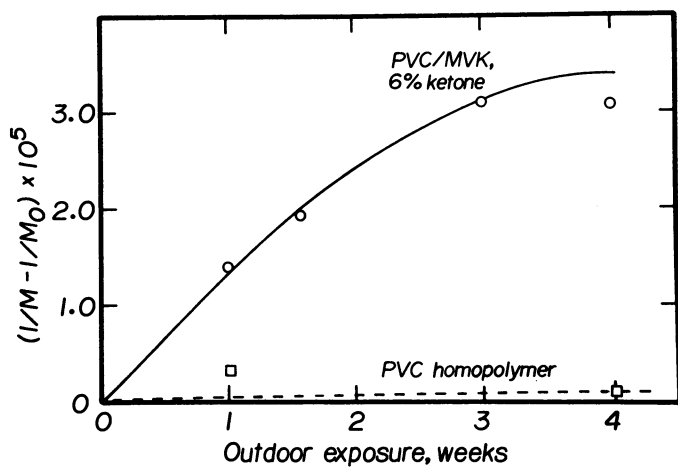
Figure 3. *Normalized chain breaks on irradiation (outdoors)*
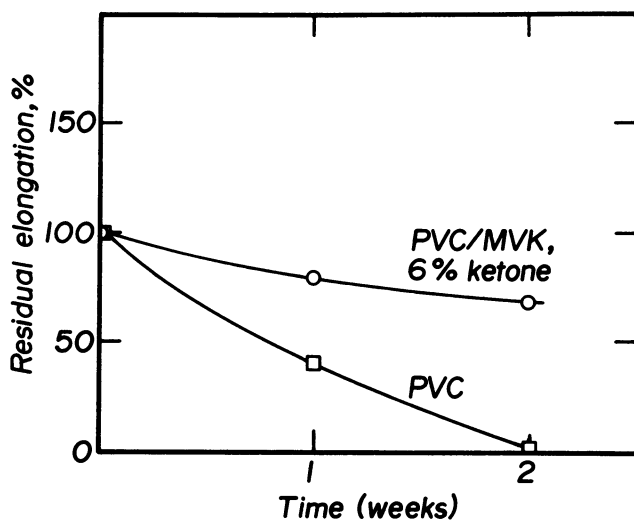
Figure 4. *Residual elongation; film thickness, 0.2 mm*
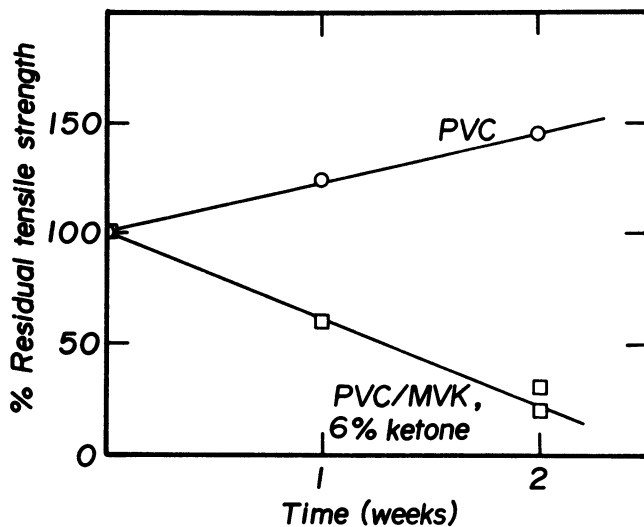
Figure 5. Percent residual tensile strength, outdoor weathering; film thickness, 0.2 mm
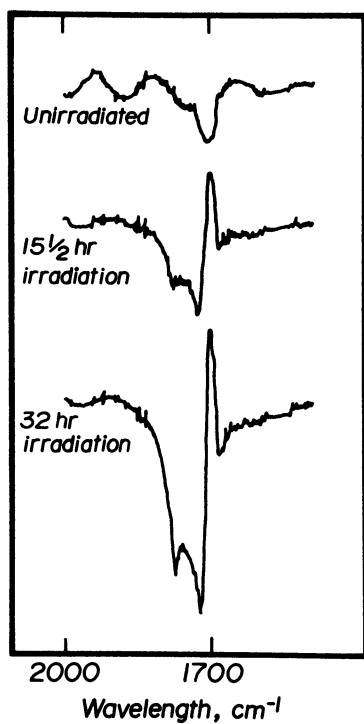
Figure 6. Photodegradation of PVC copolymer, differential infrared spectra

represented in the scheme below:

(1)

(2)
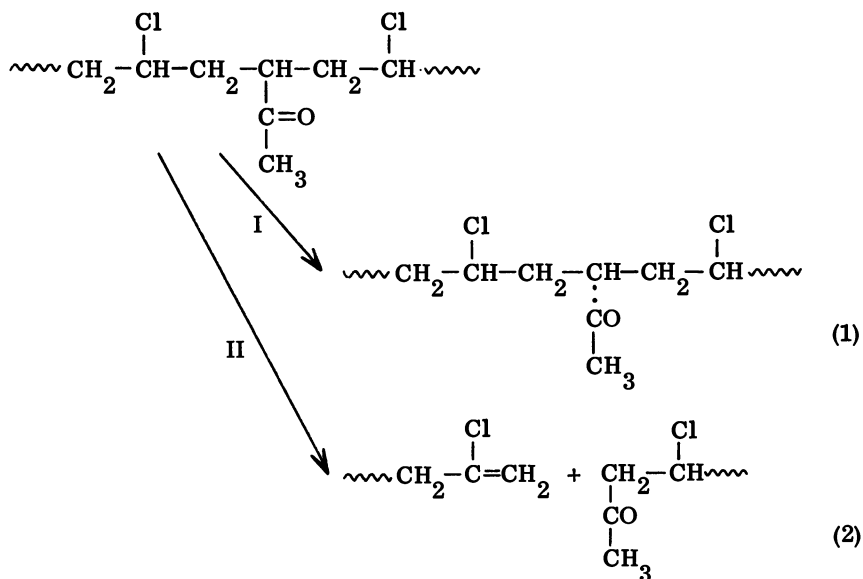
Partly because it is known that thermal stabilizers for PVC also inhibit UV degradation, it was thought that the photodegradation of PVC followed a mechanism similar to that established for its thermal degradation. This mechanism is based on the free radical initiated dehydrochlorination reaction of alkyl chloride which, in PVC, results in conjugated unsaturation. This unsaturation is responsible for the rapid discoloration of PVC on heating. In photooxidation studies it is found, however, that HCl begins to be produced only at a relatively late stage and that ketonic structures are observed at a relatively early stage. Kwei (5) has shown that these ketones are present as β chloroketones in the chain, i.e., $-CH_2-C(=O)-CH_2-CHCl-$. A simple model for this type of ketone is 4-chloro-2-butanone which undergoes type I scission. Although this type of ketone can also undergo chain scission by type II, this mode was not considered because no unsaturation was observed during photolysis.

In the MVK/PVC copolymers the type I reaction does not cause chain scission so that, for chain scission to occur, the type II or some secondary mechanism is necessary. In order to minimize the effects of the secondary mechanisms which, in these copolymers also cause crosslinking and discoloration, the polymers were irradiated in the presence of stabilizers. Under these conditions the copolymers did indeed undergo chain scission. Only a very small amount of vinyl double bond absorption was observed in IR or the irradiated films, but

even in the thermal degradation, where conjugated unsaturation is observed in the UV spectrum, it is difficult to observe unsaturation in the IR. Photolysis of chloro ketones of structure similar to the copolymers has not been reported so we have examined the photolysis of 5 chloro-2-hexanone, the simplest compound of similar structure, to see if it can undergo type II reaction. Irradiation of 5 chloro-2-hexanone in hexadecane at room temperature with 313 nm radiation results in the Norrish type II reaction, producing acetone and 2 chloropropene. Under the conditions of the experiment, the type I product observed would be expected to be 2 chlorobutane, but this was not detected. The study of the photolysis of 5 chloro hexanone is being continued and will be reported later. Although no type I product could be observed in this model compound it is probable that the type I would be significantly higher in the copolymer since in this case the carbonyl is attached to a secondary carbon instead of primary carbon and in simple ketones this increases the type I yield.

Infrared studies of the carbonyl absorption of the copolymers as photolysis proceeds indicates the appearance of two new peaks and the loss of the original peak. The new absorption at 1725 cm^{-1} can be explained by several processes. One is the change from a secondary ketone to a primary ketone as the type II reaction proceeds. A second explanation is the oxidation of free radical sites generated by type I. This is similar to the mechanism postulated by Kwei for the production of the β chloro ketones. It is also possible that this absorption is due to the acetyl fragments split off by type I photolysis. We have observed that the carbonyl absorption at 1770 cm^{-1} can be removed by reprecipitation from THF solution by methanol. This indicates that the group responsible for this absorption is not chemically attached to the molecule. The acetyl radical produced by the type I can abstract hydrogen, or chlorine, either from the polymer or the stabilizer to form either acetaldehyde or acetyl chloride which may hydrolyze to the acid.

Both acetic acid and acetaldehyde have an absorption in the 3100 cm^{-1} region of the infrared and are unlikely since no absorption in this region was observed. When the IR spectrum of homopolymer PVC impregnated with acetyl chloride was measured, two absorptions in the carbonyl region are observed at 1776 and 1722 cm^{-1}. These two absorptions correspond quite well with those of the degraded copolymer. It does however indicate that the radical has abstracted a chlorine from the polymer, a process generally considered unlikely.

Summary

Copolymers of vinyl chloride and methyl vinyl ketone undergo chain scission with concomitant rapid decreases in tensile strength and elongation when exposed to near ultraviolet light and solar radiation. Free radicals formed by the homolytic scission of the acyl group apparently deplete the stabilizers used and lead to rapid discoloration of the polymer, presumably by the usual radical chain reaction involving the production of HCl and conjugated double bonds.

Acknowledgements

Literature Cited

1. Guillet, J. E., in "Polymers and Ecological Problems", J. Guillet, ed., Plenum Publishing Corp., New York, 1973.
2. Dailer, K. and Vogler, K., Makromol. Chem.,(1952), 6, 191.
3. Hartley, G. H. and Guillet, J. E., Macromolecules, (1968) 1, 165.
4. Amerik, Y. and Guillet, J. E., Macromolecules, (1971) 4, 375.
5. Kwei, K.-P. S., J. Polym. Sci., Part A-1, (1969) 7, 1975.

Photodegradation of Styrene–Vinyl Ketone Copolymers

M. HESKINS
EcoPlastics Ltd., 201 Consumers Rd., Willowdale, Ontario, Canada M2J 4G8

T. B. McANENEY* and J. E. GUILLET
Department of Chemistry, University of Toronto, Toronto, Ontario, Canada M5S 1A1

The photolysis of copolymers containing ketone groups has both academic and practical interest since the way in which the polymeric environment affects the photochemical pathways leads to an understanding of the photodegradation of polymers in which the ketone group is present as an adventitious or intended impurity. Copolymers with vinyl ketones also provide a practical means for preparing plastics with controlled lifetimes as a means of combatting litter problems (1-3).

In this report we examine the effects of several vinyl ketone monomers on the photodegradation of polystyrene in the solid phase. Previous work (4, 5) has indicated that copolymers containing vinyl ketones undergo photolysis by the Norrish type I and type II primary reactions. Studies by Golemba and Guillet (6) and by Kato and Yoneshiga (7) have shown that these processes also occur in copolymers of styrene with methyl vinyl ketone and with phenyl vinyl ketone.
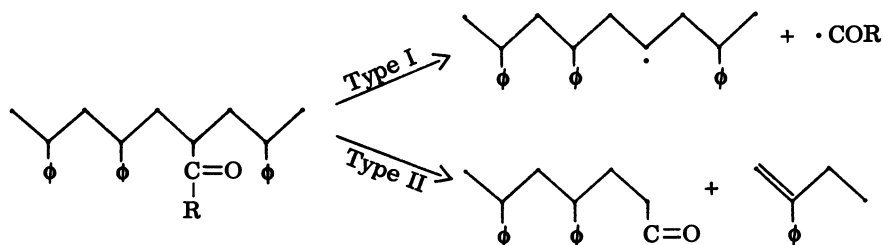
It can be seen that the type II reaction will break a C—C bond in the chain backbone, while the type I reaction will produce two free radicals without primary main chain scission. In the presence of air these radicals initiate photooxidation and therefore cause chain scission by sec-

*Present address: INCO Research, Sheridan Park, Ontario, Canada.

ondary reactions. The effect of ketone structure on the relative rates of these reactions is the subject of this investigation.

Experimental

Preparation of Monomers. Methyl vinyl ketone (MVK) was obtained from Pfizer Chemical Division, New York, and distilled to remove the inhibitor. Methyl isopropenyl ketone (MIPK) was prepared by the aldol condensation of methyl ethyl ketone and formaldehyde, according to the method of Landau and Irany (8). The major impurity in this monomer is ethyl vinyl ketone (5%). The monomer was redistilled before use. 3 Ethyl 3 buten 2 one (EB) was prepared by the aldol condensation of methyl propyl ketone and formaldehyde. Ethyl vinyl ketone (EVK) was prepared by a Grignard synthesis of the alcohol, followed by oxidation to the ketone. t–Butyl vinyl ketone (tBVK) was prepared from pinacolone and formaldehyde by the method of Cologne (9). Phenyl vinyl ketone (PVK) was prepared by the dehydrochlorination of β chloro propiophenone (Eastman Kodak). Phenyl isopropenyl ketone (PPK) was prepared by the Mannich reaction using propiophenone, formaldehyde and dimethylamine HCl.

These monomers have a tendency to dimerize on standing at room temperature and were kept at 0°F. All the monomers were at least 95% pure, except the MIPK which contained 5% EVK. The purity of this monomer was 93%.

Copolymers. The copolymers were prepared by emulsion polymerization in a "pop bottle" polymerizer at 80°C using sodium aryl alkyl sulphonate (Ultrawet K) as emulsifier and ammonium persulphate as catalyst. The polymerizations were carried to greater than 95% conversion (4-8 hr) and the feed concentrations of the vinyl ketones were taken as their concentrations in the polymer. Copolymers containing 1% and 5% by weight of vinyl ketones were prepared. The copolymers were not homogeneous in ketone concentration since the reactivity ratios indicated that the vinyl ketones would be used up before the end of the polymerizations. Thin films were prepared for irradiation by compression molding in a Carver Press at 150°C at 20,000 psi. The films were usually 0.22 mm thick.

Blends were prepared by solution blending the copolymers with a Dow general purpose molding grade (667) polystyrene, casting from solution and then compression molding film as for the copolymer.

Irradiation. The films were irradiated in air in an American Ultraviolet Co. UV Accelerometer. This uses a medium pressure mercury arc lamp enclosed in Pyrex and its major emission is at 313 nm together with less intense light at 298 and 366 nm. The lamp runs at about 40°C. The amount of near ultraviolet light absorbed by the

films during the tests is estimated to be in the order of 4×10^{-7} einstein/ sq cm/hr.

The degradation of the copolymers or blends was followed by the change in their solution viscosity in toluene at $30°$ C. The viscosity average molecular weights were calculated from the equation (10),

$$[\eta] = 1.1 \times 10^{-4} \, M^{0.725}$$

The number of breaks/chain is given by $[(M_{n_0})/(M_n)] - 1$, where M_{n_0} is the initial number average molecular weight and M_n the number average molecular weight after irradiation. The total number of chain breaks is then

$$\left(\frac{M_{n_0}}{M_n} - 1\right) \frac{g}{M_{n_0}} = \left(\frac{1}{M_n} - \frac{1}{M_{n_0}}\right) g$$

where g is the weight of irradiated sample. The results are reported here as $[(1/M_v) - (1/M_{v_0})]$ against time of exposure. Although a standard size sample is used, there is an error involved in using viscosity average rather than number average. However, since it was not possible to measure the light absorbed, we have not attempted to measure quantum yields. The expression is used to counteract the effect of differing initial molecular weights of the copolymers.

Results and Discussion

The photodegradation of 0.22 mm thick films of styrene/1% MVK and styrene/1% MIPK copolymers in the Accelerometer are shown in Fig. 1. The MVK copolymer degrades significantly faster than the MIPK copolymer. The difference in structure in the ketone units of the copolymer is that the MIPK copolymer has the acetyl group attached to a tertiary carbon on the chain, while in MVK this carbon is secondary. Studies with simple ketones of precisely this structure, i.e., acetyl group attached to secondary or tertiary carbon which can also undergo a type II reaction, have not been made. However, studies with related methyl ketones (11, 12) lead to the expectation that the MIPK copolymer will have a somewhat higher type I yield and lower type II. In the irradiation with high intensity artificial UV sources it is expected that any photooxidation will be minimized and chain scission will be principally due to the type II reaction. Figure 2 shows the effect of outdoor exposure where, although the breakdown of the MVK copolymer is initially faster, it does not maintain its rate and the MIPK copolymer eventually achieves a greater degree of chain scission. This can be ascribed to the continuing effect of photooxidation initiated by the type I free radicals in the latter case.
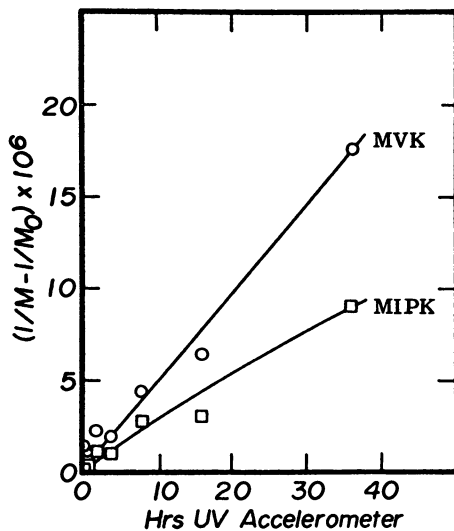
Figure 1.   Photolysis of PS containing 1%
MVK and 1% MIPK
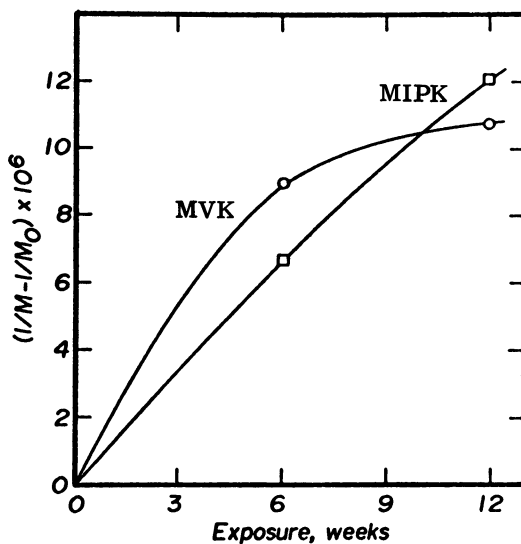
Figure 2.   Weathering of copolymer of 5% MVK
and 5% MIPK with styrene in Arizona

tert-Butyl vinyl ketone copolymers would be expected to show a low type II yield since this is observed for simple ketones of analogous structure. The 1% tBVK copolymer does indeed give a low rate of degradation compared to a similar MVK copolymer, as shown in Fig. 3.

The other two monomers chosen have an ethyl group replacing a methyl group, either in the acyl group (EVK) or on the α carbon (EB). The photolysis of these comonomers, when copolymerized at the 1% level with styrene, are intermediate between the methyl substituted analogs MVK and MIPK, as shown in Fig. 4.

The photodegradation of a 1% PVK copolymer is compared with the 1% MVK copolymer in Fig. 5. Previous studies (6, 1) have indicated that the PVK copolymer has a significantly higher quantum yield for type II reaction than MVK and the ketone group has a higher extinction coefficient in the UV region. It would therefore be expected that a faster rate of chain scission would be obtained for the PVK copolymer than the MVK. This is indeed true during the early stages of the reaction, but the rate of degradation slows down rapidly at longer exposure times. The reactivity ratios for PVK–styrene are not favourable for a random distribution of the phenone groups. In fact, calculations show that, with all monomer charged initially, nearly all the PVK is incorporated in the first 20% of polymer produced. Since chain scission is concentrated in this fraction of the copolymer, viscosity will give a poor indication of the total number of chain scissions in this case. The PIPK copolymer showed a somewhat similar effect. At high degrees of degradation there is also a color-forming reaction (related to photooxidation) which makes the polymer opaque to UV radiation. This also contributes to the retardation of the photolytic process.

Blends. The type I reaction produces free radicals which, in the presence of oxygen, initiates photooxidation which also results in a decrease in the polymer molecular weight. An indication of the relative importance of the type I reaction in these systems can be estimated from the amount of chain scission induced in a blend of the copolymers with homopolymer polystyrene. For these experiments, one part of 5% vinyl ketone copolymer was blended with four parts of styrene homopolymer to retain an overall ketone monomer concentration of 1%.

Figure 6 shows the rates of degradation for four of the copolymers. This figure shows that the overall rate is greater for MIPK than for MVK copolymer blends. It should be noted that for all these blends, the rate of degradation is greater than can be attributed to the breakdown of the copolymer in the blend. Under the conditions of the test the value of $[(1/M) - (1/M_0)]$ for the MVK copolymer blend would not rise above 1×10^{-6} if no sensitization had taken place. This was determined by irradiating the 5% MVK copolymer and the homopolymer and then preparing a solution of the degraded polymers in the correct
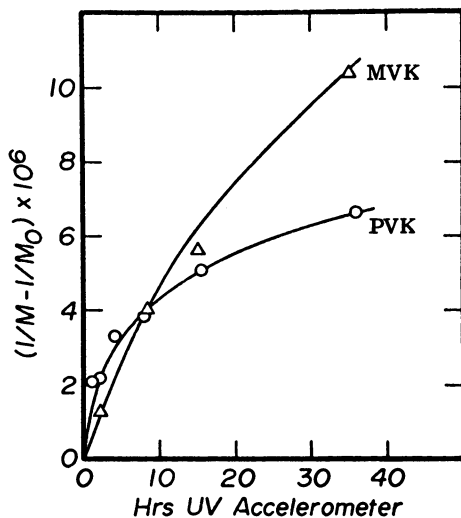
Figure 3.   Photolysis of 1% PVK copolymer
               and 1% MVK copolymer
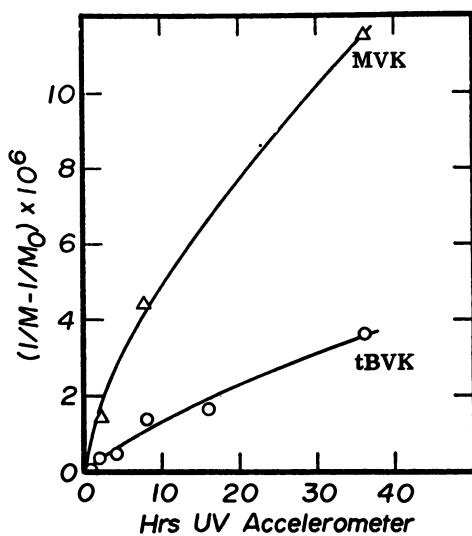
Figure 4.   Photolysis of 1% tBVK copolymer
               and 1% MVK copolymer
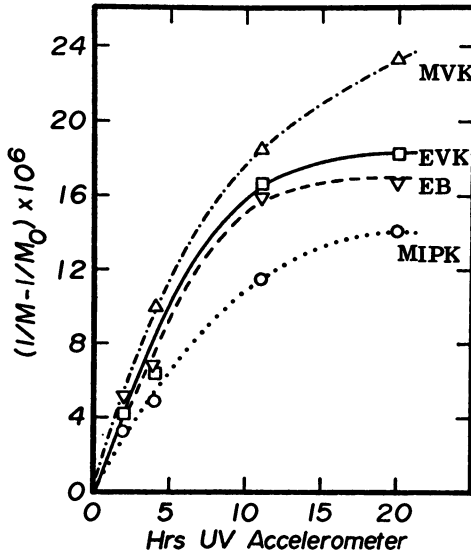
Figure 5. Photolysis of 1% copolymers with styrene
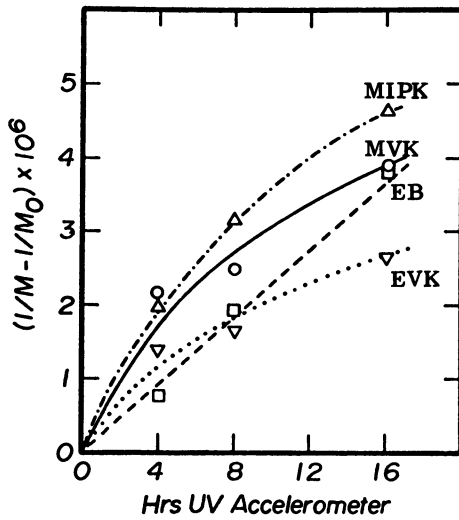
Figure 6. Photolysis of 4:1 blends of polystyrene with polystyrene 5% vinyl ketone copolymers

proportions prior to measuring the solution viscosity. The greater total degradation in the case of the MIPK copolymer is attributed to the increased photooxidation initiated by a higher type I in this system than in the MVK system. This affect is even more marked for the tBVK copolymer where the rate is comparable to that of MVK, even though the molar concentration of ketone groups is only one-half as great.

The PVK copolymer blend shows a lower rate and less sensitization of degradation in the homopolymer. The PVK copolymer is known to have a low yield of type I reaction (6) and this supports the idea that the sensitization of photooxidation is due to free radical formation rather than more elaborate mechanisms such as via formation of singlet oxygen. It also appears that the hydrogen abstraction reaction of excited phenone groups (13) which is the basis of the use of benzophenone as a prodegradant in polystyrene (14), is not as important in this system.

The determination of quantum efficiency of the photochemical reactions has not been attempted because it is difficult to separate definitely the effects of the type I and type II reactions. However, on the assumption that the type II dominates in copolymer photolyses and that the type I dominates in the photolyses of blends, the results appear to be in accord with expectations based on the photochemistry of related simple molecules.

Acknowledgements

Literature Cited

1. Guillet, J. E., in "Polymers and Ecological Problems", J. Guillet, ed., Plenum Publishing Corp., New York, 1973.
2. Guillet, J. E. and Troth, H. G., U.S. Patent 3,860,538.
3. Guillet, J. E., U.S. Patent 3,753,953.
4. Guillet, J. E. and Norrish, R. G. W., Proc. Roy. Soc., (1955) A233, 153.
5. David, C., Demarteau, W. and Geuskens, G., Polymer, (1967) 8, 497.
6. Golemba, F. J. and Guillet, J. E., Macromolecules, (1972) 5, 212.
7. Kato, M. and Yoneshige, Y., Makromol. Chem., (1973) 164, 159.
8. Landau, E. F. and Irany, E. P., J. Org. Chem., (1947) 17, 422.
9. J. Colonge, Bull. Soc. Chim., (1936) 3, 2116.

10. Danusso, F. and Moraglio, G., J. Polym. Sci., (1957) <u>24</u>, 161

11. Golemba, F. J. and Guillet, J. E., Macromolecules, (1972) <u>5</u>, 63.

12. Nicol, C. H and Calvert, J. G., J. Amer. Chem. Soc., (1967) <u>89</u> 1790.

13. Turro, N. J., "Molecular Photochemistry", W. A. Benjamin, New York, 1965, Ch. 6.

14. Ohnishi, A., Japanese Patent 71 38,687.

21

Novel Additive System for Photodegrading Polymers

DONALD E. HUDGIN and THOMAS ZAWADZKI

Princeton Polymer Laboratories, Inc., Plainsboro, N.J. 08536

Introduction and History

Many organizations in the world have been con-
cerned with the problem of disposing of plastics which
have no further use. Particularly those plastics giv-
en intense consideration are the so-called disposable
products such as wrapping films, non-reuseable con-
tainers, 6-pack holders and drinking cups and lids.
Also of consideration is the area of agricultural
mulch films, which are designed to degrade at the
proper time for maximum crop yield.
A number of solutions have been forthcoming as
evidenced by the large number of publications and
patents concerned with methods for environmentally de-
grading polymers. In a publication of the Plastics
Technical Evaluation center at Picatinny Arsenal en-
titled "Environmentally Degradable Plastics: A Re-
view" and authored by Mrs. Joan Titus, much of the
past history up to about February 1973 has been cov-
ered. Also papers presented at the conference on
"Degradability of Polymers and Plastics" in London in
November, 1973 have summarized many of the fundamental
and practical aspects of polymer degradation.
By far the greatest volume of work has involved
photodegradation. Although biodegradable has become
a popular, overused and much misused word with plas-
tics, the experts know that very few plastic products
are truly biodegradable and certainly none of the so-
called commodity resins.
Several years ago, Princeton Polymer Labs. con-
tracted with a client to develop a degradable agri-
cultural mulch film. A first generation additive
system was developed and some 12,000 sq. ft. of poly-
ethylene film containing the additive was tried out in
14 states in the U.S.A. Both black and clear films

290

were used. The average time to break up was 11 days
for the clear film and 13.9 days for the black film.
A second generation, and far more effective photo-
degrading additive system was later developed and
extensive indoor and outdoor testing was done. With
such an effective system it was obvious that its use
could go much further than just agricultural mulch
films.
     It is well known that individually, photoinitia-
tors and certain metallic organic compounds cause
hydrocarbon polymers, such as polyethylene or poly-
styrene, to photodegrade faster than the original
polymer not containing such an additive. We have
discovered that by combining both types of additives
in a plastic a striking synergistic effect occurs.
Up to a 10 fold increase in the rate of degradation
has been observed.

Testing Method

     The standard film used for screening candidate
compounds was a 1.5 mil LDPE film sold by the Union
Carbide Corp. under the name "Zendel Polyethylene
Film." Several tests were carried out on the untreat-
ed film in the UV degradation apparatus and showed
this film to fail in 1100 hours. This was the control
to which all the treated films were compared.
     In order to screen candidates as rapidly as pos-
sible the following procedure was evolved:
     Plastic film (usually LDPE) 1" x 3" and 1.5 mils
thick was dipped into a solution of the candidate
compound or mixture of compounds in chloroform at 60°C
for 10 seconds.
     After dipping in the chloroform solution, the
film was dipped into fresh cold chloroform for 1 sec-
ond to wash off any residual material from the surface
of the film. The film was then allowed to dry in the
open air at ambient temperature for at least 15 min-
utes, after which it was mounted in clamps on a holder
as described under "Test Equipment."

Test Equpment (Figure 1)

     Samples of film (1 to 5 mils) and sheet (5-50
mils) were exposed by mounting a 1" x 3" specimen in
clamps on a holder so that it was suspended about 1/4"
above the surface. Each specimen thus mounted was
placed on an 18" diameter horizontal round turntable,
which was rotated at 16 rpm. Above the table at
approximately 11 inches were 4 General Electric RS

sunlamps. All of this equipment was housed in a metal
box approximately 21" wide, 21" deep and 24" high.
On opposite sides of the box at the turntable level
were two openings 17" wide by 7" high. A fan of ad-
justable speed was used to blow through the openings
to control the turntable temperature (37° + 2°C).

The light intensity was checked periodically to
make sure that it remained fairly constant. When a
drop in intensity was observed, new sunlamps were used
to replace the used lamps.

The specimens were periodically tested by apply-
ing pressure on the suspended film or sheet. A spec-
imen was considered to have failed when it broke on
application of a slight pressure (zero elongation).

The sunlamp exposures were also correlated with
tests in outdoor sunlight. During the months from
April through September an outdoor rack was used to
expose samples of polymer film and sheet. These sam-
ples were mounted in holders similar to those used for
sunlamp exposure as previously described. The rack
faced South and was set at a 45° angle to the horizon-
tal. Although outdoor sunlight intensity is·variable
depending on haze, clouds and rain, over a period of
time reasonably good correlation was obtained.

Individual Compounds Tested

Several hundred compounds were screened by the
test method described above and·from this the most
promising candidates were derived. These fell into
two classes: metallic organic compounds and photo-
chemical activators.

Examples of metallic organic compounds are listed
in Table 1 along with their times to failure. Like-
wise examples of photoactivators are listed in Table
2. The times to failure obviously vary widely and
since only selected samples were analyzed for the ac-
tual amounts of degrading agents present, the true
amounts incorporated in the polymer film are not
known in most cases.

Obviously the amount incorporated will vary with
the particular compound. Only by melt blending will
there be precise control of the amount incorporated
into the polymer. Nevertheless, for an initial
screening this method proved quite adequate, and it
was determined that once conditions were worked out,
the results proved to be quite reproducible.
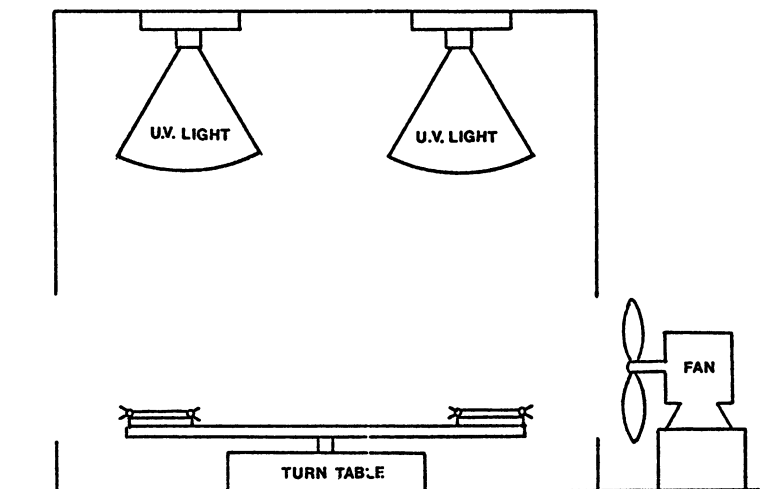
Figure 1.   Apparatus for polymer degradation

Table 1

Time to Failure of Polyethylene Film
Containing a metallic-organic compound

Metallic-Organic Compound	Time to Failure (hrs.)
Zirconium Neodecanoate	234
Cobalt Pentanedione	311
Ferric Pentanedione	141
Ferrous Dicyclopentadienyl	311
Ferrous Pentanedione	281
Titanium Pentanedione	94
Cobalt Dicyclopentadienyl	102
Vanadium Neodecanoate	448
Ferrous Stearate	115
Ferric Naphthenate	91
Control	1100

Table   2

Time to Failure of Polyethylene Film
Containing a Photoactivator Type Compound

Photoactivator	Time to Failure (Hrs.)
4-Chlorobenzophenone	214
Benzophenone	236
4-Methyl benzophenone	165
4, 4'-Dichlorobenzophenone	165
Phenyl benzoate	214
4-Methoxybenzophenone	207
Acetophenone	214
O-Dibenzoyl benzene	240
5-Chlorobenzotriazole	214
Benzil	109
4-Phenyl-2-pyridyl ketone	84

Combinations Tested

Although several of the organic-metallic compounds and the photoactivators showed good promise individually, it was felt that a more active system was desired. Selected mixtures were tried and amazingly and quite unexpectedly, a pronounced synergistic effect was discovered. One very good example is as follows:

Compound(s)	Time to Failure (hours)
Iron(+2)Pentanedione (A)	281
4-Chlorobenzophenone (B)	214
(A) + (B)	21

Thus the ability to degrade the LDPE has been increased ten fold over the single compounds.

Table 3 lists different combinations showing this remarkable synergistic effect. Some combinations gave better results than others, but since the amounts actually incorporated into the polymer was not known, in most of these examples the best synergistic effect was not always obtained.

Optimum Ratios and Amounts

All the previously reported tests were carried out using the same strength dip solutions. The strength of solutions was now varied to determine if the ratio of the two ingredients was important and how important. In a first attempt, zirconium neodecanoate was selected as the metallic organic compound and 4-chlorobenzophenone as the photoactivator. It was discovered the ratio was quite important as is shown in Figure 2. A minimum or shortest time to failure is clearly shown. Figure 2 shows an example in which the concentration of the additive, zirconium neodecanoate, is held constant while the second additive, 4-chlorobenzophenone, is varied.

Figure 3 shows the reverse of Figure 2, namely that the 4-chlorobenzophenone is held constant in solution concentration, while the zirconium neodecanoate is varied. Again as was shown on Figure 2, a minimum curve is shown, which shows that an optimum ratio is necessary to get the fastest degradation.

In Figure 4 the concentration of zirconium neodecanoate was plotted against the concentration of the 4-chlorobenzophenone and contour lines drawn for selected failure time using interpolation and

Table 3

Time to Failure of a Polyethylene Film Containing Both a Metallic-Organic Compound and a Photoactivator Type Compound

Metallic Organic Compound (A)	Photoactivator (B)	Time to Failure (hrs)		
		A	B	A + B
Zirconium Neodecanoate	4-chlorobenzophenone	234	214	142
Cobalt Pentanedione	4-chlorobenzophenone	311	214	85
Titanium Pentanedione	2-Phenylacetophenone	94	236	21
Cobalt Pentanedione	2-Phenylacetophenone	311	236	42
Ferrous Pentanedione	Benzophenone	281	236	42
Ferrous Pentanedione	Phenyl benzoate	281	214	49
Ferrous Pentanedione	Phenyl 2-pyridyl ketone	281	84	36
Ferrous Stearate	Benzophenone	115	236	98
Cobalt Pentanedione	4-chlorobenzophenone	311	214	85
Titanium Pentanedione	4-chlorobenzophenone	94	214	21
Ferric Naphthenate	4-chlorobenzophenone	91	214	49
Ferrous Neodecanoate	4-chlorobenzophenone	141	214	96
Ferrous Pentanedione	4-Methylbenzophenone	281	165	76
Ferrous Pentanedione	4-Bromobenzophenone	281	236	47
Ferrous Pentanedione	4,4'-Dichlorobenzophenone	281	165	47
Titanium Pentanedione	2-Phenylacetophenone	94	236	44
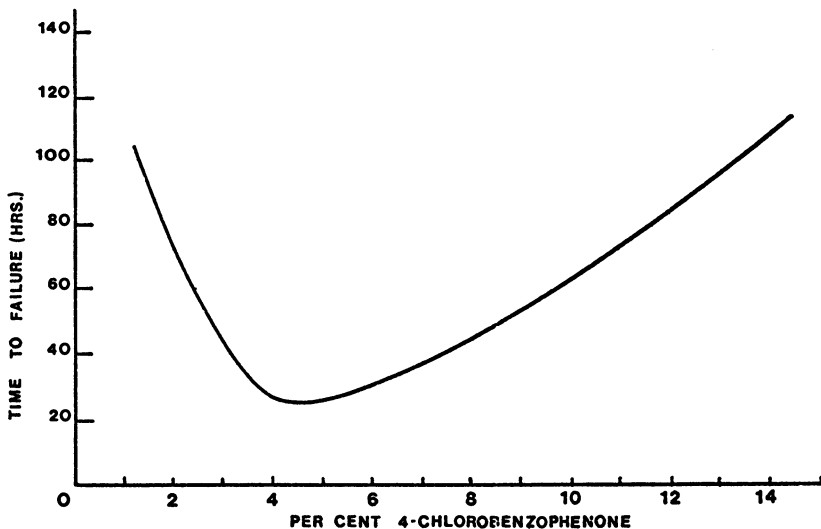
Figure 2. Chloroform dip solution contained plus 4-chlorobenzophenone as indicated
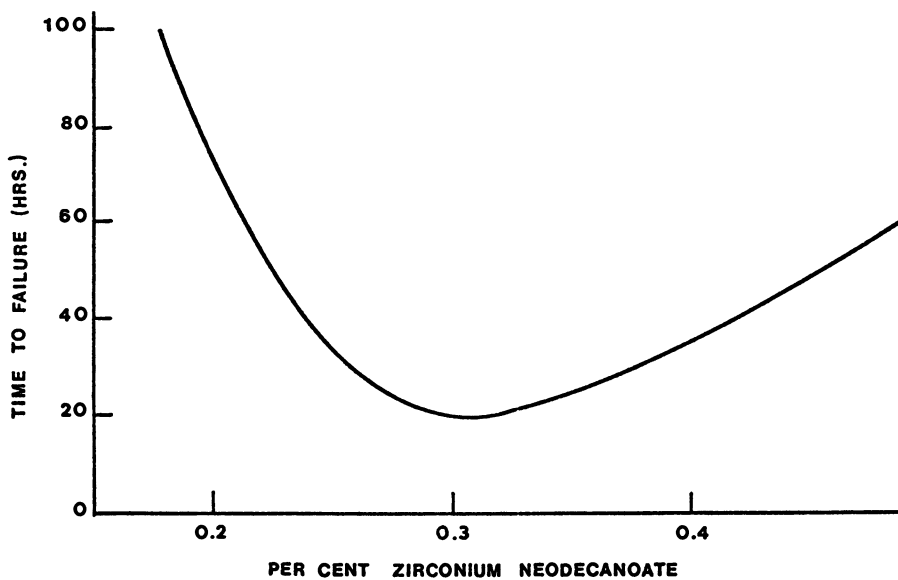
Figure 3. Chloroform dip solution contained 3.2% 4-chlorobenzophenone plus zirconium neodecanoate as indicated

extrapolation. This type of plot shows clearly the most effective area. Also this plot cannot only be useful in selecting the best ratio of ingredients for a desired failure time,but can be employed to determine the most economical combination of degrading additives.

Further evidence is shown in Figure 5 in which two levels of benzophenone are used as the concentration of ferrous stearate is varied. The two curves cross over rather abruptly. By the same token in Figure 6 the ferrous stearate is used at two levels while the benzophenone is varied.

A similar contour plot is shown in Figure 7 as was shown in Figure 4, except benzophenone and ferrous stearate are the two ingredients used. An idealized plot is shown in Figure 8. This plot illustrates the interactions between the two types of degrading additives and shows how these interactions can affect the rate of degradation as well as the economics. At point Z the most effective combination would be expected. If the ratio is held constant but the total amount of additive is decreased (going from Z toward 0) the time to failure increases as would be expected; however, if the total amount is increased (going from Z toward P) the time to failure also increases.

In a similar manner if Component B is held constant and Component A is increased (going from R to S), the time to failure decreases to a minimum, then rises. The same effect is observed by holding A constant and increasing B (going from X to Y).

Once a plot of this type is accurately established, it can be useful in determining the amounts of components A and B to bring about failure in the desired time at the lowest additive cost. For example, if component B is 10 times as expensive as component A and a 100 hr. failure time is desired, the least amount of component B to give a 100 hrs. failure time would be at point C. On the other hand if component A is 10 times as expensive as component B, the most economical combination will be at point D.

Analysis of Ingredients in Films

All of the work reported up to this point has left a big unknown and that is the actual amounts of compounds absorbed into the polymer were not known. Films were prepared using individual solutions of three metallic organic compounds and one photoactivator and the amount of compound determined for each film. The conditions for film preparation and the
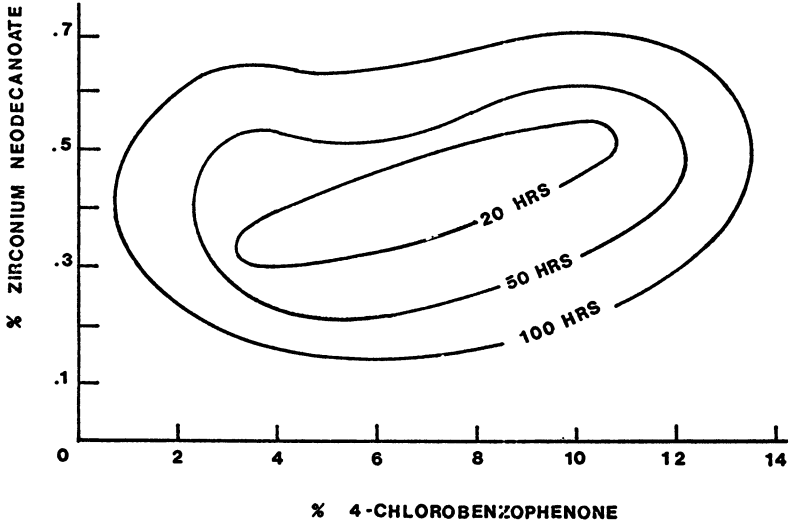
Figure 4.   Contour plot showing the time to failure
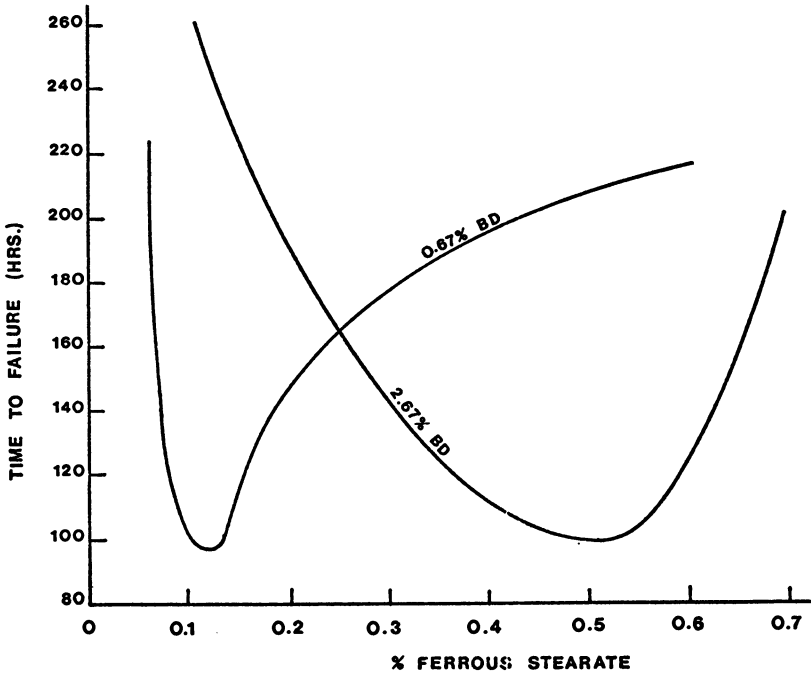
Figure 5.   Chloroform dip solutions contains amounts of compounds as indicated
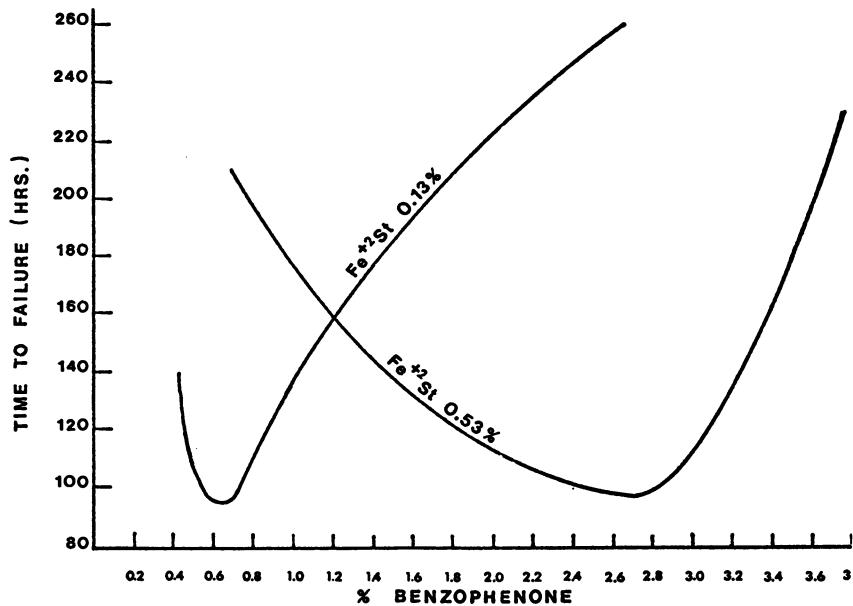
Figure 6.   Chloroform dip solutions contains amounts of compounds as indicated
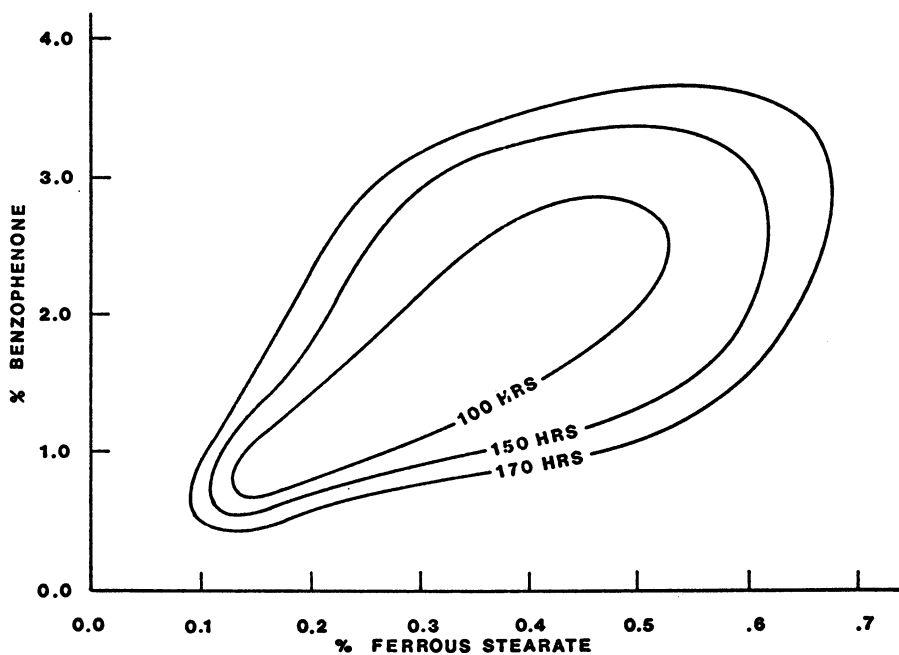
Figure 7.   Contour plot showing time to failure

analytical results are shown in Table 4. These results showed levels that offered a guide for the next step, which involved blending with precise amounts of ingredients.

Blending Studies

Two ingredients, zirconium neodeconoate and benzophenone, were blended into a low density film grade polyethylene as indicated on Table 5. The total amount of ingredients was kept at 100 mg. per kilogram of polyethylene on a roll mill at 325°F. The polyethylene was sheeted off the roll mill and a portion pressed between polished photographic plates in a press to give a 1 1/2 mil film. The films were exposed as described under Testing Method above and the time to failure recorded. The results are graphically shown on Figure 9. Thus, as with the solution dip studies, it has been emphatically shown that the ratio of the two types of ingredients is important for obtaining the maximum rate of degradation.

Comparison of Indoor and Outdoor Testing

The methods and procedure are described under Testing Method and Test Equipment. Ten film specimens were arbitrarily chosen for comparison of indoor and outdoor testing. Results are shown in Table 6. On an average the time to failure for indoor exposure was about one-third for outdoor exposure. This seemed to vary somewhat with the particular system used.

Types and Forms of Plastics Tested

A number of plastic types as well as forms were tested by the dip technique described earlier and exposed in the indoor UV testing equipment. The time to failure for the treated and untreated samples is shown in Table 7.

Continuing Research

Although the work reported in this paper has been concerned with combinations of two degrading additives, systems involving three or more additives are being investigated. Even faster rates than were obtained with dual system can be achieved. With three additives and using a typical ternary composition graph, contour lines can be plotted and the area of maximum effectiveness determined quickly. Princeton Polymer
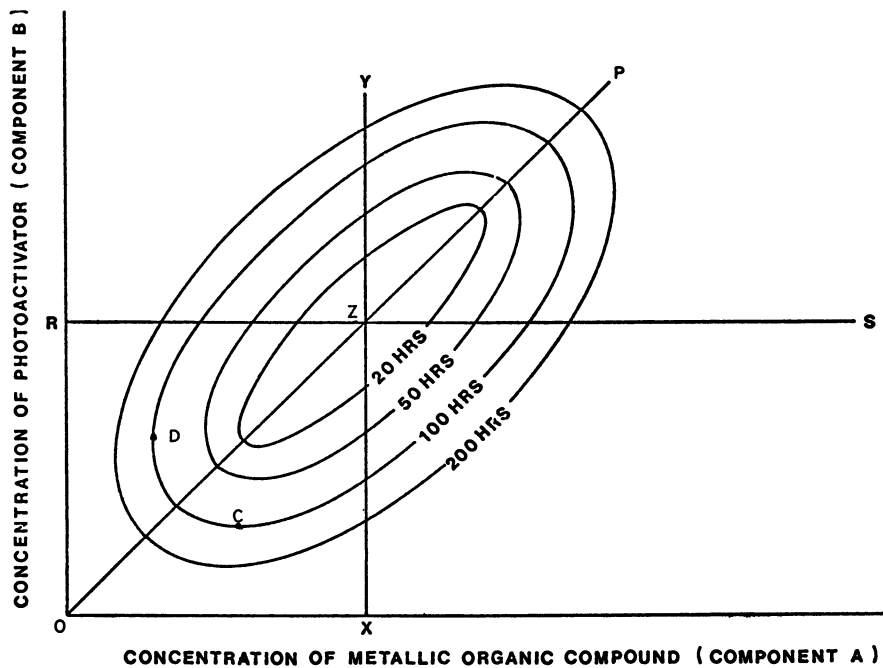
Figure 8.   Idealized graph showing failure times at various concentrations

Table   4

Analysis of Films

Compound in Film	Analytical Results
Cobalt Pentanedione	124 ppm Co
Ferrous Pentanedione	139 ppm Fe
Zirconium Neodecanoate	1000 ppm Zr
4-Chlorobenzophenone	140 ppm Cl

Table   5

Synergistic Effect

Mg. Benzophenone per Kg. Polyethylene	Mg. Zirconium Neodecanoate per Kg. Polyethylene	Time to Failure
0	100	242 hours
20	80	119 hours
40	60	46 hours
60	40	26 hours
80	20	106 hours
100	0	224 hours
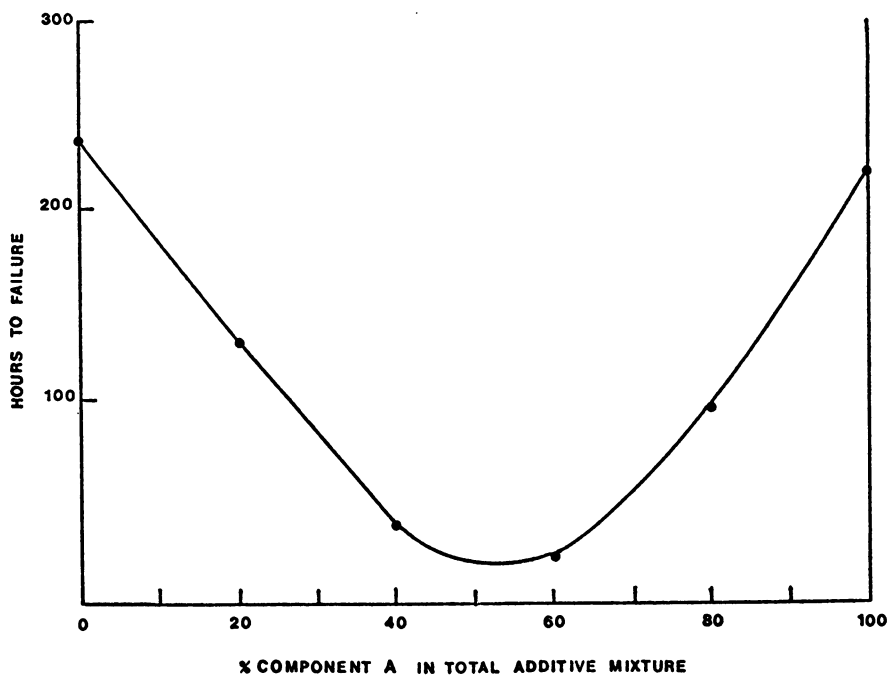
Figure 9.

Table 6

Comparison of Indoor and Outdoor Tests*

Sample	Days to Failure	
	Indoor	Outdoor
1	2	9
2	3	14
3	2	7
4	3	14
5	2	7
6	4	10
7	10	20
8	9	20
9	4	9
10	3	9
Total	42	119
Average	4	12

*Based on 24 hrs./day exposure to sunlamps (indoors) and 24 hrs./day sunlight and darkness (outdoors).

Table 7

Types and Forms of Plastics Tested

Polymer Type	Form	Time to Failure (Days)	
		Untreated	Treated
Polyethylene	Clear Film	45	1 to 4
(Low Density)	Black Film	45	2 to 5
	20 Mil Sheet	>90	21
	40 Mil Sheet	>100	10
Polyethylene	Bottle	>100	7
(High Density)	20 Mil Sheet	>100	20
Polyethylene	Bottle	>22	<22
(Medium Density)			
Polypropylene	Film	30	1
Polystyrene	Film (1 1/2 Mil)	>32	2
	Sheet (5 Mil)	13	<1
	Jar	>100	20
Polyvinyl Chloride	Sheet	>70	48
Methacrylonitrile-Styrene Copolymer	Bottle	>100	42
Polyethylene Terephthalate	Mylar Film (1 Mil) Mylar Film (2 Mil)	>100	>100
Polyamide (Nylon)	Sheet (10 Mil)	41	8
Polymethyl Methacrylate	Sheet (30 Mils)	>100	>100
Cellulose Acetate	Film (3 Mils)	22	3
Polyacetal	Film (2 Mils)	13	2
Acrylonitrile-Ethyl Acrylate Copolymer	Sheet (20 Mil)	>100	>100

Laboratories is not prepared to present data on this
work at this time, however, a paper covering this ex-
tended work might be given some time in the future.

Summary

Princeton Polymer Laboratories has discovered
that mixtures of a metallic organic compound and a
photoactivator produce a degradative effect in certain
polymers that may be as much as ten fold greater than
that produced by the individual compounds. The ratio
of the components, type of plastic and total amount of
additive are some of the important factors that affect
the time to failure. Because of this strong syner-
gistic effect, the amount of additive required is
quite small, thus resulting in a very low cost, which
has been estimated at less than 0.1 cent per pound of
finished plastic.

22

Sensitizers for Photodegradation Reactions

J. D. COONEY and D. M. WILES

Division of Chemistry, National Research Council of Canada, Ottawa, Canada K1A 0R9

Intensive research in the past eight years on sensitizers for the photodegradation of thermoplastics has led to the new concept of photodegradable plastics or Degradable Plastics. The term Degradable Plastics is commonly used to describe plastics which undergo more rapid than normal deterioration on exposure to unfiltered (although not necessarily direct) sunlight while maintaining long-term indoor stability. Owing to the action of outdoor weathering, Degradable Plastics disintegrate into tiny fragments and it is frequently claimed that these fragments are further degraded by micro-organisms (i.e., fungi, bacteria).

Realistic uses for Degradable Plastics include those applications where materials are used outdoors for a limited time only and it is not economically desirable to collect the residual materials after use. Examples are agricultural mulch, films and cordage, twine, etc. Another application is that of packaging which is stored and used indoors and discarded outdoors, in other words litter for which manual collection is not practicable.

Degradable Plastics are not inherently biodegradable but, for the most part, are slightly modified conventional resins which are intentionally made more sensitive to the erythemal (sunburn) region of the sun's spectrum. One common approach to the required modification involves the addition of a photosensitive additive, hopefully with just the right UV absorption spectrum and subsequent excited state reaction mechanisms to produce early embrittlement. The other approach involves the use of a copolymer where the conventional resin monomer is copolymerized with a small amount of another monomer containing

a functional group which absorbs UV radiation.
Ideally the light-sensitive groups absorb strongly in
that part of the sun's spectrum which passes through
the atmosphere but is not transmitted by window glass,
i.e., absorb in the region 290 to 320 nm. The use of
a masterbatch is possible with both approaches, and it
is claimed that there are no deleterious effects on
processing characteristics or on final physical
properties.
    This paper describes the effects of UV light, the
most significant aspect of outdoor weathering, on a
variety of Degradable Plastics and also discusses the
extent of biodegradability of the photodegraded
samples.

Examples of Degradable Plastics

    (a) Ecolyte Resins: EcoPlastics Ltd., Toronto,
Canada. Ecolyte resins ($\underline{1}$) are copolymers containing
a few per cent of vinyl ketone comonomer and are based
on the inventions of Professor James E. Guillet of the
University of Toronto. Quantum yield considerations
account for the efficacy of having the units
distributed randomly (and sparsely) in the backbone of
$\sim CR_1 \sim$ polymer chains. Plastics of both the addition
$\quad|$
$\quad C=O$ and condensation polymer types can be made
$\quad|$ suitably photosensitive in this way although
$\quad R_2$ polystyrene (Ecolyte PS), polyethylene (Ecolyte
PE) and polypropylene (Ecolyte PP) are the first to be
developed. Controlled outdoor lifetimes over a very
wide range of time periods (days to months) are
possible with apparent long term stability indoors.
The persistence of outdoor mechanical integrity
depends on the concentration of the ketone comonomer
and its specific structure, e.g., the nature of R_1 and
R_2. The time-to-embrittlement of Ecolyte PS and PE in
our Weather-Ometer exposures are listed in Tables I
and II.

    (b) Sty-Grade: Bio-Degradable Plastics, Inc.,
Boise, Idaho ($\underline{2}$). The approach in this case is the
incorporation of a photosensitive additive with
conventional resin, e.g., benzophenone blended with
polystyrene. The rate of degradation outdoors can be
varied by changing the amount of additive used,
although there is expected to be an upper limit beyond
which sensitivity to artificial light becomes a
problem. Benzophenone has been given FDA approval for
certain packaging end-uses. Time-to-embrittlement

TABLE I

Embrittlement Times of Degradable Polystyrenes[a]

Samples	Time to Embrittlement	
	Xe Arc (hr)	Outdoors (months)
Ecolyte "Fast" foam, 2800μ	275[b]	1.0
Ecolyte "Fast" foam, "	70[b]	-
Ecolyte "Slow" foam, 2000μ	2400[c]	>6.5
Ecolyte "Slow" foam, "	600[c]	-
Ecolyte "Fast" film	23	-
Ecolyte "Slow" film	55	-
Sty-Grade resin conc. film	6	-
Sty-Grade resin conc. let-down 5:1 film	22	-
Der Wienerschitzel coffee cup lid, a Sty-Grade product, resin conc. let-down 50:1	112	-
Control, Styron 666 film	495	-

[a]Foams are expected to be slower than films owing to thickness and opacity. The UV-degradable formulations listed here are not necessarily those which are to be used in commercial products. In addition, comparison of embrittlement times is not intended to relate to the relative merits of the various materials.

[b]Irradiated 35 hr on each side.

[c]Turned over every 24 hr.

TABLE II

Embrittlement Times of Degradable Polyolefin Films

| Samples | Time to Embrittlement | | Time to 1/10 of %E |
	Xe Arc (hr)	Outdoors (months)	Xe Arc (hr)
Control LDPE, Dupont, 110μ	1175	6.5	400
Ecoten LDPE, 51μ	2210	~11	490
Bio-Degradable Plastics Inc., LDPE, 42μ	750	4.0	215
ENDE-plast LDPE with FAM-1, Akerlund and Rausing, 58μ	1550	>4.5	375
Ecolyte #1 LDPE, EcoPlastics Ltd., 53μ	820	2.5	85
Ecolyte #2 LDPE, EcoPlastics Ltd., 63μ	1180	>4.5	230
Ecolyte #3 LDPE, EcoPlastics Ltd., 61μ	1465	–	315
Control LDPE, EcoPlastics Ltd., 64μ	2075	–	480
Control LDPE, 12μ	1820	>18	–

data for samples of this type of product are shown in
Tables I and II.

   (c) <u>Ecoten.</u>   The approach used by Professor
Gerald Scott (University of Aston, Birmingham, U.K.)
involves the use of multiple additives such as ferric
dibutyldithiocarbamate [Fe(III) DBC] or ferric stearate,
possibly with a cobalt, copper, chromium, manganese or
cerium salt.   This type of system which provides
stability during the processing and initial UV
exposure periods, has been used in polyolefins and
polystyrene, for example.   After an induction period,
Fe(III) DBC oxidizes and decomposes giving products
that catalyze the photodegradation of the polymer.   It
has been noted (<u>3</u>) that, although iron dialkyldithio-
carbamates represent delayed action UV activator
additives, sulfur-containing ligands are not essential.
Advantages claimed in addition to the induction period
are the small quantity of additive required [0.01 to
0.05% Fe(III) DBC] and the continuing oxidative
degradation in the dark following initial photo-
oxidation (during which the additive is changed from
stabilizer to pro-degradant).   It appears to be
necessary, however, to select an additive level which
is in a fairly narrow range for minimum embrittlement
time.   The performance of an Ecoten low-density
polyethylene sample in our Weather-Ometer exposure is
shown in Table II.
   The products described above were selected in
order to illustrate some of the principles associated
with the enhancement of sunlight sensitivity.   There
are, in addition, other examples (<u>2</u>) of the copolymer
approach, e.g., ethylene/carbon monoxide, and the
additive approach.

   (d) <u>Experimental Modification of Conventional
Plastic Films.</u>   We have examined numerous modification
procedures potentially capable of reducing the
embrittlement time of commercial plastic films (mainly
the polyolefins).   Partial thermal oxidation, corona
discharge in different environments, ozone treatment
and γ-irradiation were some of the procedures that
proved to be impractical.   The main effort then was to
find an additive that would make low-density poly-
ethylene a photodegradable plastic.   A few of the
additives employed were titanium dioxide, benzophenone,
4-nitrobenzophenone, 4-hydroxybenzophenone,
4-(β-hydroxyethoxy)benzophenone, anthraquinone,
anthrone, benzanthrone, xanthone, deoxybenzoin,

α-bromo-p-phenylacetophenone, (2-benzoylvinyl) ferro-
cene, ferrocenecarboxyaldehyde, and 1,1'-dibenzoylfer-
rocene. The data are summarized in Tables III, IV and
V.

Experimental

Outdoor exposures were conducted in the summers
of 1972-74 at a 45° angle facing south, latitude 45° N
in Ottawa, Canada.
A 6000W xenon arc Atlas Weather-Ometer (4)
equipped with Corning No. 7740 borosilicate inner and
outer filters was used as a laboratory light source
because its emission spectrum is similar to that of
sunlight, as illustrated in Fig. 1. The Weather-
Ometer was operated with the lamp on continuously and
the exposure chamber was maintained at a black panel
temperature of 145±5°F and a relative humidity of
30±5%.
Polymer embrittlement was determined by 180° fold
and/or pencil puncture tests. Elongation in the
transverse direction of the LDPE samples was measured
on an Instron TT-C tensile tester at 70°F and 65%
relative humidity. The time to break was 25-50 sec.
for 2 mm strips utilizing a gauge length of 0.5" and
jaw-type clamps.
The laboratory treatments listed in Tables III,
IV and V were performed by soaking the films in
solutions containing 1.0g of potential photosensitizer
in 250 ml of methylene chloride or ethanol for 3 days
at 22°C. The TiO_2 treatments, however, involved a
$TiCl_4(g)$ in N_2 treatment followed by a H_2O soak for
conversion to TiO_2.

Discussion

Degradable Polystyrenes. The Ecolyte "Fast"
polystyrene foam has a higher concentration of photo-
sensitive vinyl ketone comonomer than the Ecolyte
"Slow" foam and as a result has a shorter irradiation
time to embrittlement as listed in Table I. The
"Fast" foam was brittle after one month outdoor ex-
posure or 275 hr xenon arc irradiation. The outdoor
exposure was facilitated by wind and rain erosion.
Turning the sample over after 35 hr xenon irradiation
lowered the embrittlement time to a remarkably short
period of 70 hr considering the thickness and opacity
of the foam. Similarly the "Slow" foam had its xenon
embrittlement time reduced from 2400 hr to only 600
hr by turning the foam over after each 24 hr irradi-
ation period. To obtain a better idea of the rate of

TABLE III

Embrittlement times of Low-Density Polyethylene Films

Treatments	Hours to Embrittlement
LDPE, 110μ, control	1520
LDPE + TiO$_2$ (2.0%)	330
LDPE, 100μ, control	1350
LDPE + 1,1'-dibenzoylferrocene (1.3%)	288
LDPE + benzophenone (10%)	660
LDPE, 110μ, control	1225
LDPE + ferric dibutyldithiocarbamate	825
LDPE + 2-methylanthraquinone	920
LDPE + 1,3,5-triacetylbenzene	920
LDPE + 9-fluorenone	1030
LDPE + flavone	1030
LDPE + 4-chromanone	1030
LDPE + dibenzanthrone	1030
LDPE + carbazole	1030
LDPE + benzophenone	1030

TABLE IV

Embrittlement Times of High-Density Polyethylene Films

Treatments	Hours to Embrittlement
HDPE, 23μ, control	925
HDPE + TiO$_2$ (2.3%)	64
HDPE + anthraquinone	385
HDPE + anthrone	420
HDPE + benzanthrone	420
HDPE + 2-methylanthraquinone	450
HDPE + 1,3,5-triacetylbenzene	450
HDPE + α-bromo-p-phenylacetophenone	475
HDPE + 9-fluorenone-4-carboxylic acid	575
HDPE + flavone	650

photo-oxidation, films were prepared from the foams.
Films cast from CCl₄ solutions of the "Fast" and "Slow"
foams embrittled in 23 and 55 hr xenon irradiation,
respectively, whereas the control polystyrene film
required 495 hr irradiation to produce embrittlement.
The photosensitive vinyl ketone comonomer concentration
can be varied to control the lifetime of the Degrad-
able polystyrene to suit the desired use.

Bio-Degradable Plastics Inc. recommend that their
Sty-Grade resin concentrate be let-down 10:1 or 20:1
for use in formulating a Degradable polystyrene (2).
A film produced by employing the resin concentrate
let-down 5:1 embrittled in 22 hr while a commercial
product believed to be let-down 50:1 (5) embrittled
with a 112 hr xenon irradiation. A film of the resin
concentrate embrittled in 6 hr; therefore, variation
of the let-down ratio can control and vary the lifetime
of the polystyrene during outdoor use.

Degradable Low-Density Polyethylene (LDPE) Films.
Typical xenon arc embrittlement times for unstabilized
low-density polyethylene are 1600-2400 hrs. The con-
trols chosen for this research are listed in Table II;
the thin LDPE garment bag embrittled in 1820 hr and the
EcoPlastics LDPE control became brittle after 2075 hr
xenon irradiation. The thin garment bag was not
brittle, as determined by a fold test, after 18 months
outdoor exposure. The Dupont "Sclair" LDPE control
listed in Table II was unusual since it had short
embrittlement times of 1175 hr in the Weather-Ometer
and 6.5 months outdoors. This film was used as a
yardstick to measure the Degradable LDPE films since
a Degradable Plastic should not last more than 6
months, perhaps less, outdoors and ≤1200 hr in the
xenon arc Weather-Ometer.

Ecoten LDPE embrittled in 2210 hrs in the Weather-
Ometer and ~11 months outdoors. This sample of Ecoten
does not appear to be a satisfactory Degradable Plastic
because of the high level of TiO₂ added to the film.
Clear Ecoten film without the titanium dioxide pigment
was tested outdoors in Israel as agricultural mulch
and found to embrittle in less than four months (6).

Bio-Degradable Plastics Inc. brown LDPE film was
brittle in 750 hr xenon irradiation and four months
outdoors. This lifetime could presumably be decreased
or increased by changing the masterbatch ratio.

ENDE-plast LDPE with fortified "additive mixture
one" (FAM-1) is marketed as a Degradable Plastic by
Akerlund and Rausing in Sweden. A clear film of ENDE-
plast was brittle in 1550 hr xenon irradiation and
>4.5 months outdoors and appears to have a longer

lifetime than warranted for most uses of Degradable
Plastics. This lifetime presumably can be decreased
by lowering the masterbatch let-down ratio.

The Ecolyte LDPE films are numbered in relation
to the concentration of photosensitive vinyl ketone
comonomer present in the polymer ie. 1>>2>3. The
Ecolyte #1 LDPE containing the most vinyl ketone co-
monomer was brittle in 820 hr in the Weather-Ometer
and 2.5 months outdoors. The Ecolyte #2 was brittle
in 1180 hr and the Ecolyte #3 required 1465 hr while
the EcoPlastics Ltd. LDPE control required 2075 hr
xenon arc irradiation to reach embrittlement. This
series of Ecolytes demonstrates the varied and con-
trolled lifetimes that can be designed into Degrad-
able Plastics by controlling concentration of the
photosensitizer.

The discrepancy between xenon arc and outdoor
weathering data for the Bio-Degradable Plastics Inc.
LDPE and the Ecolyte #1 LDPE most likely occurs be-
cause the xenon arc lamp was operated with an UV en-
ergy slightly below, rather than slightly above, that
of noon summer sunlight as depicted in Fig. 1. The
lower xenon arc output would greatly reduce the energy
in the 285-315 nm region where the Ecolyte #1 absorbs
radiation but would not have as great an effect in
the 315-340 nm region where Bio-Degradable Plastics
Inc. LDPE appears to absorb radiation.

In a second experiment the functional lifetime of
the Degradable LDPE Plastics was examined. The func-
tional lifetime was defined as the xenon arc irradia-
tion time required to reduce the percent elongation
at break by 9/10. These values listed in Table II
are determined from the elongation as a function of
irradiation time curves in Figs. 2 and 3. The order
of increasing time by which films reach 10% of their
original elongation is quite similar to the order of
embrittlement times. Thus, the former can be used as
a convenient indicator of relative susceptibility to
brittleness.

A few of the photosensitive additives that we
have tried are listed in Table III, IV and V. Table
III has the hours of xenon arc irradiation to em-
brittlement of treated low-density polyethylene,
Table IV contains results for treated high-density
polyethylene while Table V contains results for
treated polypropylene films. It should be noted that
these additives were designed to increase the number
of chromophores on and near the film surfaces. In
principle the "optimal" concentration of the "right"
chromophores should enhance the absorption of light

TABLE V

Embrittlement Times of Polypropylene Films

Treatments	Hours to Embrittlement
PP, 27μ, control	240
PP + TiO₂ (5.9%)	16
PP, acetone extr.	155
PP, acetone extr. + anthraquinone	50
PP, acetone extr. + anthrone	65
PP, acetone extr. + α-bromo-p-phenyl-acetophenone	65
PP, acetone extr. + xanthone	75
PP, acetone extr. + 1,1'dibenzoyl-ferrocene (0.2%)	85
PP, acetone extr. + 2-methylanthra-quinone	<90
PP, acetone extr. + 1,3,5-triacetyl-benzene	<90
PP, acetone extr. + benzophenone (0.7%)	90
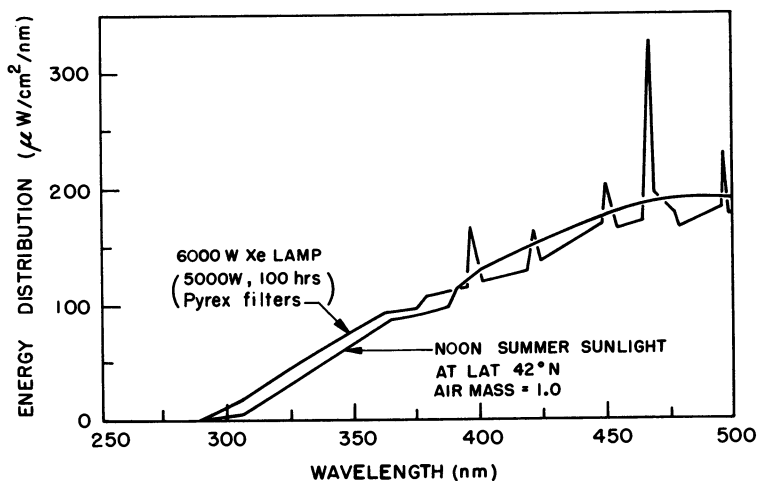
Atlas Fade-Ometer and Weather-Ometer Bulletin #1300

Figure 1. Energy distribution, as a function of wavelength, of a high pressure xenon arc lamp and noon summer sunlight (4)
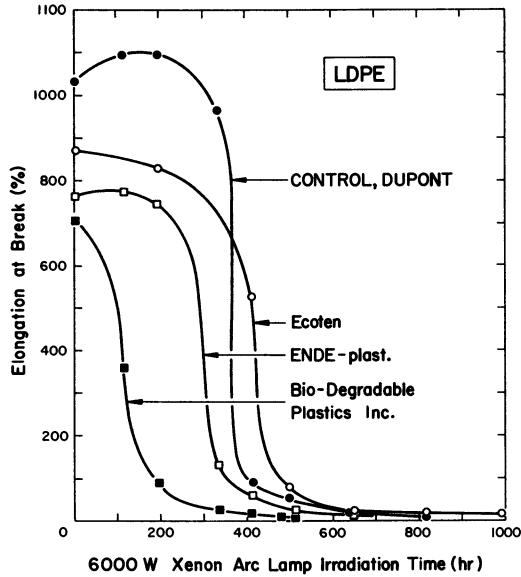
Figure 2. Elongation at break of degradable
LDPE plastics as a function of xenon arc lamp irra-
diation time
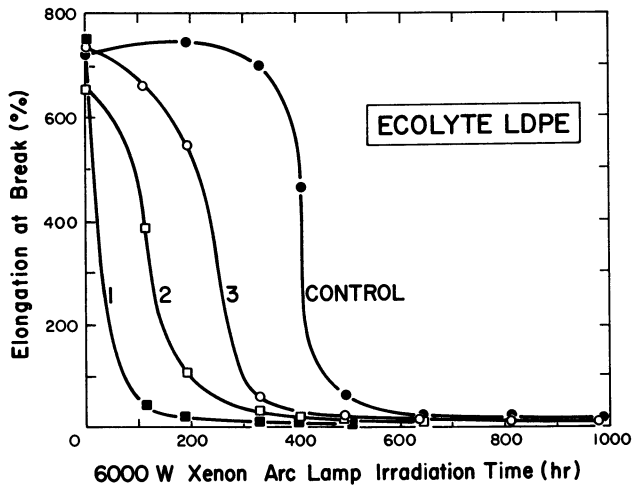
Figure 3. Elongation at break of Ecolyte LDPE degradable
plastics as a function of xenon arc lamp irradiation time

in the 290 to 320 nm region without significantly in-
creasing the absorption at longer wavelenths. Of the
approaches reported here, the titanium dioxide and
1,1'-dibenzoylferrocene additives seem promising for
LDPE while titanium dioxide, anthraquinone, anthrone,
benzanthrone, 2-methylanthraquinone and 1,3,5-tri-
acetylbenzene are promising for HDPE, but not ne-
cessarily of commercial interest.

       It is also thought that some of the additives we
used might, in addition to having the desired photo-
chemical effects, exhibit some propensity to enhance
polymer chain re-structuring during photodegradation.
Such an action (crystallization or crosslinking) could
increase the brittleness of a film for a given extent
of photo-oxidative change. There is no evidence that
this occurred.

Biodegradability

       It is a fact that actinic deterioration of
Degradable Plastic films will, in due course, lead to
the crumbling of them into fine particles. Such dis-
integration obviates the plastics litter problem and
provides the possibility of a solution to the agri-
cultural plastics residue situation. There is evi-
dence in this paper and elsewhere (2) that there are
commercially viable formulations with which packaging
(and related) plastics can be made to have controlled,
short embrittlement times outdoors but no indoor
stability problems.

       Arguments can be made to the effect that the
actinic deterioration of common plastics might make
these plastics more likely to support the growth of
micro-organisms. The reasoning has to do with shorter
polymer chains, more polar groups including end groups
and reduced hydrophobicity in the photodegraded
material, although there is good evidence (7) that
some of these factors do not enhance biodegradability.
We have shown (8) that UV-degraded commercial films
do not support surface fungal growth in specific
tests (e.g., ASTM G 21-70), and similar research (9)
indicates that the same is true for photo-oxidized
samples of the Degradable Plastics described above.

       It is possible, nevertheless, to rationalize the
apparent discrepancy between these data and the claims
that photodegraded Ecolyte (1), and Ecoten (3) and
Sty-Grade (2,10) plastics do biodegrade. In the
surface growing fungal tests, the spores from a
limited number of fungi are used even though it is
not known which fungi are likely to produce enzymes

which can degrade synthetic polymers. A 2 or 4 week
incubation period is not long enough to detect sig-
nificant microbial deterioration except in the case
of inherently biodegradable materials. Since all of
the tens of thousands of species of micro-organisms
are actually or potentially present in any bit of soil
and since synergism among these micro-flora is pro-
bable, it makes sense to use some sort of soil as a
source of microbial activity instead of the spores
from a few fungi. Relevant respiration experiments
involving the measurement of oxygen consumed and/or
carbon dioxide produced have shown that weathered
Degradable Plastics (Ecolytes (11) and Akerlund and
Rausing ENDE-plast LDPE (12)) are utilized as carbon
sources by micro-organisms. As one might expect, the
projected time scale for complete biodegradation is
probably decades, not days. It is reasonable to
assume that the effects of weathering on conventional
plastics are the same (chemically and physically) as
for Degradable Plastics; of course, much longer ex-
posures are required for the former to reach the same
stage of actinic deterioration. Thus, it could be
concluded that conventional plastics (PE, PP and PS)
may also become microbially susceptible after exten-
sive outdoor weathering.

Literature Cited

1. Guillet, J.E., "Polymers and Ecological Problems",
    Polym. Sci. Technol. (1973) 3, 1-25, ed. J.E.
    Guillet, Plenum Press, N.Y.
2. Baum, B. and Deanin, R.D., Polym. Plast. Technol.
    Eng. (1973) 2, 1-28.
3. Scott, G., ref. 1, pp. 27-44.
4. Atlas Fade-Ometer and Weather-Ometer Bulletin No.
    1300, Atlas Electric Devices Co., Chicago, 1971.
5. Chem. Eng. News, (1972) (June 19) 32.
6. Scott, G., Degradability of Polymers and Plastics
    Conference, paper #6, The Plastics Institute,
    London, U.K., Nov. 27-8, 1973.
7. Potts, J.E., Clendinning, R.A., Ackart, W.B. and
    Niegisch, W.D., ref. 2, pp. 61-79.
8. Cooney, J.D., Colin, G. and Wiles, D.M., "Disposal
    of Plastics with Minimum Environmental Impact",
    ASTM Special Technical Publication 533, pp. 17-27,
    1973.
9. Cooney, J.D. and Wiles, D.M., Society of Plastics
    Engineers 32nd Annual Technical Conference, San
    Francisco, pp. 420-422, May 13-16, 1974.

10.   Mortillaro, L., Mater. Plast. Elastomeri, (1972),
      38, 210-215.
11.   Guillet, J.E., Degradability of Polymers and
      Plastics Conference, paper #4, The Plastics
      Institute, London, U.K., Nov. 27-8, 1973.
12.   Nykvist, N.B. ibid. paper #18; Polym. Age (1974)
      5,6.

NRCC No. 14563

Effects of UV Light on the Chemical and Mechanical Properties of Fiber Forming Polymers

D. J. CARLSSON and D. M. WILES

Division of Chemistry, National Research Council of Canada,
Ottawa, Canada, K1A 0R9

I. Introduction

The aesthetic and mechanical properties of all polymers deteriorate upon exposure to terrestrial sunlight, that is UV and visible light of wavelengths $\geq$290 nm (Figure 1). The degree of susceptibility to sunlight varies enormously amongst the polymers in current commercial use. For example poly(methyl methacrylate), and poly(vinyl fluoride) are extremely stable (>5 years outdoors), poly(ethylene terephthalate) and poly(hexamethylene adipamide) are intermediate (2-3 years outdoors), whereas poly(propylene), and poly(1,3-phenylene isophthalamide) are very sensitive to sunlight exposure ($\leq$ one year) (1). Sunlight resistance also varies with physical properties such as crystallinity, orientation, applied stress, etc. for a given polymer, and resistance can be greatly improved by the use of UV stabilizers in several cases (2).
In this paper the light initiated failure of materials belonging to three different generic groups of fiber forming polymers will be discussed. The polymers are poly(propylene), PP, poly(ethylene terephthalate), PET and poly(1,3-phenylene isophthalamide), PmPiPA. PP represents a low cost material widely used in carpeting, upholstery, cordage etc., PET is extensively used in clothing and PmPiPA is a more costly specialty material restricted to applications requiring non flammability coupled with low smoke emission or good resistance to prolonged high temperature exposure (200°C and above). In this discussion of polymer photodegradation, the key initiation reactions, and oxygen dependent processes will be compared with the emphasis

on the rôle that these reactions play in the deterior-
ation of the mechanical properties of the three
polymers. The work described has employed near UV
and visible radiation which approximates sunlight.

II. Initiation of Degradation

From an inspection of the UV absorption curves
and the spectrum of terrestrial sunlight (Figure 1)
it is obvious that PET and PmPiPA strongly absorb
part of the shortwave UV component of sunlight. Pure
PP on the other hand does not itself absorb beyond
~190 nm, so that it should be extremely UV stable.
In practise there are several types of impurities in
commercial PP which can absorb above 290 nm.
Important initiating chromophores include carbonyl
and hydroperoxide groups (from oxidations during
polymerization and extrusion, and O_3 or singlet
oxygen, $^1\Delta_g$ attack) and residues from the polymeriza-
tion catalyst (Ti and possibly also Al compounds)
(3). All of these chromophores absorb beyond 290 nm,
but are present in PP at low concentrations ($<5 \times 10^{-3}$M
for >C=O and -OOH, $\leq 1 \times 10^{-3}$M for Ti). The key photo-
initiation process in a given PP sample will depend
on production and processing conditions as well as
the subsequent history of the article (3).
The important primary processes expected to
result from the absorption of near UV by the three
polymers are listed in Table I. Also shown are the
estimated absorptions due to chromophores and the
efficiencies of the primary photolysis processes.
Efficiencies are expressed as quantum yields for the
formation of certain primary products, and are
collected from published values (4, 5, 6, 7). The
cited quantum yields for PET product formation have
been recalculated from previously published data (6).
Both PP macro-ketones and hydroperoxides photo-
cleave to give free radicals in the polymer (4, 5)
(Table I). These cleavage processes are relatively
efficient but very infrequent because of the low UV
absorptions of these initiaters and their low con-
centrations in the undegraded polymer.
The primary processes in PET probably involve
scission of the C(=O)-O backbone link, a Norrish Type I
cleavage (reaction II, Table I) and an intramolecular
H-abstraction, a Norrish Type II process (reaction
III, Table I) (6). Carboxylic acid formation in

TABLE I Photodegradation Mechanisms

	Photo-initiation Process	Absorp. %a	φb	Oxidation Steps	Main Backbone Scission Step
PP	$>C=O^c$ —hν→ $R\cdot + R'\cdot + CO$	$<5 \times 10^{-6}$	0.07 (CO)	$PP\cdot + O_2$ → $PPO_2\cdot$	$CH_3-\overset{\cdot}{C}-\overset{\cdot\cdot}{O}$ ... I
	$CH_3\overset{}{C}-OOH$ —hν,d→ $CH_3\overset{}{C}-O\cdot$ $+\cdot OH$	$<1 \times 10^{-5}$	~3.0 (HO·)	$PPO_2\cdot + PPH$→$PP\cdot +$ PPOOH	$\sim C-CH_3$ ... $C=O$
PET	$O=C-O-CH\sim$ —e,hν→ II: $\sim\phi\cdot + CO +\cdot OCH_2\sim$; III: $\sim\phi COOH +CH_2=CH\sim$	100	1×10^{-4} (CO); 2×10^{-4} (COOH)	II PET R·→ $\sim\phi COO\overset{H}{\overset{\vert}{C}}CH_2\sim$ —$O_2,R'H$→ $\sim\phi COO\overset{H}{\overset{\vert}{C}}-CH_2\sim + R'\cdot$; $\sim\phi COO\overset{H}{\overset{\vert}{C}}-CH_2\sim$ OOH	$\sim\phi C-O-C-CH_2\sim$ —→ II, III and IV ; $\sim\phi COO\cdot +$ $H-C\sim$ $=O$
PmPiPA	$\sim\phi CONH\phi\sim$ —hν,f,V→ $\sim\phi\overset{\cdot}{C}O+$ $\cdot NH\phi\sim$	100	1×10^{-6} (CO); 3×10^{-7} (Fries)	$\sim\phi\overset{\cdot}{C}O+\cdot NH\phi\sim$ —O_2→ ... $\overset{O=}{\underset{\phi C}{}}-OON\phi$ —hν,VI→ $\sim\phi COOH+ON\phi\sim$	V and VI

a) Absorption at 300 nm for 10μ of commercial polymer
b) In m.einst^{-1}, for primary product in parentheses.
c) Initially $<1\times 10^{-3}$M. d) Initially $<5\times 10^{-3}$M. e) Initially ~15M. f) Initially ~12M

irradiated PET has been measured by IR spectroscopy (at 3290 cm^{-1}) and by non-aqueous titration on soluble samples (6).

PmPiPA probably undergoes photo-cleavage at the C(=O)-NH bond to give a caged radical pair. Some CO elimination from ~φ-ĊO (reaction 1) occurs before the radicals recombine. Radical combination can reform the original amide link, or produce 2-aminobenzophenone backbone units - a Photo-Fries rearrangement (reaction 2) (7). These 2-aminobenzophenone groups have been detected by their characteristic emission

$$\sim\!C(=O)\!-\!\langle \rangle\cdot \; + \; CO \qquad\qquad (1)$$

$$\sim\!C(=O)\!-\!\langle \rangle\!-\!C(=O)\!-\!N(H)\!-\!\langle \rangle\!-\!N(H)\sim \;\xrightarrow{h\upsilon}\; \sim\!C(=O)\!-\!\langle \rangle\!-\!\dot{C}(=O) \;+\; \cdot ON(H)\!-\!\langle \rangle\!-\!N(H)\sim$$

$$\sim\!C(=O)\!-\!\langle \rangle\!-\!C(=O)\!-\!\langle \rangle(NH_2)\!-\!N(H)\sim \qquad\qquad (2)$$
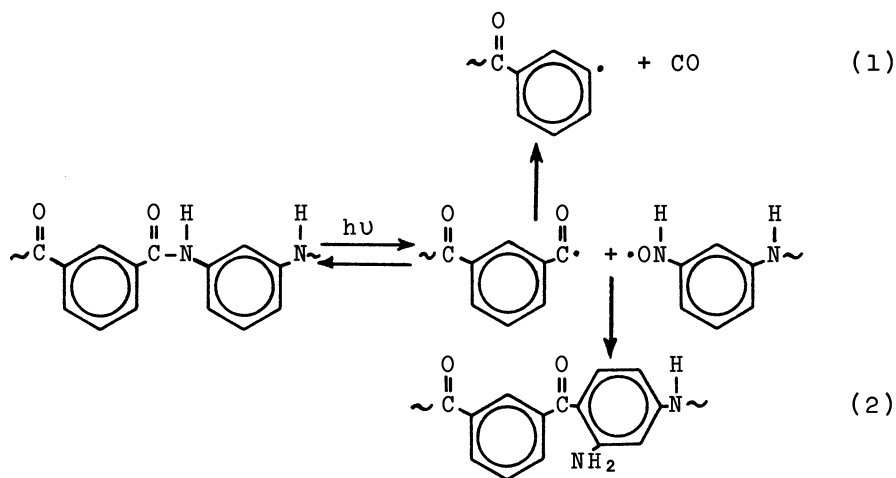
spectra (460 nm emission from ~410 nm excitation in PmPiPA) in PmPiPA films which had been irradiated in the absence of O$_2$.

From the quantum yield data in Table I and the extent of sunlight absorption by each polymer (Table I and Figure 1) it is apparent that although PET and PmPiPA absorb strongly, they have very low quantum yields for their primary reactions. PP on the other hand absorbs weakly due to low concentrations of chromophores but these chromophores give radical products by efficient processes. In addition photo-oxidation leads to a rapid build up of additional UV absorbing -OOH groups (discussed in Section III).

III. Oxygen Reactions

Oxygen can permeate amorphous regions in
polymers and intercept some of the radicals produced
in the photo-initiation steps (4, 5, 6, 8) (Table I).
In PP no more than one in six of the photo-initiation
steps can be expected to result in a free tert.-
peroxy radical (PPO$_2$. reaction 3); the remainder of
the initiation steps

$$PP \xrightarrow[\text{etc}]{\cdot OH, R\cdot} \sim CH_2-\overset{CH_3}{\underset{\cdot}{C}}-CH_2\sim \xrightarrow{O_2} \sim CH_2-\overset{CH_3}{\underset{\underset{O\cdot}{O}}{C}}-CH_2\sim \quad (PPO_2\cdot)(3)$$
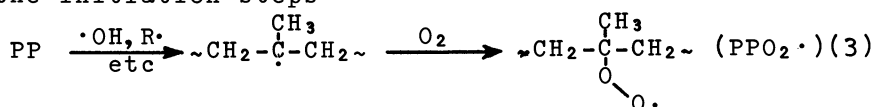
yield radical pairs which terminate in the cage (9).
The free peroxy radical (PPO$_2$·) can propagate intra-
molecularlly by hydrogen abstraction from a neigh-
boring tert-C-H site on the same backbone (reaction
4) or undergo an intermolecular tert-H- abstraction
(reaction 5) with intramolecular attack being
favored roughly thirteen fold over the intermolecular
process (10). Up to 100 propagations can then occur
before termination with another peroxy radical (9).
The overall result of a photo-initiation step is then
the generation of up to roughly 30 fresh -OOH groups,

$$\sim CH_2-\overset{CH_3}{\underset{\underset{OH}{O}}{C}}-CH_2-\overset{CH_3}{\underset{\cdot}{C}}-CH_2\sim \xrightarrow{O_2} PPO_2\cdot \text{ etc} \quad (4)$$

$$\sim CH_2-\overset{CH_3}{\underset{\underset{O\cdot}{O}}{C}}-CH_2-\overset{CH_3}{\underset{H}{C}}-CH_2\sim$$

$$\xrightarrow{PP} \sim CH_2-\overset{CH_3}{\underset{\underset{OH}{O}}{C}}-CH_2-\overset{CH_3}{\underset{H}{C}}-CH_2\sim + \sim CH_2-\overset{CH_3}{\underset{\downarrow O_2}{C}}-CH_2\sim$$

$$PPO_2\cdot \text{ etc} \quad (5)$$
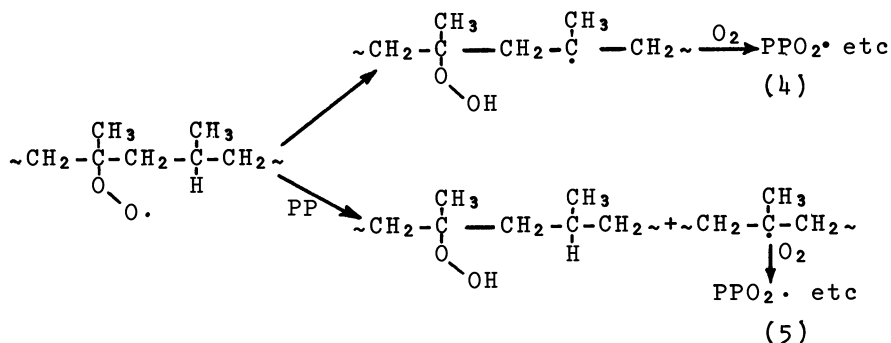
each of which can efficiently photo-cleave and so
initiate further PP oxidation.

Hydroperoxide groups have also been suggested to
be intermediates in PET photo-oxidation (6). The
build up of detectable quantities of -OOH groups has
not been directly observed, but the presence of
hydroxyterephthalate groups after UV irradiation in
air has been suggested to result from ·OH (from -OOH
photo-cleavage) addition to the PET backbone (6). The

hydroxyterephthalate groups were detected by
fluorescence spectroscopy (emission at 460 nm, from
an excitation maximum at 340 nm) (11). This
fluorescence build up was only observed during
irradiation in the presence of O_2 (6). Hydro-
peroxide groups could result from radical abstraction
from a backbone methylene group in the presence of
O_2 as shown in Table I. The photodecomposition of
these hydroperoxide intermediates to give macro-alkyl
radicals can be expected to subsequently cause
further backbone scission via reaction IV (Table I),
followed by CO_2 elimination from the $\sim\phi CO_2\cdot$ radical.
Appreciable CO_2 evolution is only observed during
the photodegradation of PET in air, when the CO_2
quantum yield reaches $\sim 1.5\times10^{-4}$m.einst^{-1}, as compared
to $\sim 2\times10^{-5}$m.einst^{-1} in the absence of O_2 [recal-
culated values from (6)].

In the presence of O_2, the photolysis of PmPiPA
gives carboxylic acid groups, possibly by O_2 in-
sertion after NH-C(=0) cleavage to give the transient
peroxide shown in Table I (reaction VI) (8).
Carboxylic acid formation [quantum yield $\sim 8\times10^{-5}$m
einst^{-1} (8)] is a much more efficient process than
CO elimination or Photo Fries rearrangement observed
during vacuum irradiation (Table I). Carboxylic acid
formation in PmPiPA films and fibers has been
observed by IR spectroscopy (at ~ 1720 cm^{-1}) and by
potentiometric titrations on dissolved samples (8).
In fact 2-aminobenzophenone units were not detected
after the irradiation of PmPiPA films in air. The
irradiation of PmPiPA fabrics in air however resulted
in the build up of both carboxylic acid groups and
2-aminobenzophenone units (12).

In all cases, O_2 enhances the degradative effects
of UV irradiation either by generating new photo-
unstable species, or as in the case of PmPiPA by
intercepting primary radicals which in the absence of
O_2 would largely recombine to reform the amide link
because of the rigidity of the PmPiPA matrix
(T_g $\sim 275^{\circ}$C). Photo-oxidation results in a progressive
shift of the UV absorption spectrum of each polymer
towards longer wavelength, even into the visible in
the case of PmPiPA, which becomes yellow-brown. UV
irradiation of all three polymers in the absence of
O_2 causes relatively little change in mechanical
properties whereas UV exposure in the presence of O_2

leads to a rapid deterioration in elongation at break and a less marked reduction in tensile strength. The difference between irradiation under vacuum and in air can be seen in Figure 2.

IV. Surface Reactions

Some of the products from the initiation and photo-oxidation steps listed in Table I can be detected (often with difficulty) by transmission IR spectroscopy. Transmission IR and stress-strain changes are shown in Figures 2, 3 and 4 for PmPiPA (8), PP (13) and PET (14) films and fibers irradiated in air. In all cases it is immediately apparent that the decrease in mechanical properties is not paralleled by the observed increase in degradation products (-OOH groups in PP, at 3400 cm^{-1}, -C(=O)OH groups in PET at 3290 cm^{-1} and -C(=O)OH groups in PmPiPA at 1720 cm^{-1}) as measured by transmission IR. This discrepancy is removed if surface IR spectra of the degraded films are measured by internal reflection spectroscopy (IRS). This technique employs an IR beam reflected from the interface between the polymer and an IR transparent reflection element (Ge or a TlI/TlBr crystal, KRS-5) at an angle of incidence greater than the critical angle for the interface. The observed IR spectrum results only from the surface layer (~0.1-2μ) of the polymer, the actual thickness monitored depending on the optical conditions (15). The IRS spectra of PmPiPA after various periods of UV exposure in air are shown in Figure 5. Photo-oxidation leads to a rapid build up in carbonyl absorption (at ~1720 cm^{-1}) in the surface IR spectra, but this change is very much less prominent in the transmission spectra (Figure 2, cf. normalized IRS and transmission data, OD_{1720}/OD_{1410}). All quantitative IR data in Figures 2-4 have been normalized to unit thickness of film in each case. Normalization involves ratioing the optical density (OD) of the product absorption to the optical density of an invariable reference band, (i.e., a band un-affected by degradation) measured under identical reflection or transmission conditions (16).

The IRS normalized optical density data shown in Figures 3 and 4 for each irradiation time were measured with several angles of incidence (30°, 45°, 60°) and on two reflection elements (Ge and KRS-5)
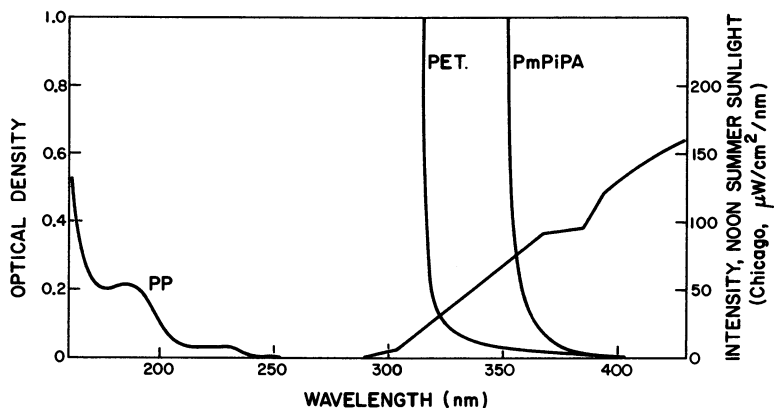
Figure 1. UV absorptions and sunlight intensity distribution. For 10μ films.
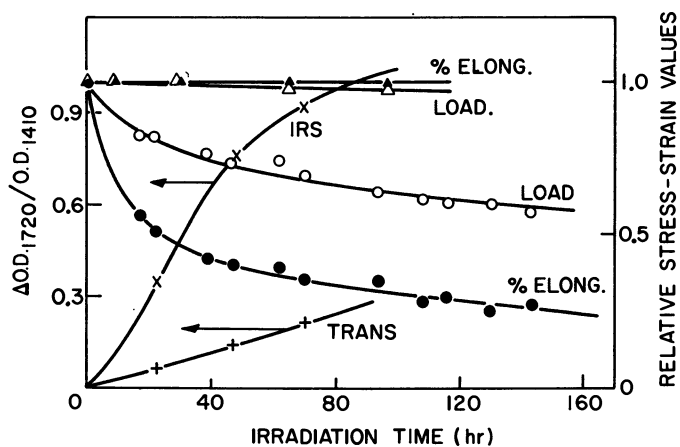
*Figure 2. IR and tensile changes: PmPiPA photodegradation.
Xenon arc Weather-Ometer stress–strain data: 44 tex, 2 ply yarn
Nomex. ▲△, vacuum irradiated; ●○, air irradiated. Initial elonga-
tion at break, 30%. Initial tensile strength, 9.0×10^7 g cm^{-2}. IR
data: 10μ films. Trans, +; IRS, x($d_p = 0.55μ$).*
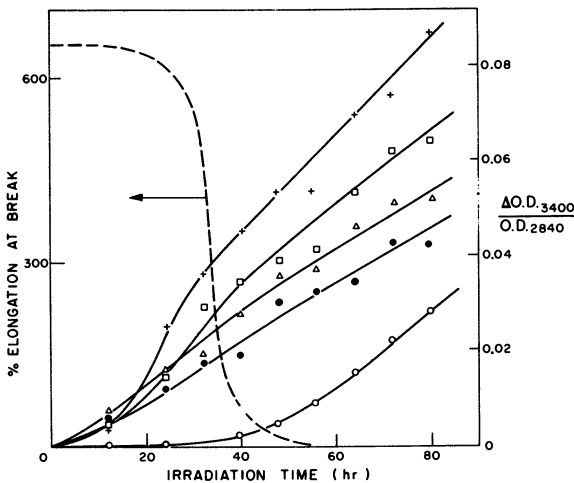
*Figure 3.   IR and brittleness changes: PP photooxidation
(24). 21μ Eastman film, irrad. 320 nm (filtered Hg arc).
0 hr tensile strength: 3.0 × 10⁵ g cm⁻². Trans. ir: ○.
IRS ir (d_p): + (0.19μ), △ (0.42μ), □ (0.22μ), ● (0.59μ).*
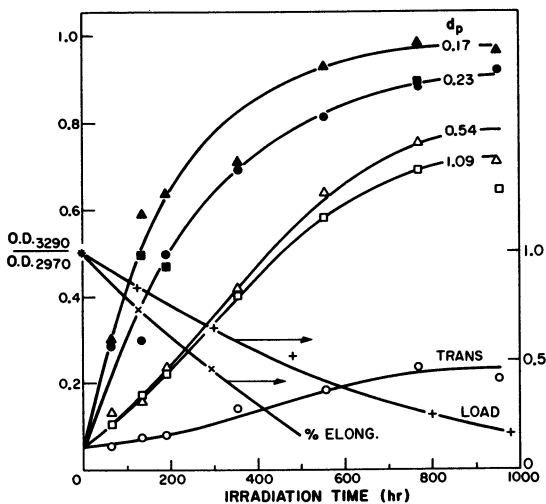
*Figure 4.   IR and tensile changes: PET photooxida-
tion. 21μ Mylar film, irradiated Xenon arc Weather-
Ometer. Initial elongation at break, 190%. Initial
tensile strength, 7.3 × 10⁵ g cm⁻². d_p = depth of
penetration for IRS ir spectra.*

so that spectra corresponding to several different
depths of penetration (d_p) of the reflected beam
could be measured for each film sample (16). From
the IRS data, degradation takes place almost entirely
in the surface layer (up to ~1μ) for each polymer,
and little in the bulk of the sample (as shown by
the transmission IR data). For PET and PmPiPA, only
the surface directly facing the light source was
extensively degraded, the obverse sides being little
changed. On the other hand, for PP, both the
directly irradiated and obverse sides of each film
showed virtually identical extents of surface
oxidations. Similar surface effects were observed
for the generation of carbonyl products (at ~1715
cm^{-1}) and the change in backbone helical content
(997 cm^{-1} absorption) of PP (13). Profiles of
normalized optical density as a function of d_p close
to one PP film surface are shown in Figure 6. These
data show that extensive relaxation of the amorphous
PP chains into the preferred helical conformation
has occurred in the surface zone as the photo-
oxidation proceeds. Initially the surface (from IRS)
and interior (from transmission IR) helical contents
were identical ($OD_{997}/OD_{974}=0.84$). Similar surface
"concentration" profiles can also be constructed for
the directly irradiated surfaces of PET and PmPiPA.
The normalized OD-d_p curves can be converted into
true profiles of product concentration as a function
of depth into the samples, but several assumptions
are required (16).

The strong absorption of short wave UV by PET
and PmPiPA films (Figure 1 and Table I) means that
the first few microns (for PET) and tenths of microns
(for PmPiPA) will absorb all of the damaging short
wave UV from the Xe arc (similar to sunlight) and
shield the remainder of the sample. Only longer
wavelengths (weakly absorbed, and lower energy) will
reach the obverse surface of each sample. In fact
irradiation of PET or PmPiPA films with longer wave-
length UV (>315 nm and >360 nm respectively) results
in virtually uniform carboxylic acid generation
throughout the films (8, 17). For PP, the front and
rear surface photo-oxidation probably stems from
surface thermal oxidation during processing when
trace amounts of >C=O and -OOH groups are generated
in the film surfaces during the brief air exposure
of the extruded melt at ≥250°C before quenching (18).
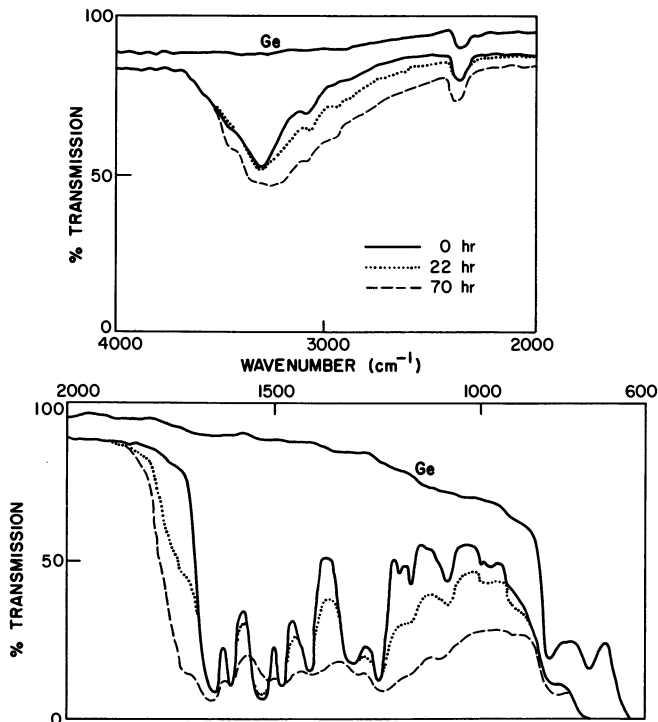
Journal of Polymer Science

*Figure 5.   IRS ir spectra of air irradiated PPiPA films. Ge re-
flection element, 45° incidence. Film surface directly irradiated
for specified times with Xenon arc Weather-Ometer. Ge curve
due to reflection element alone (8).*
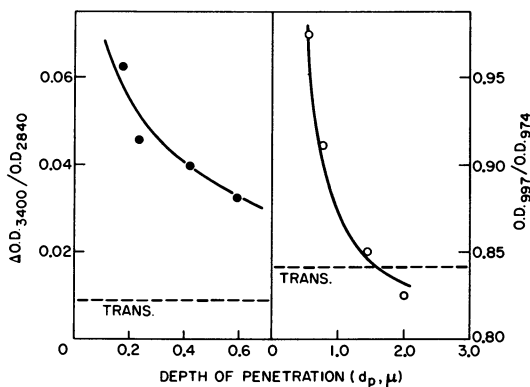
*Figure 6.   Surface changes from IRS spectra during
PP photooxidation. Film and irradiation details as in
Figure 2, 56 hr irradiation. d_p measured in from
irradiated surface.*

The UV transparency of PP and the extremely low
absorption of the chromophores (Table I) mean that
the obverse PP surface receives virtually the same
incident UV intensity as the front surface, and so
photo-oxidation proceeds at the same rate in both
surfaces.

V. Backbone Scission

The useful mechanical properties of all macro-
molecules depend on the great length of the polymer
backbone. This length allows extensive entanglement
and folding leads to the formation of crystallites
interconnected by amorphous zones. Any backbone
cleavage will result in a weakening of the polymer
structure, particularly since scission reactions occur
largely in the amorphous zones, containing tie
molecules which connect crystallites.

For PP, PET and PmPiPA, the primary photo-
initiation steps all involve backbone scission, yet
none of these polymers deteriorates appreciably in
mechanical properties during irradiation with UV
>290 nm in the absence of O_2. In fact both PET ([17],
[19]) and PmPiPA ([7]) undergo crosslinking which renders
the polymers insoluble in their usual solvents (o-
chlorophenol for PET and dimethylacetamide for
PmPiPA). Crosslinking in these aromatic polymers
probably results from radical addition to phenyl rings
in adjacent chains ([19]). For PP, even complete
photolysis of the very low concentrations of chromo-
phores can have little effect on physical properties.

In the presence of O_2, crosslinking reactions
are reduced due to O_2 interception of radical inter-
mediates, and additional backbone cleavage reactions
become important (Table I). For PP, the primary
initiation processes are very rare, but the hydro-
peroxide which rapidly builds up (Figure 3) following
the initial photo-initiation processes quickly
becomes the dominant source of free radicals. In PP,
backbone scission largely results from the β-scission
of macro-alkoxy radicals ([5]) (reaction I, Table I).
Roughly 70-80% of the PP macro-alkoxy radicals β-
scission, 10-20% hydrogen abstract from PP to give
alcohol groups and the remainder are lost by
combination with other radicals ([5],[9]). The β-scission
of a tert-alkoxy radical may occur by two routes
(reactions 6 and 7). In well characterized liquid

phase β-scissions the elimination of a secondary alkyl
radical (reaction 6) is normally favored over primary

$$\sim CH_2-C\overset{\diagup CH_3}{\underset{\diagdown O}{}} + \cdot CH_2 \sim \qquad (6)$$

$$\sim CH_2-\overset{CH_3}{\underset{O\cdot}{\overset{|}{\underset{|}{C}}}}-CH_2 \sim$$

$$\sim CH_2-\overset{}{\underset{O}{\overset{|}{\underset{||}{C}}}}-CH_2 \sim + CH_3 \cdot \qquad (7)$$
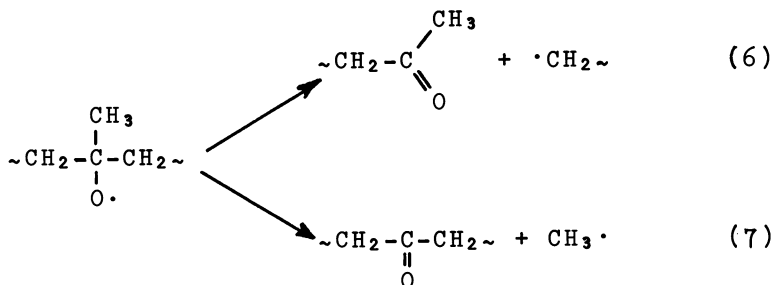
radical elimination (reaction 7) (20). From IR
analysis of the photolysis products from PP hydro-
peroxide groups, Carlsson and Wiles concluded that
backbone ketone formation via the unusual scission
reaction 7 occurred at roughly the same rate as
terminal methyl ketone formation (5). This might
imply the reversability of reactions 6 and 7 in the
rigid polymer, so that product formation by the
elimination of a small mobile radical ($CH_3 \cdot$) is
favored, but obviously needs further confirmation.
Alkoxy β-scission (reaction IV, Table I) is probably
also important in PET photo-oxidation (6), as
described previously.

The presence of extensive backbone scission
during photo-oxidative degradation has been demon-
strated by molecular weight ($\bar{M}n$) determination,
based on solution viscosities. PET with an initial
$\bar{M}n$ of ~20,000 decreased to ~14,000 after 600 hr
xenon arc irradiation (21). PmPiPA with an initial
$\bar{M}n$ of ~40,000 decreased to ~10,000 after 40 hr of
xenon arc irradiation (8). The actual extent of
backbone scission is even more startling when it is
remembered that degradation has occurred only in the
irradiated surface layer (<1μ) of each polymer, so
that $\bar{M}n$ in this surface layer will be of the order
of 1000, i.e., oligomer in each case.

V.   Surface Degradation and Brittle Failure

The surface oxidation and associated backbone
scission discussed above can be expected to result in
a drastic reduction in surface toughness and resis-
tance to stress. In fact electron microscopy of the
PP surface shows that the film becomes covered in

parallel cracks during photo-oxidation (13) (Figure
7). The film cracks (~50 nm wide and ~0.5μ deep at
35 hr irradiation) first become detectable at an
irradiation time (~24 hr) close to that at which the
rapid decrease in elongation to break (increase in
brittleness) occurs (Figure 3). The PP surface
cracks probably arise from the extensive surface re-
crystallization which results from scission of the
tie molecules in the amorphous phase. Recrystall-
ization was also indicated by the large bulk density
increase which accompanies photo-degradation
(0.8858 g.ml^{-1} initially, 0.9024 g.ml^{-1} after 80 hr
Hanovia irradiation, λ>320 nm). This change will
cause a contraction in the degraded (surface) zones,
resulting in crack formation. The increase in the
997/974 ratio (helical backbone conformation, Figure
5) is also associated with chain scission in the
amorphous zones, followed by the relaxation of the
cleaved fragments into the preferred helical con-
formation essential for PP crystallization (13).

At room temperature, PP is close to its T$_g$(0-
25°C) and well above its normal brittle-ductile
transition temperature (~ -30°C). However the
presence of surface cracks in the photo-oxidized film
is apparently sufficient to promote brittle failure
at room temperature. According to the Griffith
crack theory, once a critical crack length has been
exceeded, a critical crack velocity is required to
propagate the crack. If this velocity is not ex-
ceeded, cold drawing of the amorphous zones ensues.
At low degrees of degradation (<24 hr, Figure 3)
cracks are not detected and no decrease in sample
brittleness results. Beyond 24 hr irradiation, the
surface cracks become apparent and increase in depth
as degradation proceeds since a greater thickness of
polymer has become oxidized. Then at the strain rate
used (5.2 cm min^{-1}) plastic deformation at the crack
tip can no longer dissipate the applied energy and
the cracks propagate through the interior of the film.

Highly oriented PP monofilaments (drawn to break
at 25°) are more resistant to photo-oxidation than
medium drawn fiber (~x5 orientation at ~230°C) as
measured both by oxidation product build up and
mechanical deterioration (22). Both types of PP
monofilaments also show crack formation during photo-
oxidation (Figure 7). The lower orientation material
shows quite wide, deep cracks whereas the fully
oriented fiber shows many short, narrow cracks for
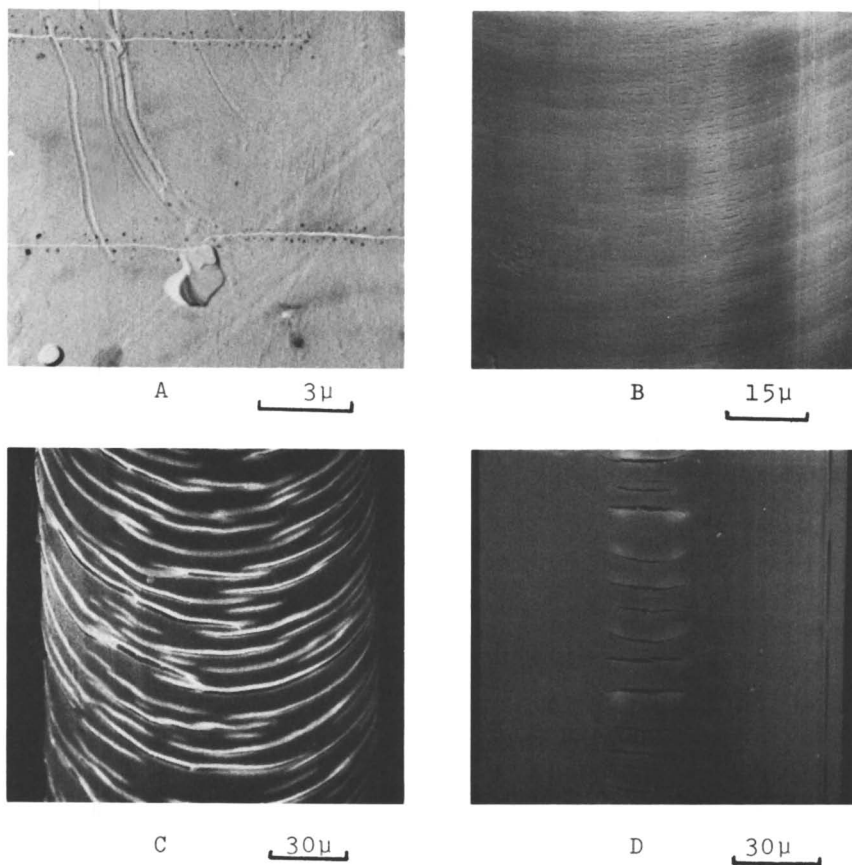
Figure 7. Surface changes during PP photooxidation electron micrographs. A, 24 hr irradiation; film and irradiation conditions in Figure 2. B, 115μ PP monofilament, fully oriented. C, D—130μ PP monofilament, medium orientation. B and D—195 hr, C—275 hr, Xenon arc Weather-Ometer.

equivalent irradiation periods. For both types of
fiber, cracks are initially detected (at ~100 hr
xenon arc irradiation) over narrow arcs (~20% of the
circumferance) on the directly irradiated zone and
the diametrically opposite zone (i.e., rear). As
photo-oxidation proceeds, the cracked zone broadens
until the whole circumference is involved (~200 hr
irradiation). The correlation between mechanical
deterioration and the detection of surface cracks is
poorer in the fiber samples than in PP films,
extensive mechanical deterioration preceding crack
detection by ~40 hr.

PET and PmPiPA show no surface changes even after
extensive photo-degradation (600 and 120 hr
respectively). However, slight flexing of these film
samples causes the convex sample surfaces to break up
into many parallel cracks (14,23). The changes shown
in Figure 8 for PmPiPA are in fact typical of PET,
but after a much longer irradiation period (~800 hr
xenon arc Weather-Ometer). The concave surface of
each flexed film (in compression) showed no visible
changes by electron microscopy. Both PET and PmPiPA
show only a small increase in density on photo-
oxidation. Cracking in the unstressed state is not
expected during degradation since inter- and intra-
molecular H-bonding forces in the polyester and poly-
amide structures will resist surface contraction.
However, the backbone scission in the surface skin is
so extensive that neither polymer can tolerate even a
small extension without the photo-oxidized layer
cracking at right angles to the applied stress. The
formation of surface cracks in PET and PmPiPA under
low stress accounts for the rapid drop in tensile
properties after photo-oxidation. For PET and PmPiPA,
both polymers are glassy at room temperature (T_g
values 67-81°C and ~275°C respectively) and on the
application of an increasing stress to the degraded
materials the cracks, initially produced at low stress
in the degraded surface layer, propagate into the
remainder of the (largely undergraded) films. The
glassy nature of each polymer precludes sufficient
plastic deformation at the crack tips, even in the
underlying undegraded polymer, to dissipate the
applied stress at the strain rate employed (5.2 cm
min^{-1}). Both PET and PmPiPA films show fracture
surfaces which indicate a different failure in the
irradiated surface zones as compared to the remainder
of the film (cf. Figure 8 for PmPiPA).
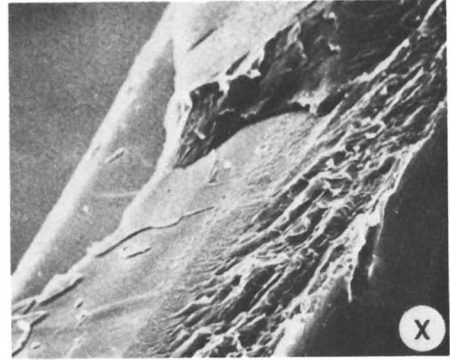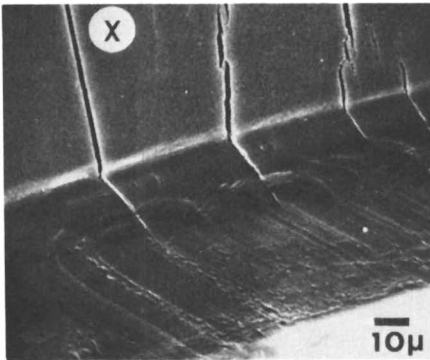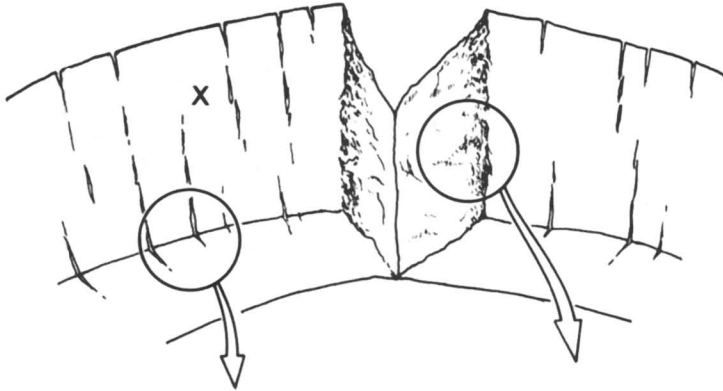
Canadian Textile Journal

Figure 8.   Scanning electron micrographs of photooxidized PmPiPA.   100μ film, 120 hr Xe arc Weather-Ometer irradiated on side X. Flexed as shown. Right, fracture surface; left, section at 90° to flex.direction (23).

Films of the aromatic polymers PET and PmPiPA show a 7-8 fold difference in stability to xenon arc irradiation, PET being the more stable (cf. Figures 2 and 4). This difference is mainly due to the differences in inherent UV absorption of the polymers (Figure 1). It can be calculated that the total energy absorptions from the xenon arc by 10μ film of PET and PmPiPA are $\sim 1 \times 10^{-9}$ einst.$cm^2 sec^{-1}$ and $\sim 14 \times 10^{-9}$ einst.$cm^2 sec^{-1}$ respectively. The larger energy absorption of PmPiPA partially offset by the slightly lower quantum yield for photo-oxidative scission ($\sim 8 \times 10^{-5}$ m.einst^{-1}) as compared to PET ($\sim 2 \times 10^{-4}$ m.einst.$^{-1}$). The very high T_g of PmPiPA can also be expected to increase the susceptibility of the polymer to crack propagation as compared to PET.

VI. Conclusions

a) Photo-oxidative degradation of PP, PET and PmPiPA occurs largely at the surfaces.

b) Oxygen enhanced scission of the polymer backbone renders the irradiated surfaces brittle, and unable to accommodate a low applied stress.

c) The formation of or presence of surface cracks in this brittle layer is responsible for the loss in elongation and tensile properties of the films.

Literature Cited

1.   Hawkins, W.L. in "Polymer Stabilization" ed. W.L. Hawkins, pp. 1-28, Wiley-Interscience (New York) (1972).

2.   Trozzolo, A.M. in "Polymer Stabilization" ibid pp. 159-214.

3.   Cichetti, O., Adv. Polym. Sci. (1970) 7 70-112.

4.   Carlsson, D.J. and Wiles, D.M., Macromolecules (1969) 2 587-597.

5.   Carlsson, D.J. and Wiles, D.M., Macromolecules (1969) 2 597-606.

6.   Day, M. and Wiles, D.M., J. Appl. Polym. Sci. (1972) 16 203-215.

7.   Carlsson, D.J., Parnell, R.D. and Wiles, D.M. J. Polym. Sci. Polym. Letters Ed. (1973) 11 149-155.

8.   Carlsson, D.J., Gan, L.H., Parnell, R.D. and Wiles, D.M. J. Polym. Sci. Polym. Letters Ed. (1973) 11 683-688.

9.   Decker, C. and Mayo, F.R., J. Polym. Sci. Polym. Chem. Ed. (1973) 11 2847-2877.

10.   Van Sickle, D.E., J. Org. Chem. (1972) 37 755-760.

11.   Pacifici, J.G. and Straley, J.M., J. Polym. Sci. Polym. Letters Ed. (1969) 7 7-9.

12.   Carlsson, D.J., Gan, L.H. and Wiles, D.M. to be published.

13.   Blais, P., Carlsson, D.J. and Wiles, D.M., J. Polym. Sci. Part A1 (1972) 10, 1077-1092.

14.   Blais, P., Day, M. and Wiles, D.M., J. Appl. Polym. Sci. (1973) 17 1895-1907.

15.   Harrick, N.J. "Internal Reflection Spectroscopy" Interscience, New York (1967).

16.   Carlsson, D.J. and Wiles, D.M., Macromolecules (1971) 4 174-179.

17.   Day, M. and Wiles, D.M., J. Appl. Polym. Sci. (1972) 16 191-202.

18.   Carlsson, D.J. and Wiles, D.M., Macromolecules (1971) 4 179-184.

19.   Marcotte, F.B., Campbell, D., Cleaveland, J.A. and Turner, D.T., J. Polym. Sci. A1 (1967) 5 481-501.

20.   Mill, T., Richardson, H. and Mayo, F.R., J. Polym. Sci. Polym. Chem. Ed. (1973) 11 2899-2907.

21.   Day, M. and Wiles, D.M., J. Appl. Polym. Sci. (1972) 16 175-189.

22.   Carlsson, D.J., Clark, F.R.S and Wiles, D.M. to be published.

23.   Blais, P., Carlsson, D.J., Parnell, R.D. and Wiles, D.M., Can. Text. J. (1973) 93-96.

24.   Carlsson, D.J. and Wiles, D.M., J. Polym. Sci. Polym. Letters Ed. (1970) 8 419-424.

24

Mechanisms of Photodegradation and Stabilization of Polyolefins

GERALD SCOTT

University of Aston in Birmingham, Gosta Green, Birmingham B4 7ET, England

Summary

The most important initiation process involved in the early stages of the photo-oxidation of polyethylene is shown to be hydroperoxide photolysis associated with the decay of vinylidene groups. This is followed by carbonyl photolysis occurring primarily by the Norrish type II process.

The most effective uv stabilisers belong to the preventive class of antioxidants. The nickel dialkyl dithiocarbamates which are important members of the peroxide decomposer class are particularly effective and are found to prevent the decay of vinyl-idene and the formation of hydroperoxide both during processing and during subsequent uv irradiation. Carbonyl triplet and oxygen singlet quenching appear to play only a minor role with typical nickel complex stabilisers. However, the nickel oximes behave both as uv screening agents and as radical trapping agents in model compounds.

Introduction

The mechanisms of thermal antioxidant action have been extensively studied over the past thirty years and can be considered to be reasonably well under-stood. Several comprehensive reviews are available (1-3), and antioxidants have been classified into two main types (4,5), namely preventive and chain-breaking. The former act

340

by interfering with the initiation step of the autoxidation
(i) and the latter with the propagation step (ii).

$$Initiator \longrightarrow X\cdot \qquad \text{Initiation (homolysis)} \qquad (i)$$

$$X\cdot + RH \xrightarrow{(a)} XH + R\cdot$$

$$R\cdot + O_2 \xrightarrow{(b)} RO_2\cdot \left.\begin{array}{l} \\ \\ \end{array}\right\} \quad \text{Propagation (chain reaction)} \qquad (ii)$$

$$RO_2\cdot + RH \xrightarrow{(c)} RO_2H + R\cdot$$

$$(2)RO_2\cdot \longrightarrow \text{Stable Molecule} \qquad \text{Termination} \qquad (iii)$$
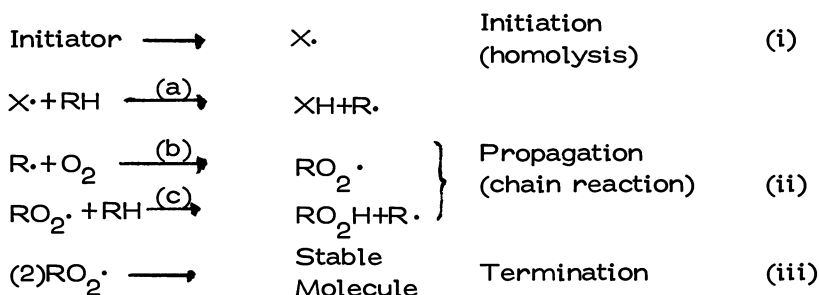
Although photo-oxidation involves the same reaction
sequence, the relative importance of the three
stages differs. In general much more energy is
available for the initiation step in the form of uv
light. This is capable of photolysing a variety of
weak bonds in polymers to free radicals or of act-
ivating double bonds to triplet states which behave
as diradicals. The rate of initiation (i) is much
higher in the case of photo-oxidation than it is in
thermal oxidation and hence the rate of termination (iii)
is also higher. Consequently the length of the kinetic
chain (ii) is shorter and chain-breaking antioxidants
are relatively less effective although it is observed
that this type of antioxidant frequently shows synergistic
behaviour with uv stabilisers.

It has been recognised, therefore, that the most
important uv stabilisers fall into the preventive
class (6) and three distinct mechanistic types of
uv stabilisers have been proposed. In chronological
order these are (a) uv absorbers (6-8) (b) peroxide
decomposers (5,6,9-12) and (c) triplet quenchers (13-20).

(a) UV Absorbers

The main classes of compound contained in this class
are the 2-hydroxybenzophenones (I) and the 2-hydroxy-
benzotriazoles (II).

I   II
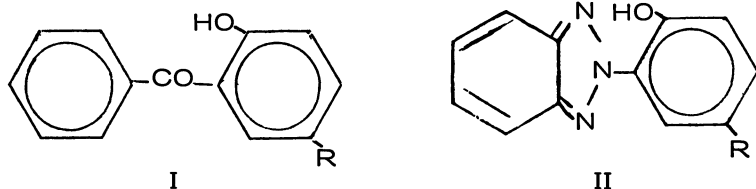
These were believed originally to function entirely as
uv screening agents (6). It was thought that, like
pigments such as carbon black or titanium dioxide, they
had the ability to absorb the uv light and dissipate this
as thermal rather than as chemical energy.
Subsequent work has shown that this class shows
some ability to behave by the chain-breaking mechan-
ism (11,21,22) and also to quench triplet states
(16,20). However, there is little doubt that uv screen-
ing is one, and probably the most important, of their
functions so that they prevent or reduce the rate of
formation of initiating free radicals in the polymer.

(b) Peroxide decomposers

Some of the most powerful uv stabilisers belong to
the class of peroxide decomposing preventive antioxidants
and it has been suggested that the mechanism of this
type of uv stabiliser is not distinguishable from their
behaviour as thermal antioxidants although all peroxide
decomposers do not behave as uv stabilisers (11). Of
paramount importance in the peroxide decomposer –
uv stabiliser class are the metal dithiocarbamates (III)
(9,22,23,24) the dithiophosphates (IV) (11,24) and the
cyclic phosphate esters (V) (11,25,26) which unlike
most antioxidants and uv stabilisers have very high
activity as both thermal and uv stabilisers. Detailed studies

III   IV

V
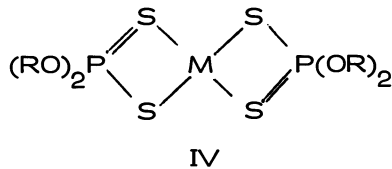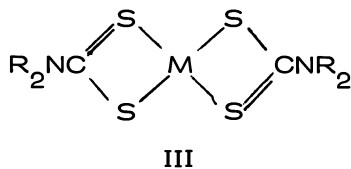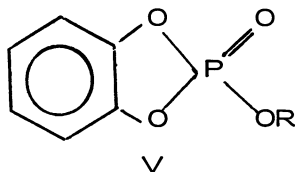
in model systems have shown that III – V give rise
to very powerful Lewis acid catalysts for the
decomposition of hydroperoxides in a pseudo–first
order decomposition of hydroperoxide (27), indica-
ting that the Lewis acid is not destroyed by oxidation
but persists in the polymer until it is deactivated or
lost by volatilisation.

(c)   Excited State Quenchers

The suggestion that some uv stabilisers may function
by deactivating photo–excited states of molecules,
particularly of triplet carbonyl and singlet oxygen,
arose largely as a result of fundamental photochemical
studies in model systems and many attempts have been
made to invoke this mechanism to explain the activity
of a variety of photo–stabilisers (13–20). Many effect-
ive uv stabilisers are indeed efficient quenchers of
photo–excited states (20), but so are many more which are
not and in some cases, notably the transition metal acetyl
acetonates (VI), (28) quenchers of triplet carbonyl are
among the most powerful photo–activators known (22).

VI
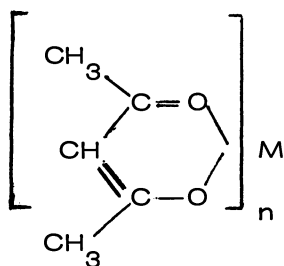
The presence of photo–activators in polymers

The failure to demonstrate a satisfactory relation-
ship between carbonyl triplet or oxygen singlet

quenching ability and uv stabilising effectiveness
necessitates a more basic approach to the question
of mechanism and in particular it is important to
understand the relative importance of photo-
activators in the various stages of thermal and
environmental history of polymers.

The polyolefins are particularly suitable subjects
for study since formally they should not absorb in
the uv above 285 nm which is the effective cut-off
point for uv light coming through the earth's
atmosphere. In practice they do absorb and it has
been a matter of conjecture since polyethylene was
first discovered as to which of the very minor
chromophoric constituents of commercial polyolefins
are responsible for their photo-sensitisation.

The possible stages in the history of a typical
polymer during which sensitisers may be introduced
are shown in Table 1.

Transition metal ions

There is considerable evidence that some transition
metal ions are powerful activators for both thermal
and uv initiated oxidation of polymers. The most
effective of these are cobalt, iron, copper and

manganese but these are not normally found as
catalyst residues from ionic polymerisation.
Titanium, the most likely contaminant, is not a very
powerful pro-oxidant. Nevertheless, its presence
in small amount may partly account for the much
lower uv resistance of HDPE as compared with
LDPE. The common transition metal ions are,
however, likely contaminants during processing and
particularly reprocessing operations when
contaminants (from biological or other sources) are
not adequately removed from waste plastics. The
effects of typical pro-oxidant transition metal ion
complexes on the uv stability of polyethylene and
polypropylene are shown in Table 2. It is clear
that cobalt and iron in soluble form have a catas-
trophic effect on the uv stability of both polymers.
Moreover, stability is affected in proportion to the

Table 1

	Stage	Possible photosensitisers
1	Polymer manufacture	Unsaturation, Transition metal ions (hydroperoxide, carbonyl compounds by adventitious oxidation)
2	Processing and fabrication	Hydroperoxides, carbonyl compounds (by high temperature oxidation, limited oxygen supply) Transition metal ions (from machinery or compounding ingredients)
3	Environmental exposure	Polycyclic hydrocarbons (atmospheric pollution) Carbonyl (by photolysis of hydroperoxides) Unsaturation (by photolysis of ketones) Singlet oxygen and derived hydroperoxides (by quenching of carbonyl triplet etc with triplet oxygen) Transition metal ions (particularly iron and copper)

Table 2

Effect of transition metal acetylacetonates on the
oxidation of LDPE during processing and on UV irradiation

Additive	Concentration mols / 100 g	Carbonyl index (before exposure)	Time to embrittlement (hrs)
Fe(acac)$_3$	2×10^{-3}	10.22	120
	1×10^{-3}	4.64	216
	0.7×10^{-5}	1.10	260
Co(acac)$_3$	2×10^{-3}	43.57	0
	1.4×10^{-4}	22.82	50
Ni(acac)$_2$	2×10^{-3}	0.51	1968
Mn(acac)$_2 \cdot 2H_2O$	2×10^{-3}	0.64	600
	1.7×10^{-4}	2.70	510
Ce(acac)$_3$	2×10^{-3}	0.48	700
Zn(acac)$_2$	1×10^{-3}	0.38	1370
None	–	0.15	2100

effect of the metal ion on the carbonyl index of the polymer as a result of oxidation during processing.

Effect of Processing on the uv Stability of Polyolefins

There has been a tendency in the past to ignore the effects of processing on the photo-stability of polymers. The technologist is concerned with the effects of photo-oxidation on fabricated articles such as film and fibres and in most published technolgical studies of polymer photo-stability, the detailed thermal history of the polymer is not specified. Consequently inter-laboratory comparisons of uv stability of polymers and the effects of uv stabilisers is normally difficult if not impossible. There is evidence that in some cases the role of photo-stabilisers has been confused with that of thermal stabilisers since the two are mechanistically related (11). Just how important can be the prior thermal history of polyethylene on its uv stability is shown in Figure 1 which relates the processing time under standard conditions to the time to embrittle-ment in a standard sunlamp / blacklamp (S/B) environmental simulator. Figure 1 also shows the effect of soluble iron on this process and illustrates the importance of controlling transition metal ion concentration during manufacture and processing.

Processing of polyethylene, as might be expected, leads to a change in functional group concentration. This is shown for LDPE in Figure 2 (29). Ketonic carbonyl increases in an auto-accelerating mode and vinylidene, which is initially the most important unsaturated group present, decays rapidly after an induction period. Vinylidene decrease is associated with the rapid formation and rapid decay of hydro-peroxide. The formation of conjugated carbonyl in the later stages of the photo-oxidation in place of vinylidene indicates that vinylidene decay is associated with the oxidation of the allylic group.

The time to embrittlement of polyolefins during photo-oxidation is not directly related to initiation carbonyl concentration (9-11). This is exemplified for HDPE in Figure 3 and a similar relationship exists for LDPE and
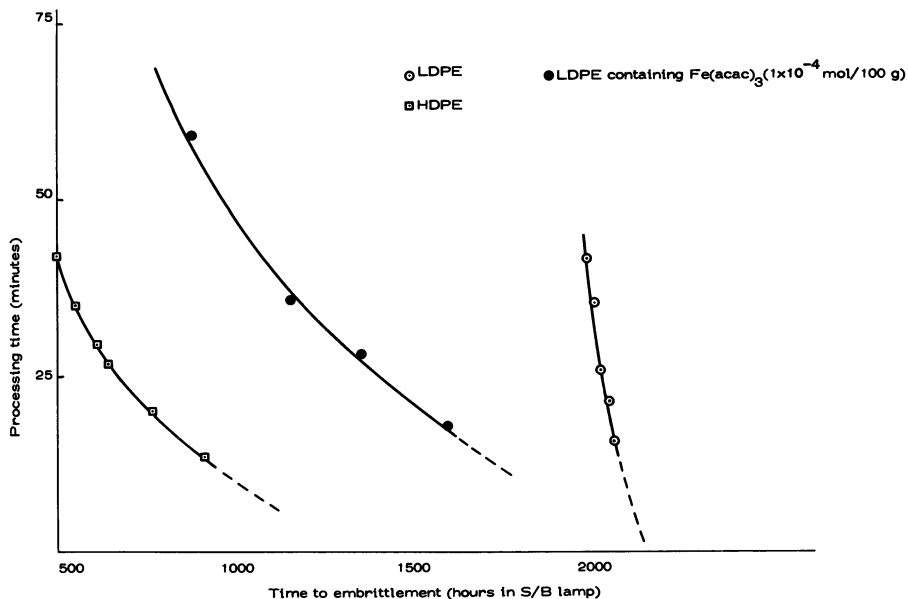
Figure 1.   Effect of melt processing in air upon the time to embrittlement of polyethylene on uv irradiation
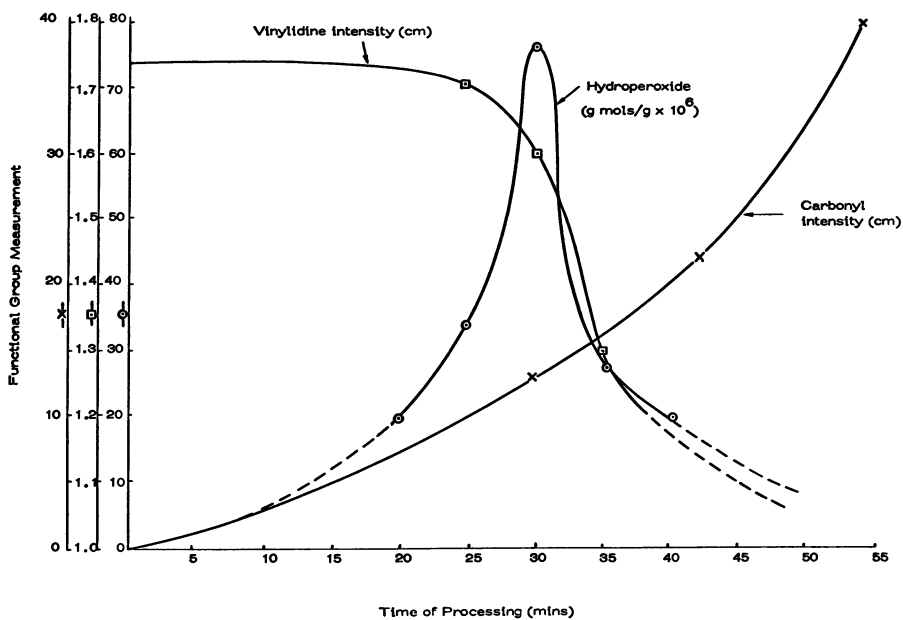
Figure 2.   Change in functional group concentrations during processing of LDPE

PP. Embrittlement times always change most rapidly in mildly oxidised polymers containing little or no carbonyl. This finding is consistant with the observation that added long chain dialkyl ketones are not sensitisers for polypropylene photo-oxidation (30) although aromatic ketones are (22,30).

Photo-oxidation of LDPE which has been subjected to a minimal processing treatment (5 mins at 160°C) leads to a very rapid decay of vinylidene and the auto-accelerating formation of ketonic carbonyl (29). Hydroperoxide cannot be measured in this system either after processing or during uv irradiation (31). More extensive processing (30 mins at 160°C) leads to the formation of hydroperoxide (see Figure 2) which on uv irradiation decays rapidly (Figure 4) (31). Vinylidene, which has been partially destroyed during the processing operation decreases more rapidly than in the normally processed polymer. The carbonyl formation curve is no longer auto-accelerating, consistent with the initial presence of hydroperoxide. LDPE processed to the optimum hydroperoxide concentration and heated in helium for 6 hours at 160°C to destroy hydroperoxide and then subjected to photo-oxidation again becomes auto-accelerating (see Figure 4). The initially higher carbonyl concentration appears to have some effect on the rate of subsequent carbonyl growth and the importance of carbonyl in the absence of hydroperoxide is being studied further.

It seems unlikely then that carbonyl (ketone and aldehyde) formed by thermal breakdown of hydroperoxides are important sensitisers for photo-oxidation of LDPE in normally processed polymers. The evidence is consistent with the theory that allylic hydroperoxide derived from vinylidene is the important photo-initiator initially present under these conditions. Vinylidene disappears as a concomitant of hydroperoxide photolysis, initiating photo-oxidation in a manner analogous to its function in thermal oxidation.

The chemistry of thermal oxidation, leading to disappearence of vinylidene after an induction period (Figure 2) is shown in scheme (iv). The physical
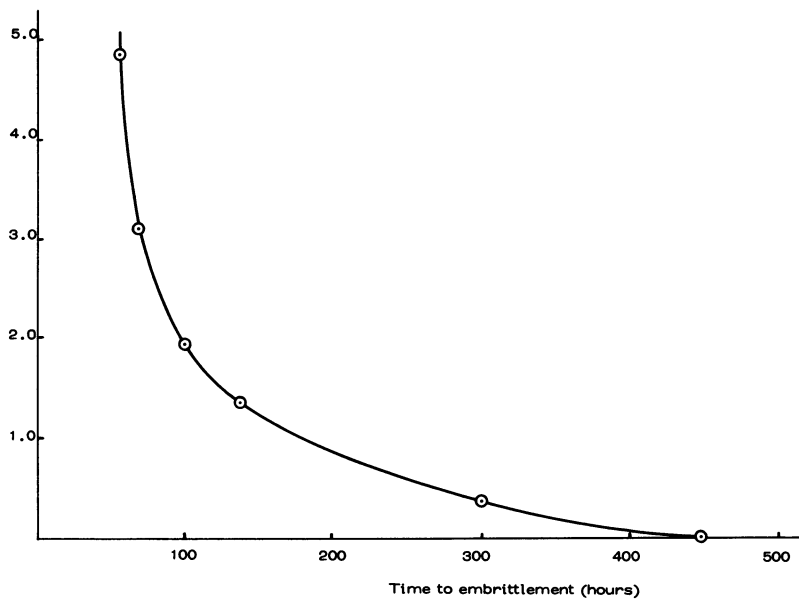
Figure 3. Relationship between carbonyl content and embrittlement time of HDPE
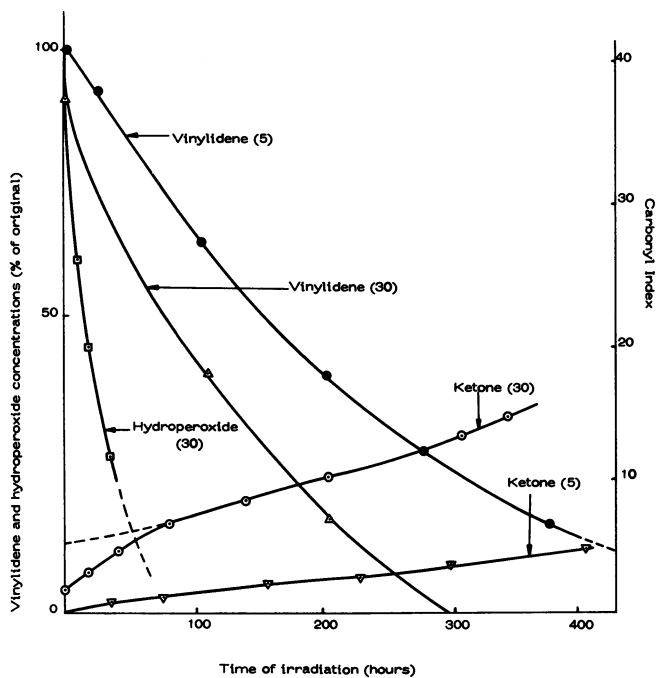
Figure 4.   Effect of irradiation time on functional group concentration in LDPE. Processing times in parenthesis.

consequence is primarily chain scission associated
with the formation of carbonyl compounds.

$$-CH_2-\underset{\underset{CH_2}{|}}{\overset{O}{\underset{||}{C}}}-CH_2-CH_2- \xrightarrow{(a)} -CH_2-\underset{\underset{CH_2}{|}}{C}-\overset{OOH}{\overset{|}{CH}}-CH_2$$

$$\xrightarrow{(b)} -CH_2-\underset{\overset{|}{O\cdot}}{C}-CH-CH_2- \qquad (iv)$$

$$\xrightarrow{(c)} -CH_2-\underset{\underset{CH_2}{|}}{\overset{O}{\underset{||}{C}}}-CHO \; + \; \cdot CH_2-$$

$$\xrightarrow{(d)} -CH_2-\underset{\underset{CH_2}{|}}{C}-\overset{O}{\overset{||}{C}}-CH_2-$$
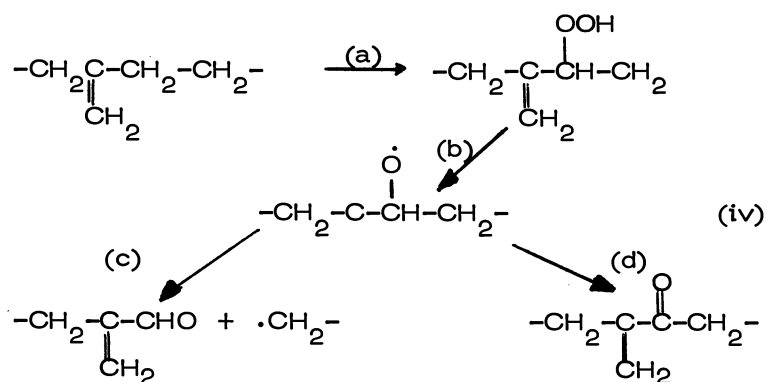
Photo-oxidation also leads to chain scission and there is
evidence for a cross-linking reaction not observed in
thermal oxidation. This leads to the formation of
chlorobenzene insoluble gel during the early stages
of photo-oxidation (31) (see Figure 5). This cross-
linking reaction is closely associated with changes
in mechanical properties during the early stages of
photo-oxidation. It is known that elongation at break
always increases before decreasing to zero and the
dynamic modulus initially decreases before increas-
ing due to oxidative crystallisation. There is,
therefore, a pronounced induction period before increase
in density occurs, presumably due to the onset of
relaxation processes in the polymer. Vinylidene
addition (v) must therefore compete with reactions
(iv (c) and (d)) in photo-oxidation.

The inflexion of the carbonyl formation curve for
LDPE oxidised during processing illustrated in
Figure 2 always occurs at about the same time
of photo-oxidation (see Figure 6). In heavily
thermally oxidised polyethylene the carbonyl index
actually decreases initially before increasing again.
Ketone carbonyl is the main product formed in the
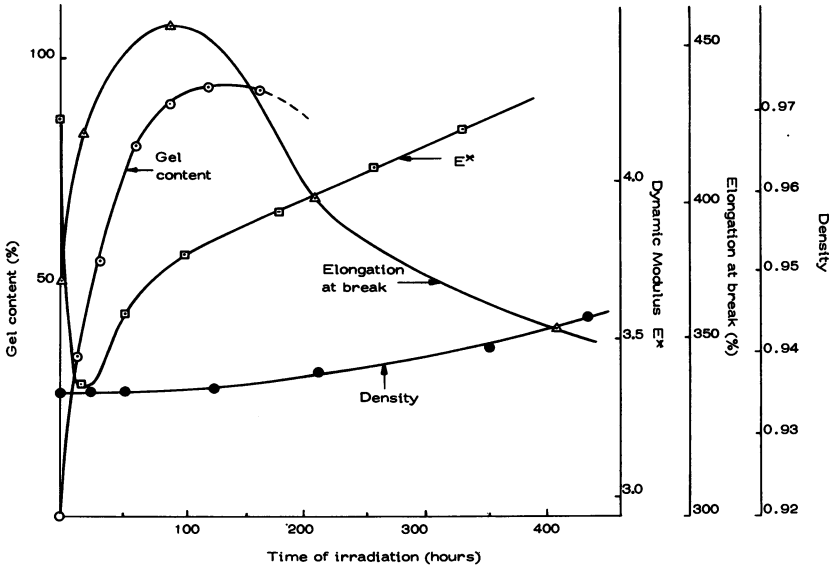
Figure 5.   Effect of irradiation on the mechanical and physical properties of
LPDE during the early stages of uv irradiation
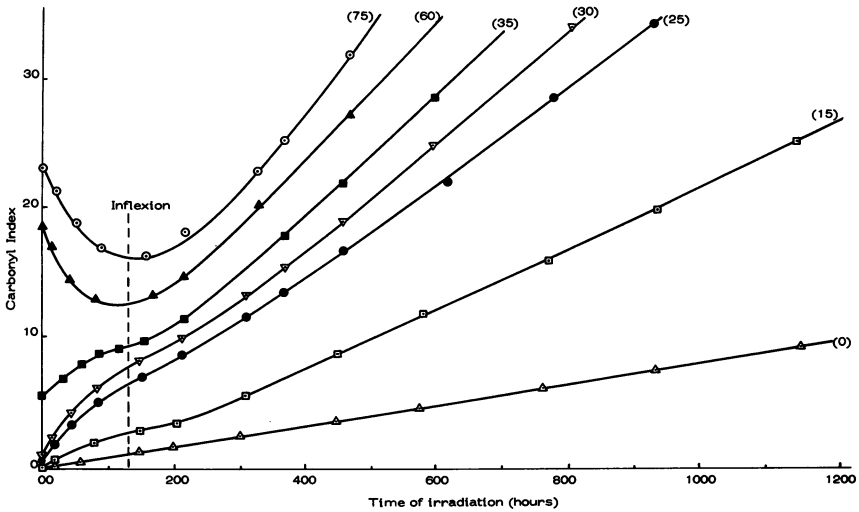
Figure 6.   Variation of carbonyl index with irradiation time for LDPE processed
for varying times. Processing times in parenthesis.
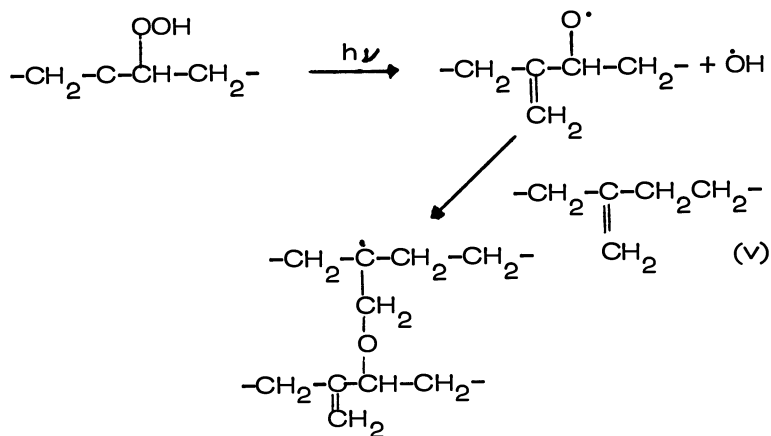
initial stages by Norrish II photolysis (vi). The
reason for this apparent decay of carbonyl has not yet
been demonstrated unequivocally but it seems likely
that it is due either to loss of carbon monoxide by
Norrish I photolysis (33) or to the broadening of the
carbonyl peak due to the formation of a new methyl
ketone (VIII) absorbing at a slightly longer wavelength than
the original ketone (VII).

The second stage of carbonyl growth appears to produce
mainly carboxylic acid by Norrish I photolysis (vii).
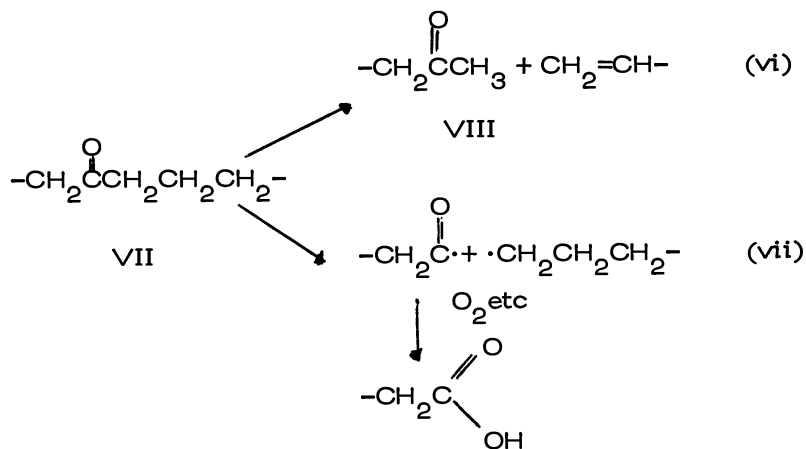
Confirmation for the changeover in mechanism is
found in the fact that during the first 100 hours, vinyl is

a major product formed in an initially zero order
reaction (see Figure 7) but this also autoretards to
give a much lower rate when the Norrish I process
becomes predominant. It has previously been
observed by Guillet and his co-workers (33) that
Norrish I photolysis is less important than Norrish II
in polyethylene-carbon monoxide co-polymers and in
model ketones at ambient temperatures. Decrease in
the viscosity of the medium, like increase in temperature
leads to an increase in the ratio of Norrish I to Norrish II
quantum yields. This has been interpreted (33) as being

due to the increase in segmental motion of the
polymer chain with decrease in caged recombination
of the radicals produced by the Norrish I process.
This restriction does not apply to the Norrish II
process which does not involve radical products.
It is significant therefore that the Norrish II process
predominates until the onset of oxidative crystallisation
which also requires mobility of the polymer segments
to permit relaxation reallignment of the polymer
chains.

If carbonyl is primarily formed as a consequence of
photolysis of hydroperoxide in thermally oxidised
polyethylene, then the rate of carbonyl formation
should be proportional to hydroperoxide concentration.
This is found to be so up to the maximum hydro-
peroxide concentration (Figure 8) but beyond this
point, photolysis of breakdown products becomes
more important.

Other possible initiation processes

The conclusion which emerges from the above studies
is that the hydroperoxide photolysis is the most
important initiating process occurring in the photo-
oxidation of lightly oxidised LDPE. The contribution
of other initiating reactions cannot, however, be
excluded since the plot of carbonyl formation rate
against hydroperoxide concentration appears to have
a positive intercept on the carbonyl rate axis (Figure 8).
A number of initiating processes have previously been
proposed which might contribute.
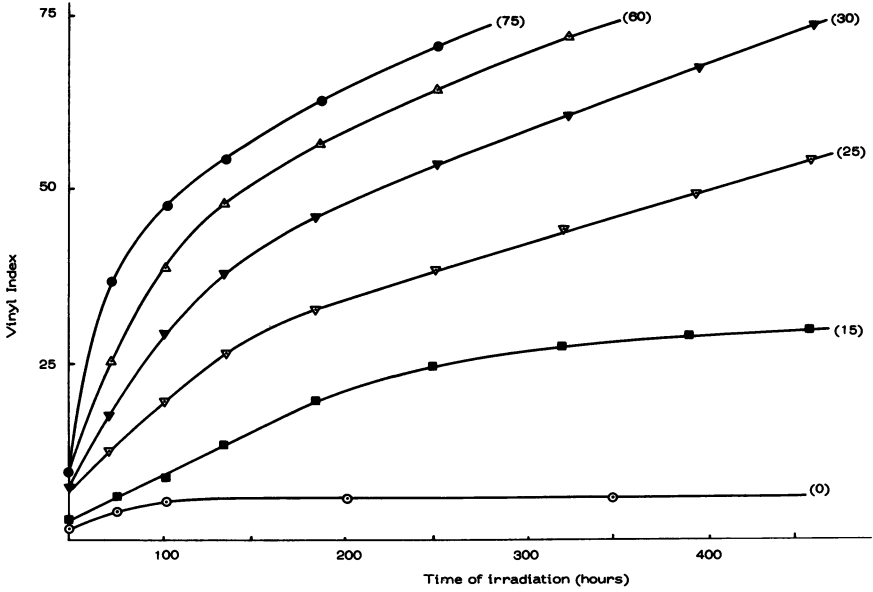
Figure 7.   Variation of vinyl index with irradiation time for LDPE processed for varying times. Processing times in parenthesis.
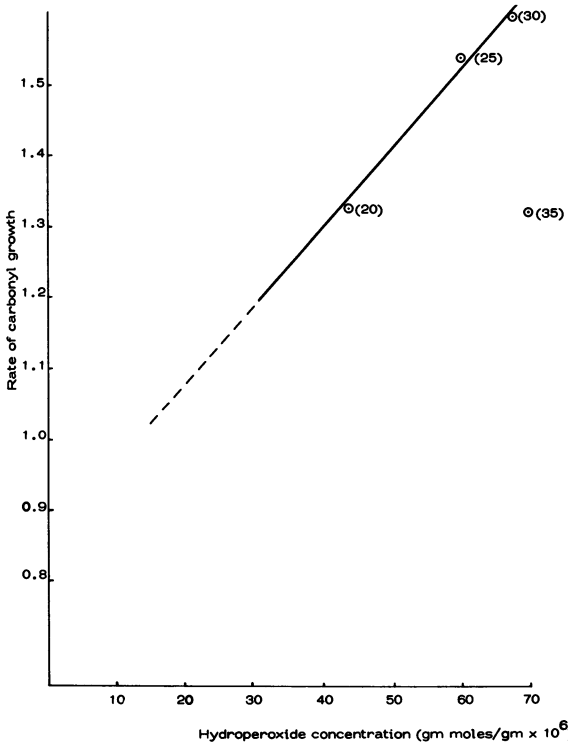
Figure 8.   Variation of carbonyl formation rate (from Figure 6) during irradiation with initial hydroperoxide content for processed LDPE. Processing times in parenthesis, mins at 160°C.

(a)   Olefin triplet and oxygen perturbed triplet
activation

There is evidence that even in the complete absence
of oxygen, double bonds may be activated by uv
irradiation (300 nm) to become much more reactive
to oxygen (34).   In the presence of oxygen this
process is probably accelerated by displacement
of the triplet absorption to longer wavelength (35).
However, if this process made a significant
contribution in practice, the disappearence of
vinylidene would show auto-accelerating behaviour (35).
This is never observed in unstabilised thermally
formed samples.   Even when formed by compression
moulding without previous mixing, the vinylidene group
disappears rapidly without an induction period
It seems unlikely then that direct activation of
polyolefins by light will be important in practice.

(b)   Singlet oxygen

It is well known that a variety of chromophores can
transfer triplet excitation energy to oxygen and it
has been suggested (15,17,18,20) that singlet oxygen
formed in this way might react with unsaturated
groups present in polyolefins, or even with the
saturated carbon atom to form hydroperoxides.   The
most likely chromophore to fulfil this function in
polyethylene would seem to be carbonyl and although
the present work suggests that this is not important
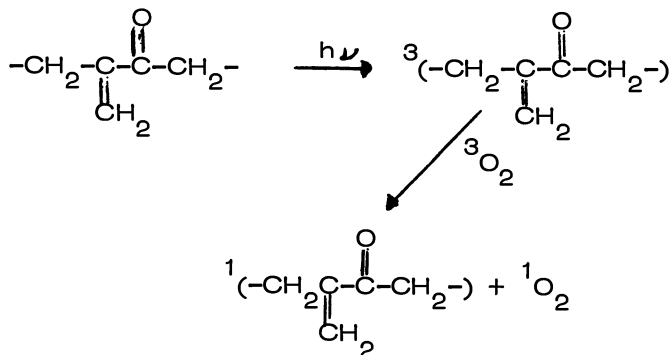
itself as a photo-initiator in processed LDPE this
could be a consequence of its effectively quenching
by triplet oxygen.

The effect of singlet oxygen on LDPE fabricated film
was therefore studied. The film was placed within a
few cms of the singlet oxygen source for six hours.
At the end of this time, no change could be observed
in the vinylidene concentration, no hydroperoxide
could be detected either by chemical analysis or by
IR spectroscopy and no additional carbonyl was
formed (31). On irradiation, vinylidene disappearence
and carbonyl formation rates were identical to the
control and the time to embrittlement was the same.
Detailed studies in model olefins have shown that
vinylidene and vinyl compounds are relatively unreactive
toward singlet oxygen compared with tri-alkyl ethylenes (36).

Ozone

Ozone reacts with double bonds to give ozonides
which are peroxidic in nature and hence might be
potential initiators for photo-oxidation. A film of
LDPE exposed to ozonised oxygen for 6 hours
showed a very rapid increase in carbonyl concentra-
tion which increased with time of exposure to ozone (31).
Vinylidene concentration was, however, unaffected
and peroxides could not be detected. On uv irradiation,
t he rate of carbonyl growth appeared to be almost
identical to the control. Although the results are
not conclusive, ozone appears to be a potentially
more important initiator than singlet oxygen and further
studies are in progress.

Effect of metal complex uv stabilisers

In view of the conclusion that hydroperoxides are
important photo-initiators it is important to
evaluate the relative contribution of uv screening,
peroxide decomposition, triplet quenching and
kinetic chain-breaking to the mechanism of action
of typical nickel complex stabilisers. Nickel
dibutyl dithiocarbamate (III, R=n.Bu, M = Ni) was
selected as representative of the peroxide decomposers

(9,22) and a nickel acetophenone oxime (IX) as
representative of the 'quenchers' (13,19).

IX

(NiOx)
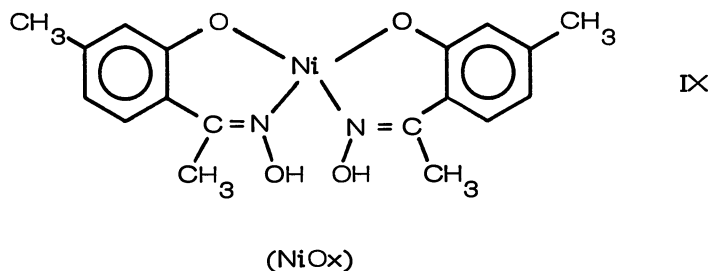
Both compounds were examined as additives (0.2%) and
as screens at equivalent screening effectiveness in HD
polyethylene (Figures 9 and 10). Both were more
effective as additives than as screening agents,
particularly so in the case of the nickel dithio-
carbamate (NiDBC). This accords with similar
studies in polypropylene. Of greater interest is
the shape of the carbonyl growth curves (Figures 9
and 10) which, except in the case of the NiDBC stabilised
film, all show the inflexion which has already been
observed in the case of LDPE without additives
(Figure 6). The NiOx seems to have a slight retarding
effect on the initial part of the carbonyl formation curve
which is due to hydroperoxide photolysis when used as
a screen. When used as an additive however, hydroperoxide
derived carbonyl is considerably retarded. NiDBC has
a similar effect to NiOx as a screen but completely
removes the hydroperoxide derived carbonyl growth curve
when it is used as an additive. This is consistent with
the known behaviour of NiDBC as a peroxide decomposing
antioxidant and indeed no hydroperoxide can be detected
in LDPE on extended processing when NiDBC is present
in the system (31). This leads to a similar induction
period in carbonyl development which is shown in
Figure 11. The lower initial carbonyl concentration
after processing is evident even for a relatively low
concentration of NiDBC. NiOx is not a peroxide
decomposer and does not show this effect. This
metal complex appears to behave similarly to other
metal complexes during processing (5 mins at 160°C)
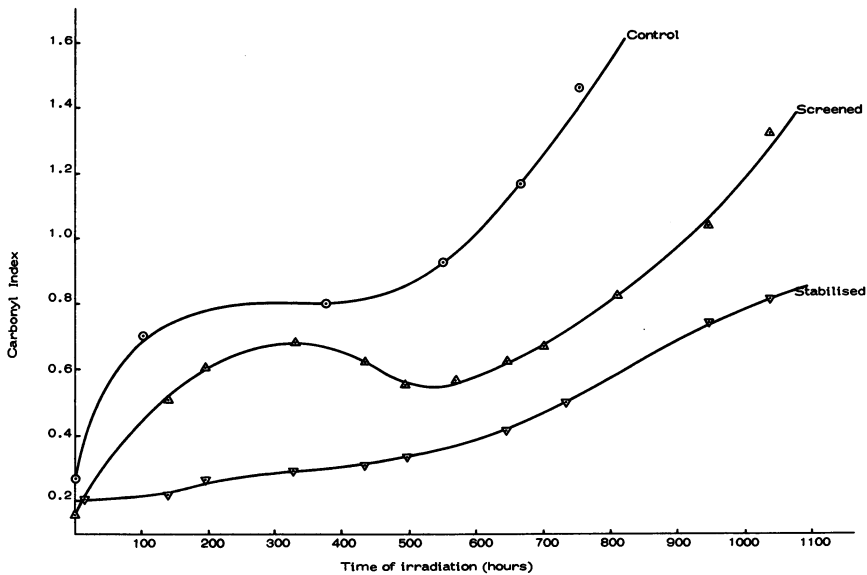
Figure 9. *Effect of NiOx as a screen and as an additive (0.2%) at equivalent screening effectiveness in HDPE*
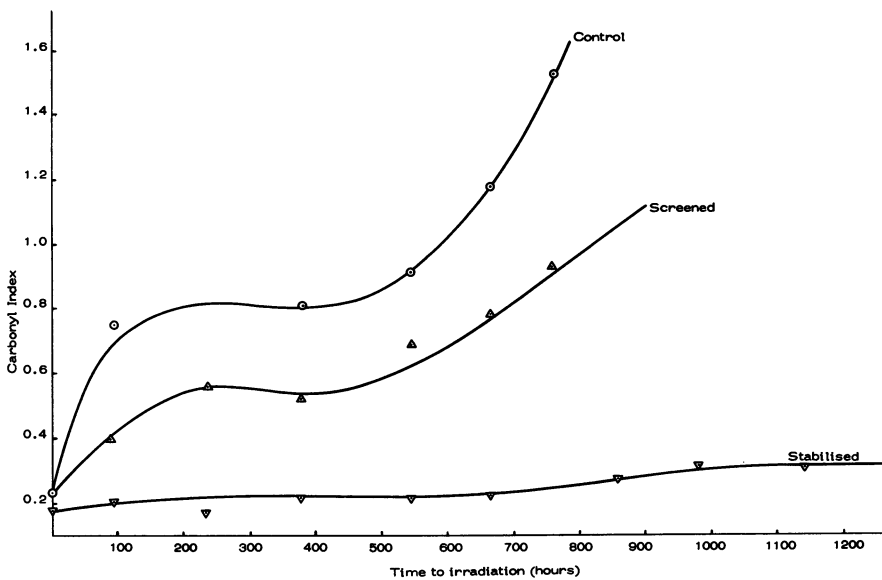
Figure 10. *Effect of NiDBC as a screen and as an additive at equivalent screening effectiveness in HDPE*

but it appears to retard photo-oxidation, although not as markedly as NiDBC at the same concentration.

The effect of the nickel complexes on vinylidene disappearence is striking (see Figure 12). NiDBC is a powerful uv antioxidant which introduces an induction period in the photo-oxidation of vinylidene even in heavily processed polymers. This induction period is related to NiDBC concentration (31) and this fact is consistant with the view previously proposed that the dithiocarbamates are powerful peroxide decomposing antioxidants in both thermal and uv oxidation (9,22). In this respect they resemble the cyclic phosphates which are again both powerful thermal stabilisers and effective uv stabilisers (25). Non-antioxidant metal complexes, of which ferric acetylacetonate (Fe(acac)$_3$) is typical, accelerate the oxidative destruction of vinylidene and the uv degradation of the polymer. Ferric dibutyl dithio-carbamate (FeDBC) shows features of both systems in that it functions as a protective agent for vinyli-dene both during processing and initially during uv exposure but is converted sharply at the end of the induction period to a powerful uv pro-oxidant (22). This behaviour parallels the function of the same additives in carbonyl formation and it appears that the effectiveness of a peroxide decomposing uv stabiliser can be predicted by a detailed study of the change in vinylidene unsaturation in the early stages of uv exposure.

Studies in model systems

Although it is evident from the above studies that the dithiocarbamate uv stabilisers function primarily as peroxide decomposers and only to a minor extent at uv absorbers, it is not clear to what extent they act as triplet quenchers. In the case of NiOx, it is known that this is not a hydroperoxide decomposer (37) and this is confirmed in Figure 11 which shows that it does not inhibit thermal oxidation to carbonyl and unlike NiDBC, its main effect in uv degradation is to retard the photo-oxidation process. In order to study the behaviour of these complexes in photo-
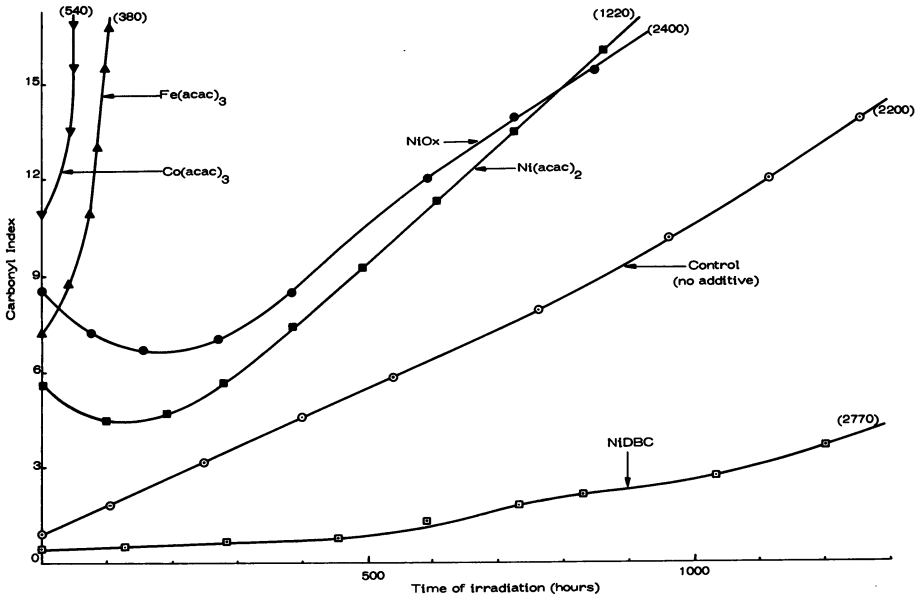
Figure 11. Effect of metal chelates (0.1%) carbonyl formation during irradiation of LDPE. Hours to embrittlement in parenthesis.
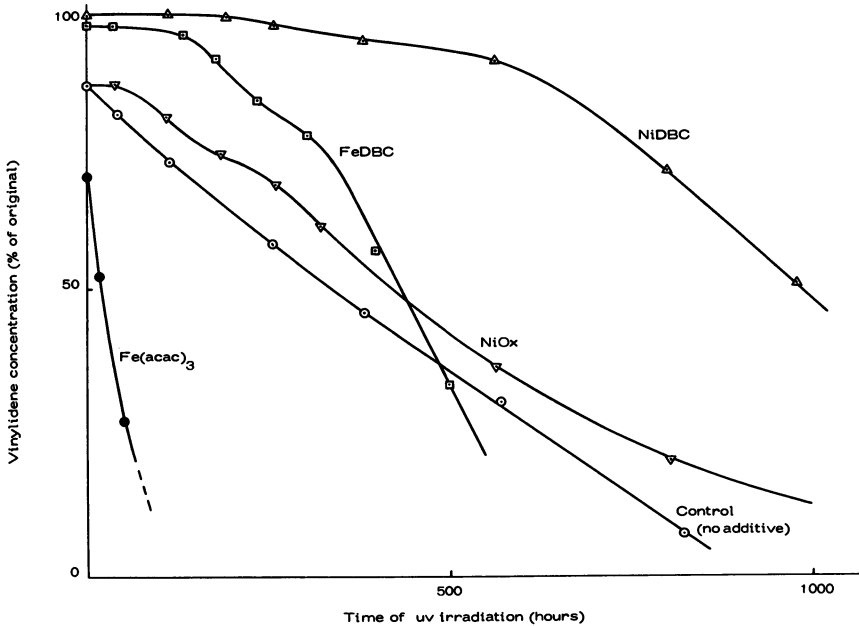
Figure 12. Effects of metal chelates (0.025%) on vinylidene concentration during photooxidation of LDPE

oxidations initiated by hydroperoxide and ketone respectively it is necessary to resort to model compounds since it is not possible to incorporate NiDBC and hydroperoxide together into polyethylene due to their rapid chemical interaction. Figure 13 compares the effectiveness of NiDBC as an external uv screen and as an additive at equivalent screening effectiveness for cumene photo-oxidation (38). Cumene hydroperoxide and benzophenone were used as initiators, the concentrations of photo-initiators in the control (non-photo-stabilised) experiments being adjusted to give the same rate of oxidation. As might be anticipated, the effect of NiDBC as an external screen was to reduce both hydroperoxide and ketone initiated oxidations by the same amount. When used as an additive, however, the behaviour was quite different. In the benzophenone initiated system it behaved as a screening agent only, whereas in the hydroperoxide initiated system it behaved initially as a screen but the photo-oxidation then auto-retarded until it eventually stopped completely. Whereas in the screening experiments the hydroperoxide concentration increased, in the additive system initiated by hydroperoxide it decreased to zero (37). This is convincing evidence that NiDBC behaves primarily as a peroxide decomposer. In a normally processed polymer, the Lewis acid catalyst known to be produced will be formed by thermal oxidation during processing. Physical screening plays a minor role and triplet quenching does not appear to be of significance.

A similar experiment was carried out with NiOx (Figure 14) (39). Again in the benzophenone initiated system this stabiliser behaved only as a screening agent and no evidence was found that either triplet carbonyl quenching or singlet oxygen quenching make a significant contribution to the mechanism. In the hydroperoxide initiated photo-oxidation NiOx shows an additional retarding effect. This behaviour is typical of the behaviour of a chain-breaking antioxidant in a peroxide initiated system. The mechanism of this chain-breaking process which has also been
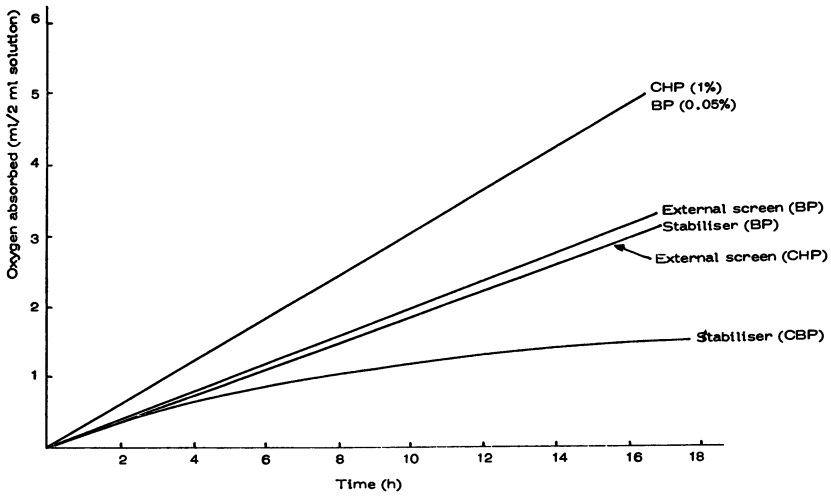
Figure 13. Effect of NiDBC as uv stabilizer (0.025%) and as an external screen at equivalent screening effectiveness in cumene
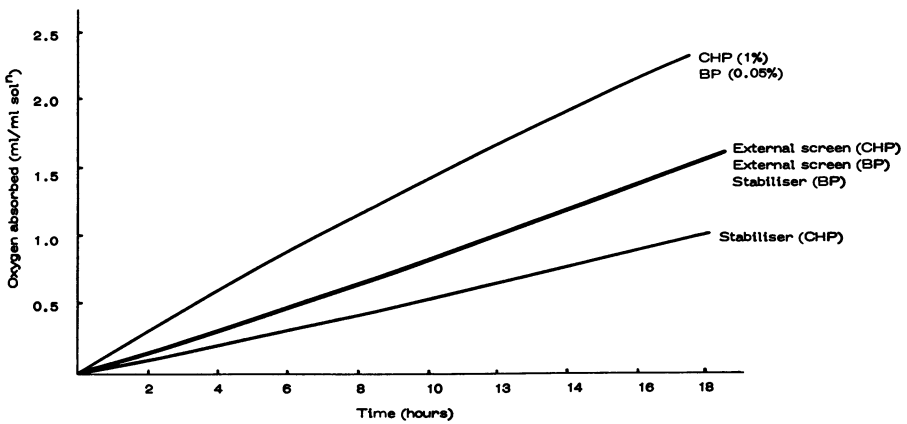
Figure 14. Effect of NiOx as uv stabilizer (0.025%) and as external screen at equivalent screening concentration in cumene

reported (<u>40</u>) for other nickel complexes derived from
phenols, is being investigated in detail.

I gratefully acknowledge the contribution made to
these studies by my colleagues Dr M U Amin,
Miss R P R Ranaweera and Mr L M K Tillekeratne.

References

1.   Autoxidation and Antioxidants, Ed W O Lundberg,
     Interscience, New York, 1961

2.   G Scott, Atmospheric Oxidation and Antioxidants,
     Elsevier, London and New York, 1965.

3.   Polymer Stabilisation, Ed WL Hawkins, Wiley-
     Interscience, New York, London, 1972

4.   Ref 2, Chapters 4 and 5.

5.   G Scott, Chem and Ind, <u>7</u>, 271, (1963)

6.   Ref 2, p 180

7.   H J Heller, Europ Polym J, Supplement,
     105, (1969)

8.   H J Heller, and H R Blattman, Macromolecular
     Microsymposia, X & XI, 141, Prague, 1972,
     (IUPAC), Pure and App Chem, No 1 & 2, <u>36</u>,
     (1973)

9.   D C Mellor, A B Moir and G Scott, Europ
     Polym J, <u>9</u>, 219, (1973)

10. G V Hutson and G Scott, Chem and Ind, 725,
     (1972)

11. G V Hutson and G Scott, Europ Polym J, <u>10</u>,
     45, (1974)

12. G Scott, Macromolecular Chemistry (IUPAC),
     <u>8</u>, 319, (1973)

13. P J Briggs and J F McKellar, J App Polym Sci, <u>12</u>, 1825, (1969)

14. J C W Chien and W P Connor, J AmChem Soc, <u>90</u>, 1001, (1968)

15. A M Trozzolo and F H Winslow, Macromolecules, <u>1</u>, 98, (1968)

16. J P Guillory and C F Cook, J Polym Sci, A1, <u>9</u>, 1529, (1971)

17. M L Kaplan and P E Kelleher, J Polym Sci, <u>139</u>, 565, (1971)

18. J Flood, K E Russell and J K Wan, Macromolecules, <u>6</u>, 669, (1973)

19. A Adamczyk and F Wilkinson, J Chem Soc, Farad II, <u>68</u>, 2031, (1972)

20. D J Carlsson, T Suprunchuk and D M Wiles, Macromolecules, <u>5</u>, 659, (1972), J Polym Sci, <u>B11</u>, 61, (1973)

21. J H Chaudet and J W Tamblyn, SPE, Trans <u>1</u>, 57, (1961)

22. M U Amin and G Scott, Europ Polym J., <u>10</u>, 1019, (1974)

23. Ref 2, p 216

24. J D Holdsworth, G Scott, and D Williams, J Chem Soc, 4692, (1964)

25. G V Hutson and G Scott, J Polym Sci, Symp No 40, 67, (1973)

26. G Scott, Pure and App Chem, <u>30</u>, 267, (1972)

27. K J Humphris and G Scott, J Chem Soc, Perkin II, 617, (1974)

28. G S Hammond and R P Foss, J Phys Chem, <u>68</u>, 3739, (1964)

29. M U Amin and G Scott and L M K Tillekeratne, Europ Polym J, <u>11</u>, 85, (1975)

30. D J Harper and J F McKellar, Chem and Ind, 848 (1972)

31. G Scott and L M K Tillekeratne, unpublished work

32. D J Carlsson and D M Wiles, Macromolecules, <u>2</u>, 587, (1969)

33. G H Hartley and J E Guillet, Macromolecules, <u>1</u>, 169, (1968), F J Golemba and J E Guillet, Macromolecules, <u>5</u>, 63, (1972)

34. A Ghaffar, A Scott and G Scott, Europ Polym J, in press

35. J C W Chien, J Phys Chem, <u>69</u>, 4317, (1965)

36. N A Khan and G Scott, unpublished work

37. R P R Ranaweera and G Scott, unpublished work

38. R P R Ranaweera and G Scott, J Polym Sci, in press

39. R P R Ranaweera and G Scott, Chem and Ind, 774, (1974)

40. D J Carlsson and D M Wiles, J Polym Sci, Polym Chem Ed, <u>12</u>, 2217, (1974)

Influence of UV Irradiation on the Stability of Polypropylene and Blends of Polypropylene with Polymethyl methacrylate

N. GRASSIE and W. B. H. LEEMING

Department of Chemistry, University of Glasgow, Glasgow G12 8QQ, Scotland

The volatile products of thermal degradation of polypropylene
(PP) under vacuum in the temperature range 300-360°C comprise a
complex mixture of saturated and unsaturated hydrocarbons. Under
u.v. radiation at these temperatures (photothermal degradation),
the general pattern of products is similar but the rate is in-
creased, ehtylene appears as a minor product and the relative
amount of methane is very much greater, especially as the tempera-
ture is decreased below 300°C. Energies of activation of the
thermal, photothermal and photoreactions are 50.1, 33.9 and 11.7 k
cal mole^{-1} respectively.
    The molecular weight of PP increases under u.v. radiation at
20°C but decreases at 200°C, the cross-over point being approxi-
mately 100°C. This irradiated polymer is less stable thermally.
    Thermal volatilization analysis (TVA) of blends or mixtures
of PP and poly(methyl methacrylate) (PMMA) reveals that the PMMA
component tends to be stabilized and the PP destabilized. Pre-
irradiation of blends strongly suppresses the yield of monomeric
methyl methacrylate but methyl methacrylate units appear in the
chain fragment fraction.
    These observations are discussed from a mechanistic point of
view.

Introduction

Interest in the susceptibility of polypropylene (PP) to deg-
radation, especially by heat, light, oxygen and combinations of
these agencies, has kept pace with the increasing commercial
application of this material. The purely photo (1-5) and thermal
reactions (6) which occur, have been studied in isolation from
one another, and it is clear that similar radicals are involved
as intermediates in the overall processes. Previous work on
acrylate and methacrylate polymers and copolymers (7-8) has dem-
onstrated that the superficial differences in overall degradation
mechanism may be attributed to the different ways in which the
same primarily produced radicals react in the solid and liquid

phases in which photo and thermal reactions respectively occur. These two aspects of degradation can be linked, however, by studying the reactions which occur under photothermal conditions (9), that is, by initiating degradation by u.v. radiation at temperatures above the melting point of the polymer and up to or even above the degradation threshold temperature. Thus, although the reaction is photoinitiated, the subsequent steps occur in the same environment as purely thermal degradation. In the acrylate and methacrylate series, combined studies of this kind have led to a more complete understanding of both photo and thermal reactions.

The reactions which are induced by pairs of different degradation agencies may also be clarified by studying the influence of one on the other. For example, the decrease in the thermal stability of poly(methyl methacrylate) (PMMA), as a result of pre-irradiation, has been clearly shown to be due to photo-induced chain scission which results in chain terminal unsaturation at which subsequent thermal decomposition is readily initiated (10).

The experiments described in the first part of this paper thus seek to extend our knowledge of the degradation processes which occur in PP, first, by linking photo and thermal processes through photothermal studies and second, by observing the effect of pre-irradiation on subsequent thermal degradation.

The comparatively recent application of polymer blends or mixtures has significantly increased the range of physical properties available to the plastics technologist. Blending has been used, for example, to improve processing characteristics and especially to increase the toughness and impact resistance of commercial materials. The high impact polystyrenes and ABS polymers are among the earliest and best known examples of an ever increasing range of products. Thus there has been considerable interest in the physical properties of these materials, but very much less is known about the chemical interactions which occur between the constituents, especially as they affect stability and degradation properties. Richards and Salter (11) have shown that in blends of polystyrene and poly(α-methyl styrene), radicals produced when the less stable poly(α-methyl styrene) thermally degrades can initiate degradation in the polystyrene at temperatures at which it is normally stable. McNeill and his colleagues have similarly reported on the changes in mechanism and products of degradation which occur when mixtures of poly(methyl methacrylate) and poly(vinyl chloride) (12-15), poly(methyl methacrylate) and polychloroprene (16), poly(vinyl chloride) and chlorinated rubber (17), and poly(vinyl chloride) and poly(vinyl acetate) (18) are thermally degraded in presence of each other.

Since commercial polymers are frequently applied outdoors in sunlight, it was clearly of interest to extend these studies by investigating the possible occurrence of interactions between the constituents of blends under ultra-violet radiation. The system PP-PMMA was chosen for study because of the known susceptibility

of both polymers to radiation, because the relationship between
the thermal and photo induced reactions with occur in PP and PMMA
are now understood and because blending with PMMA has been sug-
gested as a method of improving the poor dyability of PP (19).

Experimental

The PP was supplied by Shell Research Ltd., completely free
from additives (M_v = 222,300). The PMMA (M_n = 516,000) was pre-
pared from monomer (BDH Ltd.) which was purified by washing with
sodium hydroxide solution and distilled water, followed by drying
and vacuum degassing and distillation. It was polymerized at 60°C
under vacuum with azo-di-isobutyronitrile (0.1% w/v) as initiator
and purified by precipitation three times by methanol from toluene
solution followed by vacuum drying at 60°C.

Since there is no suitable solvent for film casting of PP at
ambient temperature, discs, 1 cm in diameter and approximately
230 mμ in thickness, were prepared by placing 80 mg of the polymer
in a continuously evacuated die and compressing to 20 tons/sq cm
for 4 minutes in a Perkin-Elmer hydraulic press. Discs prepared
in this way are opaque.

In the high temperature experiments to be described, the
discs, being molten, were amorphous and transparent. For reac-
tions below the melting point of the polymer, however, the opaque
discs were melted by heating under vacuum to 200°C and cooled at
20°C. In this way, samples with reproducible transmittance of
approximately 98% of 2537Å radiation at 20°C are obtainable.

In general, unlike molecules are incompatible in the solid
phase. This, and the fact that the degree of crystallanity of the
PP may vary according to its pretreatment, means that it is essen-
tial that blends should be prepared using a standard procedure
and the best test of the achievement of reproducible blends is
probably reproducibility of experimental degradation results.
Mizutani's (19) method was used, in which a slurry of PP in an
acetone solution of PMMA was evaporated to dryness with continuous
stirring. Samples for degradation were then prepared, as above,
by forming discs by compression, followed by melting under vacuum.
In this way, translucent samples were obtained which degraded re-
producibly, both photo and thermally.

A Hanovia chromatolite lamp was used as the source of ultra-
violet radiation. This is a low-pressure mercury arc, the main
emission comprising the resonance lines at 1849 and 2537Å. The
former is completely absorbed by 1 cm of air, while the latter is
almost completely transmitted by air and 95% by silica. Thus
virtually pure 2537Å radiation impinges on the polymer. The lamp
was connected to an L.T.H. transistorized 1 kVA voltage regulator
to ensure that fluctuations in mains output did not affect
emission.

Reactions were carried out under vacuum in silica cells in-
corporating an optically flat window through which the polymer
film could be irradiated. The film, supported on a silica disc,
was placed on the bottom of the cell which was placed in a furnace
controlled at +0.5°. The temperature of the film was measured by
a Chromel-Alumel thermocouple placed inside the reaction cell in
contact with the film.

The total products may be conveniently separated into four
fractions for separate analysis, namely, permanent gases, products
volatile at 20°C, products volatile at degradation temperatures
but involatile at 20°C (chain fragment or "cold ring" fraction)
and residual polymer.

The technique of thermal volatilization analysis (TVA) has
been developed and fully described by McNeill (20). A polymer
sample is heated through a linear temperature programme from
20-500°C at 10°/minute. The volatile products are passed through
a series of five traps maintained at fixed temperatures between
0°C and -196°C and pressure of gases passing through each trap is
measured by a Pirani gauge. The Pirani gauge responses are dis-
played on a single thermogram and measure the rates of production
of products volatile at the various trap temperatures.

Molecular weights were measured viscometrically at 135°C in
decalin with 1% of 2,6-di-tert-butyl-p-cresol as stabilizer. The
Mark-Houwink equation was applied with K and α values of 1.07 x
10^{-4} and 0.80 respectively (21).

A 10 cm gas cell was used to record the infra-red spectra of
gaseous products. The spectra of chain fragments were measured
by casting a thin film from warm toluene on a KCℓ plate. The
spectra of polymer residues were recorded using the KCℓ disc
technique. All spectra were run on a Perkin-Elmer 257 Grating
Spectrophotometer.

Ultra violet spectra were obtained using a Unicam SP800
instrument.

An AEI MS10 Residual Gas Analyzer was used to record mass
spectra of permanent gases. Spectra of other gaseous products
were obtained using an AEI MS12 instrument.

Gℓc analyses were carried out on a Microtek GC 2000R instru-
ment with dual columns, packed with 30-60 mesh silica gel, a flame
ionization detector and a linear temperature programmer.

The PP and PMMA in degraded samples were separated by dis-
solving the degraded blend in p-xylene under nitrogen and allowing
the hot solution to cool slowly. The resulting suspension was
poured into methanol and the precipitate filtered off, washed with
methanol and dried in a vacuum oven. The material thus obtained
was extracted with acetone in a Soxhlet extractor for 20 hours
under nitrogen, the PMMA being soluble and the PP insoluble.

Results

1. Comparison of Thermal and Photothermal Degradation of Poly-
    propylene (200–356°C)

Tsuchiya and Sumi (6) have thermally degraded polypropylene
in the temperature range 360–400°C and have made a detailed anal-
ysis of all products with 1–12 carbon atoms. On this basis, a
decomposition mechanism has been proposed. Initiation occurs by
random scission of the main chain. The radicals thus formed
undergo transfer reactions most readily at tertiary carbon atoms
but the distribution of products indicates that intramolecular
transfer to both third and fourth carbon atoms is particularly
important.
    In the present work, a similar complex mixture of saturated
and unsaturated hydrocarbons was obtained. Detailed analyses of
the type described by Tsuchiya and Sumi (6) were not carried out,
however. Instead, attempts were made to highlight the most sig-
nificant similarities and differences between the characteristics
and products of the thermal and photothermal reactions. The
melting point of polypropylene is in the region 165–180°C and
thermal degradation, as revealed by the evolution of volatile
products, becomes significant a little below 300°C. Thermal and
photothermal degradations were therefore studied in parallel over
the range 200–356°C in order to observe the interplay of the photo
and thermal components of the overall reaction.
    The infra-red spectra of the permanent gases from all degra-
dations showed only absorptions at 3018 cm^{-1} and 1304 cm^{-1} char-
acteristic of methane.
    Apart from an additional low intensity absorption at 950 cm^{-1},
attributed to ethylene, in the products of photothermal degrada-
tion, the infra-red spectra of products volatile at 20°C from all
thermal and photothermal degradations in the range 300–356°C were
identical and consistent with a complex mixture of saturated and
unsaturated hydrocarbons, as shown by Tsuchiya and Sumi (6). In
photodegradation at 200°C, which is below the threshold for ther-
mal degradation, the only identifiable product is methane. Gas
chromatographic separation of this product fraction confirms that
ethylene is always formed during photothermal, but never during
thermal degradation.
    Mass spectra of volatile products from photothermal and ther-
mal degradations at 354°C and of photothermal degradation at 200
and 250°C are illustrated in figure 1. They are all typical of a
mixture of hydrocarbons with the main peaks separated by 14 units
(CH_2). They are generally similar, except that as the degradation
temperature is decreased, the lines at mass numbers 15 and 16
become relatively much more intense. These two lines, as well as
forming part of the breakdown pattern of higher hydrocarbons, are
characteristic of methane. Thus it may be concluded that the
relative proportions of methane in the volatile products

progressively increases as the temperature of photodegradation is decreased below the thermal degradation threshold.

The infra-red spectra of all chain fragment fractions from photothermal and thermal degradations are similar to that of un-degraded polypropylene, apart from the fact that small additional absorptions appear at 3080 cm^{-1}, 1650 cm^{-1} and 888 cm^{-1}, all of which can be attributed to unsaturation. This is due to the inter and intramolecular transfer steps which are an integral part of the mechanism of Tsuchiya and Sumi (6), and which lead to chain scission and terminal unsaturation. The number average molecular weight of the cold ring fraction is approximately 850 (20 propy-lene units) in all cases, which suggests that it is formed pre-dominantly by intermolecular transfer.

The rate of degradation, as measured by rate of loss in weight, is always greater for photothermal than for thermal degra-dation at the same temperature. The increment of rate which may be attributed to photoiniation, calculated by subtracting the thermal from the photothermal rate, is represented in figure 2 as a function of temperature. The points at 200 and 250°C represent extents of photothermal degradation as measured, since significant thermal degradation does not occur at these temperatures. These rates are represented in the form of Arrhenius plots in figure 3. Energies of activation may thus be deduced as follows: Thermal, 50.1 k cal/mole; photothermal (300-356°C), 33.9 k cal/mole; photo (200-356°C), 11.7 k cal/mole. The data obtained at 200 and 250°C clearly give a reasonably good linear relationship with the photo increment of the overall rate at higher temperatures indicating that the photo and thermal reactions may be regarded as distinct from one another and that the total photothermal reaction is best represented by the dotted curve which is asymptotic with the pure thermal and pure photo reactions at high and low temperatures respectively.

2.   Photodegradation of Polypropylene at Low Temperature
       (20-200°C) and its Effect on Subsequent Thermal Degradation

The effects of irradiation in the temperature range 20-200°C were assessed by molecular weight analysis and from the weight loss characteristics on subsequent thermal degradation.

The molecular weight of polypropylene is found to increase on irradiation at 20°C, but to decrease at 200°C. No change due to purely thermal degradation occurs even at 200°C. In figure 4, molecular weights of samples irradiated for 41 hr are plotted as a function of temperature of irradiation. These data confirm the direction of change of molecular weight at high and low tempera-tures and indicate that the change over occurs at approximately 100°C.

Figure 5 compares Thermal Volatilization Analysis (TVA) ther-mograms for unirradiated and preirradiated polypropylene. The lack of coincidence of the traces in each thermogram indicates a
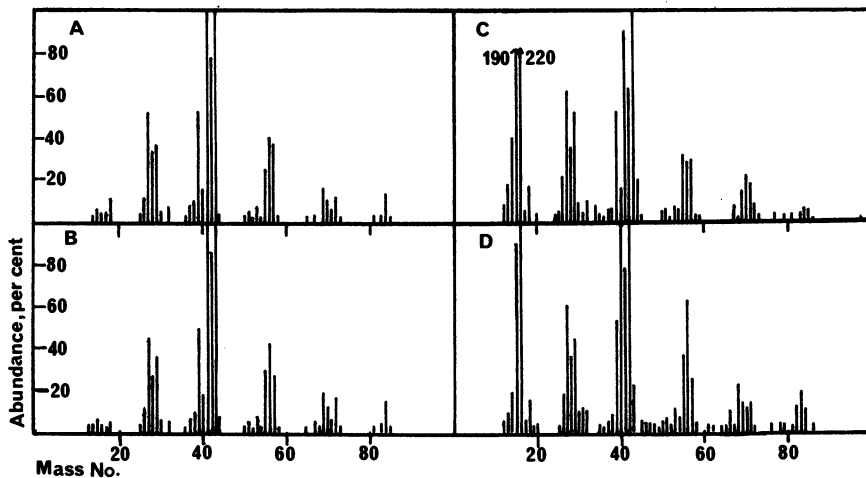
Figure 1.   Mass spectra of volatile products from photothermal and thermal degradations of PP. A, thermal at 354°C; B, photothermal at 354°C; C, photothermal at 200°C; D, photothermal at 250°C.
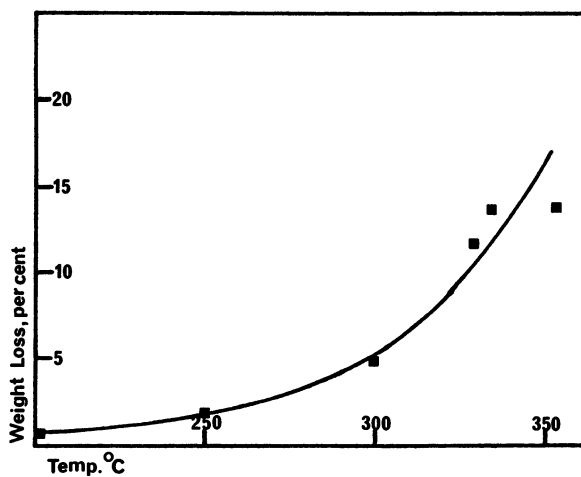
Figure 2.   Weight loss of PP after irradiation for 15 hr as a function of temperature. Points represent the difference between extents of thermal and photothermal degradations at these temperatures.
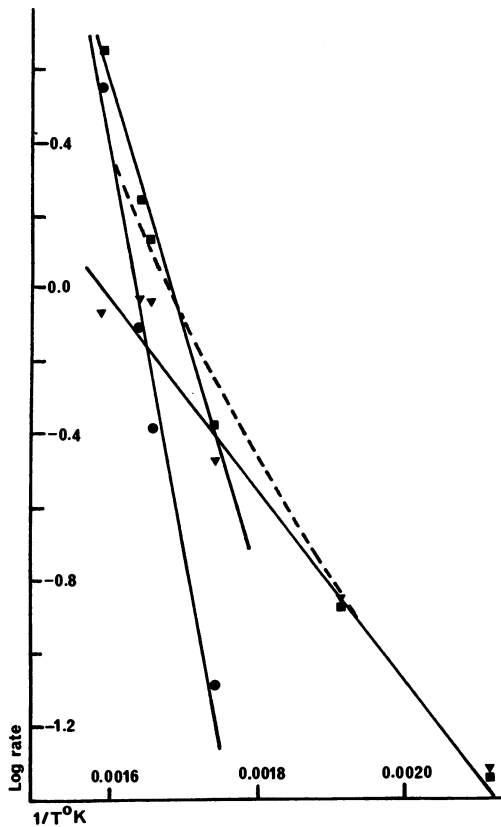
Figure 3.   *Arrhenius plots for PP degradation.* ●, *thermal*; ■ *photothermal*; ▼, *photo.*
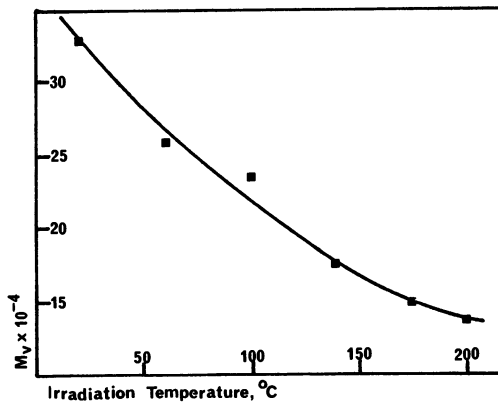
Figure 4.   *Molecular weight of PP after irradiation for 41 hr as a function of irradiation temperature*

complex mixture of products with a wide range of volatilities, but
the fact that the rate maximum on each trace occurs at the same
temperature is strong evidence that all the volatile products are
formed concurrently in reactions which follow from a common in-
itiation step. The distribution of products from the preirradi-
ated polymer is closely similar and the rate maximum occurs at
the same temperature. The only difference between the two thermo-
grams is that volatile products begin to appear at a lower tem-
perature from the preirradiated polymer. Isothermal degradation
confirms the TVA evidence that preirradiation destabilizes PP to
thermal degradation. Thus figure 6 demonstrates that weight loss
after 17 hours at 335°C increases continuously with time of pre-
irradiation and that the effect is greater the higher the tempera-
ture at which pre-irradiation was carried out.

3. Thermal Degradation of Blends of Poly(Methyl Methacrylate)
    and Polypropylene

    Mizutani and his colleagues (19) have reported that the rad-
icals produced from thermally degrading PMMA in a mixture with PP
are effective in accelerating the breakdown of PP. This effect
has been further investigated using TVA.
    It is well established that thermal degradation of PMMA gives
almost quantitative yields of monomer in a radical chain depoly-
merization process which occurs in two stages (22). At lower
temperatures, initiation occurs exclusively by scission at un-
saturated chain terminal structures. At higher temperatures,
random scission of the polymer chain occurs. The TVA thermogram
of PMMA illustrated in figure 7A, is typical of evolution of a
single volatile product and the shape and relative position of
the −75° curve is quite specific for monomeric methyl methacrylate.
The two peaks correspond to monomer production following the two
initiation modes.
    The TVA thermogram for PP, illustrated in figure 7B, has been
discussed previously. It indicates a complex mixture of products
with a wide range of volatilities, but the fact that the rate max-
imum on each curve occurs at the same temperature is strong evi-
dence that all the volatile products are formed concurrently in
reactions which follow from a common initiation step.
    The thermogram illustrated in figure 8A was obtained using PP
and PMMA in the weight ratio 90/10 but unmixed. The principal
features of the behaviors of the individual polymers are clearly
discernible by comparison with the individual thermograms in
figure 7. There are well defined differences, however, as illus-
trated in figure 8B, when TVA is carried out on a 90/10 mixture
of the polymers. Thus a new peak ($T_{max} \sim 426°C$) appears as a
shoulder on the low temperature side of the PP peak, the position
of which is unaltered. The low temperature PMMA peak has dis-
appeared, however, and the high temperature peak is slightly dis-
placed to higher temperature.
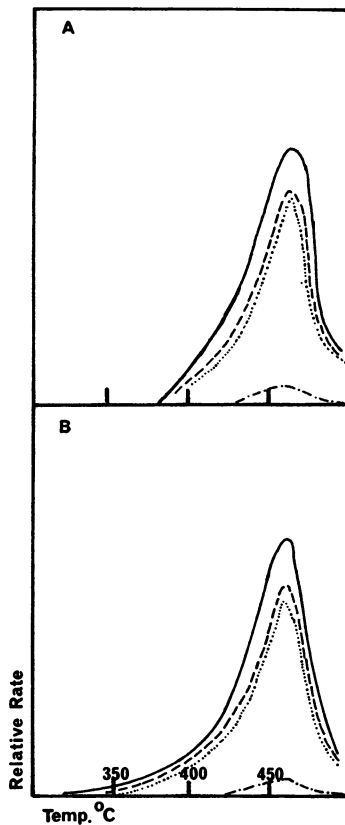
Figure 5. TVA thermograms for unirradiated (A) and preirradiated (B) PP. Trap temperatures: —, 0° and —45°C; ---, —75°C; ···, —100°C; —··—·, —196°C.
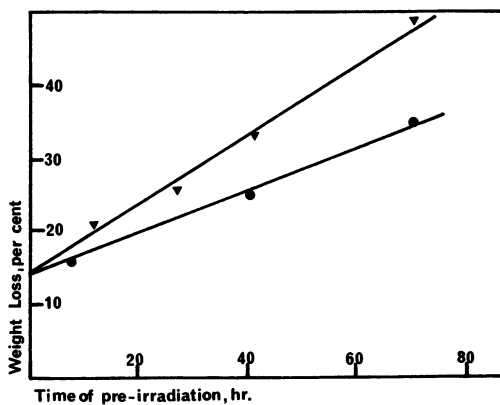
Figure 6. Weight loss in PP from thermal degradation for 17 hr at 335°C as a function of time of pre-irradiation at 20°C (●) and 200°C (▼)
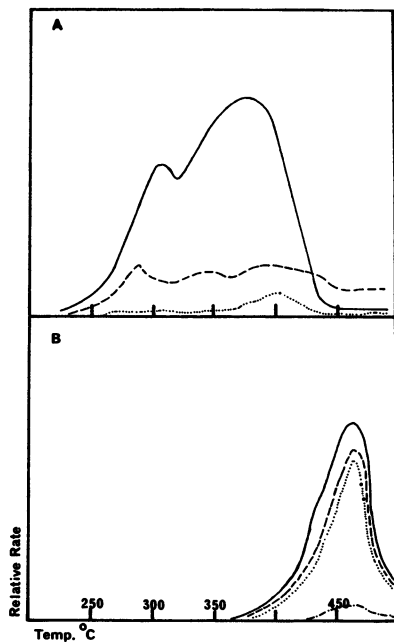
Figure 7. TVA thermograms for PMMA (A) and PP (B). Trap temperatures: —, 0° and −45°C; - - -, −75°C; ···, −100°C; -·-·, −196°C.
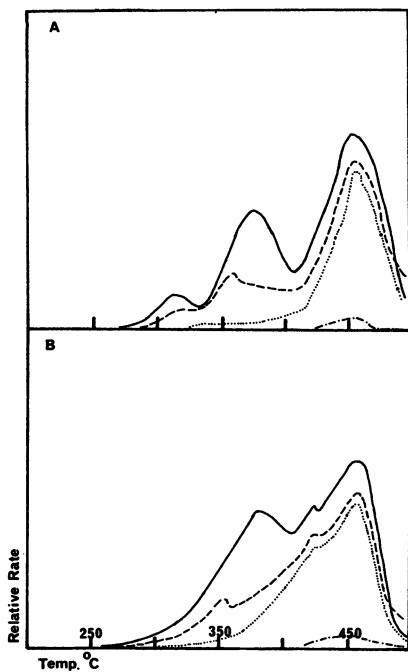
Figure 8. TVA thermograms for 90/10, PP/PMMA. A, unmixed; B, mixed.

4. Photolysis of Blends of Poly(Methyl Methacrylate) and
    Polypropylene

    At temperatures up to approximately 150°C u.v. irradiation of
PMMA in the form of thin film results in random cleavage of the
polymer molecules without depolymerization to monomer (7). The
accepted mechanism may be represented as follows:

$$\sim\!CH_2\!-\!\underset{\underset{COOCH_3}{|}}{\overset{\overset{CH_3}{|}}{C}}\!-\!CH_2\!-\!\underset{\underset{COOCH_3}{|}}{\overset{\overset{CH_3}{|}}{C}}\!-\!CH_2\!\sim$$

$$\downarrow h\nu$$

$$\sim\!CH_2\!-\!\underset{\underset{COOCH_3}{|}}{\overset{\overset{CH_3}{|}}{C}}\!-\!CH_2\!-\!\overset{\overset{CH_3}{|}}{\underset{\cdot}{C}}\!-\!CH_2\!\sim \qquad + \qquad \cdot COOCH_3$$

$$\downarrow \qquad\qquad\qquad\qquad\qquad\qquad \downarrow$$

$$\sim\!CH_2\!-\!\underset{\underset{COOCH_3}{|}}{\overset{\overset{CH_3}{|}}{C}}\!\cdot \; + \; CH_2 = \overset{\overset{CH_3}{|}}{C}\!-\!CH_2\!\sim$$
$$\qquad A$$

Volatile products
including CO, CO_2,
CH_4, methanol and
methyl formate.
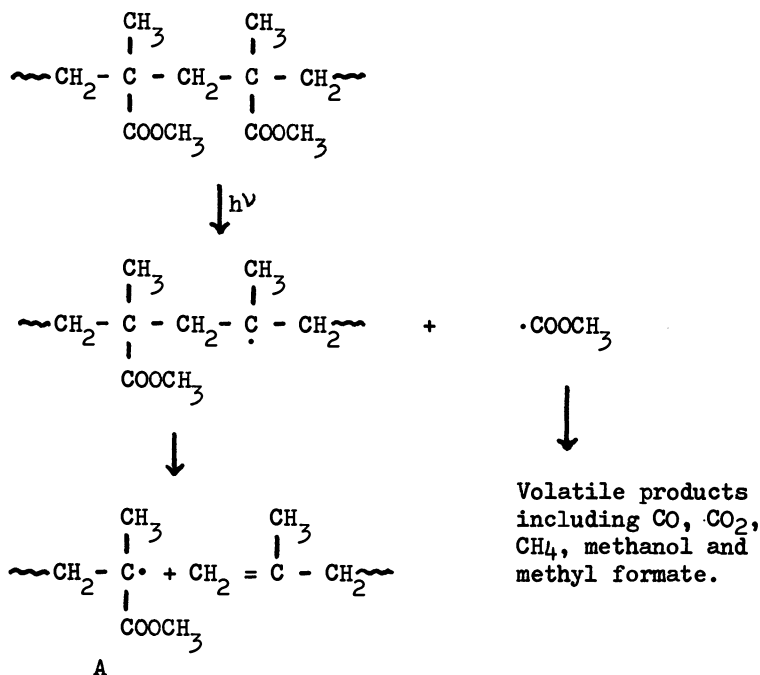
    The production of monomer by depolymerization of radical A
only occurs above the glass transition point when free diffusion
and escape become possible and at temperatures in excess of 150°C
yields of monomer become almost quantitative as in the thermal
reaction at higher temperatures.
    Similarly, volatile products are not formed in significant
quantities when PP is irradiated at temperatures up to 200°C.
However, as described above, at ordinary temperatures, the molec-
ular weight increases although the effect decreases with in-
creasing temperature until at approximately 100°C the molecular
weight remains stationary. As the temperature is further raised,
the molecular weight decreases at an increasing rate. This has
been interpreted in terms of competing combination and scission
reactions of chain side radicals

$$\text{\textasciitilde CH}_2\text{- }\overset{\bullet}{\text{CH}}\text{ - CH}_2\text{- }\overset{\displaystyle\overset{\text{CH}_3}{|}}{\text{CH}}\text{\textasciitilde}$$
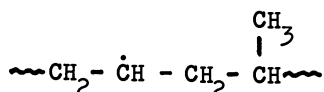
probably formed in a photocatalysis process involving chromophoric impurities in the polymer.

Irradiation of blends of PP and PMMA of various compositions at 20°C for times up to 20 hours also results in no detectable weight loss and no infra-red spectral changes. In addition, extraction by acetone is successful in removing all traces of PMMA from the irradiated blend. Thus, in spite of the fact that an increase in the molecular weight of the PP and a decrease in the molecular weight of the PMMA components indicates radical formation from both, there is no evidence of the formation of graft or block copolymers.

A blend containing 10% of PMMA was similarly irradiated at 150°C. The only significant volatile product was methyl methacrylate and the weight loss, corresponding to the amount of the PMMA blended, was complete after 5 hours. Infra-red spectral measurements indicated the complete absence of methacrylate in the residue. At all irradiation times up to 5 hours the methacrylate content of the blend is completely separable from the PP by acetone extraction. Thus, these experiments could provide no positive evidence of reaction of either PMMA radicals or methyl methacrylate monomer with PP radicals, all of which were known to be present in the system.

5.   Thermal Degradation of Pre-irradiated Blends of Poly (Methyl Methacrylate) and Polypropylene

Pure PP and blends with increasing proportions of PMMA were irradiated in vacuum at 20°C for 20 hours. The weight loss on subsequent heating for 3 hours at 354°C was used as a measure of the influence of blend composition on stability and compared with the behavior of un-irradiated materials. The results, which are illustrated in figure 9, demonstrate that while the thermal stability of pure PP is greatly reduced by pre-irradiation, the additional effect of the presence of PMMA is relatively minor.

Infra-red spectra of the products, volatile at ordinary temperatures, of the thermal degradations represented in figure 9 are a superimposition of the spectrum of methyl methacrylate monomer on that of the volatile products of the thermal degradation of polypropylene. However, the amount of methyl methacrylate, as measured by the optical density of the carbonyl peak at 1740 cm^{-1}, is strongly suppressed by pre-irradiation, as shown in figure 10.

None of the residues from these degradations had any significant carbonyl content. This is strong evidence that grafting does not occur either during pre-irradiation or subsequent thermal degradation and is at variance with Mizutani's (19) claim to have produced block and graft copolymers by thermal degradation under
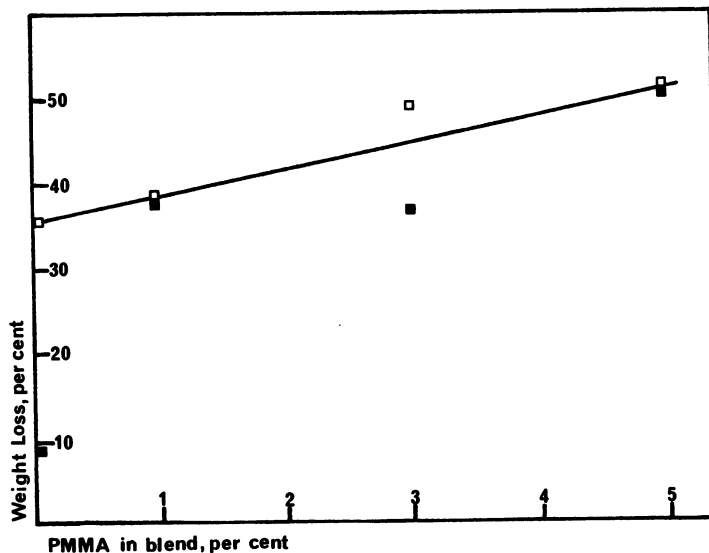
Figure 9. Weight loss, after 3 hr at 354°C, as a function of PMMA content of PP/PMMA blends. ■, unirradiated; □, pre-irradiated at 20°C for 20 hr.
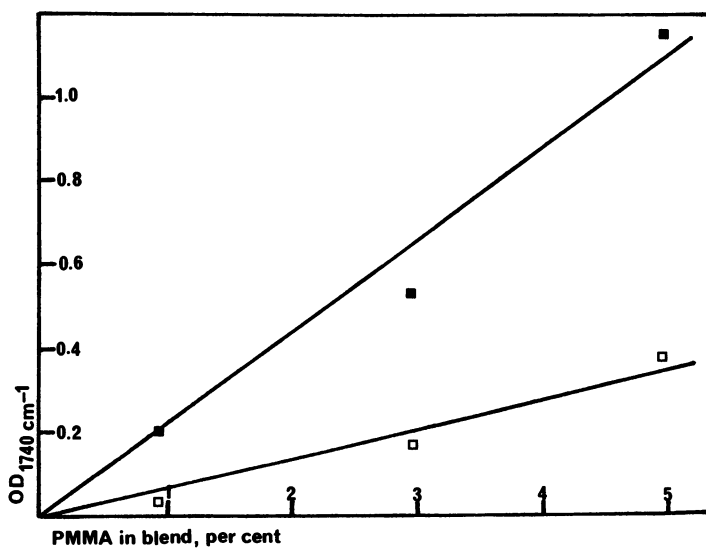
Figure 10. Optical density of the carbonyl peak at 1740 cm⁻¹ of the volatile products of degradation for 3 hr at 354°C of PP/PMMA blends as a function of blend composition. ■, unirradiated; □, pre-irradiated at 20°C for 20 hr.

similar conditions.

In the infra-red spectra of the products from these degrada-
tions, which are involatile at room temperature and which consist
of large chain fragments, the only notable differences from the
corresponding product fraction from unblended PP, are the appear-
ance of a broad band at 1735-1740 cm^{-1}, and a sharper absorption
at 1185 cm^{-1}, respectively assigned to carbon-oxygen double and
single bond stretching. The ratios of the optical densities at
1740 and 890 cm^{-1}, the latter being typical of products from un-
blended PP, were taken as a measure of the relative proportions
of methyl methacrylate and propylene residues in this fraction,
and are shown as a function of blend composition in figure 11,
from which it is clear that the effect of pre-irradiation is to
increase the methyl methacrylate unit content of the chain frag-
ment fraction.

This effect of pre-irradiation in depressing the proportion
of methyl methacrylate monomer, but increasing the methyl methac-
rylate content of the chain fragments formed during subsequent
thermal degradation, may be related to the additional observation,
illustrated in figure 12, that pre-irradiation also suppresses the
"interaction" peak (see figure 8B) which is found to contain a
high proportion of monomeric methyl methacrylate.

6.   Thermal Degradation of Blends of Polypropylene and Pre-
     irradiated Poly(Methyl Methacrylate)

In order to investigate further the role of the PMMA compo-
nent in the thermal degradation of pre-irradiated blends, a 3%
blend was prepared from unirradiated PP and PMMA which had been
photolyzed independently for 20 hours at 20°C, during which time
the number average molecular weight had decreased from 516,000 to
25,000. The TVA thermogram is illustrated in figure 13 and is
clearly more closely similar to those of non-preirradiated blends,
as in figures 8B and 12A, rather than to pre-irradiated blends, as
in figure 12B. Thus, the importance of the PP rather than the
PMMA component of the blend in determining its thermal stability
after irradiation is emphasized.

Discussion

Polypropylene. In the thermal and photothermal degradations
of PP as prepared as well as in the thermal degradation of the
pre-irradiated polymer, the general patterns of volatile products
are similar and are qualitatively accounted for in terms of the
mechanism of Tsuchiya and Sumi (6), which proposed that the com-
plex mixture of saturated and unsaturated hydrocarbons is formed
in a free radical process in which inter and intramolecular trans-
fer play a predominating role. In the photothermal reaction,
however, in addition to those products, a very much higher rela-
tive concentration of methane and an appreciable amount of
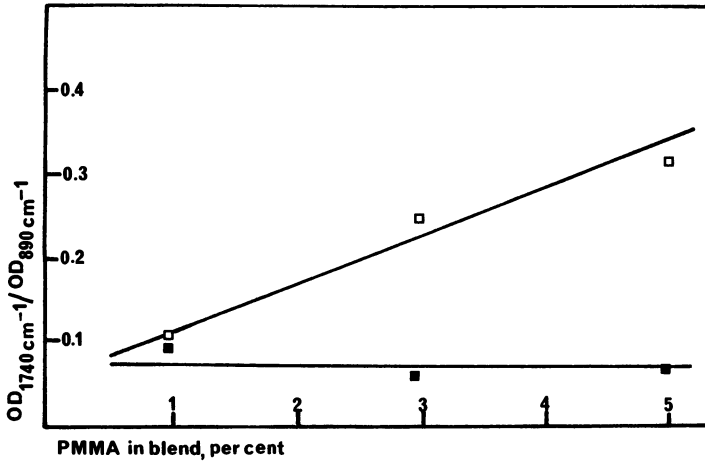
Figure 11.   Ratio of optical densities at 1740 cm⁻¹ and 890 cm⁻¹ of the chain fragment fraction from the degradation for 3 hr at 354°C of PP/PMMA blends as a function of blend composition. ■, unirradiated; □, pre-irradiated at 20°C for 20 hr.
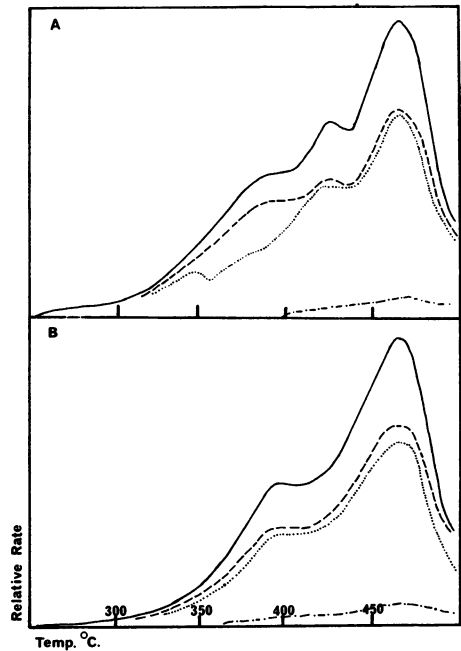
Figure 12.   TVA thermograms of a 5/95, PMMA/PP blend. A, unirradiated; B, pre-irradiated at 20°C for 20 hr.
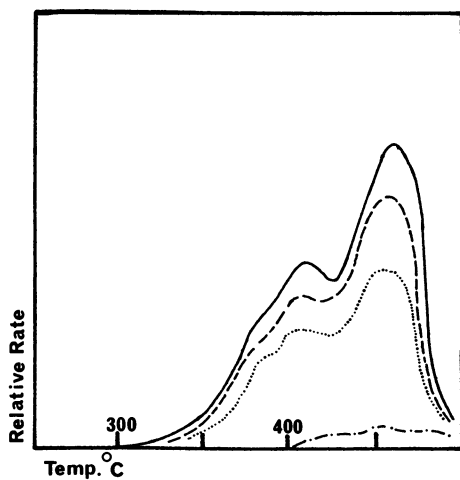
Figure 13.   TVA thermogram of a 3/97 blend of PMMA, pre-irradiated at 20°C for 20 hr, with PP

$$\sim CH_2 - CH - CH_2 - CH \cdot - CH_2 - CH - CH_2 \sim \quad (CH_3)$$

1.
$$\sim CH_2 - C \cdot + CH_2 - CH - CH_2 \sim \quad (CH_3)$$

2. / **3.** Combination (cross-linking)

$$\sim CH_2 - CH - CH_2 - CH_2 - CH_2 - CH \sim \quad (CH_3)$$

4.
$$\sim CH_2 - C \cdot - CH_2 - CH_2 - CH_2 - CH \sim \quad (CH_3)$$

5.
$$\cdot CH_2 - CH \quad / \quad \overset{CH_2}{=} CH + \cdot CH_2 - CH_2 \sim$$

6. Ethylene by Depolymerisation

7.
$$\sim CH_2 - C = CH_2 + \cdot CH_2 - CH_2 \sim \quad (CH_3)$$

8. Ethylene by Depolymerisation

Inter and intra molecular transfer leading to products as in the thermal reaction.
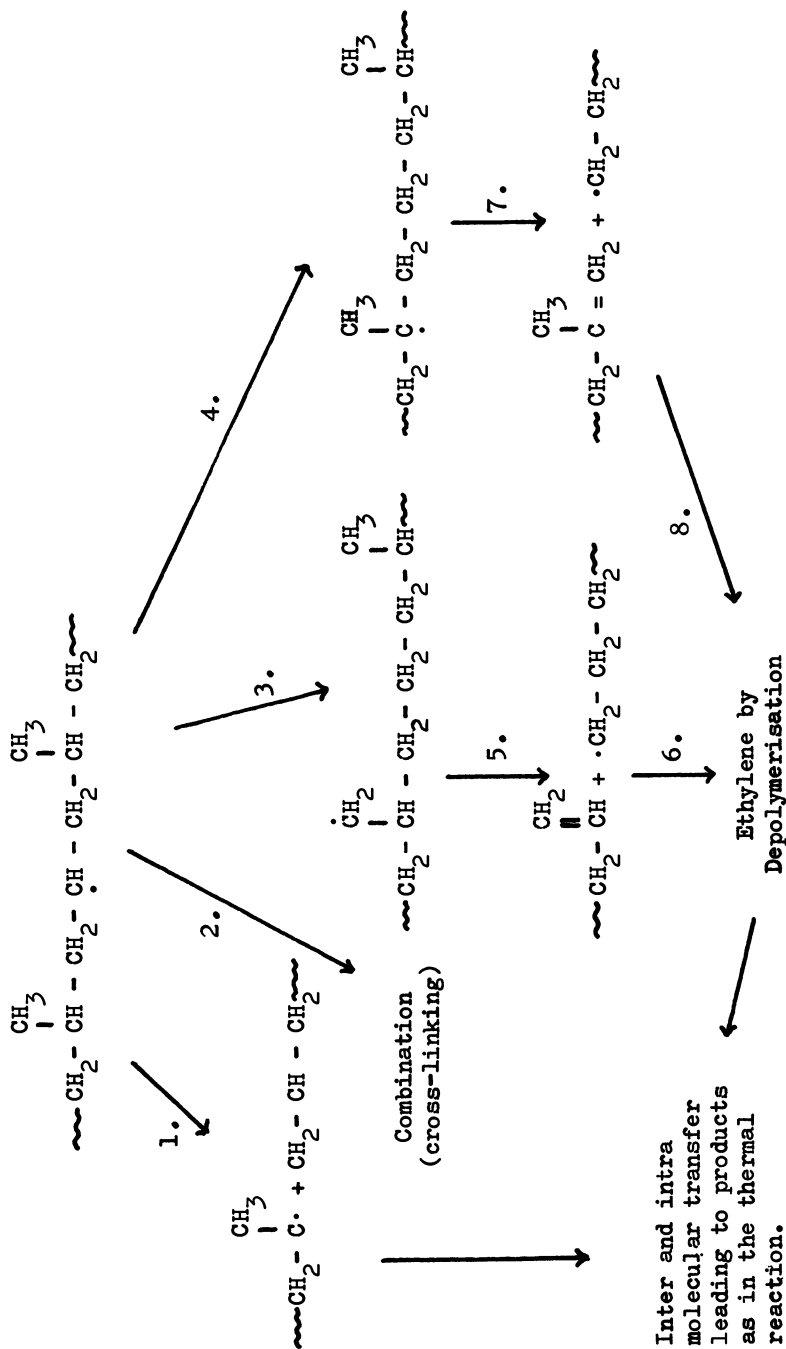
ethylene are found, which was not reported in Tsuchiya and Sumi's analysis. Ranby and Yashida (1) have reported the formation of methyl radicals on irradiation of isotactic PP with 2537Å radiation at 77°K which thus associates the formation of methane with the photoinitiation of degradation. Thus the most fundamental difference between photo and thermal degradation clearly resides in the initiation step, and the appearance of ethylene and the increased yield of methane, must be associated with this.

Since pure PP does not incorporate chromophoric groups, it is clear that photoinitiation of radical degradation processes must involve chromophoric impurities. There has been a great deal of discussion of this in the past and hydroperoxides or carbonyl structures formed by oxidation of the parent polymer and transition metal residues from the polymerization catalyst seem to be the most likely candidates. It is not appropriate to discuss this aspect in the present paper, suffice it to say that the association of methane with photoinitiation, but not thermal initiation, suggests that photoinitiation involves C–CH$_3$ bond scission to form chain side radicals in contrast to thermal initiation which involves scission of the C–C bond in the main chains.

The initial formation of chain side radicals rather than chain terminal radicals as in the thermal degradation also allows a reasonable explanation of some of the other features of the photoreaction. Thus the chain side radicals should be expected to undergo a number of competing reactions of the type shown.

The increase in molecular weight which is observed at lower temperatures is the result of reaction 2. The reactions which result directly in chain scission (reaction 1) or lead to chain scission after radical migration (reactions 3 and 4) become increasingly important as the temperature is raised. No special significance is attached to the precise temperature (100°C) at which scission begins to predominate over cross-linking. The primary steps involved in the interaction of radiation with the polymer should be virtually independent of temperature. The effect of temperature should rather be associated with the mobility of the chain segments in which these radicals are present. At low temperatures, the low mobility favors cross-linking while increasing the mobility by raising the temperature favors scission processes. A similar observation has been made in the degradation of polystyrene by high energy radiation,(23, 24) and in poly (methyl acrylate),(25) the greater chain mobility in solution compared with the solid is reflected in the dramatic change over from chain scission to cross-linking when solutions and solid respectively are irradiated with 2537Å radiation.

Scission of these chain side radicals can result in radicals terminated by sequences of methylene groups which should be capable of liberating a proportion of monomeric ethylene by depolymerization (reactions 6 and 8). This is very much less probable if radicals are initially formed by main chain scission as in the thermal reaction.

Terminally unsaturated structures are formed as in reactions 1, 5 and 7 and it is to these that thermal destabilization due to pre-irradiation must be attributed. It is well established that unsaturated structures in polymer molecules constitute thermally labile or "weak" links because the energy requirement for scission at adjacent bonds is reduced by approximately 19 k cal mole^{-1}, being the energy associated with the allylic radical thus formed.

These thermal and photoreactions clearly involve an initiation step in which radicals are formed, followed by a variety of propagation steps. It is reasonable to assume that the radicals finally disappear by reaction in pairs. In any case, only the initiation step is different in the two reactions, propagation and termination being identical. The overall energy of activation, E_o, in a kinetically simple radical reaction of this kind, which is strictly analogous to radical polymerization, is given by

$$E_o = \frac{1}{2}E_i + E_p - \frac{1}{2}E_t$$

in which E_i, E_p and E_t are the energies of activation for initiation, propagation and termination respectively. Since E_p and E_t are the same for the photo and thermal reactions, then

$$E_{ot} - E_{op} = \frac{1}{2} (E_{it} - E_{ip})$$

in which the second subscript indicates the thermal and photoreactions. But the energy of activation for photoinitiation, E_{ip}, should be expected to be close to zero, thus

$$E_{it} = 2 (E_{ot} - E_{op})$$

Using the values 11.7 and 50.1 k cal mole^{-1} deduced for E_{op} and E_{ot}, a value of 76.8 k cal may be calculated for E_{it}, the energy of activation for thermal initiation. This is close to the accepted value of approximately 80 k cal mole^{-1} for the strength of a saturated carbon-carbon bond, thus supporting the proposition that thermal initiation involves scission of normal C-C main chain bonds.

Blends of Polypropylene and Poly(Methyl Methacrylate). In seeking explanations for the experimental observations in blend degradations, it is important to consider the form in which the polymer is being degraded. Since compatibility, especially in polymers as unlike chemically as PP and PMMA, is the exception rather than the rule and since the blend samples were translucent, it seems most likely that the low concentration component, PMMA, is dispersed as discrete micelles in a matrix of PP. Thus, any interaction between the degradation reactions of the two components must occur across a fairly well defined phase boundary. Because of the severe restrictions on the motion of macromolecules

and macroradicals and thus of their interaction in a polymer melt,
it seems more probable that reaction will occur between one poly-
mer and a small radical or molecule formed in the degradation of
the other and which can diffuse more freely from one phase to the
other.

It is quite clear from the results presented above that in
mixtures of PP and PMMA, the course of the thermal degradation of
each polymer is strongly influenced by the presence of the other.
Thus a comparison of TVA thermograms in figure 8B with those in
figures 7A, 7B and 8A shows that in degrading mixtures, monomer
production in the low temperature phase of the degradation of PMMA
is suppressed.

Both types of reaction have been reported, however. The ap-
pearance of block or graft copolymers has been the usual type of
evidence for interaction of macromolecules and macroradicals.
Thus Pavlinec (26) detected grafting in a thermally degrading mix-
ture of PP and poly(vinyl acetate) and Mizutani (19) found it in
degrading mixtures of PP with PMMA, polystyrene and some related
polymers. On the other hand McNeill and Neil (13) have shown that
chlorine atoms from degrading poly(vinyl chloride) are responsible
for the accelerated decomposition of PMMA in mixtures of the two.

It is quite clear from the results presented above that in
mixtures of PP and PMMA, the course of the thermal degradation of
each polymer is strongly influenced by the presence of the other.
Thus a comparison of TVA thermograms in figure 8B with those in
figures 7A, 7B and 8A shows that in degrading mixtures, monomer
production in the low temperature phase of the degradation of PMMA
is suppressed. The high temperature methyl methacrylate peak is
displaced slightly to higher temperature and a surge of methyl
methacrylate production occurs at an abnormally high temperature.
On the other hand, figure 9 demonstrates that the rate of thermal
degradation of PP is strongly accelerated by the presence of quite
small proportions of PMMA.

Figure 7 shows that pure PP is thermally stable in the range
of temperature at which the low temperature phase of the degrada-
tion of pure PMMA occurs. Since there is no evidence of grafting
at any temperature during thermal degradation of blends, it must
be assumed that the inhibition of monomer production demonstrated
by figure 8B is due to stabilization of the primarily formed rad-
icals by hydrogen transfer from the polypropylene at the PP/PMMA
interface. The chain side PP radicals thus formed should then be
expected to undergo chain scission to form terminally unsaturated
structures and radicals which will decompose in a series of inter
and intramolecular transfer reactions to give the complex series
of saturated and unsaturated hydrocarbons typical of the degrada-
tion of pure PP at higher temperatures. Thus the accelerating
effect of the presence of PMMA on the thermal degradation of PP,
which is illustrated in figure 9, is also explained. As the tem-
perature is raised, the rate of the reaction increases and passes
through a maximum at approximately 275°C (figure 8B) due to the
consumption of PMMA through which all initiation continues to
occur. At this temperature, however, a significant proportion of
the original PMMA is still present (figure 7A) and the thermal
degradation threshold of the PP component is reached. As the
temperature is raised further, the rate of the natural degradation
of PP progressively increases and it is suggested that the radi-
cals which become available in this way are capable of initiating

degradation in the residual PMMA, thus accounting for the "inter-action peak" at approximately 420°C (figure 8), which is known to be due to volatile products containing a high proportion of mono-meric methyl methacrylate. By the time the temperature reaches 450°C, all PMMA is decomposed and the final peak has all the nor-mal characteristics of that obtained using pure PP.

Irradiation of PMMA at 20°C results in chain scission and the production of terminally unsaturated polymer molecules, but no large production of volatile products. At 150°C the increased mobility of the polymer molecules allows the primarily formed rad-icals to depropagate and monomer production is quantitative. Irradiation of PP results in chain side radicals which combine to form cross links at 20°C, but undergo scission to form terminally unsaturated molecules at 150°C. When blends are irradiated at these temperatures, there appears to be no significant interaction of the radicals formed in the two phases because there is no evi-dence of block or graft formation. Thus the two constituents appear to decompose in isolation from one another.

In view of the large effect on the thermal degradation of PP of both pre-irradiation and blending with small proportions of PMMA (figure 9), it is perhaps surprising that the rates of ther-mal degradation of blends before and after pre-irradiation are almost identical. The explanation may be found in the fact that since the stability of PP is reduced on irradiation by the forma-tion of labile cross links and unsaturated terminal structures, the thermal degradation temperature of the PP and PMMA now overlap significantly. Thus high concentrations of radicals are formed simultaneously in both phases during thermal degradation of pre-irradiated blends and a high proportion of these radicals are destroyed by mutual disproportionation at the interface at the expense of the hydrogen transfer reactions which predominate in un-irradiated blends.

In spite of the fact that pre-irradiation of blends does not markedly affect the overall rate of degradation, it does, never-theless, have a strong effect on the nature of the volatile products. Figures 10 and 11 demonstrate that the yield of mono-meric methyl methacrylate is progressively suppressed while methyl methacrylate units become incorporated into the chain fragment fraction. It is suggested that the methyl methacrylate monomer formed by depolymerization of PMMA can add to some extent to the PP radicals. However, the effective concentration of monomeric methyl methacrylate in the degrading PP must be quite small so that depropagation will be favored in the propagation/depropaga-tion equilibrium and the methyl methacrylate side chains on the PP molecules will not exceed a few units in length. A branch point of this kind should be expected to be a weak point in the molecule so that scission would occur followed by transfer processes to give fragments containing both kinds of units. Effectively, it is being suggested that short grafts of methyl methacrylate on PP are being temporarily formed, but by addition of monomer to PP

radicals rather than by their reaction with PMMA radicals and that the graft points being labile, decompose rapidly so that no significant proportion of methyl methacrylate units is found in the residue.

The importance of the reduction of the stability of the PP component by pre-irradiation in determining the course of the degradation reaction is further emphasized by the TVA thermogram in figure 13, which demonstrates that the "interaction" peak due to monomer is at least as prominent as in un-irradiated blends (figure 8B).

Thus the basic conclusions may be summarized as follows. In un-irradiated blends of PP and PMMA, the PMMA tends to be stabilized and the PP destabilized to thermal degradation. This is because the PMMA radicals react with the PP to form radicals in the latter which further decompose at the PMMA degradation temperature rather than at the higher temperature of PP degradation. Pre-irradiation destabilizes the PP so that the temperatures of the thermal degradations of the two polymers overlap and monomeric methyl methacrylate can react with PP radicals to a much greater extent than in un-irradiated materials and in such a way as to suppress monomer production and favor the production of chain fragments comprising a combination of both monomers.

Literature Cited

1. Ranby, B. and Yashida, H., J. Polymer Sci., C, $\underline{12}$, 263 (1966).
2. Kusumoto, N., Matsumoto, K. and Takayanagi, M., J. Polymer Sci., A, $\underline{7}$, 1773 (1969).
3. Hatton, J. R., Jackson, J. B. and Miller, R. G. J., Polymer, $\underline{8}$, 411 (1967).
4. Kujirai, C., Hashiya, S., Furuno, M. and Terada, N., J. Polymer Sci., A1, $\underline{6}$, 589 (1968).
5. Takeshitta, T., Tsuji, K. and Seiki, T., J. Polymer Sci., A1, $\underline{10}$, 2315 (1972).
6. Tsuchiya, T. and Sumi, K., J. Polymer Sci., A1, $\underline{7}$, 1599 (1969).
7. Grassie, N., Chem. Zvesti, $\underline{26}$, 208 (1972).
8. Grassie, N., Pure and Applied Chem., $\underline{34}$, 247 (1973).
9. Grassie, N. and Jenkins, R. H., European Polymer J., $\underline{9}$, 697 (1973).
10. McNeill, I. C. and Neil, D., Thermal Analysis p. 353. Schwenker, R. F. and Garn, P. D. (Eds.) Academic Press: New York (1969).
11. Richards, D. H. and Salter, D. A., Polymer, $\underline{8}$, 127 (1967).
12. McNeill, I. C. and Neil, D., Makromol. Chem., $\underline{117}$, 265 (1968).
13. McNeill, I. C. and Neil, D., European Polymer J., $\underline{6}$, 143 (1970); $\underline{6}$, 569 (1970).
14. McNeill, I. C., Neil, D., Guyot, A., Bert, M. and Michel, A., European Polymer J., $\underline{7}$, 453 (1971).

15. Guyot, A., Bert, M., Michel, A. and McNeill, I. C., European Polymer J., $\underline{7}$, 471 (1971).
16. Gardner, D. L. and McNeill, I. C., European Polymer J., $\underline{7}$, 603 (1971).
17. Dodson, B., McNeill, I. C. and Straiton, T., J. Polymer Sci. In the press.
18. Jamieson, A. and McNeill, I. C., J. Polymer Sci. (Chem.), $\underline{12}$, 387 (1974).
19. Mizutani, T., Matsuoka, S. and Yamamoto, K., Bull. Chem. Soc. Japan, $\underline{38}$, 2045 (1965).
20. McNeill, I. C., European Polymer J., $\underline{6}$, 373 (1970).
21. Davis, T. E., Tobias, R. L. and Peterli, E. B., J. Polymer Sci., $\underline{56}$, 485 (1962).
22. Grassie, N. and Melville, H. W., Proc. Roy. Soc., $\underline{A199}$, 1 (1949).
23. Parkinson, W. W., Bopp, C. D., Binder, D. and White, J. E., J. Phys. Chem., $\underline{69}$, 828 (1965).
24. Burlent, W. J., Neerman, J. and Serment, V., J. Polymer Sci., $\underline{58}$, 491 (1962).
25. Grassie, N. and Davis, T. I., Makromol. Chem., $\underline{175}$, 2657 (1974).
26. Pavlinec, J. and Kaloporov, N. J., European Polymer J., $\underline{7}$, 1445 (1971).

Photooxidative Degradation of Polymers by Singlet Oxygen

B. RÅNBY and J. F. RABEK

Department of Polymer Technology, The Royal Institute of Technology,
Technical University, Stockholm, Sweden

This paper is an interpretation of the primary photo-oxidation process due to singlet oxygen and some problems in photostabilization of polymers and plastics. Electronic structure, generation, properties and role of singlet oxygen in polymer chemistry are discussed. The reader is also referred to a number of review articles on the subject (1-11).

Properties of singlet oxygen

Using quantum mechanics the electronic configuration of molecular oxygen (O_2) in the ground state $^3\Sigma_g^-$ can be written as follow (12):

$$KK(\sigma_g 2s)^2(\sigma_u 2s)^2(\sigma_g 2p_x)^2(\pi_u 2p_y)^2(\pi_u 2p_z)^2(\pi_g 2p_y)(\pi_g 2p_z)$$
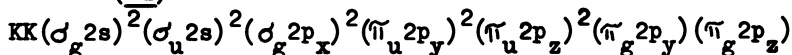
Two unpaired electrons are in orbitals each one having the orbital angular momentum on the molecular axis equal to unity but revolving in different directions. This gives a total orbital angular momentum of zero. This state has a molecular electron cloud with rotational symmetry, and it is called a sigma (Σ) state. The last two electrons have parallel spins, leading to the triplet state with paramagnetic properties. Molecular oxygen has a biradical nature and it reacts easily with other organic free radicals.

When sufficient energy is added to molecular oxygen it may change its electronic configuration. Two form of excited oxygen are formed and are known as:

1. Singlet oxygen $^1O_2(^1\Delta_g)$ which has the electronic configuration:

$$KK(\sigma_g 2s)^2(\sigma_u 2s)^2(\sigma_g 2p_x)^2(\pi_u 2p_y)^2(\pi_u 2p_z)^2(\pi_g 2p_y)^2$$
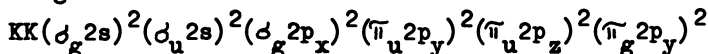
The electrons in the highest orbitals are paired and their spins are antiparallel. The first excited state-singlet oxygen $^1O_2(^1\Delta_g)$ lies above the ground state of molecular oxygen($^3\Sigma_g^-$) by 22.5 kcal/mol (0.98 eV). Because the electrons in this $^3\Sigma_g^-$ state are paired (have antiparallel spins) they

show a characteristic electron spin resonance (ESR) spectrum.

2. Singlet oxygen $^1O_2(^1\Sigma_g{}^+)$ has an identical electron configuration as molecular oxygen $(^3\Sigma_g{}^-)$. The difference is that in the $^1O_2(^1\Sigma_g{}^+)$ state the electrons in the antibonding (π^*) orbitals have antiparallel spins, whereas in the $^3\Sigma_g{}^-$ state these electrons have parallel spins. The second excited state-singlet oxygen $^1O_2(^1\Sigma_g{}^+)$ lies above the ground state of molecular oxygen $(^3\Sigma_g{}^-)$ by 37.5 kcal/mol (1.63 eV).

The two singlet oxygen states are deactivated by light emission in the range (13,14):

$$^1O_2(^1\Delta_g) - 7,882.4 \text{ cm}^{-1} \ (12.686.5 \text{ Å})$$
$$^1O_2(^1\Sigma_g{}^+) - 13,120.9 \text{ cm}^{-1} \ (7.621.4 \text{ Å})$$

The radiative lifetime of singlet oxygen $^1O_2(^1\Delta_g)$ in gas phase is extremely long (ca. 45 min)(15), whereas that of $^1O_2(^1\Sigma_g{}^+)$ is only 7 sec (16). The singlet oxygen $^1O_2(^1\Sigma_g{}^+)$ is rapidly quenched by water vapour. The lifetime of $^1O_2(^1\Delta_g)$ in solution is strongly affected by the nature of the solvent (17)(Table 1).

Table 1. The lifetime of $^1O_2(^1\Delta_g)$ singlet oxygen in different solvents (17)

Solvent	Life time μsec	Solvent	Life time μsec
H_2O	2	C_6H_6	24
CH_3OH	7	CH_3COCH_3	26
50%D_2O+ 50%CH_3OH	11	CH_3CN	30
C_2H_5OH	12	CS_2	200
C_6H_{12}	17	CCl_4	700

A detailed theory of the quenching of singlet oxygen by solvents in terms of transfer of electronic-to-vibrational energy has been given by Kearns (9,17). It has been determined that the diffusion path of singlet oxygen $^1O_2(^1\Delta_g)$ in thin film is about 115-20 Å (18).

Generation of singlet oxygen

There are three ways of preparation of singlet oxygen:
  1.Chemical reactions,e.g:

1.REACTION OF CALCIUM HYPOCHLORITES WITH HYDROGEN
   PEROXIDE

$$Cl_2 + H_2O_2 \longrightarrow {}^1O_2 + 2HCl$$

2.THERMAL DECOMPOSITION OF ADDUCT OF TRIPHENYL-
   PHOSPHITE AND OZONE (MURRAY R.W.,KAPLAN M.L.)

$$(C_6H_5O_3)P + O_3 \xrightarrow{-70^\circ} (C_6H_5O_3)P\begin{smallmatrix}O\\O\end{smallmatrix}O$$

$$(C_6H_5O_3)P\begin{smallmatrix}O\\O\end{smallmatrix}O \xrightarrow{-35^\circ} {}^1O_2 + (C_6H_5O_3)P=O$$
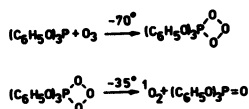
3.DISMUTATION REACTION OF SUPEROXIDE ANIONIC RADICALS
  (SCHAAP.A.P.)

$$2O_2^- \xrightarrow{+2H^+} {}^1O_2 + 2H_2O_2$$
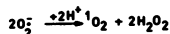
  2.Excitation by microwave frequency (2450 MHz). Oxygen under 1 torr pressure is passed through a quartz tube which is part of the discharge section which is connected to electrode-less microwave generator (Fig.1).
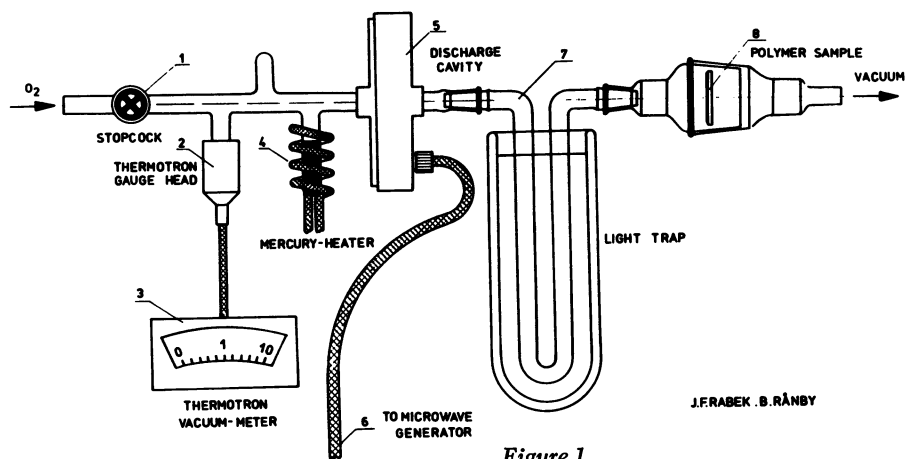
Figure 1.

Such a discharge produces at the same time atomic oxygen, ozone and singlet oxygen. The oxygen entering the discharge zone is saturated with mercury vapour and after discharge a mercuric oxide film is deposit when atomic oxygen and ozone are formed.
  3.Photosensitization method. Sensitizers can absorb light and be raised to excited states. After the initial excitation

to the lowest singlet states, a molecule may loose its excita-
tion energy in one or more of the following ways:

    i.Fluorescence - radiative conversion into the ground
      state.

   ii.Internal conversion:non-radiative conversion into the
      ground state.

  iii.Intersystem crossing:non-radiative transition involving
      a spin intercombination to the triplet state.

   iv.Photochemical reaction by unimolecular dissociation or
      by intermolecular reactions.

    v.Non radiative energy transfer to a neighbouring molecule
      e.g.molecular oxygen (Fig.2).
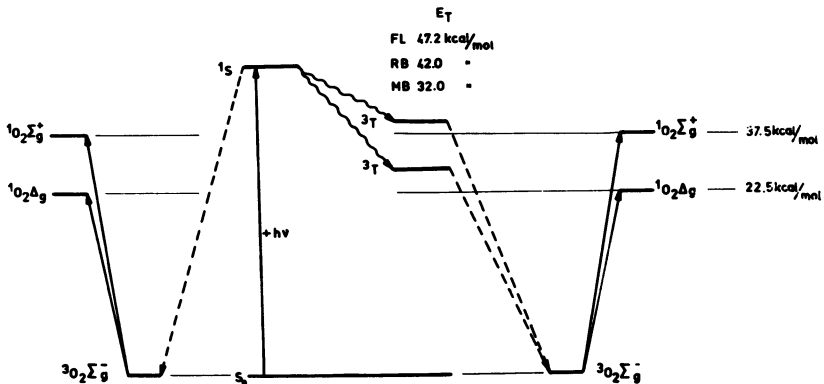
Figure 2.

After intersystem crossing to the triplet state the molecule
may react in one of the following ways:

    i.Phosphorescence - radiative inter-combination with the
      ground state.

   ii.Internal conversion:non-radiative inter-combination with
      the ground state.

  iii.Photochemical dissociation or rearrangement.

   iv.Triplet-triplet energy transfer: non-radiative transfer
      of electronic energy to a nearby molecule, e.g.molecular
      oxygen (Fig.2).

As a consequence of energy transfer from excited singlet state
or triplet state of a sensitizer to molecular oxygen may be
formed:

$$^1S + {}^3O_2 \longrightarrow {}^3T + {}^3O_2$$
$$^1S + {}^3O_2 \longrightarrow {}^3T + {}^1O_2({}^1\Delta_g, \text{and/or } {}^1\Sigma_g{}^+)$$
$$^1S + {}^3O_2 \longrightarrow S_o + {}^3O_2 + \Delta$$

$$^3T + {}^3O_2 \longrightarrow S_o + {}^1O_2({}^1\Delta_g, \text{and/or } {}^1\Sigma_g{}^+)$$

$$^{3}T + {}^{3}O_2 \longrightarrow S_o + {}^{3}O_2 + \Delta$$
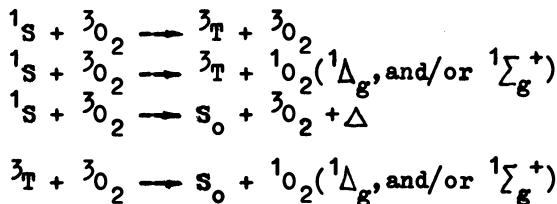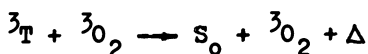
where $^{1}S, ^{3}T$ denote excited singlet and triplet state and S_o the ground state of sensitizer. The most common sensitizers for singlet oxygen generation are cyclo-aromatic hydrocarbons, carbonyl compounds and dyes,e.g.fluorescein,Rose Bengal, methylene blue (19-29):

FLUORESCEIN (FL)   ROSE BENGAL (RB)   METHYLENE BLUE (MB)
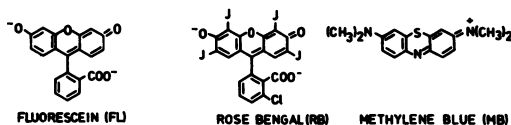
A polymer based Rose Bengal has also been reported (30). In our experiments we also developed liquid (polymer in benzene solution)-solid phase (dye sensitizer deposited on the surface of silica gel) system (Fig. 3).

30 cm

O₂

J.F.RABEK B.RÅNBY
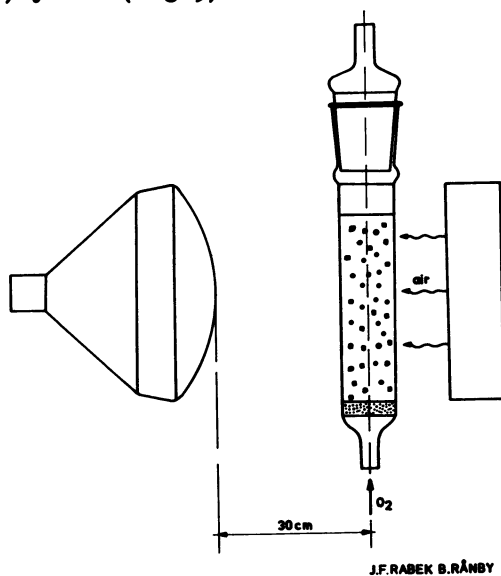
Figure 3.

We have found that this liquid-solid phase system due to efficient sensitized photo-oxidative degradation of dissolved polymer (e.g.polybutadienes).

There is only little detailed knowlidge of the photo-sensitization properties of other compounds which are commonly used in polymer chemistry,e.g.catalysts,modifiers,emulsifiers, antioxidants,pigments,dyes,etc. Some of these compounds may change their structure under processing conditions at higher temperatures. A new compound formed can also have photo-sensitizing properties. We can expect that polymers which

contain carbonyl group like polyketones or phenyl groups like polystyrene, can transfer their excitation energy to molecular oxygen and form singlet oxygen.

Recently it has been reported, that singlet oxygen can be produced by the dismutation reaction of superoxide anionic radicals (see chemical generation of singlet oxygen, page 3 of this paper)(31-33). Superoxide anionic radicals take part in several polymer reactions, and are also important species in biopolymer chemistry.

Reactions of singlet oxygen

Reactions of singlet oxygen with various organic compounds are known as "photosensitized oxidations". There are three typical reactions of singlet oxygen (1-10, 34, 35):

REACTIONS OF SINGLET OXYGEN

1. "ENE" TYPE (e.g. OXIDATION OF 2-METHYLBUTENE-2)
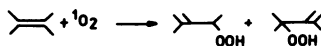
2. "DIENOPHILE" TYPE (e.g. OXIDATION OF BUTADIENE)
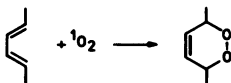
3. DIRECT ADDITION TO DOUBLE BOND
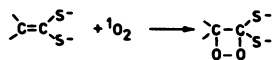
Another important reaction expected for polymers is the direct addition or the abstraction of hydrogen atoms by singlet oxygen with formation of hydroperoxides or hydro-peroxide radicals, respectively:
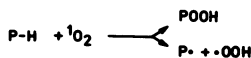
The rate constant of hydrogen abstraction by singlet oxygen depends primarily on the activation energy. The reaction can proceed rapidly only if the activation energy is small. This rule gives selectivity in the abstraction of hydrogen from polymers by singlet oxygen with a strong preference for the most weakly bonded hydrogen atom. It has been stated that singlet oxygen may react slowly with saturated hydrocarbons like n-tetracosane (36).

An important reaction from the polymer chemistry point of view is hydrogen abstraction from hydroxyl groups in

substitued phenols by singlet oxygen (<u>37-41</u>):
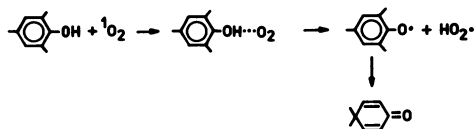
Substitued phenols are commonly applied as commercial anti-
oxidants and the above presented reaction can play a role in
the mechanism of polymer stabilization against oxidation.

Deactivation of singlet oxygen

The deactivation of singlet oxygen is known as "quenching
of singlet oxygen" and it occur in two ways:

DEACTIVATION OF SINGLET OXYGEN

1. CHEMICAL DEACTIVATION

$$^1O_2 + Q \rightarrow QO_2$$

1.3–DIPHENYL-
ISOBENZOFURAN
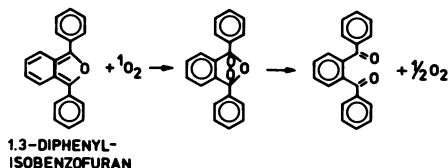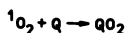
1,3-diphenylisobenzofuran has the largest rate constant known
$(8 \times 10^8 M^{-1} sec^{-1})$ for quenching singlet oxygen (<u>17</u>).

2. PHYSICAL DEACTIVATION

$$^1O_2 \rightarrow {}^3O_2 + \Delta$$

$$^1O_2 + Q \rightarrow {}^3O_2 + Q + \Delta$$
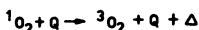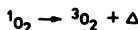
where Q is quencher and Δ means energy. The kinetics of this
process is well known (<u>42,43</u>). The most widely investigated
quenchers for physical quenching are amines (<u>14,44-49</u>):

$$R_3N + {}^1O_2 \rightarrow \left[R_3N^+ \cdots O_2^- \right] \rightarrow R_3N + {}^3O_2$$
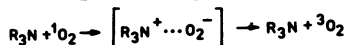
Several other compounds can quench singlet oxygen without
chemical reaction, e.g. β-carotene, where only cis-trans iso-
merization occurs (<u>50,51</u>) and metal complexes (<u>52-55</u>). It is
probable that most of these compound quench singlet oxygen by
energy transfer, but electron transfer or charge-transfer
complex formation can be taken into consideration (<u>44</u>).

The role of singlet oxygen in polymer chemistry

The importance of singlet oxygen in polymer chemistry should be considered from three aspects:
1. Formation of singlet oxygen in a polymer matrix.
2. Initation of oxidative degradation of polymers.
3. Stabilization of polymers against singlet oxygen oxidation.

1. Singlet oxygen in a polymer matrix can be formed in three ways:
   i. In a photosensitized reaction due to traces of impurities present.
   ii. In an energy transfer reaction between excited triplet state of carbonyl group and molecular oxygen ($\underline{56}$):

$$-CH_2-\overset{O}{\underset{||}{C}}-CH_2- \xrightarrow{+h\nu} -CH_2-\left[\overset{\bullet}{\underset{|}{\underset{O}{C}}}\right]-CH_2- \xrightarrow{^3O_2} -CH_2-\overset{O}{\underset{||}{C}}-CH_2- +\,^1O_2$$
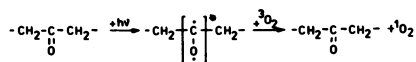
   iii. In an energy transfer reaction between excited triplet state of benzene rings, e.g. in polystyrene, and molecular oxygen ($\underline{57}$):

$$-CH_2-CH- \xrightarrow{+h\nu} -CH_2-CH- \xrightarrow{+^3O_2} -CH_2-CH- +\,^1O_2$$
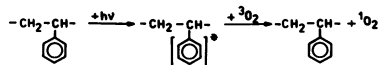
   iv. In an energy transfer reaction between photoexcited polyene double bonds and molecular oxygen ($\underline{58}$):

$$-(CH=CH)_n- \xrightarrow{+h\nu} -(CH=CH)_n^{\bullet}- \xrightarrow{^3O_2} -(CH=CH)_n- +\,^1O_2$$
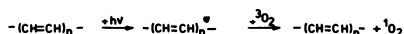
2. The role of singlet oxygen in the oxidative degradation of polymers has been pointed out by several authors, e.g. for polyethylene ($\underline{36,56}$), polypropylene ($\underline{59}$), polystyrene ($\underline{57,60}$), poly(vinyl chloride) ($\underline{58,61}$) and rubber ($\underline{62-66}$) and reviewed by Rabek and Rånby ($\underline{34,35}$).

At present time there is no good interpretation given for the initation step of the photo-oxidation reactions of polymers. A direct reaction of molecular oxygen with polymer resulting in hydrogen abstraction is improbable, because it is an endothermical reaction requiring about 30-40 kcal/mol. Several authors have estimated, that hydroperoxides present in polymers are responsible for the initation step. UV irradiation or heating can decompose hydroperoxide groups to free radicals and a subsequent disproportionation of the macroradicals may cause further degradation and oxidation of the polymer chain. The proposed mechanism seems to be correct, but there is one unanswered question: "what is the mechanism of hydroperoxide group formation" ?

The new suggestion proposed for polystyrene by Rabek and Rånby ($\underline{57}$) considers the formation of hydroperoxide groups along of polymer chain from a reaction of singlet oxygen with

polymer. These authors have also assumed that singlet oxygen
can abstract hydrogen atoms and produce hydroperoxy radicals:
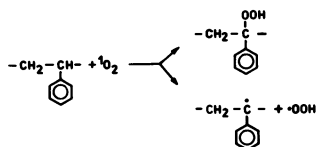
Free radicals react very fast with molecular oxygen, giving
macroperoxy radicals, which can abstract hydrogen from another
macromolecule. Ordinarily, the energy required to break a C-H
bond in a polymer is so that the reaction cannot occur
unassisted by other reactions and some bond formation may
occur in the transition state with singlet oxygen. However,
indirect evidence for that has not been found yet. In all
radical processes studied to date, the rate of hydrogen
abstraction from hydrocarbon chains increases in the order
primary < secondary < tertiary bonded. This order is the same
regardless if the attack is singlet oxygen or a free radical
because it is due to the strength of the C-H bond being
broken. Thus, tertiary C-H bonds are the weakest and tertiary
hydrogens are abstracted at the fastest rates. Two other
factors which frequently influence the rate of hydrogen
abstraction reactions are; the polar effect and the solvent
effect, which would need further discussion.

Trozzolo and Winslow (56), Carlsson and Wiles (59) and Gibb
and MacCallum (58) suggest that the formation of hydroper-
oxides results from singlet-oxygen attack on double bonds in
the polymers:
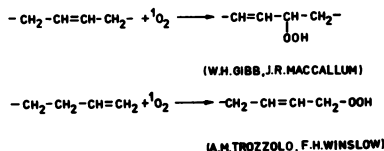
In the case of polydienes, Kaplan and Kelleher (63,64) have
shown addition of singlet oxygen to two nearest neighbour
double bonds with the formation of two allylic hydroperoxides.
Further addition of singlet oxygen to double bonds followed
the formation of cyclo-peroxide rings:
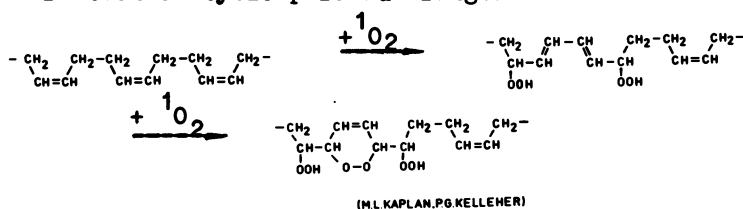
Rabek (66) has assumed that in the case of singlet oxygen
reaction with polyisoprene, double-bond shift occurs:

$$-CH_2-\underset{\underset{CH_3}{|}}{C}=CH-CH_2- +{}^1O_2 \longrightarrow -CH_2-\underset{\underset{OOH}{|}}{\overset{\overset{CH_2}{||}}{C}}-CH-CH_2-$$

(J.F RABEK)
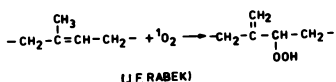
   The newest results obtained by Rabek and Rånby (67) show
that during dye sensitized singlet oxygen photo-oxidation of
cis- and trans-polybutadiene rapid degradation occur what has
been indicated by viscosity (Fig.4) and Gel Permeation
Chromatography (GPC)(Fig.5).

J.F.RABEK . B.RÅNBY
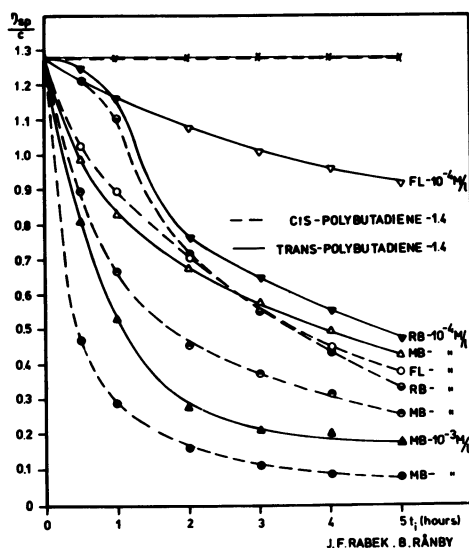
Figure 4.   Change of viscosity number of cis-
and trans-*polybutadienes-1,4 in benzene–*
methanol solution (9:1) during visible light
(Tungsten-500W, Argaphoto-BM lampe, Phil-
ips) irradiation in the presence of air and dyes:
FL-Fluorescein, RB-Rose Bengale, MB-Meth-
ylene blue. The concentration of dyes in solu-
tion was 10^{-3} or 10^{-4} M/1.
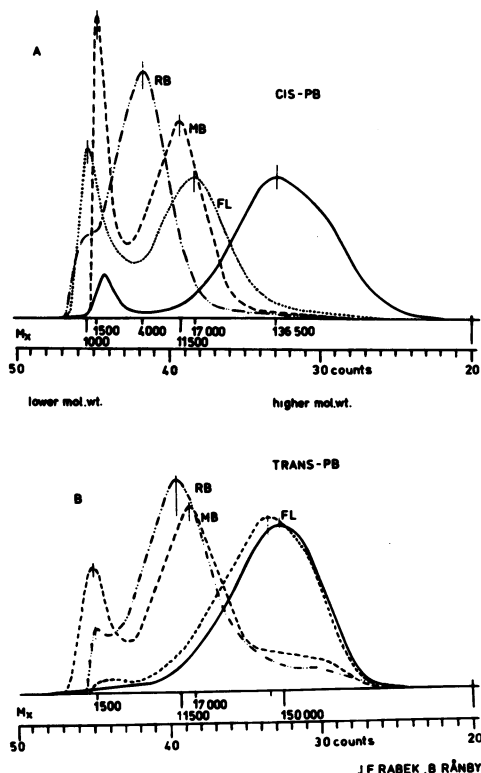
Figure 5. Gel-permeation chromatograms of (A) cis- and (B) trans-polybutadiene-1,4. (—) undegraded polymer and degraded in the presence of FL-fluoresceine, MB-methylene blue, and RB-Rose Bengal. Concentration of dyes in benzene–methanol (9:1) solution of polybutadienes was 10⁻⁴ M/1.

Breck at al (68) have recently examined the reactivities of a number of saturated and unsaturated polymers towards singlet oxygen generated by microwave generator. The saturated chain polymers as polystyrene,polyurethane and polyethylene were found to be inert within the experimental conditions with singlet oxygen,while the unsaturated polymers as polydienes were found to react quite readily.In this paper concentration of hydroperoxide groups has been measured. The similar results with oxidation of polybutadienes by singlet oxygen generated in microwave unit (Fig.1) and in dye photosensitized oxidation has been obtained by Rabek and Rånby (67). Infrared transmission spectra have been measured using film samples directly casted on KCl pellets and ATR spectra using aluminium-backed films (Fig.6).
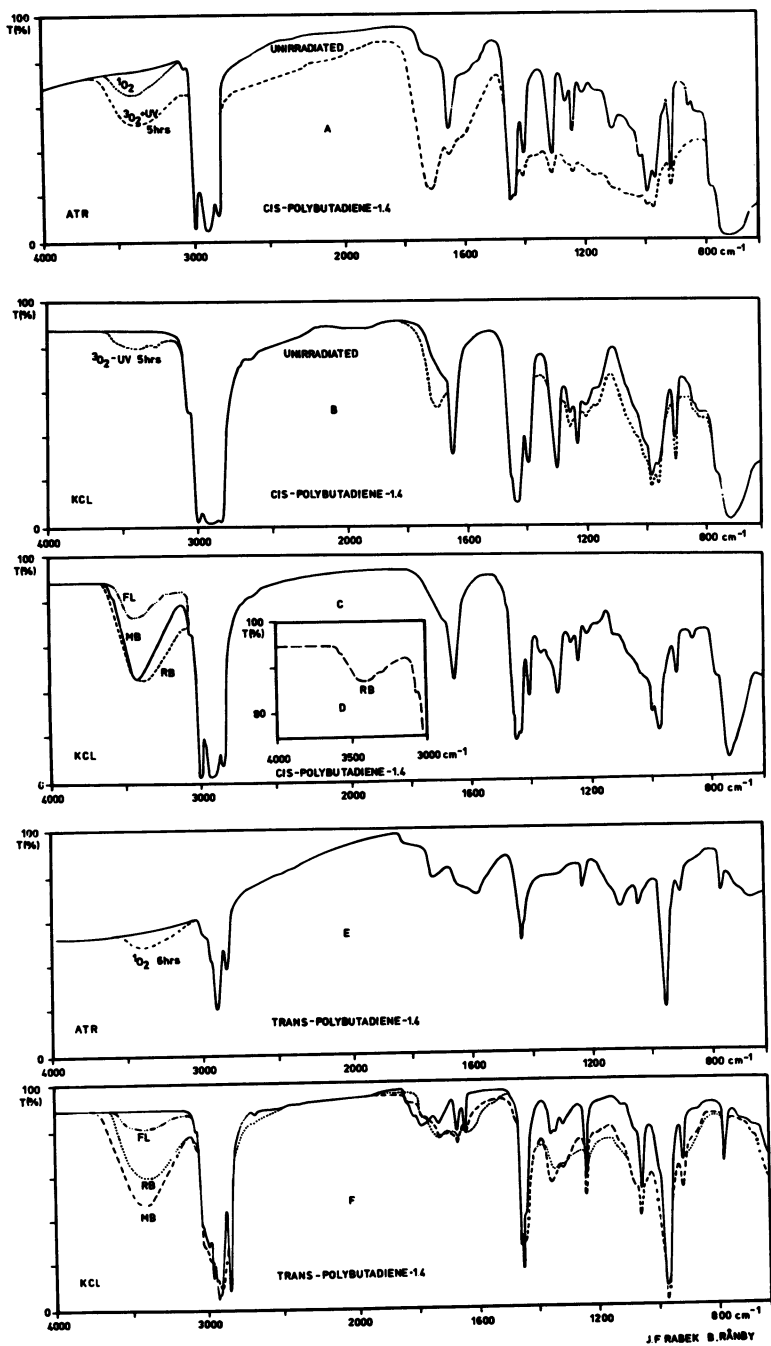
Figure 6. *(Legends on following page)*

J.F RABEK B.RÅNBY

Figure 6.   A.   ATR spectra of cis-polybutadiene-1,4 *films; (—) unirradiated; (···) exposed 6 hr to* $^1O_2$ *generated in microwave unit (MWU); (---) uv-irradiated 5 hrs in the presence of molecular oxygen. B. IR transmission spectra of* cis-polybutadiene-1,4 *films; (—) unirradiated; (---) uv-irradiated 5 hr in the presence of molecular oxygen. Films exposed 6 hr to* $^1O_2$ *from (MWU) did not give visible change in a spectrum. C. IR transmission spectra of* cis-polybutadiene-1,4 *after dye photosensitized degradation of polymer in benzene–methanol (9:1) solution; FL-fluorescein, MB-methylene blue, RB-Rose Bengal. The concentration of dye in solution was* $10^{-4}M/1$. *D. IR transmission spectra of* cis-polybutadiene-1,4 *degraded in liquid (polymer in benzene solution)–solid phase (Rose Bengale deposited on the surface of silica gel) system (Figure 3). E. ATR spectra of* trans-polybutadiene-1,4-*films; (—) unirradiated; (---) exposed 6 hr to* $^1O_2$ *generated in microwave unit (MWU). F. IR transmission spectra of* trans-polybutadiene-1,4 *after dye photosensitized degradation of polymer in benzene–methanol (9:1) solution; FL-fluorescein, MB-methylene blue, RB-Rose Bengal. The concentration of dye in solution was* $10^{-4}M/1$.

The results presented by Breck et al (68) for saturated chain polymers do not consider the possibility, that very small amounts of hydroperoxide groups can be formed along the saturated-chain polymers. Such small amounts of hydroperoxides can not be detected by common analytical methods but may be sufficient for the initiation of an oxidative degradation mechanism of polymers.

3. The third important aspects of singlet oxygen in polymer chemistry is the role of photostabilizers and antioxidants in singlet oxygen quenching. It is well known that several metal chelates efficiently quench the triplet states of many compounds (69-74). Recently it has been found that commercial photostabilizers containing nickel complexes like nickel-thiophenolate and nickel-alkyldithiocarbamate chelates are efficient singlet oxygen quenchers (52-55,68,75-77). The high quenching efficiency of singlet oxygen by Ni(II) chelates would explain their activity as polyolefin photostabilizers and is consistent with the suggestion that singlet oxygen is responsible for the initation step of photo-oxidation. Similarly it has been demonstrated that various aromatic diamines used to stabilize rubbers are effective singlet oxygen quenchers (78). The new view of the antioxidant action as a preventive mechanism of polymer oxidation involves the deactivation of singlet oxygen.

Conclusions

In this short review the authors have demonstrated the apparent role of singlet oxygen in polymer chemistry. Many areas reviewed still present important unsolved reserach problems.

References

1. R.Higgins,C.S.Foote and H.Cheng.Adv.Chem.Ser.,No.77,102 (1968).
2. A.J.Arnold,M.Kubo and C.A.Ogryzlo,Adv.Chem.Ser.,No.77,133 (1968).
3. A.U.Khan and D.R.Kearns,Adv.Chem.Ser.,No.77,143 (1968).
4. D.R.Kearns and A.U.Khan,Photochem.Photobiol.,10,193 (1969).
5. E.A.Ogryzlo,Photophysiol.,5,35 (1970).
6. D.R.Kearns and W.Fenical,Ann.N.Y.Acad.Sci.,171,34 (1970).
7. T.W lson and J.W.Hastings,Photophysiol.,5,49 (1970).
8. M.L.Kaplan,Chem.Techn.,1971,621.
9. D.R.Kearns,Chem.Rev.,71,395 (1971).
10. J.F.Rabek,Wiadom.Chem.,25,293,365,435 (1971).
11. J.F.Rabek and B.Rånby in Conference on "Degradation and Stabilization of Polymers",Bruxelles,1974,p.257.
12. E.K.Gill and K.J.Laidler,Can.J.Chem.,36,79 (1958).
13. S.J.Arnold and E.A.Ogryzlo,Photochem.Photobiol.,4,943 (1965).
14. K.Furukawa,E.W.Gray and E.A.Ogryzlo,Ann.N.Y.Acad.Sci.,171, 175 (1970).
15. R.M.Badger,A.C.Wright and R.F.Whitlock,J.Chem.Phys.,43, 4345 (1965).
16. W.H.J.Childs and R.Mecke,Z.Phys.,68,344 (1931).
17. P.B.Merkel and D.R.Kearns,J.Am.Chem.Soc.,94,7244 (1972).
18. B.Schnuriger and J.Bourdon,Photochem.Photobiol.,8,361 (1968).
19. J.Bourdon and B.Schnuriger,Photochem.Photobiol.,5,507(1966)
20. F.A.Gollmick and H.Berg,Photochem.Photobiol.,7,471 (1968).
21. K.Gollnick in "Advance in Photochemistry"(ed.W.A.Noyes, G.S.Hammond and J.N.Pitts Jr.,),Interscience-Wiley,1968, vol.6,p.2.
22. K.Gollnick,Adv.Chem.Ser.,No.77,67 (1968).
23. D.R.Kearns,R.A.Hollins,A.U.Khan,R.W.Chambers and P.Radlick, J.Am.Chem.Soc.,89,5355 (1967).
24. D.R.Kearns,R.A.Hollins,A.U.Khan and P.Radlick,J.Am.Chem.Soc 89,6456 (1967).
25. P.B.Markel,R.Nilsson and D.R.Kearns,J.Am.Chem.Soc.,94,1030 (1972).
26. R.Nilsson and D.R.Kearns,Photochem.Photobiol.,17,65 (1973).
27. R.Nilsson and D.R.Kearns,Photochem.Photobiol.,19,18 (1974).
28. J.Stauff and H.Fuhr,Ber.Bunseng.phys.Chem.,73,245 (1969).
29. T.Wilson,J.Am.Chem.Soc.,88,2898 (1966).
30. E.C.Blossey,D.C.Neckers,A.L.Thayer and A.P.Schaap,J.Am.Chem Soc.,95,5820 (1973).

31. A.P.Schaap,A.L.Thayler,G.R.Faler,K.Goda and T.Kimura, A.Am.Chem.Soc.,<u>96</u>,4025 (1974).
32. E.A.Mayeda and A.E.Bard,J.Am.Chem.Soc.,<u>96</u>,4023 (1974).
33. E.A.Mayeda and A.E.Bard,J.Am.Chem.Soc.,<u>95</u>,6233 (1973).
34. J.F.Rabek,in "Degradation of Polymers",Comprehensive Chemical Kinetics (ed.C.H.Bamford and C.F.Tipper),Elsevier Oxford,vol.14,p.265 (1975).
35. B.Rånby and J.F.Rabek,"Photodegradation,Photo-oxidation and Photostabilization of Polymers",Wiley,London,1975.
36. M.L.Kaplan and P.G.Kelleher,J.Polymer Sci.,B,<u>9</u>,565 (1971).
37. T.Matsuura,K.Omura and R.Nakashima,Bull.Soc.Japan,<u>38</u>,1358 (1965).
38. T.Matsuura,N.Yoshimura,A.Nishinaga and I.Saito,Tetrahedron Lett.,<u>1972</u>,4933.
39. M.Thomas and C.S.Foote - private communication.
40. T.Matsuura,N.Yoshimura,A.Nishinaga and I.Saito,Tetrahedron Lett.,<u>1969</u>,1669.
41. L.Taimir and J.Pospisil,Angew.Makromol.Chem.,<u>39</u>,189 (1974).
42. R.H.Young,R.Martin,K.Weherly and D.Feriozi,prepr.Div.Petrol Chem.Amer.Chem.Soc.,<u>16</u>,A89 (1971).
43. D.R.Kearns,prepr.Div.Petrol.Chem.Amer.Chem.Soc.,<u>16</u>,A9(1971)
44. R.H.Yound,R.L.Martin,D.Feriozi,D.Brewer and R.Kayser, Photochem.Photobiol.,<u>17</u>,233 (1973).
45. E.A.Ogryzlo and C.W.Tang,J.Am.Chem.Soc.,<u>90</u>,6527 (1970).
46. W.I.Smith Jr.,J.Am.Chem.Soc.,<u>94</u>,186 (1972).
47. I.B.C.Matheson and J.Lee,J.Am.Chem.Soc.,<u>94</u>,3310 (1972).
48. K.Furukawa and E.A.Ogryzlo,J.Photochem.<u>1</u>,163 (1972/1973).
49. K.Furukawa and E.A.Ogryzlo,Chem.Phys.Lett.,<u>12</u>,370 (1971).
50. C.S Foote,Y.C.Chang and R.W.Denny,J.Am.Chem.Soc.,<u>92</u>,5216, 5218 (1970).
51. C.S.Foote and R.W.Denny,J.Am.Chem.Soc.,<u>90</u>,6233 (1968).
52. J.Flood,K.E.Russel and J.K.Wan,Macromolecules,<u>6</u>,659 (1973).
53. D.J.Carlsson,T.Suprunchuk and D.M.Wiles,J.Polym.Sci.,A1,<u>11</u>, 61 (1973).
54. D.J.Carlsson,D.E.Sproule and D.M.Wiles,Macromolecules,<u>5</u>, 659 (1972).
55. D.J.Carlsson,G.D.Mendenhall,T.Suprunchuk and D.M.Wiles, J.Am.Chem.Soc.,<u>94</u>,8961 (1972).
56. A.M.Trozzolo and F.H.Winslow,Macromolecules,<u>1</u>,98 (1968).
57. J.F.Rabek and B.Rånby,J.Polym.Sci.,A1,<u>12</u>,273 (1974).
58. W.H.Gibb and J.R.MacCallum,Europ.Polym.J.,<u>10</u>,533 (1974).
59. D.J.Carlsson and D.M.Wiles,J.Polym.Sci.,B,<u>11</u>,759 (1973).
60. J.F.Rabek and B.Rånby,J.Polym.Sci.,A1,<u>12</u>,295 (1974).
61. K.P.S.Kwei,J.Polym.Sci.,A1,<u>7</u>,1075(1969).
62. G.P.Canva and J.J.Canva,Rubber J.,<u>153</u>,361 (1971).
63. M.L.Kaplan and P.G.Kelleher,J.Polym.Sci.,A1,<u>8</u>,3163 (1970).
64. M.L.Kaplan and P.G.Kelleher,Science,<u>1969</u>,1206 (1970).
65. M.L.Kaplan and P.G.Kelleher,Rubber Chem.Technol.,<u>45</u>,423 (1972).

66. J.F.Rabek,in XXIIIrd IUPAC Congress,Boston,USA July 1971,
    ed.Butterworths,London,vol.8,p.29.
67. J.F.Rabek and B.Rånby,J.Polym.Sci,in press.
68. A.K.Breck,C.L.Taylor,K.E.Russel and J.K.S.Wan,J.Polym.Sci.,
    A1,12 ,1505 (1974).
69. J.C.W.Chien and W.P.Cooner,J.Am.Chem.Soc.,90,1001 (1968).
70. H.Linschitz and L.Pekkarinen,J.Am.Chem.Soc.,82,2411 (1952).
71. G.S.Hammond and R.P.Foss,J.Phys.Chem.,68,3739 (1964).
72. R.P.Foos,D.O.Cowan and G.S.Hammond,J.Phys.Chem.,68,3747
    (1964).
73. P.J.Briggs and J.F.McKeller,Chem.Ind.,1967,622.
74. P.J.Briggs and J.F.McKeller,J.Appl.Polymer Sci.,12,1825
    (1968).
75. J.P.Guillory and C.F.Cook,J.Polym.Sci.,A1,11,1927 (1973).
76. J.P.Guillory and R.S.Becker,J.Polym.Sci.,A1,12,993 (1974).
77. A.Adamczyk and F.Wilkinson,J.Appl.Polym.Sci.,18,1225 (1974)
78. J.P.Dalle,R.Magous and M.Mousseron-Canet,Photochem.
    Photobiol.,15,411 (1972).

Photodegradation of Automotive Paints

P. C. KILLGOAR, JR., and H. VAN OENE

Research Staff, Ford Motor Co., Dearborn, Mich. 48121

Retention of gloss, color stability and resistance to embrittlement under outdoor conditions are some of the important requirements of automotive paints. Changes in gloss can be related to photochemical degradation and subsequent removal of low molecular weight fragments of the polymer binder used in the paint. New paints are usually tested for their chalk resistance and gloss retention properties by outdoor exposure in Florida or other locations for a period of two years. Therefore, there is a two years waiting period between the completion of the paint development work and the actual use of that paint.

In order to speed up paint development, accelerated testing methods have been devised. One such test method is the 500-2000 hour exposure test in the weather-o-meter using high intensity light. Accelerated weathering techniques do not always correlate well with actual outdoor exposure data, presumably the spectral distribution of the light being different from sunlight. Moreover, the actual weathering process depends on the details of the environment such as temperature, humidity and pollution levels (1), the influence of which cannot be duplicated in an accelerated test.

The process of weathering is not understood in great detail because of the complexity of paint formulations in that polymer composition, crosslinking agent, catalysts, pigments and additives all influence the photochemical processes.

Loss of gloss during outdoor exposure can be due to inadequate pigment dispersion (2). Some of the surface treatments of pigments used to obtain good pigment dispersion may also be detrimental in outdoor exposure (3). Since chalking is essentially a surface phenomena, any segregation of components of the paint during evaporation or the extensive use of surface active additives which can cause the composition of the surface region to be significantly different from that of the bulk will also influence weathering properties.

To predict the gloss retention behavior of any paint, one must know the photochemical processes taking place and the

morphology of the paint film. Morphology of the paint film and the state of pigment dispersion can be determined by electron microscopy (2). The study of photochemical changes is usually more difficult. Infrared spectroscopy successfully used for the study of photo-oxidation of polyethylene (4) is not sufficiently sensitive to study acrylic type polymers used in automotive paints. The chemical compositions of the paint film are too complicated to allow studies of their photochemistry by most of the available techniques.

In this work we have concentrated on the development of a method which can be used to study the chemical aspects of photo-degradation, specifically photoinitiation under conditions of illumination which do not differ greatly from those experienced during outdoor exposure. This method can be adapted to study photo-oxidation also.

The photoinitiated degradation of a typical melamine cross-linked acrylic enamel studied by using this technique will be discussed.

Chemistry of Photodegradation of Acrylic Polymers

The majority of the work on the fundamental processes of photodegradation of acrylic polymers has been carried out by Grassie and co-workers (5-7). For radiation with wavelength $\lambda > 300.0$ nm photodegradation is initiated by absorption of a photon by the carbonyl group of the ester side chains. Subsequent fragmentation depends on local stereochemistry and temperature. The principal modes of fragmentation are described by the Norrish I and Norrish II processes (8).

The Norrish I process can be represented by:

$$\text{\small ∿CH}_2 - \underset{\substack{| \\ \overset{\displaystyle C}{O \diagdown OR}}}{C}(x)\text{∿} \quad \overset{h\nu}{\rightarrow} \quad \text{∿CH}_2 - \underset{\cdot}{C}(x)\text{∿} \; + \; \cdot CO_2R \qquad 1(a)$$

$$\text{∿CH}_2 - \underset{\substack{| \\ CO\cdot}}{C}(x)\text{∿} \; + \; \cdot OR \qquad 1(b)$$

followed by

$$\cdot CO_2R \;\rightarrow\; CO_2{\uparrow} \; + \; R\cdot \qquad\qquad 2(a)$$

$$\text{∿CH}_2 - \underset{\substack{| \\ CO\cdot}}{C}(x)\text{∿} \;\rightarrow\; \text{∿CH}_2 - \underset{\cdot}{C}(x)\text{∿} \; + \; CO{\uparrow} \qquad 2(b)$$

$$\cdot CO_2R + H\cdot \;\rightarrow\; HCO_2R \text{ (formate ester)} \qquad 2(c)$$

In the primary process CO_2, CO or formate esters are formed plus
a polymeric macroradical and ester side chain fragments R· and
RO·.

The Norrish II process involves the participation of β
hydrogen of the alcohol segment or a γ hydrogen on the polymer
backbone in the formation of a six member ring through hydrogen
bonding with the carbonyl oxygen. This can be represented as:

$$\text{vvCH}_2 - \overset{\overset{\text{H}}{|}}{\underset{\underset{\text{Y}}{|}}{\text{C}}} - \text{CH}_2 - \text{C(x)vv} \rightarrow \text{vvCH}_2 - \overset{\overset{\text{H}}{|}}{\underset{\underset{\text{Y}}{|}}{\text{C}}} - \text{CH}_2 - \underset{\underset{\text{COOH}}{|}}{\text{C(x)vv}} \quad 3(a)$$

$$\overset{|}{\underset{\underset{\text{O} - \text{CH}_2}{\overset{\nwarrow \text{C} \nearrow}{\;}}}{\text{C} = \text{O}}} \overset{\text{H} \quad \text{R}}{\underset{\text{H}}{}}$$

$$+ \; H_2C = CHR\uparrow$$

or

$$\text{vvCH}_2 - \overset{\overset{\text{Y}}{|}}{\underset{\underset{\text{H}}{|}}{\text{C}}} - \text{CH}_2 - \underset{\underset{\overset{\diagdown}{\text{C}} - \text{OR}}{}}{\text{C(x)vv}} \rightarrow \text{vvCH}_2 - \overset{\overset{\text{Y}}{|}}{\text{C}} = \text{CH}_2 + \qquad 3(b)$$

$$\overset{\overset{\text{C(x)vv}}{\|}}{\underset{\underset{\text{HO}^{\diagup} \diagdown \text{OR}}{}}{\text{C}}} \leftarrow \rightarrow \overset{\overset{\text{HC(x)vv}}{|}}{\underset{\underset{\text{O}^{\diagup} \diagdown \text{OR}}{}}{\text{C}}}$$

Hence the Norrish II process leads to formation of an alkene
[3(a)] or chain scission [3(b)]. The fate of the polymeric macro-
radical depends on the sequence distribution of the copolymer.
Consider the macroradical:

$$\text{vvCH}_2 - \underset{\underset{\text{CO}_2\text{R}}{|}}{\text{C(x)}} - \text{CH}_2 - \overset{\overset{\cdot}{}}{\text{C(Y)}} - \text{CH}_2 - \underset{\underset{\text{CO}_2\text{R}}{|}}{\text{C(x)vv}}$$

$$\text{I}$$

As prepolymers used in crosslinking reactions of acrylic enamels
are usually copolymers of acrylic (x = H) and methacrylic
(x = CH_3) type monomers, the macroradical I can undergo a number
of rearrangements depending on the local sequence distribution.
For X = Y = CH_3 (a methacrylate sequence) one obtains:

1) Chain scission

$$\text{I} \rightarrow \text{vvCH}_2 - \underset{\underset{\text{CO}_2\text{R}}{|}}{\overset{\overset{\text{CH}_3}{|}}{\text{C}}} - \text{CH}_2 - \overset{\overset{\text{CH}_3}{|}}{\text{C}} = \text{CH}_2 + \; \cdot\underset{\underset{\text{CO}_2\text{R}}{|}}{\overset{\overset{\text{CH}_3}{|}}{\text{C}}} - \text{CH}_2 - \underset{\underset{\text{CO}_2\text{R}}{|}}{\overset{\overset{\text{CH}_3}{|}}{\text{Cvv}}} \qquad 4(a)$$

followed by depropagation

$$
\underset{\substack{| \\ CO_2R}}{\overset{\substack{·CH_3 \\ |}}{\sim\!\sim\!C}} - CH_2 - \underset{\substack{| \\ CO_2R}}{\overset{\substack{CH_3 \\ |}}{C·}} \;\rightarrow\; \underset{\substack{| \\ CO_2R}}{\overset{\substack{CH_3 \\ |}}{\sim\!\sim\!C·}} + CH_2 = \underset{\substack{| \\ CO_2R}}{\overset{\substack{CH_3 \\ |}}{C}} \uparrow
\qquad 4(b)
$$
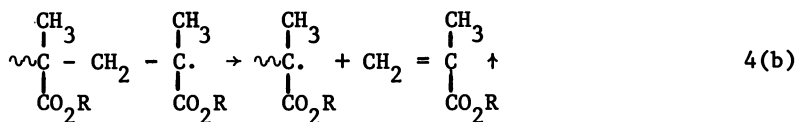
For X = Y = H (an acrylic sequence) one obtains:

1)   Chain scission:

$$
I \rightarrow \sim\!\sim\!CH_2 - \underset{\substack{| \\ CO_2R}}{CH_2} - CH_2 - \overset{\substack{H \\ |}}{C} = CH_2 + ·\underset{\substack{| \\ CO_2R}}{\overset{\substack{H \\ |}}{C}} - CH_2 - \underset{\substack{| \\ CO_2R}}{\overset{\substack{H \\ |}}{C}}\!\sim\!\sim
\qquad 5(a)
$$

followed by intermolecular transfer

$$
\sim\!\sim\!\underset{\substack{| \\ CO_2R}}{\overset{\substack{H \\ |}}{C}} - CH_2 - \underset{\substack{| \\ CO_2R}}{\overset{\substack{H \\ |}}{C·}} \;\rightarrow\; \sim\!\sim\!\underset{\substack{| \\ CO_2R}}{\overset{\substack{H \\ |}}{C}} - CH_2 - \underset{\substack{| \\ CO_2R}}{\overset{\substack{· \\ |}}{CH_2}}
\qquad 5(b)
$$
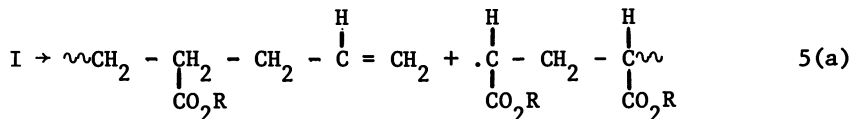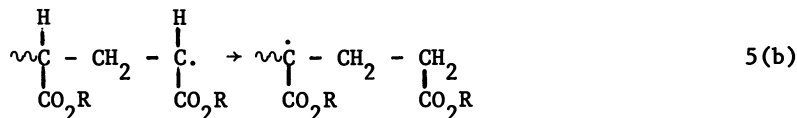
The radical remaining can undergo termination by H abstraction or recombination leading to further crosslinking. For X = CH₃ and Y = H (an alternating sequence of acrylic and methacrylate monomers).

1)   Chain scission:

$$
\sim\!\sim\!CH_2 - \underset{\substack{| \\ CO_2R}}{\overset{\substack{CH_3 \\ |}}{C}} - CH_2 - \overset{\substack{H \\ |}}{\underset{·}{C}} - CH_2 - \underset{\substack{| \\ CO_2R}}{\overset{\substack{CH_3 \\ |}}{C}} \rightarrow \sim\!\sim\!CH_2 - \underset{\substack{| \\ CO_2R}}{\overset{\substack{CH_3 \\ |}}{C}} - CH_2 - \overset{\substack{H \\ |}}{C} = CH_2 +
$$

$$
·\underset{\substack{| \\ CO_2R}}{\overset{\substack{CH_3 \\ |}}{C}} - CH_2 - \underset{\substack{| \\ CO_2R}}{\overset{\substack{H \\ |}}{C}} - CH_2\!\sim\!\sim
\qquad 6(a)
$$

followed by intermolecular transfer:

$$
\sim\!\sim\!CH_2 - \underset{\substack{| \\ CO_2R}}{\overset{\substack{H \\ |}}{C}} - CH_2 - \underset{\substack{| \\ CO_2R}}{\overset{\substack{CH_3 \\ |}}{C·}} \;\rightarrow\; CH_2 - \underset{\substack{| \\ CO_2R}}{\overset{\substack{H \\ |}}{\overset{·}{C}}} - CH_2 - \underset{\substack{| \\ CO_2R}}{\overset{\substack{CH_3 \\ |}}{CH}}
\qquad 6(b)
$$

or depropagation:

$$\sim\sim CH_2 - \underset{\underset{CO_2R}{|}}{\overset{\overset{H}{|}}{C}} - CH_2 - \underset{\underset{CO_2R}{|}}{\overset{\overset{CH_3}{|}}{C}} \cdot \rightarrow \sim\sim CH_2 - \underset{\underset{CO_2R}{|}}{\overset{\overset{H}{|}}{C}} \cdot + CH_2 = \underset{\underset{CO_2R}{|}}{\overset{\overset{CH_3}{|}}{C}} \uparrow \qquad 6(c)$$
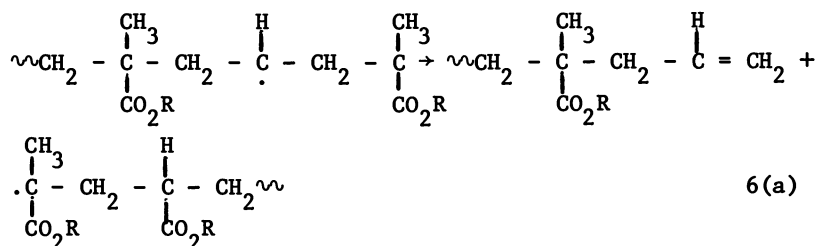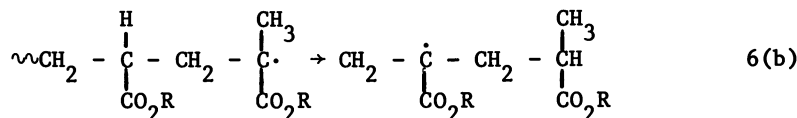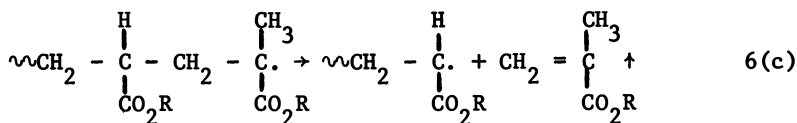
On the basis of this reaction scheme, one predicts that photochemically induced degradation results in chain scission of the prepolymers and evolution of volatile products such as CO_2, CO and abstraction or recombination products of alkyl fragments derived from the ester side chain fragments. The Norrish II process is unimportant for short chain esters, (e.g. methylmethacrylate), for longer chain esters it should be considered.

The reaction scheme as outlined is admittedly oversimplified, it nevertheless provides a guide as to what kind of degradation products can be expected. Even though we will consider the degradation of a melamine crosslinked paint, no detailed reaction scheme has been devised for the degradation of the melamine itself; this will be treated separately in a future publication.

Experimental Method

It is possible to follow the photodegradation reactions of acrylic polymers by continuously monitoring the evolution of the volatile products by means of a sensitive mass spectrometer. One is left with the task of identifying the degradation products from their fragmentation patterns. Since most of the fragmentation patterns are known (9), one gains the advantage that kinetic studies are possible, without having to condense the sample and perform GC analysis.

Figure 1 is a schematic diagram of the apparatus we have designed. A vacuum chamber holds the paint panel. This chamber is connected via a heated tube to the ion source of a Varian MAT 311 double focusing mass spectrometer. The mass spectrometer is controlled by a computer supplied by Incos Corporation which utilizes a Nova II computer with 32K of core, two 1.2 million word disks, a Tektronix 4010 scope and a specially designed interface. This system collects and stores the data and is used in the subsequent data reduction. A Bausch and Lomb high pressure mercury arc lamp is used as the light source. A water filter to remove the infrared radiation and a pyrex filter to remove radiation below 300.0 nm are used. A thermocouple behind the panel is used to monitor the panel temperature when the chamber is heated. The principle involved in getting the degradation products formed in the chamber to the ion source is differential pumping, which is accomplished by keeping the pressure in the ion source of the mass spectrometer, typically 1.33×10^{-4} Pa (10^{-6} torr), at a lower pressure than that in the chamber, usually 1.33 to 1.33×10^{-1} Pa (10^{-2} 10^{-3} torr).

Under the control of the computer a mass spectrum from M/E = 10 to M/E = 350 can be obtained as often as every 12-15 seconds. In order to analyze the results, we have the computer plot out the intensity as a function of scan number for the fragment of interest, for example M/E = 44, the CO_2 peak is shown in Figure 2.

The background intensity is observed for several hours after the chamber is interfaced to determine that it is not changing. One expects a "pumping equilibrium" to be reached between the chamber and the ion source since without the lamp on there should be no process producing material.

Figure 3 shows the behavior of the background for a period of about 1 hour after the chamber was interfaced to the ion source. When the background stabilizes, the lamp is turned on.

Description of Paint

The paint studied is a typical automotive thermosetting enamel which consists of an epoxy functional acrylic copolymer and butylated melamine crosslinking agent. The acrylic copolymer is composed of methyl methacrylate, n-butyl methacrylate, n-butyl acrylate, styrene, acrylonitrile, 2-ethyl hexyl acrylate and 2-hydroxyethyl methacrylate. Carbon black was used as the pigment.

Theory

In order to interpret the time dependence observed in Figure 2 one has to derive expressions for the rate of formation of products within the film, diffusion of these products into the reaction chamber and the pumping speed of the product to the mass spectrometer. A detailed analysis is given in Appendix I.

It is assumed that the incident radiation is absorbed by the paint film according to Beer's law:

$$I(x) = I_o \exp(-\alpha x) \tag{7}$$

where I is the intensity, x is the distance into the film, the surface being located at x = 0; $\alpha = \epsilon c$, where ϵ is the molar extinction coefficient and c the concentration of absorbing species present. It is further assumed that the products are formed by a pseudo-zero order reaction:

$$\frac{\partial c(x,t)}{\partial t} = \Phi I \tag{8}$$

where Φ is the quantum efficiency of the process. This assumption can of course be changed and a different form of the rate expression easily accommodated in our analysis.

DOUBLE FOCUSING MASS SPECTROMETER
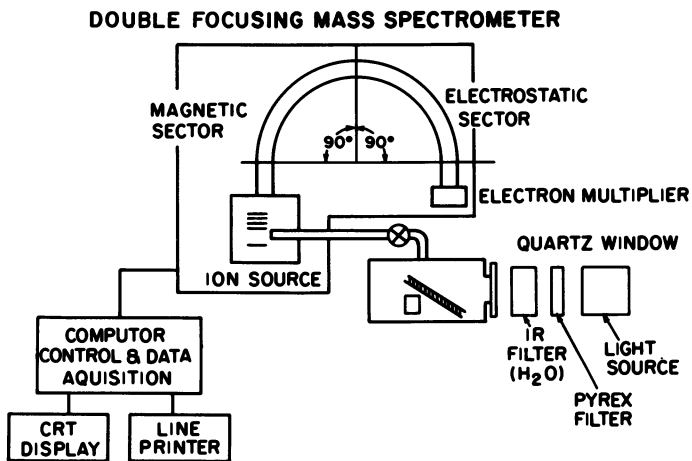
Figure 1.   Schematic of double focusing mass spectrometer

$$\frac{M}{E} = 44 \, (CO_2{}^+)$$
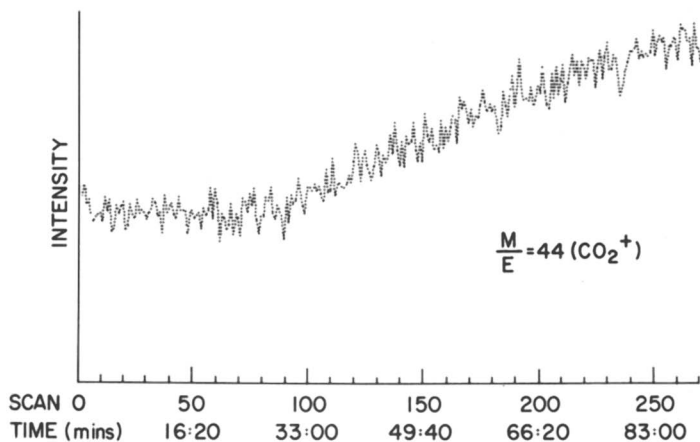
Figure 2.   Plot of raw experimental data as obtained from the computer for CO_2

The removal of products from the film is by diffusion. The rate of diffusion is given by the product:

$$D \quad \frac{\partial c(x,t)}{\partial x} \quad x=0 \tag{9}$$

where D is the diffusion coefficient of the product within the film and $\frac{\partial c(x,t)}{\partial x}$ the concentration gradient of the product at the surface (x=0) of the film.

The product distribution $c(x,t)$ within the film is determined by the diffusion equation:

$$\frac{\partial c(x,t)}{\partial t} = D \frac{\partial^2 c(x,t)}{\partial x^2} + \Phi I_o e^{-\alpha x} \tag{10}$$

The solution of 10 is given in Appendix I. The expression for the rate of evolution of product from the film is found to be:

$$D \quad \frac{\partial c(x,t)}{\partial x} \quad x=0 \quad = B \left[1 - e^{D\alpha^2 t}\right] \text{Erfc} \ (\alpha\sqrt{Dt}) \tag{11}$$

where $B = \dfrac{\Phi I_o}{\alpha}$

The time dependent diffusion term in equation 11 can be important below the glass transition temperature of the film; for most cases, however, $\alpha\sqrt{Dt} > 3$ hence erfc $(\alpha\sqrt{Dt}) \approx 0$, and the rate of product evolution from the film is essentially constant.

One can now calculate the concentration of product n_i in the reaction chamber from the equation:

$$\frac{\partial n_i}{\partial t} = B_i - \beta_i n_i \tag{12}$$

where β_i is the pumping speed to the mass spectrometer of molecule i, and obtain

$$n_i = \frac{B_i}{\beta_i} (1 - e^{\beta_i t}) \tag{13}$$

Since the signal in the mass spectrometer is proportional to the flux of molecules, the signal itself is proportional to:

$$\frac{\partial n_i}{\partial t} \quad \text{mass spectrometer} \quad = \beta_i n_i = B_i (1 - e^{-\beta_i t}) \tag{14}$$

The expression holds for a product formed by a zero order process and which does not participate in further reactions within the film. Expressions for other reaction schemes have been derived and will be published in a subsequent paper.

The quantity B_1 is interesting in that it clearly illustrates the importance of the absorption coefficient α. For a carbonyl group $\alpha \simeq 10^4 cm^{-1}$, hence degradation is confined to a region of only 2 μm. An increase in α will limit the degradation reactions to an even smaller surface region. Weakly absorbed radiation, however, will cause degradation throughout the whole film.

Results and Discussion

Utilizing the degradation scheme outlined above, one can make a prediction as to the degradation products that should be observed in the mass spectrometer. Figure 2 depicted the experimental data for one of these, CO_2. There is approximately 10% noise on this data which is due to noise in the electronics. This has since been remedied substantially. However, in order to effectively use this data, it was necessary to improve the signal to noise ratio; by averaging ten successive scans, these are acquired in approximately two minutes.

Figure 4 is a plot of the data of figure 2 averaged in this manner. The arrow in the figure denotes the time when the lamp was turned on. Notice that within two to four minutes detectable quantities of product are found, indicative of the sensitivity of this method.

From equation 14 one expects for a zero order process the time intensity curve to reach a constant value. It is also well established that the CO_2 production from the ester side chain degradation occurs in essentially one step (10) and in our case because of the large excess of reactant is independent of concentration. Therefore, the CO_2 production should exhibit a pseudo-zero order kinetic behavior. It is clear from figure 4 that the CO_2 data does indeed behave as equation 14 suggests. As a test of how well equation 14 actually describes the process responsible for the CO_2 production a non-linear least squares program (11) was used to fit the data of figure 4 to equation 14. The results are shown in figure 5; the fit is quite reasonable, indicating that this type of analysis for unraveling the kinetic behavior of the degradation is valid.

As pointed out previously, the lamp is not turned on until the background stabilizes. It is useful to monitor the background during the experiment to detect any changes in experimental conditions. Shown in Figure 4 along with the data for CO_2 is the O_2 data averaged in the same manner. There is no process which is expected to produce oxygen and, therefore, it serves as a convenient monitor for the background. The series of peaks corresponding to mercury from the pumps acts as another internal monitor of the system.

Figure 6 is a plot of two other fragments observed, M/E = 31 (CH_3O^+) and M/E = 41 ($C_3H_5^+$). These curves show a different type of time intensity behavior than that of the CO_2. There is no plateau after three and one half hours. The difference must be
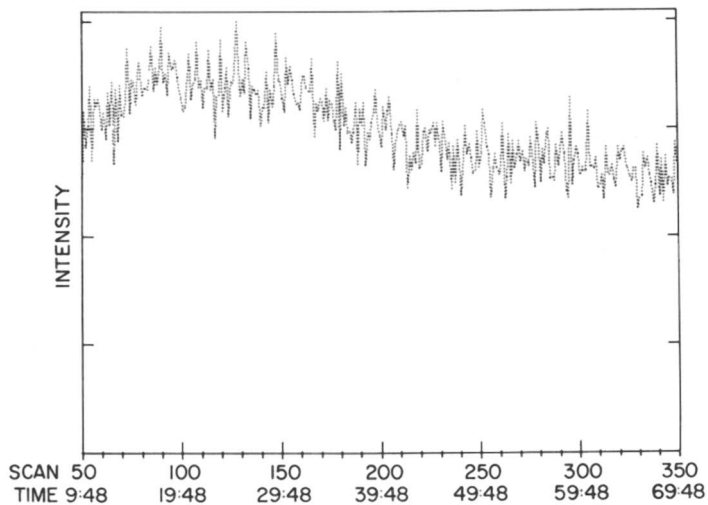
Figure 3.   Raw experimental data of background ion intensity before degradation experiment initiated
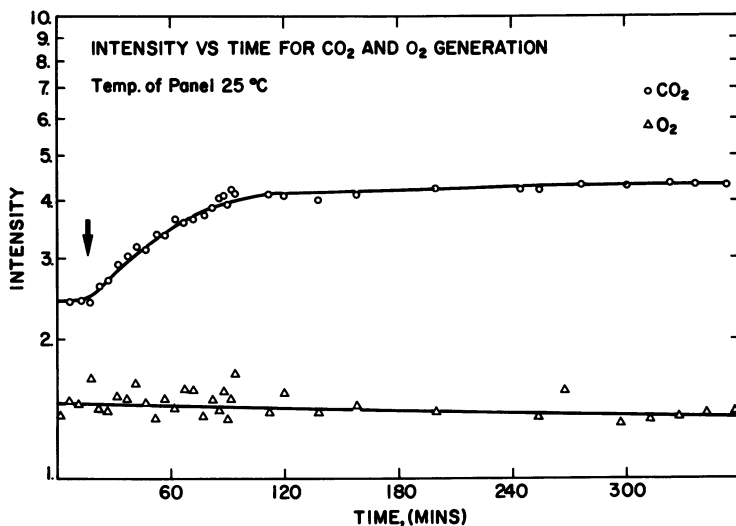
Figure 4.   Plot of experimental data for CO₂ and O₂ after averaging. Each point represents a 10-spectra average.
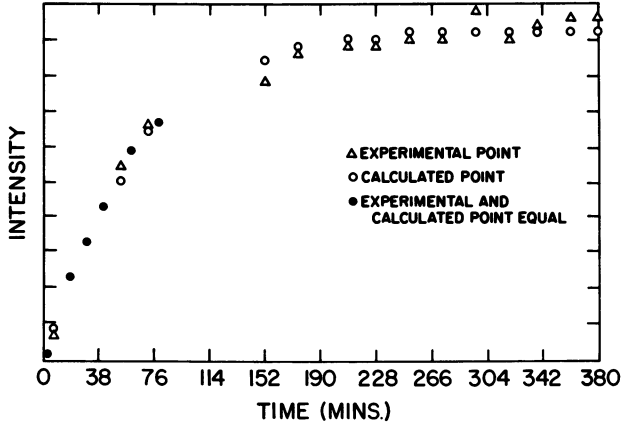
Figure 5.   Comparison of experimental data for CO_2 with a nonlinear least squares fit of this data to Equation 14
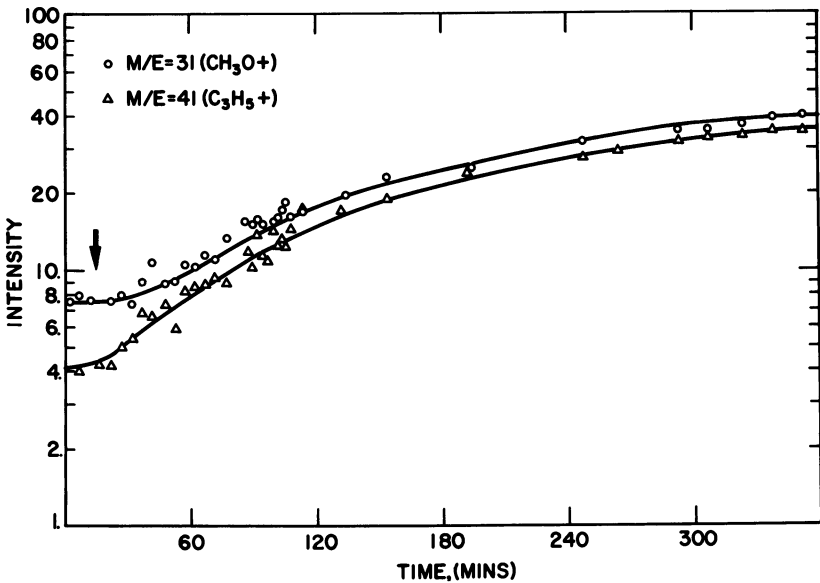
Figure 6.   Averaged data for the CH_3O+ and C_3H_5+ fragments

due to a different kinetic process being responsible for the
generation of the molecules producing these fragments. This of
course is not unreasonable because the type of molecules which
can generate these fragments are alcohols and esters (e.g.
formates) which are probably formed in a two step process. The
computer fit of the CO_2 data makes one confident that with the
proper kinetic assumptions an analytical expression can be derived
to fit the data, and therefore kinetic parameters arrived at.
One complication exists in this process, the M/E = 31 peak, for
example, may have contributions from more than one molecule (e.g.
CH_3OH and CH_4CO_2). That being the case the curve would be a sum
of two or more kinetic processes. This can be overcome by the
use of high resolution mass spectrometry.

     With high resolution capability one can find unique masses
which are attributable to each molecule and from that intensity
and a library of mass spectral data (9) one can "deconvolute"
the mass spectrum into its individual components. We currently
have the ability to acquire such data and are developing the
software needed to handle it.

     In low resolution finding unique masses for each fragment is
considerably more difficult if not impossible. However, there is
another approach which may be taken. If one examines the reaction
scheme, a prediction of which molecules will be generated can be
made. Then utilizing a library of mass spectral data a series of
simultaneous equations in contribution to intensity of given mass
spectral peaks can be written (12). The only assumption necessary
for this is we know all the molecules contributing to each peak
of interest.

     Such a procedure was followed with our data. Based on the
prepolymer composition it was decided that Butanol, Butane,
Butene, methanol and methyl formate would be the most likely
degradation products in addition to the CO_2 and CO. Utilizing
the M/E = 56, 43, 41 and 31 peaks, a set of simultaneous equations
were solved for the composition of the degradation products ob-
served at the end of the experiment. Table I lists this
composition.

TABLE I

     Calculated composition of degradation products from acrylic
paint at 25°C found at end of experiment

Component	Calculated Intensity
Butanol	3.4×10^5
Butane	4.4×10^5
Butene	2.8×10^5
Methanol	2.0×10^5
Methyl formate	1.3×10^5

Using this composition the intensity of several other peaks not used in the solution of the simultaneous equations and assumed to originate from these degradation products only were calculated. The results are tabulated in Table II.

TABLE II

Calculated vs. observed intensity for mass spectral peaks assumed to originate from the degradation products of Table I.

M/E	Calculated Intensity	Observed Intensity
27	4.3×10^5	4.4×10^5
29	4.9×10^5	8.0×10^5
39	2.2×10^5	2.5×10^5

Good agreement with the M/E = 27 and 39 peaks is obtained, but there is a fairly large discrepancy with the 29 peak. This indicates that there is another degradation product we have not considered contributing to the 29 peak. This may be a melamine fragment or some other molecule.

In any event it is clear the low resolution data can be used to gain insight into the role played by the chemistry of the film in the degradation as well as giving kinetic information.

Examination of our data for peaks due to monomer which might be formed from unzipping reactions showed no detectable amount being produced. This is not unexpected because the prepolymer composition is approximately 50% acrylate type monomers and, therefore, degradation by unzipping is unlikely.

Conclusions

It has been demonstrated that the sensitivity of the mass spectrometer makes it ideally suited for application to the study of polymer photodegradation. The basic understanding of the system makes it possible to extract useful kinetic and chemical information about the degradation reactions. Work on the roles of temperature, chemical composition and network structure is in progress.

Acknowledgments

Literature Cited

1. Hoffman, E. and Saracz, A., J. Oil Col. Chem. Assoc., <u>55</u>, 1079 (1972).
2. Colling, J. H., Cracker, W. E., Smith, M. C., and Dunderdale, J., J. Oil Col. Chem. Assoc., <u>54</u>, 1057 (1971).
3. Perera, D. Y., and Heertjes, P. M., J. Oil Col. Chem. Assoc., <u>54</u>, 774 (1971).
4. Tamblyn, J. W., Newland, G. C., and Watson, M. T., Plastics Technol., <u>4</u>, 427 (1958).
5. Grassie, N. and Farrish, E., Europ. Poly. J., <u>3</u>, 627 (1967).
6. Grassie, N., Torrence, B. J. D., and Colford, J. B., J. Poly. Sci. Al, <u>7</u>, 1425 (1969).
7. Grassie, N. and Jenkins, R. H., Europ. Poly. J., <u>9</u>, 697 (1973).
8. Calvert, J. G. and Pitts, J. N., "Photochemistry", John Wiley and Sons, Inc., New York (1966).
9. ASTM Committee E-14 on Mass Spectrometry, "Index of Mass Spectral Data", ASTM, Philadelphia, Pa. (1969).
10. Calvert, J. G and Pitts, J. N., "Photochemistry", John Wiley and Sons, Inc., New York, p. 434 (1966).
11. Dye, J. L. and Nicely, V. A., J. Chem. Ed. <u>48</u>, 443 (1971).
12. Willard, H. H., Merritt, L. L., Jr., and Dean, J. A., "Instrumental Methods of Analysis", D. Van Nostrand Co., Inc., Princeton, N. J., p. 449 (1965).
13. Bateman, H., "Tables of Integral Transforms Vol. I.", McGraw-Hill Book Co., Inc., New York, pp. 245-6 (1954).

APPENDIX I

SOLUTION OF DIFFERENTIAL EQUATION DESCRIBING TIME DEPENDENCE OF PRODUCT DETECTION

It is assumed that the film absorbs light by Beer's law

$$I(x) = I_o \exp(-\alpha x) \tag{1}$$

where the variables are defined in the text of this paper. It is also assumed that the degradation products are formed by a pseudo-zeroth order reaction:

$$\frac{\partial c(x,t)}{\partial t} = \Phi I \tag{2}$$

The products formed are removed from the film by diffusion. The rate of diffusion from the film is given by

$$D \left(\frac{\partial c(x,t)}{\partial x} \right)_{x=0} \tag{3}$$

The product distribution within the film is given by the diffusion equation

$$\frac{\partial c(x,t)}{\partial t} = D \frac{\partial^2 c(x,t)}{\partial x^2} + \Phi I_o e^{-\alpha x} \tag{4}$$

Solving equation 4 for $c(x,t)$ and then solving equation 3 yields the rate of product into the chamber. The boundary conditions imposed to solve these equations are

$$c(x,o) = 0$$
$$c(\infty,t) = 0 \tag{5}$$
$$c(o,t) = 0$$

The Laplace transform is used to solve equation 4 where:

$$\bar{c}(x,P) = \int_o^\infty c(x,t) \, e^{-pt} \, dt \tag{6}$$

hence

$$\int_o^\infty e^{-pt} \frac{\partial c(x,t)}{\partial t} \cdot dt = \int_o^\infty D \frac{\partial^2 c(x,t)}{\partial x^2} e^{-pt} \, dt +$$
$$\int_o^\infty Ae^{-\alpha x} e^{-pt} \, dt \tag{7}$$

Solving

$$\int_o^\infty e^{-pt} \frac{\partial c(x,t)}{\partial t} \, dt = \left[ce^{-pt} \right] + p\int_o^\infty ce^{-pt} \, dt = p\bar{c}$$
$$ce^{-pt} = 0 \quad \text{Since for } t = 0 \quad c(x,o) = 0$$

$$\int_o^\infty D \frac{\partial^2 c(x,t)}{\partial x^2} e^{-pt} \, dt = D \frac{\partial^2}{\partial x^2} \int_o^\infty ce^{-pt} = D \frac{\partial^2 \bar{c}}{\partial x^2}$$

and

$$\int_o^\infty Ae^{-\alpha x} e^{-pt} \, dt = \frac{1}{p} Ae^{-\alpha x}$$

Therefore the transformed differential equation becomes:

$$D \frac{\partial^2 \bar{c}}{\partial x^2} - p\bar{c} = -\frac{1}{p} Ae^{-\alpha x} \tag{8}$$

The complementary solution to equation 8 is

$$\bar{c} = A' e^{\left(\frac{P}{D}\right)^{\frac{1}{2}} x} + Be^{-\left(\frac{P}{D}\right)^{\frac{1}{2}} x} \tag{9}$$

since as $x \to \infty$ $c \to o$, A' must be zero.

The particular solution to equation 8 is

$$\bar{c} = Fe^{-\alpha x} \tag{10}$$

substituting into 8 one obtains

$$F = \frac{1}{p} \frac{A}{p - D\alpha^2}$$

and the complete solution is

$$\bar{c} = Be^{-\left(\frac{p}{D}\right)^{\frac{1}{2}} x} + \frac{A}{p(p - D\alpha^2)} e^{-\alpha x} \tag{11}$$

eliminating one of the constants with the boundary condition $c(o,t) = 0$ we obtain:

$$\bar{c} = -\frac{A}{p(p - D\alpha^2)} e^{-\alpha x} - \frac{A}{p(p - D\alpha^2)} c^{-\left(\frac{x}{\sqrt{D}}\right) p^{\frac{1}{2}}} \tag{12}$$

Using the tables of transforms (13) we rewrite equation 12 in terms of x and t:

$$c(x,t) = \frac{Ae^{-\alpha x}}{D\alpha^2} \left[e^{-D\alpha^2 t} - 1 \right] + \frac{A}{D\alpha^2} \operatorname{Erfc}\left(\frac{1}{2} \frac{x}{\sqrt{Dt}} \right) -$$

$$- \frac{1}{2} \frac{A}{D\alpha^2} e^{D\alpha^2 t} \left[e^{\alpha x} \operatorname{Erfc}\left(\frac{1}{2} \frac{x}{\sqrt{Dt}} + 2\sqrt{Dt} \right) + e^{-\alpha x} \operatorname{Erfc}\left(\frac{1}{2} \frac{x}{\sqrt{Dt}} - \alpha\sqrt{Dt} \right) \right]$$

Triplet States of Photosensitive Aromatic Azides

MINORU TSUDA and SETSUKO OIKAWA

Laboratory of Physical Chemistry, Faculty of the Pharmaceutical Sciences,
Chiba University, Chiba 280, Japan

Abstract: Although aromatic azides are believed not to emit phosphorescence, 2,4,6-tribromophenylazide was found to phosphoresce in EPA at 77°K, and the peak of the spectrum coincides with the tail of the absorption spectrum of its concentrated solution in ethyl iodide. The measurements of the $S_0 \rightarrow T_1$ absorption spectra in ethyl iodide with vibrational structures were also succeeded in the cases of ethyl p-azidobenzoate and ethyl p-azidocinnamate. The experimantal values coincided with the $(\pi \rightarrow \pi^*)^3$ transition energies estimated by SCF MO CI calculations(Pariser-Parr-Pople method); the transition energies of T_1 are 20100 cm^{-1} for the former and 18700 cm^{-1} for the latter, respectively, and that for phenylazide is 21700 cm^{-1}. The results obtained by the calculation of MIM(molecule in molocule) method showed that the contribution of the localized excitation(LE) of azide group to the state function of T_1 of p-azidobenzoate is 61.33 % and that of benzoyloxy group is only 18.22 %. However, in the case of p-azidocinnamate, the main contribution to T_1 is the LE of cinnamoyloxy group(69%)

   Aromatic azides are stable photosensitive compounds and some of them mixed in cyclized rubber are practically used as photosensitive resines.(1) Such photosensitive polymers as poly(vinyl p-azidobenzoate)(2) and poly(vinyl p-azidocinnamate)(3) are also investigated. These photosensitive resines are known to be spectrally sensitized by triplet sensitizers(1,2,3). But the energies $E(T_1)$ of the lowest triplet states T_1 of aromatic azides have not been known, because these compounds emit no phosphorescence(4) and the trials on the measurement of their $S_0 \rightarrow T_1$ absorptions are failed(4,5).
   In order to decide $E(T_1)$ of azides, Saunders et al. measured quantum yields for nitrogen evolution in sensitized photolysis of azides(4) expecting such a relationship that the rate constants k_q in the energy transfers from the triplet sensitizers to an azide might converge to a constant value provided $E(T_1)$ of sensitized were larger than $E(T_1)$ of the azide, as Hammond et al. had obtained in the sensitized cis-isomerization of trans-stilbene(7). In the cases of azides, however, k_q increases monotonously according to the increase of $E(T_1)$

of sensitizers. Saunders considered that extraporation of the lines
showing the relation log k_q versus $E(T_1)$ of sensitizers to log k_q=9
suggested the $E(T_1)$ of azides, since k_q had converged at 10^9–10^{10} 1.
$mol^{-1}.sec^{-1}$ in the sensitized cis-isomerization of trans-stilbene.
$E(T_1)$ of phenylazides was decided to be 75 Kcal/mol(26300 cm^{-1}) by
the procedure. Although we accept some of questionable points in
their discussions, the largest difficulty is that the $(n{\rightarrow}\pi *)^1$ transi-
tion(Fig.1a) of phenylazide tails to 75 Kcal/mole. Therefore, $E(T_1)$
should be lower than that of the lowest singlet state. Saunderes also
showed that sensitizers as low in $E(T_1)$ as benzophenone(68 Kcal/mol (
23800 cm^{-1})) gave appreciable reaction in the photolysis of phenylazi-
de(4), which suggests that the reaction mechanism is not so simple as
in the case of sensitized cis-isomerization of trans-stilbene. There-
fore, we cannot expect the obtaining of the exact value of $E(T_1)$ of
aromatic azides by such a procedure of simple chemical kinetics as
Saunders used.
 In this paper, we effortto determine $E(T_1)$ of aromatic azides
spectroscopically, utilizing the inner and outer heavy atom effects
along with the theoretical estimation of the $E(T_1)$ by the PPP calcula-
tions(6), and also discussed the electronic structures of aromatic
azides comparing those with the data obtained by the MIM calculations
(6).

Phenyl Azide.

 <u>Transition Energies and Spectrum</u>. The results of the PPP calcu-
lations on the transition energies and oscillator strengths of phenyl-
azide are shown in Fig.1c. The spectrum in EPA at 77°K has the same
peak at 40000 cm^{-1} as that in n-hexane solutions at room temperature
without the remarkable vibrational structure near 35000 cm^{-1} in the
former. The vibrational structure corresponds to that of $^1B_{2u}$ state
of benzene in the number of peaks and the intervals as was shown in
Fig.1a Therefore, it is considered that the transition arises from
the $^1B_{2u}$ transition of benzene. The MIM calculation justified the es-
timation as was shown in Table 1, where the contribution of the LE
function of $^1B_{2u}$ is 84 % in the S_1 state. The forbidden $^1B_{2u}$ transi-
tion becomes a weakly allowed one by the perturbation of azide.
 The S_2 transition in phenylazide shows the blue shift in polar
solvents: the peak at 40000 cm^{-1} in n-hexane shifts to 40400 cm^{-1} in
ethanol and EPA at room temperature(the spectrum in EPA shown in Fig.
1b shift from 40300 cm^{-1} to 40000 cm^{-1} again by the frozen conditions).
This is an extraordinary phenomenon in the $(\pi{\rightarrow}\pi *)^1$ transitions. The
PPP calculations reveal the reason as is shown in Fig.2. As are found
from the molecular diagrams of S_0 and S_2, the electron displacement
from azide to benzene in S_0 changes to the opposite direction in S_2
in spite of the same direction in S_1. In the case of aniline, the red
shift is observed in polar solvents and the direction of the electron
displacement is the same in each case of S_0,S_1 and S_2.
 The similarities of the absorption spectra of phenylazide and
stylene are already pointed out by the present author(10). Comparing
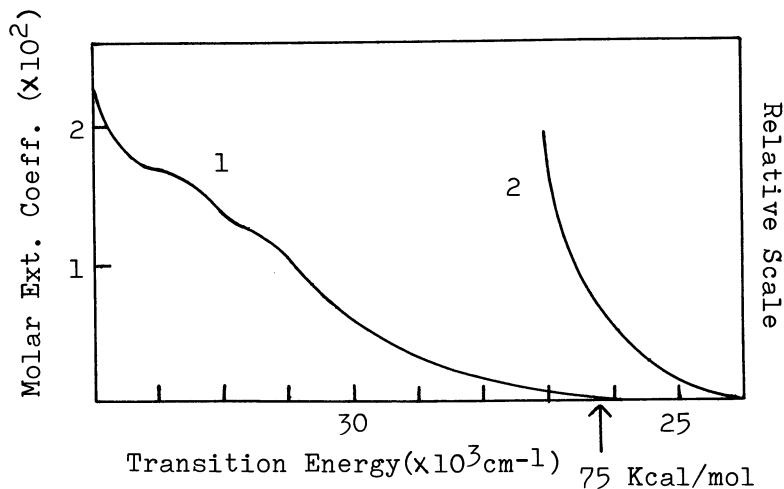
Figure 1a.   The tail of (n → π*) absorption spectrum of phenyl azide 1: 0.42 × 10⁻²M, 77°K in EPA, 2: 0.2M, 20°C in benzene
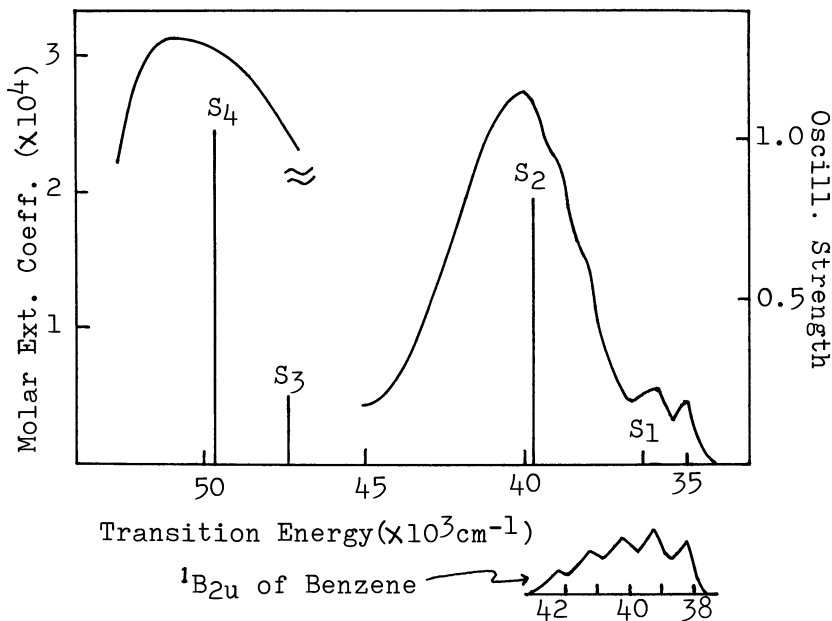
Figure 1b.   The comparison of the calculated values with the experimental ones on the electronic transition energies and oscillator strengths of phenylazide. The S₁ transition has a vibrational structure corresponding to the five peaks of ¹B₂ᵤ of benzene. The absorption spectrum lower than 45,000 cm⁻¹ was measured at 77°K in EPA. The S₄ absorption is that of neat phenylazide (thin layer).

Table 1. The Contributions of Various Electronic Configurations of the MIM model for the State Functions of the PPP model of Phenylazide = Benzene(B) + Azide(A).

Singlet State		S_0	S_1	S_2	S_3	S_4	S_5
Transition Energy(cm^{-1})			35271	39805	46624	49680	54226
LE	G	92.30	0.02	0.02	0.02	0.10	3.05
	B	0.18	86.48	39.46	80.21	74.58	41.39
	A	0.01	0.38	24.55	8.66	0.87	1.93
CT	A→B	4.62	3.77	9.22	1.71	6.20	7.96
	B→A	2.66	3.16	22.37	2.58	11.98	37.36
Total		99.78	93.81	95.62	93.18	93.73	91.69
LE+G		92.49	86.88	64.03	88.89	75.55	46.37
CT		7.28	6.93	31.59	4.29	18.18	45.32
Main Contribution			85.34 $^1B_{2u}$	24.55 A S_1 22.37 CT	62.39 $^1B_{1u}$	67.14 $^1E_{1u}$	37.36 CT 35.31 $^1E_{1u}$

Triplet State		T_1	T_2	T_3	T_4	T_5
Transition Energy(cm^{-1})		21338	28869	32814	32953	35884
LE	B	14.66	78.26	87.22	86.76	87.32
	A	64.94	14.59	0.25	3.77	0.46
CT	A→B	4.54	0.94	3.62	2.12	3.22
	B→A	11.51	0.12	2.79	1.24	2.71
Total		95.66	93.91	93.88	93.88	93.71
LE+G		79.60	92.85	87.47	90.53	87.78
CT		16.05	1.06	6.41	3.36	5.93
Main Contribution		64.94 A T_1	77.91 $^3B_{1u}$	80.15 $^3E_{1u}$	63.02 $^3E_{1u}$	69.17 $^3B_{2u}$

Figures are the squares of the coefficients in the state functions expressed as a linear combination of the electronic configurations of the MIM model. G: Ground configuration, LE: Configuration of the localized excitation, CT: Charge transfer configuration.
B_{1u}, B_{2u}, E_{1u}: The electronic states of benzene
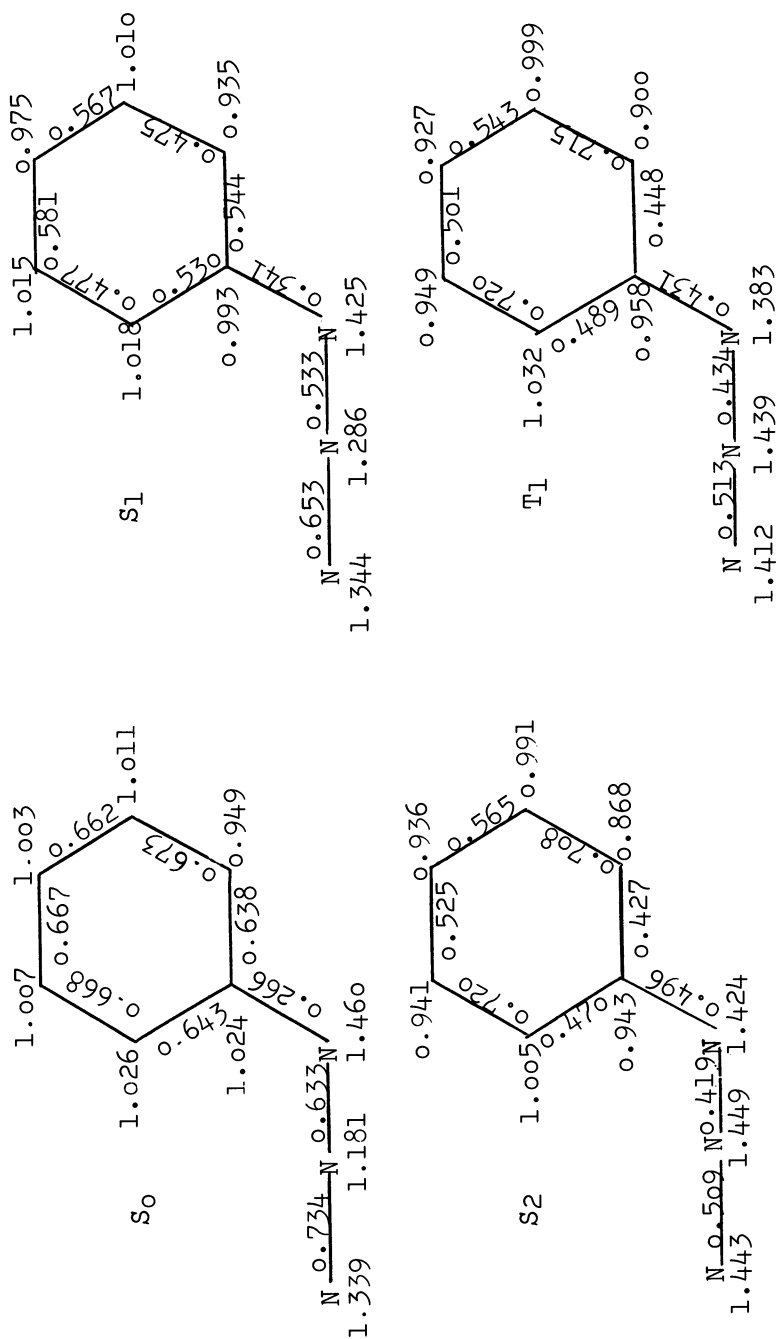
Figure 2.   Molecular diagrams of the various states of phenylazide

the results in Table 1 and Appendix 1, we can find out the remarkable
similarities of the state functions S_0, S_1, S_2, T_1, which are observed,
and other states of these two compounds. And we can also see that the
S_2 state function is similar to the S_2 function of cinnamoyloxy group
in the points of the intramolecular charge transfer character and the
large contribution of the azide(ethylene in the latter) LE function.

Triplet State. A remarkable feature of the T_1 state of phenyl
azide is the large contribution of the LE function of azide group.
The same tendency was observed in the cases of stylene, stilbene(6)
and cinnamoyloxy group(6). The calculated value of T_1 is 21700 cm^{-1}.
The $S_0 \rightarrow T_1$ absorption spectrum in EtI gives only tail near the calcu-
lated value. The emission spectrum in EPA gave such a phosphorescence
as was shown in Fig.3. The intensity increases with the irradiation
time. Therefore, it is clear that the emission spectrum is that of
the photodecomposed product, which is estimated to be aniline from the
similarity of the phosphorescence of the authentic sample.

P-Azidobenzoate.

Transition Energies and Spectrum. The UV spectrum of poly(vinyl
p-azidobenzoate) is the same as that of ethyl p-azidobenzoate. The
spectrum of the latter in n-hexane solutions is shown in Fig.4 with
the calculated transition energies and osillator strengths.
Hasegawa et al. divided the spectrum into four peaks assuming the
Gaussian distributions around the transition energies lower than 40000
cm^{-1} (11). According to our theoretical calculations, however, there
are only two peaks in this area. Assuming the Gaussian distribution
around the S_2 transition energy, we obtained the two transition peaks,
one of which, the S_1 transition, has three peaks which has the same
intervals as the S_1 transition of phenylazide. Therefore, the S_1
state is considered to arise from the $^1B_{2u}$ state of benzene. The esti-
mation is supported by the MIM calculations as is shown in Table 2 (
also see Appendix 3 and 4 in the discussions in this section). The S_2
transition also the same property as that of phenylazide. When we
performed the MIM calculations of p-azidobenzoate = phenylazide + car-
boxyl group, all the transitions which can be observed by the conven-
tional UV spectrometer($S_0 \sim S_5, T_1$) are substantially those of phenyl
azide(purterbed by carboxyl group).(Appendix 2)

The $S_0 \rightarrow T_1$ transition energy. The $S_0 \rightarrow T_1$ absorption spectrum of
ethyl p-azidobenzoate in C_2H_5I was succeeded in the measurement(Fig.
5(a)). PPP calculations show that the transition energy of T_1 is
20084 cm^{-1} and the energy difference between T_1 and T_2 is 6300 cm^{-1}.
Therefore, we can expect the vibrational structures of T_1 isolated
from T_2 if it appears. The spectrum has the progressions of about
2000 cm^{-1} which is in accordance with the stretching vibration of azi-
de group of IR spectra(2150 cm^{-1})(2a). The MIM calculation reveals
that the contribution of the LE function of azido group is 61.33 %,
and that of benzoyloxy group is 18.22 % for T_1. Therefore, we can
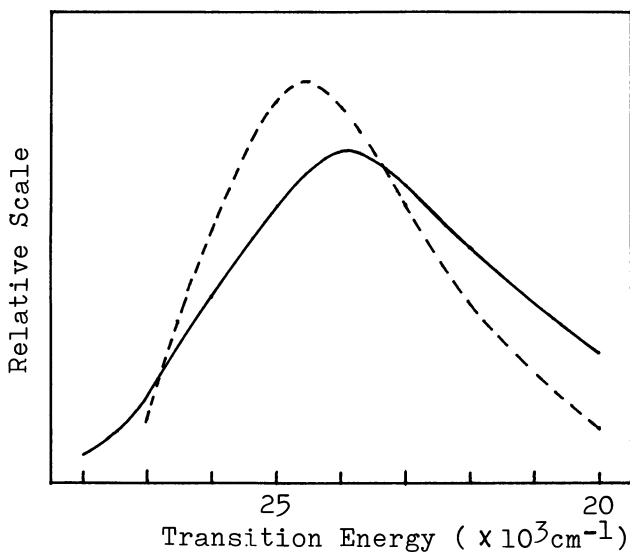
Figure 3.   Phosphorescence spectra of aniline (- - -) and the photodecomposed product of phenylazide (—) at 77°K in EPA
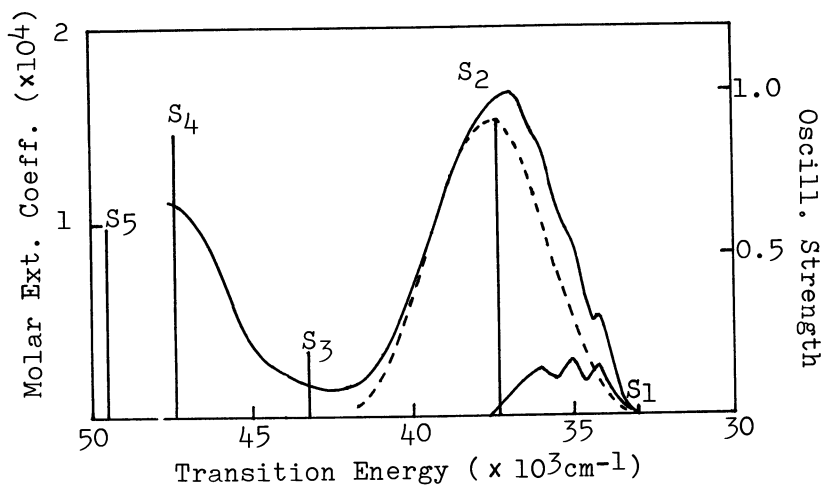
Figure 4.   Comparison of the calculated values with the experimental ones on the transition energies and oscillator strengths of p-*azidobenzoate (ethyl* p-*azidobenzoate in* n-*hexane). (- - -), the spectra divided to* S_1 *and* S_2. *Assumed Gaussian function is* $F = (A/(\sqrt{2\pi}D)) \exp (-(E - E_0)^2/(2D^2))$; E_0, *peak position;* $A/(\sqrt{2\pi}D)$, *peak height;* $\sqrt{2\ln 2}D$, *half value width.*

Table 2. The Contributions of Various Electronic Configurations of the MIM model for the State Functions of the PPP model of p-Azidobenzoyloxy Group = Benzoyloxy Group(B.A.)+Azide(A)

Singlet State		S_0	S_1	S_2	S_3	S_4	S_5
Transition Energy(cm^{-1})		33048	37142	43338	47413	49562
LE	G	90.57	0.01	0.14	0.12	0.89	0.41
	B.A.	1.76	87.07	51.95	73.20	77.49	71.02
	A	0.05	0.08	17.58	11.56	3.94	4.59
CT	A→ B.A.	5.00	3.60	11.28	3.03	5.62	1.36
	B.A.→A	2.27	2.01	13.11	4.02	3.77	14.37
Total		99.65	92.77	94.06	91.93	91.69	91.75
LE+G		92.38	87.16	69.67	84.88	82.32	76.02
CT		7.27	5.61	24.39	7.05	9.39	15.73
Main Contribution			83.05 B.A. S_1	41.41 B.A. S_2	30.18 B.A. S_2 / 34.13 B.A. S_4	37.02 B.A. S_3 / 23.65 B.A. S_5	24.18 B.A. S_3 / 20.73 B.A. S_4

Triplet State		T_1	T_2	T_3	T_4	T_4
Transition Energy(cm^{-1})		20084	26388	30169	31157	32711
LE	B.A.	18.22	72.17	89.61	89.03	84.07
	A	61.33	19.39	0.18	0.89	0.94
CT	A→ B.A.	5.21	1.23	0.62	1.79	7.22
	B.A.→A	9.31	0.27	2.60	0.41	0.24
Total		94.07	93.06	93.01	92.12	92.47
LE		79.55	91.56	89.79	89.92	85.01
CT		14.52	1.50	3.22	2.20	7.46
Main Contribution		61.24 A T_1	70.06 B.A. T_1	68.91 B.A. T_3 / 12.67 B.A. T_2	58.83 B.A. T_2 / 20.31 B.A. T_4	47.75 B.A. T_4 / 13.22 B.A. T_2

Figures are the squares of the coefficients in the state functions expressed as a linear combination of the electronic configurations of the MIM model. G: Ground configuration, LE: Configuration of the localized excitation, CT: Charge transfer configuration

conclude that the vibrational structure of the $S_0 \rightarrow T_1$ absorption arises from azide group(Table 2).

Emission Spectra. With the phosphoroscope, ethyl p-azidobenzoate in EPA at 77°K, gave an emission spectrum which is shown in Fig.6.
The spectrum is that of the decomposed product, which is estimated to be ethyl p-aminobenzoate in comparison with the phosphorescence of the authentic sample(Fig.6).

P-Azidocinnamate

Transition Energies and Spectrum. Poly(vinyl p-azidocinnamate) was prepared and investigated on the photochemical reactions by the present author(3). Since it has two photosensitive chromophores, namely azide and cinnamoyloxy group, the characters in the excited states are interesting in connection with the photochemical reactions. The absorption spectrum is the same as that of ethyl p-azidocinnamate. The PPP calculation reproduces well the UV spectrum as was shown in Fig.7. The MIM calculation reveals that the lower excited states are those of cinnamate(Table 3) and the considerations discussed in the preceeding paper(6) can be adopted in the same manner in this case. Therefore, the S_1 state arise from the $^1B_{2u}$ state of benzene and the S_2 state has a CT character(or delocalized character). These electronic states illustrate well the characteristics of the photochemical reactions of poly(vinyl p-azidocinnamate)(3), where the central double bonds react in the same way as cinnamoyloxy group.

Triplet States. The measurement of the $S_0 \rightarrow T_1$ transition energy was succeeded in the case of ethyl p-azidocinnamate, too(Fig.5(b)). The lowest triplet state energy calculated by the PPP method is 18755 cm^{-1} in accordance with the observed value. The MIM calculations show that the main contribution to T_1 is the LE of cinnamoyloxy group (69 %) and the energy difference between T_1 and T_2 is only 3200 cm^{-1}. We can understand from the small difference that the only one vibrational structure appears in Fig.5(b) and can also estimate that the vibrational structure arises from the central double bond of cinnamoyloxy group and not from azide. The T_2 state has the same character as the T_1 state of phenylazide where the contribution of the LE function of azide group is remarkable(55.02 % in this case).
The spectral sensitization by erythrosine(T_1=14700 cm^{-1}) was succeeded in poly(vinyl p-azidocinnamate)(3). The phenomena of the spectral sensitization of azide compounds by the sensitizers having the lower T_1 state energy than azides themselves, therefore, has confirmed for the first time in this paper although Lewis et al. had speculated the same thing on the unreliable data(4). The reaction mechanism may contain the exciplex formations, of which the theoretical investigations are now in progress. The observation in the erythrosine-sensitized photochemical reaction of the central double bond of p-azidocinnamate is interesting in connection with the possibility of the exciplex formation in the photodimerization of poly(vinyl cinnamate) spec-
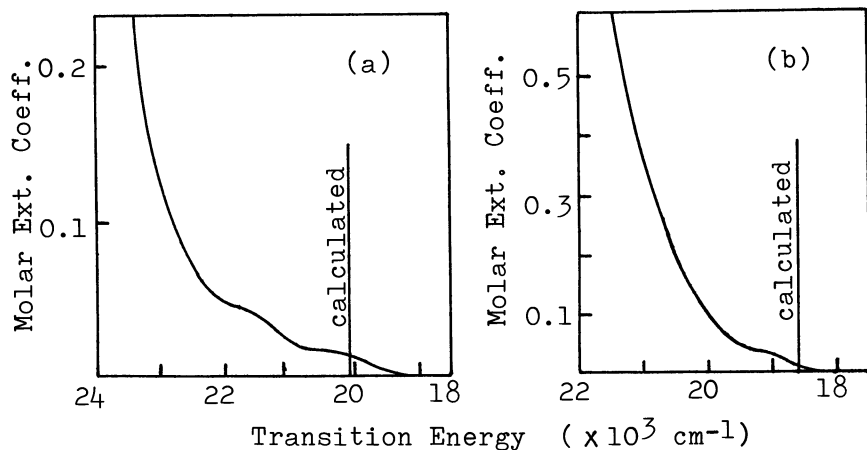
Figure 5. $S_0 \rightarrow T_1$ absorption spectra of aromatic azides 50 (vol) % EtI solutions at room temperature. The light path length is 5 cm. a, ethyl p-azidobenzoate; b, ethyl p-azidocinnamate.
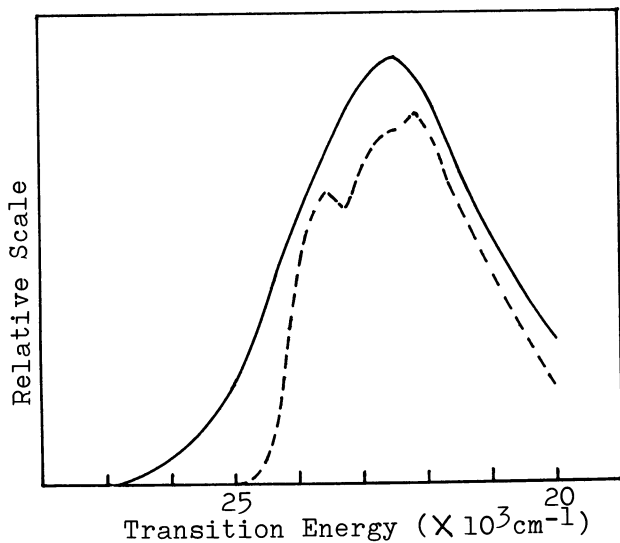
Figure 6.   Phosphorescence spectra of ethyl p-aminobenzo-ate (- - -) and the photodecomposed product of ethyl p-azidobenzoate (—) at 77°K in EPA

Table 3. The Contributions of Various Electronic Configurations of the MIM model for the State Functions of the PPP model of p-Azidocinnamoyloxy Group = Cinnamoyloxy Group(C. A.)+Azide(A)

Singlet State		S_0	S_1	S_2	S_3	S_4	S_5
Transition Energy(cm^{-1})		33151	33708	42508	43716	46988
LE	G	91.94	0.03	0.07	0.00	0.05	0.06
	C.A.	0.19	87.73	73.24	76.19	58.00	85.20
	A	0.05	0.31	7.57	4.52	19.92	3.14
CT	A→C.A.	2.47	2.30	6.16	7.10	11.95	1.27
	C.A.→A	5.11	3.08	6.88	5.43	3.55	3.03
Total		99.76	93.45	93.92	93.24	93.47	92.70
LE+G		92.18	88.07	80.88	80.71	77.97	88.40
CT		7.58	5.38	13.04	12.53	15.50	4.30
Main Contribution			82.23 C.A. S_1	63.97 C.A. S_2	58.63 C.A. S_3 19.64 A S_1	23.54 C.A. S_3	79.20 C.A. S_4

Triplet State		T_1	T_2	T_3	T_4	T_5
Transition Energy(cm^{-1})		18755	22201	29102	30270	32136
LE	C.A.	69.07	31.07	83.76	90.45	85.81
	A	16.93	55.02	8.11	0.08	3.46
CT	A→C.A.	4.23	6.30	0.26	2.71	0.29
	C.A.→A	3.59	2.06	1.04	0.23	3.83
Total		93.82	94.45	93.17	93.47	93.39
LE		86.00	86.09	91.87	90.53	89.27
CT		7.82	8.36	1.30	2.94	4.12
Main Contribution		66.96 C.A. T_1	54.93 A T_1	80.26 C.A. T_2	81.51 C.A. T_3	61.86 C.A. T_4

Figures are the squares of the coefficients in the state functions expressed as a linear combination of the electronic configurations of the MIM model. G:Ground configuration, LE:Configuration of the localized excitation, CT:Charge transfer configuration.
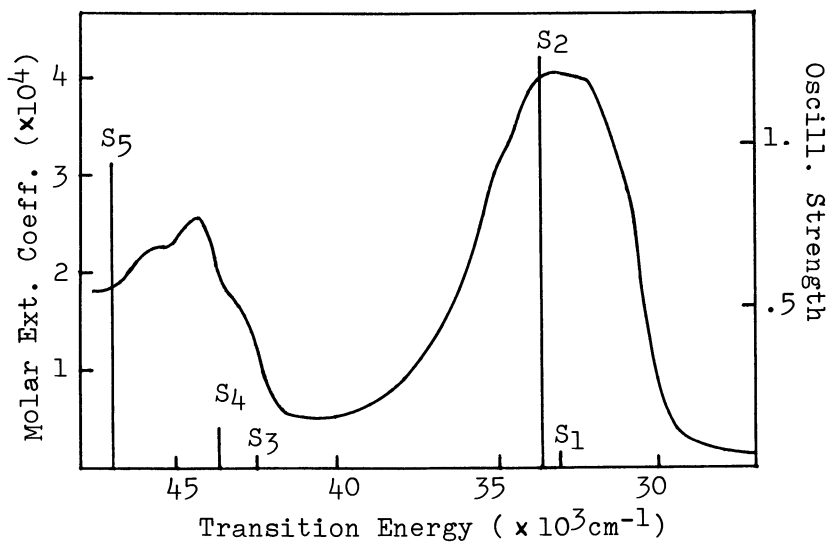
Figure 7. Comparison of the calculated values with the experimental ones on the electronic transition energies and oscillator strengths of the p-azidocinnamate (ethyl p-azidocinnamate in n-hexane)

Table 4. Parameters Used in the MO Calculations

	I_r	$(rr\vert rr)$	Z_r
N : tr^2 tr tr π (>N-)	14.12	12.34	3.9
N^+: di di π π^2(-N≡)	28.88	14.30	4.25
N : di^2 di π π (≡N)	14.18	12,52	3.9

β_{CC}: 2.34 (phenylazide)
         2.25 (p-azidobenzoate)
         2.31 (p-azidocinnamate)   (eV unit)

ulated in the preceeding paper(6).

2,4,6-Tribromophenylazide(TBA)

The absorption spectrum of TBA in EtI(0.426 mol/l) has only tail near 22000 cm^{-1}. Its phosphorescence spectrum in EPA(0.028 mol/l) was measured at 77°K. These two spectra are shown in Fig.8(a). The agreement of the phosphorescence(after corrected) and the $S_0 \to T_1$ absorption spectrum is satisfactory.

The intensity of the phosphorescence of TBA at 22200 cm^{-1} decreased along with the irradiation at 34500 cm^{-1} light according to the first order reaction rate(Fig.9). It is well known that phenyl azide photochemically decomposes in the first order reaction rate(3). The EPA matrix of TBA colored in yellowish orange by the irradiation of light showing the formation of an azo compound and a new phosphorescence peak arose at 18200 cm^{-1}(corrected), the intensity of which increased along the photoirradiation. Its excitation spectrum has a peak at 25600 cm^{-1}(corrected). From these facts we can believe that TBA emitts the phosphorescence having a peak at 22200 cm^{-1}. Since $(\pi \to \pi^*)^1$ transitions of TBA are at 45400 cm^{-1}(ε (molar extinction coefficient):7.26 $\times$ 10^4) and 40800 cm^{-1}(ε:1.9 $\times$ 10^4), and $(n \to \pi^*)^1$ transition is at 34500 cm^{-1}(ε:1.9 $\times$ 10^3), the phosphorescence(22200 cm^{-1}) is considered to arise from $(\pi \to \pi^*)^3$ transition.

The excitation spectrum(after corrected) of TBA has a shoulder near 34500 cm^{-1} which coincides with $(n \to \pi^*)^1$ transition (Fig.8b). As was shown by a few authors(3,9), the quantum yields of photocomposition of aromatic azide by the light of $(n \to \pi^*)^1$ transition were lower than those by that of $(\pi \to \pi^*)^1$ transition. The fact means that $(n \to \pi^*)^1$ transition should have more emissive property than $(\pi \to \pi^*)^1$ transition provided we assume other energy transfer processes are comparable in either case. The spectrum in Fig.8b justifies the considerations. The phosphorescence newly arisen at 18200 cm^{-1} is estimated to be that of 2,4,6,2',4',6'-hexabromoazobenzene, because the phosphorescence and the excitation spectrum of authentic 2,4,6-tribromoaniline are in the higher energy regions than those of the decomposed product(Fig.10)

Experimental

Substances: TBA: Recrystallized 2,4,6-tribromoaniline(8.5 g) was dissolved in 50 % H_2SO_4(100 ml) at 70–80°C, then cooled to 5°C. Diazotization was carried out by the addition of NaNO$_2$(2.125 g in 20 ml of water)at 5°C in the dark room, then converted to TBA by the dropping of NaN$_3$(2.8 g in 14 ml of water) for 30 min. Recrystallized from methanol-water. Calc. C:20.25 N:11.81 Br:67.37 Exp. C:20.44 N:12.20 Br:67.48; IR:N$_3$ 2140 cm^{-1}

Ethyl p-azidobenzoate and ethyl p-azidocinnamate were synthesized from p-amino derivatives in a similar manner.

Purification. Silica gel(100 mesh) was piled up to 10 cm in the glass tube(2 cm diameter) for column chromatography and adjusted by
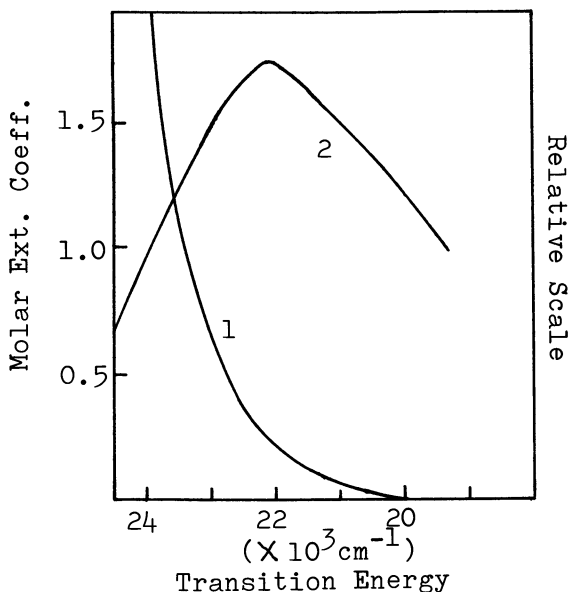
Figure 8a. S_0-T_1 absorption and phosphorescence spectra of 2,4,6-tribromophenylazide. 1, S_0-T_1 absorption of 0.426 mol/l. EtI solution at 20°C. 2, phosphorescence in EPA at 77°K, corrected according to the method of ref. (8).
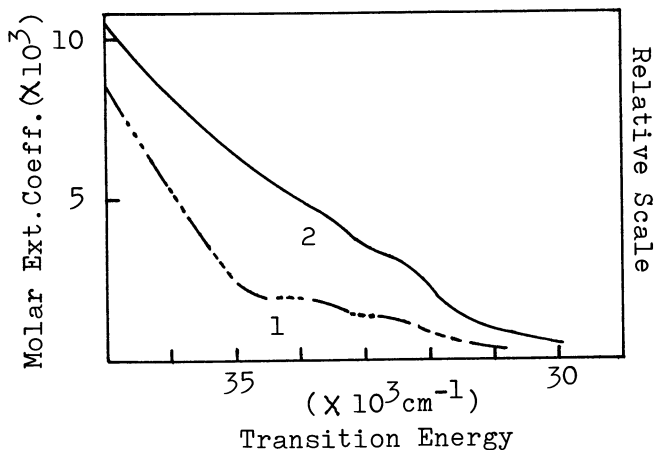
Figure 8b. $(n - \pi^*)^1$ absorption spectrum and excitation spectrum for the phosphorescence of 2,4,6-tribromophenylazide. 1, $(n - \pi^*)^1$ (30,000–35,000 cm^{-1}) and tail of $(\pi - \pi^*)^1$ absorption spectrum in n-hexane at 20°C. 2, excitation spectrum for the curve 2 in Figure 8a, corrected according to the method of ref. (8).
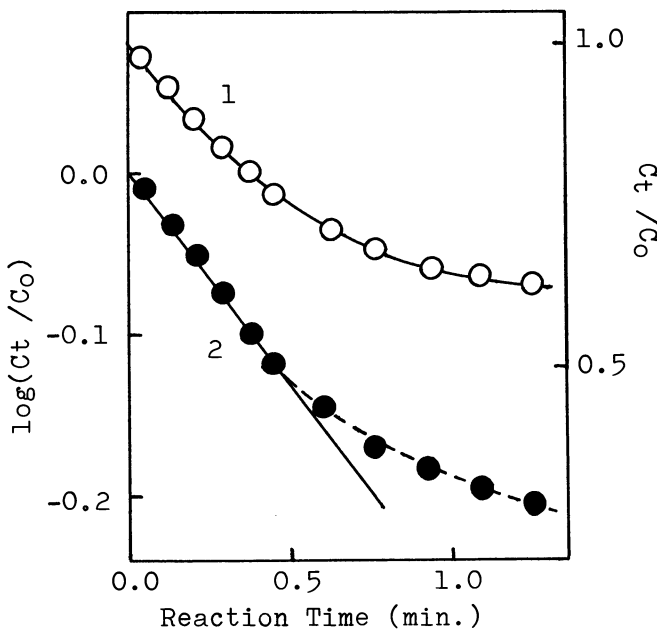
Figure 9.   The decrease (curve 1) of the intensity of phosphorescence of 2,4,6-tribromophenylazide along with the irradiation of 34,500 cm⁻¹ light following the first order reaction rate (curve 2). C₀ means initial concentration at t = 0.
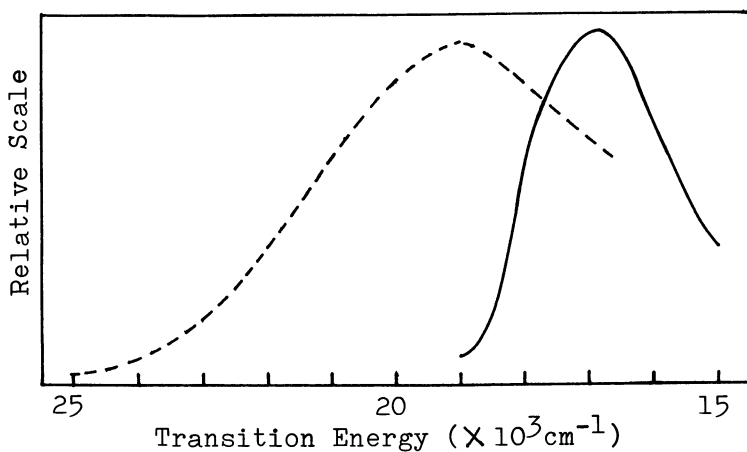
Figure 10.   Phosphorescence spectra of 2,4,6-tribromoaniline (- - -) and the photochemical product of 2,4,6-tribromophenylazide (—) at 77°K in EPA

flowing 50 ml of n-hexane. Ethyl p-azidobenzoate(6g) in spectrograde
n-hexane(50 ml) and then more 50 ml of n-hexane as the eluent were
made to flow through the column. The eluate was held at dry ice tem-
perature overnight and the crystallized product was collected. The
procedure was repeated three times in the present case. TBA and ethyl
p-azidocinnamate were purified in a similar manner.

    $S_0{\rightarrow}T_1$ Absorption. Ethyl iodide was distilled in dark room and
passed through the alumina column immediately before the spectrometry.
The most favorable ratio of sample and solvent was 1:1(in volume).
The quality of the spectrum was similar in either case of 5 and 10 cm
light-paths.

    Spectrometry. The absorption and phosphorescence spectra were
measured in the same manners as in the preceeding paper(6).

Theoretical

    The PPP and MIM calculations are performed in the same manners
as in the preceeding paper(6). The parameters used are the same ex-
cept those listed in Table 4.
    The calculations are carried out by HITAC 8700/8800 computers of
The University of Tokyo.

Literature Cited

1) Kosar,K.,"Light Sensitive Systems",Wiley,New York (1965)
2) Merrill,S.H. and Unruh,C.C., J.Appl.Polymer Sci.,(1963),7, 273;
2a) Tsuda,M.,Yabe,A. and Takanashi,H., Bull.Soc.Photo.Sci.Tech.Japan,
(1974), 23, 12
3) Yabe,A,Tsuda,M.,Honda,K. and Tanaka,H., J.Polymer Sci., (1972),
(A-1), 10, 2379
4) Lewis,F.D. and Saunders,W.H., J.Am.Chem.Soc.,(1968), 90, 7033
5) Kasha,M. and McGlynn,S.P., Ann.Rev.Phys.Chem.,(1956), 7, 403
6) See the preceding paper by Tsuda,M. and Oikawa,S.
7) Herkstroeter,W.G. and Hammond,G.S., J.Am.Chem.Soc.,(1966),88,4769
8) Tsuda,M.,Oikawa,S. and Miyake,R., J.Soc.Phot.Sci.Japan(Nippon Sha-
shingakkai-shi), (1972), 35, 90
9) Reiser,A. and Marley,R., Trans.Faraday Soc., (1968), 64, 1806
10) Tsuda,M., High polymer,Japan, (1970), 19, 109
11) Hasegawa,K. and Sano,R., Photo.Sci.Eng., (1971), 15, 309

Appendix 1. The Contributions of Various Electronic Configurations of the MIM model for the State Functions of the PPP model of Styrene = Benzene(B) + Ethylene(E)

Singlet State		S_0	S_1	S_2	S_3	S_4	S_5
Transition Energy(cm^{-1})		35800	41000	46200	50300	55900
Oscill. Strength			0.00	0.62	0.14	1.09	0.62
LE	G	90.56	0.04	0.00	0.00	0.00	0.00
	B	0.01	83.52	35.28	71.35	71.44	69.54
	E	0.00	0.00	21.60	16.21	2.81	16.12
CT	B→E	4.54	4.40	18.97	2.35	9.06	3.60
	E→B	4.54	4.40	18.97	2.35	9.06	3.60
Total		99.65	92.36	94.82	92.26	92.37	92.86
LE+G		90.57	83.56	56.88	87.56	74.25	85.66
CT		9.08	8.80	37.94	4.70	18.12	7.20
Main			83.43	21.60	54.53	62.76	62.39
Contribution			$^1B_{2u}$	E	$^1B_{1u}$	$^1E_{1u}$	$^1E_{1u}$

Triplet State		T_1	T_2	T_3	T_4	T_5
Transition Energy(cm^{-1})		22700	31000	33300	34900	35800
LE	B	30.46	70.16	83.69	76.08	83.55
	E	42.71	21.03	0.51	15.17	0.00
CT	B→E	10.81	0.43	4.16	0.84	4.43
	E→B	10.81	0.43	4.16	0.84	4.43
Total		94.79	92.05	92.52	92.94	92.40
LE		73.17	91.19	84.20	91.25	83.55
CT		21.62	0.86	8.32	1.69	8.85
Main		42.71	61.78	82.36	75.30	83.46
Configuration		E	$^3B_{1u}$	$^3E_{1u}$	$^3E_{1u}$	$^3B_{2u}$

Figures are the squares of the coefficients in the state functions expressed as a linear combination of the electronic configurations of the MIM model. G:Ground configuration, LE:Configuration of the localized excitation, CT: Charge transfer configuration B_{1u},B_{2u},E_{1u}: The electronic states of benzene

Appendix 2. The Contributions of Various Electronic Configurations of the MIM model for the State Functions of the PPP model of p-Azidobenzoyloxy Group = Carboxyl Group(COO)+Phenylazide(PHA)

Singlet State		S_0	S_1	S_2	S_3	S_4	S_5
	G	92.13	0.05	0.84	0.01	0.10	1.03
LE	PHA	0.67	88.55	82.98	85.60	84.91	62.41
	COO	0.13	0.02	1.06	1.98	2.45	13.56
CT	PHA→COO	5.84	4.68	7.29	5.28	4.88	11.34
	COO→PHA	1.02	0.40	1.37	0.18	1.42	5.20
Total		99.79	93.70	93.54	93.05	93.76	93.54
LE+G		92.93	88.62	84.88	87.59	87.46	77.00
CT		6.86	5.08	8.66	5.46	6.30	16.54
Main Contribution			86.56 PHA S_1	78.50 PHA S_2	78.03 PHA S_3	75.92 PHA S_4	34.38 PHA S_5

Triplet State		T_1	T_2	T_3	T_4	T_5
LE	PHA	91.23	85.36	85.21	88.03	91.70
	COO	0.19	2.22	0.68	1.88	0.04
CT	PHA→COO	1.29	5.32	7.29	2.82	1.52
	COO→PHA	0.26	1.15	0.33	0.65	0.59
Total		92.97	94.05	93.51	93.38	93.85
LE		91.42	87.58	85.89	89.91	91.74
CT		1.55	6.47	7.62	3.47	2.11
Main Contribution		90.79 PHA T_1	81.36 PHA T_2	62.98 PHA T_3	56.10 PHA T_4	43.07 PHA T_5 26.48 PHA T_4

Figures are the squares of the coefficients in the state functions expressed as a linear combination of the electronic configurations of the MIM model. G:Ground configuration, LE:Configuration of the localized excitation, CT:Charge transfer configuration

Appendix 3. The Contributions of Various Electronic Configurations of the MIM model for the State Functions of the PPP model of p-Azidobenzoyloxy Group = Azide(A)+Benzene(B)+Carboxyl Group(COO)

Singlet State		S_0	S_1	S_2	S_3	S_4	S_5
	G	84.77	0.00	0.96	0.00	0.31	2.37
	B	0.96	77.63	40.77	62.67	66.62	38.23
LE	COO	0.12	0.02	0.96	1.83	2.25	12.40
	A	0.04	0.08	16.36	10.94	3.68	4.42
	A→B	4.62	3.47	9.08	2.65	5.23	1.14
	A→COO	0.07	0.00	0.80	0.28	0.01	0.36
CT	B→COO	5.33	4.34	5.71	4.57	4.38	9.50
	COO→B	0.94	0.36	1.13	0.14	1.33	5.03
	COO→A	0.01	0.00	0.13	0.03	0.00	0.02
	B→A	2.14	1.80	12.73	3.59	3.55	12.77
Total		98.99	87.69	88.64	86.69	87.37	86.24
LE+G		85.89	77.73	59.05	75.44	72.86	57.42
CT		13.11	9.97	29.58	11.26	14.50	28.82
Main Contribution			75.89 $^1B_{2u}$	24.79 $^1B_{1u}$	35.96 $^1B_{1u}$	37.23 $^1E_{1u}$	19.05 $^1E_{1u}$

Triplet State		T_1	T_2	T_3	T_4	T_5
	B	16.11	60.86	76.75	79.13	77.82
LE	COO	0.17	2.04	0.62	1.73	0.04
	A	57.46	18.20	0.17	0.84	0.87
	A→B	4.79	1.06	0.60	1.51	6.97
	A→COO	0.16	0.16	0.01	0.21	0.01
CT	B→COO	0.93	4.87	6.71	2.44	1.41
	COO→B	0.17	1.06	0.30	0.59	0.53
	COO→A	0.05	0.01	0.01	0.01	0.00
	B→A	8.67	0.25	2.30	0.35	0.21
Total		88.52	88.51	87.45	86.81	87.86
LE		73.74	81.10	77.54	81.70	78.73
CT		14.77	7.41	9.93	5.11	9.13
Main Contribution		57.46 A	58.20 $^3B_{1u}$	58.29 $^3E_{1u}$	63.52 $^3E_{1u}$	57.52 $^3B_{2u}$

Figures are the squares of the coefficients in the state functions expressed as a linear combination of the electronic configurations of the MIM model. G:Ground configuration, LE:Configuration of the localized excitation, CT:Charge transfer configuration B_{1u}, B_{2u}, E_{1u}:The electronic states of benzene

Appendix 4. The Contributions of Various Electronic Configurations of the MIM model for the State Functions of the PPP model of Benzoyloxy Group = Benzene(B) + Carboxyl Group(COO)

Singlet State		S_0	S_1	S_2	S_3	S_4	S_5
Transition Energy(cm^{-1})			35400	43800	48400	50500	57100
Oscill. Strength			0.017	0.150	0.565	1.107	0.516
LE	G	92.38	0.09	0.69	0.63	0.12	0.00
	B	0.56	87.86	77.18	66.64	85.14	52.33
	COO	0.06	0.08	0.73	16.19	1.56	24.62
CT	B→COO	5.72	5.37	13.93	4.93	6.06	3.49
	COO→B	1.09	0.51	2.04	5.25	0.94	13.66
Total		99.81	93.91	94.57	93.64	93.82	94.10
LE+G		93.00	88.03	78.60	83.46	86.82	76.95
CT		6.81	5.88	15.97	10.18	7.00	17.15
Main Contribution			86.04 $^1B_{2u}$	71.04 $^1B_{1u}$	56.26 $^1E_{1u}$	77.56 $^1E_{1u}$	26.17 $^1E_{1u}$ 24.62 COO

Triplet State		T_1	T_2	T_3	T_4	T_5
Transition Energy(cm^{-1})		27100	31700	33000	36200	37400
LE	B	83.50	85.30	88.07	77.02	24.83
	COO	3.04	1.46	1.39	12.88	62.42
CT	B→COO	6.61	6.32	3.71	1.80	0.65
	COO→B	1.66	0.47	0.72	2.71	7.13
Total		94.81	93.55	93.89	94.41	95.03
LE		86.54	86.76	89.46	89.90	87.25
CT		8.27	6.79	4.43	4.51	7.78
Main Contribution		79.73 $^3B_{1u}$	59.65 $^3E_{1u}$	84.50 $^3E_{1u}$	58.59 $^3B_{2u}$	62.42 ^3COO

Figures are the squares of the coefficients in the state functions expressed as a linear combination of the electronic configurations of the MIM model. G:Ground configuration, LE:Configuration of the localized excitation, CT:Charge transfer configuration

Appendix 5. The Contributions of Various Electronic Configurations of the MIM model for the State Functions of the MIM model for the State Functions of the PPP model of Stilbene = Benzene(L.B) + Ethylene(E) + Benzene(R.B)

						Singlet State						
	S_0	S_1	S_2	S_3	S_4	S_5	S_6	S_7	S_8	S_9	S_{10}	S_{11}
Transition Energy (cm^{-1})		34000	34600	34700	43600	44400	46800	48400	49700	53800	55300	55900
Oscill. Strength		1.49	0.00	0.00	0.00	0.13	0.00	1.35	0.00	0.00	0.83	0.00
G	81.29	0.00	0.00	0.05	0.00	0.00	0.00	0.00	13.91	0.00	0.00	0.00
R.B	0.01	12.32	36.71	36.78	34.13	33.56	27.94	29.08	1.70	39.90	31.29	4.55
LE E	0.00	20.04	0.00	0.00	0.00	11.16	0.00	0.00	0.00	0.00	9.45	0.00
L.B	0.01	12.32	36.71	36.78	34.13	33.56	27.94	29.08	1.70	39.90	31.29	4.55
R.B→E	4.17	9.33	2.18	2.14	4.09	0.87	5.94	5.31	10.23	0.71	2.66	18.83
R.B→L.B	0.29	2.41	0.54	0.52	0.08	0.52	2.07	1.99	9.20	0.09	0.81	0.45
E→L.B	4.17	9.33	2.18	2.14	4.09	0.87	5.94	5.31	10.23	0.71	2.66	18.83
CT L.B→E	4.17	9.33	2.18	2.14	4.09	0.87	5.94	5.31	10.23	0.71	2.66	18.83
L.B→R.B	0.29	2.41	0.54	0.52	0.08	0.52	2.07	1.99	9.20	0.09	0.81	0.45
E→R.B	4.17	9.33	2.18	2.14	4.09	0.87	5.94	5.31	10.23	0.71	2.66	18.83
Total	98.57	86.82	83.22	83.21	84.78	83.30	83.78	83.38	76.63	82.82	84.29	85.32
LE + G	81.31	44.68	73.42	73.61	68.26	78.78	55.88	58.16	17.31	79.80	72.03	9.10
CT	17.26	42.14	9.80	9.60	16.52	4.52	27.90	25.22	59.32	3.02	12.26	76.22
Main Contribution		20.04 E	36.66x2 B_{2u}	36.73x2 B_{2u}	33.52x2 B_{1u}	29.27x2 B_{1u}	25.35x2 E_{1u}	23.86x2 E_{1u}	CT	39.38x2 E_{1u}	25.61x2 E_{1u}	CT

		Triplet State								
		T_1	T_2	T_3	T_4	T_5	T_6	T_7	T_8	T_9
Transition Energy (cm^{-1})		18600	27200	30200	32100	32100	32800	34400	34600	34700
LE	R.B	11.10	38.30	34.79	36.95	36.97	39.12	33.72	36.71	36.79
	E	37.20	0.00	12.04	0.00	0.21	0.00	15.04	0.00	0.00
	L.B	11.10	38.30	34.79	36.95	36.97	39.12	33.72	36.71	36.79
	R.B→E	6.54	1.92	0.32	2.11	2.05	1.11	0.39	2.18	2.15
	R.B→L.B	1.14	0.03	0.01	0.49	0.49	0.06	0.15	0.54	0.52
	E→L.B	6.54	1.92	0.32	2.11	2.05	1.11	0.39	2.18	2.15
	L.B→E	6.54	1.92	0.32	2.11	2.05	1.11	0.39	2.18	2.15
	L.B→R.B	1.14	0.03	0.01	0.49	0.49	0.06	0.15	0.54	0.52
	E→R.B	6.54	1.92	0.32	2.11	2.05	1.11	0.39	2.18	2.15
Total		87.84	84.34	81.62	73.90	83.33	82.80	84.34	83.22	83.22
LE		59.40	76.60	82.92	83.32	74.15	78.24	82.48	73.42	73.58
CT		28.44	7.74	1.30	9.42	9.18	4.56	1.86	9.80	9.64
Main Contribution		37.20 E	57.30x2 B1u	29.60x2 B1u	36.62x2 E1u	36.35x2 E1u	37.46x2 E1u	32.20x2 E1u	36.66x2 B2u	36.75x2 B2u

Figures are the squares of the coefficients in the state functions expressed as a linear combination of the electronic configurations of the MIM model. G:Ground configuration, LE:Configuration of the localized excitation, CT:Charge transfer configuration, B1u,B2u,E1u:The electronic state of benzene

Appendix 6. The Contributions of Various Electronic Configurations of the MIM model for the State Functions of the PPP model of Aniline = Benzene(B) + Amino Group(N)

Singlet State		S_0	S_1	S_2	S_3	S_4
Transition Energy(cm^{-1})		34300	43500	50500	51000
Oscill. Strength	X	0.000	0.081	0.000	1.167
	Y	0.047	0.000	0.925	0.000
	G	86.65	0.00	3.46	0.00	0.56
LE	B	0.75	81.60	76.21	85.56	84.81
CT	N→B	12.15	7.61	8.90	5.30	2.84
Total		99.54	89.21	88.56	90.86	88.22
Main Contribution			78.69 $^1B_{2u}$	73.07 $^1B_{1u}$	78.02 $^1E_{1u}{}^B$	80.18 $^1E_{1u}{}^A$

Triplet State		T_1	T_2	T_3	T_4
Transition Energy(cm^{-1})		26400	29200	32200	38100
Direction of Transition		X	Y	X	Y.
LE	B	81.94	78.57	84.33	90.66
CT	N→B	9.76	9.84	4.38	0.35
Total		91.70	88.41	88.71	91.01
Main Contribution		74.35 $^3B_{1u}$	49.62 $^3E_{1u}{}^B$	79.06 $^3E_{1u}{}^A$	53.94 $^3B_{2u}$

Figures are the squares of the coefficients in the state functions expressed as a linear combination of the electronic configurations of the MIM model. G:Ground configuration, LE:Configuration of the localized excitation, CT:Charge transfer configuration $E_{1u}{}^A$ and $E_{1u}{}^B$ mean the A and B representation, respectively, in the C_{2v} point group.

Molecular Diagram
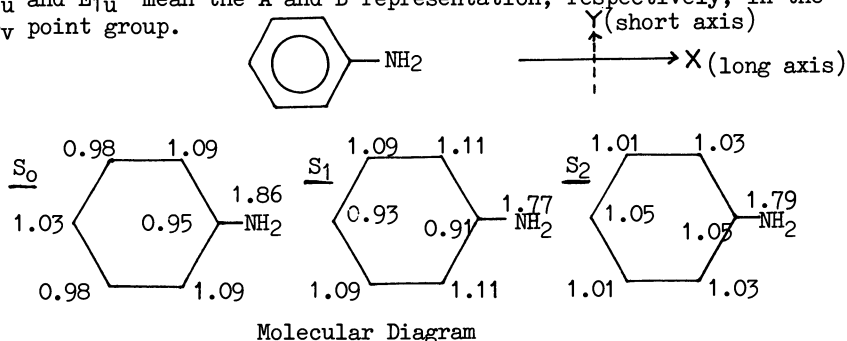
29

Electronic Structures in the Excited States of the Photosensitive Groups of Photocrosslinkable Polymers. (I) Polyvinyl cinnamate

MINORU TSUDA and SETSUKO OIKAWA

Laboratory of Physical Chemistry, Faculty of the Pharmaceutical Sciences,
Chiba University, Chiba 280, Japan

Abstract: The procedure for SCF MO CI calculation(Pariser-Parr-Pople method) was revised by introducing a new formula for the two center Coulomb repulsion integrals which reproduces well the triplet states of benzene. The application of the revised method to the calculation of the electronic states of cinnamoyloxy group was found to reproduce well the experimental values of its electronic transitions although other authors had failed in the calculations using the usual methods. On the basis of the obtained state functions, which were also rewritten in the linear combinations of the electronic configurations of MIM(molecule in molecule) method, the photochemical behaviours of cinnamoyloxy group was discussed in details. The theoretical possibility was also suggested that the singlet and triplet sensitizations by the low energy sensitizers in the mechanism of complex formation where the atomic configurations are changeable.

Since it does not suffer dark reactions, poly(vinyl cinnamate) (PVCi) is one of the most excellent and practically important photosensitive polymers and has been widely investigated[1]. Recently, it was found that a more highly photosensive polymer than PVCi was obtained by the separation of cinnamoyloxy group through $-CH_2-CH_2-O-$ from the main chain of the vinyl polymer[2]. The fact means that by
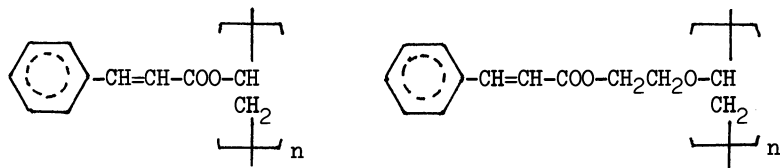
the modification of the main chain of polymer, a part of cinnamoyloxy groups wastefully used for the intramolecular reaction in PVCi can be converted to those utilizing in the formation of the intermolecular crosslinks which contribute to the photosensitivity; and it suggests

the possibilities of the wide varieties of the development of photosensitive polymers utilizing cinnamoyloxy group in future.

Few reports(**9, 11**) have been published on the electronic states of cinnamoyloxy group although there are many of those on the photochemical reactions(**1**). In this paper, the electronic structures in the excited states of cinnamoyloxy group are clarified by the molecular orbital calculations and the spectroscopic procedures, and discussed in connection with the intensity of light absorption, photochemical reaction processes and energy transfers in the sensitization which are important in the comprehensive understanding of the photosensitive polymer.

Theoretical

Pariser-Parr-Pople Method(PPP Method). The calculations are followed of the ordinary LCAO SCF MO CI method with π-electron approximation(**8,10**) where molecular wave functions, Ψ_s, of electronic cloud only are written in general as a sum of configurational functions, φ_n. φ_n are expressed as a sum of Slater determinants constructed from MO ψ_i, which are given as linear combinations of $2p\pi$AO. The considered φ_n are restricted to those arising from all the singly excited configurations and others are neglected.

In the calculations of Fock matrix elements, the zero differential overlap approximation is adopted. Then we get for a closed shell structure:

$$F_{rr} = -I_r + \tfrac{1}{2}P_{rr}(rr|rr) + \sum_{s\neq r}^{N}(P_{ss}-Z_s)(rr|ss) \tag{1}$$

$$F_{rs} = \beta_{rs} - \tfrac{1}{2}P_{rs}(rr|ss) \tag{2}$$

where $r,s=1,2,\ldots,N$ (N is the number of AO contributing π-electrons); $P_{rs}=2\sum_{i=1}^{occupied}C_{ri}C_{si}$ (C_{ri} is the coefficient of the rth AO in the ith MO ψ_i); I_r and Z_s are the ionization potential of the rth AO in the valence state and the effective core charge of the sth AO, respectively. One center Coulomb repulsion integrals $(rr|rr)=I_r-E_r$ (E_r is the electron affinity of the rth AO in the valence state), the values of which adopted in this paper are collected in Table 1 with the values I_r. Two center Coulomb repulsion integral are evaluated by the formula(**3**).

$$(rr|ss) = \tfrac{1}{2}((rr|rr)+(ss|ss)) \qquad (R_{rs}\leq 2.8\ \text{Å})$$
$$\qquad -\tfrac{1}{2}(\varsigma_r+\varsigma_s)(1.752797p-0.5922504p^2+0.0809404p^3) \tag{3a}$$

$$(rr|ss) = \frac{C}{p} \qquad (R_{rs}\geq 2.8\ \text{Å, C is a constant calculated from the formula for } R_{rs}=2.8\ \text{Å}) \tag{3b}$$

$$p = \tfrac{1}{2}(\varsigma_r+\varsigma_s)R_{rs} \tag{3c}$$

$$\varsigma_r = Z_r/n_r \qquad (n_r \text{ is the principal quantum number of rth AO;}$$
$$n_r=2 \text{ in the molecules discussed in this paper)} \tag{3d}$$

The formula(3) was newly proposed in this paper and the coefficients were so determined as the spectrum of benzene molecules in n-hexane solutions was exactly predicted in the calculations considering all singly excited electronic configurations. The core resonance integrals β_{rs} are:

$$\beta_{rs} = \frac{\beta_{cc}}{I_c S_{cc}(1-S_{cc})} \, S_{rs}(1-S_{rs}) \frac{I_r + I_s}{2} \qquad \text{(r and s are neighbors)} \tag{4a}$$

$$\beta_{rs} = 0 \qquad \text{(r and s are non-neighbors)} \tag{4b}$$

where the subscript c means that the r and sth AO are $2p\pi$ AO of carbon. β_{cc} is treated as a free parameter depending upon the size of the molecule and the contributions of heteroatoms. S_{rs} is the overlap integrals, the values of which are calculated from Roothaan's formulae based on the Slater orbitals(22). The expression $\beta \propto S(1-S)$ has already been suggested by Parr and Rudenberg relating to the "interference" between AO(8, 14). The atomic configuration of cinnamoyloxy group for the evaluations of R_{rs} are shown in Fig.1.

<u>Molecule in Molecule Method(MIM Method)</u>. In the spectra of organic molecules, an absorption band is often ascribed to one of the component groups of the molecule, a chromophore. Since photochemical reactions start at the absorption of light, a discussion of the spectra of molecules, based on the chromphores they contain, may be profitable in the researches of the reactions. In the present case, the chromophores are benzene ring, ethylenic double bond and carboxyl group, and the cyclobutane formation, to which the photosensitivity of PVCi is ascribed, is substantially the reaction of the ethylenic double bond perturbed by other chromophores. For such an investigation the state functions obtained by the MIM method may offer advisable informations than that of the PPP method. In the latter method MO is constructed by all the AO in a molecule, and the state function is expressed as a linear combination of many electronic configurations, as was shown in Table 2. Therefore, it is often difficult for us to imagine the relationship between the state function and the chemical structure or reactions, although the calculations predict well the transition energies. In order to exhibit the advantages of the both method, the state functions of the PPP method were transformed to those of the MIM method, i.e. the linear combinations of LE (locally excited state in the chromophore) and CT(the charge or electron transfer configuration from the chromophore to the other) functions.   Therefore, the parameters used in the both method are the same in this paper. Baba et al. reported that the transformation is mathematically performed when we use the same atomic orbitals as the base functions(21). In the calculations of the transformation, all the singly excited electronic configurations were considered, and the used LE functions of a chromophore are the state functions expressed as the linear combinations of all the singly excited electronic configurations obtained from the MO of the chromophore. The state wave functions resulting from the CI in the PPP
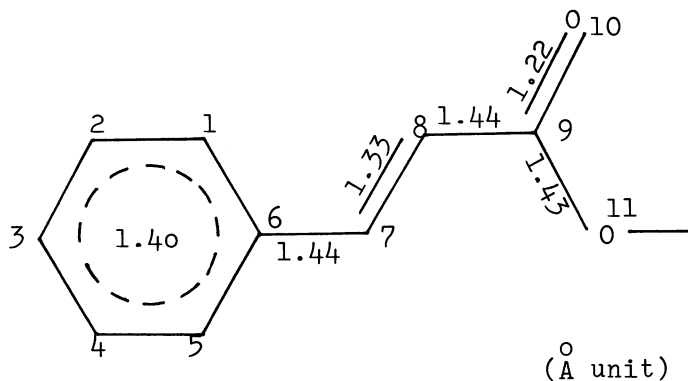
Figure 1a.   Atomic configuration of cinnamoyloxy group. All the angles are 120°.
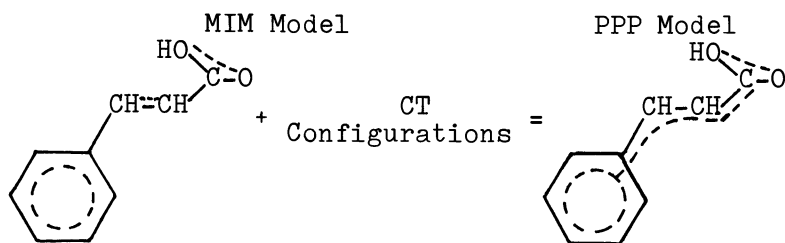
Figure 1b.   (middle) Relationship between the models of PPP and MIM methods
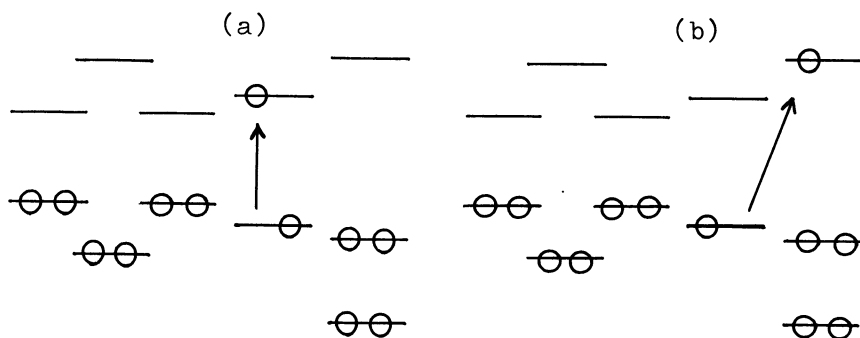
Figure 1c.   (bottom) Examples of LE and CT configurations of cinnamoyloxy group (a), LE configuration of ethylene group; (b), CT configuration from ethylene to carboxyl group

Table 1.   Parameter Used in the MO Calculations

		I_r	$(rr\vert rr)$	Z_r
C :	$tr\,tr\,tr\,\pi$ $(\!>\!C\!-)$	11.16	11.13	3.25
O :	$tr^2\,tr^2\,tr\,\pi$ $(=\!O\ )$	17.70	14.15	4.55
O$^+$:	$tr^2\,tr\,tr\,\pi^2(-\!O\!-)$	34.43	19.46	4.9

β_{cc}: 2.32   (eV unit)
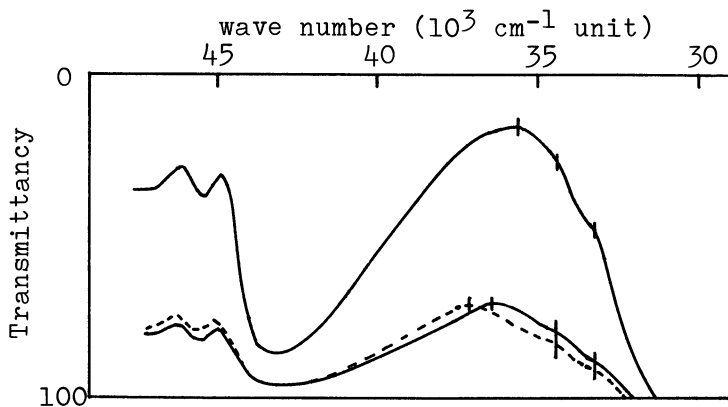
Figure 2a.   (top) UV spectrum of cinnamic acid. —, 1 mg, 5 mg/l. in
            n-hexane; - - -, 1 mg/l. in iso-PrOH.
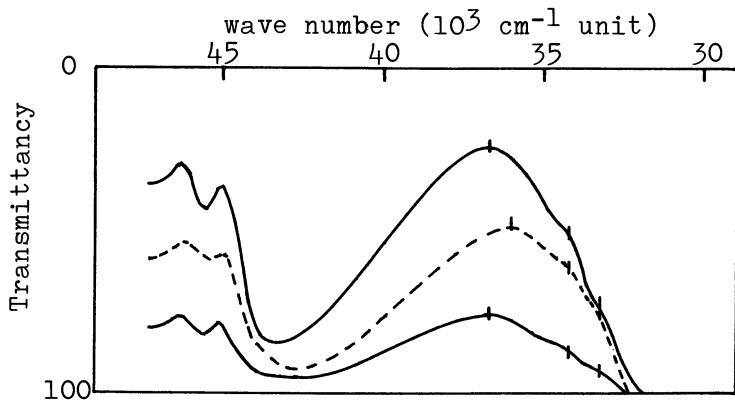
Figure 2b.   (bottom) UV spectrum of ethyl cinnamate. —, 1 mg, 5 mg/l.
            in n-hexane; - - -, 1 mg/l. in iso-PrOH.

Table 2. The State Functions and MO of trans-Cinnamoyloxy Group

Transition Energy* (cm^{-1})	Oscillator Strength*	State Functions
34165	0.022	$(S_1) = -0.6744\Psi_{5\rightarrow7} + 0.5438\Psi_{6\rightarrow8} - 0.4087\Psi_{5\rightarrow9}$ $-0.2219\Psi_{4\rightarrow8} + \cdots$
36699	0.846	$(S_2) = 0.9395\Psi_{6\rightarrow7} + 0.2354\Psi_{6\rightarrow8} + \cdots$
44202	0.074	$(S_3) = -0.6602\Psi_{5\rightarrow8} - 0.3886\Psi_{6\rightarrow9} + 0.3822\Psi_{4\rightarrow7}$ $+0.2754\Psi_{6\rightarrow8} + 0.2306\Psi_{3\rightarrow7} + 0.2203\Psi_{5\rightarrow7} + \cdots$
47514	0.754	$(S_4) = -0.6137\Psi_{6\rightarrow8} - 0.6077\Psi_{5\rightarrow7} - 0.3877\Psi_{5\rightarrow8} + \cdots$
51995	0.242	$(S_5) = 0.6337\Psi_{6\rightarrow9} + 0.4425\Psi_{4\rightarrow7} - 0.3678\Psi_{3\rightarrow7}$ $-0.2532\Psi_{5\rightarrow8} + 0.2327\Psi_{3\rightarrow9} - 0.2197\Psi_{6\rightarrow10} + \cdots$
19844		$(T_1) = -0.8876\Psi_{6\rightarrow7} - 0.2282\Psi_{4\rightarrow7} + 0.2074\Psi_{4\rightarrow9}$ $-0.2037\Psi_{3\rightarrow7} + \cdots$
29062		$(T_2) = 0.6848\Psi_{5\rightarrow8} + 0.4809\Psi_{6\rightarrow9} - 0.4159\Psi_{4\rightarrow7} + \cdots$
31132		$(T_3) = 0.7844\Psi_{5\rightarrow7} + 0.5136\Psi_{5\rightarrow9} + 0.2911\Psi_{6\rightarrow8} + \cdots$
33129		$(T_4) = -0.6841\Psi_{5\rightarrow8} + 0.4836\Psi_{6\rightarrow9} - 0.4520\Psi_{4\rightarrow7}$ $+0.2336\Psi_{6\rightarrow7} + \cdots$
35113		$(T_5) = -0.8744\Psi_{6\rightarrow8} + 0.3496\Psi_{4\rightarrow8} + 0.2735\Psi_{5\rightarrow7} + \cdots$

The Coefficient of AO

No. of MO	Occupied			Unoccupied		
	4	5	6	7	8	9
1	-0.0002	0.4939	-0.3041	-0.2824	0.4876	-0.1673
2	-0.2647	0.5057	0.1746	-0.0753	-0.5146	-0.2729
3	-0.3855	0.0183	0.4459	0.3131	0.0193	0.4977
4	-0.2734	-0.4840	0.2176	-0.1076	0.4939	-0.2946
5	-0.0135	-0.5146	-0.2691	-0.2680	-0.5027	-0.1484
6	0.2472	-0.0262	-0.4468	0.2452	0.0164	0.4667
7	0.4192	-0.0025	0.2989	0.4884	-0.0028	-0.3446
8	0.2693	0.0161	0.4558	-0.4996	-0.0068	0.1078
9	-0.1684	0.0004	0.0202	-0.3255	-0.0100	0.3649
10	-0.5837	-0.0090	-0.2464	0.2427	0.0065	-0.2063
11	0.1671	-0.0012	-0.0245	0.1416	0.0036	-0.1308
Energy Level(eV)	-13.529	-12.181	-11.532	-1.8864	-0.2333	0.3600

*Calculated value.
**The location of AO is shown in Fig.1.

method are written as

$$\Psi=(\Psi_1 \Psi_2 \dots \Psi_h)=V(U) \tag{5a}$$

where U is an h$\times$h unitary matrix and

$$V=(V_1 V_2 \dots V_h) \tag{5b}$$

are h singlet electronic configurations collected in a row vector. A similar formulation as obtained in the case of the LE and CT functions of the MIM method.

$$\Psi^o=(\Psi_1^o \Psi_2^o \dots \Psi_{h^o}^o)=V^o(U^o) \tag{6a}$$

$$V^o=(V_1^o V_2^o \dots V_{h^o}^o) \tag{6b}$$

We can write then

$$V=V^o(L) \tag{7}$$

where L is an h$^o\times$h matrix. From Eqs.(5)-(7) it can easily be shown that

$$\Psi=\Psi^o(M) \tag{8a}$$

with

$$M=(U^o)^{+}(L)(U) \tag{8b}$$

where M is an h$^o\times$h matrix and $(U^o)^{+}$ is an h$^o\times$h^o matrix defined as $(U^o)^{+}U^o=1$. Thus, we can rewrite the state functions of the PPP method to those of the MIM method if we can calculate the matrix M. U and U^o are obtained from the PPP calculations of the molecule and the chromophores. L matrix elements are the coefficients of the following expansions

$$V_o= D_o^2 V_o^o+\sum_i^{occ} \sum_k^{vac} \sqrt{2}D_o D_{ik} V_{ik}^o \tag{9}$$

$$V_{IK}= \sqrt{2}D_o D_{I'K'} V_o^o+\sum_i^{occ} \sum_k^{vac} (D_o D_{ik,I'K'}+D_{ik}D_{I'K'})V_{ik}^o \tag{10}$$

for the singlet states and

$$T_{IK}= \sum_i^{occ} \sum_k^{vac} (D_o D_{ik,I'K'}-D_{ik}D_{I'K'})T_{ik}^o \tag{11}$$

for the triplet states, respectively. V_o and V_{IK}(or T_{IK}) means the ground configuration expressed as a single Slater determinant and the singly excited electronic configuration from MO ψ_I to ψ_K in the PPP method, respectively. V_o^o and V_{ik}^o(or T_{ik}^o) have the same meanings on the LE and CT functions of the MIM method. D_o is defined as Eq.(12) using the first m rows and the first m columns of the matrix B.

$$D_0 = \begin{vmatrix} b_{11} & \cdot & \cdot & b_{1m} \\ \vdots & & & \vdots \\ b_{m1} & \cdot & \cdot & b_{mm} \end{vmatrix} \tag{12}$$

Matrix B is defined as

$$B = (C^o)^+ C \tag{13a}$$

$$(C^o)^+ C^o = 1 \tag{13b}$$

where C is an n dementional unitary matrix, the elements of which are the AO coefficients of the LCAO SCF MO obtained by the PPP method ; and C^o is also an n dimentional unitary matrix, the elements of which are obtained from the SCF MO of the chromophores where the coefficients of the AO not contributing to the chromophore are zero. n is the number of the AO contributing to the MO and m is the number of the occupied MO in the ground state. $D_{ik,I'K'}$ is the determinant of the matrix formed from the first m rows and the first m columns of the matrix B by replacing its ith row by its kth row and its I'th column by its K'th column. D_{ik} and $D_{I'K'}$ have the similar meaning, that is, the former is replaced on the row only and the latter on the column only, respectively.

Experimental

Substances. All the substances were commercial products. They were purified by the twice distillations or recrystallizations and checked by IR-spectra and melting point or boiling point measurements. n-Hexane for UV-spectra was Spectroquality grade of Matheson-Coleman & Bell Ltd. Ethyl iodide(solvent for $S_o \rightarrow T_1$ absorption spectrum): a commercial product was distilled at 72^oC and passed through 30 cm activated alumina column. All operations were carried out in a dark room and stored in the light-shielded equipment. EPA mixed solvent were a mixture of diethylether(5part), isopentane(5part) and ethanol (2part); these components were carefully purified in many steps and examined by the luminescence spectrometry.

Spectrometry. Electronic absorption spectra were measured by Hitachi EPS-3T type spectrometer using 1 cm optical path length cell. For $S_o \rightarrow T_1$ absorption spectra in C_2H_5I, 10 cm optical path length cells were used. In the latter case, the corrections were carried out for the deviation of the spectra arised from the high concentration(30wt%) of the samples. Phosphorescence spectra were measured by Hitachi MPF-2A type spectrometer at 77^oK and corrected by method published elsewhere.[20] IR-spectra were measured by Hitachi EPI-G3 type spectrometer in KBr tablets.

Results and Discussions

The Characteristics of the Absorption Spectra of Cinnamoyloxy Compound. The main peak(S_2) of cinnamic acid in UV-spectrum shows an unusual solvent effect. The peak locates at 277 nm in n-hexane, at 273 nm in iso-propanol and at 270 nm in ether, respectively. The phenomena are extraordinary in the $(\pi \rightarrow \pi^*)^1$ transitions[3]. The weak

peak at 290 nm is, however, indifferent to the species of the sol-
vents. The main peak at 277 nm in n-hexane gradually shifts to the
shorter wave length on dilution, as is shown in Fig.2(a). The 273 nm
peak observed in iso-propanol and in the diluted n-hexane solutions
shifts again to 277 nm by the addition of acetic acid. These phenom-
ena may be explained by the hydrodgen bond formation between carboxy
groups of cinnamic acid itself and between cinnamic acid and solvent;
for example $-C\langle{}^{O--HO}_{OH--O}\rangle C-$. The explanation is supported by the fact,
that these unusual phenomena are not observed in the case of ethyl
cinnamate, as is shown in Fig.2(b); where the ordinary solvent ef-
fects in the $(\pi\to\pi^{*})^{1}$ transition are observed. Therefore, we should
use the spectrum of the ester and not of the acid as the data compa-
rable with calculations.

UV Spectrum of Poly(vinyl cinnamate)(PVCi). The UV spectrum of
PVCi in tetrahydrofuran solution is identical with that of ethyl cin-
namate and it is believed to be the absorption by cinnamoyloxy group.
The main peak($\epsilon \simeq 10^{5}$) of the latter has the absorption maximum at
36750 cm^{-1} in n-hexane and is considered to be $(\pi\to\pi^{*})^{1}$ transition
from the solvent effects. There is another weak absorption near
34000 cm^{-1} which is clearly observed at low temperatures(at 77°K in
EPA solutions)(15)
     The electronic structure of cinnamoyloxy group bonded to alipha-
tic compounds is unequivocally determined in the π-electron approxi-
mation. Self-Consistent Field Molecular Orbital calculations with
Configurational Interactions(SCF MO CI) in the π-electron approxima-
tion(PPP method)(8) of cinnamoyloxy group were carried out by Nakamu-
ra(9) using the Pariser-Parr formula(10) for the two center Coulomb
repulsion integral, and Fueno(11) using the Nishimoto-Mataga formula(12)
In both cases the main peak has the lowest frequency and the second
weak transition appeares at the 1000 cm^{-1} higher frequency. These
results are in disagreement with the experimental data as was shown
in Fig.3.
     The authors revised the PPP method in a few points, especially
in the formulation for the two center Coulomb repulsion integrals, in
order to calculate the correct values of the triplet state energies(5)
The application of the revised method to the calculation of the elec-
tronic states of cinnamoyloxy group was found to reproduce well the
experimental values of its electronic transitions. The results are
also shown in Fig.3.

The Excited States of Poly(vinyl cinnamate) and their Photochemi-
cal Reactivities. The photochemical reaction of PVCi is believed to
be intermolecular crosslinking of the polymer chains by the formation
of the four-membered ring from the central double bonds of cinnamoyl-
oxy groups(6), and it is known that many experimental results from
the photochemical reaction are interpreted well(6) if we can postulate
that the reaction is the concerted cycloaddition according to the
Woodward-Hoffmann's rule(13). This means that the four-membered ring
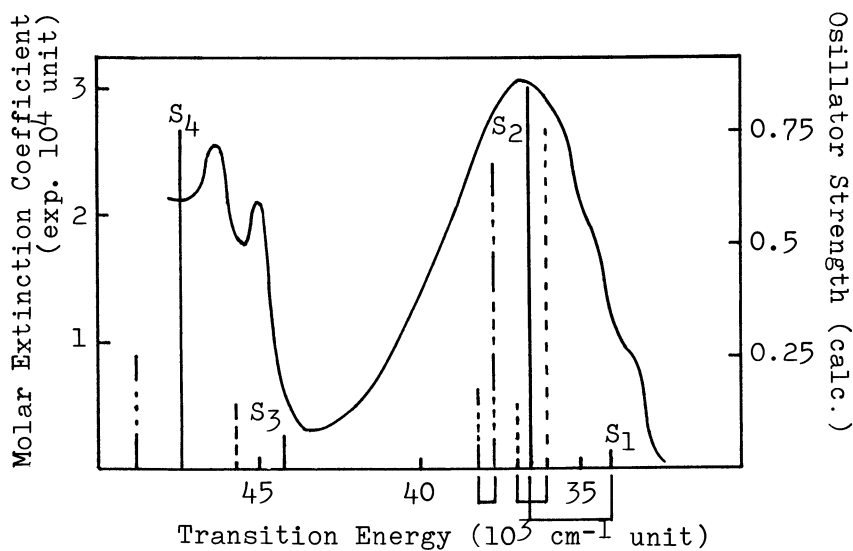
Figure 3a. Comparison of the calculated values with the experimental ones on the electronic transition energies and oscillator strengths of trans-cinnamoyloxy group *(ethyl cinnamate in* n-hexane*). ——, present work; ———, Nakamura (ref. 9); — — — — Fueno (ref. 11).*
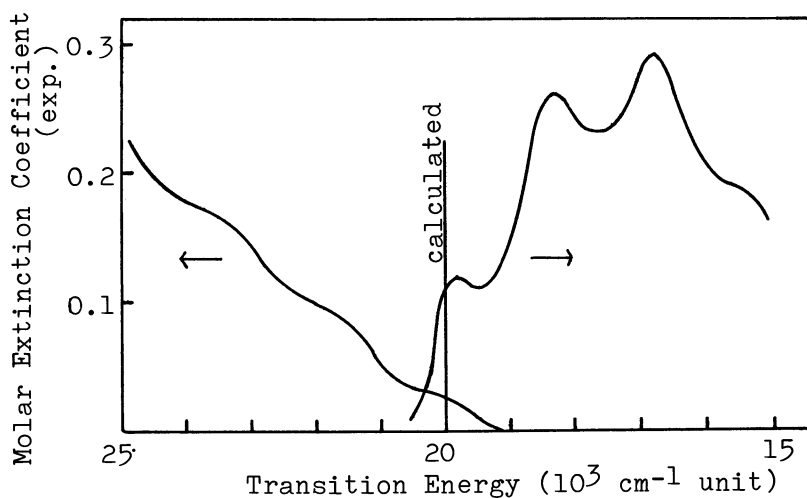
Figure 3b. $S_0 \rightarrow T_1$ absorption in ethyl iodide and phosphorescence (in EPA at 77°K) spectra of trans-ethyl cinnamate. *The emission intensity was corrected according to ref. 20. The intensity of emission is relative value. The calculated value only shows the transition energy.*

formation readily occurs if a nodal plane exist at the central double
bond in the lowest unoccupied MO(LUMO) and not in the highest occupied
MO(HOMO) of the ground state of cinnamoyloxy group within the picture
of Hückel MO or Extended Hückel MO theory.(Fig.5) In the SCF MO CI
picture the bond order at the central double bond reflects the same
meaning although the original considerations of the Woodward-Hoffmann's
rule are applicable in the special case where only one excited elec-
tronic configuration contributes mainly to the lowest excited state.
The state functions in the form of the linear combination of the elec-
tronic configurations and the MOs required in the following discus-
sions are shown in Table 2. The spatial orbital part of the lowest
triplet state T_1 corresponds to that of the second excited singlet
state S_2(the main peak) and the bond orders at the central double bond
in these two electronic states are smaller than that of the lowest ex-
cited singlet state S_1.(Fig.4) Therefore, the concerted cycloaddition
occurs favorably in thesestates. These states are also the special
cases in which one singly excited electronic configuration from the
HOMO to the LUMO contributes mainly to the state functions(see Table2)
and the HOMO and LUMO are satisfy the conditions the Woodward-Hoff-
mann's rule for the concerted cycloaddition requires. From cycliza-
tion occurs more favourably in the triplet state than in the singlet
state if the photochemical reaction takes place in the lowest energy
level of each multiplet state as in the usual way. The possibility
seems to be supported by the fact that the spectral sensitization of
PVCi is practically very effective, but is not conclusive because
there are no exact data on the quantum yields in both states. Further
discussions on this problem will be given later with another possibil-
ity obtained from the theoretical considerations.

  <u>Analyses of the Electronic Transitions of Poly(vinyl cinnamate)</u>.
The concerted cycloaddition of cinnamoyloxy group is essentially the
reaction of the central double bond. Therefore, we can expect to ob-
tain the clearer image than that hitherto considered in the photochem-
ical reaction if the contributions of the central double bond for the
excited states are calculated quantitatively. It is known that the
state functions of PPP model can be rewritten to the linear combina-
tions of LE and CT(charge transfer) functions of MIM method(**7**) when
we use the same atomic orbitals as the base functions(**21**). Using the
technique, the state functions in Table 2 are rewritten and the re-
sults are collected in Table 3. The relationship between these two
methods is illustrated in Fig.1(b),(c).

  <u>The state function of S_0</u>. The contributions of the ground state
functions of phenyl group(equivalent to benzene in the π-electron ap-
proximation), -CH=CH- (equivalent to ethylene) and carboxyl group(e-
quivalent to formic acid) are 83 % and the CT functions which connect
the LE functions in order to form the molecule, those from the OMO of
benzene to the UMO of ethylene, from ethylene(OMO) to carboxyl group
(UMO), from ethylene(OMO) to benzene(UMO) and from carboxyl group(OMO)
to ethylene(UMO) are totally 16 %. When examining the contributions of
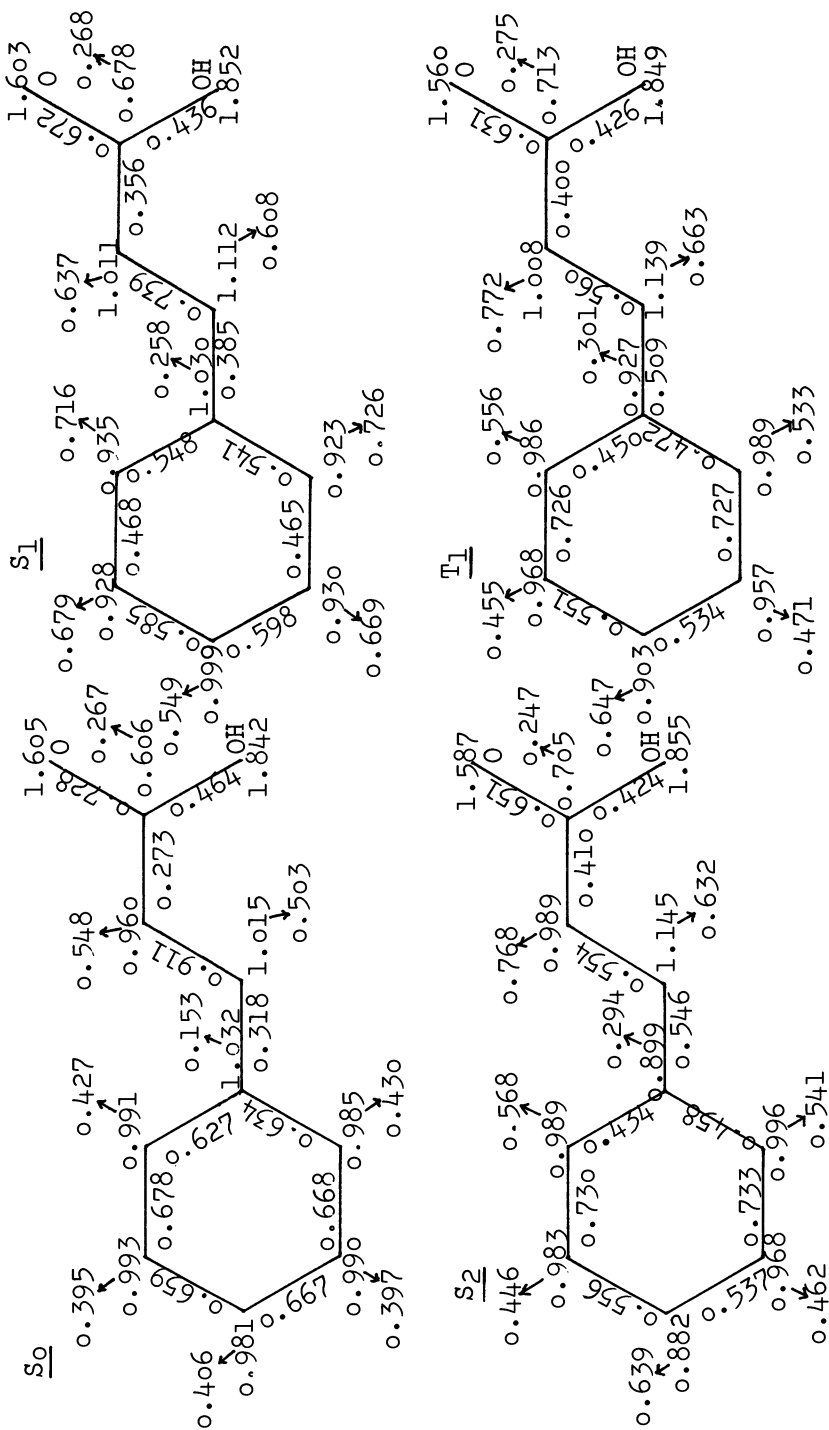
Figure 4. Molecular diagrams of various electronic states of cinnamoyloxy group in the π-electron system
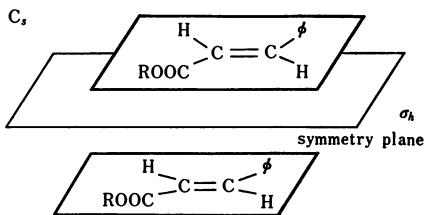
Journal of the Society of Photographic Science of Japan

Figure 5a.   (top) A pair of cinnamoyloxy groups which has C_s *symmetry*
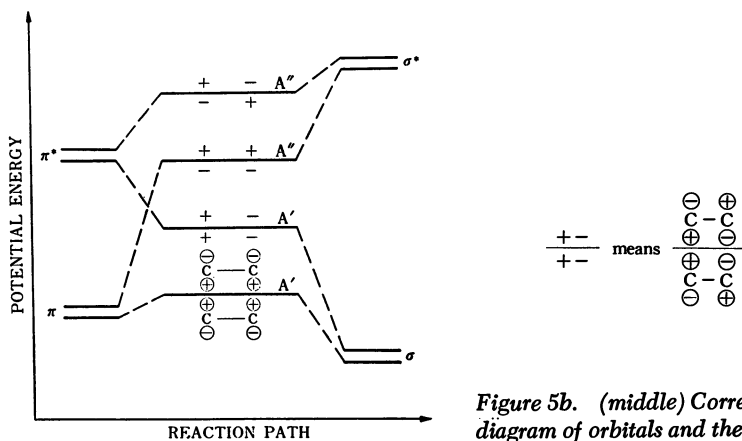
Figure 5b.   (middle) Correlation diagram of orbitals and their symmetries
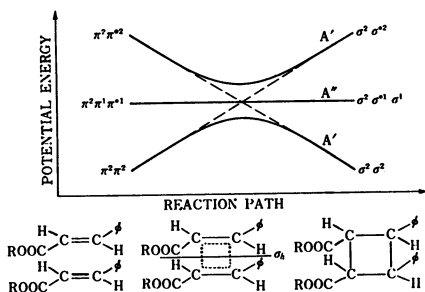
Figure 5c.   (bottom) Correlation diagram for the cycloaddition reaction of a pair of cinnamoyloxy group. The reaction occurs following the adiabatic potential curve of the A″ symmetry. The state $\pi^2\pi^1\pi^{*1}$ *is favorable for the concerted cycloadditions (see text) (23).*

Table 3. The Contributions of Various Electronic Configurations of the MIM model for the State Functions of the PPP model of trans-Cinnamoyloxy Group (%)

Singlet State		S_0	S_1	S_2	S_3	S_4	S_5
LE	G	82.72	0.20	2.43	0.00	0.24	3.87
	B	0.13	70.42	20.84	64.11	52.02	23.59
	E	0.03	0.78	21.10	11.92	1.14	1.26
	COO	0.05	0.01	0.63	0.07	0.26	15.68
CT	B→E	5.50	10.02	21.97	4.53	20.66	13.71
	B→COO	0.42	1.24	4.21	0.45	3.80	2.65
	E→COO	5.40	0.11	5.94	2.99	1.94	0.01
	COO→E	1.09	0.04	1.30	0.23	0.23	10.96
	COO→B	0.06	0.05	0.27	0.03	0.16	2.63
	E→B	3.38	1.89	8.02	1.11	4.90	9.58
Total		98.78	84.76	86.71	85.44	85.35	83.94
LE + G		82.93	71.41	45.00	76.10	53.66	44.40
CT		15.85	13.35	41.71	9.34	31.69	39.54
Main Contribution			69.04 $^1B_{2u}$	21.10 E	54.92 $^1B_{1u}$	38.68 $^1E_{1u}$	21.03 $^1E_{1u}$

Triplet State		T_1	T_2	T_3	T_4	T_5
LE	B	18.14	66.18	70.73	70.81	78.17
	E	41.72	12.95	0.40	4.16	0.00
	COO	1.52	2.21	0.14	4.58	0.01
CT	B→E	13.31	0.32	11.34	2.16	1.73
	B→COO	1.73	0.06	1.34	0.14	0.22
	E→COO	5.88	2.57	0.10	1.34	0.00
	COO→E	1.25	0.88	0.05	1.12	0.00
	COO→B	0.20	0.02	0.02	0.04	0.12
	E→B	5.75	0.12	0.62	0.75	4.87
Total		89.50	85.31	84.74	85.10	85.12
LE		61.38	81.34	71.27	79.55	78.18
CT		28.12	3.97	13.47	5.55	6.94
Main Contribution		41.72 E	64.01 $^3B_{1u}$	55.95 $^3E_{1u}$	70.41 $^3E_{1u}$	59.93 $^3B_{2u}$

Figures are the squares of the coefficients in the state functions expressed as a linear combination of the electronic configurations of the MIM model. G:Ground configuration , B:Benzene, E:Ethylene, COO:Carboxyl group. B_{1u}, B_{2u} and E_{1u} mean the LE of benzene.

each of the CT configurations in Table 3, we can find out that elec-
trons favourably distribute in carboxyl group even in the ground state
reflecting the electronagativity of heteroatoms.

The state function of S_1. The main contribution to S_1 is the LE
function of $^1B_{2u}$ state of benzene ring which occupies 69 %. The bonds
order(Fig.4) of the central double bond is substantially unchanged
compared with that in the S_0 state, because the contribution of LE func-
tion of ethylene increases only 0.75 % and that of the CT function
from benzene(OMO) to ethylene(UMO) 4.5 %, compared with those in the
S_0 state functions. Therefore, we cannot consider this state to be
highly photosensitive.

The state function of S_2. The LE function of ethylene contrib-
utes mainly to S_2(about 21 %). The result accords with the fact that
the experimental data on the photochemical reaction of PVCi are ex-
plained on the bases of Woodward-Hoffmann's rule. CT configurations
from the occupied MO(OMO) of the ground state of benzene to the unoc-
cupied MO(UMO) of ethylene and the OMO of ethylene to the UMO of ben-
zene increase 16.6 % and 4.6 %, respectively, compared with S_0.(Fig.6)
These contributions decrease the bond order of the central double bond
in S_2. In S_1 the contributions of the LE of ethylene and CT are small
Therefore, we can expect that the photochemical reaction occurs in S_2
and not in S_1, because our calculated energy levels of S_1 and S_2 are
those in the Frank-Condon state and may exchange the positions each
other in the photochemically reactive state. In order to test the
possibility, theoretical calculations of the energy level of trans-
cinnamoyloxy group with lengthening the central double bond are
carried out. The results are shown in Fig.7. As was expected, the
contribution of the electronic configuration from HOMO to LUMO in-
creases according to the lengthening of the central double bond and
the photochemical reactivity increases in the lowest excited state.
Of cource this calculation is only an approach to the possibility, al-
though the small bond order in S_2 compared with that in S_0 suggests
the lengthing of the central double bond. It is interesting that the
lowering of the transition energy following the change of the atomic
configurations suggests the possibility of the singlet and triplet sensiti-
zations by the low energy sensitizers in the mechanism of complex formations

The state function of T_1. From the results from PPP calculations
in Table 2, we can find out that the spatial part of the state func-
tion of T_1 approximately corresponds to that of S_2, and the contribu-
tion of $\varphi_{4 \to 7}$ and $\varphi_{3 \to 7}$ shows the mixing of S_3. From the results from
MIM method(Table 3), the contribution of the LE of ethylene extremely
increases in T_1 compared with that in S_2. The fact suggests that T_1
is highly photosensitive on the basis of the concerted cycloaddition
following the Woodward-Hoffmann's rule.

Analysis of the Intensity of the Electronic Transition of PVCi.
The intensities of the electronic transitions of photosensitive poly-
mers are on intimate relations with the spectral sensitivities. Most
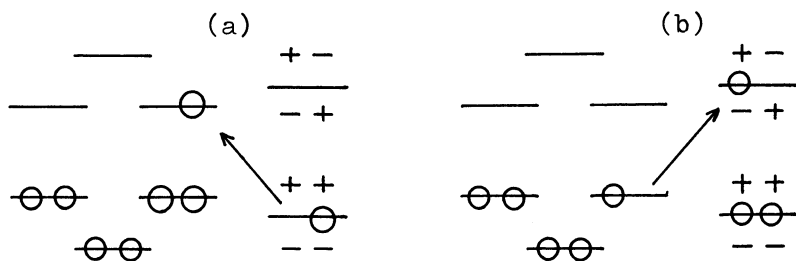
Figure 6. Decrease of the bond order of the central double bond by the contribution of CT functions a, because of the decrease of the electron occupying the HOMO of ethylene; b, because of the increase of the electron occupying the LUMO of ethylene.
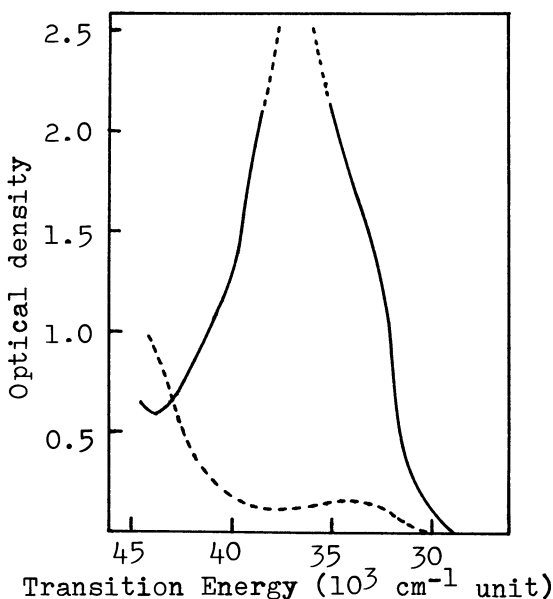
Bulletin of the Chemical Society of Japan

Figure 8c.   Polarized absorption spectrum of trans-*cinnamic acid α-form through the (010) plane. —, the light polarized parallel to the a-axis; ---, the light polarized perpendicular to the a-axis.*
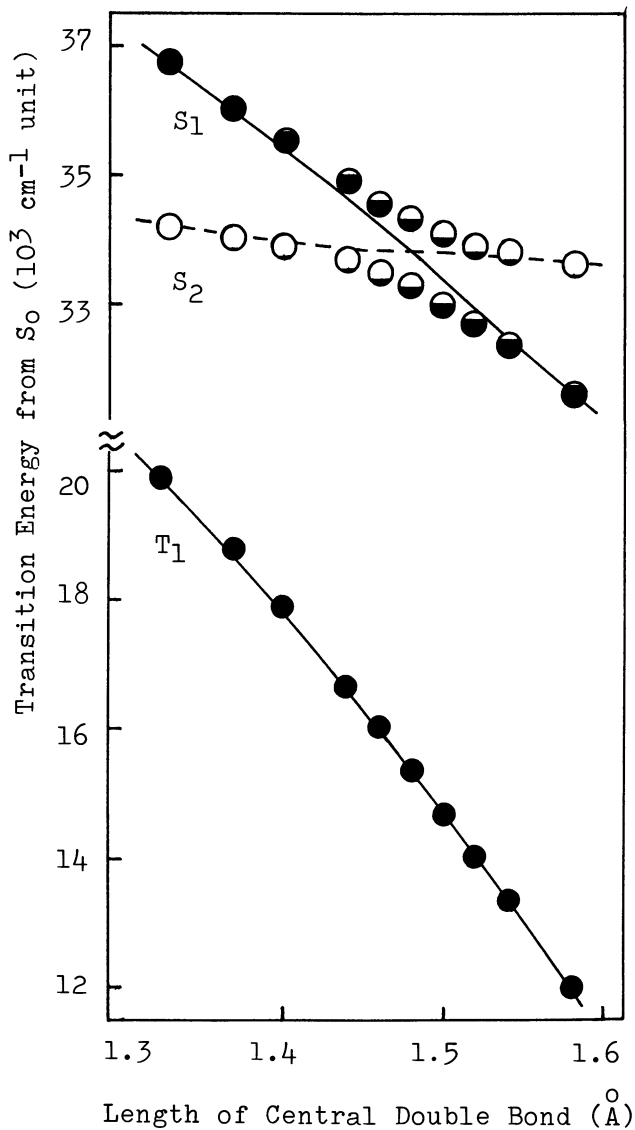
Figure 7.   The interchange of S_1 and S_2 levels of trans-cin-
namoyloxy group with lengthening of the central double bond.
The contribution of $\varphi_{6 \to 7}$ is expressed as the filled part in
circles.

Oscillator Strength

S_1

0.02

0.01

0.00

S_2

0.8

0.6

0.4

0.2

0

S_3+S_4

0.6

0.4

0.2

0

0   45   90

Rotation Angle $\theta°$
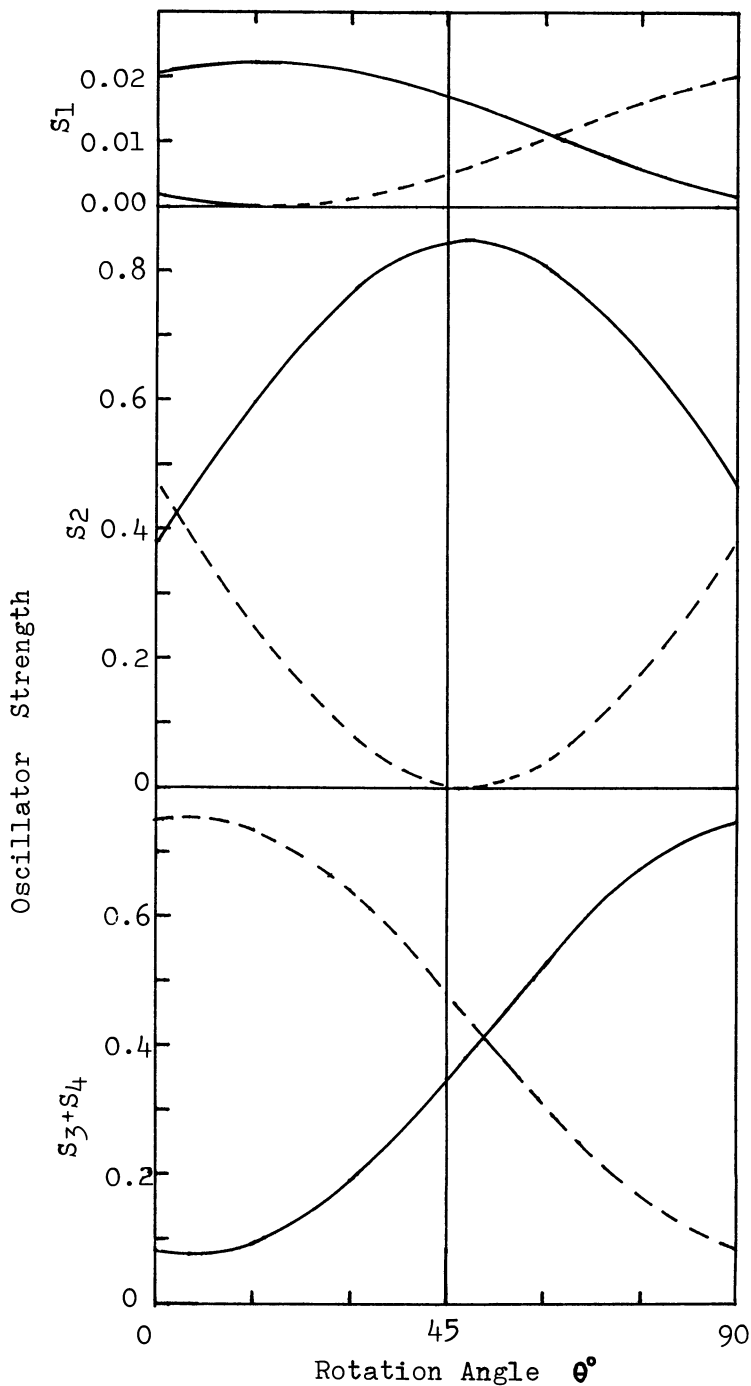
Figure 8a. Theoretical reproduction of the polarized absorption spectrum of cinnamoyloxy group. S_3 is shown in the next page. —, the light polarized to the X direction; - - -, the light polarized to the Y direction.
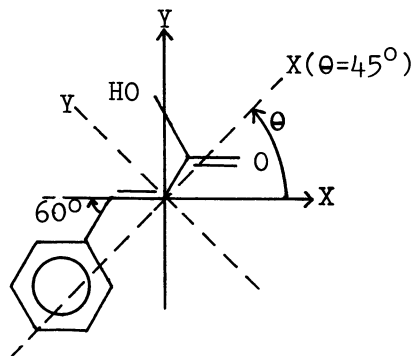
Figure 8b. Atomic configurations in the theoretical calculations of Figure 8a. The Cartesian coordinate was rotated round the Z axis.
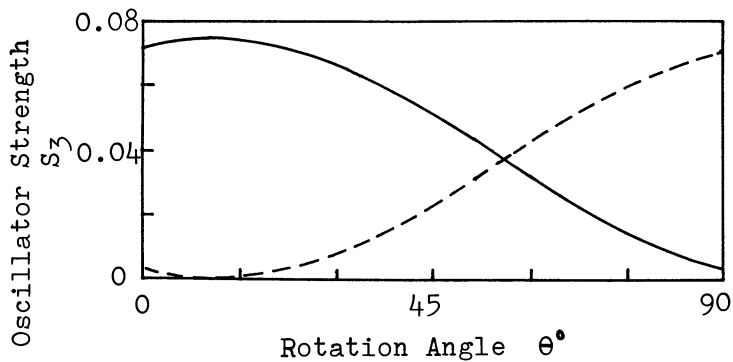
of the absorption spectra have the shapes similar to those of the
spectra of the spectral sensitivities of the photosensitive poly-
mers(15).

In this section we shall analyze the relationship between the
electronic structures and the absorption intensities in details. The
intensity of the electronic transition is experimentally obtained as
an area of the absorption spectrum displayed with the abscissa of the
energy linear scale(for example cm^{-1}, eV,etc.) and the ordinate of the
molar extinction coefficients; and the experimental value corresponds
to the theoretically obtained oscillator strength of the electronic
transition. The example is shown in Fig. 3 .

The oscillator strength(f) of a transition between two electronic
states of a molecule is given by

$$f(S_o \to S_n)= (8\pi^2 mc \, \nu(S_n)/3he^2) \, G\left|\vec{M}(S_n)\right|^2 \tag{14a}$$

where M is the transition dipole moment expressed as Eq.(14b), m and
e are the mass and charge of an electron, ν is the frequency of the
transition, and G is the number of degenerate wave functions to which
absorption can lead. The transition moment of an electronic transi-
tion in the dipole approximation, expressed in terms of the wave func-
tion of the initial and final states is

$$\vec{M} =\langle \Psi_{Sn}| \sum_p e\vec{r}_p|\Psi_G \rangle \tag{14b}$$

where Ψ_{Sn} and Ψ_G are, respectively, the wave functions of the ini-
tial and final state, $\vec{r}_p$ is the position vector of the pth electron
and the summation extends over all π-electrons. Substituting Ψ_{Sn} in
Eq.(14b) by the state functions in Table 2, we obtain

$$\vec{M} = \sum_{i \to j} c_{i \to j}\langle \varphi_{i \to j} | \sum_p e\vec{r}_p|\Psi_G \rangle \tag{14c}$$

where $c_{i \to j}$ is the coefficient of the electronic configuration $\varphi_{i \to j}$
in Table 2 and the summation extends over all the singly excited elec-
tronic configurations. Therefore, the intensity of the noticed elec-
tronic transition is obtained as the square of the vector sum of the
product of the coefficient of the electronic configuration which con-
structs the electronic state function and the transition moment of the
configuration. The values of the transition moments of the electronic
configurations required in the following discussions are collected in
Table 4.

The absorption intensity of S_1. From Table 2, we can find out
that the state function of S_1 contains $\varphi_{5 \to 7}$ and $\varphi_{6 \to 8}$ in eqivalence
as the main contributions and the signs of the coefficients are oppo-
site. On the other hand, $\langle \varphi_{5 \to 7}|\sum_p e\vec{r}_p|\Psi_G\rangle$ and $\langle \varphi_{6 \to 8}|\sum_p e\vec{r}_p|\Psi_G \rangle$ have
the same signs in each of X and Y directions and have the similar ab-
solute values as was shown in Table 4 . Therefore, the absorption in-
tensity of S_1 may be expected to be very small, because of the cancel-
lation by the two moments in the opposite directions. The exact cal-
culations considering all the singly excited configurations revealed

that the transition moment and the oscillator strength are 0.2452 and
0.0223, respectively: S_1 is a very weak transition. The prediction
is true in the experiment.(exp. f=0.02) Through these discussions we
can realize that the excited state S_1 is not expressed by such a single
electronic configuration as was done in the HMO or the Extended HMO theory.

According to the MIM calculations, the S_1 state is mainly express
ed as the LE function of $^1B_{2u}$ transition of benzene.(Table 3) The $^1B_{2u}$
transition of benzene(250 nm) is a forbidden transition and its oscil-
lator strength vanishes in the calculations although the experimental
value is f=0.002. The transition is considered to be a vibronic one
having intervals of 925 cm^{-1} of the a_{1g} vibration of benzene ring with
the singly excited e_{2g} vibration ($B_{2u} \times E_{2g} \times A_{1g} = E_{1u}$; $^1E_{1u}$ is an allowed
transition).(16). The vibrational structure is also observed in the
spectrum of PVCi.

The absorption intensity of S_2. The state function of S_2 are
mainly occupied by the configuration $\varphi_{6\to7}$, with the minor mixing of
$\varphi_{6\to8}$. $\langle \varphi_{6\to7}|\sum_p e\vec{r}_p|\Psi_G\rangle$ and $\langle\varphi_{6\to8}|\sum_p e\vec{r}_p|\Psi_G\rangle$ have the same signs in
the Y direction and the opposite in the X direction. The coefficients
of $\varphi_{6\to7}$ and $\varphi_{6\to8}$, however, have the same sign. Therefore, the
calculated value of $\langle\Psi_{S2}|\sum_p e\vec{r}_p|\Psi_G\rangle$ becomes finally smaller than
$\langle\varphi_{6\to7}|\sum_p e\vec{r}_p|\Psi_G\rangle$ in the X direction and larger in the Y direction. The
details of the oscillator strength as the function of the directions
are shown in Fig.8(a).

The state function of S_2 becomes a complicated one in the MIM
calculations(Table 3), in contrast with the single function $\varphi_{6\to7}$ in
the PPP method. On the other hand, the state function of S_1 is ex-
pressed by a simple $^1B_{2u}$ function in the MIM method although it be-
comes very complicated in the PPP method. These features reflect the
characteristic of the model adopted in each of the two methods; MO is
constructed by all the AO of the molecule in the PPP method and by the
AO of each chromophore in the MIM method.(see Fig.1) From these dis-
cussion we can realize that S_2 is a excited state spread all over the
molecule(also see MO 6 and 7 in Table 2), and S_1 is a excited state
localized in benzene ring; and also realize the importance of the se-
lection of the theoretical model in the comprehensive understanding of
the experimental phenomena.

The absorption intensities of S_3, S_4 and S_5. From Table 3 it is
found that the main contribution to S_3 is $^1B_{1u}$ of benzene ring and
those to S_4 and S_5 are $^1E_{1u}$ of benzene. The separation of the contri-
butions of S_3, S_4 and S_5 from the observed spectrum is difficult on
the absorption intensity, because the intensity of $^1B_{1u}$ of benzene is
about 50 times stronger than $^1B_{2u}$ in spite of its forbidden character.
($^1B_{1u}$ has the same progressions 925 cm^{-1} of a_{1g} as those of $^1B_{2u}$, and
is considered to be a vibronic transition with the vibrations e_{2g} and
b_{2g}(17).($B_{1u} \times E_{2g} = E_{1u}$, $B_{1u} \times B_{2g} = A_{2u}$) The intensity is f=0.1 experi-
mentally and f=0 theoretically) Therefore, the calculated intensity
of S_3 may become smaller than the experimental value. On the other
hand, the PPP calculation gives the larger value on the intensity of
$^1E_{1u}$ state compared with the experimental one; and the intensities of
S_4 and S_5 may become larger in the calculations. Recently, it was

found in our laboratory that the calculated value of the intensity of $^1E_{1u}$ became close to the experimental one when the contributions of $(\sigma \to \sigma *)^1$ transitions were considered in the calculations.

On the Absorption Spectrum of Cinnamic Acid Crystal by the Polarized light. The absorption spectra of cinnamic acid crystal(α-form) by the polarized light were measured by Tanaka(4), which was shown in Fig.8(c). Since the molecular plane of trans-cinnamic acid is nearly on the (010) plane in α-form, we can expect to reproduce well the spectra by the PPP calculations. The result is shown in Fig.8(a), from which the spectra of Fig.8(c) are considered to be those measured at the 45° rotation. At the 45° rotation S_1 has a little and S_3+S_4 has much stronger absorption intensity than S_2 in the Y direction which coresponds to that perpendicular to the a-axis. In the X direction, S_1 and S_3+S_4 have weaker intensities than S_2. The intensities of S_1 and S_2 are stronger in the X direction than those in the Y direction, and in the case of S_3+S_4 the intensity in the Y direction is stronger than that in the Y direction. These theoretical results are in accordance with the experimental observation in Fig.8(c).

The forbidden $^1B_{1u}$ and $^1B_{2u}$ transitions of benzene become allowed ones by substituting –CH=CH–COOR group for hydrogen. Provided the substituent is considered to be only an origin of the purterbation, cinnamoyloxy group can be treated as monosubstituted benzenes, for example, aniline, phenol, etc.. The assumption is the same one that is adopted in the HMO calculation, where cinnamoyloxy group belongs to C_{2v} point group. B_{1u} and B_{2u} representations in D_{6h} point group reduce to A_1 and B_1 in C_{2v}. The transitions from the ground state to A_1 and B_1 states are allowed in the direction of the long axis of the molecule for the former and the short axis for the latter. Tanaka expected that the direction of the S_1 transition should be short axis(4). The result in Fig.8(a), however, shows that the S_1 transition has both of the components in the X and Y directions at the 60° rotation. The same phenomena is also found in the S_3 transition. In the cases of aniline, phenol, etc., of which π-electron systems exactly belong to C_{2v} point group, the weak transitions arising from B_{1u} and B_{2u} of benzene are exclusively separated in the direction of long- and short-axis, respectively(18). Therefore, we can consider that the phenomena arise from the fact that π-electron system of cinnamoyloxy group belongs to C_s and not to C_{2v} symmetry.
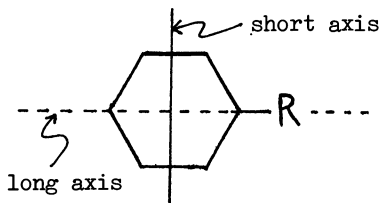
On the Spectra of the $S_0 \to T_1$ Transition. The phosphorescence spectrum and $S_0 \to T_1$ absorption spectrum are shown in Fig 3(b) with the calculated value. 0-0 Band is about 20000 cm^{-1} in the both cases and the vibrational structures also have the same intervals of about 1500 cm^{-1}. Therefore, the observed phosphorescence is concluded to be the emission from T_1 to S_0 of ethyl cinnamate and the $S_0 \to T_1$ Frank-Condon state of T_1 has the same energy level that

the longest living phophorescent T_1 state which may play an important
role in the photochemical reaction. Since the calculated value of the
transition energy in the PPP method is that of the Frank–Condon state,
these experimental facts support the exactness of the discussions on
the photochemical reaction in the triplet state based on the theoreti-
cal results by the PPP calculations.

As was shown in Table 3, the contribution of the LE function of
ethylene for the state function of T_1 is about 42 %. Therefore, we
can consider that the vibrational structures in Fig.3(b) arise from
the stretching vibration of the central double bond of cinnamoyloxy
group. The vibrational structures of $S_0 \rightarrow S_1$ absorption, $S_1 \rightarrow S_0$ fluores-
cence and $S_0 \rightarrow T_1$ absorption spectra of stilbene have the progressions
of 1599 cm^{-1}, 1635 cm^{-1} and about 1500 cm^{-1}, respectively. McClure
concluded that these progressions arose from the stretching vibration
of the central double bond of stilbene[19]. According to our results
of the MIM calculations, the LE function of ethylene is the main con-
tribution to the state functions of S_1 and T_1 of stilbene[18]. The
correlation diagram among the state functions of benzene, ethylene,
cinnamoyloxy group and stilbene is shown in Fig.9 . It illustrates
well the similarities the electronic states of cinnamoyloxy group and
stilbene

Charge Distributions---What is the Intramolecular Charge Transfer
Transition(CT Band)?. Tanaka discussed that the strong absorption
band at 36000 cm^{-1}(S_2) of cinnamoyloxy group is regarded as an intra-
molecular charge transfer band because the charge transfer from the
highest occupied orbital of the styryl group to the vacant orbital of
the carboxyl group will take place quite easily. On the other hand,
he considered that the 34000 cm^{-1} band(S_1) is dirived from the$^1B_{2u}$
state of benzene in consistent with our conclusion discussed above.

The charge distributions in the various electronic state of cin-
namoyloxy group are tabulated in Table 5 , following the results of the
PPP calculations. Although we can recognize the difference between
the charge distributions of S_1 and S_2, it is too small to distinguish
between the localized excited state and the charge transfer state.
If the consideration is concentrated on the charge distributions, the
electron transfer from ethylene to carboxyl group in S_2 compared with
S_1 should be rather recognized than that from styryl to carboxyl group
(Table.5). According to the result of the MIM calculations where cin-
namoyloxy group is divided into styryl and carboxyl, the contributions
of the charge transfer configuration from the highest occupied orbital
of styryl group to the vacant orbital of the carboxyl group(which is
only one in the π-electron approximation) are only 11.84 % and 1.8 %
in the state function of S_2 and S_1, respectively. From these discus-
sions, it seems that the change of the charge distribution or the real
occurance of the electron transfer from one chromophore to another
following the transition is independent of the real meaning of the in-
tramolecular charge transfer transition.

What is the real meaning of the intramolecular charge transfer
transition, then? We should remember the resemblance between the
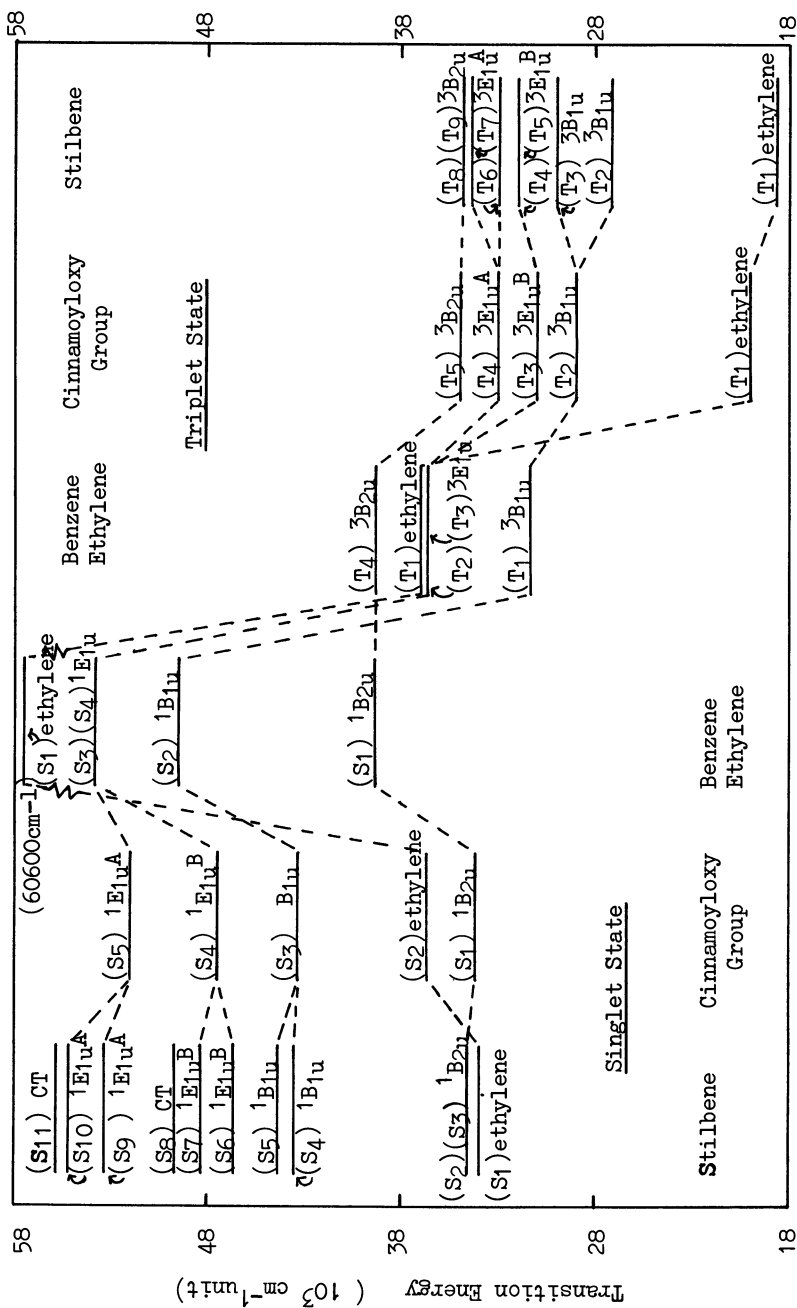
Figure 9. Correlation diagrams of the electronic states of benzene, ethylene, cinnamoyloxy group, and stilbene. E_{1u}^{A} and E_{1u}^{B} mean the A and B state, respectively, when we assume that phenyl group belongs to C_{2v} point group. CT means the charge transfer state.

Table 4. Transition Moments at the Various Electronic
Configurations $\langle \varphi_{i \to j}| \sum_p \vec{er}_p| \Psi_G \rangle^{*1}$

	Energy Level[4] (eV)	Transition Moment (Å)[2],[3]	
		X-direction	Y-direction
$\varphi_{6 \to 7}$	4.82	-1.220	-0.896
$\varphi_{5 \to 7}$	5.33	0.476	-0.394
$\varphi_{6 \to 8}$	5.67	0.658	-0.490
$\varphi_{5 \to 8}$	6.09	0.551	0.821
$\varphi_{6 \to 9}$	6.75	0.003	-0.401
$\varphi_{5 \to 9}$	6.79	0.648	-0.402
$\varphi_{4 \to 7}$	6.89	-0.515	0.214
$\varphi_{3 \to 7}$	7.31	-0.002	-0.047

*1. Atomic Configurations are expressed in Å (Fig.1)
*2. The transition moment for the Z-direction always
   vanishes in the PPP calculations because of the
   plane structure of cinnamoyloxy group
*3. The transition moment is a vector of which the sign
   depends on the sign of Ψ_{Sn}(exactly, the sign of the
   coefficient of $\varphi_{i \to j}$ of Ψ_{Sn} in Table 2). However since
   a quantum-mechanical state function does not change to
   an other state function by the change of sign, on the
   transition moment of a molecule the direction is deter-
   mined exclusively but the sign remains infinitive.
*4. Based on the energy level of S_0

Table 5. Charge Distributions in the Various Electronic States
of trans-Cinnamoyloxy Group

	Styryl	Carboxyl	Phenyl	Acrylyloxy	Total
S_0	7.946	4.054	5.971	6.029	12
S_1	7.868	4.132	5.746	6.254	12
S_2	7.853	4.147	5.720	6.280	12
S_3	7.965	4.035	5.952	6.048	12
S_4	7.898	4.102	5.852	6.148	12
T_1	7.879	4.121	5.734	6.266	12

Table 6.   The Resemblance of the S₁ State Function of Stilbene and the S₂ State Function of Cinnamoyloxy Group.

Stilbene — Total 86.82

	G & LE (44.68)				CT (42.14)					
	G	R.B	L.B	E	L.B→R.B	R.B→L.B	E→L.B	L.B→E	R.B→E	E→R.B
	0.00	12.32	12.32	20.04	2.41	2.41	9.33	9.33	9.33	9.33
subtotals		24.64		20.04	4.82		37.32			

Cinnamoyloxy Group — Total 86.71

	G & LE (45.00)				CT (41.71)					
	G	B	COO	E	B→COO	COO→B	E→B	B→E	COO→E	E→COO
	2.43	20.84	0.63	21.10	4.21	0.27	8.02	21.97	1.30	5.94
subtotals		21.47		21.10	4.48		37.23			

Figures are the squares of the coefficients of the LE and CT functions (the square of the matrix element of M of Eq. (8)), as the linear combinations of which the state functions are expressed. G: Ground States of the chromophores, E: Ethylene, B: Benzene, L.B: Left benzene of stilbene, R.B: Right benzene of stilbene, COO: Carboxyl group.

electronic states of cinnamoyloxy group and stilbene. There are no
displacements of electron in the molecule in any electronic states of
stilbene. From the correlation diagram in Fig.9, the S_2 state of cin-
namoyloxy group corresponds to the S_1 state of stilbene. The composi-
tions of the electronic configurations in the MIM calculations in
these two states are comparatively tabulated in Table 6. From this
Table, we can find out the remarkable resemblance between the two states of
the different molecules. The characteristic is that the contribution of
the charge transfer configurations is extraordinary large. (total 42%)
In the MIM method, the role of the CT configuration is the combination
of the chromophores, the components of the molecule. Therefore, the
large contribution of the CT configurations means that the electronic
state spreads all over the molecule, or is delocalized. This is the
real meaning of the intramolecular charge transfer state, to which the
intramolecular CT band appears at the transition of the molecule from
the ground state. The direction and the magnitude of the transition
moment are independent of the existence of heteroatom. The equivalent
contributions of the forward and backward charge transfer configura-
tion in stilbene are modified in cinnamoyloxy group because of the
deep ionization potential and the large electron affinity of hetero-
atoms. The contribution of the CT configutation forward the hetero-
atom becomes larger in the lower energy transitions and, on the other
hand, that backward the heteroatoms in the higher energy transitions;
and this is the cause of the occurance of the displacement of electron
in the molecule. Then, how can we explain the large displacement of
electron in S_1? From the results of the MIM calculations in Table 3
and Appendix 1, we cannot find out any reason why the charge distri-
bution in carboxyl group is large in S_1. It may be concluded that we
should consider multi-electron excited CT configurations in the MIM
calculations in order to express the S_1 state of cinnamoyloxy group in
the PPP method.

Literature Cited

1) Minsk,L.M. et al., J.Appl.Polymer Sci.,(1959),2,302,309; Tsuda,M.,
J.Polymer Sci.,(1963),B1,215, Makromol.Chem.,(1964),72,174,183, ibid,
(1973),167,183, J.Polymer Sci.,(1964),A2,2907, ibid,(1964),B2,1143,
Bull.Chem.Soc.Japan,(1969),42,905, and many others.
2) Nakane,H.,Gazô Gizyutsu,(1974),5,(5),39
3) Jaffé,H.H. and Orchin,M.,"Theory and Applications of Ultraviolet
Spectroscopy",206,Forth Ed.Wiley.,N.Y.,(1966)
4) Tanaka,J.,Bull.Chem.Soc.Japan,(1963),36, 833
5) Tsuda,M and Oikawa,S.,The 28th Annual Meeting of Chemical Soc.
Japan,Tokyo,Preprint I,1Q30,1Q31 and 1Q32 (1973)

6) Tsuda,M.,J.Scientific Org.Chem.Japan(Yukigôseikagaku),(1972),30, 589, Nippon Shashin Gakkai-shi,(1969),32,82

7) Longnet-Higgins,H.C. and Murrell,J.N.,Proc.Phys.Soc.,(1955),A68,601

8) Parr,R.G.,"Quantum Theory of Molecular Electronic Structure", Benjamin,N.Y.,(1964)

9) Nakanura,K.,Bull.Chem.Soc.Japan.,(1967),40,1027

10) Pariser,R. and Parr.,R.G.,J.Chem.Phys.,(1953),21,767

11) Fueno,T.et al.,Bull.Chem.Soc.Japan.,(1972),45,3294

12) Mataga N.and Nishimoto,K.,Z.Physik.Chem.(Frankfurt),(1957),13,140

13) Woodward,R.B.and Hoffmann,R,,"The Conservation of Orbital Symmetry",Verlay Chemie.GmbH.Weinheim,(1970)

14) Ref.331) in Ref 8)

15) Yabe,A,,Tsuda,M.,Honda,K.and Tanaka,H,,J.Polymer Sci.,(1972),(A-1) 10,2379

16) Herzberg,G.,"Electronic Spectra and Electronic Structure of Polyatomic Molecule",555,D.Van Nostrand,Princeton (1967)

17) Robinson,G.W. et al.,Annual Report Cal.Tech.(Chemistry),(1970),86

18) See the Appendix of the following paper by the authors in this book.

19) Dyck,R.H. and McClure,D.S.,J.Chem.Phys.,(1962),36,2326

20) Tsuda,M.and Oikawa,S. and Miyake,R.,J.Soc.Phot.Sci.Japan(Nippon Shashin Gakkaishi),(1972),35,90

21) Baba,H.,Suzuki,S. and Takemura,T.,J.Chem.Phys.,(1969),50,2078

22) Roothaan,C.C.J.,J.Chem.Phys.,(1951),19,1445

23) Tsuda,M.,J.Soc.Phot.Sci.Japan(Nippon Shashin Gakkai-shi),(1969), 32,82

<u>Appendix</u> The Contributions of Various Electronic Configurations
of the MIM model for the State Functions of the PPP model of
Cinnamoyloxy Group = Styrene(S) + Carboxyl Group(COO)

Singlet State		S_0	S_1	S_2	S_3	S_4	S_5
LE	G	91.82	0.03	1.14	0.04	0.15	0.12
	S	0.31	90.36	77.74	88.72	85.30	57.80
	COO	0.06	0.02	0.77	0.07	0.30	17.30
CT	S → COO	6.36	1.92	12.53	3.54	6.62	2.91
	COO → S	1.23	0.12	1.68	0.30	0.46	15.44
Total		99.78	92.45	93.86	92.67	92.83	93.57
LE+G		92.19	90.41	79.65	88.83	85.75	75.22
CT		7.59	2.04	14.21	3.84	7.08	18.35

Triplet State		T_1	T_2	T_3	T_4	T_5
LE	S	83.30	86.63	90.01	84.66	92.07
	COO	1.72	2.43	0.16	5.05	0.01
CT	S → COO	8.62	2.73	2.08	1.62	0.30
	COO → S	1.65	0.95	0.08	1.21	0.21
Total		95.29	92.74	92.33	92.54	92.59
LE		85.02	89.06	90.17	89.71	92.08
CT		10.27	3.68	2.16	2.83	0.51

Figures are the squares of the coefficients in the state functions
expressed as a linear combination of the electronic configurations
of the MIM model. G: Ground configuration, LE: Configuration of
the localized excitation, CT: Charge transfer configuration

Appendix The Contributions of Various Electronic Configurations
of the MIM model for the State Functions of the PPP model of
Cinnamoyloxy Group = Benzene(B) + Acrylyloxy Group(AC)

Singlet State		S_0	S_1	S_2	S_3	S_4	S_5
LE	G	89.42	0.16	1.31	0.09	0.04	2.89
	B	0.14	76.27	22.90	69.27	56.36	25.24
	AC	0.05	1.02	31.39	15.79	3.97	30.60
CT	B→AC	6.36	12.12	29.29	5.20	26.29	17.85
	AC→B	3.60	2.02	8.43	1.21	5.30	13.51
Total		99.57	91.59	93.32	91.56	91.96	90.09
LE+G		89.61	77.45	55.60	85.15	60.37	58.73
CT		9.96	14.14	37.72	6.41	31.59	31.36

Triplet State		T_1	T_2	T_3	T_4	T_5
LE	B	19.69	71.48	76.67	76.51	84.42
	AC	52.32	19.34	0.71	11.67	0.01
CT	B→AC	16.01	0.41	13.61	2.46	2.09
	AC→B	6.41	0.15	0.67	0.83	5.22
Total		94.43	91.38	91.66	91.47	91.74
LE+G		72.01	90.82	77.38	88.18	84.43
CT		22.42	0.56	14.28	3.29	7.31

Figures are the squares of the coefficients in the state functions
expressed as a linear combination of the electronic configurations
of the MIM model. G: Ground configuration, LE: Configuration of
the localized excitation, CT: Charge transfer configuration